Generation of transgenic lines for analysis of neural crest development in zebrafish

Carney, Tom

Award date:
2003

Awarding institution:
University of Bath

GENERATION OF TRANSGENIC LINES FOR ANALYSIS OF NEURAL CREST DEVELOPMENT IN ZEBRAFISH

Submitted by Tom Carney
for the degree of PhD of the University of Bath
2003

COPYRIGHT

Signed:.....

Date:29/12/03.....

ProQuest LLC
789 East Eisenhower Parkway
P.O. Box 1346
Ann Arbor, MI 48106-1346

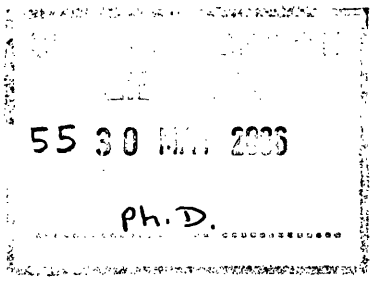
55 30 MAY 2936
Ph.D.

ABSTRACT

The neural crest is an embryonic cell type derived from the ectoderm that gives rise to a number of diverse cell types. Factors required for correct differentiation of these derivatives from the initial multipotent neural crest cell population have been described, however the interactions and roles of these factors in the neural crest are not fully understood. Zebrafish *colourless (cls)* mutants display disrupted development of non-ectomesenchymal neural crest derivatives including chromatophores and neurons and glia of the peripheral nervous system, and correspond to mutations in the transcription factor, *sox10*. Reported *cls* alleles appear to be nulls with lesions including missense and nonsense point mutations. Mutations in human Sox10 are associated with Waardenburg-Shah syndrome and Hirschsprung's Disease, whilst mouse *Sox10* mutants correspond to the *Dominant megacolon* mutant.

Here the isolation and mapping of PAC genomic clones containing zebrafish *sox10* is described, the partial sequence of which has allowed the deduction of *sox10* gene structure. Injection experiments have shown the ability of these clones to partially rescue pigment and neuronal aspects of the *cls* phenotype. This indicated that the PACs contain sufficient promoter sequence required for functional *sox10* expression.

To assist *in vivo* analysis of the role of *sox10* and other genes in neural crest development, three GFP reporter constructs have been made, including both an engineered *sox10* PAC and constructs containing 6.1 or 4.9 kb upstream promoter fragments. These all drive GFP expression in appropriate sites, including the neural crest and CNS, but also ectopically in muscle fibres in transient assays. Germline transgenics have been generated for all three reporter constructs, and show expression in premigratory neural crest, and later in certain migrating neural crest populations, in particular neural crest cells in the branchial arches and PNS glial cells. Other expression sites include cartilage cells, otic epithelia, oligodendrocytes and the olfactory bulb. Similarities and differences between the transgenic lines produced are discussed, as are some potential uses.

Two interesting *cls* alleles have been characterised. One spontaneous mutant has been shown here to be due to a transposable element, previously implicated in another spontaneous zebrafish mutant. Finally, an allele screen afforded an apparently weaker zebrafish *cls* allele with an unusual DRG-associated neurogenic phenotype. This may provide a unique insight into the mechanisms involved in DRG formation and the role of *sox10* therein.

ACKNOWLEDGEMENTS

Foremost I would like to express my sincere gratitude to my supervisor, Dr Robert Kelsh, for the opportunity to work in this field and for imparting his knowledge of zebrafish and developmental biology, as well as his guidance, support, inspiration and infectious enthusiasm.

I would also like to thank the members of the Kelsh lab, past and present, who have all assisted me at some point. A. Pauliny provided me with working *in situ* probes, PCR conditions and primers, and S. Lopes and V. Nikolić offered technical and biological opinions. In particular, I would like to thank K. Dutton for her advice and teaching me fish handling, microscopy and almost all of the embryological techniques I know. The majority of the screening work in Chapter 5 was performed by her. I am also grateful to the rest of lab 0.76 for both assistance and distraction, especially Diya for chromatography reagents and all the Duttons for supplying the lab with home-cooked food. The *in situ* in Appendix 2 was performed by Ben Steventon.

I owe much to the Postdocs of the Kelsh lab, from whom I have learnt a good deal. In particular Dr. Stone Elworthy, who taught me the virtues of the fastidious approach, and was generous with his knowledge, suggestions and encouragement. Dr. Arie Jacoby provided both helpful scientific comment and a light-hearted reminder of the Australian way. Thanks also to Dr. James Dutton for assistance with defining the transgenic expression domains and molecular techniques.

Prof. Randall Moon (University of Washington, Seattle) generously supplied the GFP plasmid XLT.GFP$_{LT}$.CS2+, whilst the Shuttle Vector and protocol for the recombinogenic targeting was recommended and kindly provided by Dr. Rosalind John (University of Cambridge), with permission from Dr. N Heintz (Rockefeller University, New York). Dr. Alan Wheals (University of Bath) was very kind in providing access to, and assistance with, the Pulsed Field Gel Electophoresis apparatus. Thanks also go to all the fish technicians who have cared for the aquarium and fish, and to the laboratory technicians for ensuring ample supplies of lab stocks.

Finally thanks to J. Savović for unwavering support, and to my family, especially to my brother and Mum.

This PhD. was funded by an ORS award (British Council) and a University of Bath studentship.

TABLE OF CONTENTS

ABBREVIATIONS

% (w/v)	percent weight per volume
A, C, G, T	adenine, cytosine, guanine, thyamine
[α–^{32}P] dCTP	alpha-labelled deoxycytosine triphosphate
bp, kb	base pairs, kilobase pairs, megabase pairs
BAC	Bacterial Artificial Chromosome
β-gal	β-galactosidase
bHLH	basic helix-loop-helix
BSA	Bovine serum albumin
°C	degrees Celsius
cDNA	deoxyribonucleic acid complementary to ribonucleic acid
CNS	Central Nervous System
C-terminal	carboxy-terminal
dATP	2'-deoxyadenosine-5'-triphosphate
dCTP	2'-deoxycytosine-5'-triphosphate
dGTP	2'-deoxyguanosine-5'-triphosphate
dTTP	2'-deoxythymidine-5'-triphosphate
DMSO	dimethylsulphoxide
DNA	deoxyribonucleic acid
dpf	days post fertilisation
DRG	Dorsal Root Ganglion
DTT	dithiothreitol
ECM	extra-cellular matrix
EDTA	ethylenediaminetetraacetic acid
ENS	Enteric nervous system
ENU	Ethylnitrosourea
g	force of gravity
mg, μg, ng, pg	milligram(s), microgram(s), nanogram(s), picograms(s)
GFP	green fluorescent protein
HMG	High-mobility group
hpf	hours post fertilisation
IPTG	isopropyl-β-D-thiogalactoside
L, ml, μl	litre(s), millilitre(s), microlitre(s)
M, mM, μM	moles per litre, millimoles per litre, micromoles per litre

MHB	midbrain-hindbrain boundary
mRNA	messenger ribonucleic acid
cm, nm	centimetre, nanometre
NCSC	neural crest stem cell
NLS	Nuclear localising signal
N-terminal	amino-terminal
PAC	P1-derived Artificial Chromosome
PCR	polymerase chain reaction
PFG	pulsed field gel
PFGE	pulsed field gel electrophoresis
PNS	Peripheral Nervous System
Prim	primordium
PTU	1-phenyl-2-thiourea
PVP	polyvinylpyrrolidine
5'-RACE	rapid amplification of 5' cDNA ends
®	Registered
RNA	ribonucleic acid
RNase A	ribonuclease A
RT	Reverse Transctiption
SDS	sodium dodecyl sulphate
SSC	saline sodium citrate
som	somite(s)
TAE	Tris-acetate-EDTA
Taq	*Thermus aquaticus*
TBE	Tris-borate-EDTA
TE	Tris-EDTA
Tris	Tris [hydroxymethyl] amino methane
™	Trademark
TUNEL	Terminal deoxynucleotidyl transferase-mediated dUTP nick end-labelling
U	unit(s) of enzyme
UTR	untranslated region
UV	ultraviolet
V, kV	Volts, kilovolts
X-gal	5'-bromo-4-chloro-3-indoyl-β-D-galactopyranoside
YAC	Yeast Artificial Chromosome

CHAPTER 1

INTRODUCTION

1.1. THE NEURAL CREST

1.1.1. Overview

The neural crest is an embryological stem cell population, and comprises the precursors to a wide diversity of cell types. Formed from the ectoderm, it exists only transiently during development as mesenchymal tissue, which arises upon delamination from the nascent neural tube during neurulation. Subsequent migration, specification and fate restriction appear to be intimately interrelated processes, which have attracted much attention, due to both the relevance to human disease aetiology and as a model of stem cell ontogeny. Upon differentiation, the varieties of cell types generated include peripheral neurons and glia (including those associated with cranial, enteric, sympathetic and sensory (dorsal root) ganglia), Schwann cells, adrenal medullary cells, pigment cells and craniofacial cartilage (Le Douarin and Kalcheim, 1999). The critical stages of neural crest cell development will be briefly discussed here.

1.1.2. Formation and induction of Neural Crest

1.1.2.1. Morphological changes involved with Neural Crest formation

Neural crest forms at the lateral edges of the neural plate at the interface with the surface ectoderm (the future epidermis). The precise timing of neural crest induction is unclear, but it probably results from a multistep mechanism, initiated during gastrulation and continuing until neural tube closure (Aybar and Mayor, 2002). In species which undergo mostly primary neurulation (amphibians, mouse and chick), induced neural crest cells delaminate from the neural folds either before they meet in the mid-line or after neural tube closure, depending on the organism and the axial position. Zebrafish instead undergo secondary neurulation, forming a neural keel, without neural folds. Subsequent to the formation of the neural keel, at approximately 15hpf, the neuroepithelium separates from the overlying the ectoderm, and concomitantly, neural crest cells can be seen segregating from the dorsal aspect of the neural keel. As in other vertebrates, the segregation and future development of neural crest cells occurs in a rostrocaudal progression (Raible *et al.*, 1992).

1.1.2.2. Molecules implicated in Neural Crest induction

There is a growing understanding as to the molecular mechanisms involved in neural crest induction, driven by a combination of techniques including confrontation of tissues *in vivo* and *in vitro*, exposure of explants to growth factors and perturbation of signalling pathways using overexpression assays and mutagenesis approaches. A critical component of these experiments is the detection of induced neural crest cells, which almost always relies on the use of early neural crest markers such as *Snail, Slug, Zic* and *FoxD3*. It has been long appreciated that interaction between the neural plate and the lateral ectoderm can induce neural crest markers (Selleck and Bronner-Fraser, 1995). One model invokes the ventral to dorsal gradient of BMP activity across the neural plate, established by a ventral source of BMP expression (in particular BMP-2/-4/-7) and a dorsal sink of BMP antagonists (such as *noggin*, *chordin* and *follistatin*) in the organiser region. The model proposes that regions of low BMP activity form neural keel, regions of high BMP activity form epidermis, whilst at intermediate levels between the two cell types, neural crest forms (Mullins *et al.*, 1998). Evidence for this comes from introducing various activators or repressors of BMP signalling directly into embryos or to explants. For example, addition of mesodermally derived BMP antagonists to *Xenopus* animal caps induces neural crest marker expression (Marchant *et al.*, 1998; Morgan and Sargent, 1997) and addition of BMP-4 expressing cells to chick neural plate explants induces neural crest markers (Liem *et al.*, 1995). Zebrafish BMP mutants support this BMP gradient model, with mutants abolishing all BMP signalling having no induced neural crest, whilst those with diminished BMP signalling show a ventral expansion of neural crest markers (Mullins *et al.*, 1998; Nguyen *et al.*, 1998).

There is clear evidence that other signalling mechanisms and factors are essential to the process of neural crest induction. For example, addition of FGFs, which constitute posteriorising signals in the neural plate, can restore the ability of *noggin* to induce neural crest markers in *Xenopus* neural plate explants (LaBonne and Bronner-Fraser, 1998), and overexpression of an FGF inhibitor in *Xenopus* embryos can inhibit crest markers (Mayor *et al.*, 1997). In chick, analysis of misexpression and grafting studies has led to the proposal that FGFs have a role in establishing the neural plate border (Streit and Stern, 1999). Wnts also act as a posteriorising signal which, like FGFs, can act with *noggin* to induce neural crest markers in neural plate explants. Inhibition of Wnt signalling prevents neural crest marker expression (LaBonne and Bronner-Fraser, 1998). However, there may be other mechanisms through which Wnts act to induce neural crest. Recently, for example, Wnt6 was shown to induce neural crest in naïve chick neural plates alone, and that its inhibition blocks neural crest formation *in vivo*. This indicated that in chick, Wnt6

is necessary and sufficient for neural crest induction. Furthermore, its expression domain is consistent with its identity as the ectodermal neural crest inducer (Garcia-Castro *et al.*, 2002). As with BMPs, later roles for Wnts in the maintenance of neural crest identity can be proposed based on functional studies and new expression domains in the dorsal ectoderm of the neural tube and neural crest (Aybar and Mayor, 2002).

An additional mechanism, which is likely to act during neural crest induction, has been demonstrated in zebrafish, where neural crest cells arise from an equivalence group with Rohon-Beard sensory neurons. *narrowminded* mutants lack both these cell types (Artinger *et al.*, 1999), and Delta-Notch signalling clearly acts to segregate one of these cell types from the other (Cornell and Eisen, 2000; see Section 5.1). Rohon-Beards or analogous cells also exist in *Xenopus* and mammals, and thus similar lateral inhibition mechanisms might also be functioning within the neural plate of these species to generate neural crest cells (Cornell and Eisen, 2000).

It is most probable that multiple signals will be involved in the steps of neural crest induction. Additional complexity is provided by the differences in the mechanisms involved and the relative importance of each signalling system between species (Aybar and Mayor, 2002; LaBonne and Bronner-Fraser, 1999).

1.1.3. Segregation of Neural Crest cells

Following their induction, neural crest cells segregate as individual cells at the dorsal midline of the neuroepithelium via an epithelial to mesenchymal transition (Le Douarin and Kalcheim, 1999). Following its early role as a ventralising signal, BMPs are later expressed in the dorsal neural tube (Sela-Donenfeld and Kalcheim, 1999). The dorsal neuroepithelial expression of BMP4 (see above), and a caudo-rostral gradient of its antagonist, *noggin,* appears to coordinate emigration of neural crest cells, via BMP4-dependant activation of *rhoB* and alteration of the expression profile of *cadherins* in the neural crest (Sela-Donenfeld and Kalcheim, 1999). *rhoB* encodes a GTP-binding protein which transduces extracellular signals and drives cytoskeletal changes. Inhibition of its function has been reported to disrupt neural crest emigration (Liu and Jessell, 1998). The expression profile of *cadherins* changes as neural crest cells leave the neuroepithelium, consistant with the known importance of *cadherin* mediated cell signalling in maintenance of tissue integrity (Akitaya and Bronner-Fraser, 1992; Inoue *et al.*, 1997). Neural crest cells themselves secrete proteases to digest the overlying basal lamina, thus permitting their own emigration (Le Douarin and Kalcheim, 1999). The zinc finger transcription factors *Snail* and *Slug*, are very early markers of the neural crest in the neuroepithelium, and appear to be required for the epithelial to mesenchymal transition, possibly through

repression of certain *cadherins* such as *E-cadherin* (Cano *et al.*, 2000; LaBonne and Bronner-Fraser, 2000). Another transcription factor involved in the induction of the neural crest and/or the segregation of the neural crest from the neuroepithelium is the winged-helix transcription factor, FoxD3. Chick and mouse studies have indicated that ectopic FoxD3 promotes formation of neural crest cells at the expense of surrounding neuroepithelial derived cells, such as interneurons. However FoxD3 must be downregulated for later neural crest cell differentiation. Although independent from the *Slug* cascade, which promotes delamination as well as specification of neural crest, FoxD3 requires Pax3 for its expression. In the mouse Pax3 mutant, *Splotch*, neural crest cells are not formed and this might be due to a specification failure due to lack of FoxD3 (Dottori *et al.*, 2001; Kos *et al.*, 2001).

1.1.4. Migration of Neural Crest cells

1.1.4.1. Pathways of Neural Crest migration

Cranial Neural Crest migration

Once delaminated from the neuroepithelium, cranial neural crest cells migrate laterally through the ECM underlying the ectoderm, and either enter the pharyngeal arches, contribute to the cranial ganglia, or migrate dorsally to produce pigment cells (Le Douarin and Kalcheim, 1999). There has been much study into the migration of the cranial neural crest, in particular, that of the neural crest at the level of the hindbrain. The hindbrain of vertebrates is segmented into rhombomeres, and the migration pattern of neural crest cells here is also segmented. Neural crest cells migrate ventrally from the dorsal hindbrain in three main streams adjacent to rhombomeres 1/2, 4 and 6-8, however they are excluded from migrating adjacent to rhombomeres 3 and 5. Neural crest cells arising from these latter regions often die, but remaining cells migrate rostrally or caudally first before entering one of the three main streams (Bronner-Fraser, 1994; Le Douarin and Kalcheim, 1999). There is good evidence that directing the neural crest cells appropriately into the streams relies on anterior-posterior identity of both the neural crest and the surrounding environment, and that this identity is established by the *Hox* code (reviewed in Le Douarin and Kalcheim, 1999).

Pathways of Trunk Neural Crest migration

After emigration from the dorsal neural tube, trunk neural crest cells are known to pause in a cell-free and ECM-rich migration staging area sited dorsolateral to the neural tube, from where they subsequently migrate away to take up the various positions in the

embryo. From this position, neural crest cells extend processes and probe the surface of the somite before migrating (Jesuthasan, 1996). In the trunk, neural crest cells migrate on either of two pathways, a dorsolateral pathway (in zebrafish termed the lateral pathway), which forms underneath the ectoderm and overlying the lateral surface of the somite, and a ventral pathway (termed the medial pathway in zebrafish), which forms between the neural tube and the medial somite surface (Le Douarin and Kalcheim, 1999; Raible *et al.*, 1992). Onset of migration occurs in a rostrocaudal sequence, with neural crest cell invasion of the ventromedial pathway preceeding that of the dorsolaterally pathway. In zebrafish the lag between medial and lateral pathway migration is approximately 4 hours (Raible *et al.*, 1992), whilst in the mouse and chick, it can be up to 1 day (Weston, 1991). Furthermore, the mechanism of migration differs such that the dorsolateral migration pathway is unsegmented, and neural crest cells will cross somite boundaries, whilst neural crest cells migrating on the medial pathway do so in a segmental pattern and at a specific rostro-caudal position relative to each somite (Bronner-Fraser, 1994; Le Douarin and Kalcheim, 1999). In chick, this is in the rostal half of each somite, whilst in zebrafish neural crest cells will migrate along the middle of the somite (Raible *et al.*, 1992). The medial pathway is also used independently by other cells and axons, namely dorsally migrating sclerotome cells and outgrowing spinal nerves (Morin-Kensicki and Eisen, 1997).

1.1.4.2. Molecules involved in controlling Neural Crest migration

Recent work has been directed towards determining the molecules underlying the control of neural crest migration. Firstly, delay of migration onto the lateral pathway correlates with deposition of inhibitory molecules in this location, namely peanut agglutinin (PNA)-binding glycoproteins and chondroitin-6-sulfate. Neural crest migration on this pathway begins after these factors are downregulated (Oakley *et al.*, 1994). Other factors are likely to play a role in migration on this pathway. c-Kit is a receptor tyrosine kinase expressed in melanoblasts and crucial to melanoblast survival, proliferation and migration (Steel *et al.*, 1992). It is bound by a soluble and membrane-bound form of its cognate ligand Steel-factor (SCF), with different roles ascribed to the different forms. The soluble form of SCF appears to be crucial in initial migration of melanoblasts onto the lateral pathway (Wehrle-Haller and Weston, 1995).

A number of factors control the segmental migration of neural crest cells on the medial pathway. Visualizing neural crest migration in chick embryos where some somites have been rotated 180°, led to the deduction that the information directing segmental migration is provided by the somites (Bronner-Fraser and Stern, 1991). The factors secreted by the somites form components of the extracellular matrix and act through integrin receptors

expressed on the neural crest cell surface to either promote or inhibit migration. This ultimately leads to funnelling of neural crest cells onto the correct path. Thus sites where neural crest cells do not migrate have been shown to contain a number of inhibitory ECM or cell adhesion molecules, including F-spondin, collagen IX, T-cadherin and versican. As with the lateral migration pathway, PNA-binding glycoproteins and chondroitin-6-sulfate also play an inhibitory role in the medial pathway (Krull, 2001).

Promoters of neural crest migration are often not localised specifically, but act as a permissive substrate for neural crest migration. Some of the molecules acting in this fashion are also required for the emigration of nascent neural crest cells from the neuroepithelium, and include fibronectin, laminin, thrombospondin and tenascin (Krull, 2001; Le Douarin and Kalcheim, 1999). Finally, the Eph family of receptor tyrosine kinases and their ligands, ephrins, play a role in segmental migration of trunk neural crest cells, along with many other roles in cell migration during development. As both receptor and ligands are located on the cell surface, their effects are mediated by direct contact between neural crest and somite cells. Analysis of expression patterns of Eph receptors and their ligands indicated that some were localised to regions of the somite corresponding to regions inhibitory to neural crest migration. For example, the EphB3 receptor was found to be expressed in the caudal half of somites, whilst its ligand ephrin-B1 was expressed on the surface of migrating neural crest cells (Krull *et al.*, 1997). Functional assays have shown that the interaction is a repulsive one, and is likely to prevent neural crest migration over the caudal half of the somites (Wang and Anderson, 1997). There is growing evidence for the role of other ephrin and Eph receptor family members in the control of neural crest migration in the trunk as well as in the hindbrain (Krull, 2001; Robinson *et al.*, 1997).

As to the precise mechanisms that pattern neural crest correctly and bring them to adopt the correct locations, little is known.

1.1.5. Specification of neural crest cells

The question as to whether neural crest cells emigrating from the neural tube are committed to a lineage as soon as they form, or whether they are initially multipotent and commit later is a fundamental question in neural crest biology. This has been addressed with four main approaches: determining heterogeneity in molecular marker expression in the neural crest at various stages, fate mapping neural crest cells by labelling *in vivo*, challenging NCSC cultures *in vitro* and altering neural crest cells' environments by *in vivo* transplantation experiments (Le Douarin and Kalcheim, 1999). Note that only the latter two approaches really test a cell's commitment, which is a function of the cell's potential. Marker analysis only comments on developmental diversity or specification of a

population of cells, whilst fate mapping makes no comment on what a cell can become, only on what cell types it contributes to under normal embryonic conditions. However a progenitor cell contributing to multiple fates, by definition, must be pluripotent for those fates at least. Conversely, a labelled progenitor cell producing only a single fate is said to be specified to that fate, but if challenged, it could potentially produce other cell types (Raible and Eisen, 1994).

A number of different experiments conducted using chick, mouse and zebrafish neural crest cells *in vivo* and *in vitro*, indicate that early neural crest cells are heterogeneous with respect to fate, some being lineage restricted, with others giving rise to a greater range of derivatives. How this heterogeneity arises is unknown, but might involve stochastic events, in combination with regulative interactions between neural crest cells (Raible and Eisen, 1996). The mechanism of restriction of potency in stem cells is also of interest, and might be brought about by either environmental signals instructing uncommitted cells to lose potency, or by intrinsic cellular events, such as asynchronous cell divisions, that alter potency and in doing so alter response to permissive environmental signals (Anderson *et al.*, 1997).

In higher vertebrates, the specification of neural crest cells migrating on the two pathways differs, such that those migrating on the lateral pathway will become pigment cells, whilst those migrating medially are fated to become neurons and glia of the PNS. This migration pattern is mostly true in zebrafish. Cells migrating laterally will only give rise to pigment cells as in chick and mammals, whilst, unlike chick and mammals, those on the medial pathway will become pigment cells as well as neurons and glia (Eisen and Weston, 1993). There is evidence in chick that melanocytes are specified prior to embarking on the lateral pathway (Wakamatsu *et al.*, 1998). Furthermore, neural crest-derived melanocyte precursors in the chick preferentially migrate to the lateral pathway, even if placed ectopically on the medial pathway. Conversely neurogenic precursors transplanted onto the lateral pathway undergo apoptosis. Thus there are environmental differences between the two pathways, which direct specified neural crest cells to migrate appropriately and which remove aberrantly migrating neural crest progenitors (Wakamatsu *et al.*, 1998).

There is evidence from analysis of molecular markers that the early neural crest does not have a homogeneous expression profile. A number of antibodies label subpopulations of early neural crest cells, which show developmental restrictions (Weston, 1991). For example the Hu antibody stains mature neurons, however at an earlier stage, it labels a subset of neural crest cells with neuronal potential (Marusich *et al.*, 1994). Similarly, only a subset of avian neural crest cells expresses the neurotrophin receptor *trkC,* putatively

those shown to have neurogenic potential *in vitro* (Henion *et al.*, 1995), although recently, more detailed analysis *in vitro* has shown that very young *trkC* expressing neural crest cells can also give rise to glia (Luo *et al.*, 2003). Such heterogeneity in expression profiles may underlie differences in neural crest specification to different lineages at this early stage. However the functional meaning of neural crest marker heterogeneity is not easy to demonstrate *in vivo*. So far establishing that the fate of a neural crest cell is different from that of a sibling cell that does not express a given marker has been limited to *in vitro* analyses of isolated cells, or immunodepletion (Le Douarin and Kalcheim, 1999). Using a GFP transgenic line to reveal heterogeneity of gene expression in live embryos would allow vital-dye labelling of the different subsets of cells *in vivo* to reveal any difference in specificity.

There is good evidence that neural crest cells in the migration staging area in all species studied to date are a mixed population of both fate restricted and multi-derivative precursor cells (Henion and Weston, 1997; Weston, 1991). Contributing to this evidence is *in vivo* fate mapping of single cells, which demonstrated that early neural crest cells are heterogeneous with respect to developmental restrictions. In chick, labelling neural crest cells demonstrated that the majority of them gave rise to more than one cell type, including DRG neurons, glia, ENS cells and pigment. This indicated multipotency of early neural crest cells. Intriguingly, not all neural crest cells labelled in this experiment gave rise to multiple-phenotype clones, indicating heterogeneity of migratory neural crest cells with respect to fate restriction (Fraser and Bronner-Fraser, 1991). Henion and Weston (1997) extended this by labelling premigratory neural crest cells in explanted chick neural tubes. This also demonstrated heterogeneity in this population, and later indicated progressive restriction of fate during neural crest development. Distinct melanogenic and neurogenic sublineages were identified, within both of which existed bipotent precursors with the added capacity to generate glia. Later, the ability of some cells to produce two alternate fates was lost and only single cell-type restricted lineage precursors could be identified.

A similar lineage analysis was performed in zebrafish *in vivo*. Comprehensive fate mapping of zebrafish cranial neural crest has been conducted and has demonstrated that the cranial premigratory crest is segmentally restricted, and crest cells are restricted at an early stage to contribute to cells of a single arch segment (Schilling and Kimmel, 1994). Thus a premigratory neural crest cell in an anterior position will form a clone in a single anterior arch element. In addition, there appears to be a medial-lateral gradient of fate-choice within the premigratory crest, such that laterally positioned crest generates mostly neurons and glia of cranial ganglia, the most medially positioned neural crest cells contribute mostly to cartilage and connective tissue, whilst intermediately positioned neural crest cells

will produce pigment cells, however all premigratory cranial neural crest cells gave rise to only a single cell type, and thus are fate-restricted (Schilling and Kimmel, 1994).

In contrast to the fate-restricted cranial neural crest cells, similar single cell labelling experiments indicated that some, but not all, premigratory trunk neural crest cells in zebrafish gave rise to multiple phenotypes. However the frequency of precursors generating multiple cell types decreased with time such that cells migrating later were all type-restricted. Additionally there was a shift in fates produced with time, with only early migrating neural crest (EMC) cells giving rise almost all neural crest trunk derivatives, whilst late migrating crest (LMC) cells only gave rise to pigment and glial cells, and not neuronal derivatives (Raible and Eisen, 1994). Thus there is compelling evidence that early neural crest cells are heterogeneous for both expression profiles and potency, and that neural crest cells become progressively more restricted in fate during development.

Zebrafish fate mapping experiments have been extended by transplantation experiments to uncover if the restrictions in fate are associated with restrictions in potency, and if environmental changes underlie changes in neural crest cell commitment, or if some intrinsic mechanism changes cell potency (Raible and Eisen, 1996). The authors demonstrated by heterochronic transplantation that EMC cells could still generate neurons if placed into an older embryo, but that LMC cells could not produce neurons when transplanted into younger embryos. This directly contrasted with similar heterochronic experiments in chick, which argued that LMC transplanted into young hosts, were still multipotent (Weston and Butler, 1966). However zebrafish LMC cells could generate neurons if EMC cells were ablated during migration or before (Raible and Eisen, 1996). It was proposed that interactions between neural crest cells establish intrinsic differences in developmental bias, although this might be conditional depending on the environment.

A fate map of the neural crest along the avian axis has been produced using isotopic grafts from quail as a marker, supported by tracer injection work described above (reviewed in Le Douarin and Kalcheim, 1999). Using heterotropic grafts where cell are placed into a different rostro-caudal site in the host has allowed production of a map of developmental potentials. To summarise, these analyses indicated that early neural crest cells grafted to different axial positions are able to generate cell derivatives appropriate for their new position. Thus although there is heterogeneity with respect to fate restriction, the neural crest appears to be highly plastic along the almost the entire length of the embryo. For example, Le Douarin *et al.*, (1978) showed that thoracic quail neural crest grafted to a vagal position in chick could contribute to the ENS, appropriate behaviour for the new location. One exception is the inability of trunk neural crest cells to contribute to cranial cartilage tissue when transplanted into the cranial region of hosts. The existence of

precursors restricted to either an ectomesenchymal (cartilage) or non-ectomesenchymal (pigment and PNS) fate has been proposed based on this and other evidence (Weston, 1991). The discovery of a zebrafish mutant with defects in only one of these sublineages (*cls* – see later) supports this notion (Kelsh and Eisen, 2000).

A final technique elucidating neural crest cell behaviour is the use of *in vitro* clonal analysis of isolated neural crest cells. This has allowed the extent of potency possessed by neural crest cells to be tested, and also the timing and mechanism of commitment and lineage segregation. So far, *in vitro* experiments have been mostly performed using cultures of isolated avian (Baroffio *et al.*, 1988) and murine (Stemple and Anderson, 1992) neural crest cells. Work in chick identified a proliferative cell population containing clones with extremely diverse potency, being able to generate neuronal, glial, pigment and cartilage precursors, with many clones able to generate more than one cell-type. As demonstrated *in vivo,* there was inherent heterogeneity in the isolated population, with a proportion of cells being monopotent, whilst others displayed intermediate developmental potentials. Development of a method for isolating and culturing of mammalian neural crest cells has revealed that some have stem cell properties such as self-renewal, and capable of generating autonomic neurons, glia and smooth muscle cells upon exposure to instructive signals from BMP2, NRG1 and TGFβ respectively (Shah *et al.*, 1996).

1.1.6. Factors involved in the specification and differentiation of neural crest cells

1.1.6.1. Soluble Factors

The factors used in the above *in vitro* neural crest culture experiments are also expressed in the embryo at sites appropriate for the type of derivatives they promote *in vitro*. For example, autonomic neurons form near the dorsal aorta, where BMPs are expressed (Schneider *et al.*, 1999), TGFβ is present in the blood vessels where smooth muscle forms and nascent neurons in ganglia express NRG1 on axons, thus directing neighbouring neural crest cells to adopt a Schwann cell fate (Leimeroth *et al.*, 2002; Shah *et al.*, 1994). In addition to the roles for these signalling molecules identified by *in vitro* analysis, other factors are likely to be involved in neural crest specification. For example, Wnt signalling has been identified as a promoter of pigment-cell formation in the zebrafish neural crest (Dorsky *et al.*, 1998). Thus fate restriction may be brought about by instructive cues present in the environment in which neural crest cells migrate. Heterogeneity in expression of certain signalling systems within the cell might then dictate whether a neural crest cell can respond to the signal or how it might interpret a combination of signals.

1.1.6.2. Transcription Factors

To effect the alteration in cell specification, signalling pathways of the above factors are likely to activate expression of certain transcription factors involved in differentiation of the various neural crest drivatives. A number of transcription factors have been identified with such roles. Many of these belong to the basic Helix-Loop-Helix (bHLH) family of transcription factors, and are implicated in the development of melanophores, sensory and autonomic neurons.

Mitf is required for melanogenesis

Firstly, there is currently strong evidence that the Microphthalmia associated transcription factor (Mitf) is a key regulator of the melanocyte lineage. Mutations in this gene are associated with the mouse mutant, *Microphthalmia*, which displays defects in eye development and has a severe deficits in neural crest-derived melanocytes (Opdecamp *et al.*, 1997). There are two zebrafish orthologues of *mitf,* with *mitfa* corresponding to the *nacre* (*nac*) locus. *nac* mutants show a complete lack of melanophores, but unlike mouse mutants, there is no eye defect (Lister *et al.*, 1999). This is due to the presence of a second orthologue in zebrafish, *mitfb*, which has assumed the role of mammalian Mitf in the eye. Mutation and overexpression studies in both mouse and zebrafish have indicated that Mitf is both necessary and sufficient for melanogenesis, and thus might act as a melanocyte master switch gene (Dorsky *et al.*, 2000; Lister *et al.*, 1999). It has been shown that the mediators of Wnt signalling, the Tcf/Lef transcriptional activators, directly activate the *mitfa* gene along with other transcription factors, demonstrating a combinatorial mechanism acting to specify pigment cells (see Section 1.2). Mitf carries out the melanocyte developmental program by activating survival and differentiation genes, such as c-Kit, ednrB and Dct (Opdecamp *et al.*, 1997).

Transcription factors involved in autonomic nervous system development

As mentioned above, BMPs provide an environmental signal promoting sympathetic neuron specification, in the same manner as Wnts promote the melanocyte lineage. MASH1 is a critical bHLH transcription factor required for autonomic neuron development, possibly to direct neuronal differentiation following commitment (Sommer *et al.*, 1995), but there is also evidence that it maintains neural crest cell competence to respond to BMP signals (Lo *et al.*, 1997). The *Mash1* knock-out mouse displays extensive loss of sympathetic, parasympathetic and certain enteric neurons (Guillemot *et al.*, 1993). It appears that BMPs themselves can induce MASH1 *in vitro* (Shah *et al.*, 1996) and are required for its expression *in vivo* (Schneider *et al.*, 1999). It is not known if MASH1 is a

direct target of BMP signalling. Other transcription factors implicated in this pathway include the Phox2 protein family. *Phox2b* knock-out mice show a more complete absence of autonomic neurons than *Mash1* knock-out mice, and *Mash1* expression is lost in these mutants (Pattyn *et al.*, 1999). Mice lacking Phox2a also show defects in the autonomic nervous system, however less severe than that of *Phox2b* knock-out mice, and Phox2a appears to be downstream of MASH1 (Stanke *et al.*, 1999). Both Phox2a and Phox2b are upregulated by BMPs and both are sufficient to promote sympathetic neuron development in chick (Stanke *et al.*, 1999). Thus it appears that Phox2b is a critical transcription factor in the ontogeny of the autonomic nervous system, and may link extracellular BMP signalling with a cascade of transcription factors necessary for its neurogenesis. MASH1 and the Phox2 proteins are all potential direct activators of other factors required during this process.

Neurogenenins are required for sensory neuron development

The bHLH proneural transcription factors neurogenin1 and 2 (ngn1, ngn2) play a central role in sensory neurogenesis. The factors involved in this process, including the neurogenins, are discussed in more detail in Chapter 5. Neurogenins are expressed in precursors of sensory neurons in mouse neural crest, and targeted mutations result in loss of DRG sensory neurons (Ma *et al.*, 1999). This study demonstrated slight temporal differences in expression between NGN1 and NGN2 in the developing DRG, as well as partial functional redundancy between them. Ectopic neurogenin expression in chick neural crest biases them to behave as sensory neurons, indicating that neurogenin acts to specify neural crest cells to a sensory neuron fate (Perez *et al.*, 1999). Reduced responsiveness of ngn2 expressing neural crest cells to BMP signalling *in vitro* indicates these cells are committed to a sensory fate (Greenwood *et al.*, 1999), however lineage tracing $ngn2^+$ neural crest cells at a very early stage indicated that this restriction occurs later, and early $ngn2^+$ cells can contribute to the autonomic nervous system (Zirlinger *et al.*, 2002). The mechanisms controlling the size of dorsal root ganglia and the proportions of neurons to glia therein are not well understood, but there is growing evidence for intimate involvement of neurogenin in Notch-Delta mediated lateral inhibition within the DRG (see Chapter 5).

1.1.7. Receptors expressed by Neural Crest cells required for survival

Instructive signalling pathways are likely to act via transcription factors to effect correct differentiation, migration and survival. There is evidence *in vivo* that neural crest cells require exposure to survival and proliferation factors during migration. Sublineages or

type-restricted precursors often express specific receptors for such factors. In particular, the receptor tyrosine kinase family play a pivotal role in many of the neural crest lineages.

Receptor tyrosine kinases of the pigment cell lineage

c-Kit is a receptor tyrosine kinase required for survival and proliferation of melanoblasts. Mutations in the c-Kit gene have been identified in mouse (*Dominant spotting, W*), zebrafish (*sparse, spa*) and humans (Piebaldism). In all cases, there is a reduction or lack of melanocytes, which has been attributed to defects in migration, survival and proliferation (Parichy *et al.*, 1999; Spritz, 1998). Luo *et al.* (2003) have shown that neural crest cells expressing c-Kit are restricted to the melanophore fate. The ligand for c-Kit has been shown to be Steel Factor, which is expressed in the environment through which melanogenic neural crest cells migrate, and mouse mutations in Steel (*Steel, Sl)* produce similar phenotypes to *W* (Steel *et al.*, 1992; Wehrle-Haller and Weston, 1995). Zebrafish mutagenesis screens have identified other tyrosine kinase receptors in other pigment cells types. For example, the *salz* mutant corresponds to a mutation in a receptor tyrosine kinase, *fms*, and shows defects in migration and survival of xanthophores, similar to the defect caused by c-Kit mutation (Parichy *et al.*, 2000).

The Schwann cell lineage requires signalling through the erbB3 receptor tyrosine kinase

Other receptor tyrosine kinase families are required for neural crest survival, migration and/or differentiation. The erbB3 receptor binds the NRG1 ligand, and is required for Schwann cell precursor survival and migration along axons (Britsch *et al.*, 2001). A mouse knock-out displays severe neuropathies due to paucity of Schwann cells, and *in vitro*, NRG1 can restrict neural crest cells to a glial fate (Shah *et al.*, 1994). *In vitro* analysis of neural crest cells has also implicated NRG1 signalling in undifferentiated, multipotent neural crest cell survival (Paratore *et al.*, 2001).

Neuronal lineage associated receptor tyrosine kinases

The *trk* receptor tyrosine kinase family, (including trkA, trkB and trkC), also plays a survival role in all neural crest derived neuronal lineages, including enteric and sympathetic ganglia (Le Douarin and Kalcheim, 1999). Associated ligands are the neurotrophin family of secreted factors. In particular, neurotrophin-3 (NT3) binds to the trkC receptor, which is expressed in a subset of neural crest cells fated to the sensory neuron lineage, and which require NT3 signalling for migration and survival (Henion *et al.*, 1995).

The role of the c-Ret tyrosine kinase receptor and its ligand GDNF has been shown to be critical for enteric neuron development from the neural crest. Humans with mutations in

c-Ret display Hirschsprungs disease, a condition characterized by absence of enteric ganglia leading to a distended colon (Hofstra *et al.*, 2000). Mice with a targeted knock-out also show similar ENS defects (Schuchardt *et al.*, 1994). c-Ret is expressed by neural crest cells in the vagal neural crest region prior to migration, a site mapped as being the origin of the ENS. They also express c-Ret as they migrate along the gut. GDNF is expressed in a complimentary fashion in the gut mesenchyme (Pachnis *et al.*, 1993). Expression of zebrafish *c-Ret* in the ENS has been described, although there is as yet no reported mutant (MarcosGutierrez *et al.*, 1997). The exact role of c-Ret signalling in the ENS is unclear, and it might be required for multiple processes in neural crest derived enteric precursor cells, including migration, survival, proliferation and/or differentiation (Lo and Anderson, 1995; Taraviras and Pachnis, 1999).

1.1.8. Waardenburg syndromes and Hirschprung's disease

Neurochristopathies are the group of diseases caused by defects of neural crest derivative. One of the most common families of these diseases is that of the Waardenburg syndromes, which often display defects in multiple neural crest cell fates, and are associated with mutations in some of the critical factors associated with neural crest ontogeny. They are classified into four subtypes depending on the combination of phenotypes presented.

1.1.8.1. Waardenburg syndrome type I (WS1)

Features of this disease include pigment anomalies (often a white forelock and heterochromatic irises), broadening of the nose due to displacement of the inner canthii of the eye (dystopia canthorum) and deafness. It shows autosomal dominant inheritance with variable severity. All cases reported so far have been due to disruptions in the *Pax3* gene, which thus makes the *Pax3* mouse mutant *Splotch* a model for WS1 (Tassabehji *et al.*, 1992). As alluded to elsewhere in this chapter, the neural crest phenotypes might thus be due to lack of *Pax3* mediated neural crest cell specification within the neuroepithelium or a later defect in regulation of downstream lineage regulating factors such as *Mitf*.

1.1.8.2. Waardenburg syndrome type II (WS2)

This autosomal dominant syndrome presents as per WS1, however without the dystopia canthorum. Thus patients present pigment anomalies, and deafness. All cases for which a lesion has been found are due to a mutation in the bHLH transcription factor, *Mitf* (Tassabehji *et al.*, 1994). Deafness has been attributed to loss of melanocytes in the ear (Nobukuni *et al.*, 1996). As mentioned earlier, mutations in this master regulator of

melanocyte differentiation are associated with the mouse mutant *microphthalmia* (*mi*) and the zebrafish mutant *nacre* (Lister *et al.*, 1999; Opdecamp *et al.*, 1997).

1.1.8.3. Waardenburg syndrome type III (WS3; Klein-Waardenburg Syndrome)

Like WS1, this disease is also caused by mutations in the *PAX3* gene, and is also inherited in a dominant manner. In addition to the hypopigmentation, facial abnormalities and deafness associated with WS1 it also presents upper limb anomalies, including hypoplasia of the musculoskeletal system, flexion contractures, fusion of the carpal bones, and syndactyly (Zlotogora *et al.*, 1995). This may be due to a secondary defect arising from lack of skeletal muscle (Tremblay *et al.*, 1998).

1.1.8.4. Waardenburg syndrome type IV (WS4; Waardenburg-Shah Syndrome)

WS4 is a multigenic condition, inherited in either a recessive or dominant manner, depending on the gene affected. Also called Hirschsprung disease with pigmentary anomaly, it combines the enteric aganglionosis of Hirschprung's disease with the pigment defects of WS2. The recessive condition has been identified as due to mutations in the endothelin-3 (Edn3) signalling molecule (Edery *et al.*, 1996; Hofstra *et al.*, 1996), or its G-protein coupled receptor endothelin receptor B (EDNRB) (Puffenberger *et al.*, 1994; Syrris *et al.*, 1999). Homozygosity for mutations in either of these genes has been shown to cause WS4, with a range of severity, presenting with some degree of hypopigmentation and aganglionosis of the gut (Edery *et al.*, 1996). Unlike WS1, deafness is relatively rare in recessive WS4, but has been reported (Puffenberger *et al.*, 1994). These phenotypes have striking similarity to those of the recessive mouse mutants *piebald-lethal* (s^l – mutant for the *Ednrb* gene) and *lethal spotting* (*ls* – mutant for the *Edn3* gene) (Kapur *et al.*, 1995), indicative of a conserved role for EDNRB-mediated signaling in both melanoblasts and ENS precursors. Recent work in mouse knockout lines clearly indicated that this role involves the correct terminal migration of these precursor cell types (Lee *et al.*, 2003). Humans heterozygous for mutations in either of these two genes have been shown to display Hirschprung's disease alone, with no pigment anomalies (Amiel *et al.*, 1996; Auricchio *et al.*, 1999; Pingault *et al.*, 2001b).

Heterozygosity at the *SOX10* locus also causes WS4, with combined pigment defects and Hirschprung's disease. Deafness is also common in this disorder. As with WS2, this is often attributed to loss of melanocytes, but as *SOX10* is expressed in the ear, a *SOX10* mutation might have a direct role here. In addition to WS4 symptoms, some SOX10 mutations produce variable dysmyelination of the CNS and PNS leading to neurological disorders (Touraine *et al.*, 2000). *SOX10* mutations will be dealt with in more detail later (see Section 1.2). Although mutations in the three genes mentioned here all result in WS4,

the aetiology is proving to be different, and the cellular defects caused by the mutation of *SOX10* are much earlier than those caused by disruption to the EDN3 signalling pathway (Lee *et al.*, 2003).

1.1.9. Zebrafish screens for neural crest mutants

Recently, the zebrafish has been employed to genetically dissect processes of vertebrate development. Mutagenesis screens have isolated numerous loci important in development of various tissues, including the neural crest (Haffter *et al.*, 1996; Henion *et al.*, 1996). As the first vertebrate species on which such large-scale mutagenesis screening has been conducted, and as positional cloning efforts are now identifying many of these mutant loci at a molecular level, the zebrafish promises to permit rapid characterization of the genes involved in formation of certain structures. Some of the mutants isolated clearly correspond to those known in humans, mice and other experimental model systems.

Neural crest derived pigment cells in zebrafish form a stereotypical pattern, and are easy to visualise and score for disrupted number, distribution or differentiation. The pigment pattern of a wild-type larva is composed of three pigment cell types, black melanophores, yellow xanthophores and the reflective iridophores and is shown in Figure 1.1. Melanophores are found in four longitudinal stripes in early larvae, namely the dorsal stripe, lateral stripe, ventral stripe and a yolk-sac stripe. Note that the only other cells to melanise in the embryo, found in the pigmented retinal epithelium, are not neural crest derived. Iridophores co-localise with melanophores in the dorsal, ventral and yolk sac stripes and migrate to cover the eye. Iridophores are also found in the lateral patch, a region lying dorsolateral to the yolk sac. Finally, xanthophores are predominantly found on the dorsal half of the embryo (Figure 1.1; Kelsh *et al.*, 1996). Due to the ease of visualising aberrations in the embryonic pigment pattern, screens readily identified a large number of mutants, each defective in some aspect of pigmentation. These mutants were classified into having reduced pigment cell number, abnormal pigment cell distribution, reduced levels of pigment in particular chromatophore(s), or abnormal pigment cell morphology (Kelsh *et al.*, 1996). In addition to pigment, the jaw cartilage also represents a readily visualised neural crest derivative. As such, screens were also able to identify a number of mutants which affect the ectomesenchymal derivatives of neural crest, in particular the jaw (Piotrowski *et al.*, 1996; Schilling *et al.*, 1996a). Subsequent screens have also been performed using PNS neuron markers to find mutants with defects in neural crest derived neuron structures (Henion *et al.*, 1996). Insertional mutation screens have also yielded interesting neural crest mutants, such as *alyron*, which show a severe deficit in

Figure 1.1 →

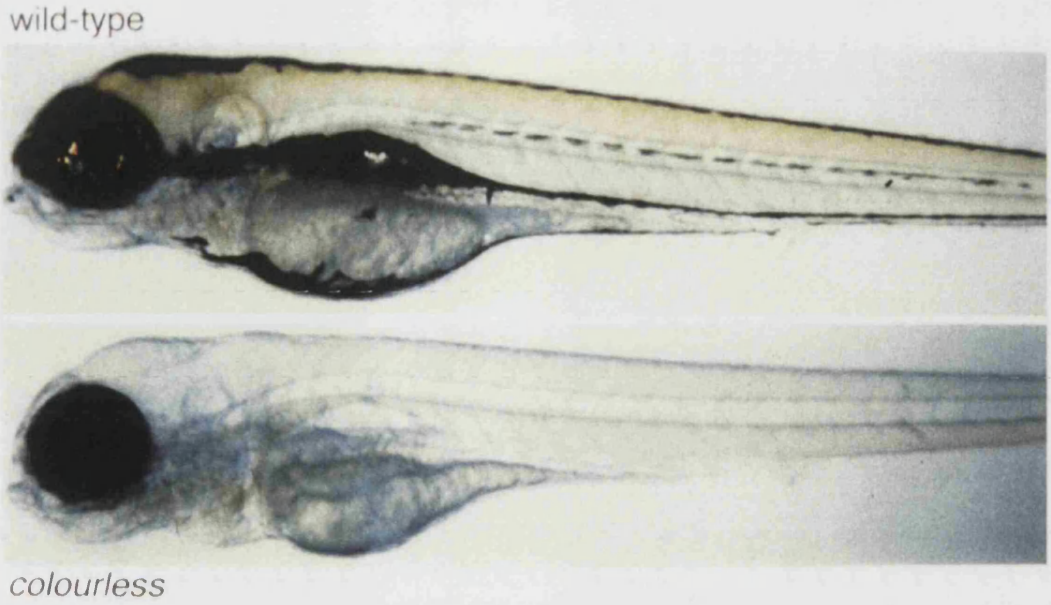

Figure 1.1 Wild-Type and *colourless* larvae pigmentation

Upper panel shows a lateral view of a 6dpf wild-type larva, viewed with transmitted light. Black melanophores are present in four longitudinal stripes, a dorsal, lateral, ventral and yolk-sac stripe. They begin to migrate to these locations at about 20 hours post fertilisation, having emerged dorsal to the neural tube. A cast of yellow xanthophores is evident dorsally, and iridophores are found with melanophores in all but the lateral stripe. In the ventral stripe, iridophores are also seen in large patches above the yolk sac termed the lateral patches, and overlying the eye.

Lower panel shows a *cls* larvae at the same stage, which displays total absence of morphologically normal body melanophores. This absence is complete for all *cls* alleles described. Note that the non-neural crest derived melanophores of the pigmented retinal epithelium are unaffected. Xanthophores and iridophores of both the body and eye are significantly reduced in *cls* individuals, however occasionally individual cells of these types are seen in *cls* larvae (Kelsh *et al.*, 1996). Other cell types not evident here are affected as well (see Section 1.2).

premigratory neural crest leading to lack of pigmentation and heart flow defects (Cretekos and Grunwald, 1999).

These screens have led to the identification of mutants disrupted for a number of the processes required during neural crest cell development. Preliminary analyses of some of the mutants' phenotypes suggested defects in neural crest induction, specification, proliferation, survival, migration or differentiation. Mutants include those with lack of or having a reduction in one type of neural crest cell derivative, for example melanophores (*nacre/mitfa*), xanthophores (*salz/fms*), iridophores (*shady*), DRG neurons (*nosedive*) and craniofacial cartilage (*chinless*) (Henion *et al.*, 1996; Kelsh *et al.*, 1996; Lister *et al.*, 1999; Schilling *et al.*, 1996b). Additionally, mutants affecting neural crest survival have also been identified, such as *sparse/c-kit* (Parichy *et al.*, 1999). Of particular interest is the *colourless* (*cls*) mutant, which shows loss of multiple neural crest derivatives. An example of a homozygous *cls* mutant is shown in Figure 1.1. Evident is the loss of all body pigment cells. Other neural crest derivatives are severely diminished as well, but not ectomesenchymal derivatives such as facial cartilage (see Section 1.2).

Thus the ability to perform mutagenesis screens in zebrafish provides a unique and novel approach to dissecting the genes responsible for the processes of neural crest development.

1.2. Sox10

1.2.1. Overview of the SOX family of transcription factors

Vertebrate embryonic development relies on the complex interactions of transcriptional regulators of gene expression. As disruptions in the activity or distribution of these factors are a cause of many human congenital diseases, understanding the associated molecular mechanisms is important, not only developmentally, but also medically. Examples demonstrating this can be found in the SOX group of transcription factors, which form a subclass of the HMG box protein superfamily (reviewed in Soullier *et al.*, 1999). Several members of the SOX family of transcription factors have essential roles in pathways governing cell behaviour and identity (Prior and Walter, 1996), and diseases exist in both humans and animals ascribed to disruption of certain *Sox* genes (Pevny and Lovell-Badge, 1997). Unlike the ubiquitously expressed HMG family, Sox proteins display tissue specific domains of expression (Pevny and Lovell-Badge, 1997).

1.2.1.1. Domains found in Sox proteins

SOX transcription factors are characterised by the presence of a conserved DNA binding domain encoded by the SRY-related HMG box, first identified in the mammalian sex-determining gene SRY (Pevny and Lovell-Badge, 1997). The HMG domain has multiple identified roles other than its DNA binding capability. There are identified motifs responsible for nuclear import (Forwood *et al.*, 2001; Sudbeck and Scherer, 1997) and export (Rehberg *et al.*, 2002) of the protein, and an ability to engage in protein-protein interactions has been noted (Melnikova *et al.*, 2000). HMG domains of some Sox proteins have also been demonstrated to have RNA splicing activity (Ohe *et al.*, 2002).

The *Sox* family comprises approximately 20 genes and are classified into ten subgroups (A- J) based on sequence similarities (Bowles *et al.*, 2000). Intriguingly, in vertebrates group A, B, C and G Sox proteins are encoded by one exon (e.g. Schilham *et al.*, 1993), whilst the few genes of the other groups characterised so far do contain intron-exon structure (eg *Sox5, 9, 10* and *17*). Generally, intron-exon boundaries are conserved within each subgroup across vertebrate species, although these cannot be extrapolated to invertebrates (Kanai *et al.*, 1996; Pusch *et al.*, 1998; Wright *et al.*, 1995; Wunderle *et al.*, 1996). Although there is a high degree of HMG domain sequence similarity between Sox proteins, there is much less conservation elsewhere in the protein. However within a subgroup certain other functional domains are conserved. These other domains include transactivation domains, mostly found in the C-terminus and shown for many Sox proteins to be able to activate transcription of target genes, as well as protein-protein binding and homodimerisation domains such as the leucine zipper motif of subgroup D (Lefebvre *et al.*, 1998; Peirano and Wegner, 2000; Wegner, 1999; Yamashita *et al.*, 1998). Repression domains have been identified in some group B Sox proteins (Uchikawa *et al.*, 1999).

1.2.1.2. DNA binding specificity of Sox proteins

All HMG domain containing proteins are able to bind to DNA, however only the subfamily containing the Sox proteins can do so with sequence specificity. This occurs through their HMG-domain, which binds DNA at the consensus sequence ($^{A}/_{T}$)($^{A}/_{T}$)CAA($^{A}/_{T}$)G (Pevny and Lovell-Badge, 1997). The structure of this DNA binding domain has been solved, indicating that it consists of three α-helices that form an L-shape. Uncommon to transcription factors, DNA binding by Sox proteins is targeted to the minor groove (Wegner, 1999). Upon binding, the DNA molecule is bent (Kamachi *et al.*, 1999; van de Wetering and Clevers, 1992), a process proposed to remodel the chromatin surrounding the gene and to bring other DNA-bound transcription factors into close

proximity to the promoter. The conformational change in the DNA might also exclude the binding of other factors to the major groove of DNA (Pevny and Lovell-Badge, 1997).

Sox proteins thus bind to a small consensus DNA recognition sequence, through a highly conserved HMG domain. Several Sox factors are expressed in more than one cell type, and many *Sox* genes are co-expressed in the same cells. This has implications for redundancy of function between Sox protein family members and also implies that there must be some mechanism to generate specificity of Sox protein recognition for, and binding to, promoters. Firstly, a degree of specificity might be produced by slight DNA recognition sequence variation. For example, Mertin *et al.* (1999) showed specificity of SOX protein binding could be altered by dinucleotide sequences flanking this target sequence. However the current favoured model relies on formation of multi-protein complexes to provide the specificity of Sox protein action. It has been well established that Sox proteins partner with other transcription factors, and this provides, to a large extent, the specificity of binding. Such interactions for Sox proteins are summarised by Wilson and Koopman (2002), and are mediated through the HMG domain itself, or other protein-protein synergy domains. For example, the Sox2 protein has multiple roles during embryogenesis, including an early role in the induction of FGF4 in mouse blastocysts, which requires the binding of both Sox-2 and the POU transcription factor Oct-3/4 to adjacent sites in an enhancer on the FGF4 gene (Ambrosetti *et al.*, 1997). Later in development, Sox2 (like Sox1 and 3) has a role in the developing CNS and lens. In this latter site, any one of Sox1, 2 or 3 can activate the δ-*crystallin* gene, but require protein-protein interaction with the partner transcription factor Pax6, which also binds to the δ-*crystallin* promoter (Kamachi *et al.*, 1995; Kamachi *et al.*, 1998). Further, domain swap experiments between SOX2 and SOX9 demonstrated that specificity of activation of the δ-*crystallin* promoter by SOX2 was mediated through a proximal portion of the C-terminal domain, a putative protein-protein binding domain (Kamachi *et al.*, 1999). Other examples of protein-protein interactions important in Sox function include the cooperative activation by Sox5, Sox6 and Sox9 of the *type II collagen* gene during chondrogenesis (Lefebvre *et al.*, 1998), and the synergistic transactivation by Sox11 and the POU protein Brn1 when adjacent binding sites were included on an artificial promoter linked to a reporter gene. Sox11 and Brn1 are co-expressed in the oligodendrocyte lineage, suggesting a real biological role in this cell type. The inability of Brn1 to act in synergy with Sox10 on the other hand suggested the presence of a combinatorial code regulating specificity of Sox protein transcriptional activation (Kuhlbrodt *et al.*, 1998a). Additionally, transcription factor partners of Sox10 have been recently identified (see below).

1.2.1.3. *Sox* genes are found throughout the animal kingdom

Sox genes can be found outside the vertebrates, and a number have been identified in *C. elegans* and in *Drosophila*, where thay also act as tissue specific transcription factors during development (reviewed in Bowles *et al.*, 2000; Cremazy *et al.*, 2001). These include the well-characterised *Dichaete* (*=fishhook),* which shows strongest sequence similarity to vertebrate *Sox2* (Russell *et al.*, 1996). Indeed the mouse *Sox2* gene can rescue *Dichaete* mutant phenotypes indicating functional conservation (Sanchez-Soriano and Russell, 1998). Less well characterised is the *Drosophila Sox100B* gene. Based on sequence comparison, *Sox100B* has been described as an invertebrate homologue of the group-E genes *Sox9* and *Sox10*, and like its vertebrate counter parts it is expressed in the developing gut, gonads and kidney (Loh and Russell, 2000). However the function of *Sox100B* remains unclear, as no mutant has yet been identified.

Of the diverse roles that Sox proteins play in different aspects of development, some have been alluded to here, and include sex determination, endoderm formation, chondrogenesis, early neural development, lens development and haematopoiesis. Of most interest to the field of neural crest biology is the group E *Sox* genes, *Sox8, 9* and *10*. All are expressed in the neural crest and/or derivatives (Wegner, 1999).

1.2.1.4. Sox8 and Sox9

Along with Sox10, Sox8 and 9 comprise the only members of Group E family of Sox proteins. All genes show a highly similar intron-exon structure and their encoded proteins have similar structure with a conserved HMG domain, and a C-terminal transactivation domain, which has been demonstrated to be functional *in vitro* (Schepers *et al.*, 2000).

Sox8 is the least well characterised member, partly because it is not associated with a human disease, although it appears to map closely to the ATR-16 mental retardation syndrome locus. Consistent with this linkage, SOX8 is expressed in human brain (Pfeifer *et al.*, 2000). In addition to the shared C-terminal domain, Sox8 has an additional potent transactivating domain immediately C-terminal to the HMG domain. *In situ* analysis in chick and mouse demonstrated *Sox8* expression beginning at E9.5 in the nasal region, and later seen in the branchial arches, limbs, eye, testes, kidney, DRGs and glia of the CNS and PNS (Cheng *et al.*, 2001; Montero *et al.*, 2002; Schepers *et al.*, 2000). A mouse lacZ knock-in reporter line confirmed much of this expression pattern and additionally described expression in the neural crest, muscle, ear, sympathetic and enteric ganglia. Although expected to generate a null allele, homozygous knock-in mice developed normally and were viable, but displayed a reduction in weight (Sock *et al.*, 2001). Possible

functional redundancy with other group E Sox proteins was proposed as a reason for the mild phenotype. Chick *Sox8* is additionally seen in the forming neural crest (Bell *et al.*, 2000). No full-length zebrafish Sox8 has yet been cloned although a partial sequence was reported by Chiang *et al.* (2001). A putative rainbow trout *Sox8* homologue, *SoxP1*, has also been identified (Ito *et al.*, 1995).

The functions of Sox9 are better understood as it is implicated in the disease Campomelic Dysplasia (CD; reviewed in Marshall and Harley, 2000). This autosomal dominant disease displays skeletal defects, in particular bowing of the long bones, sometimes with craniofacial defects and often presenting with male to female sex reversal (Foster *et al.*, 1994). A number of translocations or rearrangements affecting chromosome 17 have been identified in patients (e.g. Maraia *et al.*, 1991) as have specific mutations affecting the SOX9 coding region (Foster *et al.*, 1994). Consistent with the defects caused by SOX9 mutation, expression domains in human and mouse includes chondrogenic mesenchymal condensations, particularly in the chondrocyte preursor cells and chondrocytes of the bones and pharyngeal arches (Lefebvre *et al.*, 1997; Wright *et al.*, 1995), and in the developing genital ridges where expression is rapidly downregulated in females, but later specifically expressed Sertoli cells in males (Wagner *et al.*, 1994). A pivotal role for Sox9 in initiation of the chondrocyte differentiation program and maintenance of protein expression in differentiated chondocytes has been proposed (Bi *et al.*, 1999). This is consistent with the discovery that Sox9 is directly regulated by FGF and BMP-2 signalling, and also directly regulates collagen genes (reviewed in Marshall and Harley, 2000). Sox9 also plays a crucial role in the sex determination pathway, although the precise mechanism might vary between vertebrate species. SOX9 appears to be immediately downstream of SRY in mammals, and functions as a critical Sertoli cell differentiation factor, probably in all vertebrates (daSilva *et al.*, 1996).

Regulation of SOX9 appears to occur over a long range, with some Campomelic Dysplasia patients having breakpoints mapping up to 950kb from the *SOX9* gene (Wirth *et al.*, 1996). Evidence supporting this long distance regulation was provided by the comparative analysis of different sized SOX9 YAC reporters in transgenic mice (Wunderle *et al.*, 1998).

Animal models of CD exist, including a targeted *Sox9* knock-out which reproduces many aspects of the skeletal defects in CD patients (Bi *et al.*, 2001). In addition, two *sox9* genes exist in zebrafish, *sox9a* and *sox9b*. Both are expressed in chondrocytes of the head and fin skeleton, but whereas *sox9a* mimics mammalian *Sox9* expression in testes, *sox9b* is expressed in the ovaries. *sox9b* is also expressed in the neural crest (Li *et al.*, 2002), and overlaps with *sox10* (Pauliny, 2002). A *sox9a* mutant, *jellyfish*, has been isolated and

shows craniofacial defects similar to CD. Cell analysis indicated that specification and migration of the neural crest contributing to the pharyngeal arches was normal, but subsequent differentiation and morphogenesis was impaired (Yan *et al.*, 2002).

1.2.2. Sox10 has been cloned from a number of species

The final group E family member, *Sox10*, is of interest due to its pivotal role in development of derivatives of the neural crest. Phenotypes due to *sox10* mutations have been described in humans, mice and zebrafish, and allow mutational analysis of *Sox10* function (Kelsh *et al.*, 1996; Pingault *et al.*, 1998; Southard-Smith *et al.*, 1998). Studies in the zebrafish have suggested *sox10* may specify neural crest cell fate (Kelsh and Eisen, 2000).

*Sox*10 was first identified by virtue of its conserved DNA-binding motif - the HMG domain, characteristic of all *Sox* genes (Wright *et al.*, 1993). A full-length clone was isolated from rat primary Schwann cell cultures, and demonstrated a high degree of sequence similarity (>90%) in the HMG domain to both mouse Sox8 and 9. Regions of homology existed outside this domain, including a putative C-terminal transactivation domain. Although the HMG domain could bind DNA, no detectable autonomous activation or repression could be elicited from Sox10 protein in transcriptional assays using an artificial promoter with consensus Sox protein binding sites. Crucially, however, Sox10 could efficiently transactivate in a synergistic manner with the POU transciption factor Oct6. This synergy required both proteins to bind to adjacent sites in the promoter, with synergy mediated by the N-termini of both proteins. Similar synergy was demonstrated with the Pax3 transcription factor (Kuhlbrodt *et al.*, 1998b).

Sox10 cDNAs have been cloned from a number of other species, including mouse (Southard-Smith *et al.*, 1998), human (Pingault *et al.*, 1998), chick (Cheng *et al.*, 2000), xenopus (Aoki *et al.*, 2003; Honore *et al.*, 2003) and zebrafish (Dutton *et al.*, 2001), although zoo blot analysis has demonstrated that many other vertebrate species contain a *Sox10* gene (Southard-Smith *et al.*, 1999a). All Sox10 proteins show a high degree of sequence conservation between species, mostly confined to the HMG, synergy and transactivation domains. Only the mouse and human *Sox10* genes have been cloned to date, analysis of which has shown that gene structure (such as intron-exon boundaries) are also highly conserved (Southard-Smith *et al.*, 1999a; Southard-Smith *et al.*, 1999b). Futhermore, Sox10 in all species analysed to date have remarkably similar expression patterns. Detailed comparison of these patterns will be dealt with in a later chapter (see Section 4.1), but briefly, *in situ* analyses conducted in the species mentioned above have shown expression in the premigratory neural crest, and maintenance in a subset of neural

crest derivatives, mostly PNS glia. Ear expression during development is common to all species as is CNS expression, both at embryonic and adult stages. A lacZ knock-in mouse line has been produced, and the analysis of *Sox10*$^{lacZ/+}$ embryos has largely confirmed the *in situ* results, albeit in a *Sox10* heterozygous background (Britsch *et al.*, 2001). Mutant lesions have been identified in three species, mouse, human and zebrafish, and have provided understanding of the role of Sox10 in the neural crest.

1.2.3. Mouse, human and zebrafish Sox10 mutations

1.2.3.1. Mouse Sox10 mutants

Using a forward genetic approach, both Southard-Smith *et al.* (1998) and Herbarth *et al.* (1998) showed that a mutation in *Sox10* was responsible for the *Dominant megacolon (Dom)* mouse mutant. This strain arose spontaneously and displays, in heterozygotes, a white belly spot with white feet and concomitant megacolon, presenting as a distended abdomen. Histological analysis has demonstrated that this colon distension is due to severe reduction in enteric ganglia cells in the distal gut (Lane and Liu, 1984), caused by defective colonization by neural crest-derived neuroblasts (Kapur *et al.*, 1996). A circling behaviour, sometimes seen in *Dom* heterozygotes on certain backgrounds, suggests lack of functional Sox10 can additionally cause an inner ear defect (Pingault *et al.*, 1998). Heterozygotes do survive, with variability in survival time, depending on the background strain used. This, combined with the fact that *Dom* heterozygotes exhibit variable penetrance and expressivity of phenotypes has been attributed to modifier loci, some of which may encode co-factors that modulate Sox10 action (Southard-Smith *et al.*, 1999a). Further characterisation of these loci may afford insight into the molecular interactions and epistatic relationships of *Sox10*.

Homozygous *Dom/Dom* embryos were far more severely affected, and die around birth. Unlike heterozygous embryos, almost all cranial ganglia were disrupted with fewer *erbB3*$^+$ glia and NF$^+$ neurons present and there was a total lack of *Dct*$^+$, *Kit*$^+$ melanoblasts. Using a combination of neuronal markers including peripherin, DβH$^+$, NF and tyrosine hydroxylase to analyse *Dom/Dom* embryos, showed a rostro-caudal gradient of severity of DRG and sympathetic neurons (being completely absent caudally), and no enteric ganglia or their precursors were evident at any position along the gut at any stage (Herbarth *et al.*, 1998; Kapur, 1999). Apoptosis of *Dom/Dom* neural crest cells was evident, a proportion of which might be accounted by a lack of maintenance of *erbB3* expression, a receptor required for neural crest survival/migration (Britsch *et al.*, 2001; Kapur, 1999; Paratore *et al.*, 2001). There was no detectable defect in ectomesenchymal neural crest fates such as

the facial anatomy and the cardiac outflow tract (Kapur, 1999). This suggests that only a subset of neural crest fates are affected in *Dom.*

Preliminary (Lane and Liu, 1984) and more detailed (Puliti *et al.*, 1995) mapping analysis placed *Dom* to within 0.8cM on Chromosome 15, from which chromosome walking strategies were commenced (Herbarth *et al.*, 1998; Southard-Smith *et al.*, 1998). *Sox10* was assessed as a candidate gene, and the lesion corresponding to *Dom* was identified as an extra guanine inserted after the HMG box, and predicted to insert 99 novel amino acids before terminating (Figure 1.2). Functional analysis indicated that although the frameshift mutation did not disrupt DNA binding, it did severely abolish the ability of the Sox10 protein to synergistically enhance transactivation through Pax3 and Oct6 (Herbarth *et al.*, 1998).

A targeted mutation of mouse *Sox10* has been produced in which the *Sox10* coding region has been replaced with the *lacZ* reporter gene (Britsch *et al.*, 2001). Embryos homozygous and heterozygous for the $Sox10^{lacZ}$ allele reproduce the respective phenotypes of $Sox10^{Dom}/Sox10^{Dom}$ and $Sox10^{Dom}/+$ mice. As the $Sox10^{lacZ}$ is a null, it argues that dominance of *Sox10* mutant alleles is due to haploinsufficiency, as opposed to a dominant negative function previously proposed for $Sox10^{Dom}$ due to its retained DNA binding ability (Britsch *et al.*, 2001; Pingault *et al.*, 1998). As mentioned earlier, the lacZ reporter was expressed in appropriate sites, including premigratory neural crest, neural crest migrating into the gut, in PNS glia found associated with ganglia and axons in the head and trunk, and the otic vesicle. This line has been much used to analyse various aspects of Sox10 function in various cell types. For example, during melanocyte development, cells expressing melanoblast markers such as *mitf, c-kit* and *dct*, were decreased to 50% in heterozygous embryos, and almost totally absent in homozygous embryos, in accordance with the extent of pigmentation seen in the two genotypes and consistent with results from the *Dom* allele (Britsch *et al.*, 2001). Analysis of the glial differentiation marker B-FABP, in $Sox10^{lacZ}$ embryos demonstrated that $lacZ^{+}$ cells in the DRGs of heterozygous embryos were glial in nature (in particular PNS associated satellite glia and Schwann cells). These cells were diminished in the homozygotes, and did not appear to have differentiated into either neurons or glia (Britsch *et al.*, 2001). Decreased proliferation and increased apoptosis of undifferentiated progenitor neural crest cells in the DRG periphery is the likely cause (Sonnenberg-Riethmacher *et al.*, 2001). Similarity of mutant phenotypes between $Sox10^{lacZ}/Sox10^{lacZ}$ and $erbB3^{-/-}$ embryos, combined with loss of *erbB3* expression in homozygous *Sox10* mutants suggested that Sox10 is normally required for multipotent neural crest cell survival through maintaining *erbB3* expression (Britsch *et al.*, 2001; Paratore *et al.*, 2001). Furthermore, this paucity of differentiated glia in the DRGs of

Figure 1.2 →

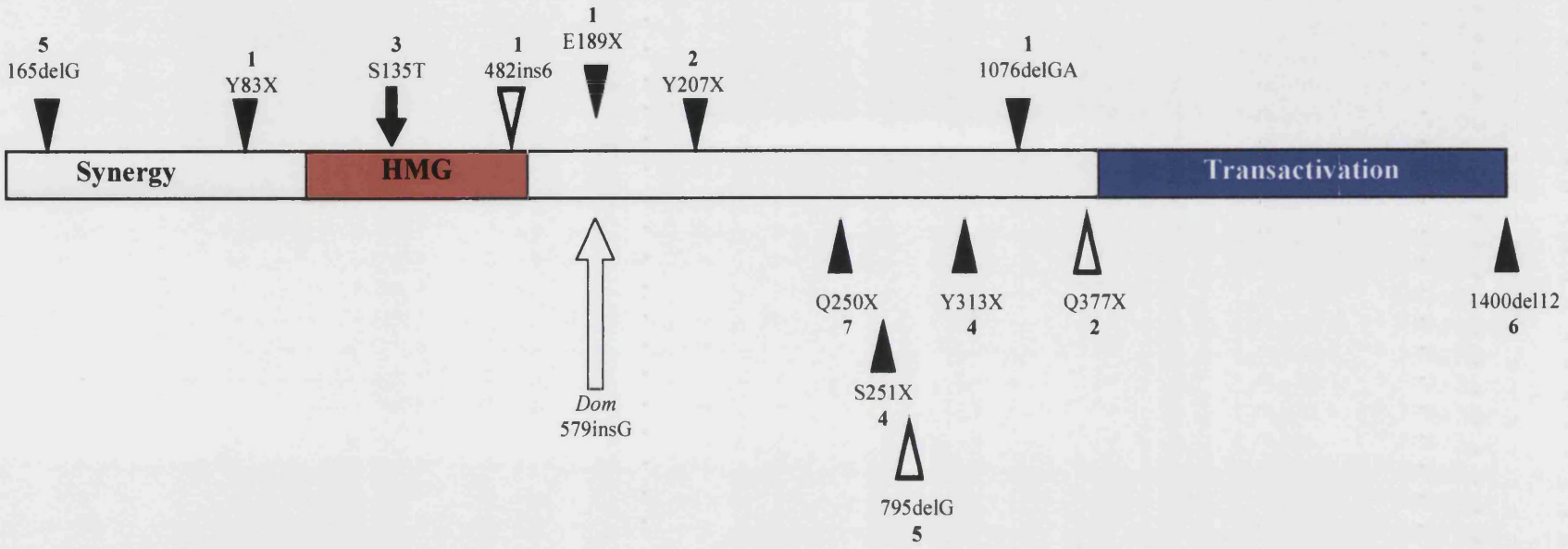

Figure 1.2: Distribution of SOX10 mutations in human and mouse

Schematic of the Sox10 protein with synergy, HMG and transactivation domains marked. Mutations in human SOX10 resulting in WS4 only are given above the protein schematic, whilst mutations that additionally produced dysmyelination of the PNS and/or the CNS are presented below. Numbers above or below each lesion refers to the reference listed below. Open arrow marks the lesion in the mouse Sox10 mutant, *Dom*.
Black-filled arrowheads refer to patients displaying deafness, hypopigmentation and Hirschprung's.
Open arrowheads indicate patients which display deafness and enteric abnormalities, but not hypopigmentation.
The filled arrow indicates a patient with hypopigmentation and deafness, but no enteric aganglionosis (Yesemite deaf-blind hypopigmentation syndrome).
References: **1:** Pingault *et al.*, 1998, **2:** Southard-Smith *et al.*, 1999a, **3:** Bondurand *et al.*, 1999, **4:** Touraine *et al.*, 2000, **5:** Pingault *et al.*, 2001, **6:** Inoue *et al.*, 1999, **7:** Inoue *et al.*, 2002.

Sox10^{lacZ}/*Sox10*^{lacZ} embryos was proposed to be the cause of the degeneration of DRG and motorneurons (Britsch *et al.*, 2001). No overt DRG phenotype has been seen in either *Sox10*^{lacZ} or *Sox10*^{Dom} heterozygotes.

Localisation and morphology of lacZ^{+} cells in the CNS of *Sox10*^{lacZ}/+ embryos was consistent with expression in oligodendrocytes and oligodendrocyte precursors, confirmed by double labelling analysis with oligodendrocyte lineage markers such as myelin basic protein (MBP) and PDGF receptor α. Sox10 CNS expression was restricted to these cells, and no neuronal or astrocytic expression was noted. Whereas PNS glial progenitors appear diminished and disorganised, oligodendrocyte progenitors appear unaffected in *Sox10*^{lacZ}/*Sox10*^{lacZ} embryos. However these mutant oligodendrocytes fail to ever express terminal differentiation products such as MBP when assessed in various *in vivo* contexts, indicating that Sox10 is required for terminal differentiation in the oligodendrocyte lineage, but not oligodendrocyte progenitor formation (Stolt *et al.*, 2002).

Paratore *et al.* (2002) demonstrated aganglionosis of the distal, but not proximal, gut in *Sox10*^{lacZ}/+ embryos. This was accounted for by reduction in the multipotent enteric progenitor pool populating the gut. Unlike *Sox10*^{lacZ}/*Sox10*^{lacZ} embryos, this was not due to apoptosis of trunk neural crest cells. Instead, through use of progenitor and neuronal markers, combined with fate mapping of initially *Sox10*$^{+}$ neural crest cells using perdurance of β-gal activity, this defect in colonising the distal gut was shown to be due to precocious adoption of neuronal traits by previously *Sox10*$^{+}$ enteric progenitors. A model for the effect of *Sox10* mutation on the enteric neurons was proposed. Neural crest cells require Sox10 for correct specification and migration to the gut; this very early step is defective in *Sox10*^{lacZ}/*Sox10*^{lacZ} embryos. However in *Sox10*^{lacZ}/+ embryos, neural crest cells survive and migrate to the gut to form the enteric progenitor pool. Due to altered Sox10 levels in heterozygotes, these cells are unable to properly interpret their environment, and thus fail to maintain their proliferative, progenitor status, and subsequently aberrantly adopt a neuronal fate. This dramatically reduces the migratory, progenitor pool, leading to insufficient numbers available to colonise the disal gut. This link between altered Sox10 levels, and responsiveness of the cell to external signals is a growing theme in describing the cellular role of Sox10, as is the link between Sox10 and maintenance of multipotency (see below).

In vitro cultures of neural crest stem cells derived from both wild-type and Sox10 mutant mice have recently been employed to better understand the role of Sox10 in mouse neural crest ontogeny. These undifferentiated cells can be challenged with soluble growth factors to produce neurons, Schwann cells or smooth muscle (Anderson, 1997). Consistent with *in vivo* expression patterns, only the uncommitted stem cells, and cells of the glial

lineage express Sox10 in this system (Paratore *et al.*, 2001). Survival of these explanted cells, and subsequent direction to a glial fate depended on presence of NRG1 (=Glial growth factor II, GGFII) in the medium, response to which requires cellular expression of wild-type Sox10, presumably through Sox10 dependant expression of the NRG1 receptor ErbB3. Absence of Sox10 not only led to increased apoptosis of these stem cells, but the surviving clones were unable to adopt a glial fate. Wild-type clones however survived, proliferated and differentiated into arrays of glia. Paratore *et al.* (2001) then demonstrated that Sox10 haploinsufficiency does not affect this NRG1 mediated survival, but did disrupt the fate choice of the neural crest stem cells. Thus, although the majority of wild-type clones always differentiated as glial cells in response to NRG1, clones heterozygous for Sox10 did not, and instead produced non-neural/smooth muscle cells. At higher culture densities, which allowed cell-cell interactions, heterozygous clones become mostly neuronal in the absence of NRG1, but supplying NRG1 restores these clones ability to become glia. Thus not only does Sox10 promote neural crest stem cell survival and acquisition of a glial fate through the NRG1 signalling pathway, but its gene dose (and presumably level of functional protein) is critical in determining how a cell interprets a combination of signals, mirroring conclusions drawn from analysis of enteric progenitors in Sox10 heterozygous embryos (Paratore *et al.*, 2001; Paratore *et al.*, 2002). The authors predict that an increase in neurogenesis in DRGs might be expected in Sox10 heterozygotes. That this is not the case argues for some compensation or redundancy in the combinatorial signalling mechanism employed in forming correct cell numbers in DRGs. This area is revisited later in further detail (see Chapter 5). This model would be strengthened greatly by the identification of a Sox10 mutant showing enhanced neurogenesis in DRGs.

Kim *et al.* (2003) have extended this *in vitro* analysis of the cellular role Sox10 plays. Using a neural crest stem cell system, in which autonomic neurons, glia and smooth muscle can be produced, they showed that transient exposure of wild-type neural crest stem cells to factors promoting neuronal differentiation (such as BMP2), abolished the ability to subsequently direct these cells to glial fates using NRG1. Similar loss of neurogenic potential after exposing the neural crest stem cells to the smooth muscle promoting factor, TGFβ, was noted. Forced expression of SOX10 in the stem cells, however, protected them from this loss of potential, through permitting subsequent induction of MASH1 and PHOX2B by BMP2. However, although SOX10 maintained neurogenic potential, it inhibited neurogenic differentiation by repressing PHOX2A, thus keeping the cells in a multipotent, proliferative state. Thus, in *Dom/Dom* embryos, although the early differentiation transcription factor PHOX2A is derepressed in neural

crest cells, early specification transcription factors (MASH1 and PHOX2B) are not, blocking neurogenesis. Curiously in the heterozygous state, derepression of PHOX2A still occurs, but unlike in the homozygotes, the early transcription factors are expressed normally. This caused inappropriate and precocious neuronal marker expression exclusively in *Dom/+* embryos. The authors conclude that, consistent with other studies (Paratore *et al.*, 2001; Paratore *et al.*, 2002), a higher level of SOX10 is required for delaying neuronal differentiation than to maintain neurogenic potential, and thus haploinsufficiency alters a cells response to combinatorial signalling (Kim *et al.*, 2003). It is dangerous to extrapolate the results from this study using these limited NCSCs to other neuronal cell types affected in Sox10 mutants, however it might indicate a theme underlying the role of Sox10 in PNS development.

1.2.3.2. Human *SOX10* syndromes

Due to striking phenotypic similarities, the *Dom* mouse mutant has been proposed as a model for the human syndromes, Waardenburg-Shah syndrome (WS4) and Hirschsprung's disease (Herbarth *et al.*, 1998; Southard-Smith *et al.*, 1999a). Both diseases display aganglionosis of the distal colon, with Waardenburg-Shah syndrome additionally presenting hypopigmentation, and in some cases deafness (Pingault *et al.*, 1998). Deficiency in glial cell mediated myelination, leading to severe neuropathy of the PNS (Charot-Marie-Tooth disease) in a Waardenburg-Shah case has also been reported (Inoue *et al.*, 1999), as has CNS dysmyelination which may account for the added mental retardation and neurological phenotypes seen in some patients (Inoue *et al.*, 2002; Pingault *et al.*, 2001a; Touraine *et al.*, 2000). SOX10 mutations have been associated with these syndromes (Pingault *et al.*, 1998). Additionally, Yemenite deaf-blind hypopigmentation syndrome, which combines pigment, inner ear and cornea anomalies, has been attributed to Sox10 dysfunction (Bondurand *et al.*, 1999a). Lesions in other genes have also been described for WS4 and Hirchprung's disease, including RET, EDNRB and ET-3 (Auricchio *et al.*, 1999; Bidaud *et al.*, 1997; Edery *et al.*, 1996; Kapur *et al.*, 1995; Syrris *et al.*, 1999). The multigenic nature of Waardenburg-Shah syndrome and Hirschsprung's disease supports the hypothesis that Sox10 acts in concert with other factors to correctly form each non-ectomesenchymal derivative. Mice homozygous for mutations in either Et-3 or EdnrB are phenotypically similar to *Dom* heterozygotes (Kapur *et al.*, 1995; Zhan *et al.*, 1999).

All human SOX10 mutations have so far appeared in the heterozygous state, and a patient homozygous for a SOX10 mutation has never been reported. As described above, the associated phenotypes present in SOX10 mutations include deafness, pigmentary

abnormalities, aganglionosis leading to bowel dysfunction, and dysmyelination of the PNS and/or CNS. So far, 13 SOX10 lesions in WS4 cases have been identified. The penetrance of each phenotype varies such that some patients only displayed a subset of defects. As in the *Dom* model, this suggests the involvement of modifying loci. However each described lesion probably disrupt SOX10 function to differing extents, so an alternative model might invoke altered transactivation of downstream targets by SOX10. In support of the former proposal, the same mutation (Q377X) occurs in siblings displaying vastly different aganglionosis severity (Southard-Smith *et al.*, 1999a). All described lesions discovered to date are presented in Figure 1.2, with presence or absence of associated myelin deficiency noted. Lesions include 7 nonsense mutations (at amino acids 83, 189, 207, 250, 251, 313 and 377), three frameshifts leading to addition of novel amino acids and premature termination, one substitution (S135T), a duplication of two amino acids within the HMG domain, and a deletion of the last 12 nucleotides of the coding region, which caused the normal stop codon to be skipped, and extended the protein by 82 novel amino acids. This last mutation does not affect the coding region, so loss of function might be due to abnormal folding of the protein or steric hindrance caused by the extra amino acids (Bondurand *et al.*, 1999b; Inoue *et al.*, 2002; Inoue *et al.*, 1999; Pingault *et al.*, 1998; Pingault *et al.*, 2001a; Southard-Smith *et al.*, 1999a; Touraine *et al.*, 2000). The variable expressivity of the same mutation within a family, argues that it is difficult to correlate position and nature of a lesion within the protein with the severity of phenotypes presented.

The transactivational potency of human wild-type SOX10 was tested using an artificial SOX-responsive reporter. The wild-type protein displayed weak transcriptional activity, in contrast to the rat Sox10, which showed none. Analysis of the human Y83X, 482ins6, E189X and 1076delGA mutant SOX10 proteins, and domain swap experiments localised this activity to the very C-terminus of the protein (Kuhlbrodt *et al.*, 1998c; see also Pusch *et al.*, 1998). Similar analyses with the SOX10 substitution mutation S135T, indicated that the substitution disrupted DNA binding due to steric hindrance, and that transcriptional potency of the protein was decreased (Bondurand *et al.*, 1999b). In addition, similar approaches clearly demonstrated that Sox10 can function synergistically with other transcription factors such as Oct6 and Pax3 to transactivate the reporter. This synergy however required adjacent sites on the promoter, and a synergy/dimerisation domain located in the N-terminal region of Sox10 (Kuhlbrodt *et al.*, 1998b; Kuhlbrodt *et al.*, 1998c).

1.2.3.3. The zebrafish *Sox10* locus, *colourless*

The first zebrafish *colourless (cls)* mutant allele first arose as a spontaneous mutation in a stock background. In addition to this first allele, cls^{t3}, subsequent mutagenesis screening has yielded 4 other alleles, namely cls^{tw2}, cls^{ty22f}, cls^{te275} *and* cls^{m618}. Embryos displayed a lack of all three types of neural crest derived pigment cells (melanophores, xanthophores and iridophores), due to an early reduction of pigment cell precursors (Figure 1.1). An early effect on ear development was also evident as a very reduced ear size (Kelsh *et al.*, 1996; Malicki *et al.*, 1996; Whitfield *et al.*, 1996). The non-neural crest derived pigmentation in the retinal epithelium was, however, not affected suggesting the pigment phenotype was due to some neural crest defect.

More detailed analysis of the *cls* phenotype revealed a stark reduction in the number of other cell types, including loss of Hu^+ neurons of the enteric, dorsal root and sympathetic, but not cranial, ganglia and a severe loss of $foxD3^+$ Schwann cells, cranial ganglion associated glia and $GFAP^+$ enteric glia (Kelsh *et al.*, 2000a; Kelsh and Eisen, 2000). Although the loss of neurons of the enteric and sympathetic chain is strong, loss of DRG neurons displays a rostro-caudal gradient of severity, as described for *Dom* (Kapur, 1999), with posterior neurons almost absent, whilst anterior DRG neurons were reduced and misplaced. The cause of these 'escaper neurons' is currently under investigation, but might be attributable to incomplete loss of support glia (Britsch *et al.*, 2001), or possibly due to partial functional redundancy with other zebrafish group E Sox genes, such as *sox9b* or *sox8*. Importantly the ectomesenchymal neural crest derivatives such as craniofacial cartilage and fin mesenchyme are mostly unaffected, except that older *cls* embryos showed slight retardation in branchial arch development (Kelsh and Eisen, 2000). That only non-ectomesenchymal crest derivatives are affected in *sox10* mutants suggested the hypothesis that neural crest cells are fate restricted early to either ectomesenchyme or non-ectomesenchyme, and implied a role for sox10 in the generation, survival and/or subsequent differentiation of a population of progenitors restricted to non-ectomesenchymal fates.

Furthermore, detection of premigratory neural crest with the *foxD3* and *snail-2* markers indicated that *cls* does not affect formation of nascent neural crest (Kelsh and Eisen, 2000). There was, however, an absence of melanoblast markers such as *dct, nac/mitfa* and *spa/kit* (Dutton *et al.*, 2001; Kelsh *et al.*, 2000b). Neural crest cell lineage analysis indicated that generally, non-ectomesenchymal crest fates do not form in *cls*, and the neural crest cells instead fail to migrate and differentiate and subsequently die by an apoptotic mechanism. Thus in *cls,* multipotent neural crest cells initially appear normally but the non-ectomesenchymal subset of derivatives fail to be specified correctly.

Based on phenotypic similarities, *cls* has been proposed to model Waardenburg-Shah syndrome (Kelsh and Eisen, 2000). A candidate gene approach identified *cls* as encoding a zebrafish *sox10* orthologue (Dutton *et al.*, 2001). This has been corroborated with evidence from rescue experiments with an inducible *sox10*-cDNA construct, identification of mutant lesions and physical mapping data (Dutton *et al.*, 2001). The expression pattern of *sox10* in zebrafish is consistent with the *cls* phenotype and is similar to that described for *Sox10* in other species, namely in premigratory neural crest, migrating neural crest, glial derivatives, the ear and oligodendrocytes. The zebrafish *sox10* expression pattern is described in more detail in Chapter 4. That *cls* corresponds to mutations in a transcription factor is also consistent with previous demonstration of the cell-autonomous nature of the mutation (Kelsh and Eisen, 2000).

All of the five *cls* alleles listed above are recessive and with seemingly identical phenotypic severity. In contrast to mammalian Sox10 mutants, there is no reported heterozygous phenotype. *cls* embryos fail to inflate a swim bladder and die at approximately 11dpf. A weaker allele, cls^{m241} was discovered, and showed some surviving melanophores (Malicki *et al.*, 1996). Unfortunately, this allele is no longer extant. Sequencing of *sox10* cDNA prepared from two of these alleles has identified a nonsense mutation leading to truncation of the protein directly before the putative transactivation domain (K376X – cls^{tw2}) and a missense mutation within the HMG-box leading to substitution of a highly conserved residue essential for DNA binding (L142Q - cls^{m618}; see also Section 5.1). Analysis of the other alleles, and generation of new, possibly weaker, alleles would allow a protein domain map to be developed, and may give further understanding of sox10 biology. The relative ease with which mutagenesis screens can be carried out in the zebrafish, facilitates this end.

Analysis of *cls* (*sox10*) mutant neural crest cells show that they undergo apoptosis before migration or differentiation. The loss of expression of factors required for melanophore specification and survival such as *mitfa* and *c-kit* prior to this in *cls* mutants suggests that apoptosis might be due to failure to activate genes required (directly or indirectly) for cell specification and survival. Perhaps *sox10* has a general role in specifying non-ectomesenchymal lineages, and does so by activation of master genes controlling cell fate and differentiation through downstream targets (Dutton *et al.*, 2001). The bHLH transcription factor *mitfa* plays such a role in the melanophore lineage, and has been shown to be directly activated by *sox10* in zebrafish (Elworthy *et al.*, 2003). In fact, comparative rescue analysis has demonstrated that the only essential role of Sox10 in the melanophore lineage is simply to activate the melanophore master switch gene *mifta* (Elworthy *et al.*, 2003). *mitfa* is thus regulated directly by at least two different

mechanisms acting in concert, namely *sox10* (Elworthy *et al.*, 2003) and Wnt signalling (Dorsky *et al.*, 2000). This combination may confine specific expression of *mitfa* to only a subset of neural crest cells in a particular location at a particular time.

It would be interesting to know if similar master switch genes, regulated by *sox10,* exist in the other non-ectomesenchymal cell fates, such as glia, enteric neurons, DRG neurons, xanthophores and iridophores. There is evidence that *phox2b* is lost in *cls* embryos (Elworthy *et al.*, in prep.) It is also likely that in some lineages, Sox10 promotes expression of growth factor receptors or receptors necessary for survival, such as c-Ret (see below). The function of Sox10 in the ear is unknown, but is a field of current study in the laboratory.

1.2.4. Target genes and mechanism of *Sox10* function

The roles of Sox10 in various cell lineages are only beginning to be understood. As a transcription factor, Sox10 is likely to perform these roles through its ability to directly regulate downstream targets. To date, few target genes of Sox10 have been identified. Those described so far are the α3 and β4 subunits of the neuronal nicotinic acetylcholine receptor (nACh) of the PNS (Liu *et al.*, 1999), MITF (Bondurand *et al.*, 2000; Elworthy *et al.*, 2003; Potterf *et al.*, 2000), c-Ret (Lang *et al.*, 2000; Lang and Epstein, 2003), the Connexin 32 junction protein (Cx32) of Schwann cells (Bondurand *et al.*, 2001) and the P_0 protein found in the myelin sheath of Schwann cells (Peirano *et al.*, 2000). In all cases, the promoters have been analysed and show critical Sox10 response elements, necessary for Sox10 binding. As mentioned previously, specificity of Sox protein activity on promoters is conferred by synergistic activation through a combinatorial code, and Sox10 requires synergy with other factors for enhanced transactivation potency. This has been demonstrated in all cases above (except for the P_0 promoter – see below), with the promoters always containing at least one Sox element adjacent to the recognition site for the second transcription factor in question. Thus Pax3 has been shown to act in synergy with Sox10 on the *c-Ret* and *Mitf* promoters, both of which contain Sox10 and Pax3 binding sites in close proximity (Bondurand *et al.*, 2000; Lang and Epstein, 2003). Other transcription factors have been implicated in interactions with Sox10, including EGR2, shown to enhance activation of Connexin 32 by Sox10, and the Sp1 transcription factor acts synergistically with Sox10 to activate nACh subunit genes (Bondurand *et al.*, 2001; Melnikova *et al.*, 2000). The P_0 promoter is activated by Sox10 directly. However attempts to uncover a second transcription factor acting with Sox10 in this process have so far been fruitless (Peirano *et al.*, 2000). Instead, Sox10 acts on this promoter as both a homodimer and a monomer. Dimerisation has two effects, namely decreasing the off-rate of the

protein, and increased the angle of DNA bending induced by Sox10 binding (Peirano and Wegner, 2000). As to why the P_0 promoter is only active in a subset of Sox10 expressing cells, cannot be explained by this, but might involve as yet undiscovered cell type-specific activating or repressing co-factors acting with Sox10.

Specific mutants of the Sox10 domains abort transactivation of the promoters listed above by disruption to DNA binding (the HMG domain), transactivation (the C-terminus) and/or synergistic protein-protein interaction (N-terminus and the HMG domain). In addition, a mutation in the Sox-binding element of the Cx32 promoter has been described in a patient with peripheral myelin defects (Bondurand *et al.*, 2001). One human SOX10 lesion, S135T, shows disparate effects on the synergistic activation of the *c-Ret* and *Mitf* promoters with PAX3. This mutation affects DNA binding by the HMG domain, such that the *Mitf* promoter fails to be activated; in contrast activation of the *c-Ret* promoter is indistinguishable from wild-type. This is probably due to the mechanism of assembly of the SOX10-PAX3 heterodimer and DNA complex. Medically, this is relevant as this is the only known human SOX10 lesion which does not show enteric aganglionosis, (this patient did however show hypopigmentation), and thus suggests that different Sox10 lesions can produce a different range of phenotypes depending on the particular domain affected by the lesion (Lang and Epstein, 2003). SOX10 mutations clearly produce heterogeneous phenotypes in different individuals. There is evidence in both human and mouse that this is caused by modifier loci (e.g. Southard-Smith *et al.*, 1999a). The above observation also demonstrates that the different lesions in SOX10 can produce different phenotypes due to divergent effects on downstream targets.

As the *Sox10*^{lacZ} homozygous mice display a severe reduction in the expression of *erbB3*, it has been proposed that Sox10 might regulate *erbB3*. Although induction of Sox10 in an *in vitro* system can also induce *erbB3,* this has not yet been shown to be direct (Britsch *et al.*, 2001). Similarly, activation of the DCT promoter by Sox10 protein in cell culture assays, combined with loss of DCT expression in mouse Sox10 mutants, have been interpreted as evidence of direct transactivation of DCT by Sox10 (Britsch *et al.*, 2001; Potterf *et al.*, 2001). However direct binding of the promoter by SOX10 has not been demonstrated, and this proposal remains questionable (Elworthy *et al.*, 2003).

Sox10's pivotal role in multiple neural crest lineages makes it likely that there are many other target genes. Its ability to activate both transcription factors, tyrosine kinase receptors and cell surface differentiation markers may indicate that sox10 functions in a variety of contexts to direct cell specification through activation of master switch transcription factors, to promote migration and survival as well as to maintain levels of certain proteins in terminally differentiated derivatives, such as glia. Furthermore,

identification of interacting transcription factors is clearly important for identifying potential target genes and understanding Sox10 function. Perhaps a screen such as a yeast 2-hybrid experiment could be used to isolate other transcription factors important for Sox10 function. This has been successfully implemented to isolate modulators of sox23 activity in the rainbow trout (Yamashita *et al.*, 1998).

It is worthwhile mentioning that the target genes of Sox10 described previously were all identified through a candidate approach. Candidate target genes were selected based on overlapping expression of Sox10 and either Pax3 or Tst-1/Oct6/SCIP with the putative target. This approach is severely limited, as it requires some prior characterisation of the target gene. Clearly some form of screening method to isolate downstream targets would be a far more attractive approach, and will allow identification of novel factors.

As to the question of factors upstream of Sox10, little is known. Recently however, work on *Xenopus Sox10* has revealed that *Sox10* is expressed very early in the neural crest lineage, and is activated by factors involved in neural crest induction and the early neural crest transcription factor, *Snail*. Thus addition of beads soaked with inhibitors of the canonical Wnt pathway or FGF signalling both inhibited *Sox10* expression in the neural plate. Additionally, loss of the *Slug* and *Snail* transcription factors found in the early neural crest also diminishes *Sox10* expression (Aoki *et al.*, 2003; Honore *et al.*, 2003). In the developing chick limb digits, *Sox10* expression can be enhanced by addition of BMP-7 (Chimal-Monroy *et al.*, 2003). Thus a number of different signalling pathways are probably involved at different stages in the regulation of *Sox10*, however there is, as yet, no evidence for a direct effect of specific factors.

1.3. AIMS OF THE PROJECT

Many aspects of Sox10 biology remain unresolved, including its precise role in the non-ectomesenchymal lineage, the mechanisms it uses to achieve specification and the full array of genes it regulates. Clearly, Sox10 functions through activation of downstream effectors, of which very few have been described. Other candidates can be proposed based on known functions in certain crest sub-lineages. Identification of these and other novel factors is an important step in defining the precise role of sox10 as well as understanding mechanisms of neural crest fate restriction. Characterising the molecular pathways/interactions associated with Sox10 will elucidate many aspects of neural crest cell development.

Generation of a variety of particular tools is critical in the approaching these problems. The main aim of this work involves the generation of a *sox10-gfp* reporter transgenic line.

This will prove useful for understanding the sites and times of *Sox10* expression, and allow manipulation to determine the key regulators of *sox10*. Further, this transgenic line will label live neural crest cells *in vivo*, allowing visualisation of cells' behaviour in time, and a better understanding of neural crest migration. Additionally, it offers the ability to isolate pure neural crest cells at various stages. Cloning of the *sox10* promoter will also allow examination of the regulation of *sox10* and factors involved.

Towards this, the initial aims were:

1. Isolation of genomic clones containing the zebrafish *sox10* gene and characterisation of structure, such as intron-exon boundaries and transcription start site.
2. Demonstration that the genomic clones isolated contain a functional *sox10* gene by attempting to rescue aspects of the *cls* phenotype with genomic clone injection
3. Sub-cloning the promoter region of *sox10* and generation of GFP reporter constructs
4. Assaying the reporter constructs *in vivo* for ability to drive GFP expression in the neural crest and other appropriate sites.

The ultimate aim was the generation of stable transgenic lines carrying these reporter constructs, and preliminary characterisation of the GFP expression pattern. Thus a major aim was to then compare the GFP expression sites with those previously described through *sox10 in situ* analysis. This might extend the pattern of expression described by *in situ*. Additionally it was hoped to isolate neural crest cells by FACS analysis, but this aim was not met due to lack of time.

In addition, identification of new *cls* alleles promises to afford a better understanding of the functional domains of the Sox10 protein, as well as to establish the roles and mechanisms of Sox10 activity. Thus one final aim was to help perform an allele screen to identify new *cls* alleles. Subsequent characterisation of any alleles found was hoped to reveal new information as to the mechanism of Sox10 action.

CHAPTER 2

MATERIALS AND METHODS

2.1. MATERIALS

Materials used and sources are listed below in the following categories.

2.1.1. Chemical Reagents

General laboratory chemicals were of analytical research grade and were purchased from a range of manufacturers, mostly Sigma Chemical Co., St Louis, MO, USA or Acros Organics, Geel, Belgium. Specialist reagents and their sources are listed below:

Agarose	USB Co., Cleveland, OH, USA
Bacto Tryptone	Oxoid, Basingstoke, Hampshire, UK
Bacto Agar	Difco Laboratories, Detroit, MI, USA
Chlorotetracycline	Acros Organics, Geel, Belgium
Fusaric acid	Acros Organics, Geel, Belgium
IPTG	Melford Labs Ltd., Suffolk, UK
Luria Agar/Broth Base	Invitrogen, Groningen, The Netherlands
Methylcelluose	Sigma Chemical Co, St Louis, MO, USA
Phenol/chloroform/isoamyl alcohol	Sigma Chemical Co, St Louis, MO, USA
1-phenyl-2-thiourea (PTU)	Sigma Chemical Co, St Louis, MO, USA
Tricaine (methylsulfonate)	Sigma Chemical Co, St Louis, MO, USA
TriReagent™	Sigma Chemical Co, St Louis, MO, USA
Yeast Extract	Difco Laboratories, Detroit, MI, USA

2.1.2. Antibiotics, Indicators and Dyes

Ampicillin	Sigma Chemical Co, St Louis, MO, USA
Bromophenol Blue	BDH Laboratory Supplies, Poole, UK
Chloramphenicol	Sigma Chemical Co, St Louis, MO, USA
Ethidium bromide	Sigma Chemical Co, St Louis, MO, USA
Kanamycin	Sigma Chemical Co, St Louis, MO, USA
Methylene Blue	Acros Organics, Geel, Belgium
Phenol Red	Sigma Chemical Co, St Louis, MO, USA
seeDNA™	Amersham Pharmacia Biotech, NJ , USA
Tetracycline	Sigma Chemical Co, St Louis, MO, USA
X-gal	Sigma Chemical Co, St Louis, MO, USA
Xylene Cyanol	BDH Laboratory Supplies, Poole, UK

2.1.3. Enzymes

Most restriction endonucleases (and 10 x restriction buffers) were purchased from Promega, Madison, WI, USA. Other enzymes were obtained from the following suppliers:

Lysozyme	Sigma Chemical Co, St Louis, MO, USA
Proteinase K	Sigma Chemical Co, St Louis, MO, USA
RNase A	Sigma Chemical Co, St Louis, MO, USA
RNase Inhibitor	Roche GmbH, Mannheim, Germany
Reverse Transcriptase	Invitrogen, Groningen, The Netherlands
I-*Sce*I	New England Biolabs, Beverly MA, USA
Plasmid-Safe™ DNase	Epicentre Technologies, Madison WI, USA
Shrimp Alkaline Phosphatase	USB Co., Cleveland, OH, USA
T4 DNA ligase	Promega, Madison, WI, USA
Taq DNA polymerase	Gibco Life Technologies, Paisley, UK

Reaction buffers (10 ×) were supplied with the latter four enzymes and 50 mM $MgCl_2$ was supplied with *Taq* DNA polymerase. The Reverse Transcriptase was supplied with a 5× Reaction Buffer and DTT.

2.1.4. Nucleic Acids and Radioactive Isotopes

[α-^{32}P] dCTP (3000 Ci/mmole)	Amersham Pharmacia Biotech, UK
ATP	Sigma Chemical Co, St Louis, MO, USA
Salmon sperm DNA	Sigma Chemical Co, St Louis, MO, USA
Unlabelled deoxyribonucleotides	Gibco Life Technologies, Paisley, UK
DNA ladder, 100 bp	New England Biolabs, Beverly MA, USA
DNA ladder, 1kb	New England Biolabs, Beverly MA, USA
1kb DNA ladder	Promega, Madison, WI, USA
100bp DNA ladder	Promega, Madison, WI, USA
High Molecular Weight ladder	Gibco Life Technologies, Paisley, UK
Primers (listed in Table 2.4)	Invitrogen, Groningen, The Netherlands
Random Hexamers	Promega, Madison, WI, USA

2.1.5. Bacterial Strains And Cloning Vectors

The plasmid vectors and bacterial strains used in this project are summarised in Tables 2.1 and 2.2 respectively. Figures 2.1 and Figure 2.2 show vector maps for pSV.RecA and XLT.GFP$_{LT}$.CS2+.

Table 2.1: Plasmid vectors

Vector	Source	Use	Reference
pBluescript®II SK(-)	Stratagene GmbH, Heidelburg, Germany	General cloning and subcloning vector	(Alting-Mees and Short, 1989)
pGEM®-T Easy	Promega, Madison, WI	PCR product cloning vector	http://www.promega.com/vectors/cloning_vectors.htm
pUC18 –*Eco*RI-BAP Ready To Go™ cloning kit	Pharmacia Biotech Hertfordshire, UK	Cloning of *Eco*RI products	(Norrander *et al.*, 1983)
pCYPAC-6	RZPD, Berlin, Germany	PAC Vector	(Ioannou *et al.*, 1994)
pSV.RecA	Prof. N. Heintz, The Rockefeller University	Recombination targetting vector	(Yang *et al.*, 1997)
XLT.GFPLT CS2+	Prof. Randall Moon, University of Washington	GFP reporter constructs	http://faculty.washington.edu/rtmoon/vectors.html

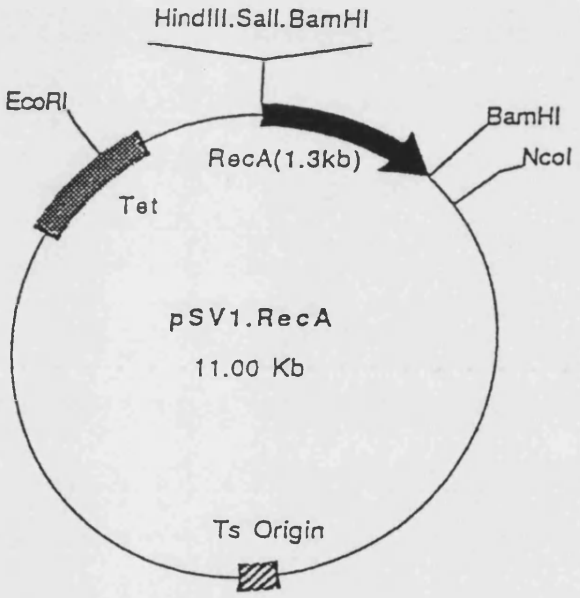

Figure 2.1: Map of pSV1.RecA

A Plasmid map showing features of the vector including the *RecA* gene, temperature sensitive origin of replication, Tetracycline resistance gene and important restriction sites. Taken from "Protocol for Targeted Modification of Bacterial artificial Chromosomes (BACs) – May 1997", a protocol released with the plasmid from the Heintz Lab at The Rockefeller University.

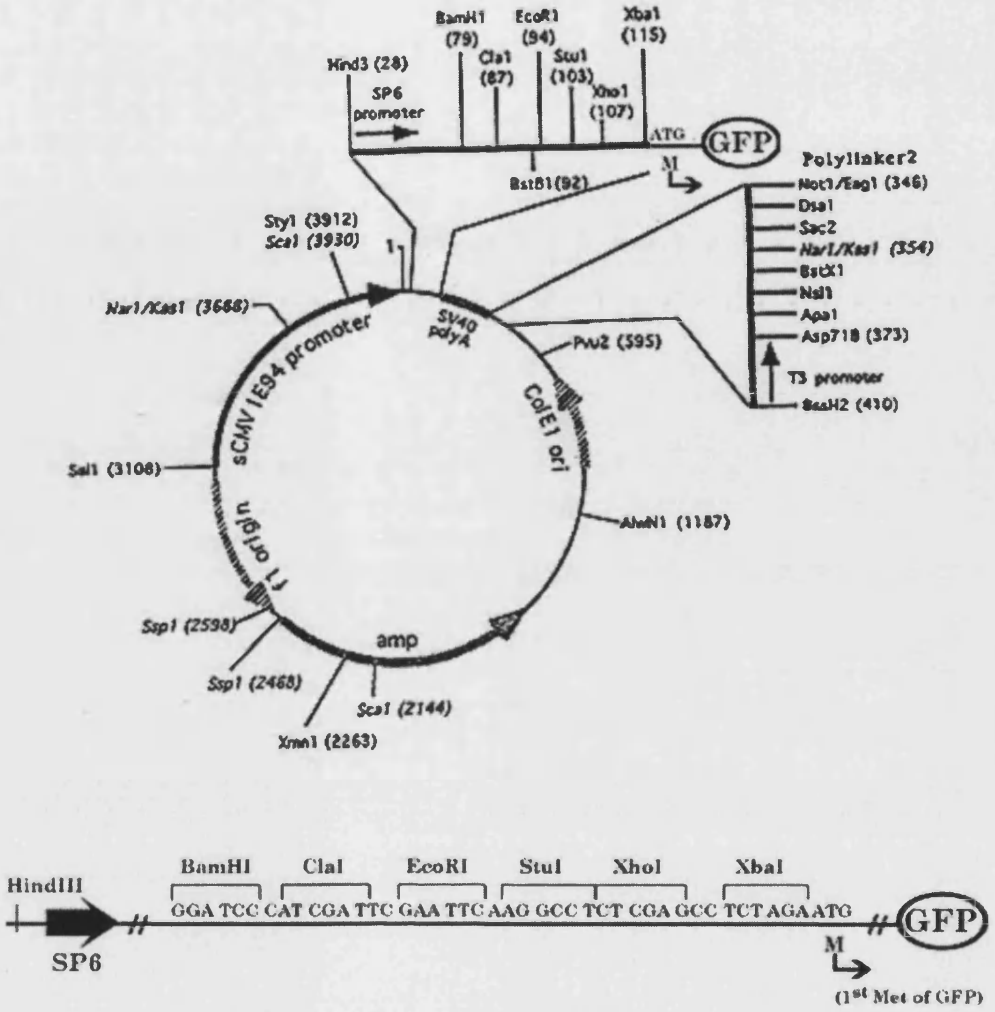

Figure 2.2: Maps of XLT.GFP$_{LT}$ CS2+

Upper part shows a plasmid map with features of the vector including CMV promoter, *gfp* gene, Ampicillin resistance gene and restriction sites. The sequence directly 5' to the *gfp* gene is given below. Adapted from http://faculty.washington.edu/rtmoon/vectors.html

Table 2.2: Bacterial strains (*Escherichia coli*)

E. coli Strain	Source	Use	Genotype and Reference
DH-5αF'	CLONTECH Labs, CA	Host for cloning into pGEM®-T and general cloning	*recA*1, *endA*1, *gyrA*96, *thi*-1, *hsdR*17 (r_K^-, m_K^+), *supE*44, *relA*1, *deoR*, Δ(*lacZYA-argF*)U169 [F', Φ80d*lacZ*ΔM15]; (Hanahan, 1983)
DH10B	RZPD, Germany	PAC clone host	F- *mcr* A Δ(*mrr-hsd*RMS-*mcr*BC) *deo*R *rec*A1 *end*A1 *ara*D139 (*ara,leu*)7697 *gal*U *galK* l- *rps*L *nup*G [F'80dlacZ ΔM15 ΔlacX74]

2.1.6. Kits and Miscellaneous Materials

Kits and other materials used in this project were obtained from the following manufacturers:

Bio-Gel P60 resin (G50 mesh)	Bio-Rad Laboratories, Richmond CA, USA
GPS™ -1 Genome Priming System	New England Biolabs, Beverly MA, USA
HighPrime™ DNA labelling kit	Roche GmbH, Mannheim, Germany
Microcon™ filter units	Millipore, Billerica, MA, USA
MSI nylon membrane	Osmonics, Minnetonka, MN, USA
QIAGEN Large Construct kit	QIAGEN, Valencia, CA, USA
QIAquick™ purification kit	QIAGEN, Valencia, CA, USA
X-ray film	Fuji X-ray Film, Fuji Co, Ltd, Japan
Wizard™ plasmid mini/midi kits	Promega, Madison, WI, USA

2.1.7. Antibodies

All antibodies used were purchased from Molecular Probes, Eugene, OR, USA, and are listed in Table 2.3.

Table 2.3: Antibodies

Antibody	Type	Use	Reference
Anti-Hu mAb 16A11 Primary Antibody	**Monoclonal Mouse IgG**	**Pan-neuronal antibody**	**(Marusich *et al.*, 1994)**
Alexa Fluor 546 goat anti-mouse	**Polyclonal Goat IgG**	**Secondary antibody for Hu primary**	**http://www.probes.com/products/**
Rabbit Anti-GFP Primary Antibody	**Polyclonal Rabbit IgG**	**Detection of GFP in fixed embryos**	**http://www.probes.com/products/**
Alexa Fluor 488 goat anti-rabbit	**Polyclonal Goat IgG**	**Secondary antibody for GFP primary**	**http://www.probes.com/products/**

2.2. SOLUTIONS, BUFFERS AND MEDIA

Solutions, buffers and media were sterilised by autoclaving or filtration through a 0.22μm filter where appropriate.

2.2.1. Solutions and Buffers

1 × Denhardt's

0.02% (w/v) Ficoll
0.02% (w/v) PVP
0.02% (w/v) gelatin

1 × SSC

0.15 M sodium chloride
0.015 M sodium citrate
Adjusted to pH 7.2 with sodium hydroxide

1 × SSPE

0.18 M sodium chloride
10 mM sodium dihydrogen orthophosphate
1 mM EDTA (pH 7.2)

1 × TAE

40 mM Tris HCl
20 mM sodium actetate
2 mM EDTA
Adjusted to pH 7.8 with glacial acetic acid

1 × TE

10 mM Tris-HCl (pH 8.0)
1 mM EDTA (pH 8.0)

1 × TNE

10 mM Tris-HCl (pH 8.0)
1 mM EDTA (pH 8.0)
10 mM NaCl

6 × Loading Buffer

0.25% (w/v) Bromophenol Blue
0.25% (w/v) Xylene Cyanol
40% (w/v) Ficoll

Antibody Blocking Solution (Block)

0.5% TritonX-100
1% DMSO
5% Horse serum
in PBS

Fix

PBS with 4% Paraformaldehyde

Genomic DNA extraction buffer

1 × TE with 1.7mg/ml Proteinase K

Lysing Solution

10 mM glucose
25 mM Tris-HCl (pH 8.0)
10 mM EDTA
4 mg/ml lysozyme

Southern Denaturing Solution

1.5 M sodium chloride
0.5 M sodium hydroxide

Southern Neutralising Solution

1.5 M sodium chloride
1 M Tris-HCl (pH 7.2)
1 mM EDTA

Southern Prehybridisation Buffer

5 × SSPE
5 × Denhardt's
0.5% (w/v) SDS
100 mg/ml denatured sonicated salmon sperm DNA

STET Buffer

0.1 M NaCl
10 mM Tris-HCl (pH 8.0)
1 mM EDTA
5% Triton X-100

Stop Buffer

0.25%(w/v) Bromophenol Blue
10 mM Tris-HCl (pH 8.0)
1 mM EDTA (pH 8.0)
0.2% (w/v) SDS

PBS

2.7 mM KCl
137 mM NaCl
0.01 M Phosphate Buffer ($Na_2HPO_4 + KH_2PO_4$) (pH 7.4)

PBTX

PBS with 0.5% Triton X-100

2.2.2. Media

Fusaric Acid and Kanamycin TB Agar

1% (w/v) Bacto tryptone
0.1% (w/v) Yeast Extract
0.1% (w/v) Glucose
0.8% (w/v) NaCl
1.5% (w/v) Bacto Agar
50μM $ZnCl_2$
50mg/L Chlorotetracycline

Autoclaved then supplemented with sterile:
72mM $NaH_2PO_4 \cdot H_2O$
12mg/L Fusaric Acid
20mg/L Kanamycin

Luria Agar (L-agar)

3.7% (w/v) Luria agar base

Luria broth (L-broth)

2.5% (w/v) Luria broth base

Zebrafish Embryo medium

0.50 μM sodium chloride
0.17 μM potassium chloride
0.33 μM calcium chloride
0.33 μM magnesium sulphate
0.1% methylene blue

2.3. GENERAL METHODS

2.3.1. Preparation of DNA samples

2.3.1.1. Bacterial Growth

Glycerol stocks or agar stabs of bacterial cell stocks were propagated by streaking on LB-agar plates containing appropriate selective antibiotics and incubated overnight at 37°C or appropriate temperature.

Bacterial cultures were grown in LB-medium supplemented with required antibiotics. Antibiotic concentrations used were as follows: Ampicillin: 50μg/ml; Chloramphenicol: 20μg/ml; Kanamycin: 25μg/ml; Tetracycline: 10μg/ml. After inoculation with a single colony, the culture was incubated overnight at appropriate temperature in a shaking incubator.

2.3.1.2. Plasmid Preparation

Rapid Boiling Lysis

Plasmid DNA for screening of putative clones was prepared using the boiling lysis method described by Holmes and Quigley (1981). Briefly, 2ml bacterial cultures were pelleted by centrifugation, resuspended in 200μl of STET buffer supplemented with 1μg/ml lysozyme and then lysed by heating at 100°C for 45 seconds. Cell debris was then pelleted by centrifugation and removed with a toothpick. The plasmid was purified from the supernatant by ethanol precipitation.

Plasmid preparation kits

High quality DNA for cloning, sequencing, embryo injection or large-scale applications was prepared using Promega mini or midi Wizard™ kits, as per manufacturer instructions. Briefly, bacterial suspensions were lysed by alkali and loaded onto the provided column. Following extensive washing of the column, the plasmid DNA was eluted with water.

2.3.1.3. Preparation of DNA from PACs

PAC DNA for embryo injection or PFGE was prepared with a QIAGEN Large Construct Kit as per manufacturer's directions.

PAC DNA for all other applications was prepared by a modified alkaline lysis method. After lysis, neutralisation and ethanol precipitation, the PAC DNA was incubated with

Plasmid-Safe™ DNAse in the supplied buffer with 1mM ATP for 3 hours. This was followed by a phenol/chloroform extraction and a final ethanol precipitation.

2.3.2. Isolation of DNA/RNA from zebrafish embryos

2.3.2.1. Isolation of genomic DNA

Genomic DNA was isolated from single zebrafish embryos by first euthanasing in Tricaine and dehydration in methanol. Embryos were desiccated by heating at 70°C for 10 minutes, and genomic DNA extracted by addition of 25µl genomic DNA extraction buffer with incubation at 55°C for 4 hours then 75°C for 10 minutes. Samples were then made up to 100µl with MilliQ water before analysis of a 5µl sample by PCR.

2.3.2.2. Isolation of total RNA

Total RNA from pooled zebrafish embryos was isolated by homogenisation in TriReagent™ following Sigma instructions and using 2ml per 60 embryos. Following phase separation by centrifugation, RNA was precipitated from the aqueous phase using isopropanol, and resuspended in water.

2.3.3. Molecular Techniques

2.3.3.1. Restriction Digests

Digestion of DNA by restriction enzymes was performed in a minimal volume, using conditions recommended by the enzyme manufacturer, for a minimum of one hour. Five units of restriction enzyme were added per µg of DNA, ensuring that the volume of enzyme never exceeded 10% of the total reaction volume. When required, RNase A and/or BSA were added to final concentrations of 20 µg/ml and 100 µg /ml respectively.

Heat inactivation of restriction enzymes was carried out by incubating the reaction at 65°C for 15 minutes.

2.3.3.2. Electrophoretic Separation of DNA

Size fractionation of DNA was performed by submarine electrophoresis on 0.8-2.0% (w/v) agarose gels in 1 × TAE supplemented with ethidium bromide to 100ng/ml, submerged in 1 × TAE running buffer. Samples were loaded with 1 × loading buffer, and electrophoresed at 15-100 V. The DNA was visualised and photographed under UV light.

2.3.3.3. Pulsed Field Gel Electrophoresis

Pulsed Field Gel Electrophoresis was performed in a CHEF-DR™ II system (Bio-Rad, Richmond, CA) through a 1% agarose gel in 0.5 × TBE. The chamber was filled with 0.5 × TBE maintained at 14°C by circulating the buffer through hosing submerged in a 9°C water bath. After loading of the samples, electrophoresis was performed at 12V/cm for 25 hours with switch times linearly ramped from 0.5s-3.0s. The gel was post-stained in ethidium bromide and DNA visualised under UV light.

2.3.3.4. Recovery of DNA from Agarose Gels

The band of interest was cut from the gel and DNA isolated using the QIAquick™ kit according to supplier instructions. Briefly, the agarose block was dissolved by heating for 10 mins at 50°C in the provided buffer, and the resulting mixture diluted with isopropanol and then loaded onto the supplied column. Following washing of the column, DNA was eluted in water or Tris buffer.

2.3.3.5. Purification of DNA

Using Phenol/Chloroform Extraction

DNA solutions were made up to a minimum volume of 100 µl with the addition of 1 × TE, and purified by mixing with an equal volume of phenol/chloroform/isoamyl alcohol. The emulsion was centrifuged at 12000 × g for 2 minutes and the upper, aqueous layer transferred to a new tube. Contaminating phenol was removed by washing with an equal volume of chloroform followed by centrifugation as above. The DNA solution was transferred to a new tube, and concentrated using a Microcon filter unit or by ethanol precipitation.

Using QIAquick™ purification kit

For purification of DNA from some enzymatic reactions, the QIAquick™ purification kit was employed as per manufacturer instructions. The reaction mix was diluted in the provided buffer, bound to the purification column and then washed with the provided buffer. DNA was subsequently eluted with water or Tris buffer.

Using Microcon™ filter units

Microcon filter units were used to concentrate, desalt and purify DNA solutions following Millipore instructions.

Precipitation of DNA and RNA

DNA and RNA samples were precipitated by addition of ammonium acetate or sodium acetate pH 5.2 to a final concentration of 0.1M and either 2.5 volumes of cold redistilled ethanol or an equal volume of isopropanol. Sometimes seeDNA™ was added to visualize the pellet. The DNA or RNA was then recovered by centrifugation at 12000 × g for 15 minutes at 4°C. The pellet was washed with cold 70% (w/v) ethanol, dried at room temperature and resuspended in a minimal volume of MilliQ water or 1 × TE.

2.3.3.6. Determination of DNA Concentration

DNA concentration was determined by comparison to DNA markers run in conjunction with the sample on an agarose gel, or by UV spectrophotometry at a wavelength of 260 nm.

2.3.4. Reverse Transcription

cDNA was synthesised from 5μg of zebrafish embryo total RNA using random hexamers and reverse transcriptase following Invitrogen instructions. Briefly, RNA was incubated with 250ng random hexamers in 11μl volume at 65°C for 5 minutes then cooled to 4°C before addition of reverse transcriptase buffer (to final concentration of 1x), 10mM DTT, 0.5mM dNTPs and 200U of SuperScript II in a 20μl reaction volume. After incubation at 42°C for 50 minutes, the enzyme was heat inactivated at 70°C for 15 minutes. Resulting cDNA was diluted 5-fold with MilliQ water before use in PCR.

2.3.5. Polymerase Chain Reaction (PCR)

PCRs were performed in 25 μl mixtures containing 0.2 mM each of dATP, dCTP, dGTP and dTTP, 1 x PCR reaction buffer, 2 or 3mM $MgCl_2$, 1.0 μM of each forward and reverse primer, 2.5 U of *Taq* DNA polymerase and template DNA. Amplification was performed in a programmable temperature controller (Techne, Cambridge, UK). Programs consisted of an initial template denaturation at 95°C for 2 minutes, followed by 35-40 PCR cycles consisting of denaturation at 94°C for 30 seconds, a 1 minute primer annealing step at temperature appropriate for the primers and final extension at 72°C for 30 -90 seconds.

All primers were purchased from Invitrogen and are tabulated below (Table 2.4).

Table 2.4: Primers

Primer name	Sequence (5'-3')	Annealing temperature	Use
PAC6F	TCG CGT AGT CGA TAG TG	47°C	Sequencing of PAC vector
PAC6R	CAC TCA ATG ACC TGA CC	47°C	Sequencing of PAC vector
Sal15	GCG TCG ACG CGC GAC ACA GAG - CAG GCA TTC AGA GC	55°C	Cloning of p2.5GFP
T7	GTA ATA CGA CTC ACT ATA GGG C	55°C	Cloning of p2.5GFP
S11	ACC GTG ACA CAC TCT ACC AAG - ATG ACC	66°C	PCR based genomic library screen
S13	CAT GAT AAA ATT TGC ACC CTG - AAA AGG	66°C	PCR based genomic library screen
S15	GCG CGA CAC AGA GCA GGC ATT - CAG AGC	66°C	PCR of *sox10* cDNA or gDNA
S17	TAT ATT CTG AGG AAG ACG GCG	66°C	PCR of *sox10* cDNA or gDNA
S19	GCA GCA AGA GCA AAC CGC ACG	68°C	PCR of *sox10* cDNA or gDNA
S20	TGG TAG GGG GCG TTG GAG GGC	68°C	PCR of *sox10* cDNA or gDNA
S21	ACC TAC CGA AGT CAC CTG TGG	58°C	PCR of *sox10* cDNA or gDNA
S22	GAT ATT GAT CCG CCA GTT TCC	58°C	PCR of *sox10* cDNA or gDNA
S24	AAT CGC ATT ACA AGA GCC TGC	56°C	PCR of *sox10* cDNA or gDNA
S25	CCA GGG AAG TGT GTT TCA CTC	56°C	PCR of *sox10* cDNA or gDNA
S26	TAT ACA TAC GGC ATC TCC AGC	56°C	PCR of *sox10* cDNA or gDNA
S27	AGT TTG TGT CGA TTG TGG TGC	56°C	PCR of *sox10* cDNA or gDNA

2.3.6. Cloning Strategies

2.3.6.1. Preparation of Insert DNA and Plasmid Vector

DNA fragments for ligation were generated by complete restriction, followed by heat inactivation of the restriction enzyme where possible. Dephosphorylation of DNA ends, when required, was achieved by addition of 2 units of Shrimp Alkaline Phospotase directly to the restriction enzyme reaction. If required, the desired fragment was purified by recovery from an agarose gel.

Vector DNA for use in ligations was digested with the appropriate restriction enzymes, and purified through a QIAquick™ column.

2.3.6.2. Ligations

Ligations were performed using 50-100 ng of vector DNA and a three molar excess of insert DNA, catalysed by 10 units of T_4 DNA ligase in a 10 µl reaction. Ligations were incubated at 16°C overnight or room temperature for 2 hours.

PCR products were cloned into pGEM-T Easy vector following Promega instructions.

2.3.6.3. Preparation and Transformation of Competent *E. coli*

Introduction of plasmid DNA into *E. coli* was performed by the two methods outlined below. Following transformation, cells were incubated in Luria Broth for one hour before spreading on LB-agar plates containing required antibiotic and overnight incubation at appropriate temperature. Where colour selection of colonies containing recombinant plasmids was desired, 200 µg/ml X-gal and 160 µg/ml IPTG were added to the plate.

Calcium chloride method

Preparation of DH5αF′ competent cells for transformation was performed using the calcium chloride method as per Sambrook (1989). Transformation of competent *E. coli* cells with plasmids was achieved using a 2 minute heat shock at either 42°C or 37°C.

Electroporation method

Preparation of electrocompetent *E. coli* was performed by culturing a sufficient volume of *E. coli* to mid-log phase, followed by extensive washes in cold 10% glycerol. After a final wash, cell pellets were resuspended in an appropriate volume of 10% glycerol and aliquoted for storage. Transformation of 100µl of thawed *E. coli* with 5ng plasmid was performed in 1mm cuvettes using a Bio-Rad Electroporator set at 1.25kV.

2.3.7. DNA Sequencing and sequence analysis

General DNA sequencing runs were performed at the Sequencing Facility, University of Bath with an ABI DNA sequencer module. Sequencing of the *t3* mutant lesion was performed commercially (Oswell Research Products Ltd, Southhampton).

Analysis of raw sequences and chromatograms, compilation of contigs and sequence comparisons were performed with the BioEdit Software package, which can be found at www.mbio.ncsu.edu/BioEdit/bioedit.html.

2.3.8. Analysis of DNA by Hybridisation

2.3.8.1. Transfer of DNA to Nylon Membranes

Southern Blotting

Following electrophoresis, DNA was transferred and UV-fixed onto a nylon membrane, following the method of Sambrook (1989). For transfer of large DNA fragments (>10kb), the gel was washed in 0.2M HCl for 15 minutes immediately before commencing the protocol.

Colony Hybridisation

Colony hybridisations were performed largely as described by (Grunstein and Hogness, 1975). Bacterial colonies were patch plated onto an L-agar plate supplemented with 100 μg/ml ampicillin and replica plated onto a Hybond-N™+ membrane which overlayed another ampicillin supplemented L-agar plate. Following overnight growth at 37°C, the filter was placed colony side up on a pad of Whatman® 3MM paper soaked in lysing solution for 20 minutes. The filter was transferred to a fresh pad of 3MM paper soaked in Southern Denaturing Solution plus 1% (w/v) SDS for a total of 20 minutes, and then on 3MM soaked in Southern Neutralising Solution, before the filter was partially air-dried and washed in 2 x SSC, during which bacterial debris was removed using absorbent cotton wool. The DNA was UV-fixed onto the filters as per Amersham instructions using a UVP CL-1000 unit (UVP, Upland CA).

2.3.8.2. Radiolabelling of DNA probes

PCR products or DNA fragments purified from an agarose gel were labelled by primer extension of random oligonucleotides using the HighPrime™ system and [α-^{32}P] dCTP. The reaction was stopped by addition of 30μl of Stop Buffer and unincorporated nucleotides were removed by column chromatography through Bio-Gel P60 resin columns made with G50 beads. Columns were packed and equilibrated with 100 μl 1 × TNE buffer by gravity flow. Labelled DNA fragments were eluted by adding the labelling reaction plus stop buffer to the top of the column and collecting the first dye fraction.

2.3.8.3. Prehybridisation, Hybridisation and Washing of filters

Prehybridisation

Filters were prehybridised in Southern prehybridisation buffer at 65°C for a minimum of one hour. The volume of Southern prehybridisation solution was approximately 0.1 ml/cm^2 of filter.

Probe Denaturation and Hybridisation

Before dilution in fresh Southern prehybridisation buffer and addition to the prehybridised filters, the radiolabelled probe was denatured by boiling for 2 minutes. Hybridisation was conducted for a minimum of 16 hours at 65°C.

Washing of Filters

Filters were normally washed twice in a solution of 2 × SSC, 0.1% SDS at 65°C for 30 minutes and then twice in 0.2 × SSC, 0.1% SDS at 65°C for 30 minutes.

Autoradiography and Stripping of Filters

Filters were covered in plastic wrap and exposed to X-ray film at -70°C for appropriate periods of time, backed by an intensifying screen (DuPont Hi-Plus).

Southern blots and colony filters were stripped of probe by boiling for 10 minutes in 0.1 x SSC, 1% SDS, then rinsed in 2 x SSC and stored in plastic wrap at 4°C.

2.4. ZEBRAFISH METHODS

2.4.1. Fish husbandry

Embryos were obtained through crosses of wild-type, mutant and transgenic zebrafish kept in the University of Bath zebrafish facility, and were raised and staged according to Kimmel *et al.* (1995). Dechorionation was performed with Watchmakers' No. 5 forceps, and embryos older than 15hpf, which were to be manipulated, fixed or live mounted, were anaesthetised by addition of tricaine (to approximately 0.2% final concentration v/v) to embryo medium.

2.4.2. Injection of zebrafish embryos

Needles for injection were made by pulling 3½" Drummond glass capillaries (Drummond Scientific Co., Broomall, PA) on a Micropipette puller (Sutter Instrument Co., Novato, CA). Zebrafish embryos were pipetted onto a 2% agarose plate in zebrafish embryo medium. Injections were performed under a dissecting microscope using a Drummond Nanoject II apparatus (Drummond Scientific Co., Broomall, PA). Phenol Red was added to DNA solutions before loading into needles backfilled with mineral oil.

2.4.3. Antibody staining

Staining of embryos with antibodies against GFP or the pan-neuronal marker Hu were performed as follows, using incubations performed at room temperature with gentle agitation. Embryos were treated with fix for 2 hours before being washed three times in PBTX for five minutes. Following three one-hour washes in MilliQ water, the embryos were pre-blocked for 2 hours by incubation in antibody blocking solution. This was replaced with primary antibody diluted 1:750 in antibody blocking solution and incubated overnight. The following day, the antibody solution was discarded and the embryos washed three times in PBTX for one hour each, then incubated overnight with appropriate secondary antibody diluted 1:800 in antibody blocking solution. The antibody was discarded and embryos washed three times in PBTX for 30 minutes each before clearing in glycerol and mounting for visualisation by microscopy.

2.4.4. Embryo mounting and microscope techniques

Mild inhibition of melanisation was performed by addition of PTU to the embryo medium to a final concentration of 0.0015%. Anaesthetised or fixed embryos were mounted either between No.1 coverslips or in 3% methylcellulose for microscopic examination on an Eclipse E800 (Nikon) microscope using Nomarski optics or fluorescence with appropriate filter.

Low power microscopic analysis and general embryo manipulation was performed on an MZ12-FL dissecting microscope (Leica) with fluorescent attachment.

GFP was visualised by epifluoresence with FITC filters, whilst the fluorescently conjugated secondary antibody for Hu staining was detected using a TRITC fluorescence filter. Photography was performed with a SPOT digital camera (Diagnostic Instruments) and images analysed and enhanced with Photoshop™ (Adobe). Confocal images were taken with a Zeiss Confocal Microscope (LSM510).

CHAPTER 3

ISOLATION AND ANALYSIS OF ZEBRAFISH *SOX10* GENOMIC CLONES

3.1. BACKGROUND: ZEBRAFISH GENOMIC LIBRARIES AND RESCUE OF ZEBRAFISH MUTANTS

3.1.1. Zebrafish genomic library resources

The advent of high throughput genome sequencing projects and the need for detailed analysis of gene structure, including identification of distant regulatory elements, have required the generation of large insert genomic libraries providing full genome sequence coverage. Additionally, large-scale mutagenesis screens in many model organisms have led to acceleration of positional cloning efforts, which depend ultimately on availability of such libraries. To this end, genomic libraries of numerous organisms, including zebrafish, have been made commercially available and are produced mostly using three vectors systems: bacterial artificial chromosomes (BACs), P1-derived artificial chromosomes (PACs) and yeast artificial chromosomes (YACs) (Amemiya *et al.*, 1999). Each of these systems show differences in insert size and culturing methods, however all offer relative ease of handling, increased cloning size capability compared to older vectors, improved stability and amenability to simple and established laboratory protocols. However each vector probably displays unique cloning biases meaning that the use of all resources is required to reduce the chance of missing regions of the genome under represented in any one system (Amemiya *et al.*, 1999).

Zebrafish YAC, BAC and PAC libraries available at the time of the commencement of this work are summarised in Table 3.1, however many more are available currently (Geisler, 2002). These four original large-insert libraries all provide approximately 4 to 5-fold coverage of the genome and were produced from the AB wild-type strain. Screening of the libraries can be performed by two methods, filter hybridisation or use of PCR pools. By arraying colony DNA of the entire library onto filters, the hybridisation approach allows rapid screening, with one round sufficient to identify positive clones. The PCR screening procedure however occurs in two rounds using gene specific PCR to detect presence or absence of the gene of interest in pools of DNA. Primary pools are prepared from DNA of genomic clones representing sections of the library, and secondary pools, corresponding to any positive primary pools, are subsequently screened to obtain plate, column and row information within the library (Geisler, 2002). The PCR approach does have the advantage of being more robust and sensitive, with little optimisation required (Amemiya *et al.*, 1999).

Resources for screening and the libraries themselves are available commercially and from public organisations such as RZPD (http://www.rzpd.de; Vente *et al.*, 1999), and have numerous important applications to zebrafish genomic analysis. These include candidate and positional cloning projects (examples include *one-eyed pinhead* (Zhang *et al.*, 1998a), *sauternes* (Brownlie *et al.*, 1998) and *mind bomb* (Itoh *et al.*, 2003)), isolation of zebrafish homologues or promoters of certain genes (e.g. the *Cx43alpha 1* gene; (Chatterjee *et al.*, 2001) and the *annexin A13* gene; (Iglesias *et al.*, 2002)), the zebrafish genome sequencing project at the Sanger centre (http://www.sanger.ac.uk/Projects/D_rerio) and rescue experiments (see below).

Table 3.1: Summary of zebrafish genomic libraries

Library name	Vector	Host Strain	Average insert size	Reference
BCH-YAC	pYAC4	AB1380	240kb	www.incyte.com
MGH-YAC	pRML1/2	J57D	470kb	(Zhong *et al.*, 1998)
BAC	pBeloBac11	DH10B™	90kb	www.incyte.com
PAC	PCYPAC6	DH10B™	115kb	(Amemiya and Zon, 1999)

3.1.2. Rescue of zebrafish mutants

Molecular genetic characterisation of zebrafish mutants begins through either a candidate or positional cloning approach. Attempts at phenotypic rescue by introduction of cloned genes, DNA constructs or synthetic mRNA into embryos is a valuable tool for both methodologies, and often allows quick dismissal of candidate genes or narrows a chromosome walk to overlapping genomic clones. Ultimately, rescue of mutant phenotype is an important criterion in the proof of gene identity of given mutants and is now routine in zebrafish gene studies.

Although first demonstrated using injection of mRNA into mutant embryos (Currie and Ingham, 1996), rescue can also be performed with genomic DNA or cDNAs driven by ubiquitous, inducible or tissue specific promoters (e.g. Liao *et al.*, 1998; Miller *et al.*, 2000). It should be noted that mosaic expression of injected DNA is far more severe than that of RNA (Gilmour *et al.*, 2002a). Thus RNA injection often provides a greater degree of rescue and is additionally a useful tool for misexpression studies and in epistasis tests. One drawback of mRNA injection (or cDNAs under ubiquitous promoters) is that expression is ectopic. This can lead to developmental defects, which may complicate interpretation of rescue success Additionally, exogenous RNA is less stable than DNA and thus rescue of later defects might prove difficult due to degradation of the mRNA (Gilmour *et al.*, 2002a). Finally, rescue by ectopic expression of a protein does not imply that it

directly corresponds to the mutation in question; it may simply be supplementing a downstream component of the pathway, indirectly disrupted by the mutation. However this cannot be the case with rescue by wild-type genomic clones as wild-type protein is produced only in the correct time and place, and only if the pathway both upstream and downstream is functional. Accordingly, rescue experiments fall into two types, those where the injected nucleic acid used for rescue corresponds to the mutated gene and those which rescue with a component downstream of the mutation. A summary of some rescue experiments conducted using nucleic acid injection in zebrafish is presented in Table 3.2.

Table 3.2: Rescue experiments in zebrafish using nucleic acid injection.

Mutation	Gene used for rescue	Method	Assessment criteria; reference
A: Rescue uses injection of nucleic acid corresponding to gene affected in mutant			
swirl	*bmp2*	mRNA	Morphology; (Kishimoto *et al.*, 1997)
one-eyed pinhead	*EGF-CFC*	mRNA	Morphology; (Zhang *et al.*, 1998a)
floating head	*znot*	BAC	*col2a1* expression in notochord cells; (Yan *et al.*, 1998)
cyclops	*ndr2*	mRNA	*twhh,shh*, and *pax2.1* expression; (Rebagliati *et al.*, 1998)
sucker	*et1*	PAC, cDNA	Alcian Blue cartilage stain; (Miller *et al.*, 2000)
nacre	*mitf*	cDNA	Melanin; (Lister *et al.*, 1999)
colourless	*sox10*	cDNA	Melanin; (Dutton *et al.*, 2001)
lost-a-fin	*alk8*	mRNA	Morphology; (Mintzer *et al.*, 2001)
spiel ohne grenzen	*pou2*	mRNA	*pax2.1* expression in MHB; (Belting *et al.*, 2001)
vlad tepes	*gata1*	mRNA, cDNA, BAC	*band3* expression; (Lyons *et al.*, 2002)
after eight	*deltaD*	Germline transgenic	Somite morphology and markers; (Hans and Campos-Ortega, 2002)
B: Rescue of Mutant uses different (downstream) gene			
cyclops	*Shh*	mRNA	Netrin1 expression; (Strahle *et al.*, 1997)
one-eyed pinhead	*mixer*	mRNA	Sox17 expression; (Alexander and Stainier, 1999)
ntl flh	*ehh*	mRNA	Muscle Pioneers (MyoD); (Currie and Ingham, 1996)
casanova	*mezzo*	mRNA	Sox17 expression; (Poulain and Lepage, 2002)
cloche	*SCL*	cDNA	Red Blood cells; (Liao *et al.*, 1998)
bozozok	*noggin*	mRNA	Otx1 expression; (Fekany-Lee *et al.*, 2000)
colourless	*mitf*	cDNA	Melanin; (Elworthy *et al.*, 2003)

Adapted and extended from Ekker, (1999).

3.1.3. Aims

Cloning and analysis of the *Sox10* genomic loci from humans and mice have been reported (Pusch *et al.*, 1998). The aims of this section of work included isolation, coarse mapping and initial sequence analysis of genomic clones containing the zebrafish *sox10*

gene, as well as demonstration that they can rescue the *cls* mutation and thus contain critical promoter elements required for *sox10* expression.

3.2. RESULTS

3.2.1. Isolation of zebrafish sox10 PAC clones

A PCR based library screen was used to isolate PAC clones containing the *sox10* gene from an arrayed zebrafish genomic library (RZPD, Berlin, Germany). Primers S11 and S13 (Table 2.4) amplify 940bp of the 3' UTR of the zebrafish *sox10* gene and were used to detect presence or absence of this fragment in 33 primary pools. Single bands of correct size were detected in seven primary pools (Figure 3.1a) as can be seen in lanes 13, 15, 18 and 30 and faintly in lanes 7, 9 and 20. Of these positive primary pools, four gave informative patterns in the secondary screen allowing identification of a row, column and plate number in the arrayed library for each clone (an example for primary pool 13 is given in Figure 3.1b). The remaining three secondary screens were not informative, as they did not give all three positive lanes required to identify position of the clone in the library (Table 3.3). The four PAC clones obtained from the screen were designated PAC G, PAC I, PAC L and PAC N, and corresponding full RZPD clone codes are presented in Table 3.3. Presence of *sox10*-like sequence was confirmed by both PCR (Figure 3.1c) and Southern analysis (Figure 3.2b, c).

3.2.2. Restriction mapping of sox10 PAC clones

A coarse restriction map of each PAC was generated by analysing *Not*I /*Sal*I single and double digests with Pulsed Field Gel (PFG) Electrophoresis, as shown on Figure 3.2a. Maps were deduced (Figure 3.3) and confirmed by probing a Southern blot of the PFG with the *sox10* 5' RACE product and a probe to the 3' UTR (provided by A. Pauliny; Pauliny, 2002; Figure 3.2b,c). The hybridisation patterns also indicated position and orientation of the coding region on each PAC shown in Figure 3.3. Note that the 3kb *Sal*I-*Not*I fragment present on all PACs (Figure 3.3) was too small to be present on the PFG or blots, however its presence has been verified on a standard agarose gel (not shown). Probing the blot with vector sequence (not shown) provided further verification of the maps.

Summing fragment sizes also allowed estimation of total insert size for each PAC, as shown on Figure 3.3 and in Table 3.3. All are smaller than the average insert size of the

Figure 3.1; Figure 3.2; Figure 3.3 ⟶

Figure 3.1: PCR based genomic library screen

a. Agarose gel of the Primary PCR based screen, showing products obtained from PCR on primary pool DNA template using Primer pair S11-S13.
PCRs were performed on Primary Pools of the RZPD BUSMP706 zebrafish PAC genomic library. Numbers at top of lanes refer to Primary Pool numbers.
PCR products of the expected size (940bp) are present in 7 of the 33 pool lanes, namely lanes numbered 7, 9, 13, 15, 18, 20 and 30 (indicated by arrowheads).
Lane M: Promega 1 kbp DNA ladder with selected fragment sizes indicated.

b. An example of an agarose gel of one informative secondary screen (corresponding to Primary Pool #13) in which 3 PCR products were obtained using Primer pair S11-S13 (again indicated with arrowhead and positive lanes highlighted with arrows). A positive control was included (lane labelled G) which used zebrafish genomic DNA as a template. In addition, a negative control PCR was included in which Secondary Pool DNA was replaced with water. This reaction gave no product (lane labelled W).
Lane M: Promega 100bp DNA ladder with fragment sizes indicated.

c. PCR of DNA template from the four PAC clones using Primer pair S11-S13. All four PACs (labelled at top of respective lanes) show a PCR fragment of correct size. A negative control PCR which used water in place of DNA template gave no product (not shown).
Lane M: NEB 100bp DNA ladder with fragment sizes indicated.

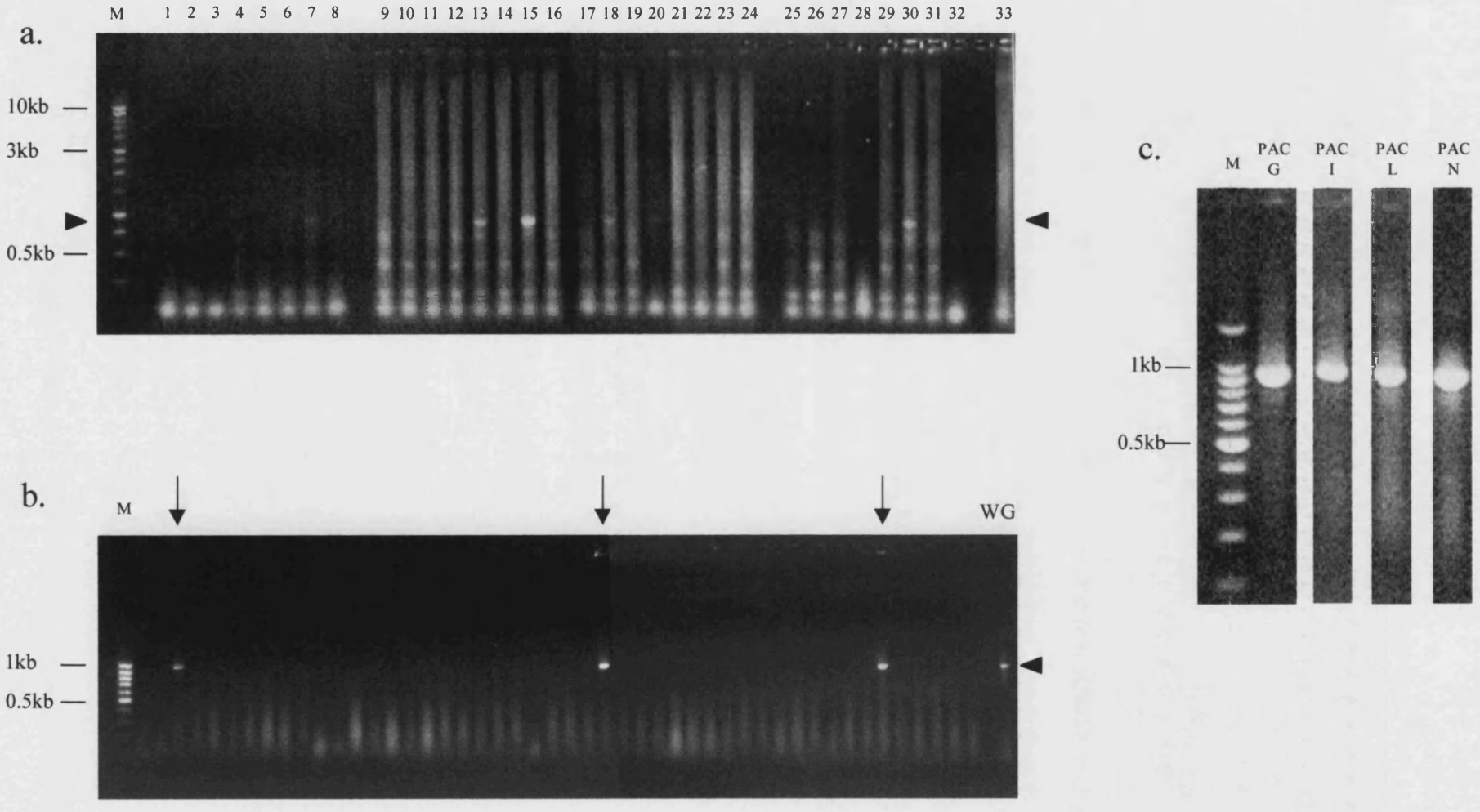
a.
M 1 2 3 4 5 6 7 8 9 10 11 12 13 14 15 16 17 18 19 20 21 22 23 24 25 26 27 28 29 30 31 32 33
10kb
3kb
0.5kb
b.
M
WG
1kb
0.5kb
c.
M
PAC G
PAC I
PAC L
PAC N
1kb
0.5kb

Figure 3.2 Physical mapping of *sox10* PAC clones

a. Pulsed field gel of single and double restrictions of PAC G, I, L and N with *Not*I and *Sal*I.

Lanes M: High Molecular Weight Marker. Some fragment sizes are indicated to the left for clarity. Sizes in kb are from top to bottom: 48.5, 38.4, 33.5, 29.9, 24.8, 22.6, 19.4, 17.1, 15.0, 12.2, 10.1, 8.6, 8.3.

Restriction digests are indicated as follows: *Not*I (N), *Sal*I (S) and *Not*I + *Sal*I (N/S).

PAC clones represented in each lane are indicated above the restriction digest title.

b. Southern blot of above gel probed with zebrafish *sox10* 5'RACE probe. Lanes as in (a.) above.

c. Southern blot of above gel probed with a region of the 3'UTR. Lanes as in (a.) above.

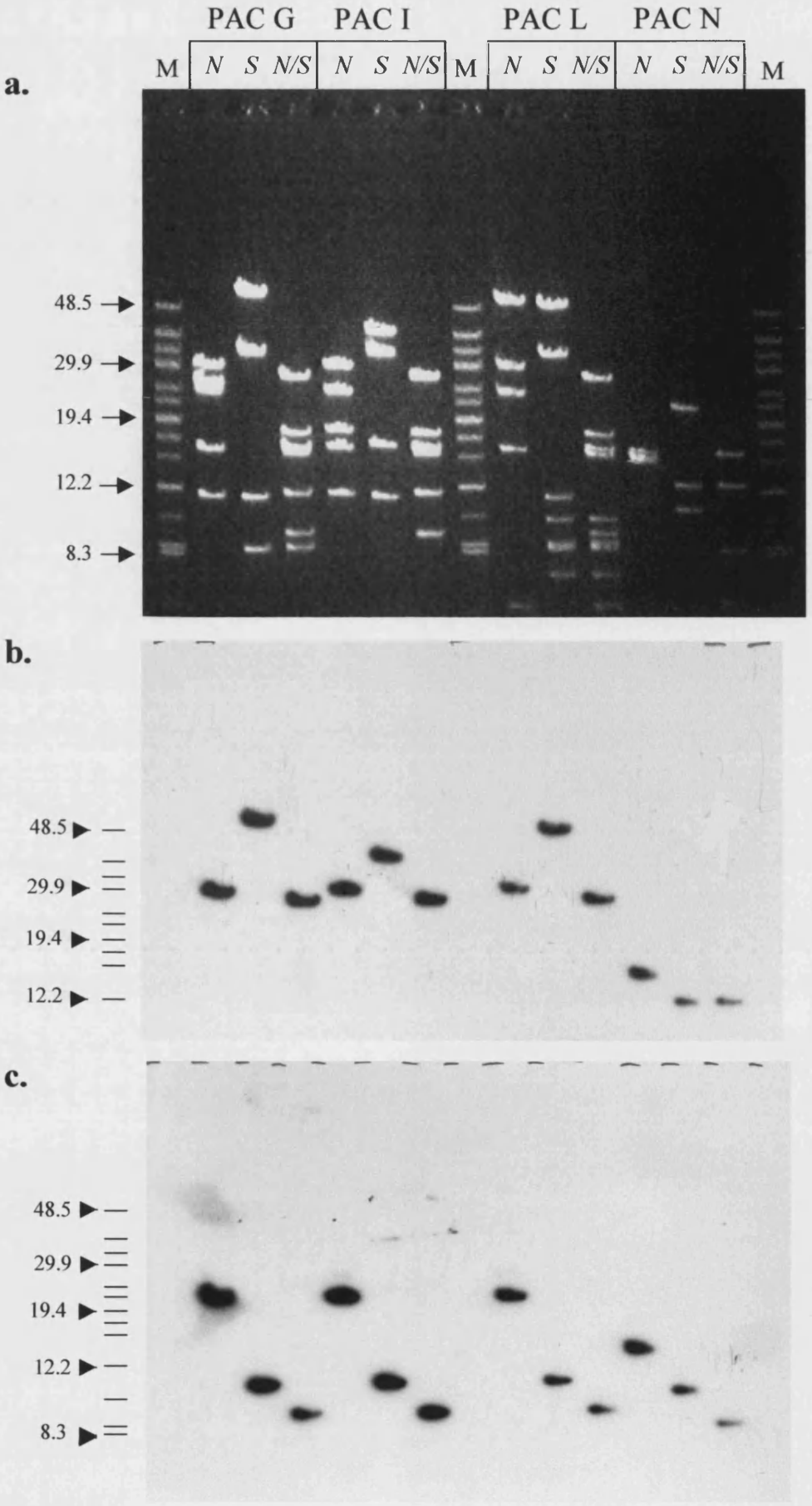
a.
PAC G
PAC I
PAC L
PAC N
M
N
S
N/S
N
S
N/S
M
N
S
N/S
N
S
N/S
M
48.5
29.9
19.4
12.2
8.3
b.
48.5
29.9
19.4
12.2
c.
48.5
29.9
19.4
12.2
8.3

Figure 3.3 Restriction Maps of the four zebrafish *sox10* PACs

*Not*I (N), *Sal*I (S) restriction maps of each PAC G, L, I and N are shown, as deduced from PFGE data and subsequent southern analysis (Figure 3.2). Estimated sizes are in kb. Sites in brackets correspond to those present on the cloning vector. The approximate position and orientation of the *sox10* gene is shown as an arrow above the maps (based on Figure 3.2b,c).

The asterisk under one fragment in PAC N indicates that this fragment appears to be approximately 1kb shorter than in the other 3 PACs (see text).

Note that the restriction digest information at the far right hand end of PAC L was uninformative. Although total size (32kb) could be accurately determined, the order of the three *Sal*I-*Sal*I fragments could not.

Also note that hybridisation of the approximately 3 kb *Sal*I-*Not*I fragment within the *sox10* gene could not be seen on either of the PFG southerns as it had run off the Pulsed Field Gel, however this has been confirmed on other gels (not shown).

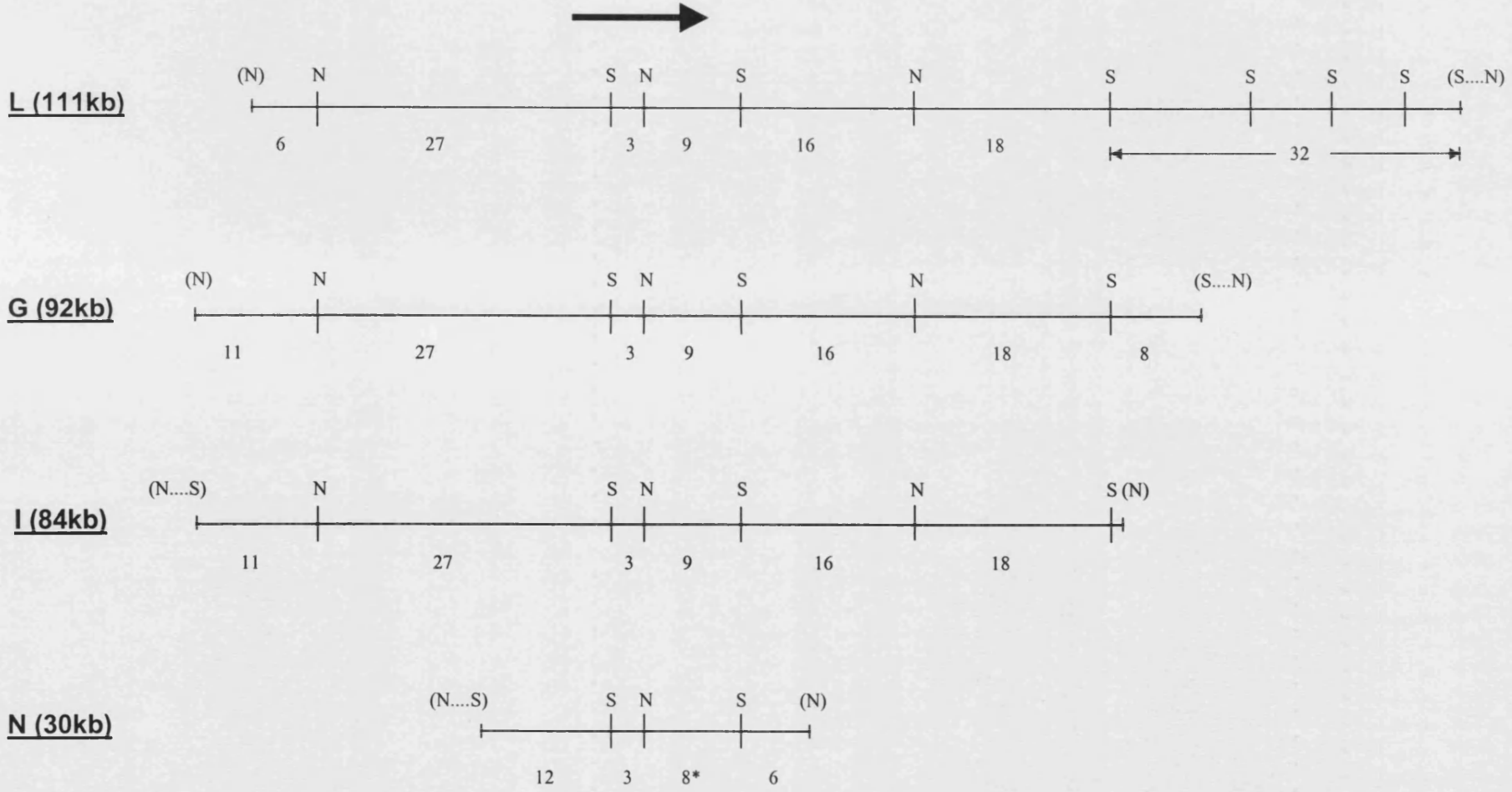
L (111kb)
(N) N S N S N S S S S (S....N)
6 27 3 9 16 18 32
G (92kb)
(N) N S N S N S (S....N)
11 27 3 9 16 18 8
I (84kb)
(N....S) N S N S N S (N)
11 27 3 9 16 18
N (30kb)
(N....S) S N S (N)
12 3 8* 6

library (~115kb; Amemiya and Zon, 1999), with PAC N being significantly so. The three largest PACs all show hybridisation of a 27kb *Not*I-*Sal*I fragment to the 5' RACE product. Further, hybridisation of a 9kb *Not*I-*Sal*I fragment to the 3' probe occurred in all three PACs, and this combined information, allowed positioning and orientation of the *sox10* coding region on the maps, also shown in Figure 3.3.

Table 3.3: Zebrafish *sox10* PACs

Positive Primary Pools (PCR signal strength)	Number Positive Secondary Pools	RZPD Clone ID	PAC Name	Insert Size
BUSMP706PP7 (+)	1	-		
BUSMP706PP9 (+)	2	-		
BUSMP706PP13 (+++)	3	BUSMP706N1498Q2	PAC N	30 kb
BUSMP706PP15 (+++)	3	BUSMP706G03116Q2	PAC G	92 kb
BUSMP706PP18 (++)	3	BUSMP706I16137Q2	PAC I	84 kb
BUSMP706PP20 (+)	3	BUSMP706L06154Q2	PAC L	111 kb
BUSMP706PP30 (+++)	2	-		

It appears that the smallest PAC (PAC N) had undergone some deletion or rearrangement during cloning, as one of the fragments 3' to the *sox10* gene in this PAC was approximately 1kb shorter than expected from the maps of the other PACs (compare band in N/S lane of PAC N with those in N/S lanes of the other PACs, Figure 3.2c). Alternatively, it could represent a polymorphism within the zebrafish sample used to construct the library, such as a small deletion or insertion, or an RFLP such as an extra *Sal*I site in the region, however this could not be detected by more detailed agarose gel electrophoresis of *Sal*I and *Not*I/*Sal*I digested PAC N, so is unlikely (not shown).

Note also that precise mapping at one end of PAC L was not possible due to uninformative restriction pattern here. Restriction mapping using a different enzyme may better resolve this region.

3.2.3. Sequence of PAC I

In collaboration with W. J. Pavan at the National Institute of Health (NIH) in Bethesda, MD, U.S.A., one of the *sox10* PACs (PAC I) was partially sequenced (unpublished). High quality sequence from an 18.5kb contig containing the putative zebrafish *sox10* gene was obtained, and used for all subsequent sequence analysis. It contained sequence with high homology to the published zebrafish *sox10* cDNA sequence (Figure 3.4), demonstrating that it probably corresponds to the gene encoding the zebrafish Sox10 protein. The overall identity between the predicted exons and the cDNA sequence is 98.6%, with the predicted

Figure 3.4 →

Figure 3.4 Intron-Exon structure and cDNA alignment

Alignment of a contig from the PAC I sequence to the published zebrafish *sox10* cDNA sequence using the Spidey program (found at http://www.ncbi.nlm.nih.gov/).

a. Intron-exon structure of the zebrafish *sox10* gene deduced from alignment to the cDNA sequence. Exons are represented as orange boxes with introns shown as blue lines. The numbers at either end refer to the position of the start of exon 1 and the end of exon 4 in the 18.5kb genomic contig sequence. Note that this 4 exon – 3 intron structure is conserved with mouse and human *Sox10* genes.

b. Table summarising the alignment by Spidey including the sites in each sequence of overlap, length of exon, percent identity within each exon, numbers of mismatches or gaps and presence of donor (d) and acceptor (a) splice sites. Overall homology is 98.6%.

c. Alignment of predicted exons with the zebrafish *sox10* cDNA sequence, with 10 bp of intron sequence either sde of each exon also shown. Intron sizes are shown at the end of exons 1-3. Note that only eight substitutions occur in the coding sequence and all are synonymous substitutions. Further, a G is present at the start of the cDNA sequence which is not present in the gene sequence, however this is likely to represent reverse transcription of the 7-methyl-guanosine cap of the *sox10* mRNA, added during mRNA processing.

Intron – exon structure and boundaries are conserved between zebrafish, human and mouse *sox10* genes, and all show canonical donor and acceptor sites.

a.

b.

EXON	Genomic coordinates	mRNA coordinates	length	identity	mismatches	gaps	Donor site	Acc. site
Exon 1	5526-5658	1-133	133	98.5%	2	0	d	
Exon 2	7764-8445	134-815	682	97.9%	14	0	d	a
Exon 3	10321-10583	816-1078	263	99.6%	1	0	d	a
Exon 4	12470-14603	1079-3202	2124	98.4%	33	14		a

c.

Exon 1: 5526-5658 (genomic); 1-133 (mRNA)

```
5526   CATGAATTGATTTTTTTCTCGCTCTTCACACAACGGGGCTCTTTAAGCCTCGACGCGCGACACAGAGCAGGCATTCAGAGCGCGAGCGAGGGGGCTGAAC
                ||||||||||||||||||||||||||||||||||||||||||||||||||||||||||||||||||||||||||||||||||||||||||||||
1              GTTTTTTCTCGCTCTTCACACAACGGGGCTCTTTAAGCCTCGACGCGCGACACAGAGCAGGCATTCAGAGCGCGAGCGAGGGGGCTGAAC

5616   CGACGGACTCTCGTGCTGGGCGGGCGACCTGCTGCACTGTAAAGTAAGTGCAT      Intron 1 (2106bp)
       |||||||||||||  |||||||||||||||||||||||||||||||
91     CGACGGACTCTCGCGCTGGGCGGGCGACCTGCTGCACTGTAAA
```

Exon 2: 7764-8445 (genomic); 134-815 (mRNA)

```
7764   ATTTTTGTAGGTTTCCATCAGATCTATATCCAGAGGAAGACGGCGGAAGGATTCCTTCTTACAAACTCGAATTATATAAAAAGAACTGTTAAGGTTTCAC
                ||||||||||||||||||| | |||||||||||||||||||||||||| ||| | |||| |  | | ||||||||||||||| |||||||
134            GTTTCCATCAGATCTATATTCTGAGGAAGACGGCGGAAGGATTCCTTCTGACAGAGTCGAGTCGTTTGAAAAGAACTGTTAAAGTTTCAC

7854   TGGATGATCTTAAATAATAAACAAAAGCACAATTATTTTACAAGAAAAAAAACATTTGTAAAGTATAAATTAATACATTTATATTTAAAATAAAATTTAAG
       ||||||||||||||||||||||||||||||||||||||||||||||||||||||||  ||||||||||||||||||||||||||||||||||||||||
224    TGGATGATCTTAAATAATAAACAAAAGCACAATTATTTTACAAGAAAAAAAACATTTGAGAAGTATAAATTAATACATTTATATTTAAAATAAAATTTAAG

7954   TGAGGAAATTAAACCTACCGAAGTCACCTGTGGCCGCAGAACTAGTGGACCGATGTCGGCGGAGGAGCACAGCATGTCGGAGGTGGAAATGAGTCCCGGG
       ||||||||||||||||||||||||||||||||||||||||||||||||||||||||||||||||||||||||||||||||||||||||||||||||||
324    TGAGGAAATTAAACCTACCGAAGTCACCTGTGGCCGCAGAACTAGTGGACCGATGTCGGCGGAGGAGCACAGCATGTCGGAGGTGGAAATGAGTCCCGGG
                                                  M  S  A  E  E  H  S  M  S  E  V  E  M  S  P  G

8054   GTGTCGGACGATGGGCACTCCATGTCCCCTGGTCACTCGTCGGGCGCTCCCGGTGGCGCGGACTCCCCTCTGCCCGGTCAGCAGTCTCAGATGTCCGGGA
       ||||||||||||||||||||||||||||||||||||||||||||||||||||||||||||||||||||||||||||||||||||||||||||||||||
424    GTGTCGGACGATGGGCACTCCATGTCCCCTGGTCACTCGTCGGGCGCTCCCGGTGGCGCGGACTCCCCTCTGCCCGGTCAGCAGTCTCAGATGTCCGGGA
        V  S  D  D  G  H  S  M  S  P  G  H  S  S  G  A  P  G  G  A  D  S  P  L  P  G  Q  Q  S  Q  M  S  G

8154   TCGGGGATGATGGAGCCGGTGTCTCCGGCGGGGTCTCAGTGAAGTCCGACGAGGAAGATGACCGGTTCCCCATCGGCATCCGCGAGGCGGTCAGTCAGGT
       ||||||||||||||||||||||||||||||||||||||||  ||||||||||||||||||||||||||||||||||||||||||||||||||||||||
524    TCGGGGATGATGGAGCCGGTGTCTCCGGCGGGGTCTCGGTGAAGTCCGACGAGGAAGATGACCGGTTCCCCATCGGCATCCGCGAGGCGGTCAGTCAGGT
       I  G  D  D  G  A  G  V  S  G  G  V  S  V  K  S  D  E  E  D  D  R  F  P  I  G  I  R  E  A  V  S  Q  V

8254   GCTGAACGGGTACGACTGGACGCTCGTGCCCATGCCCGTGCGCGTGAACTCGGGCAGCAAGAGCAAACCGCACGTCAAGCGGCCGATGAACGCGTTCATG
       ||||||||||||||||||||||||||||||||||||||||||||||||||||||||||||||||||||||||||||||||||||||||||||||||||
624    GCTGAACGGGTACGACTGGACGCTCGTGCCCATGCCCGTGCGCGTGAACTCGGGCAGCAAGAGCAAACCGCACGTCAAGCGGCCGATGAACGCGTTCATG
         L  N  G  Y  D  W  T  L  V  P  M  P  V  R  V  N  S  G  S  K  S  K  P  H  V  K  R  P  M  N  A  F  M

8354   GTGTGGGCGCAGGCCGCGCGCAGGAAACTGGCGGATCAATATCCGCACCTGCACAACGCCGAGCTCAGCAAAACACTGGGGAAGCTGTGGAGGTGAGCGCGC
       ||||||||||||||||||||||||||||||||||||||||||||||||||||||||||||||||||||||||||||||||||||||||||||||||||
724    GTGTGGGCGCAGGCCGCGCGCAGGAAACTGGCGGATCAATATCCGCACCTGCACAACGCCGAGCTCAGCAAAACACTGGGGAAGCTGTGGAG          Intron 2
       V  W  A  Q  A  A  R  R  K  L  A  D  Q  Y  P  H  L  H  N  A  E  L  S  K  T  L  G  K  L  W  R          (1876bp)
```

Exon 3: 10321-10583 (genomic); 816-1078 (mRNA)

```
10321  CATGTTTCAGACTGCTGAACGAGACGGATAAGCGGCCGTTTATCGAGGAGGCCGAGCGCTTGAGGAAGCAGCATAAGAAAGATTATCCCGAGTACAAGTA
                ||||||||||||||||||||||||||||||||||||||||||||||||||||||||||||||||||||||||||||||||||||||||||||||
816            ACTGCTGAACGAGACGGATAAGCGGCCGTTTATCGAGGAGGCCGAGCGCTTGAGGAAGCAGCATAAGAAAGATTATCCCGAGTACAAGTA
                 L  L  N  E  T  D  K  R  P  F  I  E  E  A  E  R  L  R  K  Q  H  K  K  D  Y  P  E  Y  K  Y

10411  CCAGCCACGTCGACGCAAGAACGGCAAACCGGGTTCCAGCTCAGAGGCCGACGCCCACTCTGAGGGCGAGGTCAGCCACAGCCAATCGCATTACAAGAGC
       |||||||||||||||||||||||||||||||||||||||||||||||||||||||||||||||||||||||||||||||||||||||||||||||||
906    CCAGCCACGTCGACGCAAGAACGGCAAACCGGGTTCCAGCTCAGAGGCCGACGCCCACTCTGAGGGTGAGGTCAGCCACAGCCAATCGCATTACAAGAGC
         Q  P  R  R  R  K  N  G  K  P  G  S  S  S  E  A  D  A  H  S  E  G  E  V  S  H  S  Q  S  H  Y  K  S

10511  CTGCACCTGGAGGTGGCGCACGGCGGGGGCTGCAGGGTCACCATTGGGTGATGGACACCACCCTCACGCTACAGGTGAGATACA      Intron 3 (1887bp)
       |||||||||||||||||||||||||||||||||||||||||||||||||||||||||||||||||||||||||||||||||
956    CTGCACCTGGAGGTGGCGCACGGCGGGGGCTGCAGGGTCACCATTGGGTGATGGACACCACCCTCACGCTACAG
         L  H  L  E  V  A  H  G  G  A  A  G  S  P  L  G  D  G  H  H  P  H  A  T
```

ctd...

Exon 4: 12470-14603 (genomic); 1079-3202 (mRNA)

```
12470  GTTTGCTCAGGTCAGAGTCACAGCCCTCCAACGCCCCCTACCACCCCCAAGACGGAACTGCAGGGAGGAAAATCAGGCGAGGGCAAGCGTGAGGGCGGAG
                ||||||||||||||||||||||||||||||||||||||||||||||||||||||||||||||||||||||||||||||||||||||||||||||||||||||
1079            GTCAGAGTCACAGCCCTCCAACGCCCCCTACCACCCCCAAGACGGAACTGCAGGGAGGAAAATCAGGCGAGGGCAAGCGTGAGGGCGGAG
                G  Q  S  H  S  P  P  T  P  P  T  T  P  K  T  E  L  Q  G  G  K  S  G  E  G  K  R  E  G  G

12560  CCTCTCGGAGTGGACTGGGGGTGGGAGCAGATGGAAGCTCCGCCTCATCGTCTGCCAGCGGGAAACCGCACATCGACTTCGGTAACGTGGACATTGGCGA
       ||||||||||||||||||||||||||||||||||||||||||||||||||||||||||||||||||||||||||||||||||||||||||||||||||||||
1169   CCTCTCGGAGTGGACTGGGGGTGGGAGCAGATGGAAGCTCCGCCTCATCGTCTGCCAGCGGGAAACCGCACATCGACTTCGGTAACGTGGACATTGGCGA
       A  S  R  S  G  L  G  V  G  A  D  G  S  S  A  S  S  S  A  S  G  K  P  H  I  D  F  G  N  V  D  I  G  E

12660  AATCAGCCATGACGTGATGGCCAACATGGAGCCGTTCGACGTGAACGAGTTCGACCAGTATCTCCCACCCAATGGCCACCCGCAGGCGTCCGCCACTGCC
       ||||||||||||||||||||||||||||||||||||||||||||||||||||||||||||||||||||||||||||||||||||||||||||||||||||||
1269   AATCAGCCATGACGTGATGGCCAACATGGAGCCGTTCGACGTGAACGAGTTCGACCAGTATCTCCCACCCAATGGCCACCCGCAGGCGTCCGCCACTGCC
         I  S  H  D  V  M  A  N  M  E  P  F  D  V  N  E  F  D  Q  Y  L  P  P  N  G  H  P  Q  A  S  A  T  A

12760  AGCGCAGGATCTGCAGCGCCATCGTATACATACGGCATCTCCAGCGCGCTAGCGGCCGCTAGTGGCCACTCCACCGCATGGCTGTCCAAGCAGCAACTGC
       ||||||||||||||||||||||||||||||||||||||||||||||||||||||||||||||||||||||||||||||||||||||||||||||||||||||
1369   AGCGCAGGATCTGCAGCGCCATCGTATACATACGGCATCTCCAGCGCGCTAGCGGCCGCTAGTGGCCACTCCACCGCATGGCTGTCCAAGCAGCAACTGC
        S  A  G  S  A  A  P  S  Y  T  Y  G  I  S  S  A  L  A  A  A  S  G  H  S  T  A  W  L  S  K  Q  Q  L

12860  CGTCCCAGCAGCATTTGGGCGCAGATGGCGGAAAAACGCAGATAAAGAGTGAAACACACTTCCCCGGGGATACAGCGGCGAGCGGTTCACACGTCACATA
       ||||||||||||||||||||||||||||||||||||||||||||||||||||||||||||||||||||||||||||||||||||||||||||||||||||||
1469   CGTCCCAGCAGCATTTGGGCGCAGATGGCGGGAAAACGCAGATAAAGAGTGAAACACACTTCCCTGGGGATACAGCGGCGAGCGGTTCACACGTCACATA
       P  S  Q  Q  H  L  G  A  D  G  G  K  T  Q  I  K  S  E  T  H  F  P  G  D  T  A  A  S  G  S  H  V  T  Y

12960  CACGCCGCTAACACTGCCGCACTACAGCTCCGCCTTCCCCTCGCTGGCGTCCCGCGCACAGTTCGCCGAATACGCCGAGCACCAGGCCTCGGGATCCTAC
       ||||||||||||||||||||||||||||||||||||||||||||||||||||||||||||||||||||||||||||||||||||||||||||||||||||||
1569   CACGCCGCTAACACTGCCGCACTACAGCTCCGCCTTCCCCTCGCTGGCGTCCCGCGCACAATTCGCCGAATACGCCGAGCACCAGGCCTCGGGATCCTAC
         T  P  L  T  L  P  H  Y  S  S  A  F  P  S  L  A  S  R  A  Q  F  A  E  Y  A  E  H  Q  A  S  G  S  Y

13060  TACGCCCACTCCAGCCAGACCTCAGGCCTCTACTCCGCCTTCTCCTACATGGGCCCCTCACAGCGGCCCCTGTACACCGCCATTCCGGATCCGGGATCCG
       ||||||||||||||||||||||||||||||||||||||||||||||||||||||||||||||||||||||||||||||||||||||||||||||||||||||
1669   TACGCCCACTCCAGCCAGACCTCAGGCCTCTACTCCGCCTTCTCCTACATGGGCCCCTCACAGCGGCCCCTGTACACCGCCATTCCGGATCCGGGATCCG
        Y  A  H  S  S  Q  T  S  G  L  Y  S  A  F  S  Y  M  G  P  S  Q  R  P  L  Y  T  A  I  P  D  P  G  S

13160  TGCCGCAGTCGCACAGCCCCACGCACTGGGAGCAGCCCGTATACACCACACTGTCTCGACCGTGACACACTCTACCAAGATGACCAGTCACGGAAGGTCC
       |||||||||| ||||||| ||||| ||||||||||||||||||||||||||||||||||||||||||||||||||||||||||||||||  |||||||
1769   TGCCGCAGTCACACAGCCCTACGCATTGGGAGCAGCCCGTATACACCACACTGTCTCGACCGTGACACACTCTACCAAGATGACCAGTCACTAAAGGTCC
       V  P  Q  S  H  S  P  T  H  W  E  Q  P  V  Y  T  T  L  S  R  P  *

13260  AACCGTAAAGTGTGTGTGTGTGTGTGTGCTAAAAATCATCGAAACACTCGCCTGCACCACAATCGACACAAACTGAGATCTGAGAAACGAGTGTGTGT
       |||||||| ||||||||||||||     ||||||||||||||||||||||||||||||||||||||||||||||||||||||||||||||||||||||
1869   AACCGTAAGGTGTGTGTGTGTG------CTAAAAATCATCGAAACACTCGCCTGCACCACAATCGACACAAACTGAGATCTGAGAAACGAGTGTGTGT

13360  GTGTGTGTGGAGATCTGCAGGGAAATATTCTCACGTGCCTCAGACGACCACCGTCCAGACCTGCTCCCTCAACGCCAATTTGAACACCAGTAGTATTTTC
       ||||||||| ||||||||||||||||||||||||||||||||||||||||||||||||||||||||||||||||||||||||||| ||||||||||||||
1963   GTGTGTGTG-AGATCTGCAGGGAAATATTCTCACGTGCCTCAGACGACCACCGTCCAGACCTGCTCCCTCAACGCCAATTTGA-CACCAGTAGTATTTTC

13460  GAAAAAGACGTATTACCAAAGTACCGAGACCAAAACATTACAGAAATACGAGAGTGCATCCATCCTTCCTGAACTCCGGATATCAGATCACACACAGACT
       |||||||||||| ||||||||||||||||||||||||||||||||||||||||||||||||||||||||||||||||||||||||||||||||||||||
2061   GAAAAAGACGTAGTACCAAAGTACCGAGACCAAAACATTACAGAAATACGAGAGTGCATCCATCCTTCCTGAACTCCGGATATCAGATCACACACAGACT

13560  TCAACACATGATGCTAGTACCAGTGCATCCGCATTTTTTATCTGTATTTGTATGAATGAATAATCTTTTTATTAACCAAAATAAGGCCATATTGTTTTTA
       ||||||||||||||||||||||||||||||||||||||||||||||||||||||||||||||||||||||||||||||||||||||||||||||||||||||
2161   TCAACACATGATGCTAGTACCAGTGCATCCGCATTTTTTATCTGTATTTGTATGAATGAATAATCTTTTTATTAACCAAAATAAGGCCATATTGTTTTTA

13660  AAAAAATAATGAGGTGTTTTTCGTTGTTGTAATCTCTTGTGTTGTCGTTACTGTTGTTATTTGTGTTGCCATAACTACACTGAAAAGTCTTCACCACTGT
       ||||||||||||||||||||||||||||||||||||||||||||||||||||||||||||||||||||||||||||||||||||||||||||||||||||||
2261   AAAAAATAATGAGGTGTTTTTCGTTGTTGTAATCTCTTGTGTTGTCGTTACTGTTGTTATTTGTGTTGCCATAACTACACTGAAAAGTCTTCACCACTGT

13760  CTAGTGTTTGTTAATGACATTTGTGTTTTATGACTTTCAGCGTGTGTAAATATCAGTGCCAGGACGCCATACACACACATGTCTCCACCCAATTAAGGTGCG
       ||||||||||||||||||||||||||||||||||||||||||||||||||||||||||||||||||||||||||||||||||||||||||||||||||||||
2361   CTAGTGTTTGTTAATGACATTTGTGTTTTATGACTTTCAGCGTGTGTAAATATCAGTGCCAGGACGCCATACACACATGTCTCCACCCAATTAAGGTGCG

13860  CTCACAGTGACGTTAATTAAATTGAGGAATTCCCAATCATGCAGATTCCTCTAGAAATGGCTATATTTCGTGAAAGCAGTAAATGTGAGCGCACCTTTAT
       |||||||||||||||||||||||||||||||||||||| |||||| ||||||||||||||||||||||||||||||||||||||||||||||||||||
2461   CTCACAGTGACGTTAATTAAATTGAGGAATTCCCAACCATGCAAATTCCTCTAGAAATGGCTATATTTCGTGAAAGCAGTAAATGTGAGCGCACCTTTAT

13960  TTCACACAAGCAGTACTGTAAAGGTAATATATTTTTACCAGATTGGAAATAGTGGACGTAATTACGAATTTTTAATAATAAATGACTATTTTTAGAGAAT
       |||||||||||||||||||||||||||||||||||| |||||||||||||| ||||||||||||||||||||||||||||||||||||||||||||||
2561   TTCACACAAGCAGTACTGTAAAGGTAATATATTTTTGCCAGATTGGAAATGGTGGACGTAATTACGAATTTTTAATAATAAATGACTATTTTTAGAGAAT

14060  ACCGCTAGTGCCTCAAGTCCATCACAAACGAATTGTCGTTTCTGATAAATTCAATTTTGATGATGTAAAATCCTTTTCAGGGTGCAAATTTTATCATGCG
       ||||||||||||||||||||||||||||||||||||||||||||||||||||||||||||||||||||||||||||||||||||||||||||||||||||||
2661   ACCGCTAGTGCCTCAAGTCCATCACAAACGAATTGTCGTTTCTGATAAATTCAATTTTGATGATGTAAAATCCTTTTCAGGGTGCAAATTTTATCATGCG

14160  TTAAGCGATGTGATTATACATCGAATATGCATATGCAAATTAATAAGTGCCATTTTTATAATTAAAAATACATCTATCAACTATCTGAAGACCTTCCTAA
       |||| ||||||||||||||||||||||||||||||||||||||||||||||||||||||||||||||||||||||||||||||||||||||||||||||
2761   TTAACCGATGTGATTATACATCGAATATGCATATGCAAATTAATAAGTGCCATTTTTATAATTAAAAATAC----ATCAACTATCTGAAGACCTTCCTAA

14260  CATTGGGTAAGTAAATAAATACATTCATTTCATTGTATTATTTTTGGTAAATACAATATTTAGCTATTCTACGTTTTGTCTCCCTTTGGTACTTTATAGT
       |||||||||||||||||||||||| ||||||||||||||||||||||||||||||||||||||||||||||||||||||||||||||||||||||||||
2857   CATTGGGTAAGTAAATAAATACATTTATTTCATTGTATTATTTTTGGTAAATACAATATTTAGCTATTCTATGTTTTGTCTCCCTTTGGTACTTTATAGT

14360  TTTGTTTTCGCCCTCTTTATTATTTAGTATTATTCAGAAACAAACAAACTCTTTTTATATATTACAGAATATTATTTATATTTGTTGTTG--TTTTTTTA
       |||||||| ||||||||||||||||||||||||||||||||||||||||||||||||||||||||||||||||||||||||||||||||  ||||||||
2957   TTTGTTTTTGCCCTCTTTATTATTTAGTATTATTCAGAAACAAACAAACTCTTTTTATATATTACAGAATATTATTTATATTTGTTGTTGTTTTTTTTTA

14458  TCAGTAGCGTTTTATTCTGTTTGTTGTAAACCTCTGTCGTGTGCTGTTGTGGTGGGTTAAAGTGCTGTTGTTTTTCTCTGTCGGTGTAAATAGAACTGAG
       |||||||||||||||||||||||| ||||||||||||||||||||||||||||||||||||||||||||||||||||||||||||||||||||||||||
3057   TCAGTAGCGTTTTATTCTGTTTGTCGTAAACCTCTGTCGTGTGCTGTTGTGGTGGGTTAAAGTGCTGTTGTTTTTCTCTGTCGGTGTAAATAGAACTGAG

14558  AGCAGTGACTAACTTTCCTCACTCTAAATAAAGCTGCAGTCTTTACGAACACGCAC
       ||||||||||||||||||||||||||||||||||||||||||||||||||||
3157   AGCAGTGACTAACTTTCCTCACTCTAAATAAAGCTGCAGTCTTTAC
```

proteins having identical sequence. Note the cDNA begins with a G, not present in the gene sequence. This is consistent with reverse transcription of the 7-methyl-guanosine cap of the *sox10* mRNA previously reported during cDNA synthesis (Hirzmann *et al.*, 1993). The presence of this cap additionally supports the notion that the reported *sox10* cDNA sequence represents a full-length transcript. This alignment to the zebrafish *sox10* cDNA sequence also allowed identification of intron-exon size, structure and boundary locations as shown in Figure 3.4, and also in the zebrafish *sox10* cDNA sequence in Appendix 1.

Percentage Identity Plots performed at the NIH, between the zebrafish *sox10* gene region and the mouse sox10 gene showed homology between coding regions (not shown), as expected from previous analysis using the zebrafish *sox10* cDNA sequence (Pauliny, 2002). With a view to revealing transcription factors important for controlling Sox10 expression, it was hoped that conserved *sox10* regulatory regions would be identified, however no homology was noted outside the coding region (J.R. Dutton, W. Pavan pers. comm.).

To identify conserved enhancer or promoter regions, which might have key binding sites for transcription factors controlling *sox10* expression, a comparison with the sox10 gene from a closer species was made. The *Fugu* genome sequencing project is nearing completion and a putative *sox10* containing scaffold was identified by blast search against the zebrafish *sox10* gene sequence. Scaffold number S002943 shows good homology to *sox10* sequence from zebrafish, mouse, chick and human, and is annotated in the *Fugu* genome database as containing a *sox10* orthologue based on a number of criteria including gene prediction software and a TBLASTX search. An alignment of the predicted *Fugu* and zebrafish Sox10 proteins is given in Figure 3.5a, demonstrating a 74% identity and 90% similarity between the two proteins. The similarity was greater than for any other protein sequence in the database, including the closely related zebrafish *sox9* genes. Although it cannot yet be proven, it is highly likely that this gene represents the *Fugu sox10* orthologue, as annotated by the gene prediction software.

A Percentage Identity Plot was produced between the putative 30.3kb *Fugu* sox10 genomic sequence and the 18.5kb *sox10*-containing contig of PAC I. This is shown in Figure 3.5b, and indicates 7 sites of homology (numbered 1 to 7 for clarity), plotted in a position relative to the PAC I contig and the degree of identity. A Dot Plot is also given in Figure 3.5c showing the position of these sites with respect to both sequences. Homology is seen in the exons and extremities of the introns, as well as 3 CA-repeats (numbered 4 in Figure 3.5b and c) and interestingly two sites found outside the exons. One of these sites occurs upstream of the start of transcription, whilst the other occurs downstream of the final exon.

Figure 3.5 →

Figure 3.5 Percentage Identity Plots of the *sox10* genomic regions from zebrafish and Fugu

a. Alignment of the predicted proteins from the zebrafish (upper) and the Fugu (lower) *sox10* genes. Percentage Identity between the two proteins is 74%, whilst the percentage similarity is 90%, with identical residues shaded in black and similar residues in grey. This indicates that this gene is most likely a true *sox10* orthologue.

b. Percentage Identity Plot (produced by the PIPMaker software (http://bio.cse.psu.edu/pipmaker/), comparing the zebrafish *sox10* gene contig with Fugu Scaffold S002943. Regions of identity are plotted with respect to position to the zebrafish PAC I contig sequence (x-axis; shown below) and degree of identity shown at the right on the y-axis. Boxes above outline predicted CpG islands. Note that homology exists at 7 loci in the zebrafish gene region, numbered 1 to 7 below plot. This includes the four *sox10* exons (#s 2, 3, 5 and 6), CA repeats (#4) and two flanking sites (#s 1 and 7) (see text and Figure 3.6).

c. Dot Plot from same output as in (b.) showing relative positions of the homology sites in (a.) with respect to both sequences. The Fugu sequence is presented on the y-axis and the PAC I contig sequence on the x-axis, with total sizes of sequences given on axes. Numbers within figure correspond to sites in (b.).

a.

b.

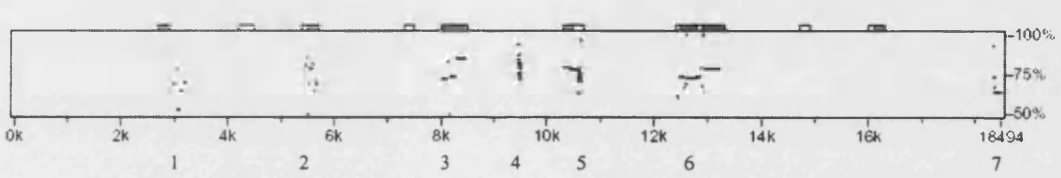

Zebrafish *sox10* PAC I

c.

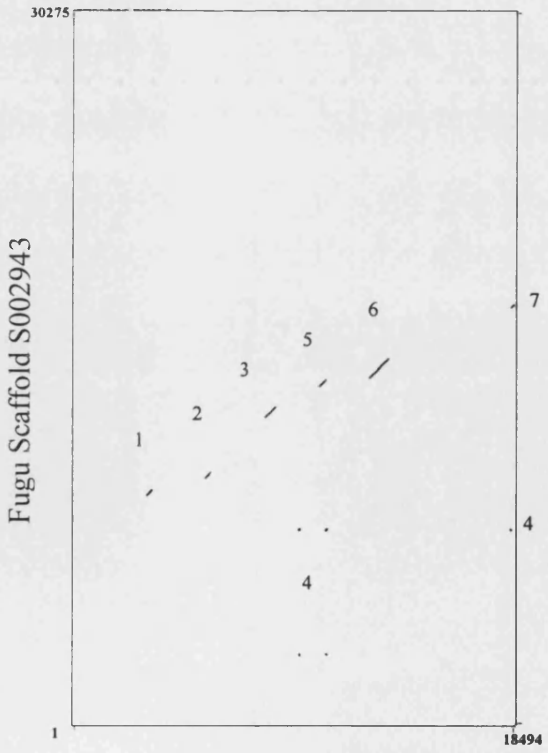

Zebrafish *sox10* PAC I

The sequence alignments for all sites (except the CA-repeats) are shown in Figure 3.6. Again, intron-exon structure and boundary position is conserved for these *sox10* genes, however notice that the *Fugu* introns are often much smaller, consistent with its compacted genome. Homology within introns is confined to short stretches at the extremities near the splice sites, and probably represents conservation of splice signal sequences. Both extragenic sites (#s 1 and 7) show no homology to sequences in the BLAST database, and the annotated *Fugu* genome browser indicates that they lie outside any recognised gene in this region (not shown). It is possible they might represent a conserved, non-coding region or conserved enhancer for the *sox10* gene in teleosts, however it is possible one or both are associated with regulation of another gene such as the *pol2rf* gene, which is found 3' to the *sox10* gene. Further functional and *in silico* analysis of these sites and the *sox10* gene region in general remains to be undertaken.

3.2.4. Rescue of *cls* by PAC clone injection

Hybridisation, PCR and sequence data imply all four PACs contain sequence highly homologous to zebrafish *sox10* cDNA, and thus were highly likely to contain the *sox10* gene. To test this, a rescue experiment was used to ask if the *sox10* sequence on each PAC represented a functional gene *in vivo* and if it corresponds to the gene affected in *cls*. Additionally, comparing abilities of each PAC to rescue all the cell types affected in *cls* allowed inferences to be made as to the size of promoter required for necessary expression in each lineage, as well as rough positioning of any enhancers for such lineages.

3.2.4.1. Chromatophore rescue

Strong *colourless* alleles never show migrating, stellate melanophores, only very small black melanised cells in the dorsal stripe, which never migrate (Kelsh *et al.*, 1996; Kelsh and Eisen, 2000). Furthermore, they show an almost complete absence of xanthophores and generally do not have any iridophores, although some embryos display a small number of iridophores in the dorsal stripe or present as a patch in the eye or lateral patch. Initial assessment of whether PAC injection could partially rescue the *colourless* phenotype focussed on melanophores, as the presence of healthy melanophores is easy to visualise and score. 1-8 cell stage embryos from *cls* $^{+/m618}$ or *cls* $^{+/ty22f}$ incrosses were injected with approximately 30-60pg of DNA from each of the four PACs. These embryos were raised at 28.5°C and inspected over the next 3 days for signs of melanophore rescue.

Figure 3.7a and b show examples of 48hr putative *cls* embryos rescued with all four PACs. By comparing to uninjected siblings (both wild-type and *cls*; see top two panels in both Figure 3.7a and Figure 3.7b), it is clear that these embryos contain an intermediate

Figure 3.6; Figure 3.7 →

Figure 3.6 Sequence alignments of homologous regions between zebrafish and fugu *sox10* genes

Regions of homology associated with the *sox10* gene were predicted and aligned by the PIPMaker software. Each site of homology is presented as boxed sequence alignment, with numbers corresponding to those designating the sites in Figure 3.5. These consist of almost all the exons of zebrafish *sox10* as well as a region upstream of the start of transcription of both genes, and a region downstream of the fourth exon, between the *sox10* gene and the *pol2rf* gene.

In each alignment box, the zebrafish sequence is given on the upper strand, with the Fugu sequence given below. Dots indicate identity and dashes indicate gaps. Exons are written in capitals and intronic sequence or putative promoter sequence written in lowercase. Predicted intron sizes are shown. The *Bam*H1 site present in the first region of homology is boxed.

Numbers on the left of each line of sequence give position number relative to the predicted start of transcription, which is shown as a large arrow. Translation start and stop codons are indicated in bold.

Note that due to lack of a full length fugu *sox10* cDNA sequence, the exact size of the first intron and 5'UTR were difficult to predict.

The other regions showing homology found by the PIPMaker software are CA repeats and are not presented here.

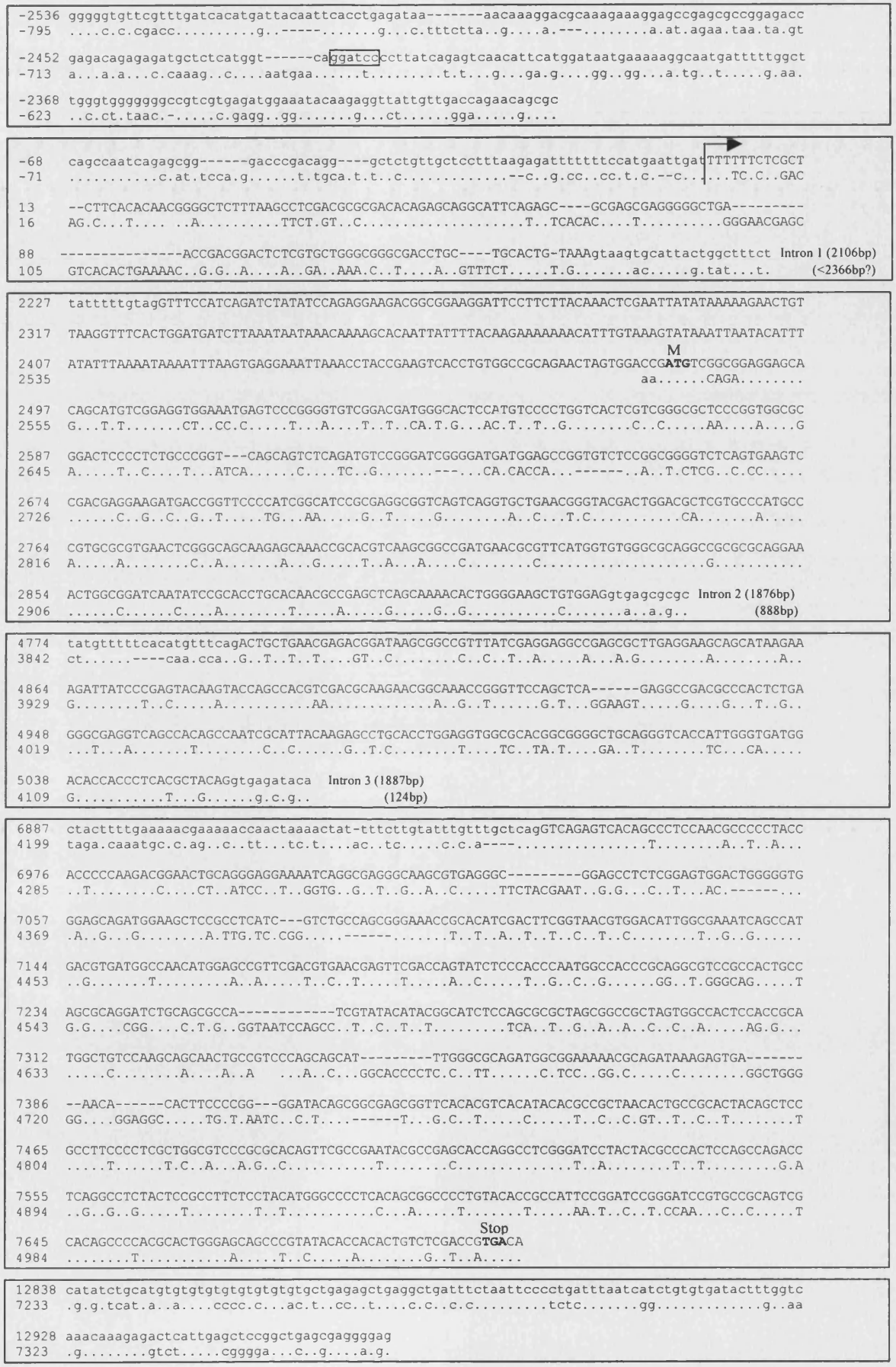
1
2
3
5
6
7
Intron 1 (2106bp)
(<2366bp?)
Intron 2 (1876bp)
(888bp)
Intron 3 (1887bp)
(124bp)
M
Stop

Figure 3.7: Rescue of melanophores in *cls* by PAC injection

a. Dorsal views of approximately 48hpf embryos showing the ability of *sox10* PACs to rescue melanophores. Upper two panels show uninjected siblings with the top panel displaying a wild-type embryo with a large number of melanophores evident. The second panel shows a *cls* embryo completely devoid of melanophores. Partial rescue of this phenotype is clear in the lower two panels showing *cls* embryos rescued by injection of PAC I (third panel) and PAC N (bottom panel). An intermediate number of melanophores are evident as is the variation of the degree of rescue seen. These melanophores appear to have normal morphology and are able to migrate to ventral parts of the embryo. This is evident in lateral views of rescued embryos.

b. Lateral views of approximately 48hpf embryos showing the ability of *sox10* PACs to rescue melanophores. Upper two panels show uninjected siblings with the top panel displaying a wild-type embryo with a large number of melanophores evident. The second panel shows a *cls* embryo completely devoid of melanophores. Again, partial rescue of this phenotype is apparent upon injection of all PACs, in this case PAC G (third panel) and PAC L (bottom panel). Examples of melanophores which have migrated to ventral positions are indicated by arrows.

a.

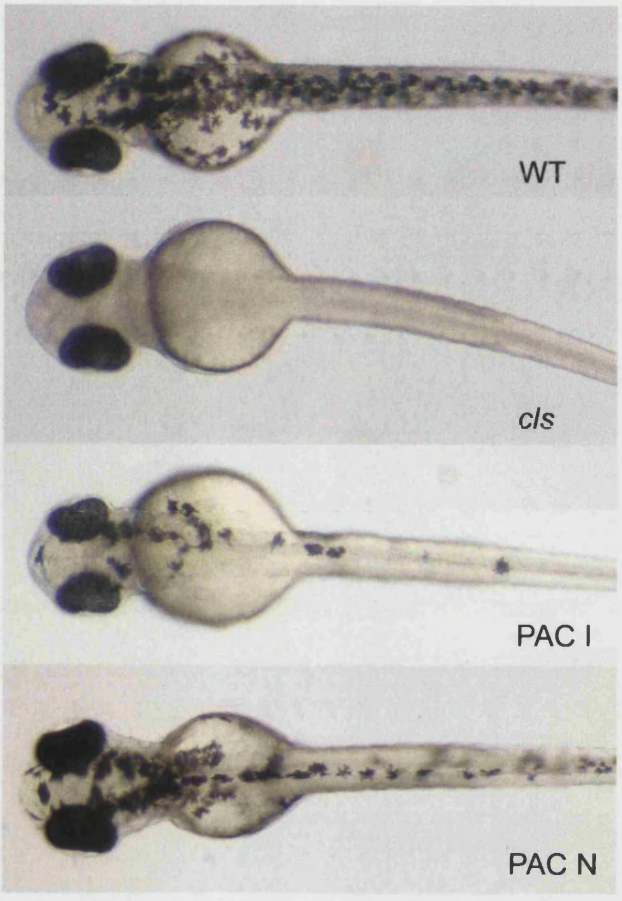

b.

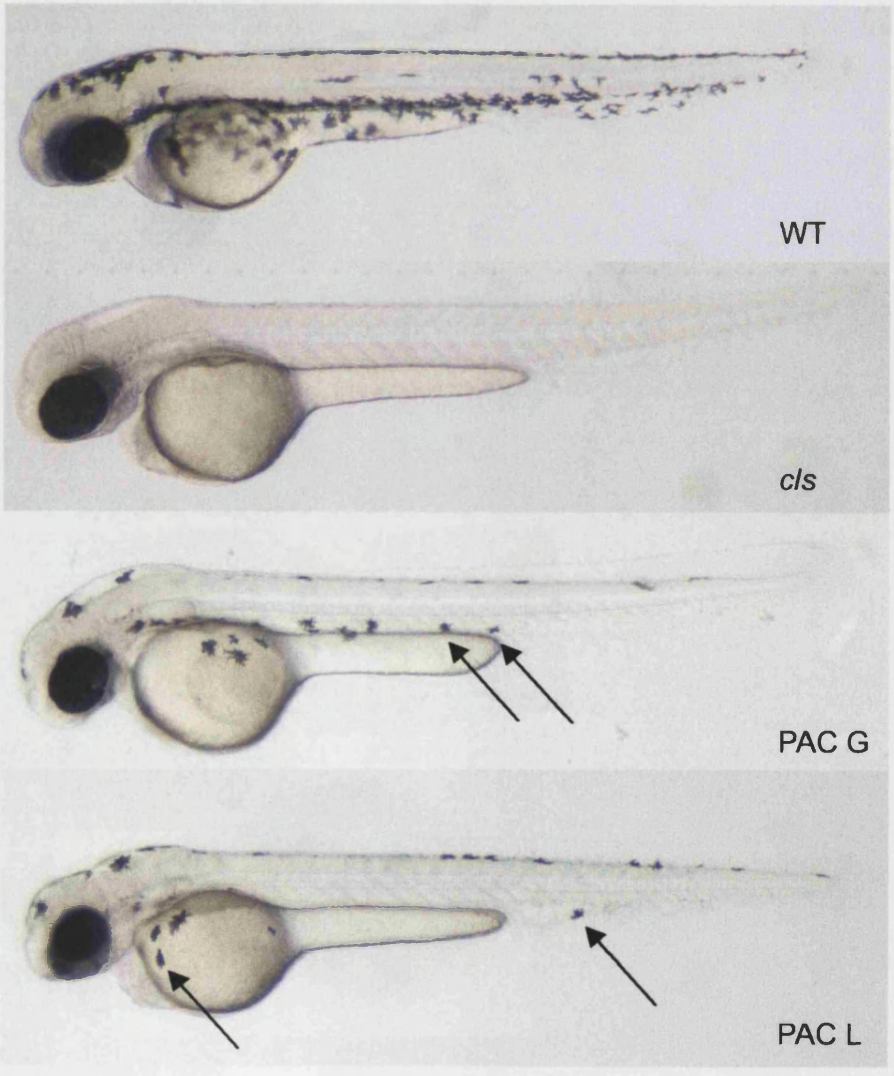

number of melanophores which display a wild-type morphology and behaviour, namely are stellate, darkly melanised and are able to migrate to ventral regions of the embryo (arrow in Figure 3.7b).

The intermediate number of melanophores seen in some injected embryos can be attributed to two different causes. Firstly, injection of the PAC DNA might have somehow reduced the number of healthy melanophores in originally wild-type embryos due to cytotoxic effects. Secondly, they could in fact represent mosaic rescue of *cls* embryos. The latter scenario predicts a decrease in the number of embryos in a batch showing zero melanophores (ie truly *cls*) from the number expected by Mendelian inheritance.

To test this, the number of strictly *cls* embryos (i.e. containing absolutely no stellate, wild-type melanophores) was compared to the numbers showing wild-type melanophores and numbers of putative rescued *cls* embryos in a batch of injected embryos at 48hpf. The proportions obtained for each PAC injection are shown graphically in Figure 3.8 as a pie chart, and compared to an uninjected batch. Whilst the latter shows, as expected, a 3:1 WT:*cls* ratio, injection of all PACs result in significant divergence from this expected Mendelian ratio (Chi-squared test results are shown in Figure 3.8), and all cause a decrease in the number of embryos with a full *cls* phenotype from the expected.. This demonstrates that the embryos showing intermediate numbers of melanophores almost certainly represent *cls* embryos partially rescued by injection of *sox10* PAC DNA.

To assess if all PACs were able to rescue to the same degree, the average number of melanophores per rescued *cls* embryo was counted. As shown in Figure 3.9, no apparent statistically significant difference between the four PACs was seen (one-way ANOVA; Figure 3.9b), and averages ranged from approximately 18 to 26 melanophores. This compares with figures reported for a heat-shock>*sox10* construct injected at similar amounts (50pg), which gave an average of 15 rescued melanophores per embryo (Dutton *et al.*, 2001). The heat-shock construct is approximately 6 to16 times smaller than the PACs, indicating that there were far fewer copies of PAC injected per embryo, yet similar rescue numbers were seen. This probably reflects the greater efficiency of the endogenous *sox10* promoter over the heat-shock promoter.

As with melanophores, all four PACs are able to rescue the other chromatophores affected in *cls*. Xanthophores are severely disrupted in strong *cls* embryos. Almost all *cls* embryos have no visible xanthophores at 5dpf (Kelsh *et al.*, 1996), however occasionally one or two xanthophores can be seen, although these appear apoptotic. The PAC injected embryos analysed for melanophore rescue at 2 days were later assessed for xanthophore rescue at 3 and 5dpf. Xanthophores can be readily visualised under transmitted light as they stain blue when the embryo is incubated in dilute Methylene Blue solution (as found

Figure 3.8; Figure 3.9 →

Figure 3.8: Comparison of the melanophore rescue abilities of each PAC

Embryos from incrosses of *cls* heterozygous fish were injected with each PAC and scored at 48hpf as either having a wild-type number of melanophores, no melanophores or an intermediate number of melanophores (putative rescued embryos). These counts are displayed graphically in the left column, represented as black, white or grey segments respectively. It is evident that the injected batches have a smaller proportion of embryos with no melanophores, and that these appear to now display an intermediate number of melanophores. The sum of embryos with no or an intermediate number of melanophores fully accounts for the expected number of *cls* embryos, arguing against an effect of injection on wild-type embryos.

The numbers of embryos in each treatment with any melanophores (i.e. wild-type + rescued embryos) were then compared to the number with no melanophores (i.e. embryos with a full *cls* phenotype). These are presented in column two with the numbers expected by Mendelian inheritance given below in brackets. The uninjected controls show a 3:1 wild-type: *cls* proportion as expected from Mendelian ratios and consistent with the recessive mode of inheritance known for the *cls* alleles used, whilst there is a deviation from this in the injected embryos. To more formally demonstrate significant rescue by PAC clone injection, a χ^2 value was calculated for each (column 3) and a probability (based on one degree of freedom) is indicated in the final column to test the null hypothesis: That divergence of the observed ratio from the expected is due to chance alone.

For the uninjected control batch, this probability is greater that 0.05, and thus there is no reason to reject the null hypothesis. Thus uninjected batches behave in a Mendelian fashion with variations due to chance.

As the probability that this is true is very small for all injection experiments ($p<0.001$), then the null hypothesis is rejected in these cases and implies that injection of the PACs is leading to a change in numbers of embryos showing any melanophores.

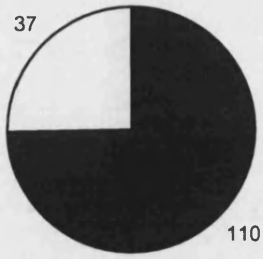

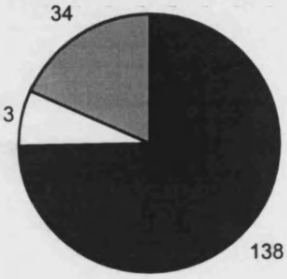

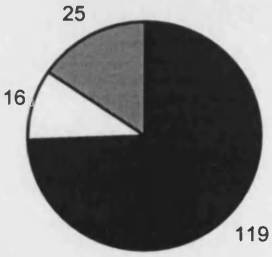

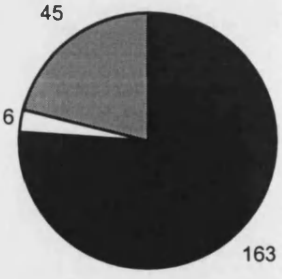

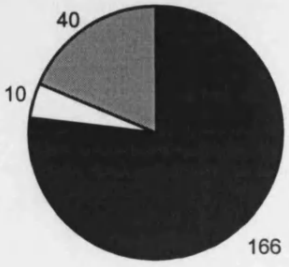

	Embryos with melanophores (expected)	Embryos without (expected)	χ^2 value	Probability
Uninjected	110 (110.25)	37 (36.75)	0.002	P>0.05
PAC G	172 (138.75)	13 (46.25)	31.872	P<0.001
PAC I	144 (120)	16 (40)	19.200	P<0.001
PAC L	208 (160.5)	6 (53.5)	56.231	P<0.001
PAC N	206 (162)	10 (54)	47.802	P<0.001

a.

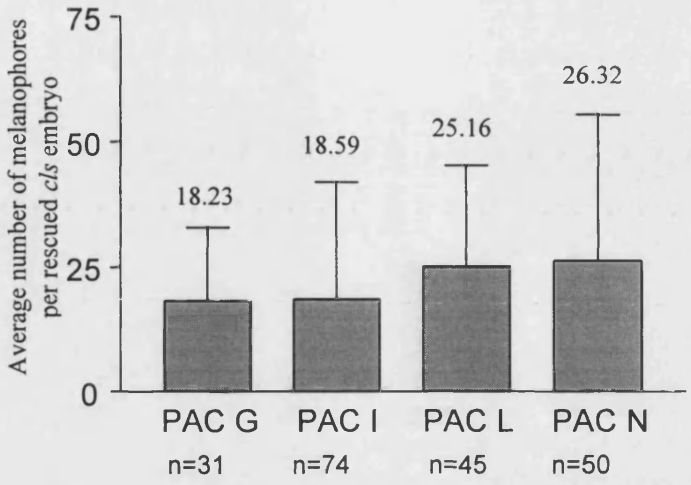

b.

Parameter	Value
Kruskal-Wallis test	
P value	0.0528
P value summary	ns
Do the medians vary signif. (P < 0.05)	No
Number of groups	4
Kruskal-Wallis statistic	7.693

Dunn's Multiple Comparison Test	Difference in rank sum	P value	Summary
PAC G vs PAC I	15.23	P > 0.05	ns
PAC G vs PAC L	-15.85	P > 0.05	ns
PAC G vs PAC N	-0.8194	P > 0.05	ns
PAC I vs PAC L	-31.09	P > 0.05	ns
PAC I vs PAC N	-16.05	P > 0.05	ns
PAC L vs PAC N	15.03	P > 0.05	ns

Figure 3.9: Average number of melanophores per rescued *cls* embryo

a. Graph showing the mean number of melanophores found per rescued *cls* embryo after injection with each PAC. Error bars show standard deviation. The large standard deviations indicate the mosaic nature of the rescue. Uninjected *cls* embryos never show any melanophores (not shown).

b. All PACs rescue to a statistically indistinguishable degree. One-way ANOVA analysis (using the Kruskal-Wallis nonparametric test) of melanophore counts of the four PACs showing that there is no difference in degree of rescue between any of them. Probabilities shown test the null hypothesis that each PAC rescues to the same degree (Left-hand table). All pairwise tests between PACs (using Dunn's Multiple Comparison test; right-hand table) indicate that there is no reason to reject this hypothesis.

in Embryo Medium). The presence of healthy stellate xanthophores in a lateral position on the trunk was clearly visible in mosaically rescued *cls* embryos as shown in Figure 3.10. Such trunk xanthophores are never seen in uninjected *cls* embryos. As xanthophores often form a sheet of cells covering the dorsal aspect of the embryo, it is difficult to distinguish individual cells, and counts of cell numbers are often impossible. Instead, quantification of xanthophore rescue by each PAC was made by simple comparison of the number of embryos with less than 5 xanthophores (considered to be unrescued *cls*) to the number showing 5 or more xanthophores (considered to be rescued *cls* or wild-type) within injected or uninjected batches. As with melanophores counts, these comparisons are represented as pie charts in Figure 3.11, and batches injected with all four *sox10* PACs show a significant deviation from the expected number of embryos showing less than 5 xanthophores (i.e. embryos with an unrescued *cls* xanthophore phenotype), demonstrated by χ^2 analysis. Thus the xanthophore phenotype of *cls* can also be rescued by injection of any of the four PACs.

Finally 5dpf injected embryos were viewed under incident light to assess rescue of the third pigment cell type, iridophores. *cls* embryos do not always have a complete lack of this cell type, and occasionally show isolated patches in an eye or the lateral patch, or cells in the dorsal stripe. Thus, in contrast to other chromatophores, rescue of this cell type was not evident on simple inspection as with other chromatophores. Figure 3.12a shows an example of a putative rescued *cls* embryo injected with PAC N and viewed under incident light at 5dpf, showing good iridophore coverage of the eye and the presence in the lateral patch. The identification of injected *cls* individuals with almost complete coverage of iridophores in one eye strongly suggested rescue of this cell type, as this is never seen in uninjected *cls* embryos. To more formally demonstrate the ability of the PACs to rescue the iridophore fate, it was necessary to perform quantitative analysis. The number of iridophores seen in the dorsal and ventral stripes, and the number of patches of iridophores seen in the eyes and lateral patches were counted. Iridophores were never seen in the yolk sac stripe in uninjected or injected *cls* embryos. The iridophore counts obtained from each injection (Figure 3.12b) show that all four PACs show rescue, to a statistically significant degree (one-way ANOVA; Figure 3.12c), given the null hypothesis that uninjected and PAC injected *cls* embryos have the same average numbers of iridophore cell and patches, with variation due to chance. Similar tests comparing each PAC injected batch indicated that no statistically significant difference of rescue between the four PACs was evident (Figure 3.12c).

Viewing injected embryos at 5dpf also allowed assessment of the viability of the other rescued pigment cells to this stage. Note from the bottom panel in Figure 3.12a that the

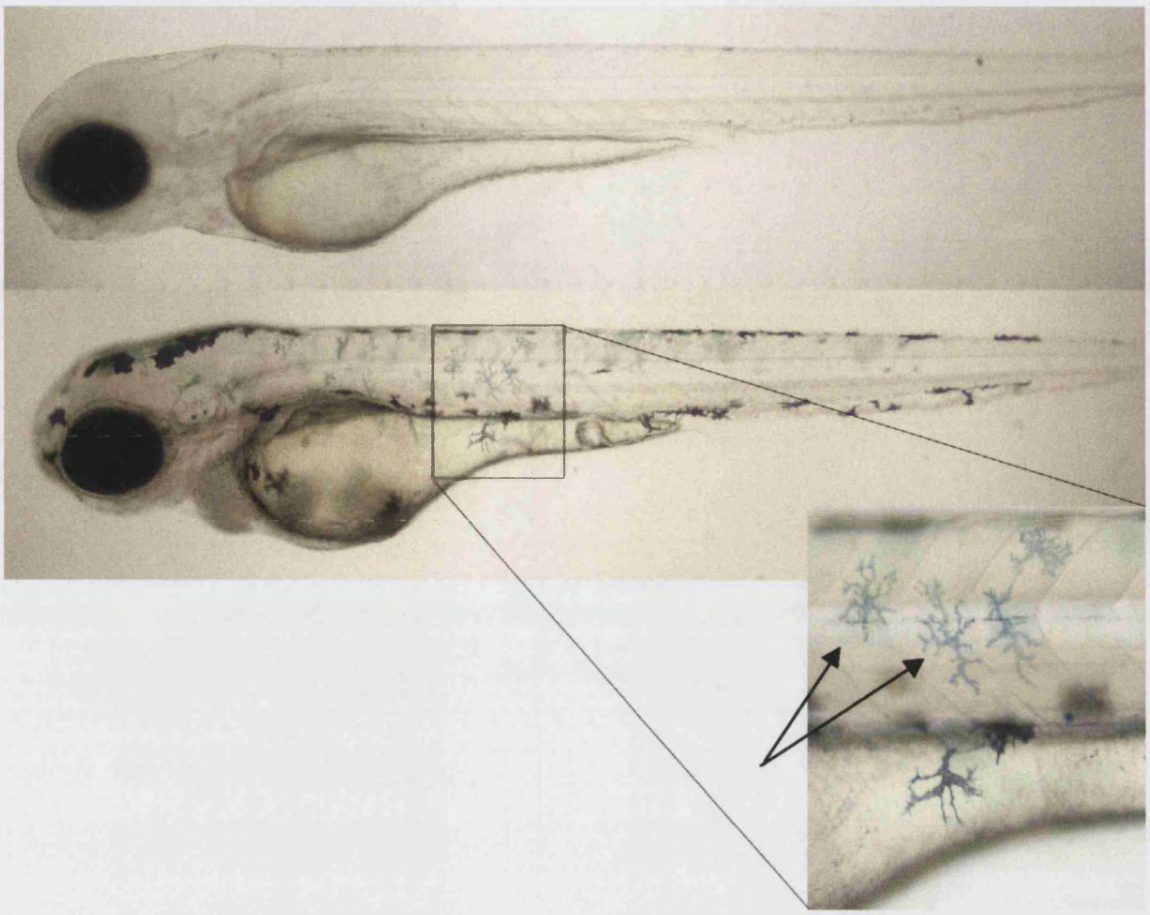

Figure 3.10 Rescue of xanthophores in *cls* by PAC injection

Top panel shows a lateral view of an approximately 72hpf *cls* embryo stained with Methylene Blue, showing a complete absence of xanthophores. A *cls* sibling injected with PAC N, similarly stained, is shown in the lower panel. Rescue of xanthophores in a mosaic manner can be seen as blue-green stellate stained cells, present on the lateral migration pathway (arrows in the higher magnification shown inset).

Figure 3.11: Comparison of the xanthophore rescue abilities of each PAC

As *cls* does not always display a complete loss of xanthophores, again a statistical approach was used to demonstrate rescue of this cell type. After counts of melanophore rescue, embryos were assessed for xanthophore rescue. Embryos from incrosses of *cls* heterozygous fish were injected with each PAC and scored at 72hpf as either having more than 5 xanthophores, or less than 5 xanthophores. The latter class were designated as *cls* whilst the others consisted of both wild-type and putative rescued *cls* embryos. These counts are displayed graphically in the left column, represented as white or black segments respectively. For simplicity, embryos with more than 5 xanthophores (i.e. wild-type and putative rescued *cls* embryos) are presented as one group.

As with melanophores, these number are presented in the table with the numbers expected from Mendelian inheritence. It is evident that whilst the uninjected controls show a 3:1 wild-type:*cls* proportion as expected from mendelian ratios and consistent with the recessive mode of inheritance known for the *cls* alleles, the injected batches of embryos have a smaller proportion of embryos showing the defined *cls* xanthophore phenotype.

χ^2 analysis was used to demonstrate that this deviation upon injection was significant for all PACs. χ^2 values are given (column 3) and probabilities (based on one degree of freedom) is indicated in the final column to test the null hypothesis: That divergance of the observed ratio from the expected is due to chance alone.

As the probability that this is true is very small for all injection experiments ($p<0.001$), then the null hypothesis is rejected in these cases and implies that injection of the PACs is leading to a decrease in numbers of embryos with a *cls* xanthophore phenotype.

For the uninjected control batch, this probability is greater that 0.05, and thus have no reason to reject the null hypothesis. Thus uninjected batches behave in a Mendelian fashion with variations due to chance.

		Embryos with >5 xanthophores (expected)	Embryos with <5 xanthophores (expected)	χ^2 value	Probability
Uninjected	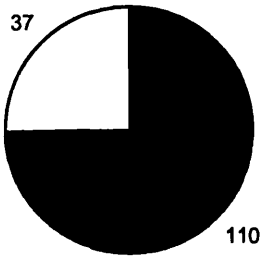	110 (110.25)	37 (36.75)	0.0023	P>0.05
PAC G	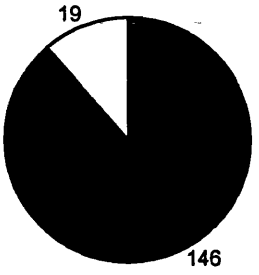	146 (123.75)	19 (41.25)	16.002	P<0.001
PAC I	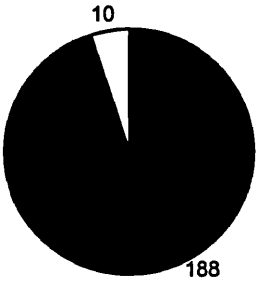	188 (148.5)	10 (49.5)	42.027	P<0.001
PAC L	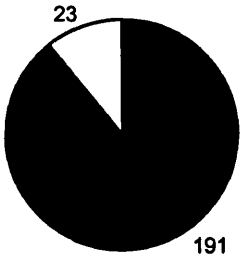	191 (160.5)	23 (53.5)	23.184	P<0.001
PAC N	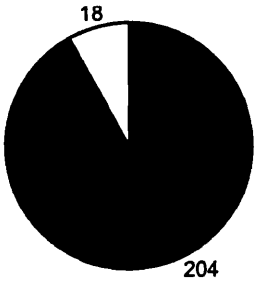	204 (166.5)	18 (55.5)	33.784	P<0.001

Figure 3.12: Rescue of Iridophores in *cls* by PAC clone injection

a. Lateral views of 5dpf embryos photographed under incident light to examine iridophores. Upper panel shows a wild-type embryo with extensive iridophore coverage over the eye and in the lateral patch (arrows). The panel below shows a *cls* embryo with deficit of iridophores on the eye and in the lateral patch apparent, but escaper iridophores are apparent on the dorsal stripe (arrowhead).

The bottom two panels show a putative *cls* embryo rescued with PAC N. The upper of these panels is photographed under incident light and shows a good coverage of iridophores over the eye, and also visible in the lateral patch (arrows). Iridophores were also noted in the dorsal and ventral stripes in this embryos but are not shown here. Bottom panel shows the same embryo photographed with transmitted light. Note that there are melanophores present in all four stripes, namely the yolk sac stripe, the ventral stripe, the medial stripe and the dorsal stripe. This indicates the ability of the rescued melanophores to survive and migrate to appropriate locations

b. Graph displaying average number of iridophores and iridophore patches for both injected and uninjected *cls* embryos. Error bars indicate standard deviations.

c. One-way ANOVA demonstrates that *cls* embryos injected with all four PACs have a significantly greater number of iridophores and iridophore patches than uninjected *cls* embryos. Left-hand table shows the results from one-way ANOVA showing there is a significant difference between mean iridophore scores of the groups. Results and probabilities from pairwise post-test (Tukey's Multiple Comparison test) is shown in the right-hand table, and shows that each PAC injection displays significantly different means to the uninjected *cls* ($p<0.01$). Meanwhile, there is no significant difference in means between each PAC injection ($p>0.05$).

a.

b.

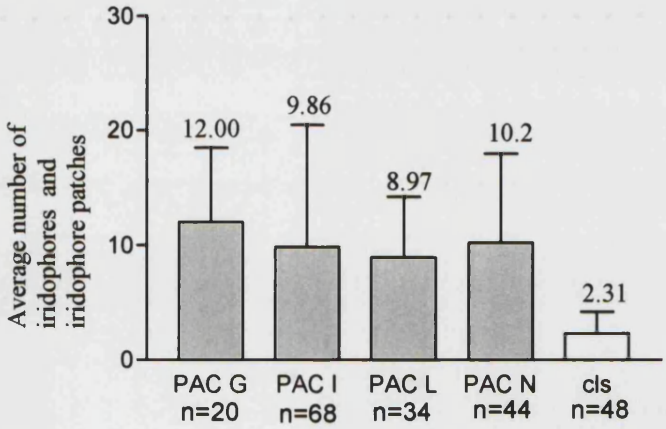

c.

One-way analysis of variance	
P value	P<0.0001
P value summary	***
Are means signif. different? (P < 0.05)	Yes
Number of groups	5
F	9.774
R squared	0.1509

Tukey's Multiple Comparison Test	Mean Diff.	q	P value
PAC G vs *cls*	9.688	6.625	P < 0.001
PAC I vs *cls*	7.548	7.507	P < 0.001
PAC L vs *cls*	6.658	5.406	P < 0.01
PAC N vs *cls*	7.892	6.882	P < 0.001
PAC G vs PAC I	2.139	1.555	P > 0.05
PAC L vs PAC G	-3.029	1.956	P > 0.05
PAC N vs PAC G	-1.795	1.212	P > 0.05
PAC L vs PAC I	-0.8902	0.7899	P > 0.05
PAC N vs PAC I	0.3438	0.3326	P > 0.05
PAC N vs PAC L	1.234	0.9835	P > 0.05

other chromatophores have survived, and have migrated to appropriate positions in the embryo. For example, melanophores can be seen in all stripes at this stage, and xanthophores are still present in the dorsal portion of the embryo. Thus PAC injection not only allows chromatophores to form in *cls* mutants, but once formed, these cells behave as wild-type cells, namely are viable, healthy and can migrate to appropriate locations.

It is clear that all four PACs are able to rescue all pigment cell types disrupted in *colourless*. This implies they all contain the promoter and enhancer elements required for *sox10* expression in the chromatophore lineages. To assess if they can also rescue the other neural crest derivatives disrupted in *cls*, such as PNS neurons, an immunofluorescent antibody stain against the Hu epitope was performed on 5dpf rescued *cls* embryos to detect neurons.

3.2.4.2. PNS rescue

Due to time constraints, only the smallest PAC (PAC N) and one larger PAC (PAC I – chosen as it was sequenced) were assayed for ability to rescue PNS neurons. As all PACs rescued chromatophores equally, it seemed likely that at least all the 3 larger PACs would rescue PNS neurons equally well, and probably all four PACs. Wild-type embryos have an iterated series of DRG neurons present in ganglia along the trunk and revealed by immunofluorescent labelling with an antibody against the pan-neuronal antigen, Hu (Figure 3.13a). In *cls* embryos this series is clearly disrupted, with DRGs almost completely absent in the posterior trunk and tail (Figure 3.13a). In the anterior trunk, DRG neuron number is reduced, and those that do form (arrows) are more disorganised. The lower panel shows a *cls* embryo injected with PAC N and immunostained with an antibody against Hu. Rescued melanophores can be seen in the dorsal head in this image. An intermediate number DRGs can also be seen, however it is not clear if this represents rescue or simply a *cls* individual displaying a less severe DRG phenotype. Other injected individuals did appear to show rescue as they formed an iterated series of DRGs in the tail with a wild-type organisation (Figure 3.13a bottom panel). To formally test if there was PAC mediated rescue of DRGs in *cls*, counts were made of DRG neurons in injected *cls* embryos and uninjected embryos, and results are displayed graphically in Figure 3.13d for both PACs. Only *cls* embryos showing pigment cell rescue were included in the DRG counts of injected embryos. This was done to eliminate any embryos that had been injected but not successfully rescued, and to maximise the chance of seeing a statistically significant effect of PAC injection on DRG neurons. A two-way students t-test was performed on data for both PACs to investigate whether there were significant difference in DRG neurons number in injected *cls* embryos compared to uninjected *cls* embryos.

Figure 3.13 ⟶

Figure 3.13 Rescue of PNS neurons in *cls* by PAC clone injection

All figures are lateral views of 5dpf *cls* embryos, uninjected or injected with PAC N and subsequently immunofluorescently stained with an antibody against the pan-neuronal marker Hu.

a. DRGs are apparent as reiterated series of labelled cells situated along the wild-type embryo (top panel; some indicated with arrows). Enteric neurons along the gut are evident as well and indicated with an arrowhead.
Second panel shows an $cls^{m618/m618}$ embryo at the same stage, showing an absence of enteric neurons (arrowhead) and a severe, but incomplete, loss of DRG neurons (some surviving neurons indicated with arrows). Note that these latter neurons are often abnormally positioned dorsoventrally.
Third panel shows a sibling *cls* embryo injected with PAC N. There appears to be a greater number of trunk and tail neurons (arrows) compared to the uninjected *cls* sibling. Bottom panel is a close-up view of the most posterior tail DRGs of a *cls* embryo rescued with PAC N. Such a regular series at the correct dorsal-ventral position is not normally seen at this axial level in uninjected *cls* embryos.

b. Close up images of enteric neurons. The top panel is a close up view of the gut of an uninjected *cls* embryo showing no enteric neurons along the gut. The lower two panels show sibling *cls* embryos injected with PAC N. Enteric neurons can be clearly seen populating the anterior half of the hindgut in the upper example, whilst the bottom panel shows an example of a rescued *cls* embryo with enteric neurons along the entire hindgut.

c. Putatively rescued neurons of the sympathetic ganglia (arrowhead) in a *cls* embryo injected with PAC N. These neurons are normally completely absent in uninjected *cls* embryos (not shown).

d. Graph displaying the average number of DRG neurons in WT embryos, uninjected *cls* embryos and PAC injected *cls* siblings. Values are given above each bar and error bars show standard deviations. * = significant p=0.03, *** = extremely significant, p=0.001, for comparison of each PAC injections versus *cls*.

e. Results from two-tailed unpaired t-test with Welch's correction for each pair of analyses. Probabilities (p) test the null hypothesis that differences between two the means are due to chance alone (* = significant, p=0.03; *** = extremely significant, p=0.001, ns = not significant)

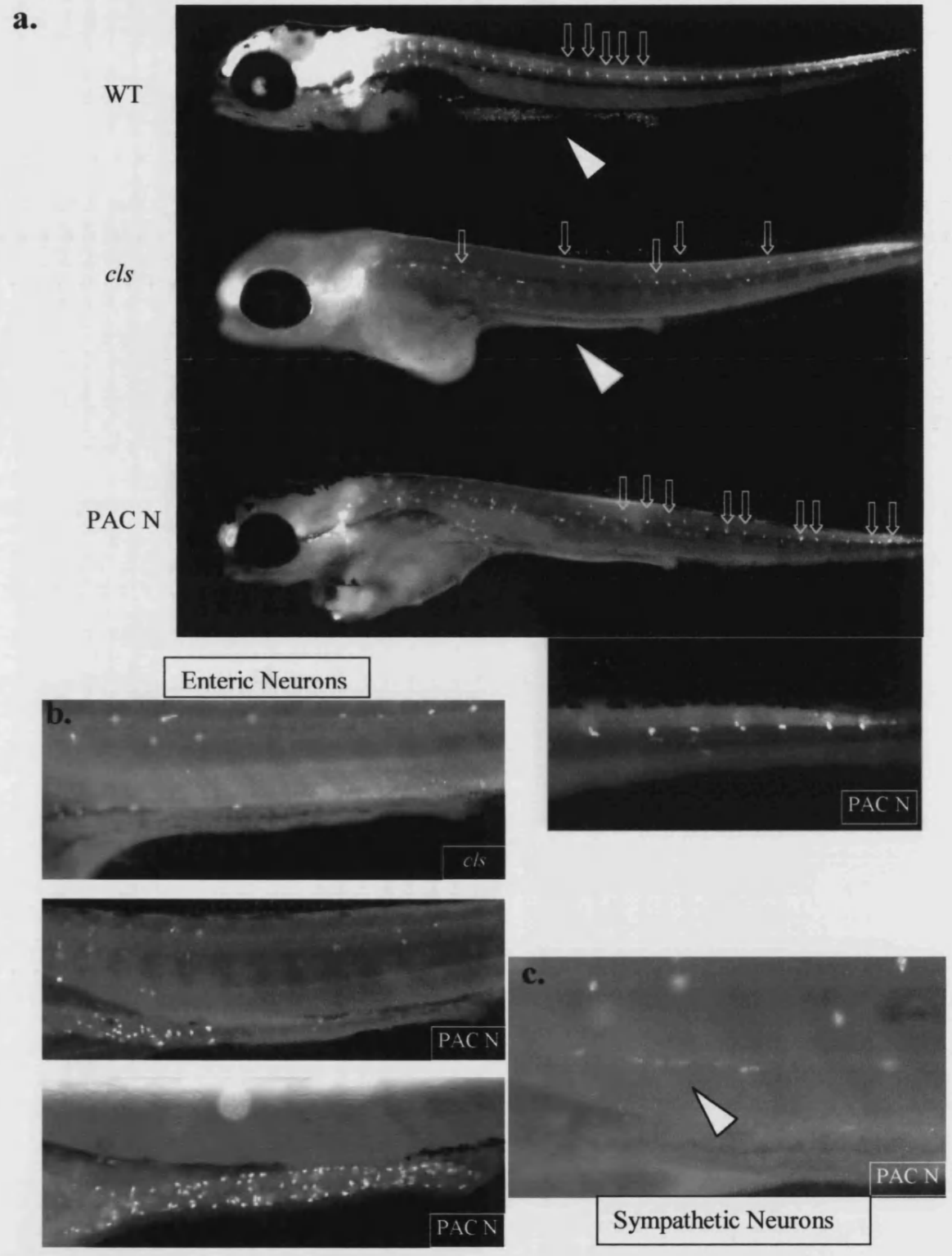

d.

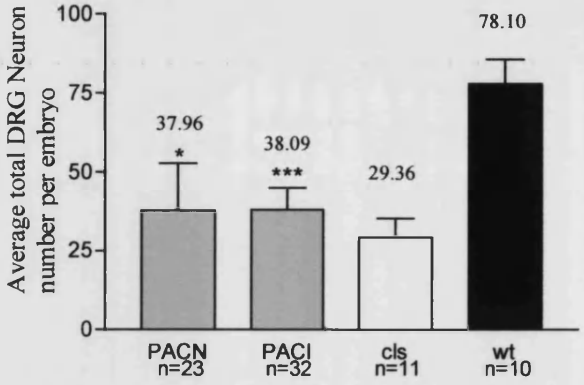

e.

Two- tailed Unpaired t test with Welch's correction	PAC N and PAC I	PAC N and *cls*	PAC I and *cls*
P value	0.9675	0.0233	0.0008
P value summary	ns	*	***
Are means signif. different? (P < 0.05)	No	Yes	Yes
Welch-corrected t, df	t=0.04105 df=28	t=2.387 df=31	t=3.995 df=19

Initially a normality test was performed, and showed that all data sets were normally distributed about a mean (not shown). This validated use of the t-test to analyse this data. As the two different data sets have been treated differently (i.e. one set has been injected), it can be expected that the deviation of the two are different. Indeed Bartlett's test for equal variance showed that both injected samples are likely to have significantly different deviations compared to uninjected *cls* controls. This then required modification of the t-test with Welch's correction. A null hypothesis for each PAC injection was proposed, namely that there was no significant difference between the number of DRG neurons in injected *cls* embryos and uninjected *cls* embryos. t-values were derived for both comparisons and are given in Figure 3.13e. It can be seen for PAC N that the t-value is greater than the critical value of 2.278 at the p=0.03 level (31df), whilst PAC I has a t-value greater than the critical value of 3.883 at the p=0.001 level (19df). Thus both null hypotheses were rejected and it could be deduced that both PACs are able to rescue the DRG neuron number. Although the probability level is different for the two comparisons, this does not mean the PACs rescue to different extents. In fact their means do not differ significantly ($p>0.05$; Figure 3.13e), and the better degree of significance seen for PAC I rescue might simply reflect stochastic differences in injection success. Alternately the slight difference in sample size between the two PAC injection experiments might alter the degree of significance seen.

Rescue of other PNS neuron types was also noted in some of the injected *cls* embryos. Figure 3.13b shows the hindgut of *cls* embryos injected with PAC N and stained for Hu (two lower panels), compared to an uninjected *cls* sibling in the top panel. $cls^{-/-}$ embryos are always almost totally devoid of enteric neurons, although an occasional Hu^{+} cell can be seen in this location. The two injected embryos presented here show clear evidence of enteric neuron rescue (arrowhead), with one individual showing good coverage along 50% of the hindgut (middle panel) and another with apparently full coverage along the hindgut (lower panel). In fact 5 out of the 23 *cls* embryos rescued with PAC N in this batch showed more than 10 enteric neurons. This reflects the success of this particular injection experiment. In all cases, rescue of enteric neurons in a posterior position along the gut was only seen if those anterior were also rescued.

Meanwhile, some individuals also appeared to have neurons in a position consistent with sympathetic ganglia (e.g. Figure 3.13c), which is never seen in *cls* embryos. Although rescue of sympathetic and enteric neurons was not noted with PAC I, this might be due to a better injection concentration or other variable of PAC N, rather than difference in DNA sequence content (see Discussion).

3.3. DISCUSSION

Four overlapping PAC genomic clones corresponding to the zebrafish *sox10* locus have been isolated by a PCR based library screen. Based on coarse restriction mapping and size estimation, the combined size of the region covered by the PACs is approximately 116kb, and it is of note that all PACs are smaller than the average insert size of the library.

A PCR of the 3'UTR of *sox10* was chosen for use in the library screen for several reasons. Firstly, it was known not to span an intron (A. Pauliny, pers.comm.). Secondly, a PCR within this region was most likely to discriminate *sox10* from other closely related Sox genes, as the target sequence was non-coding and therefore probably more divergent than coding regions of Sox family genes. This is a particularly important consideration in zebrafish as there are a number of examples of duplicated genes in zebrafish compared to mammals. This has been attributed to a genome duplication event early in the teleost lineage (Postlethwait *et al.*, 1998). For example, there appear to be two *sox11* orthologues of tetrapod *Sox11* in zebrafish, both with similar function (De Martino *et al.*, 2000). Although the possibility of two *sox10* orthologues in the zebrafish cannot yet be fully discounted, degenerate PCR, recent genome searches and genomic southern analyses have failed to show any evidence of such an occurrence (A. Pauliny, R.N.K., K. Dutton, pers. comm.). Based on evidence of rescue and sequence information, it seems highly likely that these PACs do contain the gene corresponding to both the *cls* locus and the isolated *sox10* cDNA.

A crude map of the region using rare cutting enzymes was developed, and the coding region positioned and orientated within it. The *sox10* gene was found in the central portion of all PACs, meaning it was likely they all contained the full coding sequence and a good deal of flanking sequence. The apparent small (~1 kb) deletion in PAC N is the only inexplicable result from the mapping data. Although it could represent some form of gel artefact causing aberrant band migration, or a polymorphism in the original library DNA sample, it may also be some form of internal deletion caused by instability of that PAC clone, a phenomenon which has been reported for PACs previously, albeit at a low frequency of occurrence (Ioannou *et al.*, 1994). The presence of a 30kb PAC insert is odd considering that the library was constructed by size fractionation of partially digested genomic DNA to give inserts of 100-200kb. This most likely excluded cloning such a small insert and supports the suggestion that it has undergone some form of internal deletion. The deletion occurs in an approximately 9kb fragment, which includes 420bp of sequence coding for the C-terminal of the Sox10 protein. Thus there is a low probability that the deletion might affect the Sox10 coding region. However, as this PAC can rescue as

well as other PACs, it appears that the deletion has in no way compromised the function of the *sox10* gene within this genomic clone, and thus does not appear to affect the coding region. Using the sequence data for this region might allow design of primer pairs to better localise the deletion site by PCR.

Identification of a putative *Fugu sox10* homologue has uncovered conserved regions flanking the *sox10* gene in both species. Initial analysis of these sites show that they are not recognisable coding regions, and thus might represent conserved regulatory region. This requires further analysis; however it cannot be assumed that if they are regulatory regions, that they both control *sox10* gene expression and not some other nearby gene.

It was hypothesised that these PACs contained the gene disrupted in *cls* (*sox10*). To test this, and to establish that the gene was functional, each PAC was injected into *cls* embryos, and assayed initially for melanophore rescue. An intermediate number of healthy melanophores were seen. It was proposed that this could be attributed to either mosaic rescue of *cls* embryos, or some form of cytotoxic effect on the melanophores of wild-type embryos. The latter would predict the presence of unhealthy, pale, dying melanophores in injected embryos, however this was not seen. Nor did the presence of these embryos with intermediate melanophore phenotype correlate with a deviation from the expected number of wild-type embryos; instead a decrease in the number of expected *cls* embryos was noted. This again argued against a cytotoxic effect of injection, rather that the PACs were able to rescue the *cls* melanophore phenotype. At the time, this allowed three conclusions to be drawn. Firstly, as all PACs rescued *cls*, they must all be from the same physical location in the genome. Secondly all PACs must contain a functional copy of the gene disrupted in *cls,* and lastly, as the smallest PAC was 30kb and as all PACs contained the *sox10* gene, it meant that the *sox10* gene mapped to within 30kb of the *cls* locus, which provided further evidence that *cls* does indeed correspond to mutations in *sox10.*

The success of the rescue experiments also implied there were elements present in all four PACs able to direct sufficient expression of *sox10* in the neural crest to rescue the melanophore defect in *cls*. An attempt to identify any enhancers represented in some of the PACs, but absent in others, was made by comparing the ability of the four PACs to rescue pigments cells and PNS neurons. In addition to melanophores, all PACs appear to be able to rescue the xanthophore and iridophore phenotype of *cls,* with no significant difference in success of rescue detectable. As expected, the degree of rescue between injected *cls* embryos varied within a batch, due to mosaicism obtained from DNA injection and possibly other variables such as embryo age, position of injection and precise amount of DNA injected. However no difference in rescue ability could be detected between PACs for any pigment cell type. Thus it appears that all PACs contain the elements required for

rescue of all pigment cells. Although speculation, it might be that expression of *sox10* in all pigment cell-type precursors is regulated by the same element(s).

Furthermore, there was slight but significant rescue of PNS neurons in the DRGs by the two PACs tested. That more striking rescue was not seen might be caused by a smaller contribution of neural crest cells to this derivative than compared to chromatophores, meaning that the probability that neural crest cells normally fated to become DRG neurons will contain injected PAC DNA is much lower. There is supporting evidence for this from the single neural crest cell labelling studies, which showed that DRGs represented a relatively small proportion of premigratory neural crest cell fates. Additionally, the *cls* DRG phenotype is not as severe as the *cls* chromatophore phenotype, which might cause rescue to appear less dramatic. Finally, loss of DRG neurons in the mouse *Sox10* mutants has been proposed to be a secondary effect of loss of support glia in the ganglia (Britsch *et al.*, 2001). If this is also true in zebrafish, then PAC rescue of DRG neurons is not acting cell autonomously, but through rescue of satellite glia. Thus there may be some community effect required for these neurons to survive, possibly including trophic support from sufficient numbers neural crest derived glia. In this mechanism a DRG neuron might only be rescued by the presence of a minimum number of rescued support cells, thus limiting the degree of neuron rescue seen.

Rescue of enteric neurons was also seen with PAC N (5 in 23 embryos). Although this rescue was only rarely seen, when present it was striking, with some examples showing rescue along half or even the full length of the gut length. This might indicate that only a small number of neural crest cells contribute to this cell type, and that they undergo a large number of divisions to produce the neurons along the gut. Thus, when one or more precursors are successfully targeted, extensive rescue occurs. Further, note that posterior enteric neurons were rescued if those anterior to them were also rescued. This is consistent with the notion that neural crest cells migrate in an anterior to posterior direction when populating the gut (I.T. Shepherd pers. comm.). Thus it seems likely that anterior neurons will be rescued first, and if sufficient rescued neural crest cells are present then posterior cells will be rescued. This effect is reminiscent of Sox10 haploinsufficiency in humans and mice, where enteric ganglia are nearly normal rostrally, but are absent caudally in the hindgut. This has been attributed to depletion of the pool of progenitor cells populating the gut. It seems likely that the extent of colonisation of the gut might also be proportional to the numbers of progenitors able to migrate here from the vagal premigratory neural crest position. Thus the extent of gut colonisation by neurons in rescued *cls* embryos probably reflects the number of rescued neural crest cells fated to be enteric progenitors.

Enteric neurons rescue was not seen in any PAC I injected *cls* embryos. However the mosaicism of melanophore rescue was more severe in the injection experiment with this PAC than with PAC N and it is most likely that the neural crest cells giving rise to enteric neurons, by chance, did not inherit any PAC I DNA upon injection in this particular experiment. As PAC N is almost 3 times smaller than PAC I, injection of the same mass of DNA in fact equates to almost 3 times more copies of PAC N than PAC I. This might account for the slightly better melanophore and enteric rescue seen with PAC N. As rescue of these cells was seen with the smallest PAC, it is highly likely that all four PACs would display this ability. Given that enteric rescue by PAC N was a relatively rare event, it might be that the apparent inability of PAC I to rescue could be due to insufficient experimental attempts. I predict that PAC I (and the other 2 larger PACs) would be able to rescue enteric neurons given sufficient injection experiments and good mosaic coverage of the PAC DNA upon injection. This might require increasing the amount of injected PAC I DNA so that the copy number introduced, although too much DNA might cause non-specific defects. As enteric neurons are derived from the vagal neural crest, it might be possible to predict likelihood of enteric rescue with the presence of melanophore rescue in this region.

Another explanation for the lack of enteric rescue with PAC I is that it might in fact contain an additional repressor element, missing in PAC N. This seem unlikely as it would require the existence of a further 'de-repression' element beyond the limits contained in PAC I. Without more definitive evidence that PAC I is incapable of enteric rescue, this explanation remains the less favourable.

Whether these PACs contain all the *cis*-elements controlling *sox10* expression could not be easily determined by rescue experiments, which would not be expected to reveal repressor elements for other cell types or elements responsible for fine tuning levels of expression. There is, as yet, no evidence that these PACs do not all contain the full complement of regulatory elements controlling the expression of the *sox10* gene, although this is based purely on the rescue of pigment cells and PNS neurons. Thus it is likely that most, if not all, of the important regulatory elements are contained within the region cloned in the PACs. However this is based on the ability of the PACs to rescue a limited number of cell types known to be disrupted in *cls*. Nor do rescue experiments indicate if the expression is at the wild-type levels, or if they are at lower levels, which happen to be sufficient for rescue. Rescue experiments additionally might not indicate ectopic sites of expression. If required, isolation of genomic clones containing more sequence flanking *sox10* could be achieved by either attempting to re-screen the three secondary pools that failed to give an informative PCR pattern, or alternatively screening other genomic

libraries with bigger average insert sizes, such as YAC and new generation zebrafish BAC libraries.

sox10 appears to be expressed only briefly in pigment precursors on the lateral pathway, and appears to be downregulated rapidly at around the onset of pigmentation. This indicates that the function of *sox10* in the pigment cell lineages is an early one, a notion supported by the lack of *mitfa* expression at 20hpf in *cls*, and the subsequent apoptosis of many neural crest cells in *cls* (Dutton *et al.*, 2001). Thus for the PACs to rescue pigment cells, they must be able to drive *sox10* expression in early neural crest. That we do see chromatophores rescue means that there are the necessary promoter regions for early neural crest expression present on these PACs. In addition, *sox10* expression is seen in neural crest cells migrating along the gut at around 30hpf, although its precise role here is not known, but assuming its role here is indispensable, then the enteric neuron rescue demonstrated that the PACs contain elements required for this later expression.

Furthermore, expression of *sox10* is seen in cells for which there is as yet no known phenotype, such as cartilage cells and oligodendrocytes (Pauliny, 2002). Knowledge of a detectable defect in these cell types is required before a rescue experiment could be used to assess if the PACs direct *sox10* expression here. Other cell types and structures beyond those tested here are known to be disrupted in *cls* mutants, namely the ear and glial cells of the peripheral nervous system. At the time, detailed understanding of the ear phenotype was not available, making assessment of rescue criteria difficult. Similarly, a lack of suitable markers for PNS glia made it difficult to evaluate the ability of the PACs to rescue this cell type. Thus the presence of other enhancers controlling other expression sites cannot be predicted based on these limited rescue experiments. However, subsequent experiments demonstrate that all PACs contain sequence necessary to direct *sox10* expression in these sites, as shown in the next chapter.

CHAPTER 4

PRODUCTION AND ANALYSIS OF *SOX10* REPORTER CONSTRUCTS

4.1. INTRODUCTION

4.1.1. Zebrafish reporter constructs, GFP and transgenesis

Characterisation of the regulatory regions of a gene requires investigation both *in vitro* and *in vivo* by use of a reporter gene to provide a read-out of a particular promoter's ability to drive expression in the embryo, tissue or cell type in question. The optical clarity of the zebrafish embryo, the ease with which it can be injected and the large clutch size make it amenable to such studies. A number of reporter genes have been successfully used in zebrafish and include chloramphenicol transferase (CAT; Stuart *et al.*, 1990), lacZ (Lin *et al.*, 1994), luciferase (Collas and Alestrom, 1998) and Green Fluorescent Protein (GFP; Amsterdam *et al.*, 1996). Early work relied on exogenous promoters such as the SV40 early promoter, the CMV promoter and the *ef1α* promoter from *Xenopus laevis*. Zebrafish gene cloning efforts have afforded endogenous promoters, which, not surprisingly, also drive reporter gene expression in zebrafish. Production of multiple germline transgenic lines has helped delineate critical elements in a number of zebrafish promoters (with some summarised in Table 4.1). The use of GFP has become the standard reporter gene in zebrafish. This is largely due to its ability to be visualised in live organisms without the need for fixation, staining or addition of accessory molecules, allowing a number of experiments in addition to the promoter dissection analysis offered by other reporters. GFP variants such as RFP are also starting to be used (Blader *et al.*, 2003).

One recent example of multiple GFP germline transgenic lines being used to investigate the regulatory elements of a gene focussed on dissection of the *deltaD* promoter. Production and analysis of fourteen different transgenic lines, each carrying a different amount of flanking promoter sequence, identified a number of regulatory regions directing expression in mesodermal and ectodermal domains and spanning 12.5kb both 5' and 3' to the start of transcription.

Live cell labelling by reporter genes provide a unique ability to analyse the behaviour of a cell population over time and to correlate expression patterns with cell fate (Amacher, 1999). One example of such *in vivo* analysis used a transgenic line carrying the *foxd3* promoter driving GFP, which expresses strongly in certain neural crest derivatives, namely migrating pigment cells and PNS glia. Timelapse analysis of the latter's migration along the posterior lateral line axon, coupled with laser ablation and genetic mutant studies demonstrated that these neural crest derived glia follow cues provided by the axons, rather

than leading axon pathfinding, and additionally appear to have a role in nerve fasciculation (Gilmour *et al.*, 2002b).

Screening for perturbations of reporter expression pattern through mutagenesis may also uncover loci involved in controlling a promoter's activity, or mutants of a cell type labelled by the transgene. For example, a mutagenesis screen conducted using a zebrafish endoderm specific GFP line has recently identified a number of mutations affecting specific endoderm-derived organs (H. Verkade pers. comm.). Additionally, fluorescence-activated cell sorting (FACS) can be used to isolate pure cell populations, allowing rapid production of a homogeneous cell population for transplantation or generation of expression profiles/comparisons by cDNA library analysis (Dickmeis *et al.*, 2001; Long *et al.*, 1997).

Most of these techniques described above require the use of a large number of animals, each expressing the reporter gene widely. Although microinjection of DNA constructs into large numbers of zebrafish embryos is relatively straightforward, such transient analysis is limited due to concomitant mosaicism. This means that there is a variable dose of transgene in different regions of the embryo and not all cells in an embryo will necessarily inherit a copy. Even after numerous repeated injections, a cell type arising from a small progenitor population might never be seen, and the end result is that it might not be possible to assess the full extent of expression. Additionally, some cells may inherit a dose of DNA which far exceeds the normal copy number. It is conceivable that such a dose might afford erroneous expression due to titration of transcription factors or repressor proteins required for proper gene expression and cell differentiation. Thus it is generally desirable for experimental purposes to produce transgenic animals in which the construct has integrated into the genome in moderate copy number and is thus passed through the germline to offspring in Mendelian fashion. Such inheritance produces a large number of embryos in which all cells carry equal amounts of the transgene, hence describing the complete expression pattern of the reporter consruct, and labelling the full complement of target cells. This approach has the added advantage of simply and quickly producing large amounts of labelled cells without having to perform repeated injections each time.

Nevertheless, transient transgenesis is a simple and rapid method for generating expression information for a number of different constructs. Such GFP reporter analysis has been used successfully to quickly assay for critical promoter and enhancer elements in a number of zebrafish genes including *six7* (Drivenes *et al.*, 2000), *islet-1* (Higashijima *et al.*, 2000), *insulin* (Huang *et al.*, 2001), *HuC* (Park *et al.*, 2000), *pax2.1* (Picker *et al.*, 2002) and *gata*-2 (Meng *et al.*, 1997). Germline and transient reporter analyses are often used in combination to dissect a promoter and describe a transgene's full expression

pattern. Recently, Koster and Fraser (2001) used a Gal4-UAS system to amplify GFP levels from a tissue specific promoter in transient transgenics. A marked improvement in mosaicism was noted in these embryos, with enhanced levels of expression seen throughout the embryo. Such an approach might facilitate rapid promoter dissections and mis-expression studies where germline transmission may be impossible due to dominant lethality associated with the expressed protein.

Generation of germline transgenic zebrafish has so far been achieved using simple microinjection of linear DNA into 1-cell stage embryos. However this technique shows variable efficiency, with rates often below 5% (see Table 4.1). One of the reasons for this poor efficiency might be due to large-scale concatemerisation of linear DNA when injected into early embryos (Stuart *et al.*, 1988). This could conceivably cause the injected DNA to become too large for efficient genome integration, or produce complex tandem arrays at integration sites. Such sites are often unstable, and recombination can lead to variation in expression levels (Cretekos and Grunwald, 1999). Another explanation for the poor germline transmission rate is the inability of the injected DNA to enter the nucleus. Complexing nuclear localisation signal peptides to the DNA reporters have been reported to improve germline transmission rates, although with variable success (Collas and Alestrom, 1998; but see also; Higashijima *et al.*, 1997; Long *et al.*, 1997). Due to its simplicity, simple microinjection of linearised reporter DNA remains the method of choice for generating transgenic lines. Given the poor efficiency and associated complications with this method, production of multiple transgenic lines currently remains a laborious and slow task. Numerous groups are attempting to develop more reliable methods.

One method tried is the use of retroviral infection which, when optimised, showed enhanced transmission rates, and less variable expression, however the packaging, passaging and titering proved a lengthy and time-consuming process, (Chen *et al.*, 2002; Linney *et al.*, 1999; Udvadia and Linney, 2003). Addition of adenoviral-derived flanking inverted terminal repeats to DNA constructs has been successfully used to improve uniformity of expression in transient assays and between transgenic lines, but did not improve germline transmission rate (Hsiao *et al.*, 2001). At present, the most active areas of development in zebrafish transgenesis include transposons, sperm-mediated transgenesis and co-injection with meganucleases. Firstly, a reconstructed transposon (*Sleeping Beauty*) and an active medaka transposon (*Tol2*) have both been used successfully to integrate reporter constructs into host cell DNA. Reported experiments demonstrating this are limited to *in vitro* integration into cultured cells for the former transposon (Ivics *et al.*, 1997), and transposition of both an endogenous medaka *Tol2* transposon into zebrafish (Kawakami *et al.*, 2000) and an engineered *Tol2* transposon carrying a *β-actin* GFP

reporter into medaka (Koga *et al.*, 2002). Application of this technique to reporter transgenesis in zebrafish is yet to be reported, and as such its value to the field remains unknown.

A second approach developed for efficient germline transgenesis is an adaptation of one used for Xenopus transgenesis. This involves incubation of decondensed sperm nuclei with linear DNA prior to *in vitro* fertilisation of eggs, and has been used to generate embryos expressing GFP under both exogenous (Xenopus *efl α*) and endogenous (*HuC*) promoters. These embryos showed exceptionally good coverage of expression, which might in future obviate the need for screening potential founders and establishment of transgenic lines (Jesuthasan and Subburaju, 2002). In fact all surviving fish raised to adulthood did indeed transmit the transgene to offspring indicating this method might also prove to be an efficient way of generating transgenic lines, although it might require a higher level of technical expertise than for simple microinjection.

Finally, a promising technique recently developed promotes highly efficient transgenesis using restriction enzyme mediated integration (REMI). Flanking a reporter construct with recognition sites for the meganuclease *I-SceI* and then co-injecting this into one-cell stage medaka embryos with the *I-SceI* enzyme gave much improved expression levels and rates using *actin* reporter constructs, with subsequent germline transgenesis rates of up to 50% (Thermes *et al.*, 2002). Although not yet published, others have reported similar success in zebrafish with this method.

There are currently very few GFP lines which have reported expression in the neural crest. As mentioned earlier, the *FoxD3*:GFP transgenic line shows expression in neural crest fates including pigment-cell precursors and PNS glia, however the extent of expression in premigratory neural crest cells is not reported, although its message is detectable here (Gilmour *et al.*, 2002b). Secondly, the *fli1*:EGFP transgenic line shows expression in ectomesenchymal cranial neural crest derivatives from 2dpf, including the branchial arches, and later in the jaw and pectoral fin cartilage, however no expression was reported earlier in neural crest development, nor in any other neural crest derivatives. Thirdly, both mouse and zebrafish *Cx43alpha* 1 promoters drive reporter expression in zebrafish neural crest, however this was only demonstrated in transient assays (Chatterjee *et al.*, 2001). Finally, the *Lef1/β-Catenin* dependent GFP reporter line shows a complex expression pattern throughout the embryo, due to it possessing a Wnt signalling responsive promoter. Amongst a number of other domains, expression is seen in medially (but not laterally) migrating neural crest cells, but does not appear earlier in premigratory neural crest (Dorsky *et al.*, 1998).

Thus a transgenic line showing expression in premigratory neural crest is not yet described and would prove a valuable tool to the field of neural crest research. The known expression domains of *sox10* (Section 4.1.3) make its promoter an excellent candidate for driving GFP expression in this cell type and derivatives.

Table 4.1: Summary of zebrafish germline transgenic reporter lines

Promoter	Reporter	Expression domains	Rate of transmission	Notes and References
SV40 early	Hygromycin	Not expressed	5% (by Southern)	First demonstration of germline transgenesis in zebrafish; (Stuart *et al.*, 1988)
RSV-LTR	CAT	Positive (CAT assays)	~5%	*In vivo* expression demonstrated; (Stuart *et al.*, 1990)
ef1α (Xenopus)	GFP	Ubiquitous	5-9%	First use of GFP in zebrafish; (Amsterdam *et al.*, 1995)
GATA-1 (zebrafish)	GFP	Erythroid lineage	~1%	First use of an endogenous zebrafish promoter; (Long *et al.*, 1997)
α,β-actin (zebrafish)	GFP	Muscle, ubiquitous	21%, 8%	(Higashijima *et al.*, 1997)
CMV	Luciferase	Ubiquitous	43%	Directing DNA to the nucleus via a NLS increases transgenic rate; (Collas and Alestrom, 1998)
ef1α (Xenopus)	GFP	Ubiquitous	10%	Retroviral vector infection. (Linney *et al.*, 1999) compared efficiency using this method with injection.
rag1 (zebrafish)	GFP	Lymphoid & olfactory organs	?	An engineered PAC revealed distant repression elements; (Jessen *et al.*, 1999)
shh (zebrafish)	GFP	Retina and other *shh* expression domains	?	Upstream promoter and intronic elements required for expression. Demonstrated a wave of *shh* expression across the retina; (Neumann and Nuesslein-Volhard, 2000)
HSP70 (zebrafish)	GFP	Heat Inducible	~2%	Can be induced in single cells by laser and used for fate mapping; (Halloran *et al.*, 2000)
HuC (zebrafish)	GFP	All neurons	~2%	Detected muscle repression elements; (Park *et al.*, 2000)
islet-1 (zebrafish)	GFP	Cranial motor neurons	~3%	(Higashijima *et al.*, 2000)
Histone *H2A.F/Z* (zebrafish)	GFP fusion	All nuclei and chromosomes	4%	Histone promoter driving a histone-GFP fusion; (Pauls *et al.*, 2001)
Rod opsin (zebrafish)	GFP	Rod Photoreceptors	4%	(Kennedy *et al.*, 2001)
deltaD (zebrafish)	GFP	Mesoderm, somites, neural domains	?	Numerous lines allowed detailed dissection of the promoter; (Hans and Campos-Ortega, 2002)
pax2.1(zebrafish)	lacZ, GFP	MHB, interneurons, pronephros, ear and hindbrain	9%	Used transient transgenic analysis to identify *cis*-elements, and then germline transgenics for analysis in mutants; (Picker *et al.*, 2002)
Consensus *lef* binding sites	Destabilised GFP	Wnt activity domains including ectoderm, mesoderm and neural crest	<1%	Trangene provided a readout of active Wnt signalling; (Dorsky *et al.*, 2002)
fli1 (zebrafish)	GFP	Vasculature, jaw arches	15%	(Lawson and Weinstein, 2002)
Keratin8 (zebrafish)	GFP	Skin and certain epithelia	16%	(Gong *et al.*, 2002b)
foxd3 (zebrafish)	GFP	Pigment cells, PNS glia and pineal gland	?	The first neural crest expressing line in zebrafish. Used to analyse PNS glia behaviour (Gilmour *et al.*, 2002b).

4.1.2. Introduction to PAC/BAC engineering

4.1.2.1. Recombinogenic targeting techniques

The development of large insert genomic vectors and their use in genome studies has allowed analysis of large genes, gene clusters and regulatory regions located large distances from coding sequences. Crucial to this is the ability to modify or engineer the inserts to introduce reporter genes and perform deletions or substitutions. This is particularly important in cases where conventional cloning of small promoters has failed to yield all the expression domains of a given gene. A number of techniques for modifying BACs and YACs have been developed, all based on recombination of DNA sequences (reviewed in Giraldo and Montoliu, 2001). A brief description of some of the methods developed for recombinogenic engineering of BACs and PACs is presented here.

Unlike YACs, PACs and BACs reside in recombination deficient host cells. Thus one initial requirement for recombination based engineering is either conferring homologous recombination competence to the host cell transiently, or transfer of the BAC to a new recombination competent host. The first and most successful method is detailed in Section 4.1.2.2., but other approaches have realised similar results. Jessen *et al.* (1998) have developed an approach which utilizes the capacity of short flanking DNA octamer sequences (Chi sites), engineered into a targeting vector to stimulate transfer of homologous DNA segments through the RecBCD recombination pathway. This requires the transformation of both the BAC and the targeting vector into recombination competent bacteria, but has the added advantage of only occurring through a single recombination event. The authors have used this to insert the *gfp* reporter gene into a BAC clone containing the zebrafish *GATA-2* gene (Jessen *et al.*, 1998) and into a PAC clone containing the zebrafish *rag1* gene (Jessen *et al.*, 1999). Both these successfully gave GFP expression in transient or germline transgenic analysis.

Targeted insertion of the *lacZ* reporter into a PAC containing the zebrafish *Hoxa-11b* gene was accomplished with an alternative approach. This employed capture of the PAC into yeast by a specialised Shuttle vector. Once in yeast, where homologous recombination techniques are well established, the *lacZ* gene was readily targeted to the *Hoxa-11b* gene from a targeting plasmid. The modified PAC was then shuttled back into bacteria, from where DNA was prepared and subsequently transgenic mice produced. These successfully expressed the reporter in appropriate locations, demonstrating the conservation of regulatory elements between mouse and zebrafish (Chiu *et al.*, 2000).

Other techniques employed for conferring transient recombination competence to BAC containing bacteria include the introduction of a defective λ prophage containing the λ *red*

recombination genes under a temperature sensitive promoter. Once the prophage has been introduced to a bacterial cell and induced, the targeting cassette can be electroporated in as a linear PCR or plasmid fragment, and a one-step recombination event ensues. In this manner, a transgenic mouse strain carrying the *cre* gene under the control of a neuron specific promoter was produced (Lee *et al.*, 2001).

Finally, another prophage based recombination pathway, namely RecE/RecT has also been used in a recombinogenic strategy termed "ET cloning". A plasmid carrying these genes under inducible promoters is co-transformed into the BAC host cell, along with a linear targeting cassette (Zhang *et al.*, 1998b). However this approach has proven to be technically challenging and many labs have failed to use it successfully. Attempts to improve the technique have been reported, but it does not appear to be the method of choice for modifying BACs (Giraldo and Montoliu, 2001; Muyrers *et al.*, 2001).

The most widely used method relies on introduction of RecA, and is described below. It is relatively simple to use and requires the transformation of a single construct to the original BAC host cell and has the advantage of not requiring the transformation of the PAC into a new bacterial or yeast strain as recombination is performed in the host strain.. The only slight inconvenience is the requirement of molecular detection of two subsequent recombination events.

4.1.2.2. RecA-dependant modification

Yang *et al.* (1997) were the first to report the homologous recombination based modification of a BAC, having used it to introduce the reporter gene *lacZ* into a BAC containing the mouse zinc finger gene *RU49*. Unlike conventional reporter constructs, this faithfully reproduced the endogenous expression pattern in transgenic mice. The technique has been used subsequently to produce transgenic mice containing other modified BACs, including those containing the α9 acetylcholine receptor (Zuo *et al.*, 1999), $p53^{KIP2}$ (John *et al.*, 2001), RAG2 (Yu *et al.*, 1999), *Mrf4/Mrf5* (Carvajal *et al.*, 2001), *ATP7B* (Bockukova *et al.*, 2003), and IL-8 (Wen and Wu, 2001) genes. The technique is the most widely used approach for modifying BACs and is clearly a simple and readily transferable protocol.

The technique is outlined in Figure 4.1, and uses a pop-in/pop-out approach via two successive homologous recombination events. These require the construction of a recombination cassette, which contains the sequence to be inserted into the BAC (such as a reporter gene), flanked by arms with sequences homologous to the target region on the BAC. This cassette is built in a building vector using standard cloning techniques and then transferred to a Shuttle vector (pSV1.*RecA*). Other essential features present on the latter vector include the *TetR* gene, which can be used as both a selectable and counter-selectable

Figure 4.1 →

Figure 4.1: Rec A-mediated strategy for targeted PAC modification

A shuttle vector is used to deliver the reporter gene to a precise site in the PAC via two homologous recombination steps. The GFP gene is indicated on the shuttle vector and is flanked by two homology arms, A' and B', with homology to sites A and B in the PAC. This shuttle vector is created in a building vector before being transferred to the temperature sensitive shuttle vector, which contains both positive and negative selection markers and the *RecA* gene to confer recombination capability to the host cell. After transformation into the PAC host cell, recombination events occurring at either of the homology arms can be selected. Co-integrates thus produced are then resolved via a second recombination event and, depending on the homology arm through which this occurs, produces either the original PAC or the desired modified PAC.
All molecules are depicted as linear for simplicity, but are in reality, circular.

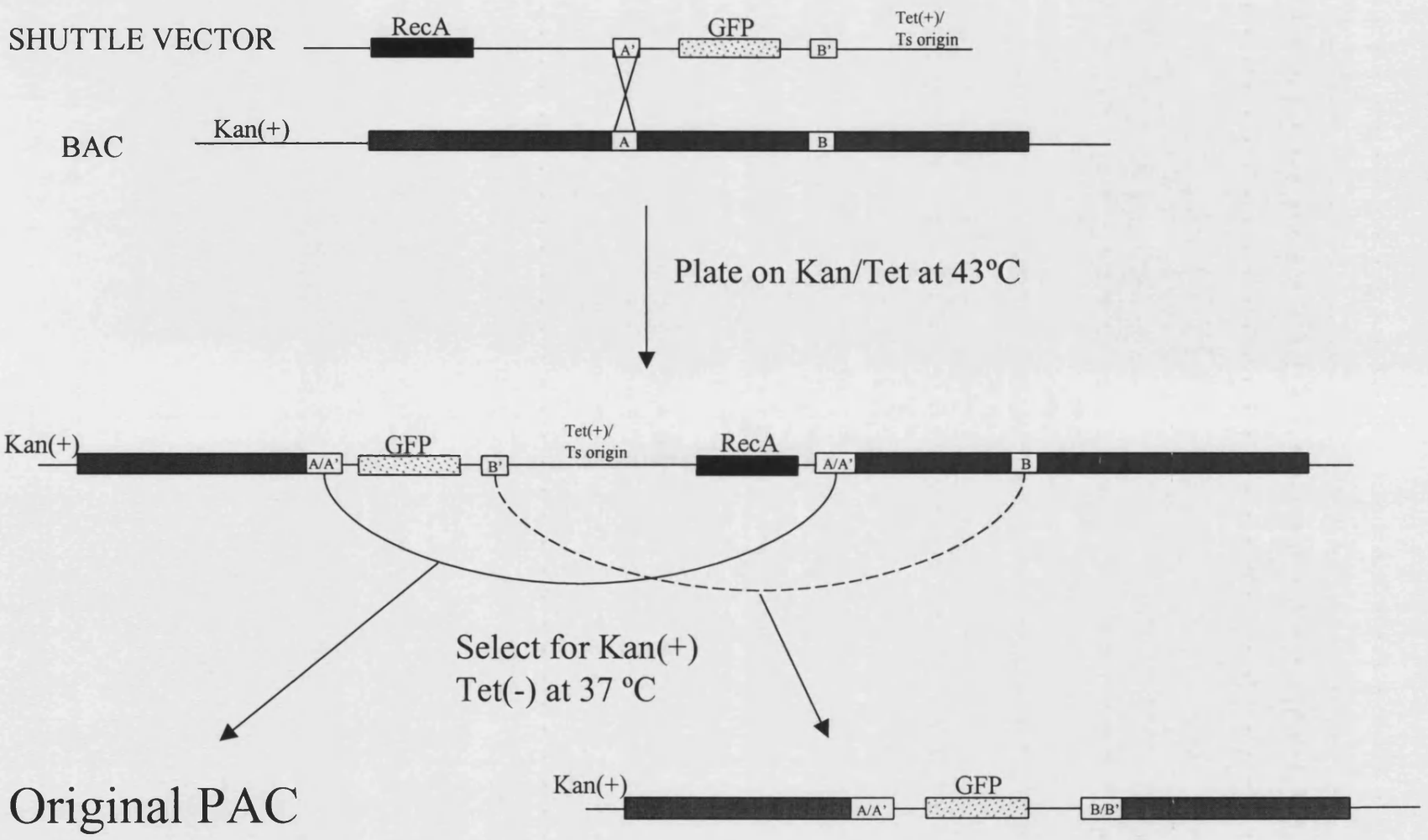
SHUTTLE VECTOR
RecA
GFP
Tet(+)/
Ts origin
A'
B'
BAC
Kan(+)
A
B
Plate on Kan/Tet at 43°C
Kan(+)
A/A'
GFP
B'
Tet(+)/
Ts origin
RecA
A/A'
B
Select for Kan(+)
Tet(-) at 37 °C
Original PAC
Kan(+)
GFP
A/A'
B/B'

marker, a temperature-sensitive origin of replication to allow for selection of co-integration events and finally the *RecA* gene, which confers homologous recombination ability to the normally recombination deficient BAC/PAC host strain.

The Shuttle vector is transformed into the BAC-containing host strain and selection of co-transformants performed using double selection of both *Tet* and the BAC selection (here, Kanamycin). Due to its temperature-sensitive origin of replication, the Shuttle vector (and hence *Tet* resistance) can only be maintained if these bacteria are grown at the permissive temperature. However integration of the vector into the BAC, mediated by *RecA* induced recombination, allows replication of these sequences from the BAC origin of replication at restrictive temperatures. Thus out of the population of co-transformants, co-integrants can be selected for by growing on both selections and at the restrictive temperature (see Figure 4.1). As integration can occur at one of two homology sites, molecular characterisation can confirm the co-integrants and indicate site of integration.

Growing the bacteria on the BAC selection only then allows some to undergo a second recombination event to resolve the co-integrants. If this recombination occurs at the same site as the first event, then the co-integrants revert to the original target BAC. However recombination at the second homologous arm of the cassette will lead to replacement of the endogenous sequence with the marker (Figure 4.1). In either case, resolved BACs will have lost all regions of the Shuttle vector outside the recombination cassette, such as the *TetR* gene, the temperature-sensitive origin of replication and the *RecA* gene. Whereas co-integrants were identified by positive selection for tetracycline resistance, resolution is now driven by selection against the *TetR* marker. This gene encodes a membrane bound protein, which acts to promote tetracycline exclusion from the cell and to aid its co-transport out of the cell. Present at high levels, this gene alters membrane properties such as structure and cation exchange rates (Stavropoulos and Strathdee, 2001). However this also confers sensitivity to certain chelating agents such as fusaric acid (Bochner *et al.*, 1980), and thus it is possible to select against tetracycline resistance by incubating the cells with the chelator fusaric acid. Colonies can then be tested for tetracycline sensitivity and should represent cells in which a second recombination event has resolved the co-integrants. These resolved BACs will include both the desired result (containing the reporter gene substituted into the BAC), and the original BAC (Figure 4.1). Identification of correctly resolved BACs is achieved through molecular analysis.

This method reported by Yang *et al.* (1997) has been recently improved by the same lab, offering an even quicker modification of BACs, and allowing efficient production of reporter constructs carrying large regions of a gene promoter sequence (Gong *et al.*, 2002a).

4.1.3. Summary of *Sox10* expression patterns

4.1.3.1. Expression in the neural crest and its derivatives

Knowledge of a gene's expression pattern is, amongst other criteria, critical to understanding its role in development. The *Sox10* expression pattern has been described in a number of species and cell lines using a combination of Northern, *in situ,* immunostaining and transgenic reporter analysis. New sites of expression are being continually uncovered, highlighting the fact that many analyses are not complete and that many domains are overlooked. A summary of *in vivo* expression patterns in all species analysed to date is given in Table 4.2, including data accrued from *in situ* analysis and information revealed by a mouse *lacZ* line. Additionally, a summary of Sox10 Northern experiments is presented in Table 4.3.

Sox10 expression patterns have been most extensively analysed in the mouse using immunostaining, Northerns, *in situ* hybridisation and a lacZ transgenic knock-in. The latter two techniques showed that expression is first seen in edges of the lateral plate and in the pre-migratory neural crest at approximately E8.5 (Britsch *et al.*, 2001; Kuhlbrodt *et al.*, 1998b). Later, expression was confined to migrating neural crest contributing to peripheral nerves and ganglia, presumably glia, whilst it was downregulated in other neural crest derivatives during migration. Thus at E9.5, expression is described in both dorsal root and a number of cranial ganglia. Of the latter, the first to indicate *Sox10* expression are the trigeminal (V), the facial (VII) and the acoustic (VIII) ganglia, and later (at E10.5) all cranial ganglia and nerves express *Sox10*, as do sympathetic ganglia. *Sox10* signal in enteric ganglia is detected from E12.5, when expression in peripheral nerve fibres of the limbs is also prominent (Herbarth *et al.*, 1998; Kuhlbrodt *et al.*, 1998b; Pusch *et al.*, 1998; Southard-Smith *et al.*, 1998).

This early *Sox10* expression pattern is well conserved with that of other species, although minor differences are described. Thus human *SOX10* expression is seen in neural crest cells at 4 weeks, including some cranial ganglia, with expression at 6 weeks seen in all cranial ganglia, DRGs, spinal nerves, the sympathetic ganglia chain and enteric ganglia. Interestingly, *SOX10* expression was also noted in the cephalic neural crest derivatives which later form cartilage rudiments of the nasal bone (Bondurand *et al.*, 1998; Touraine *et al.*, 2000).

The chick *cSox10* expression pattern reveals similar expression patterns to those of mammalian *Sox10* genes, namely expression in premigratory neural crest, as well as migratory neural crest with expression retained only in the subset of neural crest contributing to the cranial ganglia, DRGs, sympathetic ganglia, nerve fibres, and later in

enteric ganglia. Double labelling studies indicated that the cells labelled at these sites are non-neuronal (Cheng *et al.*, 2000).

Recently, the Sox10 expression pattern in *Xenopus* was reported, and again shows expression in neural crest forming regions of the lateral neural plate as demonstrated by overlap with other neural crest markers such as Slug and Sox9. Following neural tube closure, Sox10 expression remains in neural crest in a premigratory position in both trunk and cranial regions. Interestingly, in contrast to mouse, there is strong expression in migrating neural crest cells within the branchial arches (Honore *et al.*, 2003). Expression in the head is later confined to the cranial ganglia and otic vesicle, but the authors did not report maintenance of Sox10 expression in any other neural crest derivatives such as trunk PNS glia (Aoki *et al.*, 2003).

Thus Sox10 expression is seen in the neural crest from an early stage in all species studied, and appears to be maintained in glial derivatives thereof, including dorsal root, sympathetic, enteric and cranial ganglia, although expression in neuronal precursors at early stages cannot be categorically ruled out, based on current reports.

4.1.3.2. Expression outside the neural crest

Expression of Sox10 has been reported in sites outside neural crest. This includes the otic vesicle, which maintains strong expression from early stages in all species, and the CNS. Northern analysis of human samples at adult stages indicates high levels of expression at various sites as listed in Table 4.3 and includes expression in the spinal cord and brain, particularly in the medulla and corpus callosum. Weaker expression was also detected in all brain regions analysed including the cerebellum, occipital pole, frontal lobe, thalamus, hippocampus, substantia nigra, cerebral cortex, and major brain nuclei (Pusch *et al.*, 1998). Northern analysis also detected fetal expression in the developing brain, and faintly in the lung and kidney (Bondurand *et al.*, 1998; Southard-Smith *et al.*, 1999a).

Similar northern results were obtained with mouse and rat samples, with transcripts detected during embryogenesis and in adult colon, heart, lung, muscle, testes and brain (Table 4.3). At the latter site, transcripts were detected in all regions tested, in particular in the cerebellum, pons, olfactory bulb, hippocampus, cerebral cortex and midbrain (Kuhlbrodt *et al.*, 1998b; Southard-Smith *et al.*, 1999a; Southard-Smith *et al.*, 1998). Greater detail of expression patterns was obtained through *in situ* analysis of sectioned adult and embryo rodent brains, and correlated with regions containing a high content of myelinated fibres. Strong *Sox10* expression in the otic and nasal placodes is seen in mouse from E8.5 and E10.5 onwards respectively (Kuhlbrodt *et al.*, 1998b). Elsewhere in the CNS, strong expression was seen in the spinal cord, adjacent to the ventricular zone,

probably oligodendrocyte precursors (Kuhlbrodt *et al.*, 1998b). X-gal staining of the *Sox10*^{lacZ} strain confirmed this CNS expression pattern (Britsch *et al.*, 2001; Stolt *et al.*, 2002). *In situ* analysis of human fetal brain also showed expression in the otic vesicle and in nonneuronal cells of glial rich regions including the cerebellum, hippocampus (Touraine *et al.*, 2000).

Chick *in situ* analysis demonstrated expression in the ventricular zone of the spinal cord as well as in the pineal organ. In addition, strong c*Sox10* expression is also described in the otic vesicle (Cheng *et al.*, 2000). Subsequent analysis has shown expression of *cSox10* in the septa, valves and glia of the innervating nerves of the developing heart (Montero *et al.*, 2002), and expression in the condensing mesenchyme within the digits and nerves of the limbs (Chimal-Monroy *et al.*, 2003). Expression in condensing mesenchyme of the limbs has also been reported in the *Sox10*^{lacZ} strain (Britsch *et al.*, 2001).

4.1.3.3. Zebrafish *sox10* expression pattern

Analysis of *sox10* expression in zebrafish by *in situ* hybridisation has revealed a pattern which is comparable to that just described for other species. Expression is first detectable at 2 somite stage (~11hpf) as two stripes in the lateral neural plate, in a position consistent with neural crest progenitors. The two stripes meet medially and dorsal to the neural tube as the cells converge, to form premigratory neural crest cells. *sox10* expression is maintained in these cells and follows an anterior to posterior progression as neural crest develops, with the posterior extent of expression expanding towards the tail with time. By approximately 18 somite stage (~18hpf), expression in premigratory neural crest extends along the entire axis of the embryo. To determine if *sox10* labels all premigratory neural crest, double *in-situ* analysis was used with *sox10* in combination with *foxD3*, which demonstrated that *foxD3* expression precedes *sox10* in this domain and that overlap was extensive but incomplete (Dutton *et al.*, 2001). Similar analysis with *sox9a* indicated very little overlap of *sox10* and *sox9a* in the embryo, restricted to the otic vesicle. No expression of *sox9a* was evident in premigratory neural crest. *sox9b*, in contrast, mostly overlapped with *sox10* here (Pauliny, 2002). *sox10* expression is maintained in migrating neural crest cells from 14 somite stage (~16hpf) on the medial pathway, and is rapidly downregulated in cells on the lateral pathway from this stage onwards. Nonneuronal cells expressing *sox10* were also seen associated with the cranial ganglia, presumably neural crest derived glia, whilst some expressing cells remained adjacent to the notochord in a medial position within each somite segment at 35hpf, in a position consistent with Schwann cells along the spinal nerves. There was no expression of *sox10* in the neural crest streams in the branchial arches, but cranial cartilage cells did express *sox10* at 48 and 60hpf. Enteric nervous

system precursors expressed *sox10* at 24hrs and can be seen as a stream of cells migrating posteriorly along the gut (Elworthy *et al.*, in prep.). At 60hpf, *sox10* positive cells can be seen around the gut epithelium (Dutton *et al.*, 2001).

Outside the neural crest or its derivatives, strong expression in the otic placode commences at around the 12 somite stage, (~15hpf), which remains until at least 60hpf. Expression is seen in the pectoral fin endoskeletal disk at 48 and 60hpf, and additionally, is reported at 24hpf in the ventricular layer in the hindbrain. Later *sox10* is seen in the spinal cord, forebrain and midbrain, although the identity of these cells is not yet clear. There is, however, good evidence for *sox10* expression in oligodendrocytes and their precursors from 48hpf onwards, first seen where they are born in the ventral spinal cord (Park *et al.*, 2002; Pauliny, 2002).

Table 4.2: Summary of Sox10 *in situ* and lacZ expression studies

		Organism						
Expression site	Mouse Stage	Mouse (*in situ*)	Mouse *Sox10* $^{lacZ/+}$	Chick (*in situ*)	Human (*in situ*)	Xenopus (*in situ*)	Zebrafish (*in situ*)	Zebrafish Stage
Neural Plate	E7.5	-	nr	+	nr	-	+	1 som
Premigratory neural crest	E8.5	+	+	+	+	+	+	1 som -
Otic Vesicle	E8.5-	+	+	+ (NN)	+	+	+	12 som -
Migrating neural crest	E9.5	+	+	+	+	+	+	14hpf-
Neural crest in branchial arches	E9.5	-	-	-	+	+	-	20hpf
Dorsal Root Ganglia	E9.5-	+	+	+ (NN)	+	nr	nr	24hpf-
Cranial Ganglia	E9.5-	+	+	+ (NN)	+	+	+ (NN)	24hpf-
Spinal Nerves	E10.5-	+	+ (S)	+	+	nr	+	24hpf-
Sympathetic ganglia	E10.5-	+	+	+	+	nr	nr	24hpf
Cardiac autonomic ganglia	E10.5-	nr	+	+	nr	nr	nr	24hpf
Cardiac septa, valve endothelia	E10.5	nr	nr	+	nr	nr	nr	24hpf
Plexi of fore/hindlimbs	E11.5-	+	+?	+	nr	nr	nr	24hpf
Pineal organ	E11.5-	nr	nr	+	nr	nr	+	24hpf
Olfactory Bulb	E12.5	+	+	nr	+	nr	nr	24hpf
Enteric Nervous system	E12.5-	+	+*	+	+	nr	+	24hpf
Melanoblasts	E12.5	+	+	nr	nr	+	+	30hpf
Limbs/Fins mesechyme/cartilage	E12.5	+?	+	+	nr	nr	+	48hpf
Developing facial cartilage	E12.5	nr	nr	nr	+	-	+	48hpf
Spinal cord (ventricular zones)	E13.5-	+	+	+	nr	nr	+	48hpf
Brain and/or Oligodendrocytes	E14.5-	+	+	+	+	+	+	48hpf

Organism studied and method used to determine expression pattern is given above, (+) indicates expression noted in this site, (-) indicates no expression seen and (nr) indicates either not reported or not examined. (NN) designates expression is in non-neuronal cells at this site as shown by a double staining approach, and (S) indicates that this expression has been shown to be in Schwann cells. (*) indicates that this cell type is much reduced in heterozygous *Sox10*^{lacZ} mice due to haploinsufficiency. (?) marks sites where expression has been suspected or is masked by overlying expression. Sites of expression are listed on the left in approximate chronological order of commencement of Sox10 expression. Corresponding mouse and zebrafish stages are presented on the left and right respectively. See text for more detail and associated references.

Table 4.3: Summary of Sox10 Northern analysis

		Human (Northern)	Rat/mouse (Northern)
Whole Embryo	E11-12.5	nr	+
Whole Embryo	E15-16.5	nr	+
Intestine	E17-19.5	nr	+
Brain	Fetus	+	nr
Lung		+	nr
Kidney		+	nr
Brain	Adult	+	+
Cerebellum		+	+ (low)
Oligodendrocytes		nr	+
Olfactory bulb		nr	+
Small intestine		+	nr
Colon		+	+
Heart		+	-
Bladder		+	nr
Spinal Cord		+	nr
Stomach		+ (low)	nr
Pancreas acini		+ (low)	nr
Skeletal muscle		+ (low)	+
Adrenal Gland		+	nr
Lung		-	?
Prostate		+	nr
Testes		+ (low)	-

Table is presented as per Table 4.2. (?)-Indicates conflicting reports as to presence or absence of expression at this site. See text for associated references.

4.1.3.4. *Sox10* expression in *Sox10* mutants

Analysis of the *sox10* expression pattern in *cls* embryos indicated a severe disruption to neural crest migratory ability at 24hpf, with a relative increase in cells seen dorsal to the neural tube. Additionally, *sox10* positive cells associated with cranial ganglia and nerves were reduced in *cls*. Prior to this, no overt differences in expression pattern could be detected between *cls* embryos and their siblings. Later, although the lateral migration pathway showed a reduction in migrating *sox10* positive cells in *cls,* a comparable number of cells were seen migrating on the medial pathway. Maintenance of expression in segmental medial clusters of cells (putative Schwann cells) was much reduced in *cls* (Dutton *et al.*, 2001). No expression was visible in the enteric nervous system in *cls* embryos at 60hpf. Loss of *sox10* expression on the lateral pathway and in the ENS has been shown by labelling studies and use of other markers to be due to absence of cells, not just *Sox10* disregulation (Dutton *et al.*, 2001; Kelsh and Eisen, 2000).

Aside from the neural crest and its derivatives, *sox10* expression was largely unaffected in *cls* mutants. Thus expression in the spinal cord, brain and cartilage cells was not obviously affected. Ear expression, however is downregulated after 40hpf (Pauliny, 2002).

The disruption to the *sox10* expression pattern in *cls* is similar to that seen in mouse *Sox10* mutant embryos. There appears to be no difference in *Sox10* expression in early neural crest between homozygous *Dom* mutants and their siblings. The migration of mutant neural crest cells was delayed however, and *Sox10* expression was lost from all cranial ganglia and nerves, due to absence of neural crest derived cells at these sites. Some migrating $Sox10^{+}$ neural crest cells were evident in the trunk, in particular in medially placed neural crest derivatives associated with the DRGs, although at reduced levels. Although most of the wild-type expression pattern is not disrupted in heterozygous *Dom* mice, the overall level of expression appears reduced. There is a dramatic reduction in the number of $Sox10^{+}$ cells in the gut of heterozygous embryos, consistent with the dominant phenotype seen for this cell type. Similarly homozygous *Dom* embryos have no $Sox10^{+}$ cells populating the gut (Herbarth *et al.*, 1998; Southard-Smith *et al.*, 1998).

Defects in the $Sox10^{lacZ}$ mutant line reflect those found in *Dom* mutants. Again, early neural crest was unaffected in both homozygous and heterozygous embryos, as shown by β–gal staining. $Sox10^{lacZ}$/ $Sox10^{lacZ}$ embryos subsequently showed vastly reduced numbers of $\beta\text{–gal}^{+}$ cells associated with cranial ganglia and nerves, peripheral nerves, the enteric nervous system and sympathetic primordium. In heterozygotes, $\beta\text{–gal}^{+}$ cells were present in the proximal gut (at a reduced level), but absent in the distal gut (Paratore *et al.*, 2002). An anterior-posterior gradient of staining in DRGs was notable in homozygotes, with a later decrease in overall size of the DRGs (Britsch *et al.*, 2001; Sonnenberg-Riethmacher *et al.*, 2001). The otic vesicle, cartilage and oligodendrocyte precursors all express β–gal in $Sox10^{lacZ}$/ $Sox10^{lacZ}$ embryos.

4.1.4. Aims

A transgenic line containing a *sox10* GFP reporter gene would be an extremely useful tool for studying both *sox10* gene regulation and visualising neural crest behaviour *in vivo*, allowing pursuit of many of the experiments outlined above. With the ultimate aim of eventually producing such lines, isolation of the *sox10* promoter was commenced.

4.2. RESULTS

4.2.1. Generation of a fine map of the *sox10* gene region

To characterise the *sox10* genomic region in more detail and to allow subcloning of the promoter, a finer restriction map was derived from a combination of Southern analysis (not shown) and the *sox10* PAC I sequence. This map is shown in Figure 4.2, where a selection of sites found are shown, and indicates that there are a number of useful sites for promoter cloning in the upstream region of the gene. For initial sequence verification of the presence of *sox10* sequence in the PACs (not shown), a number of subclones were made from PAC L, and these are drawn in the lower part of Figure 4.2.

4.2.2. Subcloning of sox10 upstream sequence

Based on the new map information, attempts were made to clone a fragment upstream of the *sox10* gene. Note that the position of the *Spe*I site adjacent to the ATG of *sox10* (Figure 4.2) is ideal for reporter construct cloning, as it allows inclusion of almost all the 5'UTR, which has been suggested to be crucial in maximising reporter expression from other zebrafish promoters (Long *et al.*, 1997). In order to subclone part of the *sox10* promoter, the 4.9kb *BamH*I-*Spe*I fragment (Figure 4.2) was isolated from PAC L by gel purification and successfully cloned into pBluescript™ II also cut with *BamH*I and *Spe*I. The resulting plasmid, pBSp4.9, is represented in Figure 4.2, and was used for subsequent generation of a GFP reporter construct. The *sox10* gene contains a 2.1kb intron in the 375bp 5'UTR putting the estimated start of transcription 2.5kb upstream of the ATG. Thus the amount of sequence 5' to the transcription start site present in the 4.9kb *BamH*I-*Spe*I fragment is approximately 2.4kb.

4.2.3. Production of reporter constructs

4.2.3.1. p4.9:GFP

To produce a GFP reporter construct, the 5' region of the zebrafish *sox10* gene present in pBSp4.9 was cloned into the XLT.GFP$_{LT}$ CS2+ plasmid (see Figure 2.2), kindly provided by Randall Moon (University of Washington), which contains a gene encoding an enhanced GFP. Briefly, both pBSp4.9 and XLT.GFP$_{LT}$ CS2+ were digested with *Sal*I and *Xba*I, and the appropriate bands isolated by gel extraction following gel electrophoresis. These fragments were ligated together resulting in replacement of the CMV promoter from the latter plasmid with the 5' *sox10* gene sequence. This places the ATG of the GFP gene

Figure 4.2 →

Figure 4.2: Map of *sox10* genomic region

Upper Section: Depiction of total cloned region surrounding *sox10*. Known *Sal*I (S) and *Not*I (N) sites, based on combined PAC restriction maps (see Figure 3.3), are shown with sizes in kb (*Sal*I fragments at the far right are unordered, see Figure 3.3). Total cloned DNA is approximately 116kb. Dashed lines at ends represent uncloned flanking genomic DNA. As previously (Figure 3.3), arrow shows position and orientation of the *sox10* gene.

Lower Section: Detail of the *sox10* gene and upstream region. From sequence information and Southern analysis, the position of sites for certain restriction enzymes were deduced and are depicted thus: *Sal*I (S), *Spe*I (Sp), *Nco*I (Nc), *EcoR*V (RV), *BamH*I (B), *EcoR*I (E). Above this map is the predicted intron/exon structure, with exons depicted as boxes. Of these, grey boxes represent the *sox10* open reading frame, the black boxes represent regions of the gene encoding the HMG domain, whilst empty boxes represent the 5' and 3' untranslated regions. Arrow depicts the predicted start of transcription, and the relative position of the Sal15 primer is indicated with an arrowhead.

Below restriction map are the positions of the various subclones made from PAC L, with corresponding names given.

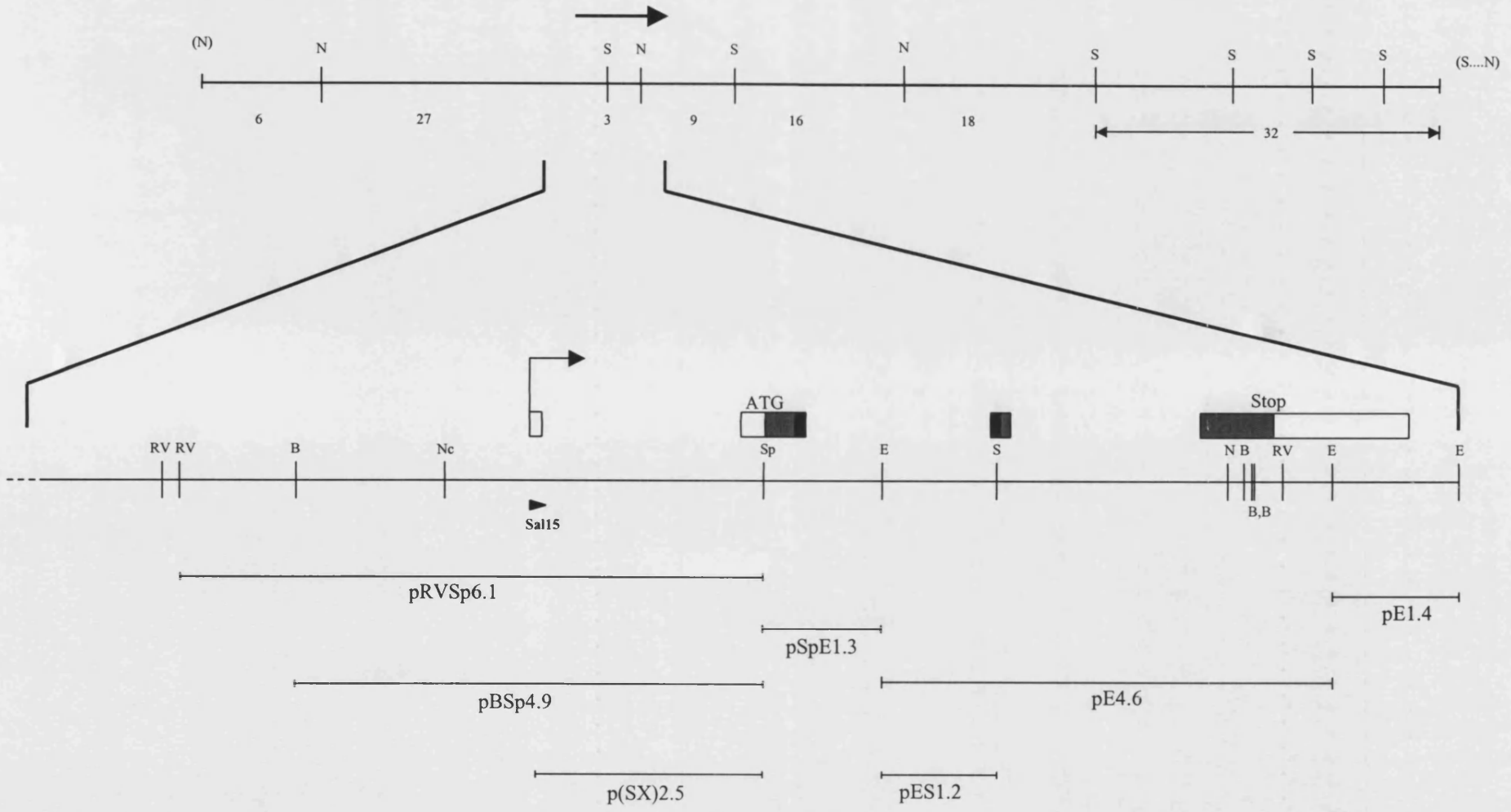
(N)
N
S
N
S
N
S
S
S
S
(S....N)
6
27
3
9
16
18
32
ATG
Stop
RV RV
B
Nc
Sp
E
S
N B
RV
E
E
B,B
Sal15
pRVSp6.1
pE1.4
pSpE1.3
pBSp4.9
pE4.6
p(SX)2.5
pES1.2

in an identical position relative to the normal position of the ATG in the *sox10* gene, thus very closely mimicking the environment found in the endogenous *sox10* promoter, however it substituted the sequence preceeding the start codon (GGACCG) with the *Xba*I recognition sequence (TGTACA). As this sequence in the *sox10* gene was non-coding and far removed from the transcription start site, it was deemed to be unlikely to have significant influence on expression of the reporter. The resulting plasmid was called p4.9:GFP and a crude restriction map is shown in Figure 4.3a.

To determine if it contains functional *sox10* promoter sequence, p4.9:GFP was injected into early cleavage embryos, and then viewed after neurulation by fluorescent microscopy for GFP expression. Figure 4.3b shows an example of a 20hpf embryo injected with 30pg of p4.9:GFP before the 1-cell stage. Neural crest cells can be seen dorsally in the head, trunk and tail in a premigratory position (arrowheads). Some of the most anterior neural crest cells expressing GFP appear to be beginning to migrate ventrally. An example of a neural crest cell is given inset in Figure 4.3b, demonstrating the stellate morphology associated with this cell type. Thus these transient analyses have shown that the promoter fragment used here appears to mimic the *sox10* expression pattern, and can drive GFP expression in the neural crest. Note however that expression is seen in muscle fibres (arrows), a site not expected based on the *in situ* pattern and which thus appears to be ectopic. This ectopic muscle expression is also shown in Figure 4.3c, d (arrows), in 24hpf and 5dpf embryos respectively. The latter embryo also shows expression in the ear as expected based on the expression of *sox10* (asterisk; Figure 4.3d). These transient analyses almost certainly do not describe the complete expression domains of this promoter. As there appeared to be ectopic expression, it was assumed that this promoter lacked repression elements and hence would render a germline transgenic line derived from this construct less useful for neural crest analysis due to masking effects by the muscle expression.

4.2.3.2. p6.1:GFP

It was hypothesised that increasing the amount of *sox10* upstream sequence in the reporter construct might lead to inclusion of repressors required for silencing promoter activity seen in muscle. An attempt to clone a larger *sox10* promoter fragment was made using the presence of the *Eco*RV site, approximately 6.1kb 5' to the start of translation (see Figure 4.2). PAC L was digested with *Eco*RV and *Spe*I and an approximately 6kb band was gel purified following electrophoretic separation. This was cloned into pBluescript cut with the same enzymes to produce pRVSp6.1 (Figure 4.2). A cloning strategy identical to that for p4.9:GFP was then employed to introduce this promoter fragment upstream of GFP

Figure 4.3 →

Figure 4.3: Map and transient transgenic analysis of p4.9:GFP

a. A map of the reporter transgene present on p4.9:GFP with restriction sites shown (abbreviations as per Figure 4.2; X-*Xba*I). Those sites not derived from the *sox10* gene but from the vector are shown in brackets. The start of transcription is shown (arrow) and the *sox10* exons of the 5' UTR depicted as open boxes. From the start of transcription to the ATG is approximately 2.5kb including 375bp 5'UTR and a 2.1kb intron. This construct thus has approximately 2.4kb of sequence upstream of the start of transcription. The *gfp* gene is shown as a green box and the polyadenylation signal sequence is given as a hatched box.
Injection of this construct into early embryos in a transient assay directs expression of GFP in a number of cell types throughout development. As expected, this is mosaic in nature, with variable degrees of expression noted.

b. Upper panel shows a lateral view of an injected embryo at 20hpf viewed under fluorescent light. Premigratory and migrating neural crest cells can be seen in both the head and trunk (upper panel, arrowheads). An enlarged picture of a migrating neural crest cell is shown inset. However ectopic expression was noted in a few sites including muscle fibres (upper panel, arrows).

c. A further example of muscle (arrow) is shown in lateral views of a 24hpf injected embryo under fluorescent light (left panel) and overlaid onto an image of the embryo viewed under Normaski optics (right panel). A single muscle fibre can be seen expressing GFP.

d. Expression in muscle cells remains until at least 5dpf. A lateral view of an injected embryo at 5dpf under fluorescent light, showing expression in muscle fibres (arrows) and the ear (asterisk).

a.

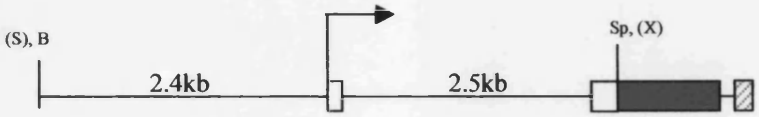

p4.9:GFP

b.

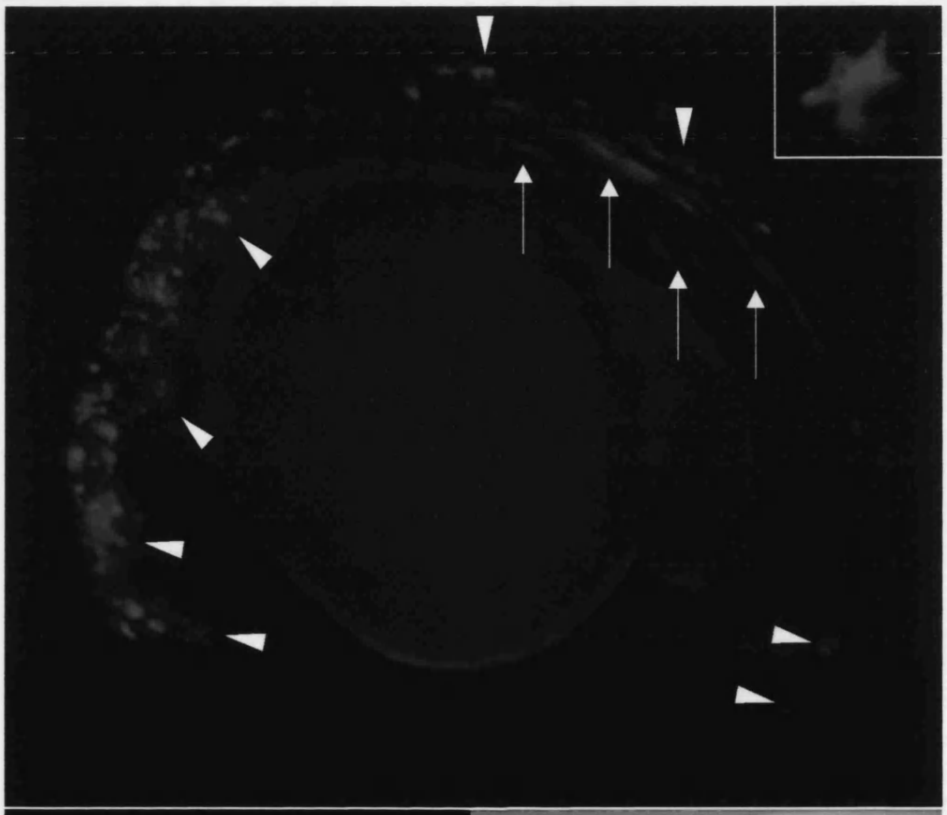

c.

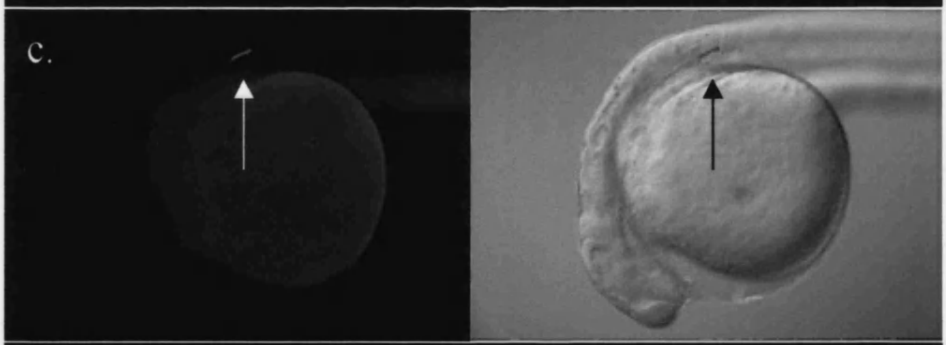

d.

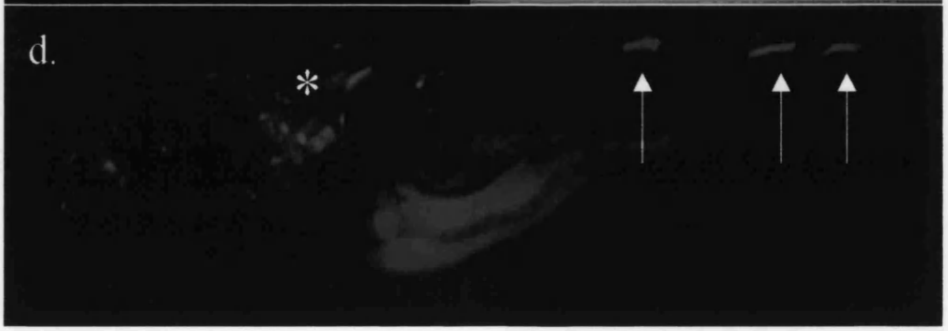

in XLT.GFP$_{LT}$ CS2+. Thus both pRVSp6.1 and XLT-GFP$_{LT}$-CS2+ were cut with *Sal*I and *Xba*I, and the appropriate bands isolated and ligated together to produce p6.1:GFP, a map of which is shown in Figure 4.4a. This construct contains approximately 50% more sequence upstream of the start of transcription compared to p4.9:GFP, with addition of an extra 1.2kb (Figure 4.4a).

As before, transient analysis was then conducted to see if this reporter could direct GFP expression in a *sox10* pattern and if it also gave ectopic expression in striated muscle cells. As can be seen in Figure 4.4b, GFP expression was again driven in neural crest cells (examples at 30hpf are shown in Figure 4.4b arrowheads; also in Figure 4.4c), however expression was also noted in muscle fibres (arrows, Figure 4.4b and c). Again, expression in the ear was evident from at least 30hpf onwards in epithelial cells of the otic vesicle (Figure 4.4c, asterisks). This expression in the ear is shown in a 5dpf embryo (Figure 4.4d, asterisk), where jaw cartilage expression was noted as well (see also Figure 4.4e). Expression at this site is in accordance with *in situ* data, which describes *sox10* expression beginning at 48hpf in this cell type and remaining until at least 60hpf (Pauliny, 2002). This transient GFP analysis thus demonstrated that the *sox10* promoter used here is probably active in the ear and jaw until later than previously described. However expression in muscle was again noted.

Due to the ectopic expression of this reporter in muscle, it was again assumed that repressor elements were not included in either the p6.1:GFP or p4.9:GFP constructs, and that the muscle expression would render any germline transgenic line produced with these reporters useless. To attempt to produce a larger reporter construct that might include all promoter and enhancer elements, a PAC engineering approach was commenced.

4.2.4. Engineering of a sox10 PAC

Due to the ectopic expression seen in the plasmid-based *sox10* promoter constructs, it was decided to attempt to increase further the amount of sequence surrounding the *sox10* reporter gene in the hope it would include repressor elements and more accurately reproduce the endogenous expression pattern. Modifying a PAC using the method outlined in Section 4.1.2 .2. above and described in Yang *et al.* (1997) was attempted. This was selected over other approaches due to a personal recommendation and an offer of necessary reagents (Dr. Rosalind John, University of Cambridge, pers. comm.).

4.2.4.1. Production of the Building and Shuttle vectors

Recombination of the GFP marker gene into a PAC first required construction of a recombination cassette, which was achieved in a building vector. The cassette needed then

Figure 4.4 →

Figure 4.4 Map and transient transgenic analysis of p6.1:GFP

a. Map of the reporter transgene present in p6.1:GFP, which includes approximately 50% more sequence upstream of the start of transcription than p4.9:GFP (now approximately 3.6kb). This was hoped to include repressors of the ectopic muscle expression seen earlier. Annotations are as per Figure 4.3.
This construct was injected into early embryos in a transient assay to assess expression domains of the larger promoter region.

b. A magnified lateral view of the anterior dorsal trunk of an injected embryo at approximately 30hpf. Again a migrating neural crest cell shows strong fluorescence (arrowhead), however this promoter also appears to direct expression in muscle fibres in transient assays (arrows).

c. A lower power image of the head of the same embryo, indicating expression in the otic vesicle (in particular, the otic epithelium, asterisks), muscle (arrow) and neural crest cell above the eye (arrowhead). Right panel shows the fluorescent image overlaid onto a brightfield image of the embryo.

d. Occasional embryos showed expression in jaw elements. This image shows a 5dpf embryo injected with p6.1:GFP in a lateral view. Expression at 5dpf is clear in the ear (asterisk), and also in the jaw (arrowhead).

e. Viewed ventrally, it is apparent that in this embryo (in **d.**), the left jaw elements (arrowhead) show good expression and coverage of the transgene. *sox10 in situ* analysis has previously indicated expression in forming jaw at 48hpf and at least until 60hpf.

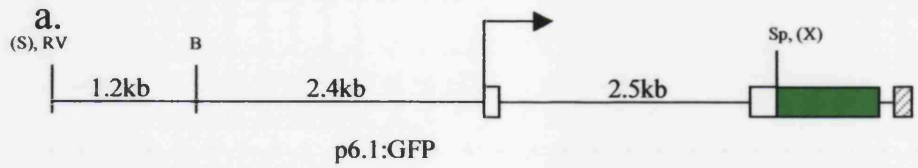
a.
(S), RV
B
Sp, (X)
1.2kb
2.4kb
2.5kb
p6.1:GFP

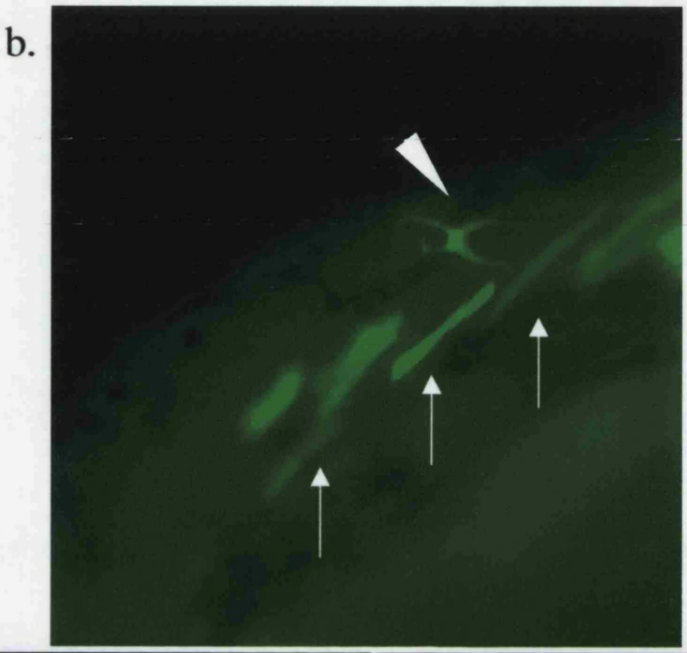
b.

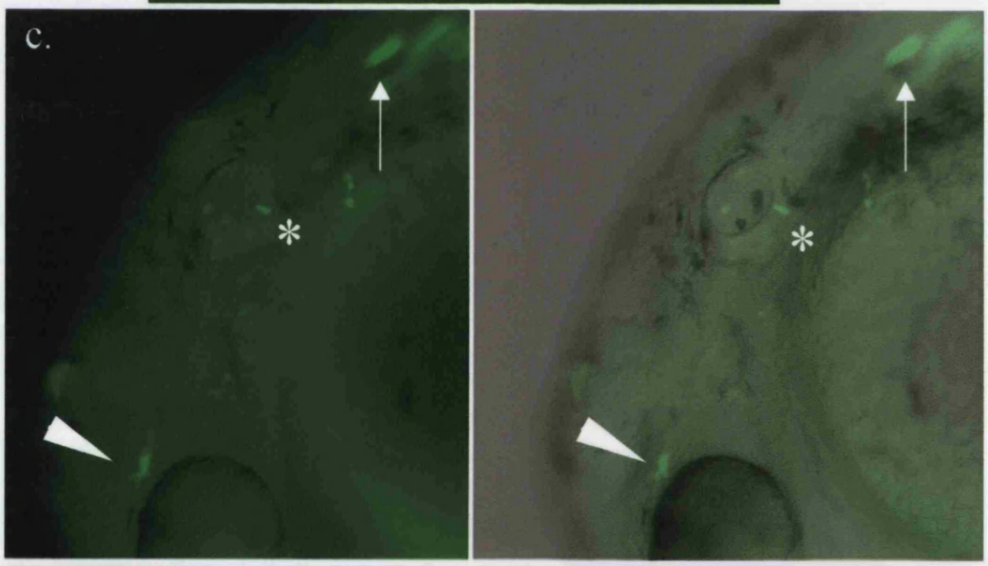
c.

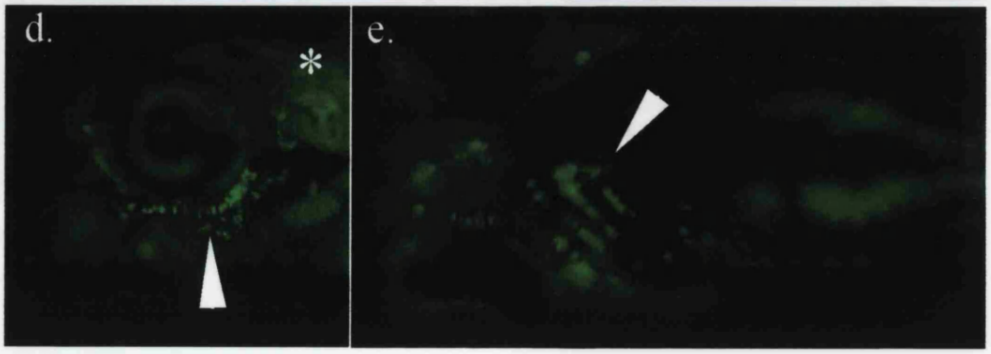
d.
e.

to be transferred into the Shuttle vector pSV1.*RecA*, kindly provided by Dr. Rosalind John (University of Cambridge) with permission granted by Nat Heintz (Rockerfeller Institute, NY). The recombination cassette contained the *gfp* gene flanked by recombination arms, which needed to be at least 500bp in size and with homology to the region flanking the target site on the PAC. It was decided to introduce the *gfp* gene at the same site as in the small constructs. This aided cloning of the cassette, as well as meaning the start of translation of the reporter is close to that of the sox10 protein as previously described. This also maximised comparability with the plasmid constructs. The cloning strategy used is presented in Figure 4.5.

The 5' homology arm ("A") was isolated by PCR from pBSp4.9. A 2.5kb fragment was amplified using the Sal15 primer and the T7 primer of the pBluescript vector, the former primer being simply the S15 primer with a 5' *Sal*I site added for later cloning purposes (see Table 2.4; position shown on Figure 4.2). The 2.5kb fragment obtained is shown in Figure 4.6a and contains some of exon 1, all of intron 1 and exon 2 up to the *Spe*I site just before the ATG of the *sox10* gene. After being cloned into pGEM-T Easy, this homology arm was cut out with *Sal*I and *Xba*I (as shown in Figure 4.6b) and gel purified. p2.5GFP was then created by ligating this fragment into the XLT.GFP$_{LT}$ CS2+ vector, also digested with *Sal*I – *Xba*I (Figure 4.6b), such that this homology arm replaced the CMV promoter in this vector and lay directly upstream of the *gfp* gene (Figure 4.5).

The 3' homology arm ("B") was a 1.2kb *EcoR*I – *Sal*I fragment which consisted of most of intron 2 and part of exon 3 up to the *Sal*I site. This was subcloned from pE4.6 by gel purification into pBluescript giving the clone pES1.2 (Figure 4.2). Fortuitously, the 1.2kb *EcoR*I – *Sal*I fragment in pES1.2 was now flanked by the *Not*I and *Apa*I site of the pBluescript multiple cloning site. These were used to cut out the homology arm from pES1.2, which was transferred to p2.5GFP, 3' of the *gfp* gene, as *Not*I and *Apa*I sites occur here in the correct orientation (Figure 4.6c). Note that this process also introduced a second *Sal*I site to the very 3' end of the recombination cassette, allowing it to be isolated as a *Sal*I fragment. The building vector thus derived was called pBV and is shown in Figure 4.5, and was checked by restriction with *Not*I and *Sal*I in comparison with p2.5GFP (Figure 4.6c).

Having produced the recombination cassette in the building vector it was now necessary to transfer it to the Shuttle vector (pSV1.*RecA*). This was done by digesting pBV with *Sal*I and gel purifying the recombination cassette. This was ligated to pSV1.*RecA* which had been cut with *Sal*I and treated with Shrimp Alkaline Phosphatase to enrich for recombinants. Transformation was performed with a 37°C 2 minute heat-shock and bacteria grown on tetracycline selection at 30°C, to allow activity of the temperature-sensitive origin of replication on the Shuttle vector. The resulting clone, pSV$_{SOX}$ was

Figure 4.5; Figure 4.6 →

Figure 4.5: Cloning strategy for generation of pBV and pSV_{SOX}

The first step towards engineering of GFP into a *sox10* containing PAC requires the generation of a shuttle vector carrying the GFP reporter gene surrounded by homology arms (see text for detail). The upstream homology arm was isolated by PCR using pBSp4.9 as a template and the T7 primer (priming from the vector) and a Sal15 primer, which represents the S15 primer with a *SalI* site added, and primes from within exon 1. The product produced (Figure 4.6a) was cloned into pGEM T-Easy (resulting plasmid p(SX)2.5 is shown in Figure 4.6b).

This product was cloned upstream of a GFP reporter, by isolating the product as a *SalI* – *XbaI* fragment and cloning into XLT-GFP_{LT}.CS2+, which has had the CMV promoter removed, also by *SalI* and *XbaI* digestion and gel purification of appropriate band. The resulting plasmid p2.5GFP is shown in Figure 4.6b, along with the donor plasmids. Fortuitously, this introduced *NotI* and *ApaI* sites in correct orientation for cloning the *EcoRI* – *SalI* fragment from pES1.2, which represents the 3' homology arm. This was achieved by digestion of both p2.5GFP and pES1.2 with *NotI* and *ApaI* and subsequent gel purification and ligation of the appropriate bands. This in effect introduces the *EcoRI* – *SalI* 3' homology arm downstream of the *gfp* gene. The resulting plasmid constitutes the Building vector, pBV. Note that the cloning steps mentioned leave *SalI* sites either side of the recombination cassette. This permitted cloning of the cassette into the pSV vector (Figure 2.1), which was also cut with *SalI* and treated with Shrimp Alkaline Phosphotase to promote recovery of recobinant clones. The resultant clone pSV_{SOX} was analysed along with pBV and pSV by digestion with *SalI*, *BamHI* single and double digests (Figure 4.6), and indicated presence of all appropriate bands.

The GFP gene is represented by a green box, with non-coding exons fragments of the *sox10* gene represented as white boxes and the coding exon fragment from exon 3 represented as a black box. Thick grey lines depict vector regions in all plasmids. On the shuttle vectors, the striped box indicates the temperature-sensitive origin of replication, the blue box indicated the tetracyline resistance gene and the yellow box shows the RecA gene. Thin black lines depict non-coding regions of the *sox10* gene such as the introns or the promoter region. The CMV promoter present on XLT-GFP_{LT}.CS2+ is similarly shown.

Note that plasmids are not drawn to scale.

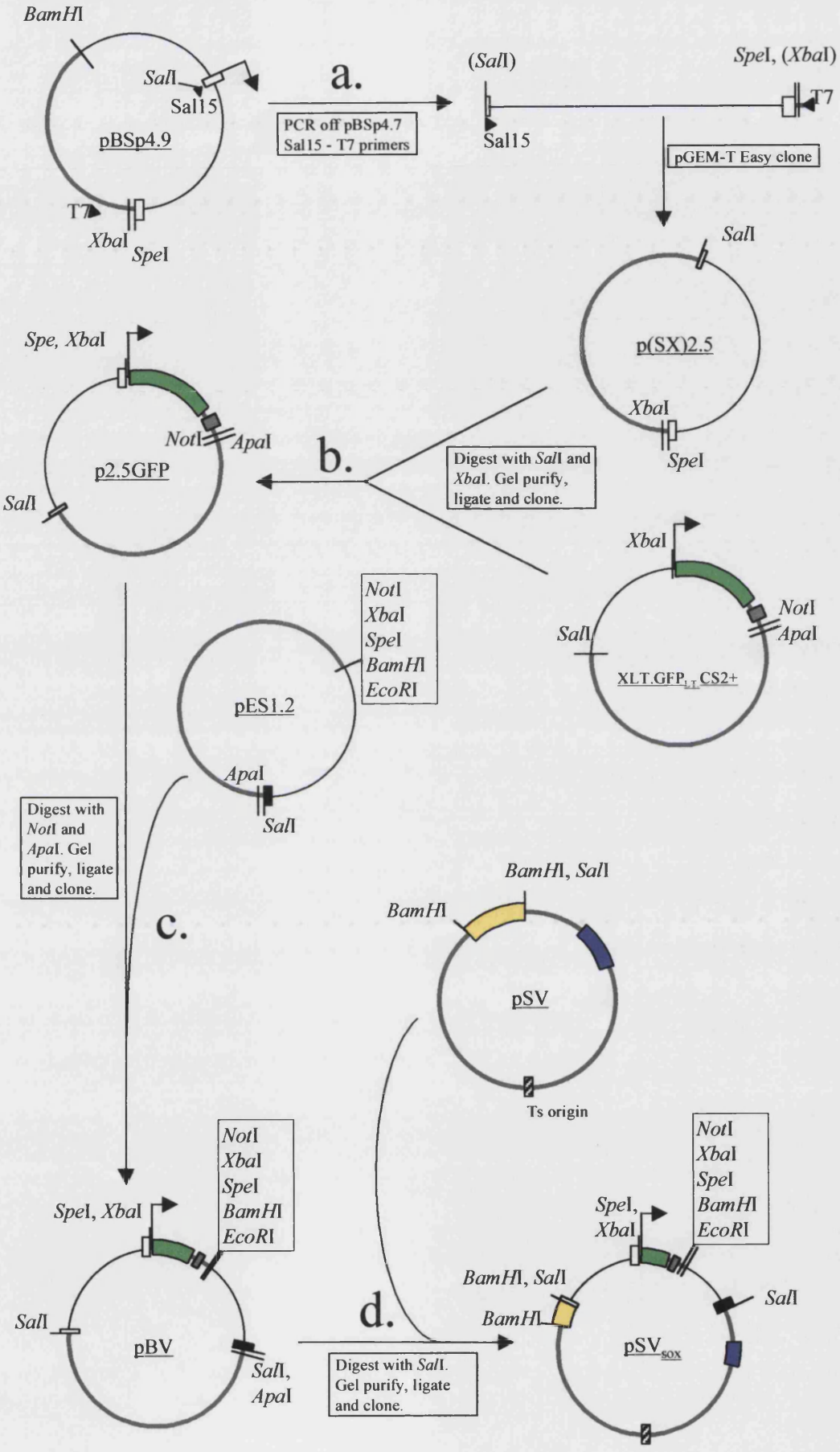
BamHI
SalI
Sal15
pBSp4.9
T7
XbaI
SpeI
a.
PCR off pBSp4.7
Sal15 - T7 primers
(SalI)
Sal15
SpeI, (XbaI)
T7
pGEM-T Easy clone
SalI
p(SX)2.5
XbaI
SpeI
Spe, XbaI
NotI
ApaI
p2.5GFP
SalI
b.
Digest with SalI and XbaI. Gel purify, ligate and clone.
XbaI
NotI
ApaI
SalI
XLT.GFP$_{LT}$.CS2+
NotI
XbaI
SpeI
BamHI
EcoRI
pES1.2
ApaI
SalI
Digest with NotI and ApaI. Gel purify, ligate and clone.
c.
BamHI, SalI
BamHI
pSV
Ts origin
NotI
XbaI
SpeI
BamHI
EcoRI
SpeI, XbaI
SalI
pBV
SalI, ApaI
d.
Digest with SalI. Gel purify, ligate and clone.
NotI
XbaI
SpeI
BamHI
EcoRI
SpeI, XbaI
BamHI, SalI
BamHI
SalI
pSV$_{sox}$

Figure 4.6 Cloning steps of pSV_{SOX}

Production of plasmids towards the cloning of pSV_{SOX}. Letters of all panels refer to the corresponding steps in Figure 4.5. In all parts, M indicates lanes containing 1kb ladder, with certain size bands indicted.

a. Lane 1: Product obtained by PCR using pBSp4.7 template and Sal15 and T7 primers. This product (arrow) contains the 3' half of exon 1, all of intron 1 and half of exon2 up to (but not including) the start of translation. This 2.5kb product will constitute the upstream ("A") homology arm.

b. This PCR product was cloned into pGEM-T Easy, producing p(SX)2.5. Digesting this plasmid with *SalI* and *XbaI* (Lane 3) allowed isolation of the PCR product (arrow) and cloning into XLT.GFP_{LT}.CS2+, similarly digested (Lane 1). This replaced the CMV promoter from the latter plasmid with the PCR product to produce p2.5GFP (shown in lane 2, also digested with *SalI* and *XbaI*).

c. Generation of pBV by introduction of the 3' homology arm into p2.5GFP. This arm comprises the 3' half of intron 2 and the 5' half of exon 3, and was isolated from pES1.2 by digestion with *NotI* and *ApaI* (Lane 3, open arrowhead). This was ligated into p2.5GFP similarly cut (not shown) to yield pBV. This latter plasmid is shown in Lane 1, digested with *NotI* and *SalI*, which releases the 1.2kb 3' homology arm, the 2.7kb vector backbone and a 3.4kb fragment containing the 5' homology arm and the *gfp* gene. p2.5GFP cut with *NotI* and *SalI* is shown in lane 2 for comparison.

d. Gel demonstrating the cloning of the approximately 4.6kb recombination cassette from pBV into pSV to produce pSV_{SOX}. This was achieved by isolating the cassette from pBV through *SalI* digestion and gel purification, and ligating to pSV similarly cut and treated with Shrimp Alkaline Phosphotase.
Lanes labelled with corresponding restriction enzyme digest above.
Lane 1: pSV_{SOX}. Lane 2: pBV. Lane 3: pSV
SalI digests of all three plasmids are shown in the first three lanes. pSV_{SOX} is composed of the 4.6kb recombination cassette from the pBV and the 11kb backbone of pSV. In addition, *XbaI* and double digests are also shown to demonstrate that all appropriate bands found in pBV are also present in pSV_{SOX}. In all cases, pSV_{SOX} is composed of the pSV backbone and bands from the recombination cassette. Note that some of the smaller bands of pSV_{SOX} are not visible on this gel due to insufficient loading, but their presence on the gel has been confirmed on other gels (not shown).

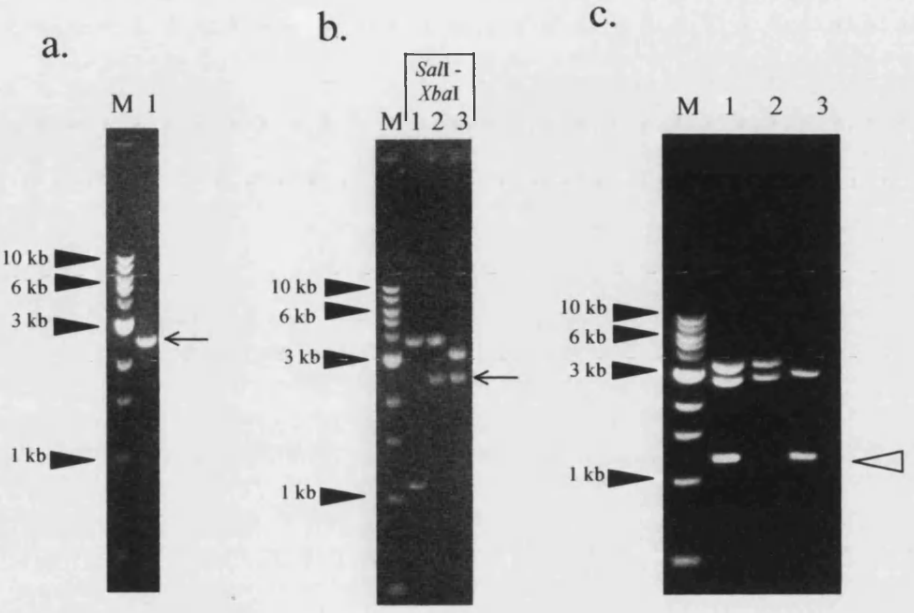
a.
M 1
10 kb
6 kb
3 kb
1 kb
b.
SalI - XbaI
M 1 2 3
10 kb
6 kb
3 kb
1 kb
c.
M 1 2 3
10 kb
6 kb
3 kb
1 kb

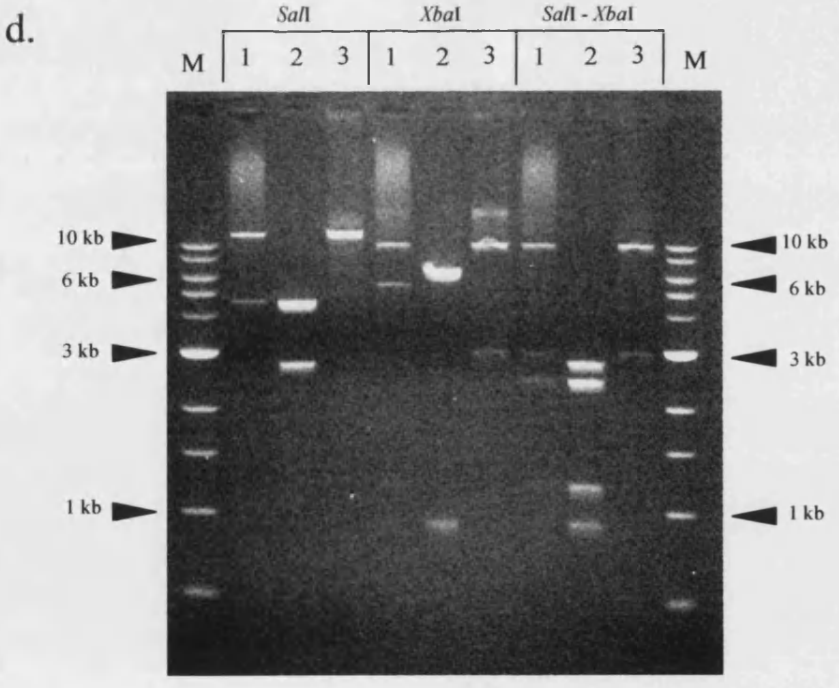
d.
SalI
XbaI
SalI - XbaI
M 1 2 3 1 2 3 1 2 3 M
10 kb
6 kb
3 kb
1 kb
10 kb
6 kb
3 kb
1 kb

checked by restriction digest (Figure 4.6d). With the Shuttle vector now ready, engineering of a *sox10* containing PAC could be attempted.

4.2.4.2. Identification of co-integrants

The first step of engineering a PAC involved introducing the Shuttle vector to the PAC host. This was achieved by making the PAC containing bacteria competent through standard calcium chloride treatment. The Shuttle vector pSV_{SOX} was now transformed in, again using a 37°C 2 minute heat shock, and co-transformants grown overnight at 30°C on dual selection (Tet and Kan). This gave a large number (~200) of colonies per plate.

To select for co-integrants where the Shuttle vector had integrated into the PAC, six co-transformant colonies were plated on dual selection and incubated at the restrictive temperature overnight (43°C). To identify correct co-integrants, PAC DNA from twenty of the large colonies obtained was prepared by miniprep, and digested with *Bam*HI. After gel electrophoresis and Southern blotting, the filter was probed with the 3' homology arm, "B". A simple schematic of the two possible co-integrant events are depicted in Figure 4.7 a, b, and allows prediction of band sizes on the Southern blot. Thus integration events at the "A" homology arm will give bands on the southern blot of 11kb and 7.8kb (Figure 4.7a), whilst recombination occurring at the other homology arm ("B") will give bands of 17kb and 3.9kb (Figure 4.7b). As can be seen on the Southern blot (Figure 4.7c), seven clones appear to represent integration at the "A" site (#s 5, 8, 11, 12, 17, 18, and 20) and only one clone has a restriction pattern indicative of recombination occurring at the "B" site (# 19). The difference in relative frequencies of recombination between the two homology arms may be due to their difference in size and/or sequence specific preference for RecA-mediated recombination. One lane (14) had two bands that did not match those expected from either recombination event, and might represent an erroneous recombination event elsewhere in the PAC or bacterial genome. All remaining lanes had a band equal in size to the original PAC, and thus probably represent clones where co-integration of the Shuttle vector did not occur. That they were tetracycline resistant might be due to the fact that pSV_{SOX} has remained in the cell, and that it might be able to replicate at a low level in the PAC host cell due to incomplete stringency of the temperature sensitive origin of replication (as reported by Gong *et al.* (2002a)). To complete the engineering of the PAC, it was necessary to resolve the co-integrants.

4.2.4.3. Resolving co-integrants

All eight correct co-integrants were streaked onto kanamycin plates and incubated at 43 °C overnight to allow resolution in some bacteria. To reveal resolved colonies, selection

Figure 4.7 ⟶

Figure 4.7: Generation and identification of co-integrants

Transformation of pBV into the host cell containing PAC I, followed by plating on dual tetracycline and kanamycin and growing at 30°C, selected for co-transformants. Co-integrants were selected for by growth of single colonies at 43°C also on dual selection. Southern analysis was used to identify successful integration events, as follows.

a. Recombination occurring at homology arm "A" will yield a co-integrant clone with *BamHI* (Ba) fragment sizes indicated. Upper plasmid on the left represents the original PAC I, whilst the lower plasmid represents pSV_{SOX}, with the temperature sensitive origin of replication and *recA* gene indicated. The targeting cassette is shown with homology arms (A', B') and the *gfp* gene. The targeted site on the PAC is similarly shown, as are two *BamHI* sites that flank the targeted region. Crossed lines depicts the site of recombination at the A homology arm. The distance between the *BamHI* sites on PAC I is approximately 10kb. The co-integrant generated is shown on the right, and expected sizes of *BamHI* fragments are shown. These are, however, only a subset of all the bands generated, as the remaining sites in the PAC are not shown. Bands that would hybridise to a homology arm "B" probe are indicated with an asterisk.

b. Recombination occurring at homology arm "B" will yield a co-integrant clone with *BamHI* fragments as shown on the right. Note that these differ from the fragments shown in **a.**, allowing differentiation of recombination events by Southern analysis.

c. Southern analysis of 20 putative co-integrant colonies. Following DNA purification, digestion with *BamHI*, gel electrophoresis and Southern blotting, correct co-integrants were identified by probing the blot with homology arm "B". Co-integrant colony numbers are indicated above lanes and run along side DNA from the original PAC I also digested with *BamHI*. As shown in **a.** and **b.**, the latter should give a hybridising band at approximately 10kb as seen in the final lane. A number of putative co-integrant lanes also show a single band of this size indicating that these do not represent clones containing the desired recombination event. However lanes 5, 8, 11, 12, 17, 18 and 20 have the two bands expected from a recombination event at site "A" (namely 11kb and 7.8kb), whilst one lane (19), had bands indicative of a recombination event at site "B" (17kb and 3.9kb). One lane (14) had two bands that did not match those expected from either recombination event, and might represent an erroneous recombination event elsewhere in the PAC or bacterial genome.

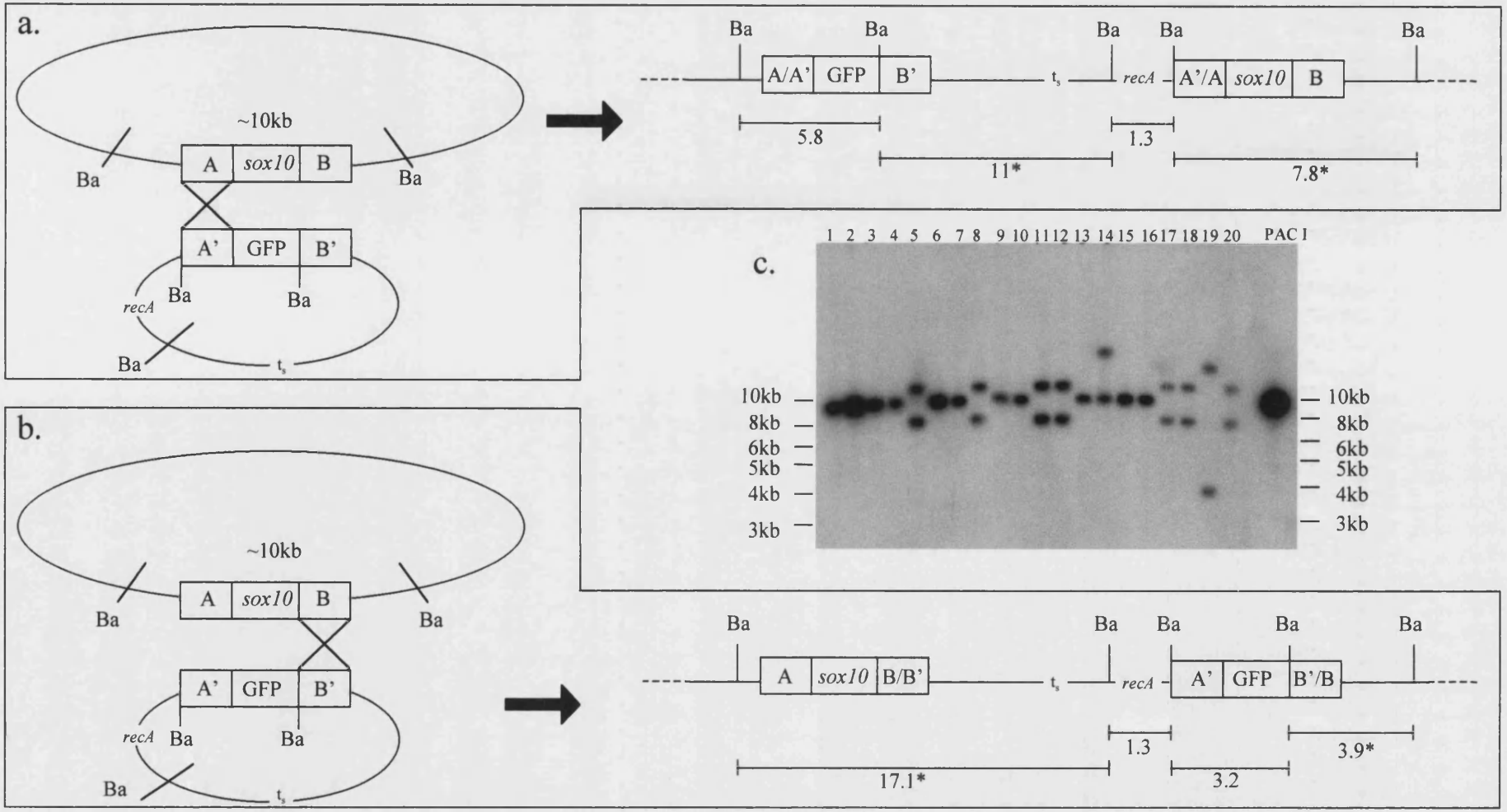
a.
~10kb
Ba
A
sox10
B
A'
GFP
B'
recA
Ba
Ba
Ba
t
A/A'
GFP
B'
A'/A
sox10
B
5.8
11*
1.3
7.8*
b.
~10kb
B/B'
A'/B
17.1*
3.2
3.9*
c.
1 2 3 4 5 6 7 8 9 10 11 12 13 14 15 16 17 18 19 20 PAC I
10kb
8kb
6kb
5kb
4kb
3kb

against the *TetR* gene was required. As previously discussed, this can be achieved by incubation with a chelator such as fusaric acid. Thus a number of putative resolved colonies from co-integrant #5 were incubated on Fusaric Acid and Kanamycin TB agar plates and derived colonies then tested for resolution (ie loss of tetracycline resistance). As all colonies grew on both Kan and Tet plates, it indicated that either the resolution did not occur or the fusaric acid mediated selection was ineffective. The latter seemed most likely as a control colony (an unresolved co-integrant) also grew on fusaric acid containing plates. Numerous attempts to optimise fusaric acid concentration for selection were undertaken. However they all proved unsuccessful and this approach was discontinued.

Another method for direct selection of Tetracycline sensitive colonies has been reported by Podolsky *et al.* (1996), who showed that the *tetR* gene confers sensitivity to nickel salts such as $NiCl_2$. Thus Kanamycin containing plates supplemented with 7mM $NiCl_2$ were made, onto which both putative resolved colonies of co-integrant #19 and an original PAC I control colony were streaked out. After overnight incubation at 37°C, both plates showed no growth, so a titration series of lower $NiCl_2$ concentrations was tried to test for differential survival based on genotype. Whereas high concentrations of $NiCl_2$ was toxic to cells irrespective of genotype, low concentrations did not seem to produce any difference in survival between the control and experimental plates. At 2.4mM, there was approximately twice the number (30) of colonies on the control plate as on the putative resolved co-integrant plate. These sixteen colonies were tested for resolution by assessing if they were tetracycline resistant. Although all were Kan^+, 5 out of the 16 were tetracycline sensitive, indicating possible resolution.

To test if this was the case, and to distinguish correctly resolved PACs from the original PAC, Southern analysis of PAC DNA from each clone was conducted. Figure 4.8a shows the sizes of some of the expected *Bam*HI and *Spe*I fragments obtained by digesting resolved PAC DNA. It is evident that a correctly resolved PAC should contain the *gfp* gene (in contrast to the original PAC), as well as showing a smaller fragments hybridising with homology arm "B". Accordingly, Southern analysis using a *gfp* probe indicated that only resolved clones #4 and 5 gave *gfp* hybridising bands of expected size, whilst the three other clones showed no hybridisation (Figure 4.8b). Stripping this blot and re-probing with the 3' homology arm, "B" (Figure 4.8b), supported the inference that colonies 1, 2 and 3 appeared to have reverted back to the original PAC I, whilst colonies 4 and 5 were correctly resolved. Thus the first three clones had *BamH*I and *Spe*I bands of approximately 10kb and 8.8kb on this blot as expected, whilst clones #4 and 5 had smaller *BamH*I and *Spe*I bands of 3.8kb and 7.5kb (Figure 4.8b).

Figure 4.8 →

Figure 4.8: Resolving co-integrants to produce PACIGFP

Resolution of co-integrants was achieved by growth in kanamycin at the restrictive temperature (43°C), followed by selection on $NiCl_2$ containing agar (see text). Five colonies were obtained from selection of bacteria obtained from resolution of co-integrant number 19 (the single co-integrant formed by recombination at site "B"), all proved to be kanamycin resistant and tetracycline sensitive as expected for resolved PACs.

a. Resolution of co-integrant #19 can occur, either through homology arm "B" again in which case it reverts to the original PAC I, or through the other homology arm "A", as shown as crossed lines between the sites. The latter produces the desired targeted clone, shown below, where the first part of the *sox10* coding region has been replaced by the *gfp* gene. This gene contains *BamH*I and *Spe*I sites at its 3' end, such that Southern analysis and restriction polymorphisms can be used to distinguish between the two possible resolved PACs, which differ by the presence of this gene and these two novel sites in the targeted PAC. The original PAC I is also shown for comparison, and sizes of certain restriction fragments which hybridise to a *gfp* probe or the homology arm "B" probe are shown.

b. Southern blot of the 5 resolved PAC clones, digested as shown and hybridised with a *gfp* probe (left panel) or the homology arm "B" probe (right panel). In both panels, lanes containing the original PAC I, similarly digested, are shown for comparison. Lanes labelled M contain a 1kb DNA ladder, with some bands and corresponding sizes indicated. The first three resolved PACs do not show hybridisation to *gfp*, whereas the last two (numbers 4 and 5) do. Fragment sizes are as expected (approximately a 5.9kb *BamH*I fragment and a 1kb *Spe*I fragment). The plasmid XLT-GFP_{LT}-CS2+ is also shown as a positive control, which has been digested with *Xba*I and *Not*I to release the *gfp* gene. Upon using the homology arm "B" probe, the expected restriction fragment polymorphisms are obtained, such that the correctly resolved PACs have approximately 3.8 and 7.5kb hybridising *BamH*I and *Spe*I fragments respectively, whilst those which have reverted to the original form show 10 and 8.8kb bands using these restriction sites (compare to the PAC I control lane).

c. To check that the engineered PAC carried the modification desired, and not any gross rearrangements, RFLP analysis was performed to compare PACIGFP with the original PAC I. This was done using *BamH*I (B), *Eco*RI (E), *Sal*I (S), *Spe*I (Sp) and *Xba*I (X), as shown. It is clear that although some bands sizes are altered, many bands are common between the two PACs, suggesting no gross rearrangement has occurred.

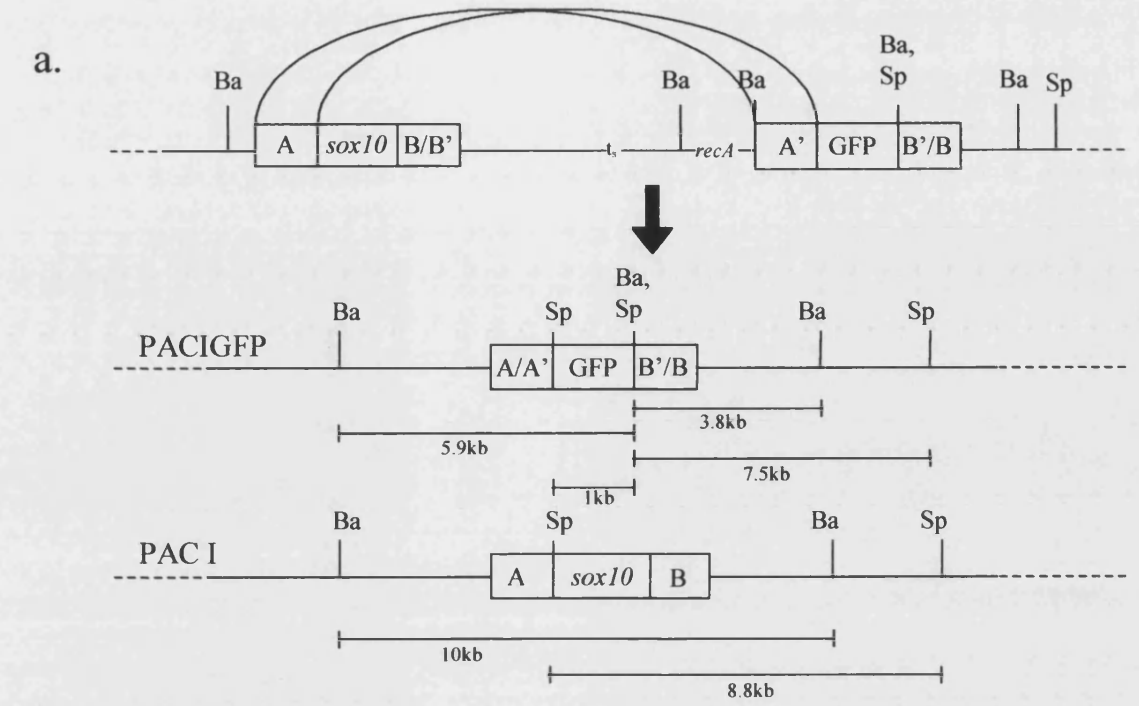
a.
Ba
Ba
Ba
Ba,
Sp
Ba
Sp
A
sox10
B/B'
recA
A'
GFP
B'/B
Ba,
Sp
Ba
Sp
Ba
Sp
PACIGFP
A/A'
GFP
B'/B
3.8kb
5.9kb
7.5kb
1kb
Ba
Sp
Ba
Sp
PAC I
A
sox10
B
10kb
8.8kb

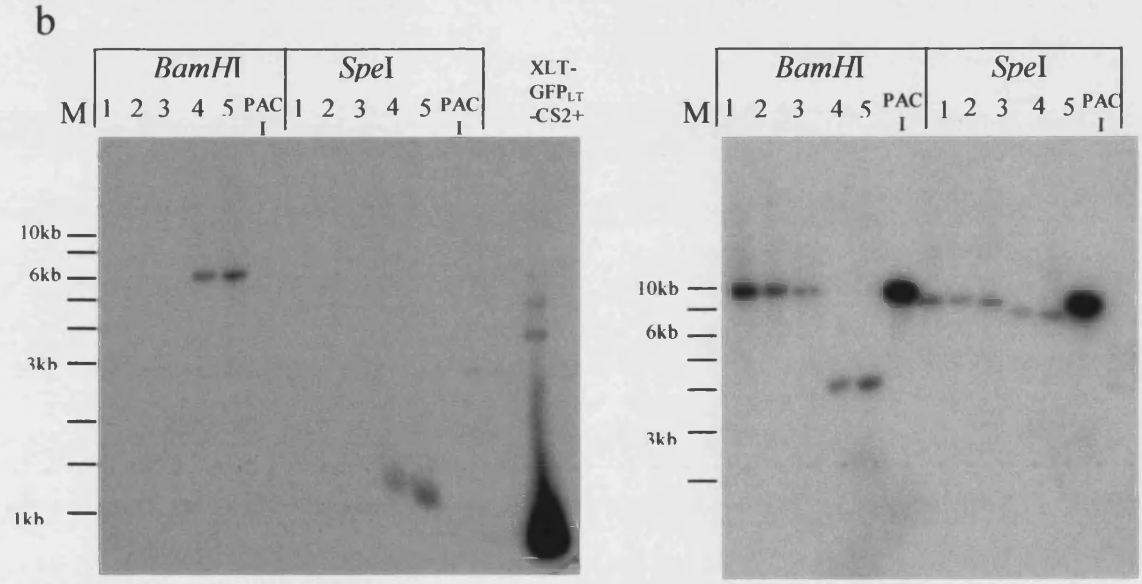
b
BamHI
SpeI
M
1 2 3 4 5 PAC I
1 2 3 4 5 PAC I
XLT-GFPLT-CS2+
10kb
6kb
3kb
1kb
BamHI
SpeI
M
1 2 3 4 5 PAC I
1 2 3 4 5 PAC I
10kb
6kb
3kb

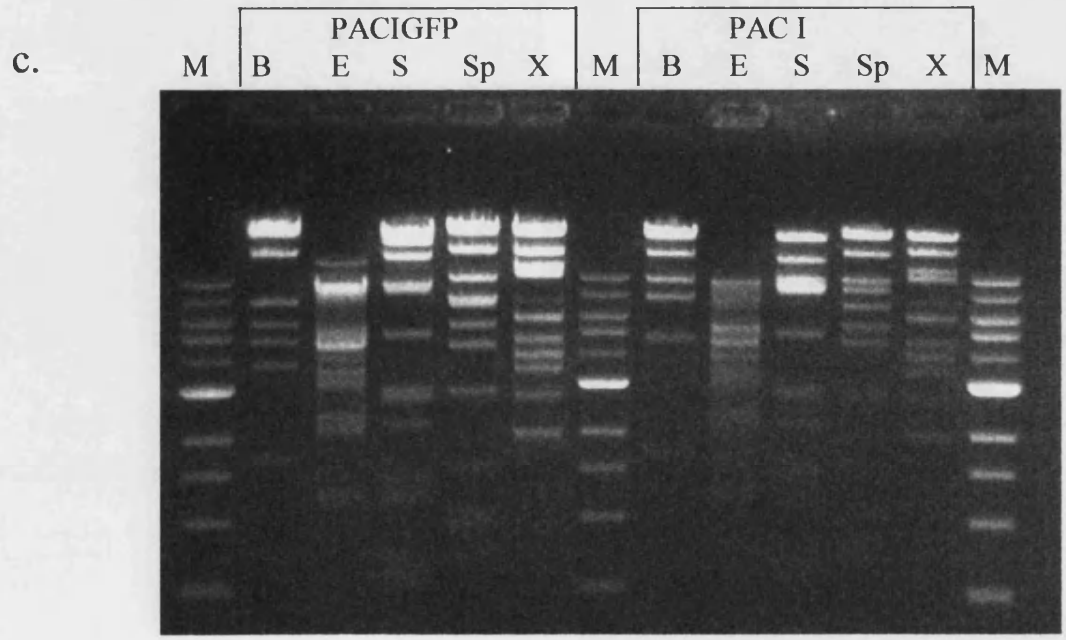
c.
PACIGFP
PAC I
M
B
E
S
Sp
X
M
B
E
S
Sp
X
M

To ensure the transient presence of the recombinase in the PAC had not caused undesired rearrangements, restriction fingerprints of one of the modified PAC clones (#4) was compared to that of the original PAC. As can be seen in Figure 4.8c, although a number of bands are different between the original and modified PACs, as expected through modification, there are also a large number of bands in common, indicating that there has not been severe rearrangement of the PAC. It was thus concluded that the PAC represents a correctly modified construct, namely a GFP reporter flanked by approximately 33kb upstream and 41kb downstream of the *sox10* transcribed region. The modified PAC was named PACIGFP and a crude map, based on the known maps of PAC I and the recombination cassettes, is shown in Figure 4.9a.

To determine if the construct is functional as a *sox10* reporter, transient analysis was performed by injecting PACIGFP into 1-cell embryos and inspecting post-neurulation for expression. Figure 4.9b shows a 24hr embryo injected with approximately 30pg of PACIGFP, showing expression in head and trunk neural crest, as well as epithelium of the ear (enlarged inset; upper panel). In one embryo, expression was also noted in Schwann cells along the posterior lateral line nerve (Figure 4.9c). Note that expression is also evident in the ear (asterisk) and in migrating pigment cells such as a presumptive xanthophore (arrow). Expression was also noted in the CNS and jaw cartilage (not shown).

Surprisingly, expression in muscle was again apparent (Figure 4.9d). This was unexpected as it was assumed that the PAC construct would contain the muscle repressor element, which was missing in the smaller two constructs. Although it is feasible that such a repressor exists and lies outside the region included in the PACIGFP construct, it seems less likely with such a large construct. This ectopic expression might have other causes, other than lack of repressor elements. It is possible that repressor elements are present, but are unable to function effectively in an unintegrated state. This might be due to these repressors acting through a chromatin remodelling mechanism, and functioning only on chromosomal DNA. Alternatively, copy number cannot be controlled for in these experiments. The number of transgene copies inherited by each cell in these transient experiments might be beyond that which can be effectively silenced. With this in mind, it was hoped that germline transgenic embryos would not show this ectopic expression.

4.2.4.4. Linearising PACIGFP – Generating PACIGFP2

To produce stable transgenic zebrafish carrying the PACIGFP construct, it was necessary to linearise the PAC. There are two rare cutting restriction sites reported in the backbone of the original PAC genomic library vector (pCYPAC6), *Not*I and I-*Sce*I. The former site is present within both the *sox10* gene sequence (see Fig. 3.3), and in the

Figure 4.9 ⟶

Figure 4.9: Crude map and transient analysis of PACIGFP

a. A crude map of the engineered reporter PACIGFP is shown. This flanks the reporter gene (green box) with approximately 33kb of upstream and 41kb of downstream sequence surrounding the *sox10* transcription region. Sites for *Not*I (N) and *Sal*I (S) are shown, with those present on the vector sequence given in brackets. The approximate transcription start site is given as an arrow.

b. Images photographed under fluorescent light of transient assays performed using the PACIGFP construct to assess ability of the reporter to drive GFP expression, and the domains yielded.
An anterio-lateral image of an injected embryo at approximately 24hpf. Migrating neural crest cells are evident (arrowheads), as is expression in the otic placode (asterisk; magnified inset).

c. An example of an injected embryo at 2dpf. GFP is seen strongly in the ear (asterisk), as well as in migrating pigment cells in the head, over the eye and in the trunk. Striking expression is also seen in cells along the posterior lateral line. This was seen very rarely in transient analyses, but is consistent with the known expression of *sox10* in this cell type. Fluorescent image is shown in the left panel, which is overlaid on a brightfield image in the right panel. The fluorescent image is magnified in the bottom panel, showing expression in cells with a morphological appearance of Schwann cells. Expression in a single xanthophore is also evident (arrow).

d. Surprisingly, muscle fibres were again GFP^+. Fluorescent image is presented in the left panel of an embryo at 24hpf, with an overlay onto a brightfield image in the right panel.

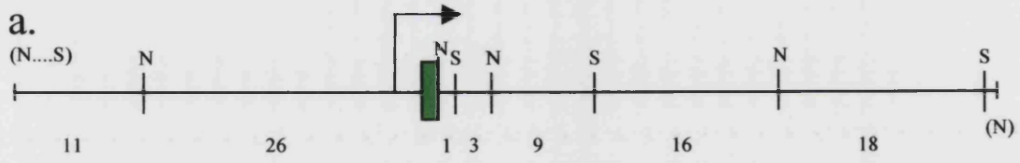

b.

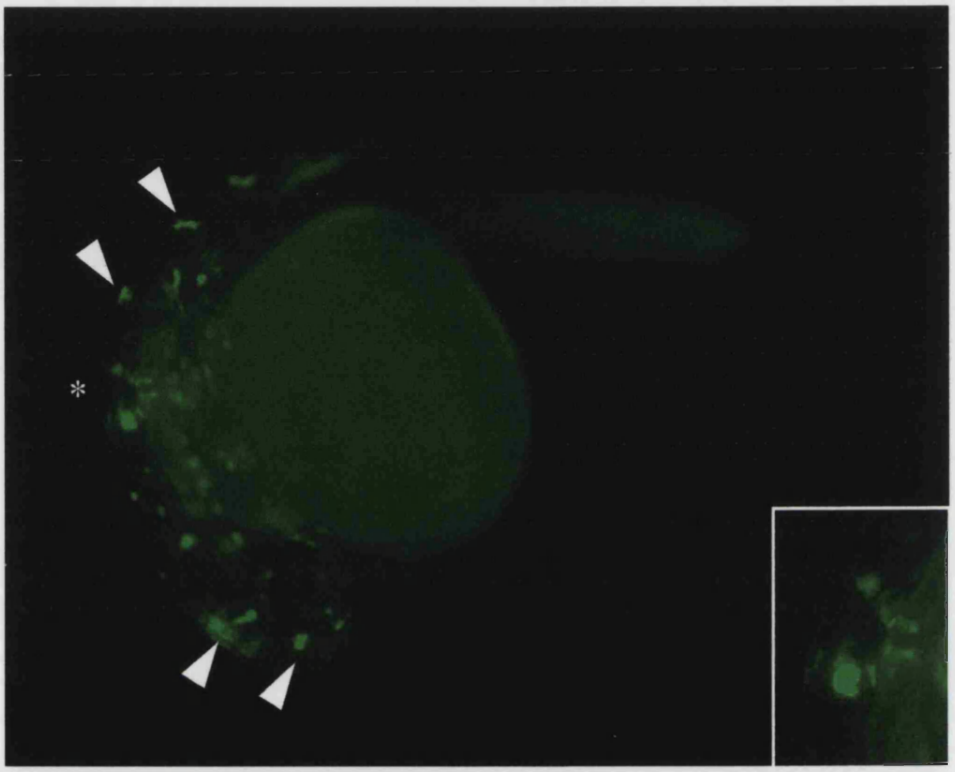

c.

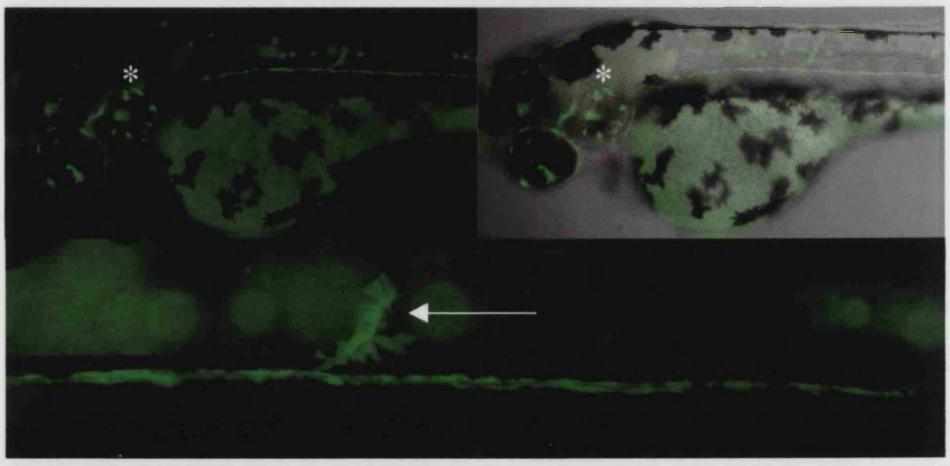

d.

transgene engineered into the PAC (Figure 4.5), and thus cannot be used to linearise the construct. The latter site is a 25bp recognition site for the intron-encoded meganuclease, I-*Sce*I. Attempts to cut PACIGFP with this enzyme failed, despite the enzyme successfully cutting control DNA supplied by the manufacturer (not shown). It was decided to check the integrity of the site in the vector by sequencing. Primers PACF and PACR were designed to allow amplification of the region containing this site on the vector, and the resulting PCR product was sequenced directly (Figure 4.10a). There are clear discrepancies between the published sequence of pCYPAC6 and the derived sequence as shown by alignment in Figure 4.10a. The sequence boxed represents the I-*Sce*I site and is clearly missing in the sequence obtained from direct sequencing of the vector. The likeliest explanation for this discrepancy is that the genomic library used was actually built in an earlier vector (such as pCYPAC2), which does not posses this meganuclease site (Figure 4.10a).

To introduce restriction sites into the vector backbone of PACIGFP, the GPS™ -1 Genome Priming System from NEB was employed. This is a transposon-based system which uses a transposase to transfer an engineered transposon from a donor plasmid randomly into a target plasmid, BAC or PAC. The transposon contains the chloramphenicol antibiotic resistance gene, allowing selection of product DNA molecules, as well as the meganuclease sites, I-*Sce*I and I-*Ceu*I, the introduction of which should allow easy linearisation of PACIGFP.

The reaction was performed as per manufacturers instructions using pGPS2.1 donor plasmid and the PACIGFP construct as a target, although with modification of product selection criteria. As insertion site is random, it was desirable to select for product molecules where the transposon integrated into the vector backbone of PACIGFP. Otherwise the transposon might disrupt a crucial regulatory region of the transgene and could affect the expression pattern. This directed approach was achieved by targeting the kanamycin resistance gene in the PAC vector. Thus, after transformation of the completed reaction into electrocompetent bacteria, selection for product molecules was performed solely on chloramphenicol, and not on dual selection of kanamycin plus chloramphenicol as recommended. The 115 colonies thus obtained were then tested for kanamycin sensitivity by replica plating on kanamycin plates. This identified any colonies which were chloramphenicol resistant but kanamycin sensitive due to insertion of the transposon into the Kan^R gene, thus disrupting its action and replacing it with Cm^R. As the kanamycin resistance gene is approximately 1kb and PACIGFP is in total about 110kb, an insertion in the kanamycin gene was expected once approximately every 110 insertion events. This

Figure 4.10 ⟶

Figure 4.10: Linearising PACIGFP via production of PACIGFP2

a. The integrity of the I-*Sce*I site in the PAC vector was checked by PCR amplification of the region using primers PACF and PACR (Table 2.4), and subsequent sequence analysis of the product. Part of the sequence obtained is presented on the top line, and is compared to the corresponding sequence from the library vector (reported as pCYPAC6, lowest sequence) and an earlier version of the vector (pCYPAC2, middle sequence). It is clear that the PACIGFP vector lacks the I-*Sce*I site as reported. It follows that the zebrafish PAC library was probably created in an earlier vector. To linearise the engineered PAC, a transposon-mediated introduction of unique sites was undertaken.

b. Following the re-engineering of PACIGFP to produce PACIGFP2, the ability to linearise the vector with I-*Sce*I was tested. Shown is a PFG of single and double digests of PACIGFP2 cut with *Xba*I and/or I-*Sce*I, along with uncut PACIGFP2 DNA.
Lane M: High Molecular Weight Markers; certain sizes shown.
Lane 1: Undigested PACIGFP2
Lane 2: PACIGFP2 digested with I-*Sce*I
Lane 3: PACIGFP2 digested with I-*Sce*I and *Xba*I
Lane 4: PACIGFP2 digested with *Xba*I
Whereas the undigested lane shows three bands, with additional bands due to supercoiled DNA species, the I-*Sce*I cut DNA shows only one band of approximately correct size. Double digestion with *Xba*I showed a difference compared to the single *Xba*I digest lane, with a 38kb band (asterisk) present in the *Xba*I lane cut by I-*Sce*I into 24 and 14kb bands (arrows), further demonstrating successful digestion of the vector by I-*Sce*I. No other *Xba*I bands were digested. Linearisation allowed attempts to generate a transgenic line carrying this construct.

a.

```
PAC PCR GACAGTGCTCCGAGAACGGGTGCGCATAGAAATTGCATCAACGCATATAGCGCTAG----------------------CA
pCYPAC2 ..................................................................----------------------..
pCYPAC6 ..................................................................TAGGGATAACAGGGTAATCTAG..
                                                                          I-SceI

PAC PCR GCACGCCATAGTGACTGGCGATGCTGTCGGAATGGACGATATCCCGCAAGAGGCCCGGCAGTACCGGCATAACCAAGCCT
pCYPAC2 ...........................................................................................
pCYPAC6 ...........................................................................................

PAC PCR ATGCCTACAGCATCCAGGGTGACGGTGCCGAGGATGACGATGAGCGCATTGTTAGATTTCATACACGGTGCCTGACTGCG
pCYPAC2 ...........................................................................................
pCYPAC6 ...........................................................................................

PAC PCR TT-AGCAATTT-AACTGTGATAAACTACCGCATTAAAGCTTATCGATGATAAGCTGTCAAACATGAGAATTGATCCGGAA
pCYPAC2 ..T........T.....................................................................C......
pCYPAC6 ..T........T.....................................................................C......

                    loxP
PAC PCR CCCTTAATATAACTTCGTATAATGTATGCTATACGAAGTTATTAGGTCCCT
pCYPAC2 ..................................................
pCYPAC6 ..............C...................................
```

b.

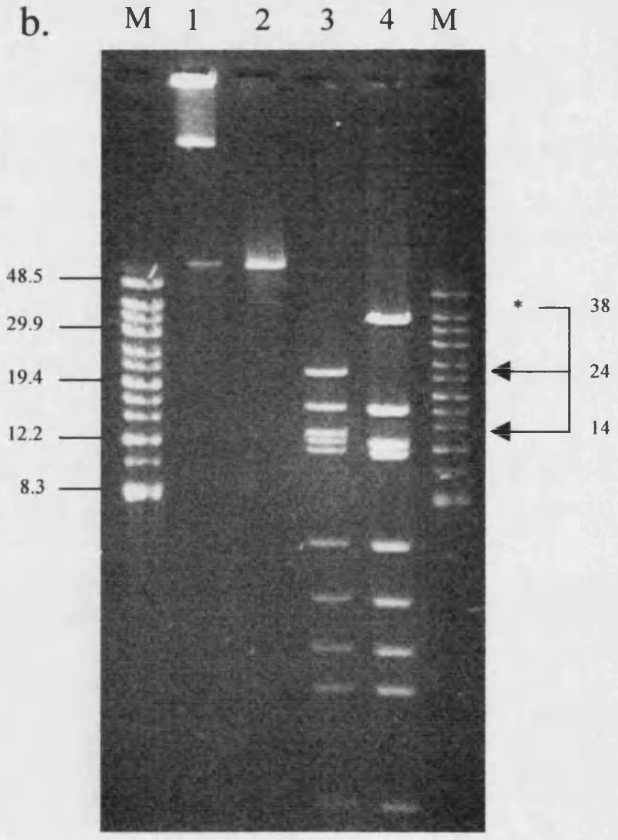

compares to the rate achieved experimentally as two of the 115 colonies tested were Kan sensitive.

The presence of the transposon in the vector of PACIGFP was confirmed by molecular techniques. PACIGFP2 DNA was digested singly with I-*Sce*I and *Xba* and also doubly with both enzymes. These reactions were run on a PFG along with uncut PACIGFP2 DNA to check for the I-*Sce*I site. This gel is shown in Figure 4.10b and clearly demonstrates both the presence of the site and that it can be used to linearise the construct successfully. This new construct was checked for functional ability to direct GFP expression in appropriate sites in the embryos. No difference in GFP expression pattern between PACIGFP and PACIGFP2 was evident in transient analyses (data not shown).

4.2.5. Production of transgenic zebrafish

As stated earlier, production of germline transgenics carrying a *sox10* GFP reporter would be of benefit to understanding the functions of sox10 as well as a live label of neural crest cells. Towards this end, 3 reporter constructs have been produced and all show correct expression in a number of *sox10* domains in transient analyses. Unfortunately, they also drive expression ectopically in certain cell types such as skeletal muscle, and it was considered that this might be problematic for some of the experiments planned if this was still seen in the germline transgenics (e.g. GFP expression in all skeletal muscle might obscure visualisation of neural crest cells).

What could cause this expression in muscle? It could be argued that the muscle expression seen here is not in fact ectopic, but that the GFP reporter assay is more sensitive at detecting sites of low promoter activity than the *sox10 in situ*. This would mean that promoter activity in muscle would be at far lower levels than that in neural crest, but there is no evidence for this from any of the transient GFP analyses, as expression in muscle cells is often just as bright as expression in neural crest cells. It might also be argued that the vector DNA could be influencing promoter expression, although transient analyses, where the vector is removed completely also produce muscle expression (not shown). If the muscle expression is truly ectopic, then lack of effective repression can be the only explanation. While it is possible that repressor elements necessary for silencing expression in ectopic cell types lie beyond the regions used in these reporters, it would mean they exist outside sequences found in PACIGFP (i.e. more than 37kb upstream and 40kb downstream of the *sox10* gene). If true this would require the engineering of a much larger *sox10*-containing genomic clone such as a YAC, an undertaking beyond the scope of this work. Another explanation for the ectopic expression seen could be that the normal repressor elements are present, but not able to function properly during the transient

transgenic assay. There may be two reasons for this. Firstly, repression might depend on some form of chromatin remodelling and thus need integration of the transgene into chromosomes for effective silencing. Secondly transgene copy number is variable in transient experiments due to mosaicism. It might be that the cells showing ectopic expression have, by chance, inherited a very large dose of the transgene, swamping or titrating out any repressor complexes needed for silencing. Whereas the endogenous *sox10* promoter is present in two copies per cell, the reporter transgene might be present in thousands of copies, conceivably more than can be silenced. It was hoped that integration of a moderate number of transgene copies could allow repession to work correctly in germline transgenics.

Attempts to produce transgenic lines carrying the three reporters followed a simple procedure. Following linearisation by restriction digestion, the DNA was purified with Microcon™ filter units and diluted to approximately 6ng/µl. Embryos from wild-type incrosses were injected as early after fertilisation as possible, and no later than 2-cell stage. Injection amounts were such as to obtain about 70% deformity rates, generally around 50 to 80 pg of DNA per embryo. A total of approximately 3000 embryos were injected for each construct and, after discarding malformed embryos, those with the best coverage of transgene as assayed under a fluorescent dissecting scope, were selected for rearing. These numbered approximately 100 to 150 embryos per construct and, allowing for some death of larvae during rearing, provided between 80 and 100 adult fish per construct. To identify transgenic founders, a batch of fish injected with each construct were crossed *inter se* and their progeny screened between 1 and 3 days under a fluorescent dissecting scope, ensuring at least 50 offspring per pair were screened. Positive founders have been identified for each construct mentioned above, however expression levels are quite divergent, and due to time constraints, not all lines have yet been firmly established or thoroughly analysed.

4.2.5.1. p4.9 :GFP

The p4.9:GFP construct, prepared as described above, was injected into one-cell stage embryos. Embryos with the best coverage of GFP positive cells were selected during later embryogenesis, and raised to adulthood. Almost all of the surviving adults were successfully screened for germline transmission. Out of 77 screened, one female founder produced offspring showing GFP expression in a *sox10* pattern. The average percentage of transgenic embryos this female founder produced per clutch was 6.5% indicative of the mosaic nature of the integration in the germ cells. All these F1 embryos transmitted the transgene in Mendelian fashion when outcrossed, with an average of 47% transgenics in

the F2 generation. Mendelian ratios have been observed in all subsequent generations, and the line, now named sox10-4.9:GFP, is now into its fourth generation.

All analysis reported for this line was conducted on hemizygous embryos produced by outcrossing F2 adults. First expression of GFP was detectable at approximately 1-2 somite stage (~10.5hpf), in anterior regions of the neural plate, identical to the first site of *sox10* expression detected by *in situ* (Pauliny, 2002). This is shown in a lateral view of a 3 somite stage (~11hpf) embryo under both transmitted and fluorescent light in Figure 4.11a. Viewing dorsally demonstrates that GFP^+ cells lie in lateral positions of the neural plate, in a position consistent with nascent neural crest. These cells appear to be converging dorsally, into a more medial position (Figure 4.11b, left panel). Slightly later, at approximately 5 somite stage (~12hpf), this domain of GFP expression has extended posteriorly, following the anterior-posterior direction of neural crest generation. A magnified view of this domain is shown in Figure 4.11c showing these cells near to the neural tube. Viewed dorsally these cells can be seen almost covering the neural tube at this axial level (Figure 4.11b, right hand panel). Coverage is not complete however, and "holes" in GFP expression are apparent in this last panel. Whether this indicates an absence of a neural crest cell at this site, or a GFP^- neural crest cell, remains to be determined.

As development proceeds, the premigratory neural crest expression domain broadens and extends more posteriorly (Figure 4.11d). Viewing dorsally at this stage, the GFP^+ neural crest can be seen covering the neural tube, extending anteriorly to the axial level of the eye field (Figure 4.11e). The expansion of GFP expression in the neural crest continues to extend further posteriorly during somitogenesis (Figures 4.11f and g), until GFP^+ premigratory neural crest can be seen the entire length of the embryo at approximately 18hpf.

At approximately the 11 somite stage (~14.5hpf), cranial neural crest can be seen beginning to migrate ventrally away from this position (indicated on Figure 4.11f). Trunk neural crest also begins to migrate not long afterwards (beginning at approximately 14 somite stage (16hpf; not shown). This compares closely with the timing of migration in the trunk reported previously as approximately 15.5-16hpf (Raible *et al.*, 1992). Due to its distribution throughout almost the entire cell, GFP allows visualisation of cellular processes and filopodia. An example of such a process in a premigratory neural crest cell from a 12 somite stage (~15hpf) embryo is indicated in Figure 4.12a. There have been some limited studies on the behaviour of these filopodia during neural crest migration in zebrafish (Jesuthasan, 1996); that they are readily visible in live embryos derived from this

Figure 4.11; Figure 4.12 →

Figure 4.12: Expression of sox10-4.9:GFP from 15hpf to 22hpf

GFP expression pattern in the sox10- 4.9:GFP line at certain stages between 12 somite stage (15hpf) and 22hpf. All figures are lateral views with dorsal up and anterior to the left. Parts **a.**, **b.**, and **d.** are projections of individual z-series taken by confocal microscopy. Parts **c.** and **e.** show images taken by both fluorescent microscopy and under Nomarski optics, and include overlays of the former onto the latter. In all parts, the stage of the embryo is given.

a. GFP expression in premigratory cranial neural crest cells at the 12 somite stage (15hpf) allows visualisation of filopodia (arrows), just as these cells begin to migrate.

b. Slightly later at 16hpf, GFP^+ cranial neural crest cells can be seen migrating and dispersed in the head, and neural crest cells beginning to migrate in the anterior trunk, whilst the tail neural crest cells remain in a dorsal, premigratory position.

c. By 20hpf, GFP^+ trunk neural crest can be clearly seen migrating on the medial pathway in the trunk (arrows), whilst GFP^+ cranial neural crest can be seen both dispersed in the head, and present in the nascent branchial arches (arrowheads). Notable is the absence of expression in the ear, highlighted by an asterisk. An embryo photographed under fluorescence (top panel) and Nomarski optics (middle panel) is shown with the combined overlay (bottom panel).

d. Enlarged view of the GFP^+ cranial neural crest cells in the head of a 20hpf embryo. Crest cells are starting to migrate over the eye, and can be seen populating the branchial arches (arrowhead).

e. Trunk and tail neural crest cells migrating medially follow well-defined paths alongside the somites, and generally do not cross over into the neighbouring somite axial level. Fluorescent (left panel), Nomarski (middle panel) and overlaid images of the posterior trunk neural crest cells of a 22hpf embryo are shown. GFP^+ cells can be seen migrating ventrally in stripes aligned with the myotomes.

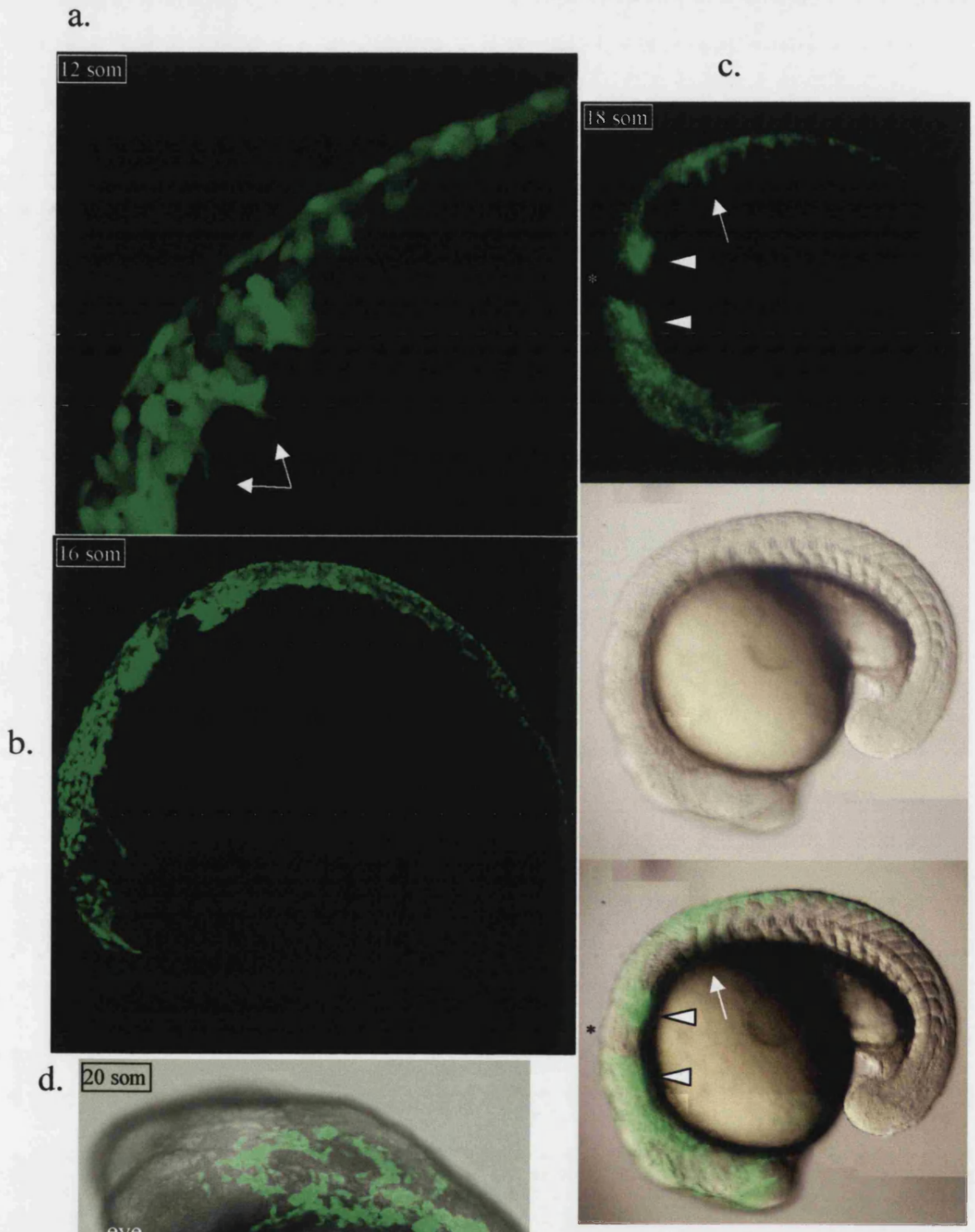
a.
12 som
c.
18 som
16 som
b.
d.
20 som
eye
e.
22hfp

GFP line suggests that it might prove a useful resource for future work in this area, and in detailed analysis of cellular behaviour in response to chemoattractive or repulsive stimuli.

By 20hpf, migrating cranial neural crest cells are clearly visible with GFP (Figure 4.12b, c and d). It is also apparent that whilst the anterior neural crest is migrating, the tail neural crest cells remain GFP^+ and in a premigratory position at this stage. Medially migrating crest cells in the trunk, do so at a specific rostro-caudal position relative to each somite as shown in Figures 4.12c and e, and as previously reported (Raible *et al.*, 1992). At this stage there is also clear expression in neural crest migrating within the branchial arches (Figure 4.12d). This is surprising, as *sox10* message cannot be detected here by *in situ* hybridisation (Pauliny, 2002). Additionally, whilst there is apparent ectopic expression in branchial arches, there is no visible expression in the ear at this stage. This is also surprising as the ear represents the strongest site of *sox10* expression during this period when analysed by *in situ* (Pauliny, 2002), and the transient analysis showed strong expression at this site (see previously).

At 24hpf, the expression domains remain essentially the same as that of the 20hpf embryo. Anteriorly in the head and trunk, neural crest cells are labelled with GFP and migrating ventrally, whilst premigratory cells are still apparent in the tail (Figure 4.13a and b). As mentioned earlier, medially migrating neural crest cells follow well-defined paths alongside each somite, and can be seen in the anterior trunk (Figure 4.13b). Neural crest cells migrating on the lateral pathway can also be seen in the trunk, and unlike those migrating medially, these cross projected somite boundaries (Figure 4.13c). Meanwhile, premigratory neural crest in the tail is developing filopodia as it starts to migrate (Figure 4.13e). Expression in neural crest migrating in the branchial arches is also clear at this time (Figure 4.13d). This image also displays GFP expression in other sites including migrating neural crest cells (including one beginning to melanise as indicated by the presence of melanin granules), and cells surrounding the forming posterior lateral line ganglion. The interior of this ganglion is populated by neurons and is GFP^-. Expression in Schwann cells of the posterior lateral line nerve can be seen at this stage as well (not shown), providing an easy method for prim staging these embryos.

Low levels of GFP expression in epithelial cells of the otic vesicle are also evident (Figure 4.13d). Thus this promoter element appears to drive GFP expression strongly in the neural crest, but only weakly in the otic epithelium. This is in direct contrast to *sox10* mRNA levels, which appear to be stronger in the otic vesicle than the neural crest (Pauliny, 2002).

Putative neurons of the olfactory bulb also start to express GFP at about 24hpf, (Figure 4.13f). This was first noted during transient reporter analyses (J. Dutton, pers. comm.).

Figure 4.13 ⟶

Figure 4.13: Expression of sox10-4.9:GFP at 24hpf

GFP expression pattern in the sox10- 4.9:GFP line at 24hpf. All figures are lateral views with dorsal up and anterior to the left. All images were taken by confocal microscopy except for those in **a.** and **e.**

a. Overview of the expression pattern in a 24hpf embryo, showing GFP expression viewed under fluorescence (left panel), a DIC image (middle panel) and an overlay of the two (right panel).

b. A confocal projection of GFP expression in a 24hpf embryo showing sites of expression, including streams of medially migrating neural crest cells in the anterior trunk (solid arrows), premigratory neural crest in the tail (open arrow) and neural crest cells in the branchial arches (solid arrowheads). Lack of expression in the ear (asterisk) and ectopic muscle expression (open arrowheads) was surprising and in contrast to *in situ* data.

c. Magnified image of the muscle expression seen in the anterior trunk at this stage (open arrowheads). Neural crest cells migrating on the lateral pathway can be seen (solid arrows).

d. Magnified image of the otic vesicle region in a sox10-4.9:GFP embryo at 24hpf. Relatively faint expression in the otic vesicle (o) is apparent at this magnification, but in contrast to the abundant *sox10* signal obtained by *in situ* analysis. Cells (probably some form of glia) encapsulating the posterior lateral line ganglion (g) are also labelled, whilst the core of the ganglion (comprised of neurons) is GFP^-. Migrating neural crest cells are also apparent with one labelled (mc). Cells beginning to melanise (evident by melanin granules) are also labelled by GFP (m). Expression in the neural crest cells migrating through the branchial arches (a) is also clear in this image.

e. Image of the tail of a transgenic embryo at 24hpf in which GFP^+ tail neural crest cells are beginning to extend filopodia and migrate away fom the premigratory position.

f. Putative olfactory sensory neurons can be seen from approximately this stage in the olfactory bulbs anterior to the eye (arrows).

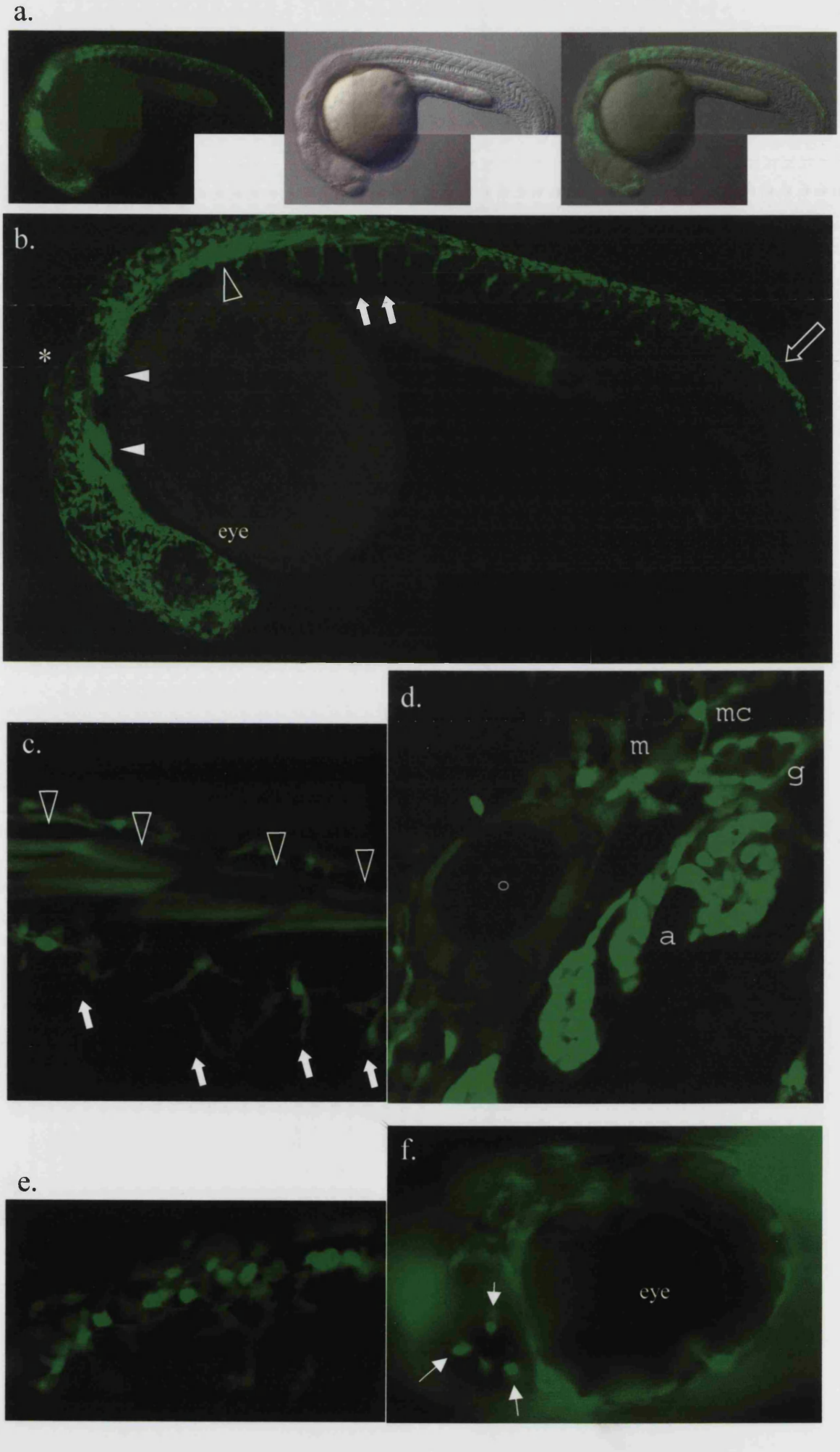
a.
b.
*
eye
c.
d.
mc
m
g
o
a
e.
f.
eye

Although this was not initially described by *in situ* analysis in zebrafish, olfactory bulb expression was reported in mice and humans. More thorough analysis of the zebrafish *sox10 in situ* pattern has shown that *sox10* is in fact expressed in the olfactory bulb (R.N.K. pers. com.) GFP expression in the ventral CNS (in particular the brain and anterior spinal cord) is visible at these stages as well (not shown). This is consistent with *in situ* data, which detected *sox10* in the ventricular layer upon transverse sectioning of the hindbrain (Pauliny, 2002). Transverse sections of the sox10-4.9:GFP transgenics are required to demonstrate precise recapitulation of the *sox10* pattern at this site.

Strikingly, beginning at around this time, clear muscle fibre expression begins to be seen, restricted to the anterior trunk (Figure 4.13b). It is not known why this expression in this cell type is only present in this axial region, and not seen in more posterior muscle. A magnified image of muscle fibres labelled with GFP is shown in Figure 4.13c. Presence of GFP^+ muscle in both transient and germline transgenics argues that lack of integration itself was not the sole cause of the ectopic expression in transient analyses.

Later, at 2dpf, almost all neural crest cells in the trunk and tail have begun to migrate. Figure 4.14a shows two confocal planes of the tail region of a 2dpf embryo, with both laterally migrating (upper panel) and medially migrating (lower panel) neural crest cells. Cells remaining dorsally might later become pigment cells of the dorsal stripe. Figure 4.14b shows a projected confocal stack of the head of a 2dpf embryo. Neural crest cells migrating through the branchial arches still show strong GFP expression at 2dpf. Unlike previously, when this expression was ectopic at this site, expression at this stage is consistent with *in situ* experiments in which *sox10* transcripts can be detected from 2dpf onwards (Pauliny, 2002). Neural crest cells in the head not associated with the branchial arches such as pigment cells have a much fainter GFP signal than earlier, possibly indicating cessation of promoter activity in these cell types. It must be remembered however, that xanthophores and iridophores are autofluorescent. Thus it is not clear that there is maintenance of promoter activity in these cell types, although it has been documented that *sox10* transcripts are not detectable in pigment cells (Pauliny, 2002). Neural crest derived cells associated with the posterior lateral line ganglion and nerve (Schwann cells) remain GFP^+.

In the CNS, GFP expression can be seen in cells in the ventral fore, mid and hindbrain (possibly oligodendrocyte precursors and neurons), consistent with reported *sox10* expression at these sites (Pauliny, 2002). As at 24hpf, the transgene is also active in the olfactory bulb. Putative cartilage cells of the endoskeletal disc in the pectoral fin are also visibly expressing GFP at this stage (Figure 4.14b) and ectopic muscle expression can still be seen in the anterior trunk.

Figure 4.14 ⟶

Figure 4.14: Expression of sox10-4.9:GFP at 2dpf

GFP expression pattern in the sox10- 4.9:GFP line at 24hpf. All images were taken by confocal microscopy.

a. Two single plane confocal images of the tail region of a 2dpf transgenic embryo, showing a lateral plane (top panel) and a more medial plane (bottom panel) at the same axial level. By this stage, most of the tail neural crest has migrated or begun to migrate from its premigratory position, and does so in the same manner as trunk neural crest. Thus neural crest cells first embark upon the medial pathway, and migrate ventrally respecting somite boundaries as shown in the lower panel. Lateral pathway migrating neural crest cells lag behind and extend processes across somites.

b. A confocal projection of GFP expression in the head of a 2dpf embryo. Expression is maintained in a number of sites seen at 24hpf. These include the olfactory bulb (arrow), muscle (open arrowhead), branchial arches (a), posterior lateral line ganglion (g) and in Schwann cells along the posterior lateral line nerve (underscored with a brace). The otic vesicle (o) is indicated and does not show strong GFP presence. Expression is also seen in the cartilage cells of the forming pectoral fin (p). First visible from approximately 24hpf, expression in the CNS is prominent by 2dpf, sited in unidentified cells of the ventral fore- and midbrain (labelled by fb and mb respectively), and more extensively in the hindbrain (hb). Similarly, expression in the spinal cord (sc), first noticed at approximately 24hpf, is clear by this stage. Faint fluorescence is visible in some pigment cells, possibly due to perdurance of the GFP protein or autofluorescence reported for xanthophores and iridophores.

a.

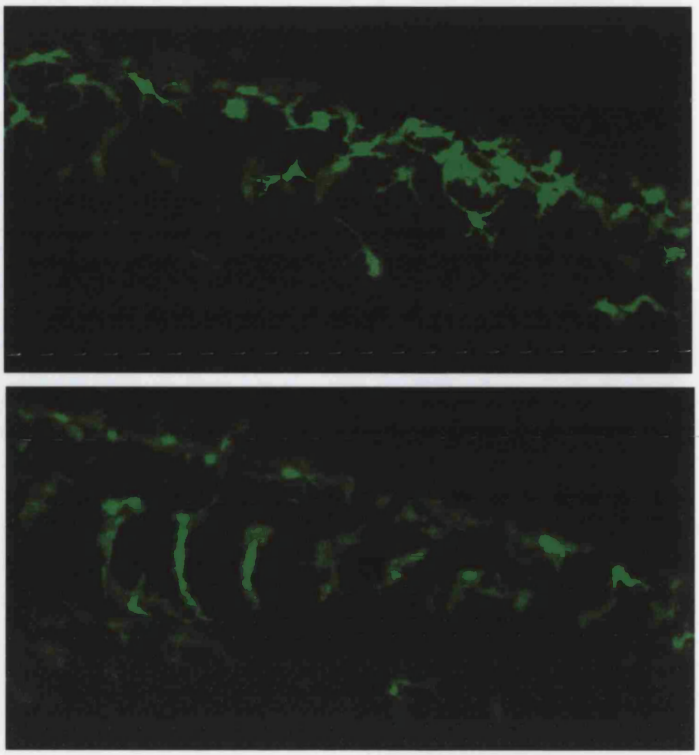

b.

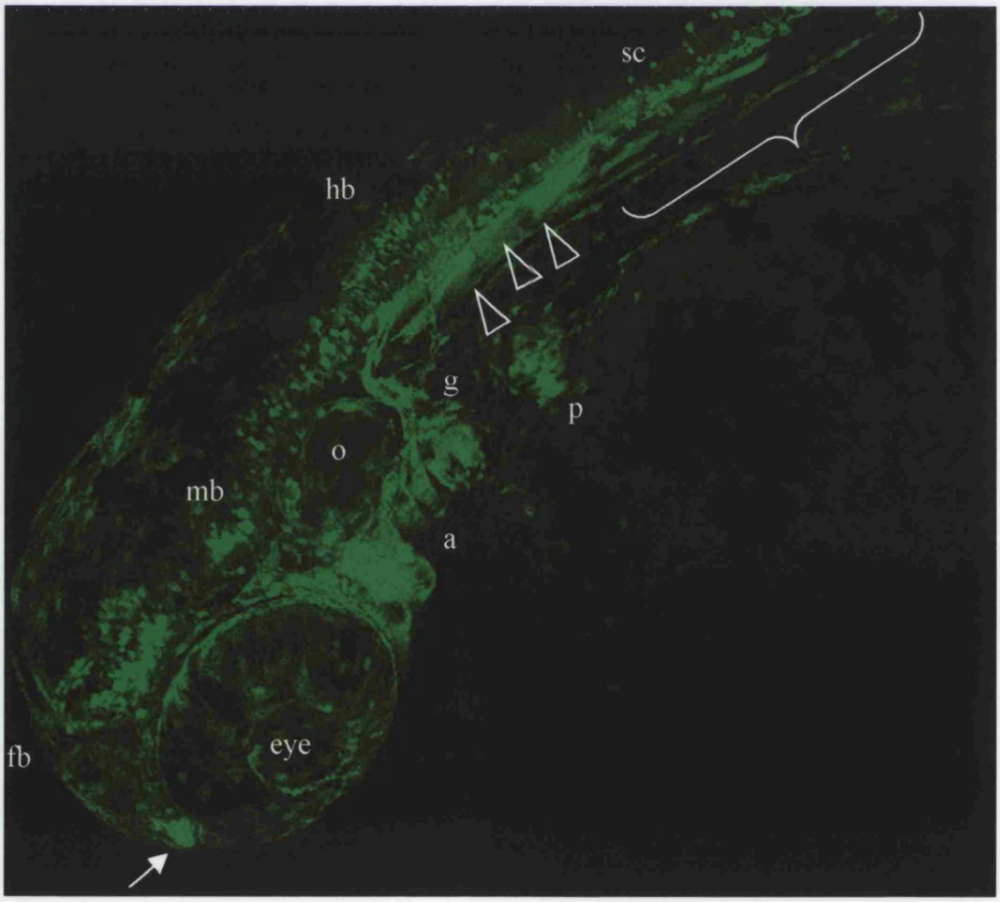

Slightly later at 56hpf, GFP^+ cells are found arranged segmentally and medial to each somite, forming chains of cells running ventrally alongside the notochord (Figure 4.15a). These cells could be either cells still migrating on the medial pathway as seen earlier, or more likely, neural crest cells that have migrated to, and remained in, a medial position forming spinal nerve associated glial cells. GFP^+ cells appear at the dorsal end of this chain of cells, and might be satellite glia surrounding the neurons of the DRGs (Figures 4.15a, b and d). Verification of the identity and differentiation status of these cells could be achieved through double labelling with other molecular markers such as *foxD3*, however there are few differentiated peripheral glial markers in zebrafish (see also Discussion). Schwann cells along the posterior lateral line nerve are GFP^+ as soon as they form at around 24hpf, and continue to express GFP until at least 20dpf. Examples showing expression in this cell population at 2-3dpf (Figure 4.14b and Figure 4.15a) and 4dpf (Figure 4.15f) are presented.

A ventral view of the head of a 3dpf transgenic embryo is shown in Figure 4.15c. Expression in cartilage cells of the forming jaw elements and pectoral fin is evident. Previously it was shown by *in situ* that *sox10* was expressed strongly at this site from 48hpf to at least 60hpf. Attempted *in situ* analysis beyond this timepoint has not been reported, possibly due to increased difficulty in the *in situ* protocol in older embryos. Analysis of this GFP line has no such restriction on age, and allows investigation of *sox10* in later embryos.

Expression within the neural tube can be seen (Figure 4.15a and at higher magnification in b). Putative interneurons, with axons projecting ventrally and laterally, express GFP, as do cells in a ventral position, consistent with their identity as oligodendrocyte precursors (also J. Dutton, pers. comm.). Olfactory bulb expression is also visible in Figure 4.15c, with a confocal projection of the olfactory bulbs at 3dpf showing cell bodies, most likely of olfactory sensory neurons, strongly expressing GFP. The axons of these cells can also be seen in a dorso-medial position in glomeruli, where they defasciculate and synapse with brain neuronal projections (Figure 4.15e). Labelling in this cell type is reminiscent of that derived from the *rag1* and *rag2* GFP transgenics (Jessen *et al.*, 2001).

The 5dpf expression pattern remains essentially identical to that at three days, and the only neural crest derivatives to have retained GFP expression are the cartilage cells of the jaws and Schwann cells of the PNS (e.g. on the posterior lateral line, Figure 4.16a). A confocal projection of a ventral view of the head shows the strong expression in the jaw elements (Figure 4.16b). Although not neural crest derived, cartilage cells in the forming fin also show GFP expression. For example, elements of the pectoral fin, including the

Figure 4.15; Figure 4.16 →

Figure 4.15: Expression of sox10-4.9:GFP from 56hpf to 4dpf

GFP expression pattern in the sox10- 4.9:GFP line between 56hpf and 4dpf. All images were taken by confocal microscopy, except **c.** and **f.** Ages of embryos are given in each image.

a. Low power lateral view of the trunk of a 56hpf, generated by projection of a confocal stack. Expression sites evident include the CNS, in particular in putative interneurons (i) and more ventrally located cells, possibly oligodendrocyte precursors (ol). Fluorescence, possibly due to autofluorescence, is visible in certain pigment cells such as iridophores (ir) and xanthophores (x). Glial cells of the peripheral nervous system are also labelled with GFP such as Schwann cells of the posterior lateral line nerve (plln), DRG and spinal nerves (sn).

b. A higher magnification view of the trunk expression domains, also generated by projection of a confocal stack. Many features shown in **a.** are indicated.

c. Ventral fluorescent image of a 3dpf transgenic embryo showing expression in cartilage cells of jaw elements, pectoral fin (p) and olfactory bulbs (arrows). Expression in catilage cells of the scapulocoracoid supporting the pectoral fin is also highlighted (arrowhead).

d. Single confocal image of lateral view of putative DRG satellite glia in the trunk.

e. Confocal projection of an anterior view of the head of a 56hpf embryo, with dorsal up. Strong expression in sensory neurons of the olfactory bulbs is indicated with arrows. Associated axons visible dorso-medially to the bulb in the glomeruli are indicated with arrowheads. Ventro-medial positioned GFP^+ cells (asterisks) are presumably cartilage cells in anterior jaw elements.

f. Expression in Schwann cells along the posterior lateral line nerve in a 4dpf embryo.

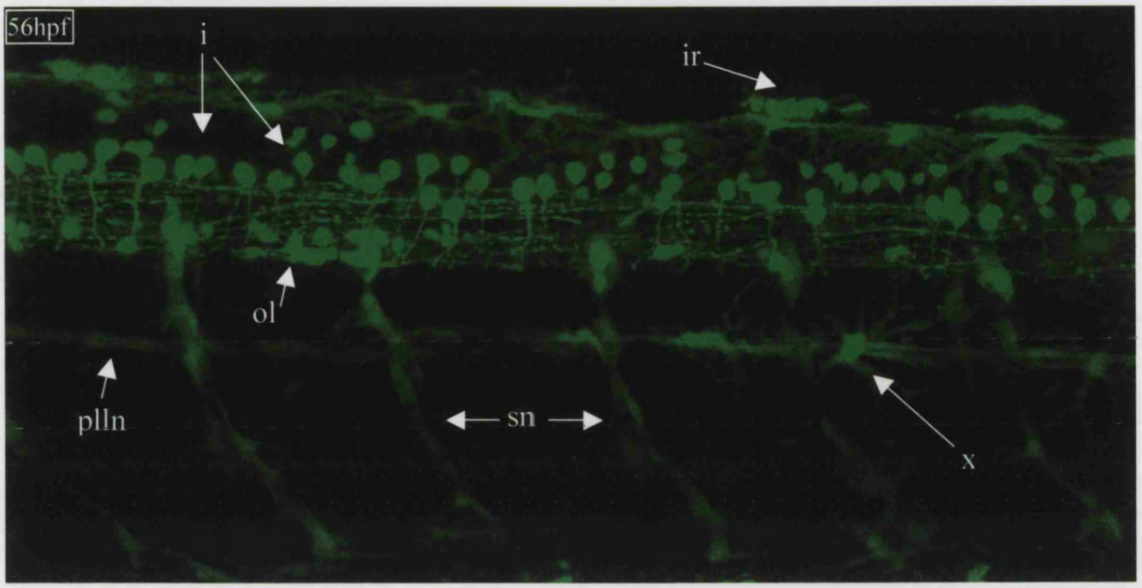
a.
56hpf
i
ir
ol
plln
sn
x

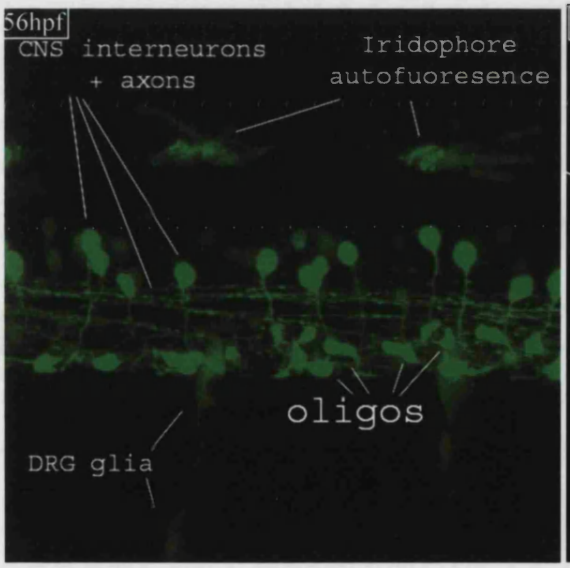
b.
56hpf
CNS interneurons
+ axons
Iridophore
autofuoresence
oligos
DRG glia

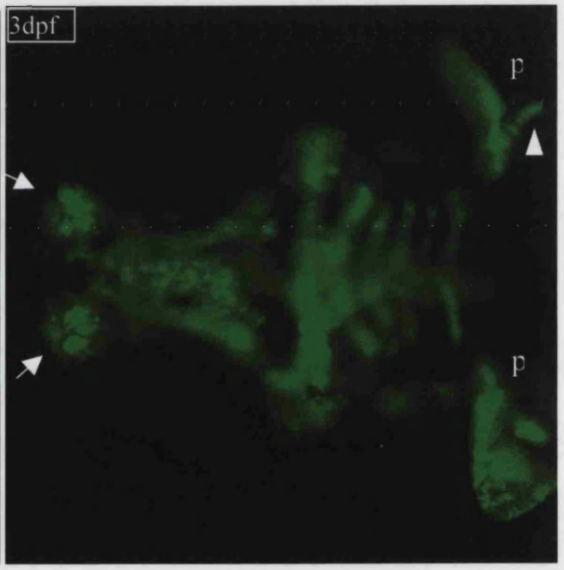
c.
3dpf
p
p

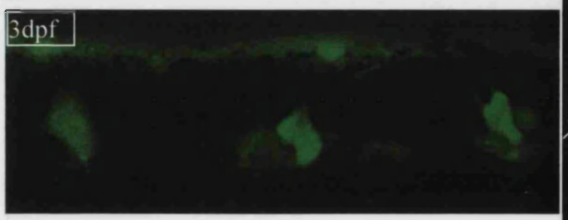
d.
3dpf

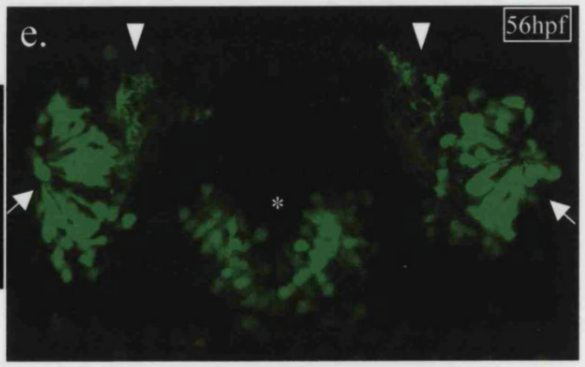
e.
56hpf
*

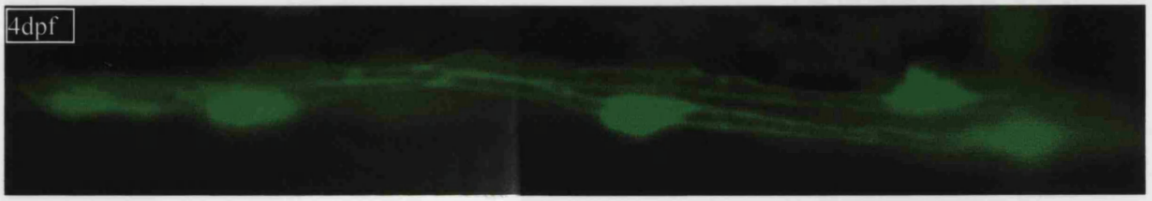
f.
4dpf

Figure 4.16: Expression of sox10-4.9:GFP at 5dpf

GFP expression pattern in the sox10- 4.9:GFP line at 5dpf.

a. Low power lateral views of a 5dpf sox10- 4.9:GFP transgenic embryo under fluorescent light.
Top Panel: By this stage, GFP expression is restricted to pectoral fin and craniofacial cartilage elements, including the jaw and gill arch elements, as well as certain glia types of the CNS and PNS, including cells in the brain and spinal cord.
Bottom Panel: Magnified view of the spinal cord of the same embryo, showing expression in putative oligodendrocytes distributed throughout the spinal cord but predominant ventrally. Schwann cells along the posterior lateral line are also apparent in this image (arrow).

b. A ventral view of the head generated by projection of a confocal stack. Expression in cartilage cells in all jaw elements is evident, as is expression in the cartilage cells of the endoskeletal disk (arrowhead) and scapulacoracoid (arrow) of the pectoral fin.

c. Single confocal image of the pectoral fin showing the tessalated pattern of cartilage cells in the endoskeletal disk. The GFP expression in cartilage cells appears to be variable and patchy.

Double immunofluorescence was used to detect neurons in the PNS (red channel - using antibodies against the Hu epitope) and GFP^+ cells (green channel - using and antibody against GFP). Both images are lateral views of 5dpf sox10- 4.9:GFP transgenic embryo.

d. Two channel fluorescent image showing that GFP^+ cells surround the DRG neurons (arrows) and line the nerves emanating from this ganglion (arrowheads). This localisation is further evidence that the *sox10* promoter is active in satellite glia and Schwann cells of the peripheral sensory nervous system.

e. Single confocal image showing the expression pattern in the DRGs, taken using two fluorescent channels. Again the GFP^+ cells can be seen surrounding the Hu^+ neurons. The distribution of signal is such that there is no overlap of expression in the two cell types. GFP expression in Schwann cells can be seen extending below the ganglion along the spinal nerve, until it ventures outside the confocal plane.

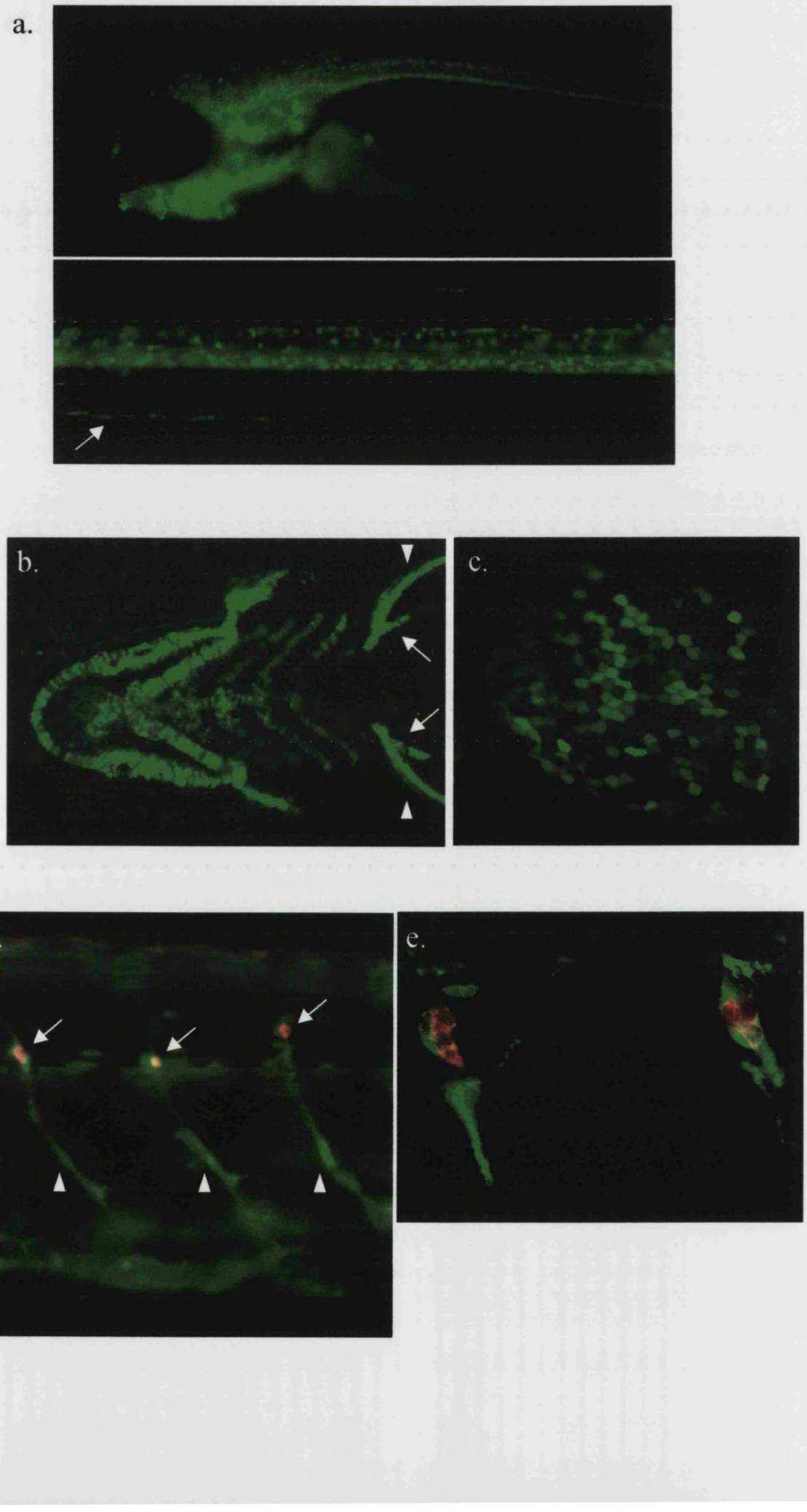
a.
b.
c.
d.
e.

scapulocoracoid and endoskeletal disc show transgene activity (Figure 4.16b). Confocal images of the endoskeletal disc show the characteristic tessellated pattern of cartilage cells (Figure 4.16c). It is clear in this image that the expression level of the transgene in individual cartilage cells is highly variable. Expression in cartilage cells of the head and pectoral fin is still apparent at 20dpf, with large cartilage cells now also apparent in the hypurals of the forming tail fin (not shown). Thus this GFP analysis confirms the *in situ* analysis, which indicated expression in forming cartilage.

The low powered lateral views of a 5dpf embryo given in Figure 4.16a also show the strong expression in the CNS, including the ventral brain and neural tube. Nasal expression is still seen (not shown), whilst the majority of interneuron expression appears to have disappeared by this stage. The expression remaining in the neural tube consists of GFP^+ cells in a position consistent with oligodendrocytes. Maintenance of transgene activity in both these myelinating cells of the CNS, and the myelinating PNS cells (Schwann cells) has been noted until at least 20dpf (not shown). Muscle expression is still evident at this stage and can be seen in Figure 4.17a.

To better establish the relationship of the cell types expressing GFP to other cells, a double antibody labelling approach was commenced. Immunofluorescence using antibodies against the pan-neuronal epitope, Hu, was used to label neurons. This was done in conjunction with immunofluorescence to detect GFP, thus allowing assessment of the proximity or overlap of the GFP^+ cells with neurons in 5dpf sox10-4.9:GFP embryos.

Figure 4.16d shows DRG neuron expression (red fluorescence) with GFP expression in surrounding cells. GFP expression was also seen in putative Schwann cells along the spinal nerve projecting ventrally from the ganglion. At this low power, it appeared that GFP was not present in the neurons, but in cells immediately encapsulating the neurons, namely satellite glia. This non-overlapping expression is better shown by two channel confocal microscopy (Figure 4.16e). Here, close proximity of the GFP signal with the neuron of the DRG is clear, as is absence of GFP expression in the neuron itself.

Further analysis of these double labelled 5dpf embryos have shown that GFP^+ cells were closely associated with neurons in other peripheral ganglia, including the posterior lateral line ganglion as shown in Figure 4.17a. Here GFP^+ Schwann cells along the lateral line can be seen emanating from the Hu^+ ganglion core. Although GFP is excluded from these neuronal cells, there appears to be GFP^+ cells surrounding some cells within the ganglion.

GFP expression is additionally seen in cells along the sympathetic chain. Figure 4.17c shows Hu^+ neurons positioned ventrally in the anterior trunk, and connecting these neurons is a chain of GFP^+ cells, lying medially to the spinal nerves and running in an anterior-

Figure 4.17 ⟶

Figure 4.17: PNS expression of sox10-4.9:GFP at 5dpf

Further double immunofluorescence images of 5dpf sox10- 4.9:GFP transgenic embryos, again using an antibody against Hu to detect neurons in the PNS (red channel) and a GFP antibody (green channel).

a. Single plane confocal image taken using dual channel detection showing the posterior lateral line ganglion with the neurons in red (arrows), and GFP^+ Schwann cells of the posterior lateral line branches (arrowheads). There appear to be some GFP signal surrounding, but not overlapping with, the neurons within the ganglion, most likely satellite glia (asterisk). Muscle fibres (m) can be seen in the top right of the figure.

b. Confocal slice through the eye, showing two neuronal layers to the retina. Image is a dorsal view with anterior up. Within the outer layer, GFP^+ cells are apparent, with putative axons. The identity of these cells, and if they are true sites of *sox10* expression, remains to be determined.

c. Lateral view of the anterior trunk. Green (top panel) and red (middle panel) fluorescent images are shown with an overlay in the bottom panel.
GFP expression can be seen in cells linking the sympathetic chain. A chain of GFP^+ cells can be seen in the ventral half of the anterior trunk (open arrowheads), underlying the Schwann cells of the segmentally arranged spinal nerves. This chain is closely associated with the location of the sympathetic neurons, as shown by Hu staining (filled arrowheads, middle panel). Comparison of these two images with a combined overlay image indicates that these neurons do not express GFP, but are closely surrounded by GFP^+ cells. Additionally GFP expressing cells appear to connect these neurons, consistent with them surrounding axons of the chain.

d. Lateral views of the hindgut. Faint GFP expression is seen in the enteric nervous system at 5dpf. GFP^+ cells can be seen in the gut (top panel), and comparing this to the neuron expression pattern (middle and bottom panels) indicates that there appears to be a large, but incomplete, overlap of expression. One example of a GFP^+, Hu^- cell is indicated with an open arrowhead. Apparent co-expression might indicate that GFP is present in neuronal cells, or that each neuron is surrounded by GFP^+ cells and that microscopy at this level is unable to resolve the positional differences in fluorescent signals.

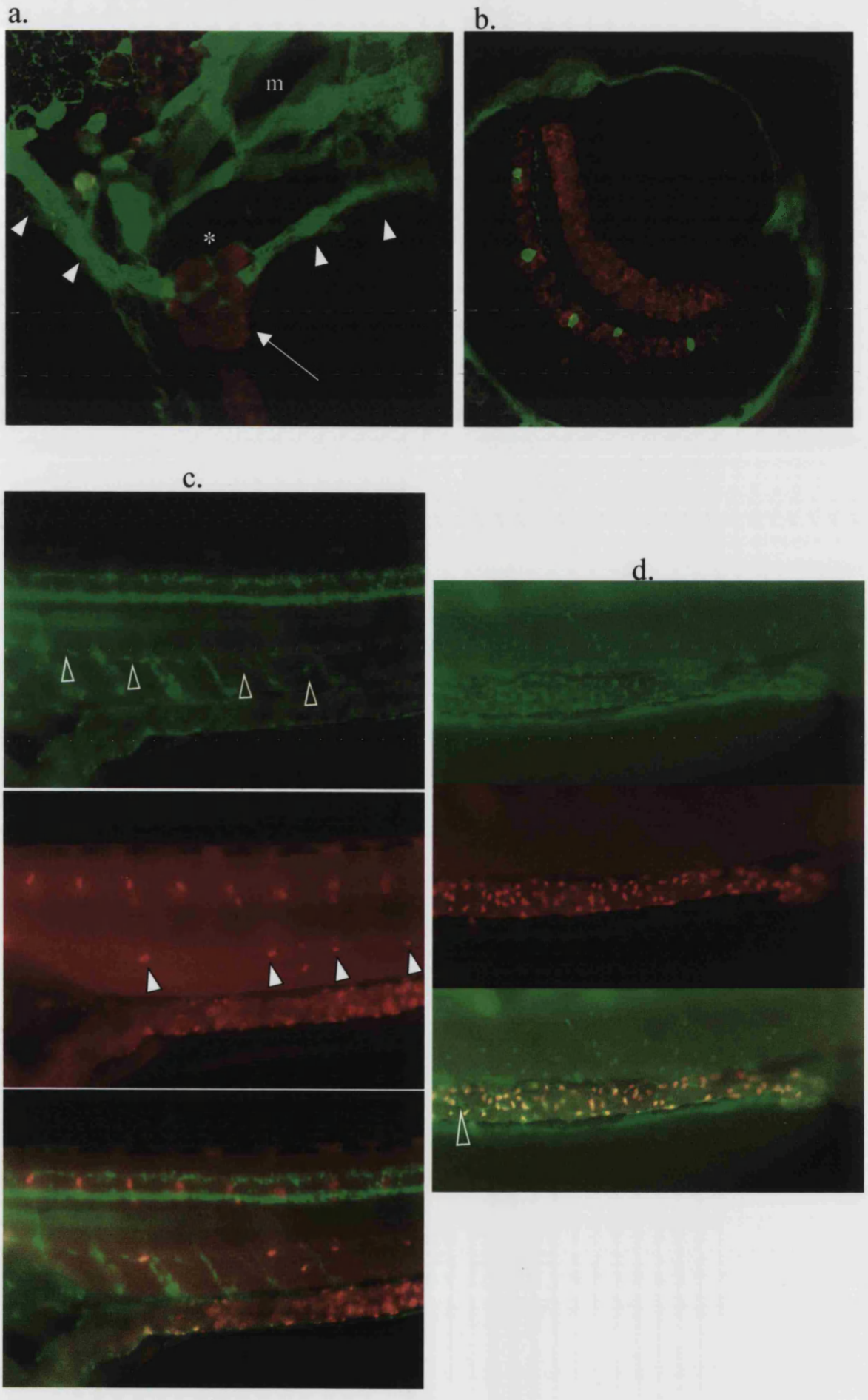
a.
m
*
b.
c.
d.

posterior direction. Closer inspection of the expression pattern shows that the GFP is not expressed in the neurons, but in cells around each neuron (not shown). An overlay of the two fluorescent images highlights the connection between the sympathetic neurons and the GFP cells along the chain connecting them. Thus the transgene is probably active in Schwann cells associated with the sympathetic chain as well, consistent with a requirement for expression of *sox10* in myelinating cells.

Expression in the enteric nervous system was seen at 5dpf. Figure 4.17b shows fluorescent images of the hindgut of a sox10-4.9:GFP transgenic embryo, immunostained for Hu and GFP. Faint GFP signal can be seen in cell bodies along the gut, and appear to mostly overlap with the Hu^+ enteric neurons. However occasionally, GFP^+, Hu^- cells are evident (indicated with arrowhead).

Finally, a confocal slice through the eye of this embryo showed GFP^+ expression in a subset of cells in the retina of the eye (Figure 4.17b). Although these cells, unlike most of their neighbours, do not appear to express Hu, axonal like projections can be seen associated. The identity of these cells remains to be determined.

The GFP expression pattern of this sox10-4.9:GFP line has been described here in some detail, although there are some expression sites that require further investigation, and some apparently ectopic domains (see Section 4.3). This line should prove useful in a number of future experiments, some of which are also outlined in Section 4.3. One simple experiment already realised, has been to establish the state of promoter activity in melanophores during development. To achieve this, sox10-4.9:GFP transgenic embryos were lightly treated with PTU to mildly inhibit melanin formation and then inspected between 26hpf to 4dpf. At each time point, an estimate of the percentage of GFP^+ melanophores was made, with at least 20 melanophores assessed for GFP signal per embryos. The resulting counts were plotted (Figure 4.18), and a non-linear regression curve plotted using Prism statistical software version 5.1 (GraphPad software, San Diego, CA, USA). The model producing the best line of fit was an exponential decay curve, as expected for a drop off of GFP signal due to protein degredation (R^2 value = 0.9415). Examples of melanophores both with and without GFP expression are shown at given timepoints (Figure 4.18).

Immediately obvious is that activity of the *sox10* promoter fragment present on the transgene is not maintained in melanophores throughout development. Although the promoter is active in melanophores at or just before the onset of neural crest melanogenesis (24hpf), it appears to be downregulated from this point onwards. Reported loss of *sox10* transcript in all differentiating pigment cell types is consistent with this analysis (Pauliny, 2002). This result has important implications for proposing a role for Sox10 in

Figure 4.18 ⟶

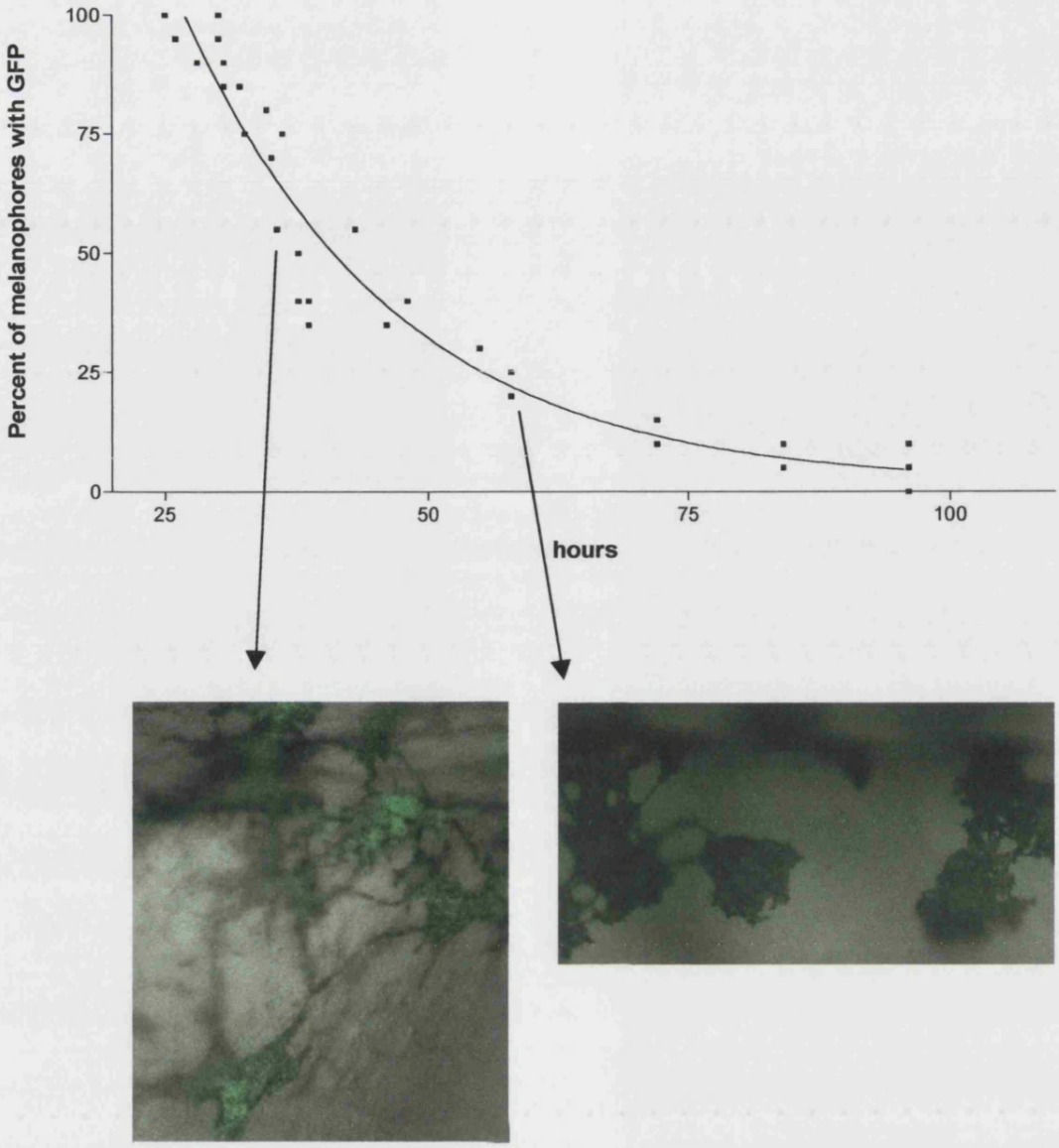

Figure 4.18: GFP signal is lost from melanophores over time

To determine whether the *sox10* promoter is active in melanophores throughout development, the percentage of GFP^+ melanophores as assessed at various time points in embryos from the sox10-4.9:GFP line. At their formation at around 25hpf, GFP is detectable in almost all melanophores. By 4dpf very few melanophores express GFP. Panels below show confocal images using a fluorescent and a white light channel at given stages. GFP expression can be seen through the melanin deposits in the melanophores early, but not later, indicating cessation of promoter activity in this cell type.

melanophore development, and suggests that *sox10* plays only an early role and is dispensable at later stages. This further supports the theory that *sox10* is only essential very early in melanophore development to activate *mitfa* (Elworthy *et al.*, 2003).

4.2.5.2. sox10-6.1:GFP

In addition to those using p4.9:GFP, attempts to produce transgenic lines carrying the p6.1:GFP construct were made. As before, the construct was linearised and injected into 1-cell stage embryos, with the best expressing embryos sorted and raised. Of the surviving adults, four out of a total of 33 screened to date gave embryos with GFP expression, and were named sox10-6.1a:GFP, sox10-6.1b:GFP, sox10-6.1c:GFP and sox10-6.1d:GFP. Presently, there are yet more potential founders to screen. The average percentage of transgenic embryos produced per founder was 12.9, 5.9, 4.6 and 15.4% respectively. All four lines are currently into the F3 generation and all have behaved in a Mendelian fashion. Curiously, all four identified so far express very weakly, much more weakly than the sox10-4.9:GFP line. This low level of expression has made visualisation of the expression domains difficult, and due to time constraints, not all four lines have been examined or documented in detail. Brief analysis of two lines, sox10-6.1c:GFP and sox10-6.1d:GFP, is presented here, but all four lines are largely identical in expression domains.

The earliest time of expression has not yet been established, however expression in premigratory neural crest in the tail of a 28hpf embryo has been seen, as well as in neural crest cells that have commenced migration (Figure 4.19b). Viewing these embryos at 28hpf reveals a similar cranial neural crest expression pattern to that of the sox10-4.9:GFP line, namely expression in the branchial arches. A hint of faint expression in migrating neural crest cells outside the branchial arches is also evident (Figure 4.19a and c). Strikingly, whereas otic vesicle expression was much weaker than branchial arch expression in the sox10-4.9:GFP line, in all sox10-6.1:GFP lines it is at a comparable level to the branchial arches (Figure 4.19a, c). This suggests that although the overall levels of expression in the sox10-6.1:GFP lines are low, the comparative expression level in the forming ear is much stronger (Figure 4.19b). Transgene promoter activity is also evident in the olfactory bulb, as with the sox10-4.9:GFP line (Figure 4.19a). Unlike transient analyses with the p6.1:GFP construct, no muscle cell expression is obvious in these lines.

Later, at 2dpf, GFP expression can be seen in cells associated with the posterior lateral line ganglion, Schwann cells (Figure 4.19d) and very faintly in cells surrounding the DRGs (Figure 4.19e). Detectable levels of GFP are also prominent in the ear, the hindbrain and in the nascent cartilage cells of the pectoral fin (Figure 4.19d). In the neural tube at this stage, the strongest expression is seen in putative oligodendrocytes, found predominantly

Figure 4.19 ⟶

Figure 4.19: Expression pattern of sox10-6.1:GFP lines

GFP expression in the sox10- 6.1c:GFP and sox10- 6.1d:GFP lines from 28hpf to 5dpf. Ages and genotype of embryos are given in each image.

a. Left Panel: Lateral image of the head of an approximately 28hpf sox10- 6.1d:GFP transgenic embryo taken under fluorescent light. Expression is faint, compared to the sox10- 4.7:GFP line, but evident in the branchial arches (a), the olfactory bulb (arrow) and clearly in the otic vesicle (o). A magnified image of the branchial arch and otic vesicle expression is shown in **c.** This image is overlaid onto a DIC image in the right panel.

b. Expression can also be seen in premigratory neural crest cells. Lateral image of the dorsal tail of a 28hpf sox10- 6.1d:GFP transgenic embryo taken under fluorescent light, showing faint expression in neural crest cells positioned dorsally as well as in cells beginning to migrate (arrowheads).

c. Magnified fluorescent image of the otic region. GFP expression is present in the otic vesicle (o), migrating neural crest cells (arrowheads) and neural crest cells in the branchial arches (a).

d. Lateral confocal projection of a 2dpf sox10- 6.1c:GFP transgenic embryo. Expression can be seen in the developing ear (e), cells in the hindbrain (hb), cartilage in the pectoral fin (p), cells associated with the posterior lateral line ganglion (g) and Schwann cells along the dorsal branch of the posterior lateral line (s).

e. Expression in the spinal cord at the same stage shows very low levels of GFP in putative interneurons (i), whilst putative oligodendrocye precursors (ol), prominent ventrally, show strong expression. Diffuse expression is also detectable in DRG glia (arrows).

f. Lateral view of GFP expression in the ear of a 5dpf sox10- 6.1d:GFP transgenic embryo viewed under fluorescent light.

g. The same embryo viewed ventrally under fluorescent light showing jaw cartilage expression

h. Lateral views of the heart of a 5dpf sox10- 6.1c:GFP transgenic embryo, viewed under fluorescent (left panel) and nomarski (centre panel) optics, with an overlay (right panel). Expression in jaw elements can be seen (arrowheads). Unique to this line, expression in the heart is also evident (arrow).

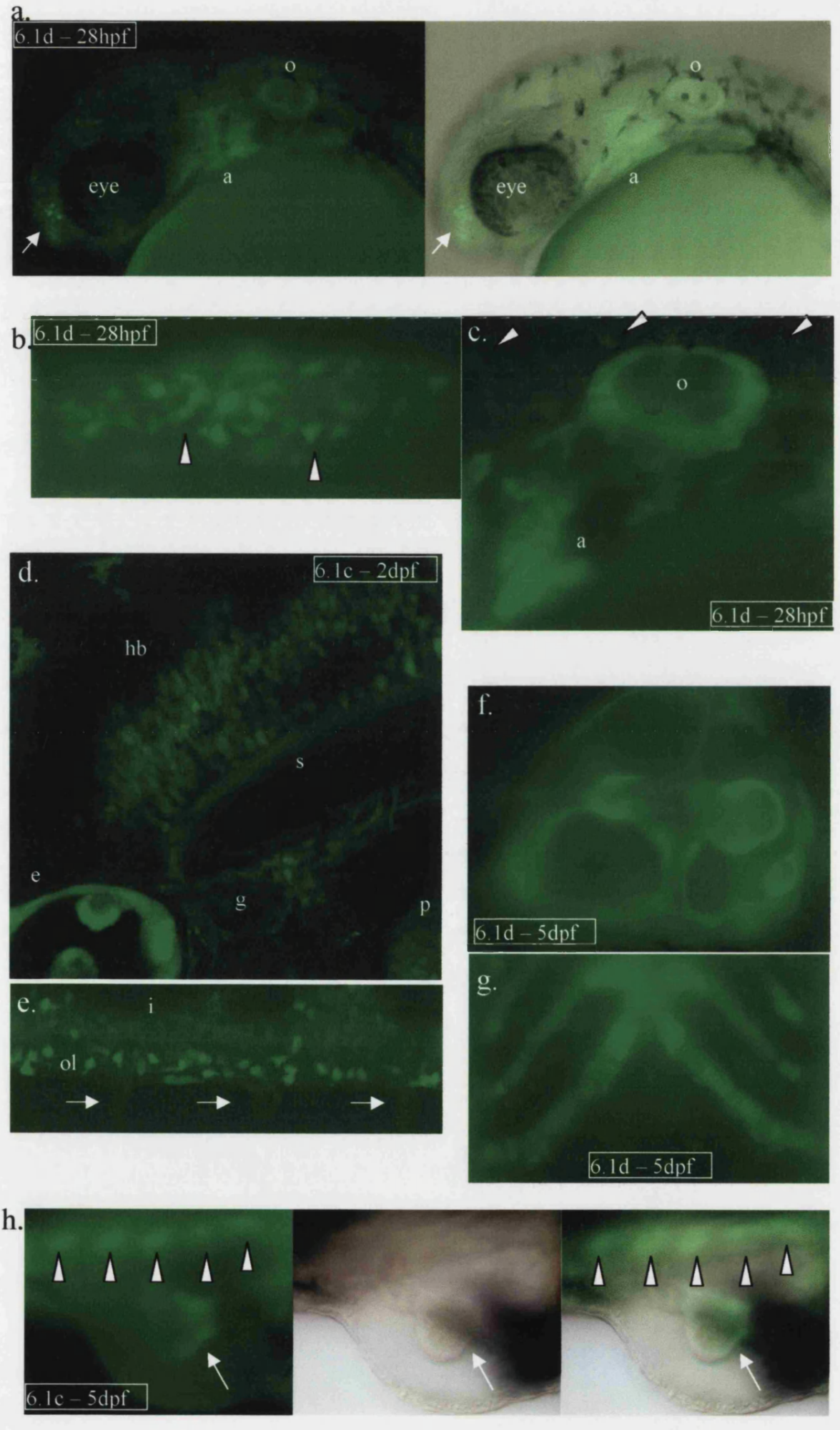
a.
6.1d – 28hpf
o
eye
a
o
eye
a
b.
6.1d – 28hpf
c.
o
a
6.1d – 28hpf
d.
6.1c – 2dpf
hb
s
e
g
p
f.
6.1d – 5dpf
g.
6.1d – 5dpf
e.
i
ol
h.
6.1c – 5dpf

ventrally and dispersed in more dorsal parts, but faint expression can be seen in other cells of the neural tube, probably interneurons (Figure 4.19e). These expression sites, with the exception of the strong ear expression, are reminiscent of the sox10-4.9:GFP expression pattern at this stage, although the levels are much lower.

Cartilage cells of the jaw elements and the ear retain GFP expression until at least 5dpf (Figure 4.19f, g).

Curiously, the sox10-6.1c:GFP line has clear expression in the heart at 5dpf (Figure 4.19h). This appears to be in cells surrounding the entire heart. Closer inspection is required to ascertain whether these cells are endo-, myo-, or epicardial in nature. A neural crest contribution to the heart outflow tract has been demonstrated in zebrafish (Li *et al.*, 2003). It is not yet known if these cells do, or ever did, express *sox10*. Additionally *sox10* in the chick has been shown to be expressed in glial cells of nerves innervating the heart as well as in septa and valves of the heart. The expression shown in Figure 4.19e appears to be too broad to correspond to any of these specific sites, although much more analysis is required. As this expression pattern is unique to this line, and not seen in any of the other sox10-6.1:GFP lines, it is possible that this is due to some form of enhancer trap. Analysis of the integration site might reveal proximity to a gene expressed in the heart.

4.2.5.3. PACIGFP2

The final construct used to produce a transgenic line was the PACIGFP2 reporter construct. Approximately 85 injected embryos have been successfully raised to adulthood, of which, 64 have been screened for transmission of the transgene. One founder male was identified that produced GFP^+ embryos. The transmission rate was approximately 6.3%, with the F1 individuals nearing breeding age. As the identification of this line is only recent, detailed documentation of the expression sites of this line has not yet been performed. The line does however show strong GFP expression in a number of locations expected for a *sox10* reporter construct.

Thus expression is seen in nascent neural crest at around 1-2 somite stage (10.5hpf; not shown) and by 24hpf is seen in migrating neural crest cells in the head (Figure 4.20a) and trunk (Figure 4.20b). Expression in the branchial arches is also evident in 24hpf PACIGFP2 transgenic embryos. In the trunk, neural crest cells migrating on both the medial and lateral pathways are GFP^+, and there appears to be some neural tube expression in a subset of neuronal cell bodies and their axons, possibly interneurons or Rohon-Beards (Figure 4.20b). Interpretation and biological significance of this neuronal expression is under investigation. Clear in Figure 4.20a is the strong expression in the otic vesicle. Expression in the olfactory bulb is also apparent at this stage (not shown). No muscle

Figure 4.20 ⟶

Figure 4.20: Expression pattern of the PACIGFP2 line

GFP expression in the PACIGFP2 line, from 24hpf to 5dpf. Ages of embryos are given in each image.

a. Confocal projections of a 24hpf embryo.
Left Panel: Lateral image of the head showing expression in migrating neural crest in the head and trunk (arrowheads) and in the branchial arches (a). The otic vesicle (o) is also strongly labelled.
Right Panel: The same image overlaid onto bright light image of the same embryo.

b. Images at higher magnification of the anterior trunk of a 24hpf PACIGFP2 embryo also generated by confocal projection. Medially and laterally migrating neural crest cells are GFP^+, as are the cell bodies and axons of interneurons or Rohon-Beards in the neural tube (arrowheards). Shown in the three panels are fluorescent (left panel), white light (middle panel) and an overlay (right panel).

c. Top Left Panel: Single confocal fluorescent image of a lateral view of the spinal cord of a 4dpf PACIGFP2 transgenic embryo, overlaid onto a brightfield image. Expression in putative oligodendrocytes can be seen predominantly in the ventral portion. Neuronal expression is absent.

d. A lower powered fluorescent image of the same region of the embryo, at a more lateral plane. Satellite cells (arrowheads) in each DRG can be seen, as can the Schwann cells (arrows) of the ventrally and dorsally projecting spinal nerves.

e. A lateral confocal image of the ear of the same embryo showing that strong expression is maintained in this organ.

f. Ventral fluorescent image showing expression in the jaw elements of an 8dpf PACIGFP2 transgenic embryo.

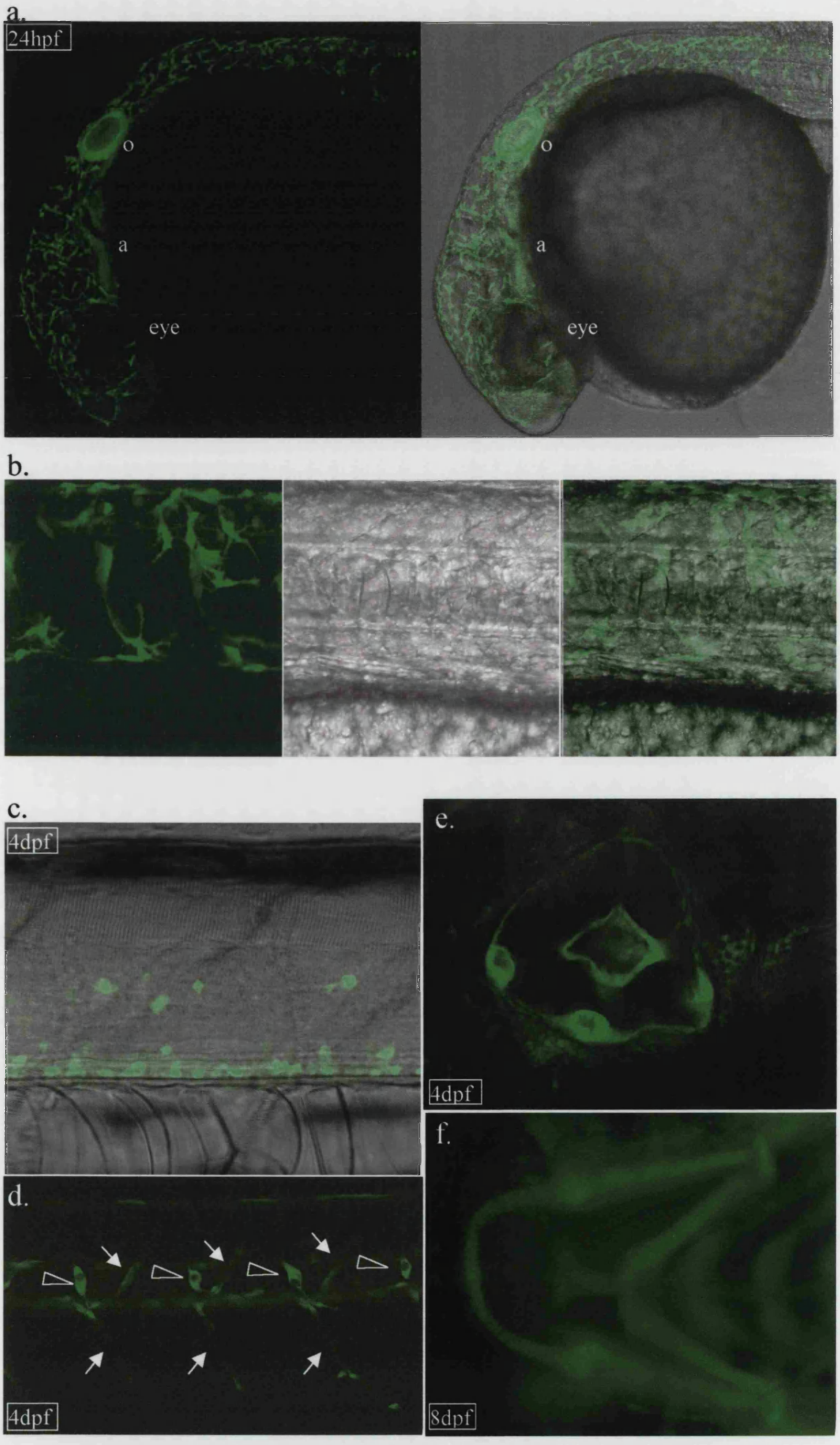
a.
24hpf
o
a
eye
o
a
eye
b.
c.
4dpf
e.
4dpf
d.
4dpf
f.
8dpf

expression is seen in this line. This is in contrast to the transient reporter assays performed with this construct, which did occasionally produce muscle expression. Thus integration of the reporter appears, in this case, to have permitted effective silencing in this cell type.

At 4dpf, PNS expression can be seen in posterior lateral line Schwann cells (not shown), and glia associated with DRGs and the spinal nerves. This is shown in Figure 4.20d, with cells in a position and of a shape reminiscent of the satellite glia surrounding DRG neurons (shown for sox10-4.9:GFP; Figure 4.17). In addition to the satellite glia, Schwann cells lining the nerves emanating from the DRG are also GFP^+ (Figure 4.20d). At this stage, GFP expression in the neural tube is confined to putative oligodendrocytes (Figure 4.20c). Expression in the ear is still very strong (Figure 4.20e), as is expression in the craniofacial cartilage. An example of GFP^+ jaw cartilage at 8dpf is shown in Figure 4.20f. The variable expression levels notable with the sox10-4.9:GFP line at this site is not evident in the PACIGFP2 line.

4.3. SUMMARY AND DISCUSSION

This chapter describes the subcloning of the *sox10* genomic region, isolation of the upstream region including the promoter and generation of GFP reporter constructs. The targeted modification of a *sox10* PAC to produce a PAC reporter construct was also achieved. A scale diagram of the three constructs is shown in Figure 4.21, and clearly demonstrates the much larger amount of flanking DNA present in the PAC reporter. The number of transgenic lines generated for each construct, and a summary of the expression sites seen in both transient and transgenic analyses are presented, compared to known *sox10* expression sites.

Unfortunately the transient analysis of these promoters was limited due to time constraints, and presence or absence of GFP expression in all expected sites was not established for all constructs. Detailed transient analysis of these, and smaller promoter fragments, was initiated as part of a promoter dissection project by others in the lab. Subsequently, transient and transgenic GFP analyses in combination should allow identification of the regulatory elements controlling *sox10* expression. Full description of a reporter's expression profile is difficult solely with transient analyses, due to associated mosaicism. As only a fraction of cells will inherit copies of the transgene, only a subset of the expression domains might be seen, even upon using a large sample size of injected embryos, and some cell types might be missed. Furthermore, it has been established here that a reporter can behave disparately in transient and transgenic environments (Figure

Figure 4.21 ⟶

Figure 4.21: Summary of the reporter constructs produced and their expression patterns

The three *sox10*:GFP reporter construct produced are depicted on the left side, with the amount of surrounding *sox10* promoter sequence shown as a horizontal line and to scale. The *gfp* gene and polyadenylation signal are presented as a green box. The approximate start of transcription for the *sox10* gene is presented as an arrow, and *Not*I (N) and *Sal*I (S) sites are presented on the PAC reporter.

A table summarising the GFP expression analyses for each reporter is presented on the right. For each reporter, the top row represents a summary of results from transient analysis, whilst the bottom row represents results from germline transgenic analysis. The number of transgenic lines produced so far for each construct is also presented. The major sites of expression are listed at the top of the table, be they endogenous or ectopic. They are listed in approximate chronological order of first appearance from left to right. The following key applies:

+: Expression is seen in this location.

-: Expression is not seen at this location.

?: presence or absence of GFP expression at this location has not been properly assessed.

Symbols are also colour coded such that:

Red: presence (or absence) of GFP expression is in contrast to the *sox10 in situ* pattern.

Green: presence (or absence) of GFP expression concurs with the *sox10 in situ* pattern.

Yellow: Presence of GFP in this cell contrasts with the *in situ* pattern, but may be due to perdurance from an earlier stage of correct expression.

Black: No conclusive *in situ* data is reported for this site yet.

Notes:

(1): Ear expression in this line is far weaker than expected from *in situ* analysis

(2): Schwann cells in all lines analysed have been seen on the PLL nerve and spinal nerves. Only in sox10-4.9:GFP have they been searched for in the sympathetic chain as yet.

(3): Late expression in the ENS is seen in both *in situs* and in transgenics. It is unclear in both analyses precisely which cell types (neuronal or glial) are labelled. Nor can an argument for GFP perdurance in the transgenic be discounted (see text).

(4): Premigratory neural crest has only been inspected in the tail of the sox10-6.1:GFP lines at 28hpf. Earlier inspection has not been conducted.

(5): Ectopic heart epithelium expression is seen in only one of the four sox10-6.1:GFP lines.

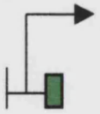

	Number of transginic lines		Premigratory crest	Migrating crest	Ear	Branchial Arches	Olfactory bulb	Brain neurons	Ventricular zone	Muscle	Enteric ganglia	Pineal gland	Interneurons	Oligodendrocytes	PLL Ganglion	Other cranial ganglia	Pigment cells	Satellite Glia	Schwann cells	Facial Cartilage	Pectoral fin cartilage	ENS	Heart Epithelia
sox10-4.9:GFP	1	Transient Analysis	+	+	+	?	?	?	?	+	?	?	+	?	?	?	+	?	?	?	+	?	-
		Transgenic Analysis	+	+	-[1]	+	+	+	?	+	-	-	+	+	+	?	+	+	+[2]	+	+	+[3]	-

sox10-6.1:GFP	4	Transient Analysis	+	+	+	?	?	?	?	+	?	?	+	?	?	?	+	?	?	+	+	?	-
		Transgenic Analysis	+[4]	+	+	+	+	+	?	-	?	?	+	+	+	?	+	+	+[2]	+	+	?	+[5]

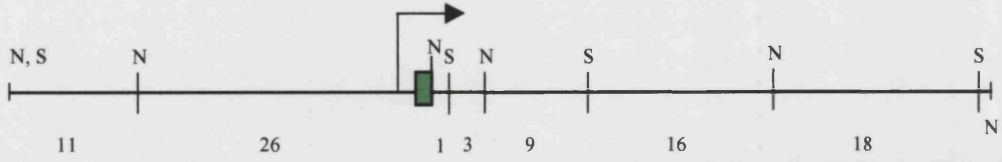

PACIGFP2	1	Transient Analysis	+	+	+	?	?	?	?	+	?	?	+	?	?	?	+	?	+	+	+	?	-
		Transgenic Analysis	+	+	+	+	+	?	?	-	?	?	+	+	+	?	+	+	+[2]	+	+	?	-

4.21). For example, the two larger constructs (p6.1:GFP and PACIGFP2) show expression in muscle in transient analyses, but not in their respective transgenic lines. Thus it is possible that, in certain circumstances, transient analyses afford erroneous expression patterns. Thus identification of an expression site in transient transgenics requires substantiation through other means, including inspection of germline transgenics and *in situ* data.

The transient analyses performed were, however, crucial in quickly demonstrating that the reporter constructs produced could direct GFP expression in the neural crest and other *sox10* expressing sites. This information argued that if introduced into the germline, these constructs could produce useful and informative transgenic zebrafish lines. Of concern, however, was the presence of ectopic expression in the muscle. More detailed transient analyses with these and other promoters have uncovered other ectopic expression sites, namely notochord and skin (J. Dutton pers comm.). If present in the transgenic lines as well, this ectopic expression might obscure the neural crest expression, and interfere with further experiments aimed at observing or manipulating labelled cells. Fortunately the muscle expression was only found in the anterior muscle blocks of the sox10-4.9:GFP line, and has not been seen in other lines. It has not hampered the analysis or use of this line so far. Others have reported ectopic expression in muscle and notochord in transient reporter analyses, including those made from the zebrafish tyrosinase promoter (Camp *et al.*, 2003). Thus this phenomenon might not be uncommon in zebrafish transient transgenic studies.

A modification to a PAC recombinogenic targeting method was also used successfully, which invoked an alternate, $NiCl_2$, method for selecting against the *tetR* marker. This was necessary as the original method based on fusaric acid proved difficult. This modification is unlikely to have any serious use in further development of recombinogenic targeting methods as the new generation of Shuttle vectors employ better selectable markers. It should be remembered however, that the Building Vector might still be useful for future modification of *sox10* containing PACs or BACs. The GFP gene present between the homology arms is flanked by *Xba*I sites, which would allow easy replacement with other reporters or coding sequences. Subsequent transfer as a *Sal*I fragment to the new generation of Shuttle vectors should allow for much easier PAC/BAC modification.

4.3.1. On the relative strength of GFP expression in the different transgenic lines

Generally, all the transgenics reproduced much of the zebrafish *sox10 in situ* pattern and, as such, correlated well with the expression patterns known in other species. Of all

constructs injected, the rate of successful germline transmission appears to vary, with the p6.1:GFP construct being the most successful (4/33 injected fish screened so far are founders). Unfortunately all four lines appear to express only weakly. Meanwhile, only one founder has been identified for each of the other two constructs injected. These two lines both express GFP strongly, however. Why might all the sox10-6.1:GFP lines express weakly? It is possible that the p6.1:GFP construct includes a general repressor element, absent in the p4.9:GFP construct and overridden in the PACIGFP2 construct by extra enhancers. Alternatively, integration of p6.1:GFP in all four sox10-6.1:GFP transgenics may have been at a relatively low copy number, leading to weak GFP expression. The difference in copy number integrated could depend on the degree of concatemerisation of the transgene upon injection into the embryo. It has been reported that linear DNA, upon introduction into 1-cell stage zebrafish embryos, is both concatemerised and amplified up to 10-fold (Stuart *et al.*, 1988). Estimation of the transgene copy number by Southern analysis remains an important goal in the characterisation of all the transgenic lines reported here.

As to why concatemerisation might have been lower upon injection of the p6.1:GFP construct remains unknown, but might involve variations in DNA quality, age of embryos injected, amount and concentration of DNA injected or location of injection within the embryo (i.e. into the yolk or cell). Additionally, the lower degree of concatemerisation might also account for the increased rate of transgenesis. With less concatemerisation, it can be envisaged that mosaicism might be less problematic as DNA can be better distributed between cells. This might increase the probability that DNA is incorporated in primordial germ cells and thus able to integrate into the germline. Thus concatemerisation might be a critical factor in balancing the rate of transgenesis with the level of expression. This is the basis for the new transgenesis technique employing co-injection of a meganuclease. The authors proposed a mechanism in which the enzyme counteracts the natural ligase activity present in the cytoplasm, and thus provides more recombinogenic ends that facilitate integration events (Thermes *et al.*, 2002).

Of all the lines, the PACIGFP2 line looks the most promising. Unlike the sox10-4.9:GFP line, it expresses in the otic vesicle strongly and does not appear to have the highly variable expression levels, seen with the smaller plasmid construct. Furthermore, it is much brighter than the sox10-6.1:GFP lines. It might be that the PACIGFP2 line expresses well due to high copy number, but it could be that it has more enhancer elements present on it that direct much stronger expression.

4.3.2. High transgene copy number might result in ectopic muscle expression

It appears strange that while all three reporters drive ectopic muscle expression in transient transgenic analysis, only the sox10-4.9:GFP transgenic line expresses here. Although it might be that this construct lacks a repressor present on the others, and that this repressor requires germline integration for it to function efficiently, a simpler explanation involves copy number. As proposed earlier, if a cell inherits a very large dose of the transgene, any repressor complexes needed for silencing may be swamped or titrated out, leading to ineffective silencing in that cell. Other evidence supports this theory. Whereas linear DNA injected into embryos can be concatemerised and amplified, this is not possible in circular injected DNA. Thus it can be predicted that the transgene copy number in cells of embryos injected with linear DNA would be greater than in cells injected with the same amount of circular DNA. It follows that if the ectopic muscle expression is due to excess transgene copy number, then it should be more prevalent in embryos injected with linearised reporter constructs compared with circular DNA. This has been observed as indeed being the case (J. Dutton, pers. comm.).

This observation strengthens the proposal that the reason all constructs show ectopic muscle expression in transient analyses is due to excess copy number. It might be that only the sox10-4.9:GFP transgenic line has a large enough copy number to swamp the repressor complexes and show muscle expression, and thus is the only transgenic line of all six produced to show this ectopic expression. Again, the crucial experiment to test this proposal is to obtain an estimate of the transgene copy number in each transgenic line using Southern analysis. The arguments outlined above predict that the sox10-4.9:GFP line will show a much greater copy number than any of the other lines.

Finally, it is worth mentioning that the PACIGFP2 reporter construct contains loxP sites. This provides a means for resolving tandem arrays at integration sites to fewer copies via exposure of transgenic embryos to Cre recombinase, and thus avoiding any adverse effects of multiple tandem arrays on transgene expression sites. No such adverse effect has been seen in hemizygous PACIGFP2 embryos as yet.

4.3.3. GFP expression is seen in premigratory neural crest

Aside from muscle, much of the expression pattern described for sox10-4.9:GFP is in accordance with the *sox10 in situ* pattern. First, GFP expression is seen in premigratory neural crest, at the same time as the *in situ* signal is evident. No overt differences between the GFP and *sox10 in situ* patterns are evident at this stage, and it is not obvious that the

GFP is expressed in more or less neural crest cells than *sox10* itself. "Holes" in the GFP expression pattern are visible (see Figure 4.11b), but *sox10 in situ* analysis at the same stage also uncovered very occasional *sox10*$^-$ neural crest cells (Pauliny, 2002), arguing that the "holes" could conceivably be due to promoter inactivity in some neural crest cells. It follows that the transgene might be faithfully reporting the status of the endogenous *sox10* promoter. Currently, double labelling studies are being conducted to compare the *sox10 in situ* pattern with the GFP pattern, using fluorescent *in situ* detection of *sox10* transcript and immunofluorescent detection of GFP protein in transgenic embryos. This is an important experiment for investigating how well the transgene mimics the expression of *sox10* in the premigratory neural crest, and whether it faithfully reports on the status of the *sox10* promoter. It will also indicate whether all GFP$^+$ cells at this stage are also *sox10*$^+$, and might help resolve the nature of such "holes" in the GFP pattern. It is also possible that they are artefactual and due to variegation in transgene activity rather than real variation in *sox10* promoter activity in the neural crest. The biological significance or fate of the *sox10*$^-$ cells has not yet been established, but might be uncovered using the GFP line, by fate mapping the GFP$^-$ (and presumably *sox10*$^-$) neural crest cells at an early stage with lineage tracing dyes.

Other double fluorescent analyses which might be informative, include use of other neural crest *in situ* markers such as *crestin* (Luo *et al.*, 2001), *foxD3* (Odenthal and Nusslein-Volhard, 1998) and *sox9b* (Li *et al.*, 2002). Such experiments might reveal subsets of neural crest with divergent expression profiles, knowledge of which is important to the understanding of the mechanism and timing of neural crest specification. Double *in situs* using these markers combined with *sox10* have been performed previously, however this could not be performed with dual fluorescence (Pauliny, 2002). This hindered interpretation of the degree of overlap of signals. Using the GFP line in place of the *sox10 in situ* probe allows dual fluorescence to be used more readily which, combined with confocal microscopy, may improve visualisation of the overlap of expression of these markers with *sox10*$^+$ cells. As an alternative to the combination of fluorescent *in situ* detection and immunofluorescence against GFP, dual immunofluorescence could be attempted using antibodies against GFP in combination with antibodies against other neural crest proteins, such as *foxD3*.

In agreement with sox10-4.9:GFP, there is evidence that the other lines reported here direct expression in premigratory neural crest. Firstly, the sox10-6.1:GFP lines expresses GFP in premigratory neural crest in the tail at 28hpf, however this line has not yet been fully analysed. It seems highly likely that inspecting these embryos at an earlier stage would also reveal expression in premigratory neural crest from the 1 somite stage as seen

in the sox10-4.9:GFP line. Meanwhile, neural crest expression at an early stage (1-2 somites) has been seen in the PACIGFP2 line.

4.3.4. GFP perdurance allows cell lineage analysis in transgenic lines

Later, GFP expression can be seen in migrating neural crest and, as shown previously, this allows processes and filopodia to be visualised. At 24hpf, medially migrating neural crest cells are GFP^+, as are laterally migrating neural crest cells and those migrating through the branchial arches. Expression at these latter two sites is in contrast to the *in situ* data, which suggests that only neural crest cells on the medial pathway retain strong *sox10* expression (Dutton *et al.*, 2001). As with the muscle expression, this could represent ectopic promoter activity in this cell type, however a more attractive explanation is perdurance of the GFP protein after the promoter has been switched off. The stability of the GFP protein has been demonstrated experimentally in the lab by direct introduction of the protein into zebrafish embryos, with GFP fluorescence noted at least 48 hours after injection, indicating the high degree of stability of the protein (A. Jacoby, pers. comm.). Thus it is possible that the apparent ectopic expression in laterally migrating neural crest (pigment precursors) and neural crest migrating in the branchial arches (jaw precursors) at 24hpf actually represents perdurance of the GFP protein expressed in premigratory neural crest. It appears that the *sox10* mRNA is present early on in premigratory neural crest fated to the cartilage lineage, is rapidly lost as they migrate through the branchial arches, and then is re-expressed in these cells at 48hpf as they begin chondrogenesis. Perdurance of GFP protein means that the phase of promoter inactivity is not seen in the transgenics.

As mRNA is generally turned over at a more rapid rate than protein, it follows that *gfp* transcripts might not be visible in GFP^+ cells in these ectopic locations. Preliminary use of a *gfp in situ* as a more accurate read-out of promoter activity has indicated that at 24hpf there is no detectable *gfp* transcript in the branchial arches, despite the presence of GFP protein (see Appendix 2). This supports the argument for perdurance of the protein, rather than inappropriate expression. In this manner, the GFP protein acts as a lineage tracer, and allows fate mapping of cells in which the *sox10* promoter has been active earlier (i.e. premigratory neural crest). One conclusion that can thus be drawn is that cells contributing to head ectomesenchyme (jaw cartilage) were $sox10^+$ at an earlier stage, along with other neural crest fated to become pigment and glial derivatives. This indicates that the cells forming all these fates are homogeneous with respect to *sox10* expression, a fact suggested but unproven by *in situ* analysis. This is despite there being no overt jaw phenotype in *cls*, a fact previously used to argue that the neural crest undergoes a restriction of fate to either the ectomesenchymal or non-ectomesenchymal lineage (Weston, 1991). It is now evident

that *sox10* may be expressed in both, but not necessary for the ectomesenchymal lineage. Perhaps this can be accounted for by redundancy of function with other transcription factors such as *sox9b,* which is also expressed in premigratory neural crest. This GFP perdurance argues that Sox10 is expressed in both lineages, or prior to the fate restriction. In addition, there is currently some speculation as to the origin of ectomesenchymal fates, and whether they form from true neural crest or from mesodermally derived cells (R. N. Kelsh pers. comm). This result argues that ectomesenchymal fates are indeed descended from the same population of precursor cells as other neural crest fates.

It is well known that DRG neurons are neural crest derived, however there has not been any evidence that the neural crest cells fated to become DRG neurons express *sox10* at any point during their development. It has been argued that the DRG neuron phenotype in homozygous *Dom* mice is a secondary consequence of loss of trophic glial support (Britsch *et al.*, 2001). Evidence that *Sox10* plays a direct role in the development of DRG neurons requires demonstration that these cells expressed *sox10* at some stage in their history. Use of GFP perdurance in the sox10-4.9:GFP line as a lineage tracer might allow this to be addressed. If, using dual immunofluorescence, cells co-expressing GFP and an early DRG neuron-specific marker are seen, then it would argue that these cells are specified to becoming sensory neurons, and at some stage expressed *sox10.* This is crucial to any argument for the direct role of *sox10* in controlling DRG neuron specification, survival or differentiation. Early sensory neuron markers which could be used include the *neuroD in situ* probe, the *Hu* epitope, or perhaps the *ngn1:rfp* transgenic line (Blader *et al.*, 2003).

Perdurance might account for other unexpected sites of GFP expression, including pigment cells, putative interneurons in the neural tube, and in enteric neurons. Reported *sox10* expression in the CNS is limited to the ventricular zone at 24hpf, and later in oligodendrocytes (Pauliny, 2002). The GFP expression seen in interneurons is unexpected, as it has not been described for *sox10.* Although expression in this cell type might have been undetected by *in situ,* it remains possible that the expression is either ectopic, or perdurance from earlier expression in the ventricular zone or the neural plate. Interneuron expression is lost after approximately 3dpf. Ventricular zone expression in the *sox10* transgenic lines has not yet been established, but will probably require the use of transverse sections to accurately determine GFP localisation. Further evaluation of the significance of GFP expression in this cell type is currently being undertaken. If perdurance is the cause of the interneuron expression, it seems strange that more cell types in the CNS do not express GFP. Interneurons share a common precursor with astrocytes in other vertebrates, whilst oligodendrocytes arise from the same precursor cell as motor neurons. Thus if this is true in zebrafish, and interneuron expression is due to perdurance prior to specification, then it

might be expected that astrocytes are also GFP$^+$, however this is not the case. That only oligodendrocytes, and not motor neurons have GFP expression supports the observation that *sox10* is only activated in oligodendrocytes after they have specified from the bipotent precursor cell (Park *et al.*, 2002).

GFP expression is seen in cells of the enteric nervous system (possibly neurons) at 5dpf. This expression pattern is surprising as it is known in mouse that enteric neurons do not express *Sox10* once differentiated (Paratore *et al.*, 2002). It cannot be ruled out that *sox10* is not expressed in ENS neurons at 5dpf, as *in situ* analysis has not been performed this late. However the zebrafish gut is populated by *sox10*$^+$ precursor cells from 24hpf to 60hpf at least (Dutton *et al.*, 2001). If *sox10* is not expressed at this later stage, then the GFP signal seen is erroneous. The cause of this could be that the expression here is ectopic. Alternatively, the GFP signal seen in the gut in these 5dpf embryos might represent perdurance of GFP from this earlier stage. Consistent with this, persistence of *lacZ* protein in differentiated neurons after cessation of promoter activity has been shown to occur in *Sox10*^{lacZ}/+ mice. If GFP expression in the enteric neurons at 5dpf is true perdurance then it should be dramatically reduced at later stages. Assessment of GFP in this location at mid-larval stages (14dpf onwards) should be relatively straightforward, and would ascertain if promoter activity is maintained. However presence or absence of GFP in enteric chain precursors prior to this stage has not been thoroughly assessed. It is interesting to note that although *sox10* mRNA can be readily detected in enteric chain precursors by *in situ* at 30hpf, GFP expression here was strikingly absent (not shown), possibly indicating lack of an enhancer element in the reporter construct. It remains to be seen if the other transgenic lines express in this cell population. This lack of earlier expression argues against perdurance, and might support an alternative reason for the apparent expression of GFP in enteric neurons, but not in precursors, namely that the later expression is due to ectopic activity of the promoter. Finally the GFP might in fact not be expressed in neurons, but simply in cells closely associated with them, and the imaging used to analyse this did not have the resolution to distinguish the two fluorescent signals. Use of two-channel confocal microscopy would be a worthwhile approach towards resolving this issue. In support of this last theory it appears that the shape of the cells differs between the two different fluorescent images, with the GFP signal appearing in processes emanating from the cell bodies, whilst the Hu signal is seen in much more compact bodies (Figure 4.17d). Although this might reflect differences in subcellular distribution of the two epitopes detected, it might also indicate that they are in fact present in two distinct, but closely associated, cell types.

Pigment cells represent a further cell type where GFP appears to perdure, with recent *gfp in situ* analysis showing that lateral pathway neural crest, which do show GFP protein, have no *gfp* transcript. Detection of presence or absence of GFP in differentiated xanthophores and iridophores is hampered by autofluorescence in these cell types. Often fixation of embryos can destroy autofluorescence. It might be possible to use this, combined with subsequent immunofluorescent detection of GFP to differentiate between autofluorescence and actual presence of GFP. Alternatively, xanthophore autofluorescence is rapidly quenched by exposure to fluorescent light. Thus a bleaching approach might indicate if the fluorescence is due to GFP protein or otherwise.

4.3.5. Further analysis of the GFP expression pattern in all transgenic lines is required

Due to time constraints, full analysis of GFP expression in all transgenic lines has not yet been performed. A summary of sites where expression might be seen, but has not yet been thoroughly evaluated is shown in Figure 4.21. Some of these sites, and others, are briefly discussed here.

sox10 in situ analysis demonstrated expression in the pineal gland, however this has not been observed in any transgenic line as yet, and thus requires closer examination. Expression is also seen in all cranial ganglia, but GFP expression in cells associated with the posterior lateral line ganglion only has been identified so far. Expression pattern in other cranial ganglia and nerves has not yet been fully assessed. All lines have GFP expression in Schwann cells along the segmental nerves and posterior lateral line, however only the sox10-4.9:GFP line has been examined for Schwann cells associated with the sympathetic ganglion. As this line clearly showed expression here, it will be interesting to see if the other lines do as well.

In situ analysis of *Sox10* in mouse and chick also revealed *sox10* expression in septa and nerves of the heart, the pancreas and in oligodendrocytes along the optic nerve. These sites in the zebrafish transgenic lines also need to be checked for GFP and *sox10* expression.

The identity of the cell types expressing GFP in the PNS and CNS is currently speculative, based on cell morphology, cell position and previously known expression patterns for *sox10*. Confirmation of these cells' identity could be achieved using molecular markers. For example, oligodendrocytes are labelled with the *olig2* bHLH transcription factor and are known to co-express *sox10* (Park *et al.*, 2002). Thin GFP^+ strands seen in the CNS are interneuron-derived axons. Double labelling experiment using an axon marker

such as α-tubulin could be used to confirm this premise. Unfortunately there are very few markers for peripheral glia available in zebrafish. However much of this expression pattern confirms the previously reported *in situ* results, including expression in certain glial cells of the PNS and oligodendrocytes of the CNS. Use of dual immunofluorescence has shown that DRG and sympathetic neurons are surrounded closely by GFP^+ cells. This proximity identifies these cells as satellite glia. Identification of *sox10* expression in satellite glia surrounding DRGs had not previously been demonstrated in zebrafish, and is consistent with the expression of *sox10* in this cell type in other species (eg mouse; Britsch *et al.*, 2001). Previous visualisation of satellite glia may have been difficult by *in situ* due to lack of mRNA distribution within the cell. The ability of GFP to label almost the entire cell aids visualisation and assessment of cell morphology and identification of cell type. In this respect, this GFP line might provide a complimentary method for analysing the expression pattern of the *sox10* protein.

The GFP antibody might also allow staining of GFP^+ cell type in adult sections. Assessment of the GFP expression pattern for these transgenic lines would be of interest in comparison with sites of maintenance of *Sox10* expression in mouse and humans.

4.3.6. Downregulation of the promoter supports a model in which Sox10 has only an early role in melanophore development

As *sox10* is required cell-autonomously in the melanophore lineage, and all neural crest cells lacking *sox10* (*cls* mutants) fail to show early melanophore lineage markers (such as the master switch gene, *mitfa*), it is likely that the *sox10* promoter is active in neural crest cells before they melanise (Dutton *et al.*, 2001; Kelsh and Eisen, 2000). Furthermore, recent rescue experiments have shown that forced expression of *mitfa* rescues melanophores in *cls* mutant embryos equally as well as in *nacre* mutants (Elworthy *et al.*, 2003). This indicates that the essential role for *sox10* in melanophore development is the early induction of *mitfa*, and that *sox10* is not required in melanophores after this stage. As *mitfa* is expressed widely at 24hpf in melanoblasts, and is downregulated in differentiated melanophores (Lister *et al.*, 1999), it would appear that *sox10* would only be required in melanophores at this early stage, at around 24hpf. This is consistent with the GFP analysis presented here, as it appears that all melanophores express *sox10* at 24hpf, but a reduction in GFP signal occurs over time. It is likely that *sox10* plays a similar early role in other pigment cells, and thus is not required (or expressed) at later stages.

That this reduction is not rapid (low level expression is still detectable at 4dpf) can be accounted for by stability of the GFP protein. The half-life of GFP protein in melanophores

estimated by this analysis is approximately 14 hours. A better assessment of transgene promoter activity could be afforded through use of *in situ* detection of the GFP transcript, or by generation of a transgenic line carrying a destabilised GFP variant. Preliminary analysis of *gfp* transcripts in 24hpf embryos indeed shows absence of nascent transcript in laterally migrating neural crest cells (i.e. pigment precursors; not shown). It should be noted that similar conclusions were drawn from *sox10 in situ* analysis. Most melanising melanophores did not express *sox10,* and those that did only showed weak expression. However these *in situs* were not developed very far, nor was a detailed timecourse established.

4.3.7. Sox10 promoter activity is retained in cartilage cells and glia

Although, no *sox10* transcripts are present in the branchial arches at 24hpf, *sox10* does come on in these cells later at 48hpf. Analysis of these GFP lines indicates that the Sox10 promoter is active in cartilage cells until at least 20dpf. Thus, the later GFP expression in developing jaw cartilage cells most likely reflects the status of the endogenous *sox10* promoter. It would be interesting to use this transgenic reporter line to ascertain when, if ever, the promoter is inactivated in this cell type.

Apparent in the sox10-4.9:GFP line is the highly variable expression levels in individual cartilage cells, particularly evident in the pectoral fin at 5dpf. This is not apparent in other sox10:GFP transgenic lines, and thus is most likely due to some form of instability of the DNA at the transgene integration site, or some form of position effect variegation. The PACIGFP2 line is just as bright as the sox10-4.9:GFP line, but does not show variable expression levels in cartilage cells. This, combined with the knowledge that it is expressed correctly in the ear, and not in muscle cells, might make this a more reliable *sox10* reporter line, and thus more useful for future experiments

The role of *sox10* in chondrogenesis is currently poorly understood, despite known expression in the facial cartilage of humans and limb cartilage of mice and chicks. One possible role might be to confer competence to respond to BMP signals instructing the onset of chondrogenesis (Chimal-Monroy *et al.*, 2003). Both the two other Group E Sox proteins have known roles in chondrogenesis, and the zebrafish *sox9a* mutant, *jellyfish*, displays severely disrupted chondrocyte morphogenesis and differentiation (Yan *et al.*, 2002). Possible functional redundancy between these closely related proteins might account for lack of an overt cartilage phenotype in *cls*. Alternatively, the *sox10* phenotype might only present much later, beyond the time of embryo death. Transplantation of a few *cls* neural crest cells into wild-type hosts would allow evaluation of a later cartilage neural

crest cell phenotype, as the early death of the embryo would be circumvented, allowing any cartilage cells derived from the donor to be examined *in vivo* at a later stage.

Long-term maintenance of GFP expression is seen in various glial populations. For example satellite glia, oligodendrocytes and Schwann cells express GFP until at least 20dpf. This corresponds to the known role of human and mouse *Sox10* in the direct transcriptional control of a number of glial differentiation genes and myelin associated proteins. No such direct regulation of glial differentiation genes has yet been investigated in zebrafish, but it appears likely given that the *sox10* promoter is active in these cells at mid-larval stages, and possibly throughout life. Thus these GFP transgenic lines strongly suggest that, as in the mouse, *sox10* is expressed in differentiated glial cells, probably with a conserved role. Use of dual immunofluorescence has demonstrated the relationship between GFP expressing cells and neurons of the peripheral nervous system. It would be worthwhile extending this approach to analyse other markers of the PNS, for example using an antibody against axons such as α-tubulin.

Expression of *sox10* in satellite cells had not previously been definitively shown, although it had been strongly suggested (Pauliny, 2002), and is consistent with known expression at this site in mice (Sonnenberg-Riethmacher *et al.*, 2001). The only other known zebrafish gene expressed in this cell type is *foxD3* (*fkd6*; Kelsh *et al.*, 2000a), however expression in this cell type was not reported in the *foxD3*:GFP transgenic line (Gilmour *et al.*, 2002b). Thus the sox10-4.9:GFP line might prove to be a unique tool for analysing development of satellite glia.

4.3.8. Identification of a possible ear enhancer?

Curiously, the sox10-4.9:GFP line showed much weaker expression in the ear than in the neural crest cells or other sites (see Figure 4.13c). This is in contrast to all other transgenic lines and the *in situ* data, which all showed equally strong (or stronger) expression in the ear as in the neural crest. It is tempting to speculate that this latter construct lacks an ear-specific enhancer that directs higher-level expression in this tissue. Unfortunately there is only one sox10-4.9:GFP line discovered so far, meaning that verification of this weak ear expression from this construct is not yet possible. It cannot be discounted that this expression is some form of unusual and specific repression in this site due to a position effect, or to integration near some repressor element. However, this seems unlikely to affect only the ear and it remains possible that an ear enhancer is missing or disrupted in the p4.9:GFP construct. By chance, the *BamH*I site at the 5' end of this construct and used for sub-cloning purposes, occurs in the middle of an extragenic region

with high homology to an upstream region of the Fugu *sox10* gene (see Figure 3.6), which might represent a conserved enhancer. As faint ear expression is seen in the transgenic line carrying a reporter construct containing only half of this region, it is tempting to speculate that this site indeed represents an ear enhancer. Inclusion of the entire region as in the slightly larger 6.1:GFP construct, appears to produce much stronger absolute and relative levels of expression in the ear. A second independent sox10-4.9:GFP line would be extremely useful in validating this observed decrease in ear expression, as would transgenic lines carrying smaller sox10:GFP constructs, excluding this entire conserved domain. Attempts to produce these lines are currently underway (J. Dutton, pers. comm). Further complicating this observation is the strong ear expression of p4.9:GFP in transient assays, however, the strength of this expression may be misleading due to high transgene copy number in the cells.

4.3.9. Potential uses of these GFP reporter lines

A number of experiments using these lines have been proposed already (see above). These involve use of the transgenic lines to fate map GFP^+ (and presumably *sox10*$^+$) premigratory neural crest cells, and to ascertain the *sox10* promoter status in various cell types. A series of other applications are envisaged. Foremost is a genome-wide analysis of neural crest cells' expression profiles. This has recently been conducted in chick using induction of neural crest in explants in combination with subtractive array analysis. A number of gene expressed specifically in the neural crest were identified (Gammill and Bronner-Fraser, 2002). The transgenic lines described here are the first zebrafish GFP transgenic lines to strongly express GFP broadly in premigratory neural crest. This expression pattern should allow isolation of relatively pure neural crest from embryos using FACS. Analysis of the expression profile of these cells using microarrays will provide the first detailed evaluation of genes critical to proper neural crest development. Subtractive or differential screens using GFP labelled neural crest cells in various mutant contexts might further identify specific subsets of genes activated by certain signalling pathways or transcription factors. Such information will allow better understanding of the mechanisms involved in migration, specification and differentiation of neural crest.

At later stages, these transgenic lines appear to label PNS glia, oligodendrocytes and catilage cells. Use of FACS on older embryos, combined with similar microarray based expression profiling will also provide new markers of these cell types. Currently, markers of PNS glia are scarce, and mostly limited to transcription factors previously expressed at premigratory neural crest stages, which renders them unhelpful for establishing the differentiation status of the cells in various genetic contexts (Gilmour *et al.*, 2002b). Thus

markers specific to the different glial cell types labelled in these lines would be of great benefit to the field. Similarly, the PACIGFP2 line labels the ear strongly, whereas the sox10-4.9:GFP line does not. Some form of differential or subtractive screen of FAC sorted cells from both lines could exploit this to isolate ear specific transcripts at various stages.

Further uses of these lines include performing mutagenesis screens to isolate mutants affecting the various cell types labelled. Performing mutant screens using transgenic lines will become more prevalent in the future. The main advantage is that cell types of interest are labelled without the need for lengthy and laborious *in situ* or antibody stainings. Thus structures or cells not readily visible with DIC optics can be assessed. In this manner, use of these *sox10* :GFP reporter lines will allow the isolation of mutants specifically affecting PNS glia, cartilage cells, the otic vesicle, olfactory sensory neurons and/or oligodendrocytes. Additionally, this screen might reveal mutants in which GFP expression is diminished, and thus identify loci that regulate the *sox10* promoter. Knowledge of the regulation of *sox10* is also critical to understanding the mechanisms involved in neural crest specification. There has been no reported examination of the regulation of *sox10* in any species to date.

4.3.10. Analysis of *sox10*:GFP transgenic lines in mutant backgrounds

Finally, these *sox10*:GFP transgenic lines will also allow further analysis of identified mutants. Firstly, the line provides a simple means for labelling a number of different cell types, the development of which can be scored in different genetic contexts. Further, as the transgenics label living cells, cellular behaviour can be followed with timelapse microscopy. One elegant example where GFP transgenics were employed to study previously described mutants used the *foxd3*:GFP line to label posterior lateral line Schwann cells, and to study their behaviour over time using timelapse microscopy in different genetic contexts, including wild-types, *cls* and *shh* (Gilmour *et al.*, 2002b). Similar timelapse studies conducted in the *sox10*:GFP lines could include premigratory neural crest cell behaviour and migration in both wild-type and various mutants. This would constitute a novel and informative approach in the neural crest field. Previously unknown contributions of zebrafish neural crest cells to various organ systems, or better understanding of neural crest cell behaviour in specific mutants might ensue.

The first mutant strain it would be worthwhile analysing with the transgenics might be *cls* itself. One immediate question which could be answered by the transgenics is whether satellite glia occur in *cls* DRGs. This is an important question as some anterior DRG neurons survive at 5dpf, whereas most die. Britsch *et al.*, (2001) has argued that in mice,

loss of DRG neurons is secondary to loss of satellite cell-derived trophic support. The very early DRG neuron phenotype in zebrafish argues that this is not the sole cause of DRG neuron loss in *cls*, but that there is a direct effect due to lack of *sox10* itself in a neuronal precursor. The extent of loss of satellite glia is not known in *cls*. Use of the transgenic line to label these cells promises to answer this, although if present, no comment could be made as to their ability to provide trophic support. However, discovery of a surviving DRG neuron with absolutely no surrounding satellite cells would prove that DRG neurons can form in the absence of this trophic support, and therefore that their loss is not purely secondary to lack of glia.

Other analyses in *cls* using the transgenic lines can be envisaged, and include detailed analysis of the migratory defect of the neural crest cells, and investigations into the sympathetic and enteric nervous system defects.

In summary, the production and characterisation of *sox10*:GFP transgenic reporters has been achieved. These should provide a useful resource for the study of a number of cell-types labelled by the line. A number of labs have recently requested the line for such analyses.

CHAPTER 5

CHARACTERISATION OF TWO *COLOURLESS* ALLELES

5.1. INTRODUCTION

5.1.1. Previous characterisation of *colourless* alleles

The first identified *colourless* allele, cls^{t3}, arose spontaneously in a Tübingen stock (Kelsh *et al.*, 1996). Subsequent large-scale zebrafish mutagenesis screens yielded 6 further *cls* alleles (Kelsh *et al.*, 1996; Malicki *et al.*, 1996), of which 5 remain extant, namely cls^{te275}, cls^{ty22f}, cls^{tw2}, cls^{tw11} and cls^{m618}. The *cls* locus has been shown to closely map to the *sox10* gene (Dutton *et al.*, 2001). As the mutagenic agent used in the screens, ENU, mostly induces point mutations in DNA (Mullins *et al.*, 1994), these alleles, therefore, were expected to display point mutations in the Sox10 protein, leading to non-synonymous amino acid substitutions or nonsense mutations. This has indeed been demonstrated, with the latter three alleles being characterised as either a nonsense mutation leading to a premature stop codon (cls^{tw2} and cls^{tw11}) or as an amino acid substitution (cls^{m618}) (Dutton *et al.*, 2001).

Thus cls^{tw2} and cls^{tw11} both show the lesion K376X in the Sox10 protein, and probably represent independent isolations of the same original mutation event (Figure 5.1a). The introduced stop codon leads to truncation of the Sox10 protein, N-terminal to a domain showing conservation to a transactivation domain in human SOX10 (Dutton *et al.*, 2001). Accordingly, this loss dramatically disrupts the protein's ability to transactivate a reporter construct *in vitro* (Pauliny, 2002).

Meanwhile, the cls^{m618} allele displays the lesion L142Q in the Sox10 protein (Figure 5.1a). This substitutes a highly conserved leucine residue in the DNA binding domain with a glutamine, and also disrupts protein transcriptional potency when assayed *in vitro* (Dutton *et al.*, 2001; Pauliny, 2002). As this mutation occurs in the DNA binding domain, the reason for this reduced transactivation of a target promoter would appear to be due to a compromised ability to bind to DNA. Indeed, computer modelling (done by M. Baker, University of Bath) of a DNA oligo representing a consensus Sox-binding site with the *m618* protein indicates that the substitution alters an amino acid with close association to the DNA sequence, and consequently might significantly alter binding affinities. *In vitro* analysis has confirmed that the same mutation in the human protein reduced its DNA binding activity (Rehberg *et al.*, 2002). This contrasts with gel shift experiments performed in our lab, which did not detect a reduced DNA binding ability compared to wild-type protein (S. Elworthy, pers. comms.). Thus the matter of the DNA binding capability of the $Sox10^{m618}$ protein requires further attention. Interestingly, Rehberg *et al.* (2002)

Figure 5.1 →

Figure 5.1: Summary of characterised *cls* alleles

a. Diagram showing the putative domains of the Sox10 protein including the HMG domain (red) and the transactivation domain (blue). The two described point mutations (*cls*^{m618} and *cls*^{tw2} (=*cls*^{tw11})) are indicated with arrowheads above. Two putative Nuclear Localisation Signals (NLS1 and NLS2) and the Nuclear Export Signal (NES) are shown below with sequences in brackets and the leucine disrupted in *cls*^{m618} is in bold. Adapted from Rehberg *et al.*, 2002.

b. Reduced *sox10* expression levels in the *cls*^{t3} allele as revealed by *in situ* hybridisation. Above panel shows a lateral view of a wild-type embryo (WT) at 18 somites with a *cls*^{t3} sibling at the same stage in the lower panel. Unlike other alleles at this stage, the amount of message is clearly reduced (indicated by arrows in the head and trunk). o, otic vesicle; e eye. Taken from Pauliny, 2002.

a:

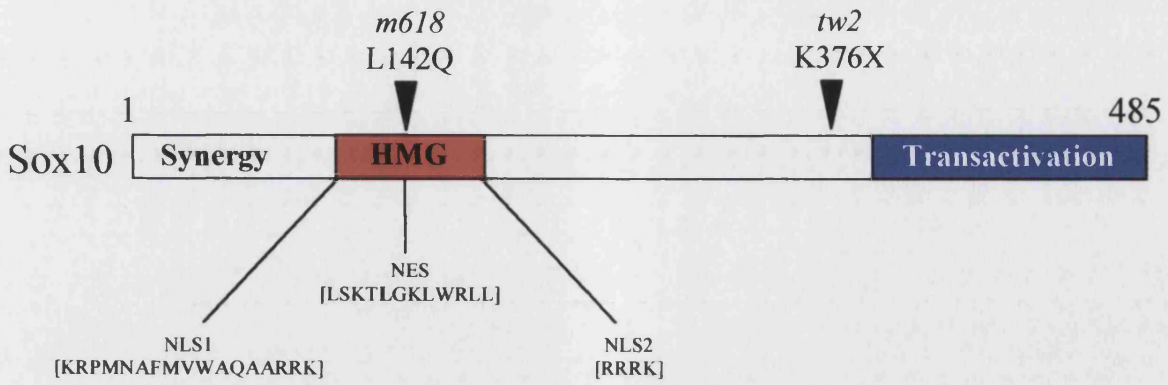
m618
L142Q
tw2
K376X
1
485
Sox10
Synergy
HMG
Transactivation
NES
[LSKTLGKLWRLL]
NLS1
[KRPMNAFMVWAQAARRK]
NLS2
[RRRK]

b:


WT
o
e
t3
o
e

demonstrated that substituting the equivalent leucine with alanine in human Sox10 produced a protein that was able to bind a consensus Sox binding sequence strongly. However, they also showed that unlike wild-type Sox10 protein, which shuttles between the nucleus and the cytoplasm, this protein could not be exported from the nucleus. The mutation deliberately targeted a consensus nuclear export sequence identified in the protein sequence (shown in Figure 5.1a), and largely abolished shuttling of the protein. This shuttling was shown to be critical for the transactivational potency of Sox10 protein possibly due to post-translational modifications effected in the cytoplasm. The authors also substituted the leucine with glutamine as in the *m618* mutation, and again noted defective shuttling, in addition to the compromised DNA-binding ability previously mentioned. Analysis of the sub-cellular localisation of the $Sox10^{m618}$ protein *in vivo* is necessary to establish this in zebrafish, and further *in vitro* experiments are required to determine if lack of export contributes to its inability to transactivate. It is worth remembering that the HMG domain of Sox proteins also mediates protein-protein interactions, necessary for transactivation (see Section 1.2).

Of the remaining alleles, cls^{te275} and cls^{ty22f} are not characterised, however it was desirable to identify the cls^{t3} mutation as it displayed unusual *sox10 in situ* patterns compared with the other *cls* alleles (Figure 5.1b; Pauliny, 2002). Whereas embryos homozygous for the characterised *cls* alleles show a strong *sox10 in situ* signal, cls^{t3} mutants show much lower levels of *sox10* mRNA, and RT-PCR attempts failed (Pauliny, 2002). Although this might be caused by a single point mutation disrupting transcription or transcript stability it is more likely due to some gross disruption at the locus such as a rearrangement, deletion or insertion event.

It should be noted that all alleles mentioned so far seem to show equally strong phenotypes, despite being due to different mutations in the gene. This might suggest that all are null alleles; otherwise it would require the unlikely event that all are hypomorphic to a similar degree (Dutton *et al.*, 2001). The validity of this claim is currently unresolved. A weak *cls* allele (*m241)* was discovered in the Boston screen (Malicki *et al.*, 1996), however this has since been lost, and attempts to re-establish the stock from frozen sperm samples have failed. This is unfortunate as it displays an incomplete loss of dorsal melanophores, and a less severe ear phenotype, but was not fully analysed. Potentially this allele could uncover subtle functions of Sox10 in the neural crest masked by the early apoptosis of these cells.

The aim of this area of work comprised the molecular characterisation of the *t3* allele and also to assist in recovery and characterisation of novel *cls* alleles with the hope of

domain mapping the protein and/or better understanding the roles of Sox10 during neural crest development.

5.1.2. Repetitive elements and transposons in zebrafish

A proportion of spontaneous mutations identified in various organisms can be attributed to transposons, which form a class of mobile, repetitive element found in higher eukaryotes. A summary of repetitive elements and transposons described to date in the zebrafish genome is presented as a tree diagram in Figure 5.2. Transposable elements fall into two groups, defined by the type of intermediate their transposition occurs through. RNA transposons (retroelements or retrotransposons) use an RNA intermediate and thus require reverse transcriptase for their amplification in the genome, whilst DNA transposons are mobilised or replicated through a DNA intermediate produced by the enzyme transposase using a "cut and paste" mechanism (Ivics *et al.*, 1999).

Apart from a small family of Miniature inverted-repeat transposable elements (MITES), DNA transposons identified in zebrafish so far are of the TcE superfamily, which can be divided into two subfamilies, Tdr1 and Tdr2 (Ivics *et al.*, 1999). All DNA transposons identified so far are non-autonomous in that they do not encode a functional transposase. Although there has not yet been direct demonstration of a functional, endogenous reverse transcriptase or transposase in the zebrafish genome, the existence of an active transposase has been inferred by Lam *et al.* (1996) through a hybridisation strategy using a probe to Tdr2. A frequency of Tdr2 transposition per generation was estimated by the authors, which, after extrapolation, led them to conclude that this forms a significant proportion of the background mutation rate. The validity of this claim is questionable as a TcE induced spontaneous mutation is yet to be demonstrated. Direct evidence at the sequence level, such as an induced mutation or identification of a DNA intermediate, is required for conclusive proof of TcE transposition.

RNA transposons are characterised by either the presence or absence of long terminal repeats (LTRs). One LTR containing retrotransposon, *bhikhari*, is present at approximately 100 copies in the genome and is actively transcribed (Vogel and Gerster, 1999), although there is no evidence that it has retained the ability to subsequently transpose. Both classes of non-LTR retrotransposons, namely LINEs (long interspersed nuclear elements) and SINEs (short interspersed nuclear elements), have been described in zebrafish. The first zebrafish SINE identified was named DANA (also called mermaid; Shimoda *et al.*, 1996), which, like most SINEs, appears to be partially derived from tRNA species (Izsvak *et al.*, 1996). DANA elements have been estimated to comprise as much as 10% of the zebrafish genome, approximating 40 000 – 50 000 copies in a haploid genome. They contain a

Figure 5.2 →

Figure 5.2 Tree diagram showing the Repetitive Elements found in zebrafish.

Repetitve elements fall into two main classes, namely Nonmobile, Tandemly repeated elements, which are comprised of high-copy transcribed genes and non-transcribed elements, including structural components of chromosomes (telomeres and centromeres), Variable number tandem repeats (VNTRs) and microsatellites. The other class of repetitive elements are the interspersed transposable elements assigned to two groups based on their method of transposition, namely DNA transposons or RNA transposons. The former include autonomous transposons, which encode their own transposase, and non-autonomous transposons, which rely on an external source of transposase for transposition. The former has not been conclusively demonstrated in zebrafish yet, but foreign transposases have been shown to be functional when introduced into zebrafish (in brackets and indicated with asterisks). Non-autonomous DNA transposons fall into two families: MITES (Minature Inverted-repeat Transposable Elements) and *TcEs* (*Tc1-like* transposable elements).
RNA transposons consist of those with long terminal repeats (LTRs) and those without (non-LTRs). The latter are divided into LINEs (Long Interspersed Nuclear Elements) and SINEs (Short Interspersed Nuclear Elements), to which the retroposon DANA belongs. A DANA-like element has inserted into some other transposable element to form the $DANA_{ntl}$ composite transposon. The method of transposition of this composite transposon is unknown thus cannot strictly be allocated to one of the two classes of transposon. Assembled from Ivics *et al.*, 1999.

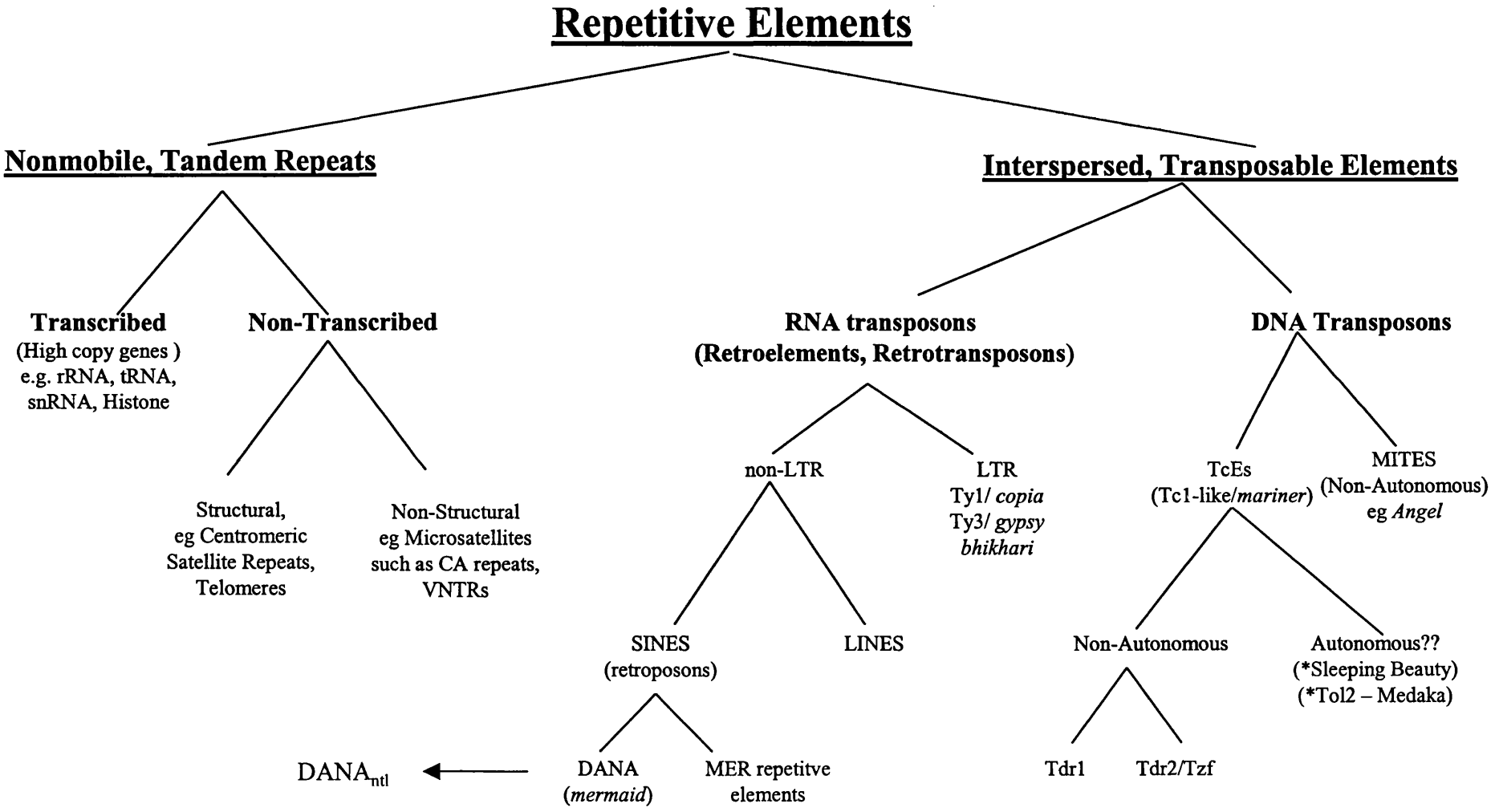
Repetitive Elements
Nonmobile, Tandem Repeats
Interspersed, Transposable Elements
Transcribed
(High copy genes)
e.g. rRNA, tRNA,
snRNA, Histone
Non-Transcribed
Structural,
eg Centromeric
Satellite Repeats,
Telomeres
Non-Structural
eg Microsatellites
such as CA repeats,
VNTRs
RNA transposons
(Retroelements, Retrotransposons)
DNA Transposons
non-LTR
LTR
Ty1/ copia
Ty3/ gypsy
bhikhari
TcEs
(Tc1-like/mariner)
MITES
(Non-Autonomous)
eg Angel
SINES
(retroposons)
LINES
Non-Autonomous
Autonomous??
(*Sleeping Beauty)
(*Tol2 – Medaka)
DANA
(mermaid)
MER repetitve
elements
Tdr1
Tdr2/Tzf
DANA ntl

distinct structure of cassettes containing (up to) four constant (C) regions each separated by an associated variable (V) domain to produce Cv blocks. The number of Cv blocks found in DANA elements varies, and not all four are always present. Composite transposable elements have been formed by DANA elements inserting into other transposable elements, exemplified by a transposon found in a *no tail* allele (Izsvak *et al.*, 1996).

5.1.3. Lateral inhibition functions during zebrafish development

Critical to organogenesis is the production of different cell types in appropriate numbers from a group of equivalent cells. During *Drosophila* neurogenesis, for example, only a subset of ventral neurectoderm cells are specified to form neuroblasts whilst adjacent cells form epidermoblasts (Technau and Campos-Ortega, 1987). Here, regulation of cell specification occurs through lateral inhibition and is mediated by interactions of the trans-membrane Delta ligand with its receptor Notch on neighbouring cells (reviewed in Muskavitch, 1994). Initially, expression of proneural genes acts to define an equivalence group, a group of cells all of which have equal potential to adopt a particular fate. In *Drosophila* neurogenesis, this is termed the proneural cluster, within which a lateral inhibition mechanism acts to select only single cells to become a neuroblast. This occurs through a regulatory feedback loop, with slight stochastic differences in amounts of Notch - Delta signalling amplified to result in a regular repeated pattern of cells expressing relatively high levels of Delta, surrounded by cells expressing Notch. Consequently, the initially equivalent cells are specified to two alternate fates. The Delta expressing cells adopt a primary fate whilst the surrounding Notch expressing cells are inhibited from adopting this primary fate, and later form a cell of alternate fate. Notch or Delta loss-of-function mutations, result in neurogenic phenotypes, with excess cells adopting the primary (neuroblast) fate at the expense of the later fates (reviewed in Chitnis, 1995). For example both Notch and Delta *Drosophila* mutants show overproduction of neuroblasts with concomitant loss of epidermoblasts (Muskavitch, 1994). It appears that this mechanism is widely used in animals, with *Notch* and *Delta* homologues identified in *C. elegans* (Seydoux and Greenwald, 1989) and numerous vertebrate model organisms, including zebrafish (Bierkamp and Campos-Ortega, 1993; Haddon *et al.*, 1998; Westin and Lardelli, 1997).

There are a number of modulators and downstream effectors of this signalling system in both vertebrates and invertebrates. Numb, for example, represses Notch function (reviewed in Struhl and Greenwald, 1999), while cleavage of Notch by presenilins (Chan and Jan, 1999) allows translocation of the Notch signal to the nucleus where, upon binding to the Suppressor of Hairless (Su(H)) protein, activates transcription of bHLH transcription

factors, namely the HES genes (homologues of the hairy and Enhancer of Split genes; Iso *et al.*, 2003). A large number of these components have been identified in zebrafish. In particular, the *Notch* and *Delta* genes of *Drosophila* both have four homologues in zebrafish, namely *notch1a, notch1b, notch2* and *notch3* (Bierkamp and Campos-Ortega, 1993; Westin and Lardelli, 1997), and *deltaA, deltaB, deltaC* and *deltaD* (Haddon *et al.*, 1998; Smithers *et al.*, 2000). Summaries of the expression domains and associated mutant loci of these genes are given in Tables 5.1 and 5.2.

Table 5.1: Expression domains and mutants of zebrafish *delta* genes

Process	Structure	*deltaA*	*deltaB*	*deltaC*	*deltaD*
Gastrulation	Epiblast	✓	✓		
	Hypoblast/margin	✓		✓	✓
Somitogenesis	Tail bud	✓		✓	✓
	Pre Somitic mesoderm			✓	✓
	Paraxial mesoderm /hypochord	✓		✓	✓
	Anterior of formed somites				✓
	Posterior of formed somites			✓	
1° neurogenesis	Trigeminal ganglia	✓	✓		✓
	Rohan-Beards	✓	✓(subset)		✓
	Motorneurons	✓	✓(subset)		✓
	Interneurons	✓	✓(subset)		✓
Later neurogenesis	Cranial ganglia			✓	
	Ear	✓	✓	✓	✓
	Spinal chord/hindbrain			✓	✓
	Retina			✓	
	Lateral Line neuromasts	✓	✓(subset)	✓	✓
	Arteries			✓	
	Pronephros			✓	
	Notochord			✓	
	Epidermal Cells			✓	
	Mutant locus	*dlA*	?	*beamter (bea)*	*after eight (aei)*

Summarised from: (Appel *et al.*, 1998; Dornseifer *et al.*, 1997; Haddon *et al.*, 1998; Holley *et al.*, 2000; Itoh and Chitnis, 2001; Riley *et al.*, 1999; Smithers *et al.*, 2000).

Table 5.2: Expression domains and mutants of zebrafish *notch* genes

Process	Structure	*notch1a*	*notch1b*	*notch2* (*notch6*)	*notch3* (*notch5*)
Cleavage	Maternally derived mRNA	✓			
Gastrulation	Epiblast		✓		✓
	Hypoblast/margin	✓		✓	
	Notochord precursors		✓		
	Hypochord precursors				✓
	Prospective floorplate				✓
Somitogenesis	Tail bud		✓		
	Pre Somitic Mesoderm	✓		✓	✓
	Tail fin primordium		✓		✓
	Anterior of formed somites			✓	
	Posterior of formed somites		✓		✓
° neurogenesis	Neural Rod		✓		✓
	Late Notochord		✓	✓	✓
	Late Hypochord				✓
Later neurogenesis	Neural tube	✓	✓		✓
	Lateral Line neuromasts/primordium				✓
	Anterior lateral line				✓
	Dorsal aorta/arteries				✓
	Endocardium		✓		✓
	Myocardium				✓
	Ear			✓	
	Mutant locus	*deadly seven (des)*	?	?	?

Summarised from: (Bierkamp and Campos-Ortega, 1993; Holley *et al.*, 2002; Itoh and Chitnis, 2001; Westin and Lardelli, 1997).

Although this is unlikely to represent the full expression pattern of these genes, it is apparent that expression patterns often overlap, and may indicate functional redundancy of these genes. Lateral inhibition in *Drosophila* sensory neurogenesis is required at two distinct stages, firstly to select sensory organ precursors and secondly to control cell specification of sibling cells within the developing sensory organ (Jan and Jan, 1994). Detailed analysis of expression of these genes in zebrafish secondary neurons, DRGs and during neural crest development is yet to be conducted, and is critical for understanding control of lineage specification in these domains.

Lateral inhibition has been shown to be critical in regulating both somitogenesis and various aspects of neurogenesis in zebrafish. For example, in both *deadly seven* and *after eight* mutants, only the first few (7-8) anterior somites form correctly (Gray *et al.*, 2001; Holley *et al.*, 2000). Further, the importance of lateral inhibition in neurogenesis is

conserved in zebrafish. Both *delta* mutants, *dlA* and *aei*, display hyperplasia of primary sensory neurons (Rohon-Beard cells) (Cornell and Eisen, 2000; Holley *et al.*, 2000). It was shown for the *dlA* mutant that this is at the expense of neural crest, which was proposed to be the secondary fate of an equivalence group with Rohon-Beards. The inappropriate neurogenesis resulting in the *dlA* mutants is preceeded by an increase both in cells exiting the cell cycle and cells expressing the proneural bHLH gene, *neurogenin1 (ngn1),* which is necessary and sufficient for sensory neuron development (Appel *et al.*, 2001; Blader *et al.*, 1997; Cornell and Eisen, 2002). This is consistent with a role for Notch signalling in maintaining cells in a proliferative state and inhibiting differentiation of the primary fate.

Other phenotypes of the *dlA* mutant include an increase in primary motorneurons and certain interneurons whilst late specified motorneurons were diminished (Appel *et al.*, 2001). *dlA* has an effect on midline structures, showing an excess of notochord cells concomitant with a deficit in hypochord and floorplate cells (also seen in the *aei* mutant and *deltaC* morphants) (Appel *et al.*, 1999; Latimer *et al.*, 2002). Finally, a five-fold increase in hair cells (sensory cells) of the inner ear has been reported for *dlA* mutants by Riley *et al.* (1999). Examination of hair cells in the lateral line system of these mutants has not been conducted, but is likely to reveal a similar over production, as *deltaA* is expressed here, and blocking Delta signalling genetically produces supernumerary hair cells (Itoh and Chitnis, 2001).

The zebrafish *des/notch1a* mutant shows an intriguing neuron phenotype apart from the somite defect previously mentioned (Gray *et al.*, 2001). Although *des* is similar to the *dlA* mutant in showing supernumerary primary motorneurons and early interneurons (Mauthner Cells), it had an opposite effect on sensory neurons. While it displays a decrease in the number of Rohon-Beards, it has a measurable increase in secondary (DRG) neuron number (but not of other neural crest fates) (Gray *et al.*, 2001). This strongly suggests a critical role for lateral inhibition in controlling cell number within DRGs. Due to a scarcity of markers for PNS glia, the authors could not test the relative numbers of these cells in *des*. If the increase in DRG neurons is at the expense of associated glia in the ganglia, it would be compelling evidence of these cell types belonging to an equivalence group, where Notch1a activity is required to stop all cells adopting the neuron fate and instead form glia; failure in this signalling (as in *des*) leads to the inappropriate numbers of cells specifying as the primary fate (neurons). That only a mild neurogenic effect was seen might be due to retained partial function in the mutant or functional redundancy with another zebrafish Notch orthologue. Similar arguments for a Notch/Delta mediated neuron/glia fate choice within DRGs have been made following experimental evidence in chick (Wakamatsu *et al.*, 2000; see below).

Note that replication of many of these mutant phenotypes by experimental manipulation of Delta-Notch signalling has confirmed that they occur through failure of the lateral inhibition mechanism. Injection of synthetic RNA encoding a dominant negative Delta protein phenocopies the primary neuron phenotype of *dlA* mutants (Appel and Eisen, 1998; Cornell and Eisen, 2000), and artificial stimulation of the Notch pathway by introduction of RNA encoding wild-type Delta proteins or constitutively active Notch causes an opposite effect with respect to primary neurogenesis, as well as midline mesoderm and somite defects (Appel *et al.*, 1999; Dornseifer *et al.*, 1997; Haddon *et al.*, 1998). Such an approach is useful when establishing a role for this system in a developmental context, in the absence of an identified mutant, and also in overcoming the effects of functional redundancy. The drawback to this is that it can be non-specific, and thus cause complicated phenotypes which are difficult to interpret, and will often only reveal early phenotypes, masking later roles for Notch-Delta signalling. Scheer *et al.* (2001) have circumvented this by establishing a GAL4-UAS system in zebrafish to spatially and temporally control the misexpression of a constitutively active Notch receptor. They conclude that Notch signalling in the retina prevents neuronal differentiation and instructs cells to become glia and were able to establish a critical period in which Notch-Delta signalling dictated fate choice. Such a genetic system could have wider uses in elucidating the role of lateral inhibition in other domains such as secondary neurogenesis.

5.1.4. Notch and Delta activity directs cell fate choice in DRGs

It is apparent that Notch-Delta mediated lateral inhibition functions in many aspects of zebrafish development, including segregation of neural crest from the neural plate and possibly within developing DRG sensory neurons, and that disruption in this process can cause neurogenic phenotypes. There is growing evidence from other species that it does indeed control fate choice in DRGs and neural crest. Firstly, molecules involved in this signalling system are expressed in neural crest and nascent DRGs in rat, mouse and chick. For example, both Notch1 and Delta1 are expressed in mouse neural crest cells and DRGs (Bettenhausen *et al.*, 1995; Morrison *et al.*, 2000; Williams *et al.*, 1995) as well as in NCSCs isolated from rodent spinal cords or nascent DRGs (Kubu *et al.*, 2002). The HES family transcription factor, *hes6* can be seen in mouse DRGs (Pissarra *et al.*, 2000), where Numb is also expressed (Zilian *et al.*, 2001). Finally, Wakamatsu *et al.* (2000) have shown that *Delta1* and *Notch1* are expressed in migratory neural crest cells in chick and later in nascent DRGs, where neurons within the core of the DRG express Delta1 and are

surrounded by proliferating Notch1 positive cells. Interestingly, asymmetric localisation of NUMB protein was seen in some of the mitotic cells in the periphery of the DRG.

Strong evidence exists that Notch signalling is functional in these domains and has a role in determining neuronal versus glial fate choice in NCSCs. Activation of the Notch signalling pathway in chick and in cultured rat NCSCs promotes gliogenesis, possibly instructively, and concomitantly inhibits proliferation and neuronal differentiation (Morrison *et al.*, 2000; Wakamatsu *et al.*, 2000). As mentioned previously, a similar role for Notch signalling was reported in zebrafish retina by Scheer *et al.* (2001), but unfortunately the authors did not analyse the effect of activated *notch1a* in the PNS. Rat NCSCs become increasingly responsive to Delta signals during DRG development as Notch levels increase and levels of the Notch inhibitor Numb decrease, biasing differentiation from neurogenesis to gliogenesis (Kubu *et al.*, 2002). Further evidence of a role for Numb in this process arises from the Numb knock-out mouse which has no DRG sensory neurons whilst presumptive glia were present (Zilian *et al.*, 2001).

Hence control of relative numbers of cell types found in DRGs relies on Notch-Delta signalling. This is likely to also be true in zebrafish, but has not yet been directly demonstrated. In other vertebrates, this has been achieved through perturbing the notch signalling system artificially during DRG development. Use of appropriate promoters to drive constitutively active Notch, dominant negative Delta or other members of the signalling system in DRGs is feasible in zebrafish. An inducible constitutive *Notch1a* transgenic line is available and chemical inhibitors of Notch signalling have been shown to be effective in zebrafish (Geling *et al.*, 2002). If lateral inhibition regulated cell fate choice in zebrafish DRGs, downregulation of Notch signalling in wild-types would be predicted to produce a neurogenic effect, whilst its induction would lead to lack of neurogenesis.

Production of sensory neurons and glia also requires other factors and regulatory proteins, but understanding how these different influences on NCSCs are integrated into a developmental program is currently limited. Glial differentiation is promoted *in vitro* over neuronal differentiation through interaction of a neuregulin1 (NRG1) isoform (glial growth factor2) with its co-receptors ErbB2/3 within NCSCs (Britsch *et al.*, 2001; Leimeroth *et al.*, 2002; Shah *et al.*, 1994), an interaction that also appears crucial for neural crest cell survival (Paratore *et al.*, 2001). *In vivo,* NRG1 and ErbB3 knock-out mice have no Schwann cells precursors or peripheral nerve associated Schwann cells, later resulting in peripheral nerve cell death (Riethmacher *et al.*, 1997).

Meanwhile, as mentioned earlier, sensory neurons of the DRGs rely on the bHLH proteins, Neurogenin (ngn)-1 and –2, which are necessary and sufficient for specification of sensory neurons. They are expressed in migrating neural crest cells and in early dorsal

root gangliogenesis in both chick and mouse (Ma *et al.*, 1999; Perez *et al.*, 1999), with ngn-2 expression slightly preceeding ngn-1. Mice lacking both neurogenins are devoid of any DRG sensory neurons, and forced expression of ngn1 in migrating chick neural crest cells directs them to migrate to DRGs and induces expression of sensory neuron markers. Zebrafish *neurogenin1* has similar expression patterns and behaves in the same way in functional studies. *ngn1* is expressed in the neural progenitors in the neural plate, including transiently in the neural crest cells and in nascent Rohon-Beards. Later expression is seen in nascent DRG neurons (Blader *et al.*, 1997; Cornell and Eisen, 2002). Reduction of *ngn1* function by use of morpholino injection resulted in a severe reduction in both primary and secondary (DRG) sensory neurons (Cornell and Eisen, 2002), indicating a conservation of roles between higher and lower vertebrates. Additionally, overexpression of *ngn1* in zebrafish leads to ectopic formation of primary neurons (Blader *et al.*, 1997). Neurogenins have also been shown to inhibit gliogenesis directly (Korzh and Strahle, 2002).

Regulatory interactions between proneural factors and Notch signalling have been demonstrated in *Drosophila* (Jan and Jan, 1994), with proneural bHLH transcription factors intimately involved with both the enhancment of lateral inhibition and the read-out through activation of downstream transcription factors responsible for neuronal differentiation (Kunisch *et al.*, 1994). This appears to be conserved in vertebrates, as Notch ligands are co-expressed with neurogenins in mouse (Ma *et al.*, 1997). Further, experiments in lower vertebrates including zebrafish have demonstrated that the proneural gene, *ngn1,* is both a regulator of, and regulated by, lateral inhibition. Induction of ectopic Notch signalling by injection of *Delta* or *her4* RNA leads to strong reduction of *ngn1* expression (Blader *et al.*, 1997; Takke *et al.*, 1999), and ablation of Notch signals through overexpression of a dominant negative form of Delta or in the *dlA* mutant leads to an increase in *ngn1* expression (Appel *et al.*, 2001; Blader *et al.*, 1997). Thus *ngn1* is negatively regulated by Notch activity and consistent with a role in negative feedback, it is also a positive regulator of neurogenic genes. *ngn1* injected embryos show increased levels of *deltaA, deltaD* and *her4,* and this activation, for *deltaD* at least, is probably due to direct binding of *ngn1* to the promoter (Hans and Campos-Ortega, 2002; Takke *et al.*, 1999).Thus a critical gene in sensory neuron specification is intimately involved with the lateral inhibition machinery, providing further evidence that this process is likely to be involved in specifying the correct number of neurons within DRGs.

The mechanisms involved in integrating lateral inhibition and other signalling systems in DRG neurogenesis are poorly understood. Analysis of zebrafish mutations where this process has been perturbed might elucidate how cells interpret these signals. With the *cls* phenotype including severe disruption to DRGs, it is likely that Sox10 plays some role in

this integration of signals, and a more detailed evaluation of the cellular defects in forming DRGs in *cls* embryos is required.

5.2. RESULTS

5.2.1. The *cls*^{t3} allele contains a transposable element

The spontaneous *cls*^{t3} allele displays a curious reduction in transcript levels in homozygotes. With the hypothesis that the *cls*^{t3} allele was due to an insertion, deletion or rearrangement at the *sox10* locus, assessment of the integrity of the gene was required. PCR was used to amplify sections in the 5' and 3' regions of the *sox10* gene from genomic DNA prepared from 5dpf *cls*^{t3} homozygous embryos or sibling embryos. The position of PCR primer combinations are summarised in Figure 5.3a, and conditions used are summarised in Table 2.4. As can be seen in Figure 5.3b and c, PCR products from the 3' region of the *sox10* gene, namely those amplified by S11-S13 and S26-S27 are identical in size between *cls*$^{t3/t3}$ mutant embryos and their siblings. Thus no large insertions or deletions were evident in these regions in the *cls*^{t3} allele. However PCRs using Primers S15-S22 and S17-S22 failed for the *cls* samples (but not siblings; Figure 5.3d) and using Primers S21-S22, there is an approximate 1.4kb increase in the size of the PCR product apparent in *cls*^{t3} homozygous embryos when compared to sibling embryos (Figure 5.3d). This implied that *cls*^{t3} was due to an insertion or duplication event in this 5' region of the *sox10* gene. It seems likely that this increased size of PCR product caused reactions with some of the primer pairs to fail. Additionally it is possible that some of the lanes labelled WT represent products obtained from heterozygous individuals. Although these should in theory show two different sized products with the S21-S22 PCR, it is likely that the shorter of the two products will be amplified with greater efficiency and might preclude amplification of the longer product. To identify the nature of the insertion/duplication via sequencing, the PCR product from the *cls*$^{t3/t3}$ S21-S22 reaction was cloned into pGEM-T Easy™ (Promega) to produce the plasmid pt3-GEMT.

A number of attempts to sequence the insert at the University of Bath sequencing facility failed, with the sequencing reactions prematurely ending a short way into a novel sequence found in the *sox10* gene. Thus it was decided to sequence the insert of pt3-GEMT commercially at Oswell Research Products Ltd. (Southhampton U.K.). The obtained sequence is given in Figure 5.4 and is available in Genbank (Accession Number: AF404490). The insert is 1397bp in size and occurs at position 631 of the cDNA. It shows

Figure 5.3; Figure 5.4 →

Figure 5.3: Assessment of the *sox10*^{t3} gene integrity by PCR

a. Schematic of the *sox10* gene including positions of primers used to assess gene integrity by PCR. Boxes depict exons interrupted by lines (introns), and shaded boxes show coding region with translation start and stop codons marked. Arrowheads with primer names indicate position and direction of priming. Large arrow shows the start of transcription.

b. Agarose gel showing the products obtained from PCR using Primers pair S11-S13.
Lane M: 100bp DNA ladder with selected fragment sizes indicated.
PCRs were performed on single embryo genomic DNA preparations from two *cls* embryos (lanes labelled *cls*) and on four siblings (lanes labelled WT). A negative control PCR was included in which template DNA was replaced with water. This reaction gave no product (lane labelled –ve).
It is clear that PCR products of the expected size (940bp) are present in all lanes corresponding to both mutant and sibling embryos, indicating no overt disruption to this part of the gene.

c. Agarose gel showing the products obtained from PCR using Primer pair S26-S27.
Lane M: 100bp DNA ladder with fragment sizes indicated PCR performed and labelled as in **b.**, with negative control included. Again, PCR products of the expected size (546bp) are present in reactions of both mutant and sibling embryos.

d. Agarose gel showing the products obtained from PCR using Primer pairs S15-S22, S17-S22 and S21-S22. Lanes M: 100bp DNA ladder (left lane) and 1kb DNA ladder (right lane), both with indicated fragment sizes. PCR performed and labelled as in **b.**, each with negative control included.
PCR reactions using Primer pair S15-S22 amplifies across an intron to give an expected fragment size of 2825bp. Note this product is only obtained from WT embryos. Only reactions using *cls*$^{t3/t3}$ embryo template fail to produce a product.
PCR reactions using Primer pair S17-S22 behave similarly. Although a product of the expected size is obtained in WT embryos (597bp), this reaction fails for *cls*$^{t3/t3}$ genomic template.
PCR reactions using Primer pair S21-S22 identify an increased product size in *cls*$^{t3/t3}$ genomic DNA in this region. The fragments obtained from WT embryos are 432bp as expected but those obtained from *cls*$^{t3/t3}$ embryos are approximately 1.8kb (indicated with asterisks). These products were cloned into pGEM-T Easy™ for sequence analysis.

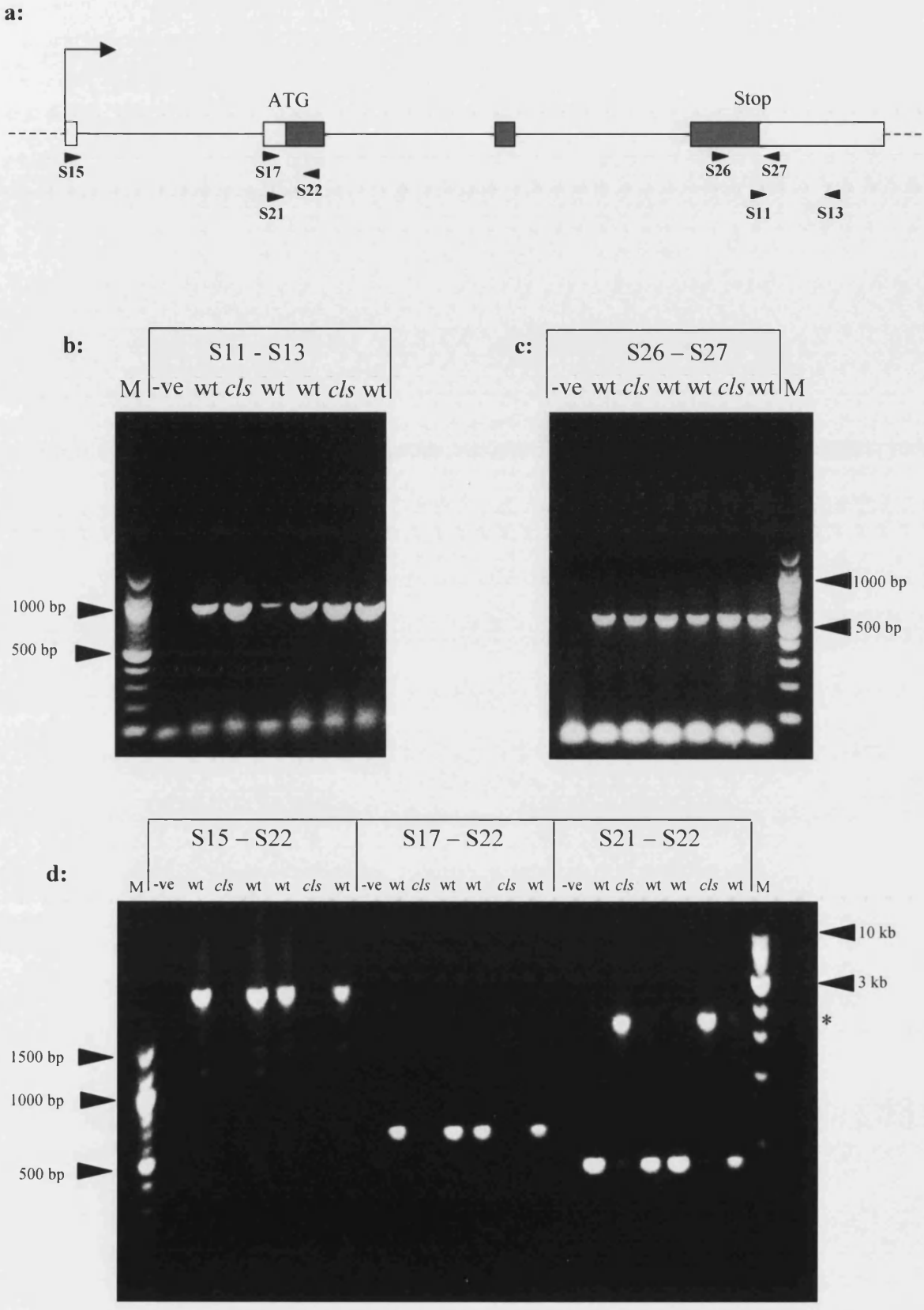
a:
ATG
Stop
S15
S17
S22
S21
S26
S27
S11
S13
b:
S11 - S13
M -ve wt cls wt wt cls wt
1000 bp
500 bp
c:
S26 – S27
-ve wt cls wt wt cls wt M
1000 bp
500 bp
d:
S15 – S22
S17 – S22
S21 – S22
M -ve wt cls wt wt cls wt -ve wt cls wt wt cls wt -ve wt cls wt wt cls wt M
1500 bp
1000 bp
500 bp
10 kb
3 kb
*

Figure 5.4: Sequence and features of the *cls*^{t3} insertion

Sequence of the 1397bp insertion found in the sox10 gene in *cls*^{t3} (sequenced from the plasmid pt3-GEMT). Duplication of host sequence at both ends of the insertion are shown in bold, the two 9bp direct repeats are shown with a solid arrow (▬▬▶), and the six 10bp inverted repeats are depicted by thin arrows (——➔). Additionally, the two Conserved boxes #3 and #4 are underlined and double underlined respectively, and both are shaded in grey. Variable regions #3 and #4 are underscored by asterisks (*) and circumflexes (^) respectively. Bracketing duplications surrounding these Conserved and Variable blocks are in italics and depicted with filled arrowheads above (▬▬▬). A conceptual translation in frame with that of the host *sox10* sequence is given above the corresponding sequence with the novel amino acids in bold and the introduced stop codon boxed.

```
      V  L  N  S  G  A  P  R  K  F  S  *

   1 GGTGCTGAAC AGTGGCGCCC CCAGAAAATT TTCTTAGGGG TGGCCAGAAG AGGCCGCACC

  61 AAATCTTGGG GTGGCACACA AAAAAAATTA TGAATTCAGT GTAATGTTAT ATTTTTGTTT

 121 TTGGTAAATG TAATAATGTA GTTTTTAAAT AAAATTTATT TTATTTTATA ATGTATTTTT

 181 ATTTTTATTT TCAATTTTAA CTAATTTATT TAATTAGTTT ATTATTCCCG GAGATGGGTT

 241 GCAGCTGGAA GGGCATCCAC TGTGTAAAAA TGTGCTAGAT AAGTTGGCAG TTCATTCCAC
                              *****

 301 TGTGGTGACA CTGGATTAAT AAAGGGACTA AGCTGACAAG AAAATGAATG AAAGAATAAT
                                    ^^^^^^ ^^^^^^^^^^ ^^^^^^^^^

 361 GAGTTTATTA ATAACCCAAA CAAATGAACA AACTGAACAA AAGGCATTAC TATACACACT

 421 CACTATACCT AATAATATTA TTTATCCATA TTGCTTTTTG AGCCATTTTA TTAATGCAGC

 481 TTCTTCTATT GATATACTGT ACCTTAAGGT AAATATTAAA ATTGCCATTG CTGTCTATTG

 541 AAGGTGTGTG CGTGCTGTCA ACGACGATCG GGGAGGGTAG TGGCGGTTCT AGTTTAAATG

 601 ACACCCTGGG CGAACCACCC TATACACCCC CACCTCTCTT GAATTGTTAG ATTTGTTATT

 661 CAATAAATAT AACAATTTAT TTATATTTAT TTATTTTACA ATTAATATTA TTATACAATT

 721 ATTATTCTGA ATAAATAACA GAAATCAGTC CTAAATAATA CTGGAAAACA ACAACTGGAG

 781 TGATATGCCA AGATCACTTA AGAAACCTTT TGCATGAAAA TTAATTATGA CAATTCTAAA

 841 GAATACAAAA AATGTATTAT AGAATCATCT GTGGTCTTAG ACCAGATCAT GGCTGAGAAA

 901 TCATGTTATA AAGTATTACC TCCCTGACTC ATTATCCCTC CTTTCTGCTT TAAAGGCATG

 961 CTTAGTGAAA TTAACATCAA CATCATCATC ATCATCATCA TATTATATAA ACTTTAGTCG

1021 ACTTTCACCT CTGCACAAAA GGCTGTTACT CCGTTTCACG GCGCATGAGC GGCGCGTATT

1081 TTGTCGGCGT GCATGCAAAC AACCAACCGG GATGCGTGAG GCGCGCGGGA ATGGTTTTCT

1141 GCGCGCATGC GTCAGTTTGC TTTCACCAGC ATTCAGCATT GAACCAGCAC TAAGGGGGAG

1201 AGACAATGAA TCAGCTACGT CAGTAAAACC AACAATAATT TAGTGGCTGC ATTTTATTTA

1261 TTTAAACAAT GGGAATTTAT AAGTGCATTT AAATCAATAA TGTCAACAGC AAAATTATAT

1321 TGGGGTGGCC ACAGGGGTGG CCAGAGTTTA CTGAGGGGTC CGTGGCCACC CCCTGGCCAC

1381 CCCTTGGGGG CGCCCCTGGT GCTGAAC
```

79% sequence homology to a type of transposon, first identified in the *no tail* allele ntl^{b138} (Figure 5.5; Schulte-Merker *et al.*, 1994). Features of this transposon include duplication of 10bp of host sequence at both ends of the insertion site (Figure 5.4, in bold), a large number of 10bp inverted repeats (Figures 5.4 and 5.5, small arrows) and 9bp direct repeats at the termini (Figures 5.4 and 5.5, solid arrows).

The *t3* and *no tail* insertions contain a region belonging to a family of retroposons called DANA (for Danio retroposon A, Izsvak *et al.*, 1996), and must represent members of a family of composite transposable elements present in the genome. DANA elements are characterised by a consensus structure composed of (up to) four constant domains, each followed by a variable domain (Cv blocks). However not all DANA elements contain all four Cv blocks, and the *no tail* insertion contains only the C_3v_3 C_4v_4 blocks (Izsvak *et al.*, 1996). These are also present in the *t3* insertion and are indicated in Figures 5.4 and 5.5 (underlined and double underlined in both). Conserved direct repeats flanking this region of DANA blocks (termed bracketing duplications) are indicated in italics in both Figure 5.4 and 5.5.

The *t3* insert interrupts the *sox10* gene upstream of the HMG domain and adds eight novel amino acids before introducing an in-frame stop codon (shown in Figures 5.4 and 5.5). This reduces the conceptual Sox10 protein from 485 amino acids in wild-type to only 93 amino acids as represented in Figure 5.12c. A summary diagram of all the features of the insertion is presented in Figure 5.6.

5.2.2. A *sox10* allele screen realizes two new alleles

5.2.2.1. Screen Methodology

The analysis of weak *cls* alleles would be of great interest as such alleles often reveal a range of subtle or later roles of the protein, normally masked by early cell or embryo death. Further, generation of an allelic series for *cls*, with mutations located throughout the protein would facilitate domain mapping. Finally, previously mentioned *cls* alleles do not show any temperature sensitivity. Temperature sensitive alleles have proven enormously informative for enhancer screening and as inducible mutants to reveal adult phenotypes or to define temporal requirements of protein function. An inducible *cls* allele would help to answer a number of questions about Sox10 such as highlighting when function was critical, if there were any later phenotypes and what other loci interact genetically. With this in mind a screen for novel *cls* alleles was embarked on.

The allele screen methodology is depicted in Figure 5.7. Previously, 15 male fish founders (P generation) were mutagenized and mated to wild-type females of the AB

Figure 5.5; Figure 5.6; Figure 5.7 →

Figure 5.5: Sequence alignment of the insertions in *cls*^{t3} and *ntl*^{b195}

Alignment of the transposon insertions found in the *cls*^{t3} and *ntl*^{b195} alleles. These show 79% homology overall, with the *cls*^{t3} being 148bp shorter than the *ntl*^{b195} allele. Features of the transposon are depicted as in Figure 5.3, including Conserved blocks, variable regions, repeats (solid and line arrows), bracketing duplications (in italics) and amino acids introduced in the *t3* allele in bold above their respective codons.

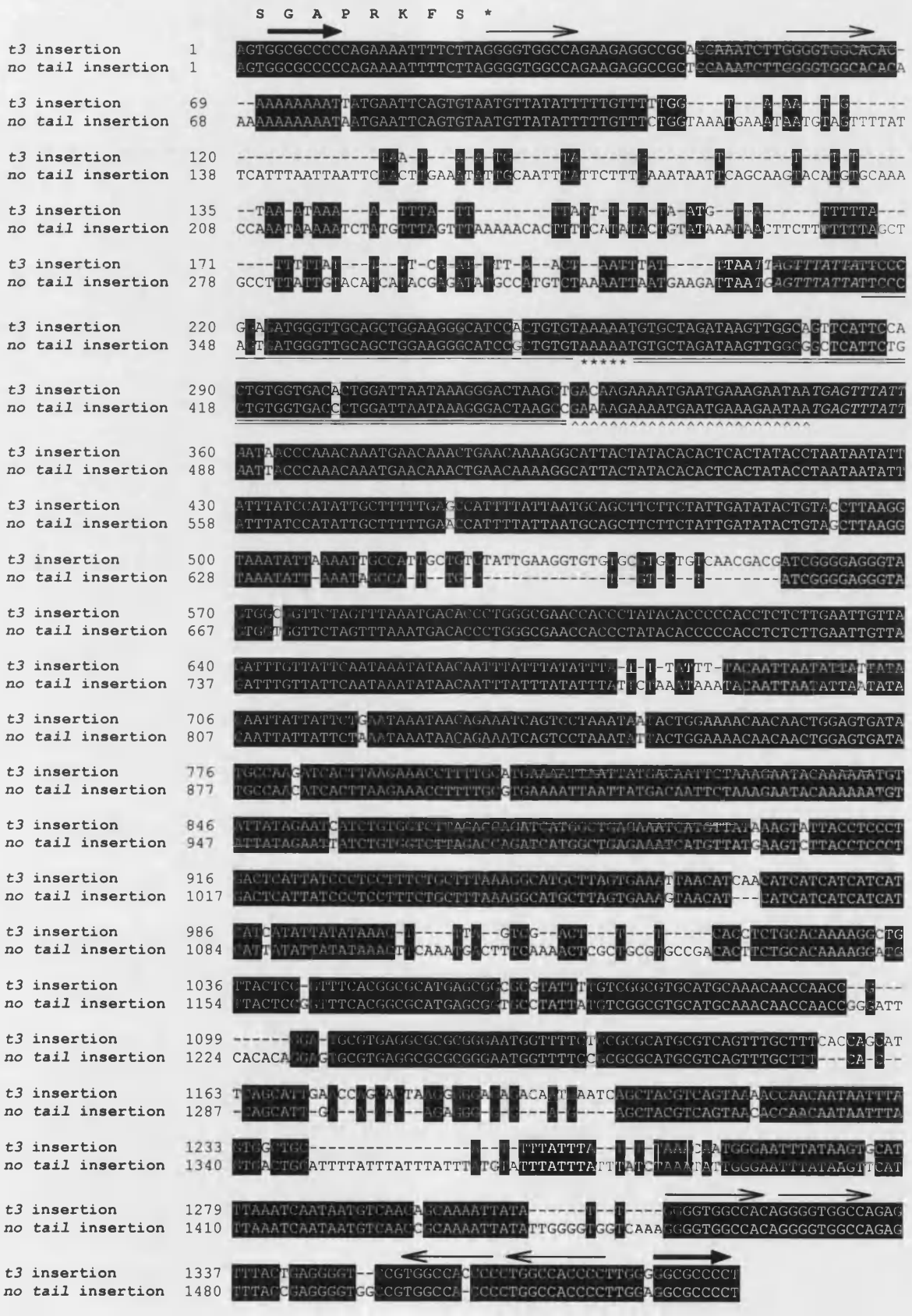
S G A P R K F S *
t3 insertion
no tail insertion

Figure 5.6: Summary diagram of features present on the *cls*^{t3} insertion

Schematic indicating the position and features of the insertion in the sox10^{t3} gene. Lower portion depicts the sox10 gene as per Figure 5.2, where exons are presented as boxes with coding region as black boxes and UTRs as open boxes. The HMG domain is presented as dark grey boxes, and the insertion has occurred in the second exon, 5' to the HMG box. Upper portion depicts features of the insertion largely as per Figure 5.3. Position of the insertion site duplication is shown by line arrows with solid arrowheads (➔). The 9bp direct repeats (➔), 10bp inverted repeats (⟶) and bracketing duplications (►) are also indicated. Cv blocks are numbered and shown as stippled boxes with variable regions as open boxes. The TAG marks the position of the introduced stop codon.

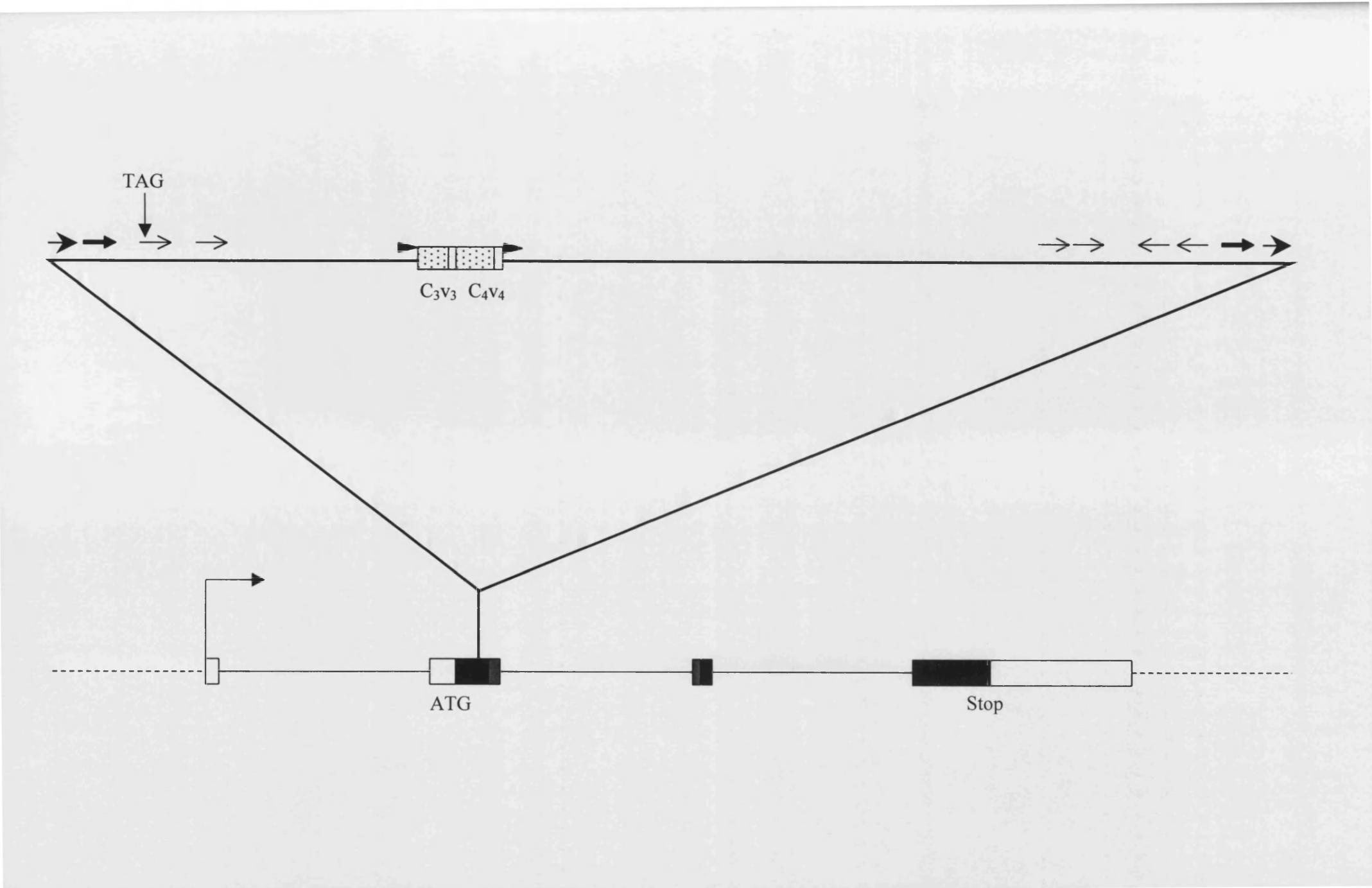
TAG
C3v3 C4v4
ATG
Stop

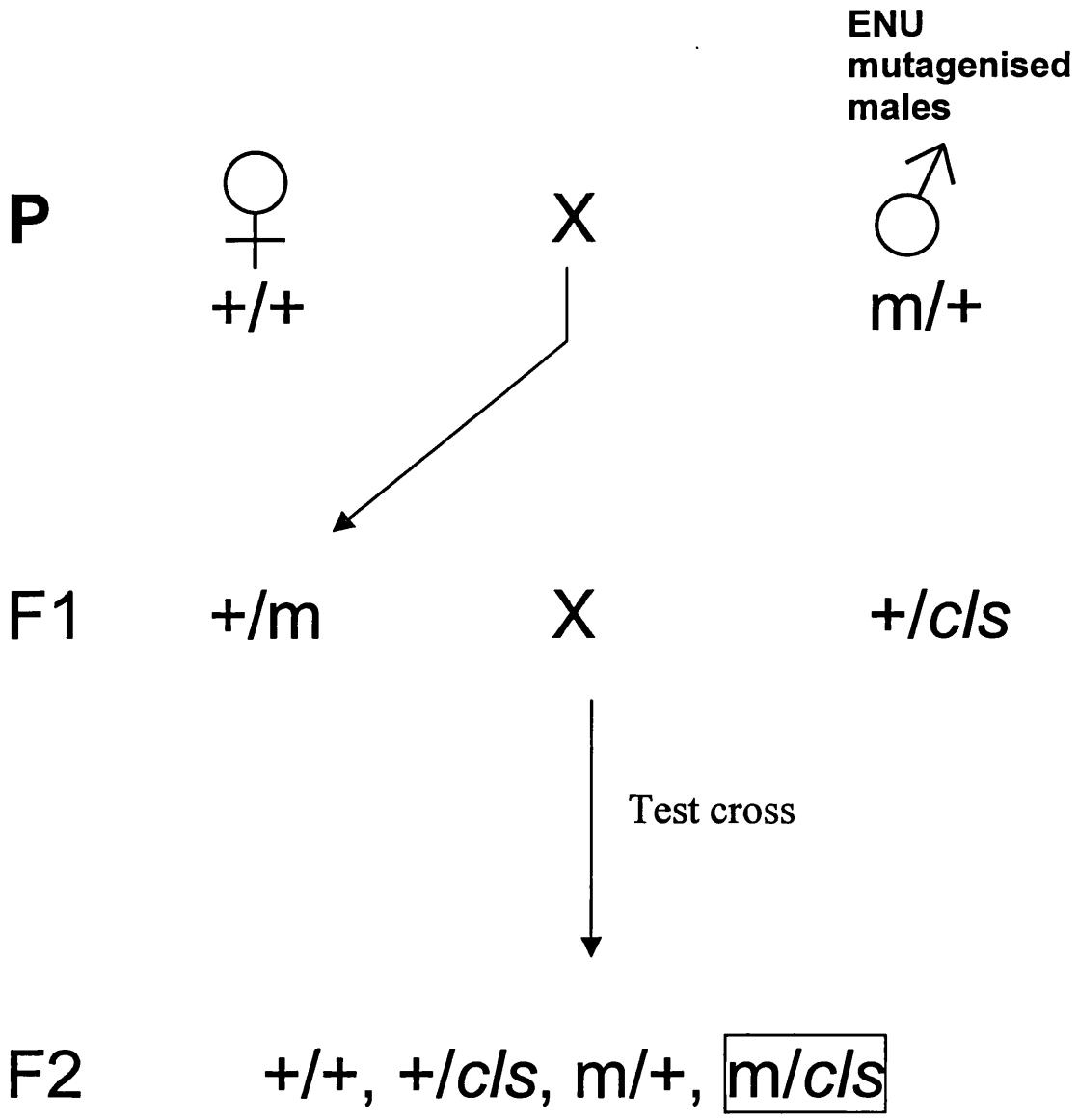

Figure 5.7: Crossing scheme for *cls* allele screen

Males mutagenised with ENU were mated to wild-type females. F1 offspring were thus heterozygous for any mutation, **m**. These fish were test crossed against known *cls* heterozygotes. Any F1 fish bearing a deleterious mutation (**m**) at the *cls* locus would fail to complement and hence present 3:1 wild type:*cls* mutant larvae in F2. Such F1 fish were thus considered "putants", and then outcrossed to wild-type fish.

background. The resulting F1 progeny were raised to adulthood and can be considered to be heterozygous for one mutagenized genome (this mutagenesis stock was produced by K.A. Dutton). To identify any carrying mutations in the *sox10* gene, these were then test-crossed by mating with known *cls* heterozygotes. As *cls* is recessive, any random mutation at this locus will fail to complement and hence present embryos at a 3:1 wild-type:*cls* ratio. In addition to alleles at the *cls* locus itself, it is also possible that a mutation acting as a dominant enhancer of the *cls* mutant allele could also be isolated in this screen.

Using this method, approximately 1800 F1 fish were test-crossed to screen for a *cls* mutant phenotype in the F2 generation. We found 5 putative mutants ("putants"), named *Jupiter, Mercury, Alpha, Zeta* and *Kappa.* All these mutants appear to be as strong as *cls* by appearance of the F2 generation, however this is possibly misleading as these mutants are transheterozygotes, and the weakness of any new allele may be masked by the strength of the established allele. The *Mercury* putant, it should be noted, originally did not shown Mendelian inheritance; only 2 mutants out of approximately 50 embryos showed the *cls* mutant phenotype. Although this could be due to incomplete penetrance, it more likely represents contamination of embryos during collection. Failure to obtain *cls* embryos from this individual when further test-crossed suggested that this latter explanation may be the case, and the *Mercury* putant was discarded. Of the remaining 4 putants, *Zeta* and *Kappa* were successfully outcrossed to wild-type fish, whilst *Jupiter* and *Alpha* were unfortunately lost either due to death, or inability to successfully outcross.

Of the remaining two putants, *Kappa* is yet to be incrossed and extensively examined, whilst *Zeta* has displayed some unique phenotypes.

5.2.2.2. *sox10*^{baz1} (*Zeta*) allele displays a weaker chromatophore phenotype

Having been established, the *sox10* allele *Zeta* was renamed *baz1* (for Bath Zeta 1). Incrosses of *baz1* hetereozygotes produced 25% of embryos with a *cls* appearance as expected (Figure 5.8a). At 5dpf, *baz1* embryos showed no melanophores (Figure 5.8a), although some small melanophores were occasionally seen in the head at an earlier stage such as 3 days (Figure 5.8b), shown migrating behind the ear. However these died by 5 days, and were never seen in other strong *cls* alleles (Kelsh *et al.*, 1996). Large stellate melanophores have been seen in the dorsal stripe of 5dpf *baz1* embryos very rarely (not shown).

Xanthophores were also severely reduced in *baz1*, as shown in Figure 5.8a by the lack of blue/yellow cast over the dorsal portion of the embryo (compare to the wild-type sibling above). Unlike stronger *cls* alleles, a couple of xanthophores were occasionally seen in the anterior head at 5dpf (not shown).

Figure 5.8 ⟶

Figure 5.8: *baz1* pigment phenotype

a. *baz1* shows a strong melanophore and xanthophore phenotype.
Top panel shows a lateral view of a 5dpf wild-type embryo viewed under transmitted light, with melanophores evident in all stripes.
Lower panel shows a $cls^{baz1/baz1}$ sibling, which clearly shows a complete absence of melanophores. Note also that the blue/yellow dorsal cast of xanthophores evident in the wild-type is also missing in the $cls^{baz1/baz1}$ embryo. Dark cells in the lateral patches, dorsal and ventral stripes (highlighted by arrowheads) are iridophores (see below). Compare with lateral view of a strong *cls* allele at 5dpf shown in Introduction chapter.

b. Small melanophores (arrowhead) are sometimes seen in *baz1* migrating ventrally in the head. These have not been reported in other strong *cls* alleles. These cells do not survive to 5dpf.

c. Iridophores are only weakly affected in *baz1*. Lateral view of 5dpf embryos viewed under incident light.
Top panel shows a wild-type embryo with iridophores apparent in the eye, lateral patches, dorsal and ventral stripes (arrowheads), whereas a strong *cls* mutant (e.g. $cls^{t3/t3}$) is mostly devoid of these cells (one is highlighted, middle panel).
Lower panel shows a *baz1* mutant embryo at the same stage, with iridophores clearly present in the eye, lateral patches and both dorsal and ventral stripes, as well as the yolk sac stripe (indicated with arrowheads).

d. Semi-quantitative (see text) comparison of average iridophore score at different sites in *baz1* and *t3* mutant embryos at 5dpf, indicating *baz1* has a generally better coverage of iridophores, which is not confined to any particular site. Error bars show standard deviations.

a.

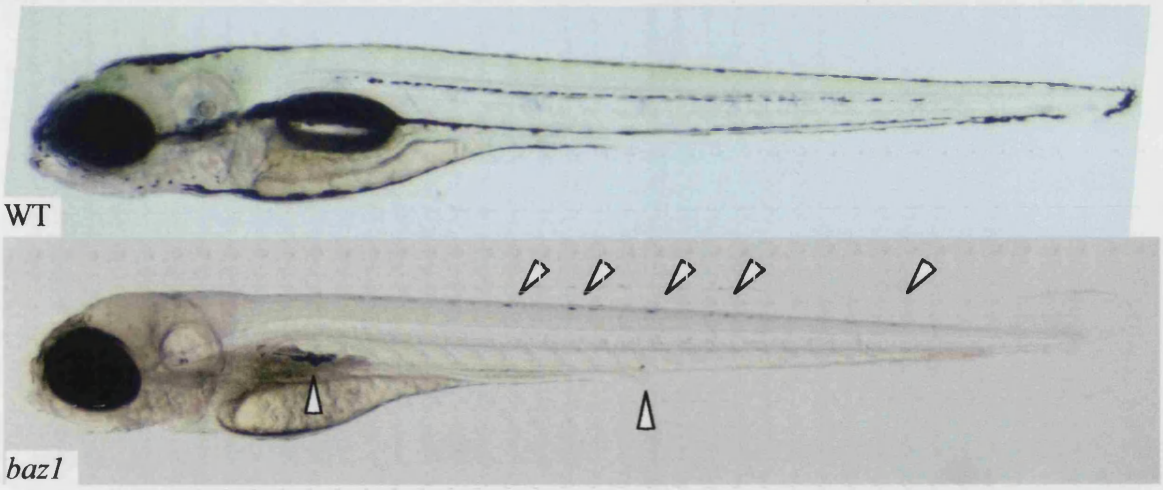
WT
baz1

b.

c.

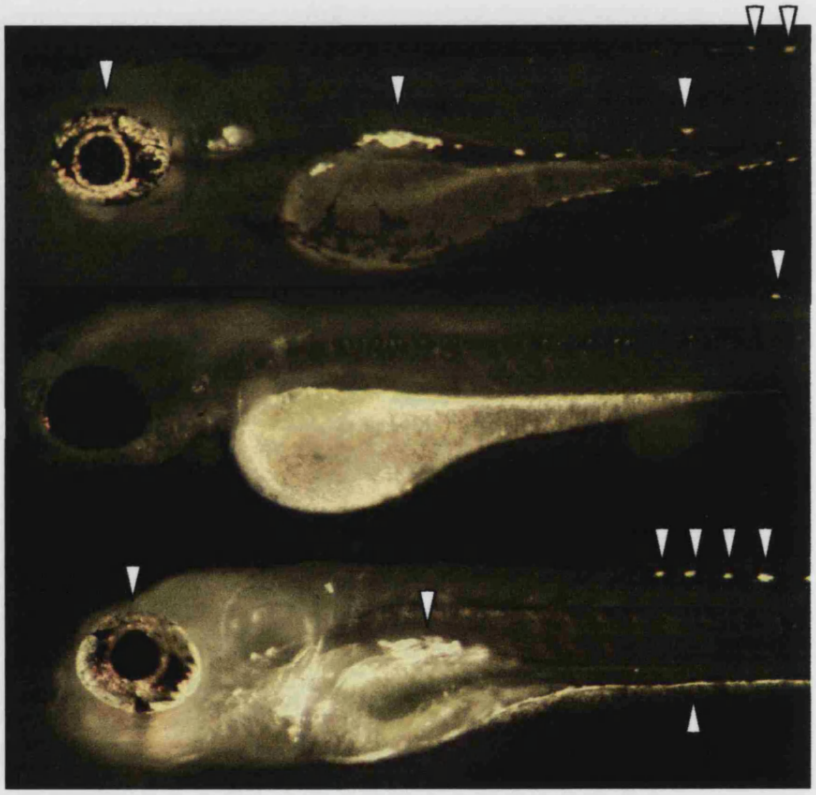
WT
t3
baz1

d.

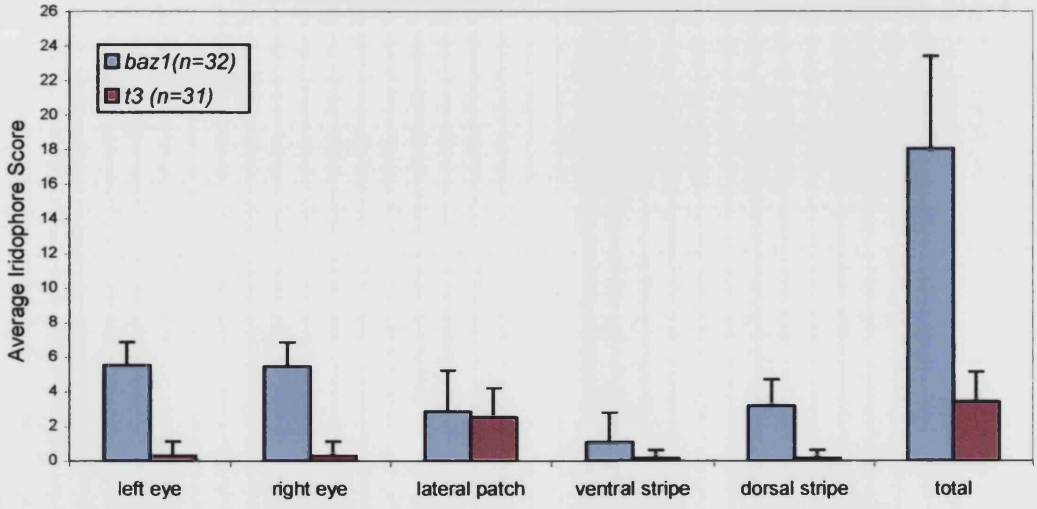
Average Iridophore Score
baz1(n=32)
t3 (n=31)
0
2
4
6
8
10
12
14
16
18
20
22
24
26
left eye
right eye
lateral patch
ventral stripe
dorsal stripe
total

A number of dark cells were seen in the dorsal stripe, lateral patch and often ventrally in *baz1* embryos. Looking at these with incident light revealed that they were in fact iridophores. Figure 5.8c shows a comparison of iridophores in *baz1* with wild-type and *t3* embryos. Clearly *baz1* has a less severe iridophore phenotype than that of *t3*. Note the almost wild-type coverage of iridophores in the *baz1* eye, and presence of iridophores in the lateral patch and dorsal stripe, as well as on the ventral stripe. These latter three regions show an intermediate number of iridophores, clearly being less than in wild-type embryos. Although iridophores are occasionally seen in stronger *cls* alleles, they are limited to a very few on the dorsal stripe, a single patch in one eye or on the lateral patch (an example on the dorsal stripe is indicated with an arrowhead in Figure 5.8c).

The severity of the irdophore phenotype in *baz1* was quantified by assigning an iridophore score out of 6 for each iridophore location over 30 *baz1* and *t3* embryos. This score comprised counts of iridophores on the dorsal and ventral stripes, as well as iridophore patch size in the eyes and lateral patches. Although slightly subjective, the counting criteria were consistent for all embryos. The results from these counts are displayed graphically in Figure 5.8d, and demonstrate the clear difference in iridophore phenotype, when compared to *t3* or other strong *cls* alleles (not shown).

Thus it can be seen that although *baz1* has a strong reduction in melanophore and xanthophore numbers approaching that for the strong *cls* alleles, it displays only a clear weak iridophore phenotype in contrast to the strong alleles. To further examine the *baz1* phenotype it was decided to look at other neural crest fates affected in *cls*.

5.2.2.3. *sox10*^{baz1} has supernumerary peripheral sensory neurons

To analyse the effect of the *baz1* allele on peripheral nervous system neurons derived from the neural crest, immunofluorescence with an antibody to the Hu antigen was performed on 5dpf *baz1* embryos. An example is shown in Figure 5.9a with wild-type and *tw2* embryos for comparison. It was seen that, as with the stronger allele, *baz1* has no enteric neurons were evident along the gut (arrowheads in all panels, compare with wild-type). However where other alleles showed a reduction, *baz1* displayed supernumerary dorsal root ganglia neurons (highlighted by arrows), above the numbers shown for wild-type embryos. Quantitation of this neurogenic effect showed an approximate doubling of DRG neurons compared to wild-type (K.A. Dutton pers. comm.). DRGs were seen in every somite block, with no gaps along the length of the embryo, and, as in other alleles, neurons were not always positioned correctly dorso-ventrally often being sited outside ganglia. Magnified images of adjacent DRGs from *baz1*and *tw2* are shown in Figure 5.9b. Not only were supernumerary neurons seen, but ectopic neurons were prominent too, with Hu^+ cells

Figure 5.9 →

Figure 5.9: *baz1* mutants show supernumerary DRG neurons

a. Lateral view of 5dpf embryos stained with the pan-neuronal marker Hu. DRGs are apparent as reiterated series of labelled cells situated in the middle of each somite in the wild-type (top panel; indicated with arrows). Enteric neurons along the gut are evident as well and indicated with an arrowhead.

Middle panel shows a *tw2* embryo at the same stage, showing an absence of enteric neurons (arrowhead) and a severe, but incomplete, loss of DRG neurons (surviving neurons indicated with arrows). Note that these neurons are often abnormally positioned dorsoventrally, and sometimes occur in mega-ganglia or ectopically on the posterior lateral line (not shown).

Lower panel shows a *baz1* mutant at 5dpf stained with the Hu antibody. Lack of enteric neurons is also apparent as with the stronger alleles (arrowhead), but a greater number of trunk neurons is indicated (arrows). These are present in every somite, and also abnormally positioned.

b. Close up confocal images of posterior trunk DRGs from 5dpf embryos stained with the anti-Hu antibody.

Left panel shows neurons in three DRGs in a wild-type embryo.

Middle panel shows a *tw2* embryo, with a clear reduction of neurons apparent

Right panel show the increase per somite of DRG neurons associated with the *baz1* mutant.

a.

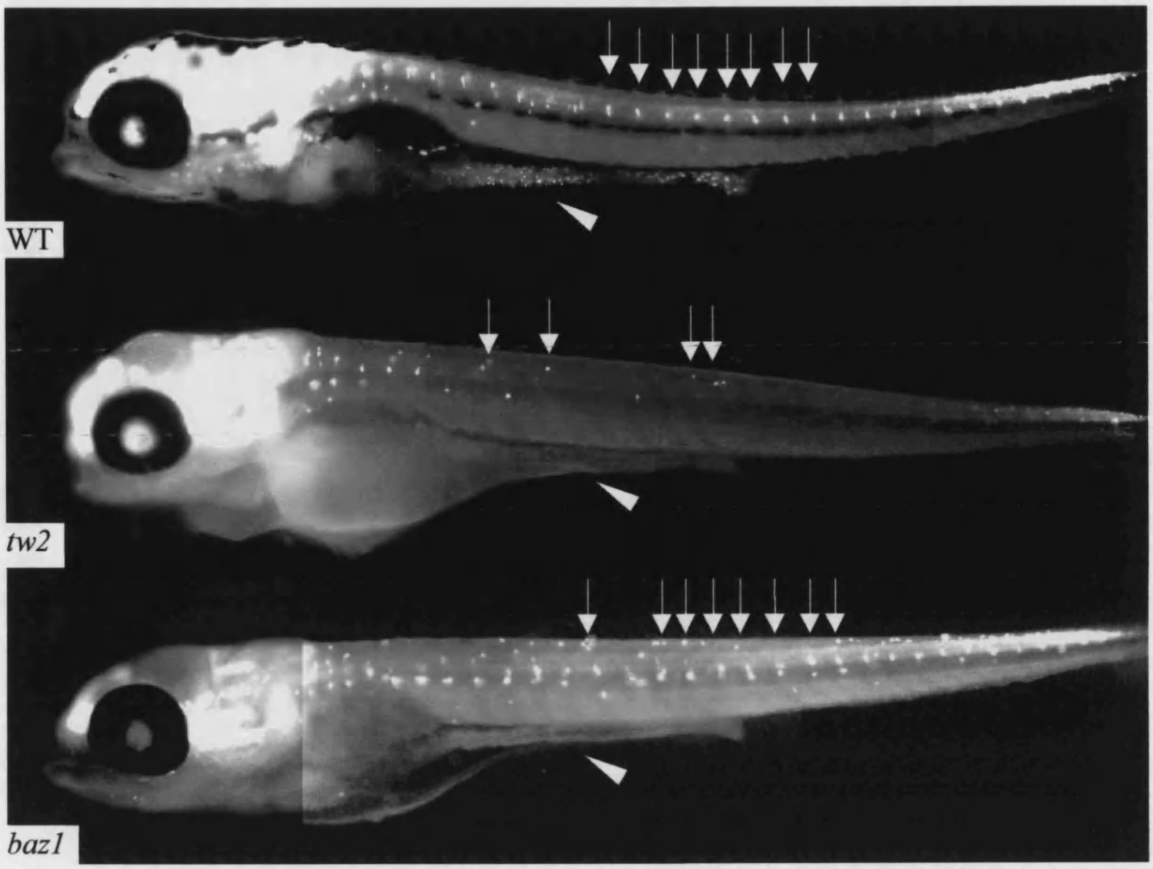

b.

WT *tw2* *baz1*

positioned on the posterior lateral line of a 5dpf *baz1* homozygous embryo (not shown). Analysis at earlier stages indicated that the appearance of these neurons in the DRGs is precocious (K.A. Dutton pers. comm.).

The supernumerary neuron phenotype is not only in contrast to the other *cls* mutant alleles, which all show a strong (but not complete) reduction in DRG neuron numbers, but is also in contrast to known mouse *sox10* homozygous mutants, which also display a severe loss of DRG neurons (Britsch *et al.*, 2001; Kapur, 1999). Whether this reduction in neurons in the mouse mutants is due directly to lack of Sox10 in neural precursors or is secondary to a lack of glial derived trophic support is an area of current debate (Sonnenberg-Riethmacher *et al.*, 2001).

It is important to note that these phenotypes are all recessive, and all sibling embryos appear normal for both chromatophores and DRG neuron number and position. This indicates that the *baz1* mutation is less likely to be due to gain-of-function. This is important to consider when proposing an explanation for the *baz1* phenotypes.

5.2.2.4. The *sox10*^{baz1} molecular lesion occurs in the DNA binding domain

Due to its unique hypermorphic nature with respect to DRG neurons, it was of interest to establish the molecular lesion of *baz1*. To achieve this, four RT-PCR reactions were performed on RNA extracted from 60 30hpf *sox10*$^{baz1/baz1}$ embryos. Primer pairs used are indicated in Figure 5.10a and were designed to produce partially overlapping products corresponding to the entire *sox10* coding region (Pauliny, 2002). PCR products obtained can be seen in Figure 5.10b and are all of the expected size. These were purified using QIAquick columns, including a 35% Guanidine HCl column wash and then sequenced at the University of Bath Automated DNA Sequencing Facility using appropriate PCR primers as a sequencing primer.

The sequences obtained were aligned using BioEdit software and compared to the wild type *sox10* cDNA sequence as shown in Figure 5.11. There are 17 nucleotide substitutions evident, 16 being present in the coding region. The reason for this large number of substitutions is probably that the mutagenesis was conducted in the *leo* background whilst all previous sequencing of *sox10* has been conducted on the AB background. Of these substitutions, only one is non-synonymous, namely a G to A conversion at position 724 of the full cDNA sequence (G→A at 724), which is shown on a chromatogram section in Figure 5.12b. This gives a Valine to Methionine change at amino acid number 117 (V117M) (Figure 5.12a), which occurs in the DNA binding HMG box (underlined in Figure 5.12a), at a position fully conserved between human, mouse and chicken Sox10 protein sequences. This position is also within one of two nuclear localisation sequences in

Figure 5.10; Figure 5.11; Figure 5.12 →

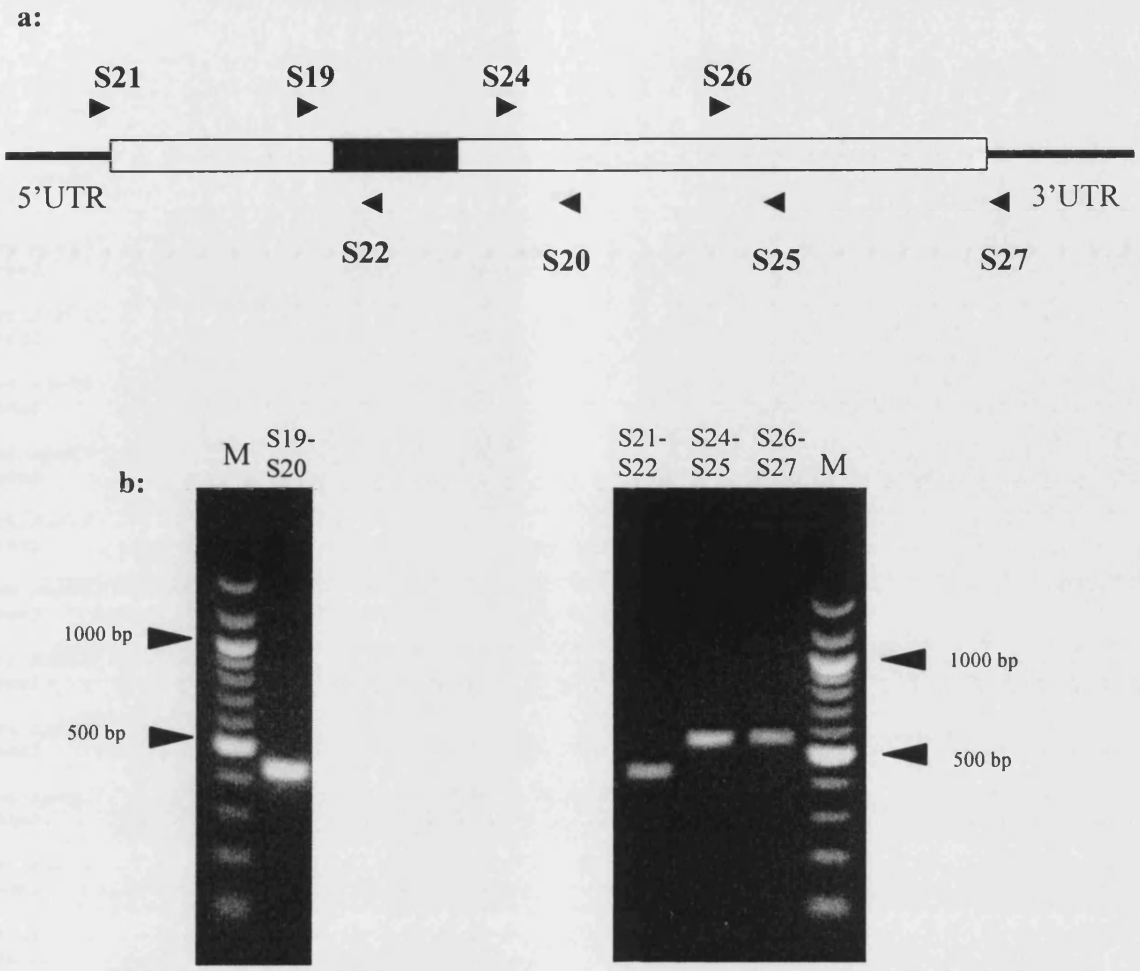

Figure 5.10: RT-PCR of the *baz1* mutant allele

a. Schematic showing the position of primer pairs on the sox10 cDNA used to PCR the coding region of *sox10*^{baz1}. Four overlapping primer pairs were used (arrowheads) and names of primers are given. Coding region is shown as an open box with the HMG box shaded, and the 5' and 3' UTR indicated. Following amplification, sequence of products were obtained and compared to the wild-type sequence (Pauliny, 2002; Genbank Accession number AF402677).

b. Agarose gel showing PCR products obtained from all four PCRs using *baz1* cDNA as template. Both gel images show 100bp DNA Ladder (lane M) with fragment sizes indicated.

Left hand gel image shows the PCR product obtained using Primer pair S19-S20, which yielded a fragment of 435bp as expected

Right hand gel image shows PCR products obtained using Primer pairs S21-S22, S24-S25 and S26-S27. Expected fragment sizes were obtained in each case, being 423bp, 545bp and 550bp respectively.

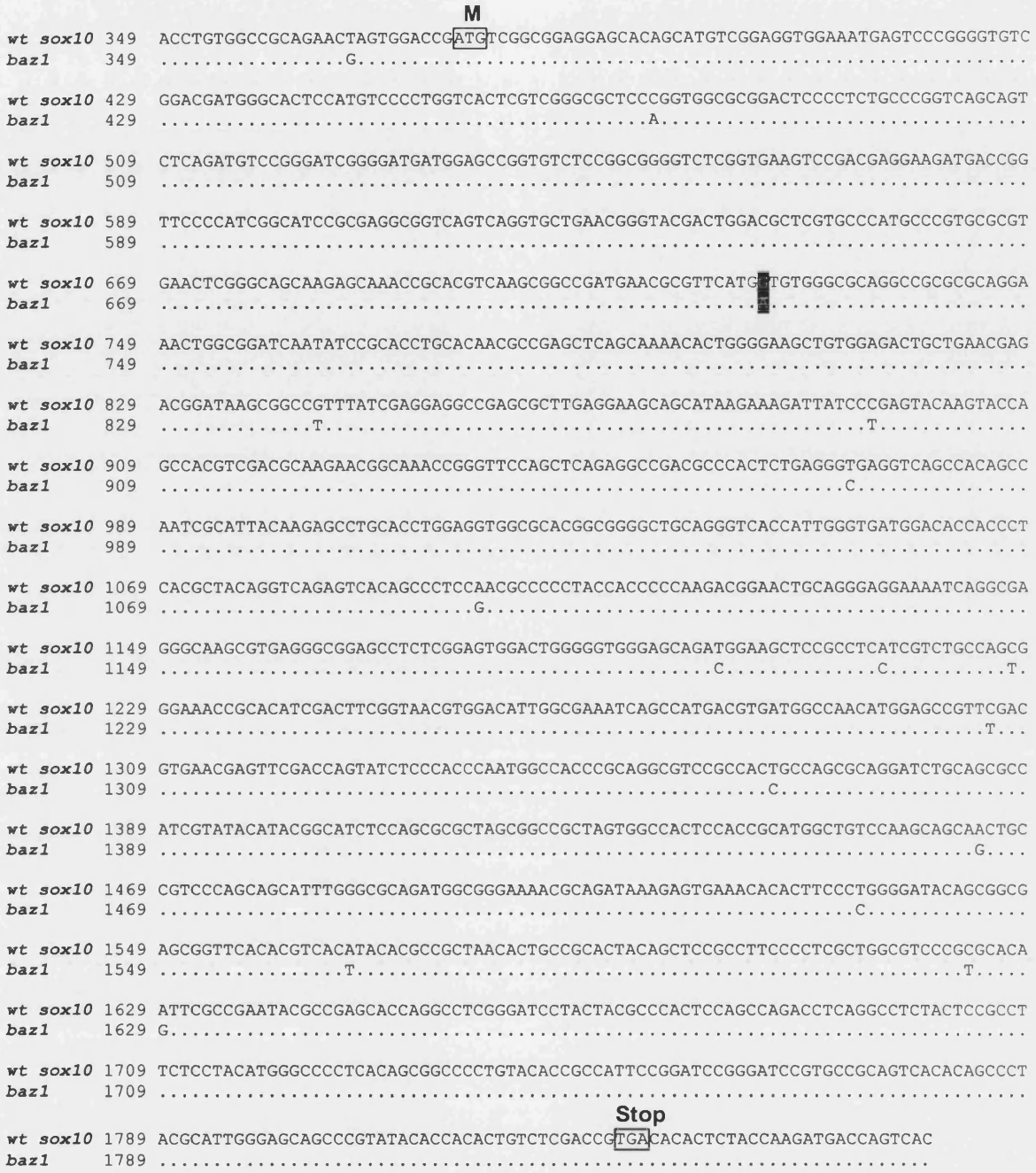

Figure 5.11: cDNA sequence of wild-type and *baz1 sox10* coding region

Sequence of *sox10* cDNA from *baz1* aligned to the wild-type *sox10* cDNA sequence. Numbers on the left correspond to that of the full-length *sox10* cDNA. Dots indicate identical nucleotides and the 17 substitutions found are shown. The non-synonymous substitution at position 724 leading to the amino acid substitution is highlighted. The start and stop codons are boxed and marked as **M** and **Stop** respectively.

Figure 5.12: Amino acid substitution in the *baz1* mutation

a. Alignment of wild-type and *baz1* Sox10 conceptual protein sequences. Numbers on the left correspond to amino acid position. The sole amino acid substitution (V117M) in the *baz1* protein is highlighted. This occurs in the HMG box (underlined) and within one of two sequences with high homology to Nuclear Localisation Sequences described in human SRY and SOX9 (both boxed).

b. Chromatogram traces displaying the nucleotide change producing the amino acid substitution in the $sox10^{baz1}$ coding region. The G to A at position 724 is marked with arrows.

c. Summary of the changes to the Sox10 protein sequence induced by the mutations described in this chapter. The WT protein (top) is compared to the *baz1* mutant protein (middle) where the V117M mutation is shown in the HMG box (red). The 1397bp *t3* insertion at position 631 of the cDNA sequence introduced 8 new amino acids (yellow box) before introducing a premature stop codon.

a.

```
wt Sox10 1    MSAEEHSMSEVEMSPGVSDDGHSMSPGHSSGAPGGADSPLPGQQSQMSGIGDDGAGVSGGVSVKSDEEDD
baz1     1    ............................................................
wt Sox10 71   RFPIGIREAVSQVLNGYDWTLVPMPVRVNSGSKSKPHVKRPMNAFMVWAQAARRKLADQYPHLHNAELSK
baz1     71   ...........................................................
wt Sox10 141  TLGKLWRLLNETDKRPFIEEAERLRKQHKKDYPEYKYQPRRRKNGKPGSSSEADAHSEGEVSHSQSHYKS
baz1     141  ...........................................................
wt Sox10 211  LHLEVAHGGAAGSPLGDGHHPHATGQSHSPPTPPTTPKTELQGGKSGEGKREGGASRSGLGVGADGSSAS
baz1     211  ............................................................
wt Sox10 281  SSASGKPHIDFGNVDIGEISHDVMANMEPFDVNEFDQYLPPNGHPQASATASAGSAAPSYTYGISSALAA
baz1     281  ............................................................
wt Sox10 351  ASGHSTAWLSKQQLPSQQHLGADGGKTQIKSETHFPGDTAASGSHVTYTPLTLPHYSSAFPSLASRAQFA
baz1     351  ............................................................
wt Sox10 421  EYAEHQASGSYYAHSSQTSGLYSAFSYMGPSQRPLYTAIPDPGSVPQSHSPTHWEQPVYTTLSRP* 485
baz1     421  ............................................................* 485
```

b.

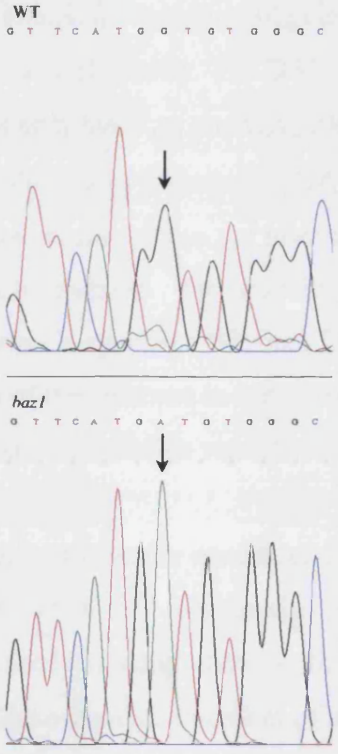

c.

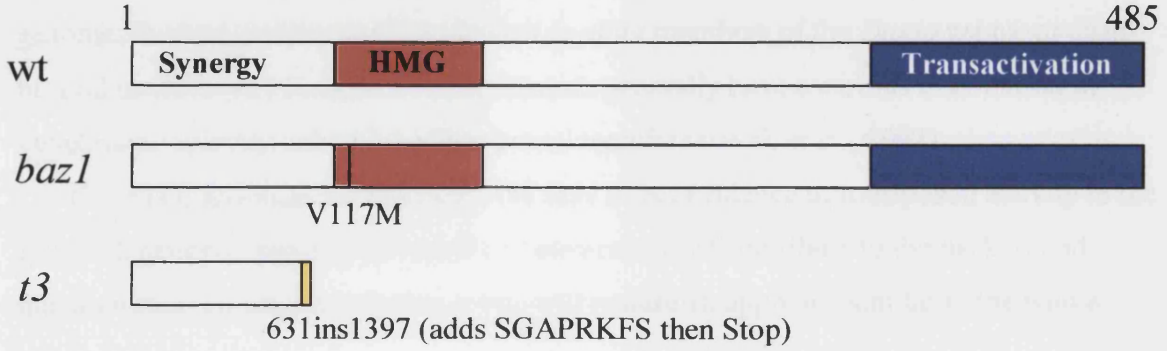

genome hybridisation display as used by Lam *et al.* (1996) for Tdr2. RT-PCR experiments have shown that at least one actively transcribed LTR-retrotransposon, *bhikhari,* exists in zebrafish. It is not known if the transposon present in *t3* is a retroposon or a DNA transposon. A similar RT-PCR approach could be used to detect any corresponding transcript from the *t3* insertion family thus indicating that it transposes through an RNA intermediate and imply that the genome contains an active reverse transcriptase.

Attempting to sequence the cls^{t3} insertion proved difficult, and this may be due to the nature of the sequence it contains. Sequencing the related insertion in the ntl^{b138} allele also proved difficult (S. Schulte-Merker, pers. comm.), and it should be noted that the cls^{t3} sequence reactions failed exactly where the inverted 10bp repeats are found. This could be due to induced secondary structure. Indeed the insert seemed refractory as a template for other polymerases. PCR of the region was problematic, and *in vivo*, levels of *sox10* transcripts appeared to be reduced in $cls^{t3/t3}$ embryos compared to siblings or homozygous *cls* embryos of other alleles when assayed by an *in situ* probe 3' to the insertion site (Pauliny, 2002). This reduction could be due to either decreased processivity of the RNA polymerase complex leading to attenuation of transcription or reduced stability of the entire transcript due to the transposon. To differentiate between these two possibilities it was decided to attempt to detect transcripts using a 5' *sox10 in situ* probe, corresponding to the region upstream of the insertion site. It was hypothesised that if the insertion was destabilising the transcript, then both 5' and 3' ends of the *sox10* transcript would be equally affected. However if the insertion was causing attenuation of transcription, then only a short 5' transcript would be produced, and differently positioned *in situ* probes might reveal relative differences in signal between $cls^{t3/t3}$ and sibling embryos. Although this was attempted, the 5' probe was short and did not give as strong a signal as the 3' probe. Unfortunately this complicated interpretation of the relative *in situ* strengths and the experiment requires repeating, perhaps with more concentrated riboprobe.

Is the cls^{t3} allele a null allele? This is an important question as such alleles reveal the effect of full loss of gene function, whereas alleles with partial protein function remaining are less informative about a genes full function. With the knowledge that the transposon present causes both a dramatic reduction of full-length *sox10* transcript, and also introduces a premature stop codon to give a severely truncated protein, it seems probable that it is a null. However the N-terminal protein-protein synergy domain of Sox10 remains unaffected (see Figure 5.12c), and conceivably might retain some function in the cell. Alternatively, cryptic splicing around the insertion might occur, similar to that seen in a viral insertional mutant of zebrafish *sox9a* (*jellyfish*; Yan *et al.*, 2002), but this remains untested for cls^{t3}. As mentioned previously, the similarity of a number of strong *cls* alleles

argues they are all null; the genetic test would be to combine each allele with a strain carrying a deletion of the locus and assess if this displays a more severe *cls* phenotype. A strain with an appropriate gamma-ray induced deletion in this region of LG3 exists (C1033) produced by the zebrafish deletion project (http://zfin.org).

Finally, use of DNA transposons in the production of zebrafish transgenics through the coordinate use of exogenous transposases and engineered TcE-type constructs are active fields of research. The transposase sources mostly used are *Tol2* isolated from medaka (Kawakami *et al.*, 2000), *Mos1* (from the *mariner* element of *Drosophila mauritiana*; (Fadool *et al.*, 1998) or a phylogenetically reconstructed fish transposase called Sleeping Beauty (Ivics *et al.*, 1997). Development of such a system in zebrafish will be extremely useful, providing a resource similar to the P-element system of *Drosophila*. This will facilitate transgenesis, insertional mutagenesis and enhancer/gene trapping strategies. It has been demonstrated here that there exists an active transposon in zebrafish capable of carrying a sizable amount of DNA (1.4kb), although its method of transposition remains unknown. Perhaps this transposon could also be exploited and modified to produce a potent system for transposition in zebrafish.

5.3.2. *sox10*^{baz1} has divergent effects on certain neural crest derivatives

The phenotype produced by the *sox10*^{baz1} allele is unusual, as it appears to strongly affect some neural crest cell fates, but only weakly affects others. This suggests that the Sox10 protein it produces has an intermediate level of activity. For example, while melanophores and xanthophores are strongly reduced, iridophores are only weakly affected. In other *cls* alleles all pigment cells are strongly affected, although occasional iridophores are seen. Underlying this might be that different levels of Sox10 activity are required by different pigment cell precursors for correct specification, survival or differentiation. In this case, it appears that the threshold of Sox10 activity required for a production of iridophores is less than that required for production of melanophores or xanthophores.

A similar situation occurs in the mouse Sox10 mutant, *Dom*. Haploinsufficiency promotes the loss of only some of the cell types disrupted in homozygous mutants (Kapur, 1999). This indicates that certain cell types are disrupted to different extents than others, depending on the level of Sox10 present. The mechanisms underlying haploinsufficiency of *Sox10* are not well understood. It has been proposed that altered transcriptional synergy due to insufficient amounts of protein is an underlying cause (Veitia, 2002). The resulting dominant phenotype can then be explained by insufficient occupancy of enhancers on target genes by transcription factor-complexes. If different promoters have differing

dosage sensitivities, then pleiotropic effects would be expected to present with different modes of inheritance. The author suggests that hypomorphic alleles in homozygosity might behave like an allele that displays haploinsufficiency, presumably also due to altered extent of enhancer occupation (Veitia, 2002).

What might cause different chromatophores to have different dependency on Sox10 activity? Conceivably, partial functional redundancy of Sox10 with another gene product might account for the increased tolerance of iridophores to loss of Sox10. For example, the *cls* DRG neuron phenotype can be strengthened by ablation of sox9b expression by use of morpholinos, suggesting that sox gene redundancy might cause incomplete sensory neuron loss in *cls* (K.A.Dutton pers. comm.).

An alternative model proposes that different functions of Sox10 are dependent on different levels of Sox10 activity. As alluded to above, this might be realised at the level of the promoter, with different master switch genes triggered at different levels of Sox10 activity. If the affinity of a mutant Sox10 protein to different target gene promoters is not identical then they will be activated to different extents (rheostatic enhancers) or have altered probabilities of becoming active (binary enhancers). Extending this, the nature of the *sox10*^{baz1} molecular lesion might cause differential effects on target promoters. The lesion is found in the DNA binding domain of the protein at a site fully conserved in human, mouse and chicken Sox10 (Cheng *et al.*, 2000), as well as in the other murine E-group sox gene, sox9 and sox8 (Dutton *et al.*, 2001). Computer modelling (done by M. Baker, University of Bath) of a DNA oligo representing a consensus sox-binding site with *baz1* protein has shown that the substituted amino acid does not have close associations with the DNA. Nevertheless, it is predicted to cause a slight conformational change in the protein-DNA complex and could conceivably alter the Sox10 binding affinities or DNA recognition ability. Consequently the Sox10^{baz1} protein might bind to its target promoters with altered affinity, and the differential effects on cell types might be due to differential binding to master gene promoters. This model predicts that *baz1* mutants would be expected to express target genes associated with promoting iridophore development to a more normal level than the *t3* mutants, but like *t3*, would be mostly unable to activate melanophore switch genes. This proposed differential transcriptional activity of the Sox10 mutant proteins requires experimental demonstration *in vivo* through *in situ* analysis of candidate downstream genes and use of *in vitro* transcriptional assays of the associated target promoters. Pigment cell specification genes or other early markers are not well characterised in zebrafish and the only known direct target of zebrafish Sox10 so far is *mitfa* (Elworthy *et al.*, 2003). Other candidates that have been identified include *mbp, ngn1* and *notch1a,* but further targets must exist and need to be identified.

The *baz1* mutation occurs in one of two consensus nuclear localisation motifs, which have been shown to direct the SRY and SOX9 proteins to the nucleus (Sudbeck and Scherer, 1997). In this work, the authors did not mutate the valine residue substituted in *baz1*, however mutation of both motifs was required to completely abolish transport into the nucleus. It is highly likely that Sox10 proteins use these conserved motifs to localise to the nucleus, however this remains to be experimentally demonstrated for Sox10 in any species including zebrafish. Whether the Sox10^{baz1} protein is able to nuclear localise also requires testing, although the work with SOX9 predicts it can. The intermediate activity of the Sox10^{baz1} protein could thus be due to either compromised DNA binding ability, insufficient amounts of the protein entering the nucleus or a combination of both effects.

In contrast to the stronger alleles, *sox10*$^{baz1/baz1}$ displays a neurogenic phenotype with respect to DRG neurons. This divergent phenotype could be explained in four main ways. Extra neurons could be produced by increased proliferation, insufficient culling of neurons or neuroblasts, aberrant migration of other neurons to the DRG location or by inappropriate adoption of the neuronal fate by cells within the nascent DRG. Arguing against increased proliferation or decreased survival, is the detection of neurons in ectopic locations, namely on the posterior lateral line, which could not be produced purely by increased proliferation or enhanced survival. Furthermore, the precocious appearance of the DRG neurons cannot be accounted for by increased proliferation, which would be predicted to produce more neurons later, rather than earlier. A time course of BrdU incorporation in mutant and wild-type DRGs could be used to measure levels of proliferation. Conversely, the relative levels of apoptosis of cells in the ganglia could be analysed with a time course of TUNEL staining to assess if increased survival or lack of normal apoptosis led to the neurogenic phenotype.

As Hu is a marker for all neurons, the precise identity of these supernumerary neurons is yet to be established. Although their position along the entire embryo length and the time they arise is consistent with them being sensory in nature, it cannot be ruled out that they may be ectopic sympathetic neurons that have migrated inappropriately. Molecular markers specific to sensory and sympathetic neurons exist, namely *ngn1* and tyrosine hydroxylase (TH) respectively (An *et al.*, 2002; Cornell and Eisen, 2002), and could be used to characterise these neurons in more detail. Use of an acetylated tubulin antibody could be used to ascertain if the neurons project axons correctly. Preliminary analysis with a TH *in situ* indicated that these supernumerary neurons do indeed express sensory markers (R. N. Kelsh pers.comm.), thus suggesting that these neurons are probably not abberently migrated neurons from other ganglia.

All four hypotheses proposed above rely on different roles of Sox10 requiring different levels of activity, possibly through critical target genes of Sox10 being activated to different extents in *baz1*. This assumption predicts that in stronger *cls* alleles, no critical genes are activated in almost all neural crest cells and all Sox10 functions fail including survival of neural crest stem cells. However, in *baz1*, subsets of genes and thus functions are activated, allowing some form of altered specification, proliferation, survival or migration of some progeny. Observations outlined above argue against a defect in survival, proliferation or migration as the cause of ectopic DRG neurons in *baz1*. It remains that specification of fate might be aberrant in *baz1* DRGs. As neurogenic phenotypes are classically associated with defects in the process of lateral inhibition, production of excess neurons might be brought about by an imbalance in this mechanism within the neural crest cells fated to the DRG lineage, leading to inappropriate neuronal fate adoption by some cells.

5.3.3. The *baz1* allele might indicate a role for Sox10 in establishing or interpreting lateral inhibition within DRGs

Given that there is strong evidence that lateral inhibition occurs in zebrafish and is critical for DRG patterning in vertebrates, it is tempting to speculate that the neurogenic DRG phenotype seen in $Sox10^{baz1}$ mutants is due to disruption in Notch-Delta signalling. If true, this suggests a role for Sox10 in regulation of lateral inhibition, a function not previously attributed to this transcription factor. To determine how suitable this proposed role is, it is necessary to assess the known behaviour of Sox10 in neural crest. Importantly, it appears that Sox10 has multiple roles at different times in certain cell lineages, and that different roles require different doses of *sox10* function.

Firstly, *sox10* is expressed in migratory multipotent NCSCs in mouse and rat, when analysed both *in vivo* and *in vitro* (Kim *et al.*, 2003; Kuhlbrodt *et al.*, 1998b; Paratore *et al.*, 2001), and is also expressed in undifferentiated neural crest cells isolated from mouse DRGs (Paratore *et al.*, 2001). These multipotent DRG associated cells undergo increased apoptosis in $Sox10^{-/-}$ mice but not in heterozygous $Sox10^{+/-}$ mice, suggesting a survival role for Sox10 in NCSCs. Survival of these cells appears to require only one copy of *sox10*, and is NRG1 dependant, exerted through Sox10's ability to positively regulate levels of ErbB3 (Britsch *et al.*, 2001; Kim *et al.*, 2003; Paratore *et al.*, 2001). As mentioned in Section 1.2, recent work in rat has uncovered a role for Sox10 in maintenance of multipotency in NCSCs. Exposing NCSCs *in vitro* with neurogenic or smooth muscle promoting signals irreversibly blocked their potential to later become glia or neurons respectively. However

forced expression of Sox10 protected them against this loss of potency, and additionally maintained their proliferative activity. Interestingly, Sox10 not only maintained NCSCs in a multipotent state, but also inhibited the differentiation of neuronal fates, leading to a delay in neurogenesis. Critically, this latter role requires a higher level of Sox10 than maintenance of neuronal capacity. NCSCs from homozygous *Dom/Dom* embryos display no neuronal capacity and never express neuron markers, whereas NCSCs derived from heterozygous *Dom/+* embryos have neurogenic potency but display neural differentiation markers earlier than wild-type cells (Kim *et al.*, 2003). This reflects the situation in the gut of *sox10* heterozygous mice where distal gut aganglionosis can be attributed to inappropriate initiation of neural differentiation and concomitant depletion of neural progenitors from a proliferative, colonising state (Paratore *et al.*, 2002). In contrast, in homozygous *sox10* mutants, neural crest derived enteric progenitor cells die very early leading to total gut aganglionosis. To summarise, Sox10 has two roles in undifferentiated neural crest cells, firstly a role in their survival and maintenance of potency, which requires a single gene dose and is thus unaffected in heterozygotes, and a role in inhibition of neural differentiation, which requires two copies of Sox10 gene and thus is aberrant in heterozygotes. It is important to note that most of the *in vitro* neural crest experiments use NCSC restricted to the autonomic or smooth muscle lineages. It is not known if these properties of Sox10 activity and function are general or lineage specific.

There is compelling evidence for a subsequent role for Sox10 in glial fate acquisition and differentiation. Upon differentiation, NCSCs downregulate *sox10* in all cell types generated, except glia (Kim *et al.*, 2003; Paratore *et al.*, 2001). Analysis of *sox10*$^{-/-}$ NCSCs in culture demonstrate that not only do they have severely compromised survival, but also those cells that do survive are unable to differentiate as glia, in contrast to wild-type NCSCs (Paratore *et al.*, 2001). This indicates a role for Sox10 in glial fate acquisition and is supported by evidence that surviving neural crest cells in *sox10*$^{-/-}$ embryos also fail to differentiate to glia (Britsch *et al.*, 2001). It is of interest to note that Sox10 is required for Notch expression in mice, which in turn is instructive for gliogenesis (see above). In addition Sox10 is also reported to directly regulate P_0, a myelin gene expressed in differentiated Schwann cells (Peirano *et al.*, 2000). It is yet to be determined whether Sox10 induces these genes in zebrafish, and if so, whether they are direct targets of Sox10.

Finally, although neurons and glia of DRGs appear normal in *sox10*$^{+/-}$ mice, undifferentiated DRG neural crest cells isolated from these mice behave differently to those isolated from wild-type mice in culture. Sox10 heterozygous NCSCs displayed different fate preference away from generation of glia, which was only corrected by both supply of NRG1 signals and allowing cell-cell interactions (Paratore *et al.*, 2001). The

authors concluded that Sox10 levels alter how a cell interprets a combination of external signals, but that there was a degree of redundancy within the integrated signalling networks *in vivo*. The mechanisms involved have not been elucidated, and it is not clear if the nature of the cell-cell interactions include Notch-Delta signalling. As mentioned earlier, dosage of a transcription factor such as *Sox10* could alter levels of protein in such a way as to affect different promoters to different extents, and this effect might be indistinguishable from simply reduced ability to occupy enhancers (Veitia, 2002).

Thus Sox10 activity levels alter responsiveness to extracellular environments. Given the importance of Notch-Delta signalling in patterning DRGs and in gliogenesis, and given that Sox10 is necessary for Notch1 expression in nascent DRGs of mice, it is conceivable that Sox10 levels alter the effectiveness of lateral inhibition. This may be through direct regulation of Notch1 by Sox10, or by Sox10 augmenting the activity of other transcription factors required for Notch expression. Alternatively Sox10 levels could alter a cell's sensitivity to Notch signals by modulating other signalling systems integrated in the lateral inhibition process. Disruption of lateral inhibition within the DRG invoked by reduced Sox10 function might then lead to neurogenic phenotype as in *baz1*.

The production of a neurogenic phenotype through deficiency of a transcription factor implicated in regulating lateral inhibition has been seen previously in zebrafish. The *no isthmus* mutant is deficient for *pax2.1* and displays a neurogenic inner ear hair cell phenotype, having twice the normal number (Riley *et al.*, 1999), a phenotype similar to that of the *dlA* mutant. Expression of *deltaA* and *deltaD* are also perturbed in these mutants indicating *pax2.1* is required for optimal expression of *delta* genes. Thus in this example of neurogenesis in zebrafish, proper lateral inhibition requires regulation by transcription factor activity.

A model explaining why *baz1* mutant embryos, uniquely for *sox10* alleles, produce a neurogenic phenotype can be proposed, and relies on early and late roles for Sox10 in neural crest, as well as the dependence on an integration and interpretation of lateral inhibition signals for appropriate neurogenesis and gliogenesis within DRGs. Firstly, Sox10 has an early role *in vivo* for the survival/maintenance of NCSCs restricted to a DRG fate, requiring relatively low amounts of Sox10 activity. Stronger *cls* alleles do not have sufficient activity for this and so the stem cells fated to become neurons or glia of DRGs apoptose, either before migration or once in a DRG position. *baz1* however has intermediate activity sufficient for survival of these stem cells, but does not have sufficient activity for the later role in gangliogenesis. Analysis of heterozygous stem cells in culture reveals that Sox10 gene dose (and hence presumably amount of activity) alters a cells interpretation of surrounding signals. So the undifferentiated neural crest stem cells in *baz1*

might show less sensitivity to lateral inhibition, either due to a direct lack of Sox10 mediated Notch expression, or an indirect effect on a signal that somehow increases effectiveness of the Notch-Delta signalling system. It is failure of this late role for Sox10 that accounts for its neurogenic phenotype.

This model predicts that further reduction in the levels of Sox10 activity in *baz1* embryos to below a critical level should reverse the neurogenic effect due to increased early loss of NCSCs. Use of varying doses of morpholinos directed against Sox10 might reveal this, alternatively production of transheterozygotes achieved by crossing *baz1* heterozygous fish to heterozygotes of a stronger Sox10 allele would reduce effective levels of Sox10, possibly to below the threshold required for NCSC survival. Furthermore, direct perturbation of Notch-Delta signalling using chemical inhibitors of Notch, or cell-specific promoters driving constitutively active Notch, dominant negative Delta or other members of the signalling system in *baz1* mutants, might enhance or rescue the *baz1* phenotype, and would provide strong evidence that the *baz1* phenotype is due to a defect in lateral inhibition.

The model presented above also predicts that any escaping NCSCs in strong Sox10 mutants might go on to produce supernumerary DRG neurons due to uncovering of the late role for Sox10. This is indeed often the case, with "mega-ganglia" commonly seen in strong *cls* embryos (K.A. Dutton pers. comm.). That they are not the rule for formed DRGs in *cls,* might indicate that only a proportion of NCSCs that contribute to a normal ganglion ever survive, or that there is some additional level of apoptosis due to lack of glial derived trophic support associated with these DRGs.

It is also critical to ascertain if Schwann cells and satellite glia are associated with the supernumerary neurons. If the model is correct, and a failure in lateral inhibition causes supernumerary neurons to form at the expense of glia, then a reduction of glial cells would be evident.

To summarize, the *baz1*mutant appears to have an intermediate level of Sox10 activity, giving divergent effects on neural crest fates. This might be due to different tolerance of critical target promoters to reduced occupation of enhancer sites by transcription factor complexes containing Sox10. It is likely, but remains to be directly shown, that regulation of cell number in zebrafish DRGs is partially controlled by Notch-Delta mediated lateral inhibition. This remains unproven however. The neurogenic phenotype of *baz1* is consistant with this hypothesis and reveals a role for Sox10 in integrating and interpreting lateral inhibition signals during the developmental program of dorsal root gangliogenesis.

CHAPTER 6

CONCLUSIONS

Many aspects of neural crest cell induction, specification, patterning and differentiation are poorly understood. It is evident from mutational studies in a number of vertebrate species that Sox10 is one of the many key factors in this process, although detailed investigation of its function and role during neural crest development is in its infancy. The zebrafish offers new approaches to elucidating the mechanisms involved in neural crest ontogeny. A number of mutants have already been identified, demonstrating that many genes and their functions are conserved between mammals and zebrafish. For example, homozygous Sox10 mutants in mouse, human and zebrafish all show a severe loss of non-ectomesenchymal neural crest derivatives. Evidence from zebrafish indicates that this is primarily due to a failure to specify neural crest progenitor cells to individual fates, most likely due to a failure to activate master switch genes in individual lineages, such as *mitfa* in the melanophore lineage. The complete array of Sox10 target genes is mostly unknown, and the identification of downstream effectors of Sox10 function, such as master transcription factors, remains a critical goal for determining its role in neural crest development. Furthermore, how crest cells integrate the environmental signals presented to them to effect a specific downstream transcription factor cascade is not known, but is crucial to understanding neural crest cell specification and commitment. There is *in vitro* evidence that Sox10 plays a further role in the interpretation of extrinsic signals, and alteration of *Sox10* gene dose alters the response of neural crest cells to their environment, however this has not been well documented *in vivo*. Much of the work in this thesis has been directed towards generating tools to allow these questions, amongst others, to be addressed.

The zebrafish *sox10* genomic region has been cloned and is present on four overlapping PACs. From one of these PACs, high quality sequence of an 18.5kb contig containing the *sox10* gene has been obtained. The predicted amino acid sequence from the gene sequence was identical to that of the published zebrafish *sox10* cDNA. Intron-exon boundaries within the coding region appear conserved with humans and mouse arguing for orthology. Further, evidence that the gene isolated corresponded to the described *sox10* zebrafish mutant, *cls*, was obtained through rescue experiments. The ability of all four PACs to rescue the *cls* pigment defect was demonstrated. Many aspects of the neuronal defects were also rescued but at a much lower frequency. For example, enteric neurons rescue was only identified upon injection of PAC N, although at a low success rate. This low rate of rescue probably means that no conclusions can yet be drawn from the fact that a larger PAC (PAC I) has so far not demonstrated enteric rescue. As the entire genomic region present on the smallest PAC is also present on all the larger PACs, it would be highly surprising if the latter could not rescue enterics. Sympathetic neurons are

completely absent in *cls*, and their presence in a mosaically rescued *cls* embryo, demonstrates that rescue of this cell type is also possible. Less dramatic, nonetheless measurable, was the rescue of DRG neurons. That rescue of DRGs appeared less striking could be attributed to the fact that the DRG phenotype is much less severe in *cls* mutants. Additionally, it is known from lineage analysis that the number of cells giving rise to the DRGs is relatively small, thus restricting the chances of a DRG fated neural crest cell inheriting the injected PAC. It has been proposed from mouse Sox10 mutant analysis that the DRG neuron phenotype is secondary to lack of differentiated glia. It cannot be ruled out by the injection experiments presented here that the DRG neuron rescue is not secondary to glial rescue. The extent of DRG-associated glia hypoplasia has not been fully addressed yet, but glia are not present on the posterior lateral line in *cls* (Kelsh *et al.*, 2000a). Use of the sox10-4.9:GFP transgenic line to visualise glia could be used to determine if any glial cells with normal morphology are present in rescued *cls* embryos. However this would not determine if these cells express appropriate differentiation markers. Attempts to measure the ability of the PACs to fully rescue glia then also require use of the only PNS glial differentiation marker reported so far, namely myelin basic protein (MBP; Brosamle and Halpern, 2002). Similarly, a precise oligodendrocyte defect in *cls* is yet to be established, but the increasing number of oligodendrocyte and myelin markers available could be used towards this end (Park *et al.*, 2002). The mouse *Sox10*^{lacZ} mutants show a terminal differentiation defect in oligodendrocytes (Stolt *et al.*, 2002), and a similar defect might be true in *cls*. Molecular marker analysis could then be used to evaluate the ability of each PAC to rescue any uncovered oligodendrocyte defect.

These rescue experiments were important, not only for establishing that all four PACs map to the *cls/sox10* locus, but also to demonstrate that all four PACs contained sufficient promoter elements to drive Sox10 expression in the neural crest to effect rescue. For the melanophore lineage, the earliest defect in *cls* can be seen at 20hpf, namely loss of the essential melanophore lineage transcription factor, *mitfa*. Thus to rescue melanophores, the PACs must contain elements necessary for driving expression in this early stage of melanophore development. The presence or absence of elements controlling expression in other sites such as in the ear, oligodendrocytes, differentiated glia and cartilage could not be established by rescue experiments, due to a lack of known measurable molecular or morphological defect in *cls*.

Potential *sox10* enhancer sites were identified by sequence comparison of the zebrafish *sox10* gene with a putative *sox10* orthologue from *Fugu* (obtained via the *Fugu* genome sequencing project). As expected the coding sequence and intron-exon boundaries are conserved, but the sequence comparison was also able to detect two conserved regions

outside the transcribed region, one 5' and one 3' to both *sox10* genes. It is not yet known if these conserved regions are significant, or if they are both involved in *sox10* regulation. It would be worthwhile repeating the comparison using a greater amount of flanking sequence in an attempt to identify other conserved regions. Further it is important to scan the conserved regions for consensus transcription factor binding sites, which might reveal information about what might be upstream of Sox10. Finally, a simple functional test demonstrating that the zebrafish and *Fugu sox10* genes are conserved would involve attempting to rescue *cls* with a *Fugu sox10* containing genomic clone. This simple and quick assay would indicate that both gene regulation and protein function are conserved. Similar analysis using a mouse *Sox10* genomic clone would also be of interest. Demonstrating an ability to rescue *cls* with the mouse *Sox10* gene would allow knowledge of the regulation and function of *Sox10* to be transferred between the two species with more confidence.

Having established from the rescue experiments that functional regulatory sequence was present on all 4 PACs, a portion of promoter was subcloned upstream of the GFP reporter. This also included all of the first intron such that the ATG codon of GFP was positioned in an identical position with respect to that of the endogenous Sox10 protein. It has been reported previously that inclusion of the 5'UTR can be important for maximising gene expression, and that genes can contain regulatory regions upstream of the translation start site, but downstream of the transcription initiation site (Gilmour *et al.*, 2002a; Long *et al.*, 1997). Indeed, promoter dissection experiments have recently suggested that a necessary enhancer element is found within intron1 of the zebrafish *sox10* gene (J. Dutton pers. comm.).

Three different sized reporter constructs were produced, two of which were plasmid based, whilst a recombinogenic technique was employed to engineer GFP into PAC I, creating a PAC based reporter. All the reporter constructs described in this work direct GFP expression in domains consistent with the *in situ* data, and which are also conserved with sites of Sox10 expression in other species, including neural crest cells, the ear, oligodendrocytes, cartilage cells and PNS glia. This supports the argument that Sox10 plays similar roles in these species. Some unexpected domains were also revealed for all constructs in transient analyses, namely muscle and interneurons. Presence or absence of the latter has not been definitely demonstrated by *in situ*, and as such might not be ectopic, however the muscle expression was unexpected. Although all constructs showed muscle expression in transient transgenics, only the smallest 4.9:GFP construct consistently did so when integrated into the germline. It has been argued that this inappropriate expression could be due to a combination of copy number and/or insufficient repressor elements. With

regard to the latter possibility, it is of interest that, by chance, the 5' end of the promoter in this construct lies within the region showing sequence conservation with the *Fugu* sequence. Thus the 4.9:GFP reporter only contains half of this conserved region, whilst the larger two constructs contain the entire conserved region. This might have implications for the anomalous expression pattern seen in the sox10-4.9:GFP line, possibly indicating that this region contains a muscle repressor element.

Furthermore, the 4.9:GFP reporter shows strong ear expression in transient analysis, but remarkably weak expression in the transgenic line, where the GFP expression in the ear is at a relatively much lower level than in the neural crest. There are a number of explanations for the faint ear expression, but one attractive explanation is that there are insufficient ear enhancer elements present to direct full GFP expression in the ear. The strong ear expression shown in transient analyses could thus be erroneous and might be due to extremely high copy numbers of transgene inherited by the cells, producing an additive effect and causing low levels of promoter activity to give a very high, but misleading, GFP signal.

Transgenic lines carrying the two larger constructs, p6.1:GFP and PACIGFP2, both show increased absolute levels of GFP expression in the ear compared to the sox10-4.9:GFP. Additionally, in both lines, the relative levels of GFP expression in the ear and neural crest are approximately the same, supporting the notion that the smallest construct lacks an ear specific enhancer. Correlation of the presence of relatively strong ear expression with the conserved sequence region in the promoter mentioned above has been used to suggest the presence of an ear enhancer here.

It should be noted that all four 6.1:GFP lines isolated show only weak GFP expression overall, whilst the 4.9:GFP and PACIGFP2 lines both express strongly. It is difficult at this stage to conclude anything about the strengths of the promoters. Establishing the copy number present in each of these lines is an important task for determining the relative strengths of each of the reporters, and for some of the arguments outlined above. This would easily be achieved through Southern analysis. Further characterisation of the spatiotemporal expression patterns of each of these lines is required, including better understanding of the PNS glial expression and the phases and sites of the CNS expression. It is important to better understand the nature of the ENS expression pattern in all GFP lines. Lack of detectable expression in migrating enteric precursors but later expression in presumptive enteric neurons, directly contrasts with the expression pattern predicted from *in situ* studies and Sox10 expression patterns in other species. It was documented by *in situ* analysis that *sox10* is expressed in cartilage and certain glial cells up to 60hpf. Inspection of the transgenic lines has indicated that this expression is maintained until much later,

being evident in certain glial lineages and cartilage cells until at least 20dpf. The role of *sox10* in the latter site is not yet well understood, but studies in chick have suggested that it permits cells to remain competent to respond to BMP signals (Chimal-Monroy *et al.*, 2003). It is well documented that *Sox10* is required for expression of myelin-associated proteins in differentiated glia, but this has not been demonstrated in zebrafish. Thus there is much to learn about the early and late roles for Sox10 during development.

The sox10:GFP transgenic lines offer a valuable tool for better understanding these roles of Sox10 and the mechanism of neural crest ontogeny. They appear to be the first transgenic line in any species that allow live imaging of both premigratory and migratory neural crest, and thus should prove useful in a number of experiments. Firstly, if combined with cell lineage analysis, they offer a means of determining the fate specification of *sox10* expressing cells from a very early stage. Thus it appears that Sox10 labels prospective neural crest cells before delamination from the neuroepithelium, and might mark these cells before they can be identified by DIC optics. If this is the case, it will allow lineage marking of neural crest precursors to occur at an earlier stage than previously, and thus could demonstrate a cell with less fate restriction than seen with later cells. For example, identification of a clone containing both ectomesenchymal and non-ectomesenchymal derivatives would prove the existence of a neural crest cell potent for both lineages. This has not yet been demonstrated in any organism *in vivo*. Additionally, there appeared to be a degree of heterogeneity present in the premigratory neural crest population with respect to GFP (and presumably *sox10*) expression, with some GFP^- 'holes' present in the neural crest population. This was reminiscent of similar holes seen in the *sox10 in situ* pattern (Pauliny, 2002). It is not known if the heterogeneity of *sox10* expression reflects heterogeneity of fate specification. This is readily testable using the GFP line to allow labelling of GFP^+ (=$sox10^+$) cells and comparing the resulting fates to those of GFP^- (=$sox10^-$) cells, although it first needs to be established by dual labelling that the GFP^- cells are also reliably $sox10^-$. This would prove a novel approach toward the correlation of marker heterogeneity with fate specification.

Due to protein perdurance, GFP itself proved a useful lineage marker, in that it was retained in cells that used to, but no longer, express GFP (=*sox10*). For example, branchial arch expression was prominent in all transgenic lines, but not seen in the *sox10 in situs*. Furthermore, recent *in situ* analysis using a *gfp in situ* probe demonstrated that although the protein was present, the mRNA was not (see figure in Appendix 2). This strongly argued that the *sox10* promoter was not active in these cells at this stage, but had been at an earlier time point, namely at the premigratory stage. This was the first direct evidence that *sox10* expressing premigratory neural crest cells in zebrafish are fated to give rise to jaw

cartilage, and current cell labelling studies are attempting to conclusively demonstrate this. It is also important to identify other cell types which at one stage expressed *sox10* during their development. In particular, DRG neurons are known to be affected in Sox10 mutants in a number of species, but it has not been well documented if their precursors at any stage express Sox10. It has been proposed that the DRG neuron defect is due to lack of glia, as opposed to a cell-autonomous defect caused by lack of Sox10 function. For the latter proposal, it is necessary to demonstrate Sox10 activity at some stage in the cells giving rise to DRG neurons. This could be done using the sox10:GFP line, by lineage labelling GFP^+ ($=sox10^+$) premigratory neural crest cells and showing they can contribute to DRG neurons or simply by showing co-expression of perduring GFP with early sensory neuron markers. Conversely, demonstrating that DRG neurons derive from cells that never express Sox10 would conclusively show that the latter proposal could not account for the DRG phenotype, and would support the alternative trophic model for DRG degeneration.

The observation that GFP expression is not maintained in the melanophore lineage is consistent with preliminary *in situ* analysis which also demonstrated that the *sox10* promoter is inactivated in differentiated melanophores. This supports the recent demonstration that the essential role for *sox10* in the melanophore lineage is to activate *mitfa* (Elworthy *et al.*, 2003). The status of the promoter in other pigment cell types is yet to be established. Fluorescence is seen in these cell types at later stages, but it cannot yet be ruled out that this is not autofluorescence. It is also conceivable that GFP might be more stable in some cell types, or might perdure to different extents in different cell lineages, thus meaning that although GFP signal is lost in melaonophores, it is maintained in xanthophores and iridophores for longer. Preliminary *in situ* analysis, however, hinted that *sox10* was not maintained in any pigment cell type (Pauliny, 2002). Although *sox10* appears to have only an early role in the melanophore lineage, it is likely that it does as well in xanthophores and/or iridophores; however it cannot yet be ruled out that it does not have a later function as well.

The perdurance of GFP in the embryo, exemplified by the expression in the branchial arches, makes the absence of signal in the migrating ENS progenitors even more curious. It would be predicted that even if promoter activity was not maintained in the ENS progenitors, GFP would be seen here as it would have perdured from the earlier expression in premigratory neural crest cells, as seen in the branchial arches. Two explanations can be proposed for this difference. Firstly, the premigratory neural crest cells fated to the ENS might never express GFP, however arguing against this is the observation that all neural crest cells in the vagal region appear to express GFP. There is growing evidence that neural crest cells fated to the ENS do express *sox10* at a premigratory stage, as there is a very

early defect in ENS progenitors in *cls* (Elworthy *et al.*, in prep.). The second explanation might be that perdurance of GFP is different in different neural crest cell lineages. This might conceivably be a function of the number of cell divisions that occur within each lineage. Thus the ENS progenitors might undergo a much greater number of cell divisions, which would be expected to dilute the GFP signal much quicker.

Aside from lineage analysis, other uses for these lines are numerous. Firstly as they live-label a number of developmentally interesting cell types and tissues including premigratory neural crest, migrating neural crest, otic vesicle, cartilage and glial cells, these lines would prove extremely useful for following cell behaviour under wild-type and various mutant conditions. Combined with timelapse microscopy, this might yield a simple means for observing the morphogenesis of certain structures and cell types, such as condensation of jaw elements, migration of neural crest cells or wrapping of axons by myelinating glia. Investigating how these are affected by disruption of certain genes' function would provide a crucial link between molecular and cellular processes. Extending this, these lines will also form the basis for more specific mutagenesis screening by permitting easy visualisation of cell types normally difficult to see. Screens aiming to isolate genes with essential function in these cell types could be readily performed. Mutants that abolish GFP expression altogether might correspond to candidate upstream factors involved in the regulation of *sox10*. A current *sox10* promoter dissection is currently underway and offers a further means of investigating the regulation of *sox10*.

One of the first mutants that needs to be analysed using this line is *cls* itself. The sox10-4.9:GFP line has already been crossed to a *cls* allele, however analysis is only preliminary at this stage. One main hypothesis this might help to test is again the proposal that the DRG neuron defect in *Sox10* mutants is due to loss of glia, and not a direct effect. This model would then predict that all surviving DRG neurons in *cls* will have an associated glial cell adjacent to provide trophic support. Combined use of a neuronal marker and GFP signal in $cls^{-/-}$;sox10-4.9:GFP embryos allows investigation of the presence of GFP^{+} glial cells surrounding neurons. It is important to note however that this does not demonstrate that these glial cells function normally to provide trophic support.

Finally, these GFP lines also offer a powerful means of isolating pure populations of cell types by FACS analysis, as has been previously performed in zebrafish (Long *et al.*, 1997). This will allow expression profiling of specific cell populations at specific developmental stages and in different mutant backgrounds. Combined with microarray analysis, now emerging in the zebrafish field, this will allow identification of cell specific markers and downstream targets of transcription factors such as *sox10*. Markers of certain cell types in zebrafish such as PNS Schwann cells and satellite glia are scarce, and remain

a much needed resource in the neural crest field (Gilmour *et al.*, 2002b). The full repertoire of signalling systems functioning in the neural crest is also not yet determined. Identifying the molecules present at different stages during neural crest specification will allow better understanding of how neural crest cells respond to different signals, and integrate these with intrinsic biases within each cell to achieve fate restriction. Furthermore, detailed understanding of the role of *sox10* in various cell lineages requires determination of its downstream targets. This could be achieved through comparison of the expression profiles of neural crest cells isolated from wild-type and *cls* embryos via microarray analysis. Isolation of neural crest cells by FACS analysis might also facilitate cell biology experiments. One such experiment might involve neural crest heterochronic and heterotopic transplant experiments to be performed, to follow the degree of potency of neural crest cells closely over time. It would be interesting to establish if the *sox10* expressing cells retain greater potency than other non-sox10 expressing neural crest cells. This would provide an *in vivo* test of the proposals made by Kim *et al.* (2003), who showed *in vitro* that SOX10 maintains cells in a multipotent state.

Thus the generation of sox10:GFP transgenic lines should prove a valuable tool to better understanding the ontogeny of various cell types, and the role of Sox10, and only a handful of possible experiments have been outlined here. Of the six lines produced, the PACIGFP2 line appears to be the most promising as it expresses strongly and in sites appropriate for *sox10*. A number of other labs are currently employing these lines for analysing different aspects of neural crest lineages.

The final part of this work involved characterising two unusual *cls* alleles. Firstly, the original *cls* allele, cls^{t3}, which arose spontaneously, has been shown to be due to a transposon insertion event. The transposon was closely related to one previously identified in a *no tail* allele, indicating that these are members of a family of composite transposons active in the zebrafish genome. Although similar, the two transposons were not identical. This might indicate that they are members of separate subfamilies. The number of copies of this family in the genome has been predicted to be around 100. Identification and sequencing of more members of these families might allow estimation of the time they arose in zebrafish. It is not yet known the mechanism of transposition, be it through a DNA or RNA intermediate. The insertion occurs 5' to the HMG box, and appears to disrupt *sox10* transcription or message stability, leading to severe decrease in full length *sox10* mRNA. Furthermore the transposon adds 8 novel amino acids before introducing a stop codon. This reduces the conceptual Sox10 protein to only 93 amino acids. It would thus appear that cls^{t3} represents a null allele, however this is disputed by morpholino

experiments, which appeared to further enhance the $cls^{t3/t3}$ phenotype, arguing that it is not a null (K.A. Dutton pers. com.). The validity of this claim is currently unresolved.

A screen for novel *sox10* alleles yielded an unusual *cls* allele, namely *baz1*. This displayed a strong defect in some neural crest derivatives, but only a weak effect in others. For example, no melanophores with wild-type morphology survived in *baz1* homozygous embryos, but iridophores were only weakly affected. In the PNS, no enteric neurons were evident, however there appeared a striking increase in the number of DRGs. With the knowledge that the molecular lesion in *baz1* is a substitution in the HMG domain, it has been proposed that the $Sox10^{baz1}$ protein might have partially reduced ability to transactivate downstream targets, and might bind to different promoters with different affinities. The precise mechanism producing this difference in activity is not known. It might be that assembly of transcription factor complexes including Sox10 occurs through a different mechanism on different target promoters. For example, if the DNA binding ability of the $Sox10^{baz1}$ protein is compromised by the lesion, then transcription factor complexes that absolutely require Sox10 binding to DNA for assembly will never attach to the DNA. Conversely, transcription factor complexes that only require protein-protein interactions mediated by Sox10 could conceivably form as normal on a target promoter. A similar effect has been noticed previously for the human SOX10 mutation S135T, also found in the HMG domain. Although this protein cannot form a transcription complex bound to the *MITF* promoter, it is able to transactivate the c-RET promoter, but only in the presence of the PAX3 protein, indicating that DNA binding in the latter, but not former case is mediated by PAX3 and not SOX10. The identification of more direct target genes of Sox10 will allow the status of the different downstream promoters in *baz1* to be established.

Thus it is conceivable that partial $Sox10^{baz1}$ protein function could produce disparate effects on different pigment cell types. Similarly, activation of genes involved with DRG formation might also be affected to different extents. Could this produce a neurogenic phenotype? Firstly, DRG progenitors clearly survive in *baz1*, whereas in other stronger alleles they either fail to specify or die at an early stage. This might be because genes required early in progenitors for survival are transcribed in *baz1*, but not in other *cls* alleles. Secondly, there is evidence that levels of Sox10 alter a cell's interpretation of the extrinsic signals in forming DRGs. Sox10 haploinsufficiency has been shown to lead to an excess production of DRG neurons from cultures of neural crest cells *in vitro*. This appears to require cell-cell communication and the absence of NRG1 signalling (Paratore *et al.*, 2001). Further, it has been shown that Notch-Delta signalling functions in both chick DRGs and the neural crest lineage of zebrafish (Cornell and Eisen, 2002; Wakamatsu *et*

al., 2000). A link between Sox10 and Notch-Delta signalling is currently not well established. In $Sox10^{lacZ}/Sox10^{lacZ}$ mice, Notch expression is absent in the DRGs, and induction of ectopic Notch signalling in zebrafish leads to an increase in $sox10^{+}$ cells (possibly glia) located on the medial pathway (Britsch *et al.*, 2001; Park and Appel, 2003). Thus it might be that Sox10 mediates the strength of lateral inhibition in ganglia, and that in *baz1* embryos, this does not occur due to an absence of Notch. DRG neurons thus form at the expense of glia. To test that the supernumerary DRG neurons are produced at the expense of glial fates, it is necessary to show that there is a reduction in the number of glia associated with these neurons. This could be achieved by using sox10:GFP line crossed onto the *baz1* background to visualise glia, or alternatively the inspection of glial specific markers, such as *mbp*. Preliminary analysis using an *mbp in situ* has shown that this marker is absent from the PNS in *baz1*, consistent with a deficit of glia, however this result could simply mean that the glial cells simply do not express differentiation markers. Thus a detailed analysis using the sox10:GFP lines might provide a better examination of the development over time of the two cell types. Perturbing Notch-Delta signalling in zebrafish DRGs will also be important to test the hypothesis that it plays a role in DRG formation. Attempting to rescue the *baz1* DRG phenotype by re-introduction of Notch signalling would strengthen an argument for a failure of lateral inhibition in *baz1*. Although it would be best to perform these analyses *in vivo*, it might be that analysis of neural crest cells isolated from *baz1* and wild-type embryos in culture would permit a more detailed study.

Thus the *baz1* mutant phenotype might represent a unique *in vivo* demonstration of some of the roles of Sox10 proposed by *in vitro* studies. A new idea in murine Sox10 studies is the concept that Sox10 maintains neural crest cells in a "stem cell state", in particular conferring multipotency and proliferative ability. Its levels appear to be critical to how a cell interprets its surroundings. Much of the mouse analysis has been confined to *in vitro* analysis, but the *baz1* mutant might offer an important *in vivo* confirmation of the models proposed by the mouse work, and also demonstration of the numerous roles Sox10 plays during neural crest development, including how it integrates a number of different signals presented to neural crest cells during development.

Both the sox10:GFP transgenic lines and *baz1* represent useful means of dissecting the processes involved in zebrafish neural crest ontogeny, and the role of Sox10 during development.

APPENDICES

Appendix 1: Zebrafish *sox10* cDNA sequence and features

Nucleotide sequence of the full-length zebrafish *sox10* cDNA, as deposited in Genbank (Accession number AF402677; Dutton *et al.*, 2001). Primers are indicated above the sequence as horizontal arrows, certain restriction sites present within the sequence are boxed and intron sites are indicated with vertical arrows. The conceptual translation is shown below the nucleotide sequence, with the start and stop codons underlined. The HMG box and HMG domain are both in bold. The mutant lesions are indicated with the nucleotide substitution written above the nucleotide sequence, and the incurred amino acid change in a bracket above the corresponding conceptual translation. Introduction or destruction of a restriction site in the cDNA sequence by the nucleotide substitution is also indicated. The sequence duplicated by the *t3* insertion event is bracketed, and the novel amino acids presented in a text box.

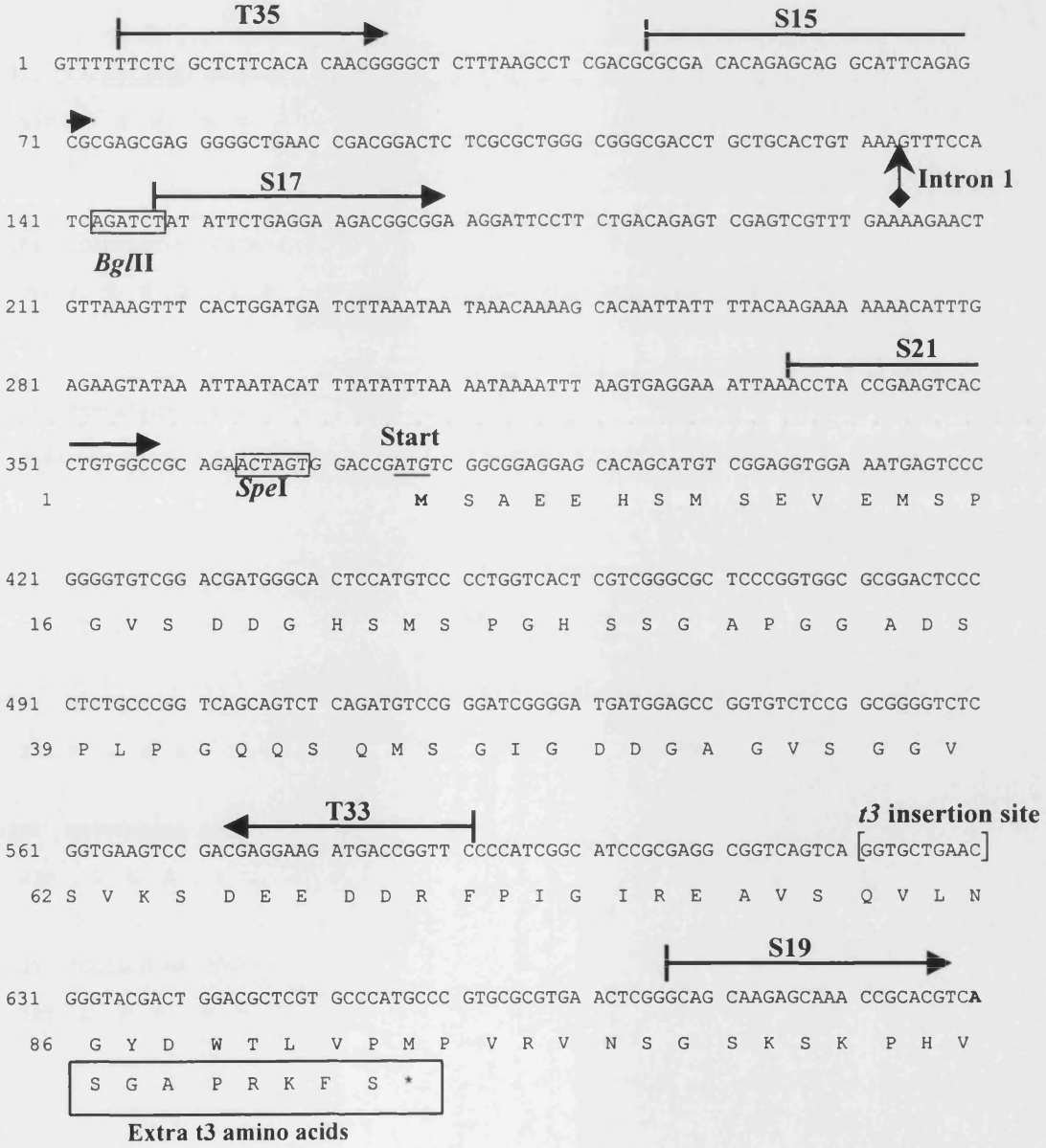

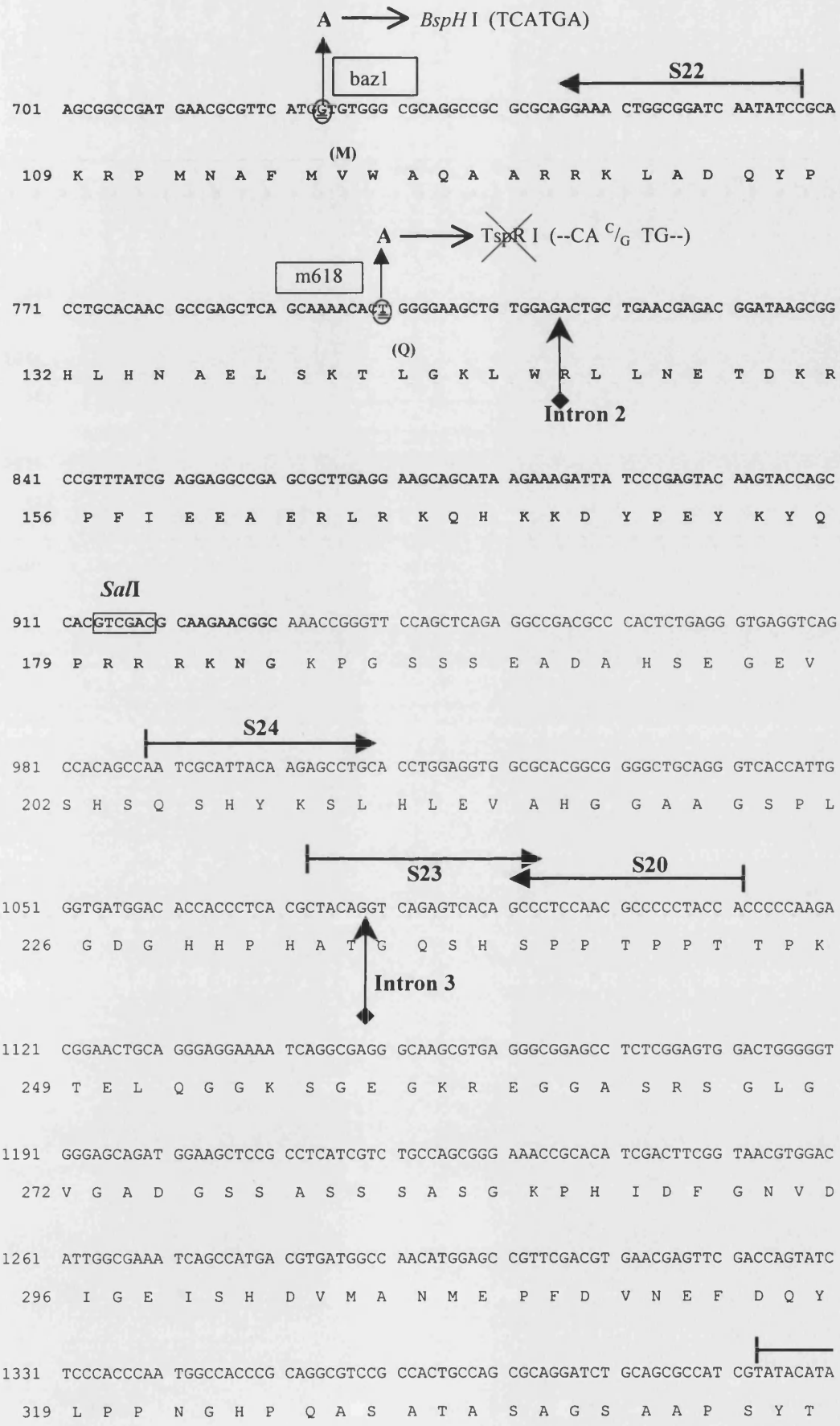
A → BspH I (TCATGA)
baz1
S22
701 AGCGGCCGAT GAACGCGTTC ATGGTGTGGG CGCAGGCCGC GCGCAGGAAA CTGGCGGATC AATATCCGCA
(M)
109 K R P M N A F M V W A Q A A R R K L A D Q Y P
A → TspR I (--CA C/G TG--)
m618
771 CCTGCACAAC GCCGAGCTCA GCAAAACACT GGGGAAGCTG TGGAGACTGC TGAACGAGAC GGATAAGCGG
(Q)
132 H L H N A E L S K T L G K L W R L L N E T D K R
Intron 2
841 CCGTTTATCG AGGAGGCCGA GCGCTTGAGG AAGCAGCATA AGAAAGATTA TCCCGAGTAC AAGTACCAGC
156 P F I E E A E R L R K Q H K K D Y P E Y K Y Q
SalI
911 CACGTCGACG CAAGAACGGC AAACCGGGTT CCAGCTCAGA GGCCGACGCC CACTCTGAGG GTGAGGTCAG
179 P R R R K N G K P G S S S E A D A H S E G E V
S24
981 CCACAGCCAA TCGCATTACA AGAGCCTGCA CCTGGAGGTG GCGCACGGCG GGGCTGCAGG GTCACCATTG
202 S H S Q S H Y K S L H L E V A H G G A A G S P L
S23
S20
1051 GGTGATGGAC ACCACCCTCA CGCTACAGGT CAGAGTCACA GCCCTCCAAC GCCCCCTACC ACCCCCAAGA
226 G D G H H P H A T G Q S H S P P T P P T T P K
Intron 3
1121 CGGAACTGCA GGGAGGAAAA TCAGGCGAGG GCAAGCGTGA GGGCGGAGCC TCTCGGAGTG GACTGGGGGT
249 T E L Q G G K S G E G K R E G G A S R S G L G
1191 GGGAGCAGAT GGAAGCTCCG CCTCATCGTC TGCCAGCGGG AAACCGCACA TCGACTTCGG TAACGTGGAC
272 V G A D G S S A S S S A S G K P H I D F G N V D
1261 ATTGGCGAAA TCAGCCATGA CGTGATGGCC AACATGGAGC CGTTCGACGT GAACGAGTTC GACCAGTATC
296 I G E I S H D V M A N M E P F D V N E F D Q Y
1331 TCCCACCCAA TGGCCACCCG CAGGCGTCCG CCACTGCCAG CGCAGGATCT GCAGCGCCAT CGTATACATA
319 L P P N G H P Q A S A T A S A G S A A P S Y T

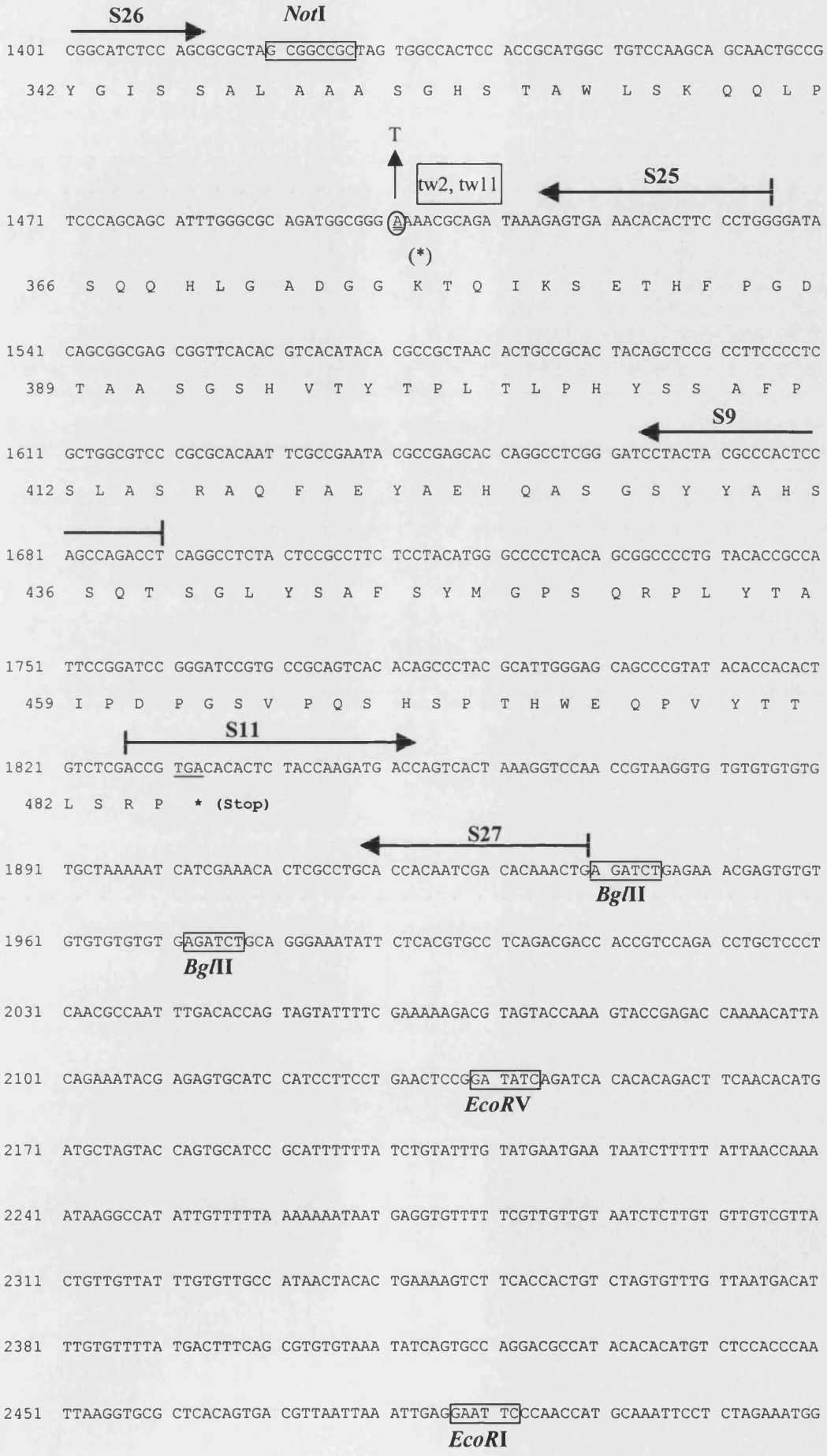
S26
NotI
1401 CGGCATCTCC AGCGCGCTAG CGGCCGCTAG TGGCCACTCC ACCGCATGGC TGTCCAAGCA GCAACTGCCG
342 Y G I S S A L A A A S G H S T A W L S K Q Q L P
T
tw2, tw11
S25
1471 TCCCAGCAGC ATTTGGGCGC AGATGGCGGG AAAACGCAGA TAAAGAGTGA AACACACTTC CCTGGGGATA
(*)
366 S Q Q H L G A D G G K T Q I K S E T H F P G D
1541 CAGCGGCGAG CGGTTCACAC GTCACATACA CGCCGCTAAC ACTGCCGCAC TACAGCTCCG CCTTCCCCTC
389 T A A S G S H V T Y T P L T L P H Y S S A F P
S9
1611 GCTGGCGTCC CGCGCACAAT TCGCCGAATA CGCCGAGCAC CAGGCCTCGG GATCCTACTA CGCCCACTCC
412 S L A S R A Q F A E Y A E H Q A S G S Y Y A H S
1681 AGCCAGACCT CAGGCCTCTA CTCCGCCTTC TCCTACATGG GCCCCTCACA GCGGCCCCTG TACACCGCCA
436 S Q T S G L Y S A F S Y M G P S Q R P L Y T A
1751 TTCCGGATCC GGGATCCGTG CCGCAGTCAC ACAGCCCTAC GCATTGGGAG CAGCCCGTAT ACACCACACT
459 I P D P G S V P Q S H S P T H W E Q P V Y T T
S11
1821 GTCTCGACCG TGACACACTC TACCAAGATG ACCAGTCACT AAAGGTCCAA CCGTAAGGTG TGTGTGTGTG
482 L S R P * (Stop)
S27
1891 TGCTAAAAAT CATCGAAACA CTCGCCTGCA CCACAATCGA CACAAACTGA GATCTGAGAA ACGAGTGTGT
BglII
1961 GTGTGTGTGT GAGATCTGCA GGGAAATATT CTCACGTGCC TCAGACGACC ACCGTCCAGA CCTGCTCCCT
BglII
2031 CAACGCCAAT TTGACACCAG TAGTATTTTC GAAAAAGACG TAGTACCAAA GTACCGAGAC CAAAACATTA
2101 CAGAAATACG AGAGTGCATC CATCCTTCCT GAACTCCGGA TATCAGATCA CACACAGACT TCAACACATG
EcoRV
2171 ATGCTAGTAC CAGTGCATCC GCATTTTTTA TCTGTATTTG TATGAATGAA TAATCTTTTT ATTAACCAAA
2241 ATAAGGCCAT ATTGTTTTTA AAAAAATAAT GAGGTGTTTT TCGTTGTTGT AATCTCTTGT GTTGTCGTTA
2311 CTGTTGTTAT TTGTGTTGCC ATAACTACAC TGAAAAGTCT TCACCACTGT CTAGTGTTTG TTAATGACAT
2381 TTGTGTTTTA TGACTTTCAG CGTGTGTAAA TATCAGTGCC AGGACGCCAT ACACACATGT CTCCACCCAA
2451 TTAAGGTGCG CTCACAGTGA CGTTAATTAA ATTGAGGAAT TCCCAACCAT GCAAATTCCT CTAGAAATGG
EcoRI

2521 CTATATTTCG TGAAAGCAGT AAATGTGAGC GCACCTTTAT TTCACACAAG CAGTACTGTA AAGGTAATAT

2591 ATTTTTGCCA GATTGGAAAT GGTGGACGTA ATTACGAATT TTTAATAATA AATGACTATT TTTAGAGAAT

2661 ACCGCTAGTG CCTCAAGTCC ATCACAAACG AATTGTCGTT TCTGATAAAT TCAATTTTGA TGATGTAAAA

S13

2731 TCCTTTTCAG GGTGCAAATT TTATCATGCG TTAACCGATG TGATTATACA TCGAATATGC ATATGCAAAT

S14

2801 TAATAAGTGC CATTTTTATA ATTAAAAATA CATCAACTAT CTGAAGACCT TCCTAACATT GGGTAAGTAA

2871 ATAAATACAT TTATTTCATT GTATTATTTT TGGTAAATAC AATATTTAGC TATTCTATGT TTTGTCTCCC

2941 TTTGGTACTT TATAGTTTTG TTTTTGCCCT CTTTATTATT TAGTATTATT CAGAAACAAA CAAACTCTTT

3011 TTATATATTA CAGAATATTA TTTATATTTG TTGTTGTTTT TTTTTATCAG TAGCGTTTTA TTCTGTTTGT

S16 S18

3081 CGTAAACCTC TGTCGTGTGC TGTTGTGGTG GGTTAAAGTG CTGTTGTTTT TCTCTGTCGG TGTAAATAGA

3151 ACTGAGAGCA GTGACTAACT TTCCTCACTC TAAATAAAGC TGCAGTCTTT ACTAAAAAAA AAAAAAAAAA

3221 AAAAAAAAAA

Appendix 2: Perdurance of GFP protein in the Branchial Arches

GFP protein perdurance in the branchial arches as shown by comparison of GFP protein levels and GFP RNA levels. All figures are confocal images of lateral views of a 24hpf embryo. In both **a.** and **b.**, the left-hand panels shows immunofluorescence using antibodies against the GFP protein (green channel), whilst the middle panels show detection of the *gfp* RNA message (red channel), by *in situ* hybridisation using the fluorescence of the Fast Red stain (Roche, IN, USA) and according to Kelsh and Eisen (2000). An overlay of the two fluorescent images is shown in the right hand panels.

a. At a lateral focal plane, strong GFP protein signal is evident in the branchial arches (arrow – left panel). However there is no detectable transcript evident (arrows, middle panel and overlay in far right panel).

b. GFP promoter activity is detectable by *in situ* at a more medial focal plane, in neurons of the olfactory bulb (arrows) and ventral midbrain (red channel middle panel). GFP protein is also detectable at these sites, as shown in the first panel (again arrow indicates the olfactory neurons) and as an overlay in the right panel. detection of *gfp* mRNA acts as an internal positive control to show that the *gfp in situ* is capable of detecting *gfp* mRNA, and thus that the GFP protein present in the arches is not due to low active promoter activity, rather due to perdurance from an earlier phase of GFP expression.

a.

b.

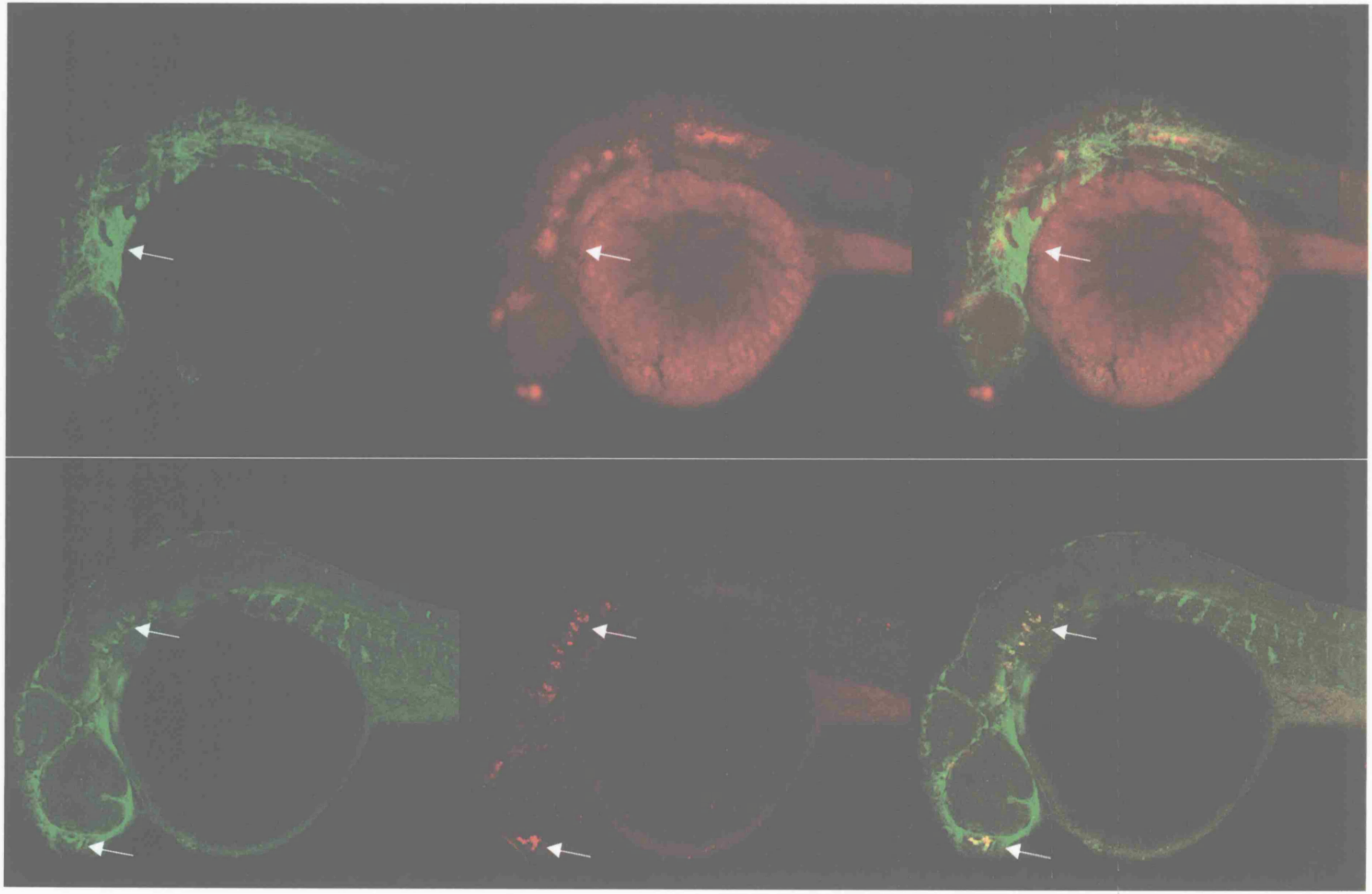

REFERENCES

Akitaya, T. and Bronner-Fraser, M. (1992). Expression of Cell-Adhesion Molecules During Initiation and Cessation of Neural Crest Cell-Migration. *Developmental Dynamics* **194:** 12-20.

Alexander, J. and Stainier, D. Y. R. (1999). A molecular pathway leading to endoderm formation in zebrafish. *Current Biology* **9:** 1147-1157.

Alting-Mees, M. A. and Short, J. M. (1989). pBluescript II: gene mapping vectors. *Nucleic Acids Res* **17:** 9494.

Amacher, S. L. (1999). Transcriptional regulation during zebrafish embryogenesis. *Current Opinion in Genetics & Development* **9:** 548-552.

Ambrosetti, D. C., Basilico, C. and Dailey, L. (1997). Synergistic activation of the fibroblast growth factor 4 enhancer by Sox2 and Oct-3 depends on protein-protein interactions facilitated by a specific spatial arrangement of factor binding sites. *Molecular and Cellular Biology* **17:** 6321-6329.

Amemiya, C. T., Zhong, T. P., Silverman, G. A., Fishman, M. C. and Zon, L. I. (1999). Zebrafish YAC, BAC, and PAC genomic libraries. In *Methods in Cell Biology, Vol 60*, vol. 60, pp. 235-+.

Amemiya, C. T. and Zon, L. I. (1999). Generation of a zebrafish P1 artificial chromosome library. *Genomics* **58:** 211-213.

Amiel, J., Attie, T., Jan, D., Pelet, A., Edery, P., Bidaud, C., Lacombe, D., Tam, P., Simeoni, J., Flori, E. *et al.* (1996). Heterozygous endothelin receptor B (EDNRB) mutations in isolated Hirschsprung disease. *Human Molecular Genetics* **5:** 355-357.

Amsterdam, A., Lin, S. and Hopkins, N. (1995). The Aequorea-Victoria Green Fluorescent Protein Can Be Used As a Reporter in Live Zebrafish Embryos. *Developmental Biology* **171:** 123-129.

Amsterdam, A., Lin, S., Moss, L. G. and Hopkins, N. (1996). Requirements for green fluorescent protein detection in transgenic zebrafish embryos. *Gene* **173:** 99-103.

An, M., Luo, R. S. and Henion, P. D. (2002). Differentiation and maturation of zebrafish dorsal root and sympathetic ganglion neurons. *Journal of Comparative Neurology* **446:** 267-275.

Anderson, D. J. (1997). Cellular and molecular biology of neural crest cell lineage determination. *Trends in Genetics* **13:** 276-280.

Anderson, D. J., Groves, A., Lo, L., Ma, Q., Rao, M., Shah, N. M. and Sommer, L. (1997). Cell lineage determination and the control of neuronal identity in the neural crest. *Cold Spring Harbor Symposia On Quantitative Biology* **62:** 493-504.

Aoki, Y., Saint-Germain, N., Gyda, M., Magner-Fink, E., Lee, Y. H., Credidio, C. and Saint-Jeannet, J. P. (2003). Sox10 regulates the development of neural crest-derived melanocytes in *Xenopus*. *Dev Biol* **259:** 19-33.

Appel, B. and Eisen, J. S. (1998). Regulation of neuronal specification in the zebrafish spinal cord by Delta function. *Development* **125:** 371-380.

Appel, B., Fritz, A., Westerfield, M., Grunwald, D. J., Eisen, J. S. and Riley, B. (1998). A zebrafish deltaA mutation disrupts specification of spinal cord neurons and floorplate. *Developmental Biology* **198:** 194.

Appel, B., Fritz, A., Westerfield, M., Grunwald, D. J., Eisen, J. S. and Riley, B. B. (1999). Delta-mediated specification of midline cell fates in zebrafish embryos. *Current Biology* **9:** 247-256.

Appel, B., Givan, L. A. and Eisen, J. S. (2001). Delta-Notch signaling and lateral inhibition in zebrafish spinal cord development. *BMC Dev Biol* **1:** 13.

Artinger, K. B., Chitnis, A. B., Mercola, M. and Driever, W. (1999). Zebrafish narrowminded suggests a genetic link between formation of neural crest and primary sensory neurons. *Development* **126:** 3969-3979.

Auricchio, A., Griseri, P., Carpentieri, M. L., Betsos, N., Staiano, A., Tozzi, A., Priolo, M., Thompson, H., Bocciardi, R., Romeo, G. *et al.* (1999). Double heterozygosity for a RET substitution interfering with splicing and an EDNRB missense mutation in Hirschsprung disease. *American Journal of Human Genetics* **64:** 1216-1221.

Aybar, M. J. and Mayor, R. (2002). Early induction of neural crest cells: lessons learned from frog, fish and chick. *Current Opinion in Genetics & Development* **12:** 452-458.

Baroffio, A., Dupin, E. and Ledouarin, N. M. (1988). Clone-Forming Ability and Differentiation Potential of Migratory Neural Crest Cells. *Proceedings of the National Academy of Sciences of the United States of America* **85:** 5325-5329.

Bell, K. M., Western, P. S. and Sinclair, A. H. (2000). SOX8 expression during chick embryogenesis. *Mechanisms of Development* **94:** 257-260.

Belting, H. G., Hauptmann, G., Meyer, D., Abdelliah-Seyfried, S., Chitnis, A., Eschbach, C., Soll, I., Thisse, C., Thisse, B., Artinger, K. B. *et al.* (2001). *spiel ohne grenzen/pou2* is required during establishment of the zebrafish midbrain-hindbrain boundary organizer. *Development* **128:** 4165-4176.

Bettenhausen, B., Deangelis, M. H., Simon, D., Guenet, J. L. and Gossler, A. (1995). Transient and restricted expression during mouse embryogenesis of *Dll1*, a murine gene closely related to *Drosophila Delta*. *Development* **121:** 2407-2418.

Bi, W. M., Deng, J. M., Zhang, Z. P., Behringer, R. R. and de Crombrugghe, B. (1999). Sox9 is required for cartilage formation. *Nature Genetics* **22:** 85-89.

Bi, W. M., Huang, W. D., Whitworth, D. J., Deng, J. M., Zhang, Z. P., Behringer, R. R. and de Crombrugghe, B. (2001). Haploinsufficiency of Sox9 results in defective cartilage primordia and premature skeletal mineralization. *Proceedings of the National Academy of Sciences of the United States of America* **98:** 6698-6703.

Bidaud, C., Salomon, R., VanCamp, G., Pelet, A., Attie, T., Eng, C., Bonduelle, M., Amiel, J., NihoulFekete, C., Willems, P. J. *et al.* (1997). Endothelin-3 gene mutations in isolated and syndromic Hirschsprung disease. *European Journal of Human Genetics* **5:** 247-251.

Bierkamp, C. and Campos-Ortega, J. A. (1993). A Zebrafish Homolog of the *Drosophila* Neurogenic Gene *Notch* and Its Pattern of Transcription During Early Embryogenesis. *Mechanisms of Development* **43:** 87-100.

Blader, P., Fischer, N., Gradwohl, G., Guillemot, F. and Strahle, U. (1997). The activity of Neurogenin1 is controlled by local cues in the zebrafish embryo. *Development* **124:** 4557-4569.

Blader, P., Plessy, C. and Strahle, U. (2003). Multiple regulatory elements with spatially and temporally distinct activities control neurogenin1 expression in primary neurons of the zebrafish embryo. *Mechanisms of Development* **120:** 211-218.

Bochner, B. R., Huang, H. C., Schieven, G. L. and Ames, B. N. (1980). Positive selection for loss of tetracycline resistance. *J Bacteriol* **143:** 926-33.

Bockukova, E. G., Jefferson, A., Francis, M. J. and Monaco, A. P. (2003). Genomic studies of gene expression: regulation of the Wilson disease gene. *Genomics* **81:** 531-542.

Bondurand, N., Girard, M., Pingault, V., Lemort, N., Dubourg, O. and Goossens, M. (2001). Human Connexin 32, a gap junction protein altered in the X- linked form of Charcot-Marie-Tooth disease, is directly regulated by the transcription factor SOX10. *Human Molecular Genetics* **10:** 2783-2795.

Bondurand, N., Kobetz, A., Pingault, V., Lemort, N., Encha-Razavi, F., Couly, G., Goerich, D. E., Wegner, M., Abitbol, M. and Goossens, M. (1998). Expression of the *SOX10* gene during human development. *Febs Letters* **432:** 168-172.

Bondurand, N., Kuhlbrodt, K., Pingault, V., Enderich, J., Sajus, M., Tommerup, N., Warburg, M., Hennekam, R. C. M., Read, A. P., Wegner, M. *et al.* (1999a). The Yemenite deaf-blind hypopigmentation syndrome revisited: SOX10 dysfunction causes different neurocristopathies. *American Journal of Human Genetics* **65:** 1599.

Bondurand, N., Kuhlbrodt, K., Pingault, V., Enderich, J., Sajus, M., Tommerup, N., Warburg, M., Hennekam, R. C. M., Read, A. P., Wegner, M. *et al.* (1999b). A molecular analysis of the Yemenite deaf-blind hypopigmentation syndrome: SOX10

dysfunction causes different neurocristopathies. *Human Molecular Genetics* **8:** 1785-1789.

Bondurand, N., Pingault, V., Goerich, D. E., Lemort, N., Sock, E., Le Caignec, C., Wegner, M. and Goossens, M. (2000). Interaction among SOX10 PAX3 and MITF, three genes altered in Waardenburg syndrome. *Human Molecular Genetics* **9:** 1907-1917.

Bowles, J., Schepers, G. and Koopman, P. (2000). Phylogeny of the SOX family of developmental transcription factors based on sequence and structural indicators. *Developmental Biology* **227:** 239-255.

Britsch, S., Goerich, D. E., Riethmacher, D., Peirano, R. I., Rossner, M., Nave, K. A., Birchmeier, C. and Wegner, M. (2001). The transcription factor Sox10 is a key regulator of peripheral glial development. *Genes & Development* **15:** 66-78.

Bronner-Fraser, M. (1994). Neural Crest Cell-Formation and Migration in the Developing Embryo. *Faseb Journal* **8:** 699-706.

Bronner-Fraser, M. and Stern, C. (1991). Effects of Mesodermal Tissues on Avian Neural Crest Cell- Migration. *Developmental Biology* **143:** 213-217.

Brosamle, C. and Halpern, M. E. (2002). Characterization of myelination in the developing zebrafish. *Glia* **39:** 47-57.

Brownlie, A., Donovan, A., Pratt, S. J., Paw, B. H., Oates, A. C., Brugnara, C., Witkowska, H. E., Sassa, S. and Zon, L. I. (1998). Positional cloning of the zebrafish *sauternes* gene: a model for congenital sideroblastic anaemia. *Nature Genetics* **20:** 244-250.

Camp, E., Badhwar, P., Mann, G. J. and Lardelli, M. (2003). Expression analysis of a Tyrosinase promoter sequence in zebrafish. *Pigment Cell Research* **16:** 117-126.

Cano, A., Perez-Moreno, M. A., Rodrigo, I., Locascio, A., Blanco, M. J., del Barrio, M. G., Portillo, F. and Nieto, M. A. (2000). The transcription factor Snail controls epithelial-mesenchymal transitions by repressing E-cadherin expression. *Nature Cell Biology* **2:** 76-83.

Carvajal, J. J., Cox, D., Summerbell, D. and Rigby, P. W. J. (2001). A BAC transgenic analysis of the *Mrf4/Myf5* locus reveals interdigitated elements that control activation and maintenance of gene expression during muscle development. *Development* **128:** 1857-1868.

Chan, Y. M. and Jan, Y. N. (1999). Presenilins, processing of beta-amyloid precursor protein, and Notch signaling. *Neuron* **23:** 201-204.

Chatterjee, B., Li, Y. X., Zdanowicz, M., Sonntag, J. M., Chin, A. J., Kozlowski, D. J., Valdimarsson, G., Kirby, M. L. and Lo, C. W. (2001). Analysis of Cx43 alpha 1

promoter function in the developing zebrafish embryo. *Cell Communication and Adhesion* **8:** 289-+.

Chen, W. B., Burgess, S., Golling, G., Amsterdam, A. and Hopkins, N. (2002). High-throughput selection of retrovirus producer cell lines leads to markedly improved efficiency of germ line- transmissible insertions in zebra fish. *Journal of Virology* **76:** 2192-2198.

Cheng, Y. C., Cheung, M., Abu-Elmagd, M. M., Orme, A. and Scotting, P. J. (2000). Chick *Sox10*, a transcription factor expressed in both early neural crest cells and central nervous system. *Developmental Brain Research* **121:** 233-241.

Cheng, Y. C., Lee, C. J., Badge, R. M., Orme, A. T. and Scotting, P. J. (2001). Sox8 gene expression identifies immature glial cells in developing cerebellum and cerebellar tumours. *Molecular Brain Research* **92:** 193-200.

Chiang, E. F. L., Pai, C. I., Wyatt, M., Yan, Y. L., Postlethwait, J. and Chung, B. C. (2001). Two *sox9* genes on duplicated zebrafish chromosomes: Expression of similar transcription activators in distinct sites. *Developmental Biology* **231:** 149-163.

Chimal-Monroy, J., Rodriguez-Leon, J., Montero, J. A., Ganan, Y., Macias, D., Merino, R. and Hurle, J. M. (2003). Analysis of the molecular cascade responsible for mesodermal limb chondrogenesis: *Sox* genes and BMP signaling. *Developmental Biology* **257:** 292-301.

Chitnis, A. B. (1995). The Role of Notch in Lateral Inhibition and Cell Fate Specification. *Molecular and Cellular Neuroscience* **6:** 311-321.

Chiu, C. H., Amemiya, C. T., Carr, J. L., Bhargava, J., Hwang, J. K., Shashikant, C. S., Ruddle, F. H. and Wagner, G. P. (2000). A recombinogenic targeting method to modify large-inserts for *cis*-regulatory analysis in transgenic mice: construction and expression of a 100-kb, zebrafish *Hoxa-11b-lacZ* reporter gene. *Development Genes and Evolution* **210:** 105-109.

Collas, P. and Alestrom, P. (1998). Nuclear localization signals enhance germline transmission of a transgene in zebrafish. *Transgenic Research* **7:** 303-309.

Cornell, R. A. and Eisen, J. S. (2000). Delta signaling mediates segregation of neural crest and spinal sensory neurons from zebrafish lateral neural plate. *Development* **127:** 2873-2882.

Cornell, R. A. and Eisen, J. S. (2002). Delta/Notch signalling promotes formation of zebrafish neural crest by repressing Neurogenin 1 function. *Development* **129:** 2639-2648.

Cremazy, F., Berta, P. and Girard, F. (2001). Genome-wide analysis of Sox genes in Drosophila melanogaster. *Mechanisms of Development* **109:** 371-375.

Cretekos, C. J. and Grunwald, D. J. (1999). *alyron*, an insertional mutation affecting early neural crest development in zebrafish. *Developmental Biology* **210:** 322-338.

Currie, P. D. and Ingham, P. W. (1996). Induction of a specific muscle cell type by a hedgehog-like protein in zebrafish. *Nature* **382:** 452-455.

daSilva, S. M., Hacker, A., Harley, V., Goodfellow, P., Swain, A. and LovellBadge, R. (1996). Sox9 expression during gonadal development implies a conserved role for the gene in testis differentiation in mammals and birds. *Nature Genetics* **14:** 62-68.

De Martino, S., Yan, Y. L., Jowett, T., Postlethwait, J. H., Varga, Z. M., Ashworth, A. and Austin, C. A. (2000). Expression of sox11 gene duplicates in zebrafish suggests the reciprocal loss of ancestral gene expression patterns in development. *Developmental Dynamics* **217:** 279-292.

Dickmeis, T., Aanstad, P., Clark, M., Fischer, N., Herwig, R., Mourrain, P., Blader, P., Rosa, F., Lehrach, H. and Strahle, U. (2001). Identification of nodal signaling targets by array analysis of induced complex probes. *Developmental Dynamics* **222:** 571-580.

Dornseifer, P., Takke, C. and CamposOrtega, J. A. (1997). Overexpression of a zebrafish homologue of the *Drosophila* neurogenic gene *Delta* perturbs differentiation of primary neurons and somite development. *Mechanisms of Development* **63:** 159-171.

Dorsky, R. I., Moon, R. T. and Raible, D. W. (1998). Control of neural crest cell fate by the Wnt signalling pathway. *Nature* **396:** 370-373.

Dorsky, R. I., Raible, D. W. and Moon, R. T. (2000). Direct regulation of nacre, a zebrafish MITF homolog required for pigment cell formation, by the Wnt pathway. *Genes & Development* **14:** 158-162.

Dorsky, R. I., Sheldahl, L. C. and Moon, R. T. (2002). A transgenic Lef1/β-catenin-dependent reporter is expressed in spatially restricted domains throughout zebrafish development. *Developmental Biology* **241:** 229-237.

Dottori, M., Gross, M. K., Labosky, P. and Goulding, M. (2001). The winged-helix transcription factor Foxd3 suppresses interneuron differentiation and promotes neural crest cell fate. *Development* **128:** 4127-4138.

Drivenes, O., Seo, H. C. and Fjose, A. (2000). Characterisation of the promoter region of the zebrafish *six7* gene. *Biochimica Et Biophysica Acta-Gene Structure and Expression* **1491:** 240-247.

Dutton, K. A., Pauliny, A., Lopes, S. S., Elworthy, S., Carney, T. J., Rauch, J., Geisler, R., Haffter, P. and Kelsh, R. N. (2001). Zebrafish *colourless* encodes *sox10* and specifies non- ectomesenchymal neural crest fates. *Development* **128:** 4113-4125.

Edery, P., Attie, T., Amiel, J., Pelet, A., Eng, C., Hofstra, R. M. W., Martelli, H., Bidaud, C., Munnich, A. and Lyonnet, S. (1996). Mutation of the endothelin-3 gene in the Waardenburg- Hirschsprung disease (Shah-Waardenburg syndrome). *Nature Genetics* **12:** 442-444.

Eisen, J. S. and Weston, J. A. (1993). Development of the Neural Crest in the Zebrafish. *Developmental Biology* **159:** 50-59.

Ekker, M. (1999). Saving zebrafish mutants. *Bioessays* **21:** 94-98.

Elworthy, S., Lister, J. A., Carney, T. J., Raible, D. W. and Kelsh, R. N. (2003). Transcriptional regulation of *mitfa* accounts for the *sox10* requirement in zebrafish melanophore development. *Development* **130:** 2809-2818.

Fadool, J. M., Hartl, D. L. and Dowling, J. E. (1998). Transposition of the *mariner* element from *Drosophila mauritiana* in zebrafish. *Proceedings of the National Academy of Sciences of the United States of America* **95:** 5182-5186.

Fekany-Lee, K., Gonzalez, E., Miller-Bertoglio, V. and Solnica-Krezel, L. (2000). The homeobox gene *bozozok* promotes anterior neuroectoderm formation in zebrafish through negative regulation of BMP2/4 and Wnt pathways. *Development* **127:** 2333-2345.

Forwood, J. K., Harley, V. and Jans, D. A. (2001). The C-terminal nuclear localization signal of the sex determining region Y (SRY) high mobility group domain mediates nuclear import through beta 1. *Journal of Biological Chemistry* **276:** 46575-46582.

Foster, J. W., Dominguezsteglich, M. A., Guioli, S., Kwok, C., Weller, P. A., Stevanovic, M., Weissenbach, J., Mansour, S., Young, I. D., Goodfellow, P. N. *et al.* (1994). Campomelic Dysplasia and Autosomal Sex Reversal Caused by Mutations in an Sry-Related Gene. *Nature* **372:** 525-530.

Fraser, S. E. and Bronner-Fraser, M. (1991). Migrating Neural Crest Cells in the Trunk of the Avian Embryo Are Multipotent. *Development* **112:** 913-920.

Gammill, L. S. and Bronner-Fraser, M. (2002). Genomic analysis of neural crest induction. *Development* **129:** 5731-5741.

Garcia-Castro, M. I., Marcelle, C. and Bronner-Fraser, M. (2002). Ectodermal Wnt function as a neural crest inducer. *Science* **297:** 848-851.

Geisler, R. (2002). Mapping and cloning. In *Zebrafish : a practical approach*, (ed. C. Nuesslein-Volhard and R. Dahm), pp. 175-212. Oxford: Oxford University Press.

Geling, A., Steiner, H., Willem, M., Bally-Cuif, L. and Haass, C. (2002). A gamma-secretase inhibitor blocks Notch signaling in vivo and causes a severe neurogenic phenotype in zebrafish. *Embo Reports* **3:** 688-694.

Gilmour, D. T., Jessen, J. R. and Lin, S. (2002a). Manipulating gene expression in the zebrafish. In *Zebrafish : a practical approach*, (ed. C. Nuesslein-Volhard and R. Dahm), pp. 121-143. Oxford: Oxford University Press.

Gilmour, D. T., Maischein, H. M. and Nusslein-Volhard, C. (2002b). Migration and function of a glial subtype in the vertebrate peripheral nervous system. *Neuron* **34:** 577-588.

Giraldo, P. and Montoliu, L. (2001). Size matters: Use of YACs, BACs and PACs in transgenic animals. *Transgenic Research* **10:** 83-103.

Gong, S. C., Yang, X. W., Li, C. J. and Heintz, N. (2002a). Highly efficient modification of bacterial artificial chromosomes (BACs) using novel shuttle vectors containing the R6Kγ origin of replication. *Genome Research* **12:** 1992-1998.

Gong, Z. Y., Ju, B. S., Wang, X. K., He, J. Y., Wang, H. Y., Sudha, P. M. and Yan, T. (2002b). Green fluorescent protein expression in germ-line transmitted transgenic zebrafish under a stratified epithelial promoter from *Keratin8*. *Developmental Dynamics* **223:** 204-215.

Gray, M., Moens, C. B., Amacher, S. L., Eisen, J. S. and Beattie, C. E. (2001). Zebrafish *deadly seven* functions in neurogenesis. *Developmental Biology* **237:** 306-323.

Greenwood, A. L., Turner, E. E. and Anderson, D. J. (1999). Identification of dividing, determined sensory neuron precursors in the mammalian neural crest. *Development* **126:** 3545-3559.

Grunstein, M. and Hogness, D. S. (1975). Colony hybridization: a method for the isolation of cloned DNAs that contain a specific gene. *Proc Natl Acad Sci U S A* **72:** 3961-5.

Guillemot, F., Lo, L. C., Johnson, J. E., Auerbach, A., Anderson, D. J. and Joyner, A. L. (1993). Mammalian Achaete-Scute Homolog-1 Is Required for the Early Development of Olfactory and Autonomic Neurons. *Cell* **75:** 463-476.

Haddon, C., Smithers, L., Schneider-Maunoury, S., Coche, T., Henrique, D. and Lewis, J. (1998). Multiple *delta* genes and lateral inhibition in zebrafish primary neurogenesis. *Development* **125:** 359-370.

Haffter, P., Granato, M., Brand, M., Mullins, M. C., Hammerschmidt, M., Kane, D. A., Odenthal, J., vanEeden, F. J. M., Jiang, Y. J., Heisenberg, C. P. *et al.* (1996). The identification of genes with unique and essential functions in the development of the zebrafish, *Danio rerio*. *Development* **123:** 1-36.

Halloran, M. C., Sato-Maeda, M., Warren, J. T., Su, F. Y., Lele, Z., Krone, P. H., Kuwada, J. Y. and Shoji, W. (2000). Laser-induced gene expression in specific cells of transgenic zebrafish. *Development* **127:** 1953-1960.

Hanahan, D. (1983). Studies on transformation of *Escherichia-Coli* with plasmids. *Journal of Molecular Biology* **166:** 557-580.

Hans, S. and Campos-Ortega, J. A. (2002). On the organisation of the regulatory region of the zebrafish *deltaD* gene. *Development* **129:** 4773-4784.

Henion, P. D., Garner, A. S., Large, T. H. and Weston, J. A. (1995). trkC-mediated NT-3 signaling is required for the early development of a subpopulation of neurogenic neural crest cells. *Developmental Biology* **172:** 602-613.

Henion, P. D., Raible, D. W., Beattie, C. E., Stoesser, K. L., Weston, J. A. and Eisen, J. S. (1996). Screen for mutations affecting development of zebrafish neural crest. *Developmental Genetics* **18:** 11-17.

Henion, P. D. and Weston, J. A. (1997). Timing and pattern of cell fate restrictions in the neural crest lineage. *Development* **124:** 4351-4359.

Herbarth, B., Pingault, V., Bondurand, N., Kuhlbrodt, K., Hermans-Borgmeyer, I., Puliti, A., Lemort, N., Goossens, M. and Wegner, M. (1998). Mutation of the Sry-related *Sox10* gene in *Dominant megacolon*, a mouse model for human Hirschsprung disease. *Proceedings of the National Academy of Sciences of the United States of America* **95:** 5161-5165.

Higashijima, S., Hotta, Y. and Okamoto, H. (2000). Visualization of cranial motor neurons in live transgenic zebrafish expressing green fluorescent protein under the control of the *Islet-1* promoter/enhancer. *Journal of Neuroscience* **20:** 206-218.

Higashijima, S., Okamoto, H., Ueno, N., Hotta, Y. and Eguchi, G. (1997). High-frequency generation of transgenic zebrafish which reliably express GFP in whole muscles or the whole body by using promoters of zebrafish origin. *Developmental Biology* **192:** 289-299.

Hirzmann, J., Luo, D., Hahnen, J. and Hobom, G. (1993). Determination of Messenger-RNA 5'-Ends by Reverse Transcription of the Cap Structure. *Nucleic Acids Research* **21:** 3597-3598.

Hofstra, R. M. W., Osinga, J., TanSindhunata, G., Wu, Y., Kamsteeg, E. J., Stulp, R. P., vanRavenswaaijArts, C., MajoorKrakauer, D., Angrist, M., Chakravarti, A. *et al.* (1996). A homozygous mutation in the endothelin-3 gene associated with a combined Waardenburg type 2 and Hirschsprung phenotype (Shah- Waardenburg syndrome). *Nature Genetics* **12:** 445-447.

Hofstra, R. M. W., Wu, Y., Stulp, R. P., Elfferich, P., Osinga, J., Maas, S. M., Siderius, L., Brooks, A. S., Von der Ende, J. J., Heydendael, V. M. R. *et al.* (2000). RET and GDNF gene scanning in Hirschprung patients using two dual denaturing gel systems. *Human Mutation* **15:** 418-429.

Holley, S. A., Geisler, R. and Nusslein-Volhard, C. (2000). Control of *her1* expression during zebrafish somitogenesis by a *Delta*-dependent oscillator and an independent wave-front activity. *Genes & Development* **14:** 1678-1690.

Holley, S. A., Julich, D., Rauch, G. J., Geisler, R. and Nusslein-Volhard, C. (2002). *her1* and the *notch* pathway function within the oscillator mechanism that regulates zebrafish somitogenesis. *Development* **129:** 1175-1183.

Holmes, D. S. and Quigley, M. (1981). A rapid boiling method for the preparation of bacterial plasmids. *Analytical Biochemistry* **114:** 193-197.

Honore, S. M., Aybar, M. J. and Mayor, R. (2003). *Sox10* is required for the early development of the prospective neural crest in *Xenopus* embryos. *Dev Biol* **260:** 79-96.

Hsiao, C. D., Hsieh, F. J. and Tsai, H. J. (2001). Enhanced expression and stable transmission of transgenes flanked by inverted terminal repeats from adeno-associated virus in zebrafish. *Developmental Dynamics* **220:** 323-336.

Huang, H. G., Vogel, S. S., Liu, N. G., Melton, D. A. and Lin, S. (2001). Analysis of pancreatic development in living transgenic zebrafish embryos. *Molecular and Cellular Endocrinology* **177:** 117-124.

Iglesias, J. M., Morgan, R. O., Jenkins, N. A., Copeland, N. G., Gilbert, D. J. and Fernandez, M. P. (2002). Comparative genetics and evolution of annexin A13 as the founder gene of vertebrate annexins. *Molecular Biology and Evolution* **19:** 608-618.

Inoue, K., Shilo, K., Boerkoel, C. F., Crowe, C., Sawady, J., Lupski, J. R. and Agamanolis, D. P. (2002). Congenital hypomyelinating neuropathy, central dysmyelination, and Waardenburg-Hirschprung disease: phenotypes linked by SOX10 mutation. *Annals of Neurology* **52:** 836-842.

Inoue, K., Tanabe, Y. and Lupski, J. R. (1999). Myelin deficiencies in both the central and the peripheral nervous systems associated with a SOX10 mutation. *Annals of Neurology* **46:** 313-318.

Inoue, T., Chisaka, O., Matsunami, H. and Takeichi, M. (1997). Cadherin-6 expression transiently delineates specific rhombomeres, other neural tube subdivisions, and neural crest subpopulations in mouse embryos. *Developmental Biology* **183:** 183-194.

Ioannou, P. A., Amemiya, C. T., Garnes, J., Kroisel, P. M., Shizuya, H., Chen, C., Batzer, M. A. and Dejong, P. J. (1994). A New Bacteriophage P1-Derived Vector For the Propagation of Large Human Dna Fragments. *Nature Genetics* **6:** 84-89.

Iso, T., Kedes, L. and Hamamori, Y. (2003). HES and HERP families: Multiple effectors of the Notch signaling pathway. *Journal of Cellular Physiology* **194:** 237-255.

Ito, M., Ishikawa, M., Suzuki, S., Takamatsu, N. and Shiba, T. (1995). A rainbow trout SRY-type gene expressed in pituitary glands. *Febs Letters* **377:** 37-40.

Itoh, M. and Chitnis, A. B. (2001). Expression of proneural and neurogenic genes in the zebrafish lateral line primordium correlates with selection of hair cell fate in neuromasts. *Mechanisms of Development* **102:** 263-266.

Itoh, M., Kim, C. H., Palardy, G., Oda, T., Jiang, Y. J., Maust, D., Yeo, S. Y., Lorick, K., Wright, G. J., Ariza-McNaughton, L. *et al.* (2003). Mind bomb is a ubiquitin ligase that is essential for efficient activation of Notch signaling by delta. *Developmental Cell* **4:** 67-82.

Ivics, Z., Hackett, P. B., Plasterk, R. H. and Izsvak, Z. (1997). Molecular reconstruction of *Sleeping beauty*, a *Tc1*-like transposon from fish, and its transposition in human cells. *Cell* **91:** 501-510.

Ivics, Z., Izsvak, Z. and Hackett, F. B. (1999). Genetic applications of transposons and other repetitive elements in zebrafish. In *Methods in Cell Biology, Vol 60*, vol. 60, pp. 99-131.

Izsvak, Z., Ivics, Z., GarciaEstefania, D., Fahrenkrug, S. C. and Hackett, P. B. (1996). DANA elements: A family of composite, tRNA-derived short interspersed DNA elements associated with mutational activities in zebrafish (*Danio rerio*). *Proceedings of the National Academy of Sciences of the United States of America* **93:** 1077-1081.

Izsvak, Z., Ivics, Z. and Hackett, F. B. (1997). Repetitive elements and their genetic applications in zebrafish. *Biochemistry and Cell Biology-Biochimie Et Biologie Cellulaire* **75:** 507-523.

Jan, Y. N. and Jan, L. Y. (1994). Genetic-Control of Cell Fate Specification in Drosophila Peripheral Nervous-System. *Annual Review of Genetics* **28:** 373-393.

Jessen, J. R., Jessen, T. N., Vogel, S. S. and Lin, S. (2001). Concurrent expression of recombination activating genes 1 and 2 in zebrafish olfactory sensory neurons. *Genesis* **29:** 156-162.

Jessen, J. R., Meng, A. M., McFarlane, R. J., Paw, B. H., Zon, L. I., Smith, G. R. and Lin, S. (1998). Modification of bacterial artificial chromosomes through Chi-stimulated homologous recombination and its application in zebrafish transgenesis. *Proceedings of the National Academy of Sciences of the United States of America* **95:** 5121-5126.

Jessen, J. R., Willett, C. E. and Lin, S. (1999). Artificial chromosome transgenesis reveals long-distance negative regulation of *rag1* in zebrafish. *Nature Genetics* **23:** 15-16.

Jesuthasan, S. (1996). Contact inhibition collapse and pathfinding of neural crest cells in the zebrafish trunk. *Development* **122:** 381-389.

Jesuthasan, S. and Subburaju, S. (2002). Gene transfer into zebrafish by sperm nuclear transplantation. *Developmental Biology* **242:** 88-95.

John, R. M., Ainscough, J. F. X., Barton, S. C. and Surani, M. A. (2001). Distant cis-elements regulate imprinted expression of the mouse $p57^{KiP2}$ (Cdkn1C) gene: implications for the human disorder, Beckwith-Wiedemann syndrome. *Human Molecular Genetics* **10:** 1601-1609.

Kamachi, Y., Cheah, K. S. E. and Kondoh, H. (1999). Mechanism of regulatory target selection by the SOX high- mobility-group domain proteins as revealed by comparison of SOX1/2/3 and SOX9. *Molecular and Cellular Biology* **19:** 107-120.

Kamachi, Y., Sockanathan, S., Liu, Q. R., Breitman, M., Lovellbadge, R. and Kondoh, H. (1995). Involvement of Sox Proteins in Lens-Specific Activation of Crystallin Genes. *Embo Journal* **14:** 3510-3519.

Kamachi, Y., Uchikawa, M., Collignon, J., Lovell-Badge, R. and Kondoh, H. (1998). Involvement of Sox1, 2 and 3 in the early and subsequent molecular events of lens induction. *Development* **125:** 2521-2532.

Kanai, Y., KanaiAzuma, M., Noce, T., Saido, T. C., Shiroishi, T., Hayashi, Y. and Yazaki, K. (1996). Identification of two Sox17 messenger RNA isoforms, with and without the high mobility group box region, and their differential expression in mouse spermatogenesis. *Journal of Cell Biology* **133:** 667-681.

Kapur, R. P. (1999). Early death of neural crest cells is responsible for total enteric aganglionosis in $Sox10^{Dom}/Sox10^{Dom}$ mouse embryos. *Pediatric and Developmental Pathology* **2:** 559-569.

Kapur, R. P., Livingston, R., Doggett, B., Sweetser, D. A., Siebert, J. R. and Palmiter, R. D. (1996). Abnormal microenvironmental signals underlie intestinal aganglionosis in Dominant megacolon mutant mice. *Developmental Biology* **174:** 360-369.

Kapur, R. P., Sweetser, D. A., Doggett, B., Siebert, J. R. and Palmiter, R. D. (1995). Intercellular Signals Downstream of Endothelin Receptor-B Mediate Colonization of the Large-Intestine By Enteric Neuroblasts. *Development* **121:** 3787-3795.

Kawakami, K., Shima, A. and Kawakami, N. (2000). Identification of a functional transposase of the *Tol2* element, an *Ac*-like element from the Japanese medaka fish, and

its transposition in the zebrafish germ lineage. *Proceedings of the National Academy of Sciences of the United States of America* **97:** 11403-11408.

Kelsh, R. N., Brand, M., Jiang, Y. J., Heisenberg, C. P., Lin, S., Haffter, P., Odenthal, J., Mullins, M. C., van Eeden, F. J. M., Furutani-Seiki, M. *et al.* (1996). Zebrafish pigmentation mutations and the processes of neural crest development. *Development* **123:** 369-389.

Kelsh, R. N., Dutton, K., Medlin, J. and Eisen, J. S. (2000a). Expression of zebrafish *fkd6* in neural crest-derived glia. *Mechanisms of Development* **93:** 161-164.

Kelsh, R. N. and Eisen, J. S. (2000). The zebrafish *colourless* gene regulates development of non- ectomesenchymal neural crest derivatives. *Development* **127:** 515-525.

Kelsh, R. N., Schmid, B. and Eisen, J. S. (2000b). Genetic analysis of melanophore development in zebrafish embryos. *Developmental Biology* **225:** 277-293.

Kennedy, B. N., Vihtelic, T. S., Checkley, L., Vaughan, K. T. and Hyde, D. R. (2001). Isolation of a zebrafish rod opsin promoter to generate a transgenic zebrafish line expressing enhanced green fluorescent protein in rod photoreceptors. *Journal of Biological Chemistry* **276:** 14037-14043.

Kim, J., Lo, L., Dormand, E. and Anderson, D. J. (2003). SOX10 maintains multipotency and inhibits neuronal differentiation of neural crest stem cells. *Neuron* **38:** 17-31.

Kimmel, C. B., Ballard, W. W., Kimmel, S. R., Ullmann, B. and Schilling, T. F. (1995). Stages of embryonic development of the zebrafish. *Dev Dyn* **203:** 253-310.

Kishimoto, Y., Lee, K. H., Zon, L., Hammerschmidt, M. and Schulte-Merker, S. (1997). The molecular nature of zebrafish *swirl*: BMP2 function is essential during early dorsoventral patterning. *Development* **124:** 4457-4466.

Koga, A., Hori, H. and Sakaizumi, M. (2002). Gene transfer and cloning of flanking chromosomal regions using the medaka fish *Tol2* transposable element. *Marine Biotechnology* **4:** 6-11.

Korzh, V. and Strahle, U. (2002). Proneural, prosensory, antiglial: the many faces of neurogenins. *Trends in Neurosciences* **25:** 603-605.

Kos, R., Reedy, M. V., Johnson, R. L. and Erickson, C. A. (2001). The winged-helix transcription factor FoxD3 is important for establishing the neural crest lineage and repressing melanogenesis in avian embryos. *Development* **128:** 1467-1479.

Koster, R. W. and Fraser, S. E. (2001). Tracing transgene expression in living zebrafish embryos. *Developmental Biology* **233:** 329-346.

Krull, C. E. (2001). Segmental organization of neural crest migration. *Mechanisms of Development* **105:** 37-45.

Krull, C. E., Lansford, R., Gale, N. W., Collazo, A., Marcelle, C., Yancopoulos, G. D., Fraser, S. E. and Bronner-Fraser, M. (1997). Interactions of Eph-related receptors and ligands confer rostrocaudal pattern to trunk neural crest migration. *Current Biology* **7:** 571-580.

Kubu, C. J., Orimoto, K., Morrison, S. J., Weinmaster, G., Anderson, D. J. and Verdi, J. M. (2002). Developmental changes in Notch1 and Numb expression mediated by local cell-cell interactions underlie progressively increasing Delta sensitivity in neural crest stem cells. *Developmental Biology* **244:** 199-214.

Kuhlbrodt, K., Herbarth, B., Sock, E., Enderich, J., Hermans-Borgmeyer, I. and Wegner, M. (1998a). Cooperative function of POU proteins and SOX proteins in glial cells. *Journal of Biological Chemistry* **273:** 16050-16057.

Kuhlbrodt, K., Herbarth, B., Sock, E., Hermans-Borgmeyer, I. and Wegner, M. (1998b). Sox10, a novel transcriptional modulator in glial cells. *Journal of Neuroscience* **18:** 237-250.

Kuhlbrodt, K., Schmidt, C., Sock, E., Pingault, V., Bondurand, N., Goossens, M. and Wegner, M. (1998c). Functional analysis of Sox10 mutations found in human Waardenburg-Hirschsprung patients. *Journal of Biological Chemistry* **273:** 23033-23038.

Kunisch, M., Haenlin, M. and Campos-Ortega, J. A. (1994). Lateral Inhibition Mediated by the *Drosophila* Neurogenic Gene- *Delta* Is Enhanced by Proneural Proteins. *Proceedings of the National Academy of Sciences of the United States of America* **91:** 10139-10143.

LaBonne, C. and Bronner-Fraser, M. (1998). Neural crest induction in Xenopus: evidence for a two-signal model. *Development* **125:** 2403-2414.

LaBonne, C. and Bronner-Fraser, M. (1999). Molecular mechanisms of neural crest formation. *Annual Review of Cell and Developmental Biology* **15:** 81-112.

LaBonne, C. and Bronner-Fraser, M. (2000). Snail-related transcriptional repressors are required in Xenopus for both the induction of the neural crest and its subsequent migration. *Developmental Biology* **221:** 195-205.

Lam, W. L., Lee, T. S. and Gilbert, W. (1996). Active transposition in zebrafish. *Proceedings of the National Academy of Sciences of the United States of America* **93:** 10870-10875.

Lane, P. W. and Liu, H. M. (1984). Association of Megacolon With a New Dominant Spotting Gene (Dom) in the Mouse. *Journal of Heredity* **75:** 435-439.

Lang, D., Chen, F., Milewski, R., Li, J., Lu, M. M. and Epstein, J. A. (2000). Pax3 is required for enteric ganglia formation and functions with Sox10 to modulate expression of c-ret. *Journal of Clinical Investigation* **106:** 963-971.

Lang, D. and Epstein, J. A. (2003). Sox10 and Pax3 physically interact to mediate activation of a conserved c-RET enhancer. *Human Molecular Genetics* **12:** 937-945.

Latimer, A. J., Dong, X. H., Markov, Y. and Appel, B. (2002). Delta-Notch signaling induces hypochord development in zebrafish. *Development* **129:** 2555-2563.

Lawson, N. D. and Weinstein, B. M. (2002). In vivo imaging of embryonic vascular development using transgenic zebrafish. *Developmental Biology* **248:** 307-318.

Le Douarin, N. M. and Kalcheim, C. (1999). The Neural Crest. New York: Cambridge University Press.

Le Douarin, N. M., Teillet, M.-A., Ziller, C. and Smith, J. (1978). Adrenergic differentiation of cells of the choloinergic ciliary and Remak ganglia in avian embryo after *in vivo* transplantation. *Proc Natl Acad Sci U S A* **75:** 2030-2034.

Lee, E. C., Yu, D. G., de Velasco, J. M., Tessarollo, L., Swing, D. A., Court, D. L., Jenkins, N. A. and Copeland, N. G. (2001). A highly efficient *Escherichia coli*-based chromosome engineering system adapted for recombinogenic targeting and subcloning of BAC DNA. *Genomics* **73:** 56-65.

Lee, H. O., Levorse, J. M. and Shin, M. K. (2003). The endothelin receptor-B is required for the migration of neural crest-derived melanocyte and enteric neuron precursors. *Developmental Biology* **259:** 162-175.

Lefebvre, V., Huang, W. D., Harley, V. R., Goodfellow, P. N. and deCrombrugghe, B. (1997). SOX9 is a potent activator of the chondrocyte-specific enhancer of the pro alpha 1(II) collagen gene. *Molecular and Cellular Biology* **17:** 2336-2346.

Lefebvre, V., Li, P. and de Crombrugghe, B. (1998). A new long form of Sox5 (L-Sox5), Sox6 and Sox9 are coexpressed in chondrogenesis and cooperatively activate the type II collagen gene. *Embo Journal* **17:** 5718-5733.

Leimeroth, R., Lobsiger, C., Lussi, A., Taylor, V., Suter, U. and Sommer, L. (2002). Membrane-bound Neuregulin1 type III actively promotes Schwann cell differentiation of multipotent progenitor cells. *Developmental Biology* **246:** 245-258.

Li, M., Zhao, C. T., Wang, Y., Zhao, Z. X. and Meng, A. M. (2002). Zebrafish sox9b is an early neural crest marker. *Development Genes and Evolution* **212:** 203-206.

Li, Y. X., Zdanowicz, M., Young, L., Kumiski, D., Leatherbury, L. and Kirby, M. L. (2003). Cardiac neural crest in zebrafish embryos contributes to myocardial cell lineage and early heart function. *Developmental Dynamics* **226:** 540-550.

Liao, E. C., Paw, B. H., Oates, A. C., Pratt, S. J., Postlethwait, J. H. and Zon, L. I. (1998). SCL/Tal-1 transcription factor acts downstream of *cloche* to specify hematopoietic and vascular progenitors in zebrafish. *Genes & Development* **12:** 621-626.

Liem, K. F., Tremml, G., Roelink, H. and Jessell, T. M. (1995). Dorsal Differentiation of Neural Plate Cells Induced by Bmp- Mediated Signals from Epidermal Ectoderm. *Cell* **82:** 969-979.

Lin, S., Yang, S. and Hopkins, N. (1994). *lacZ* Expression in Germline Transgenic Zebrafish Can Be Detected in Living Embryos. *Developmental Biology* **161:** 77-83.

Linney, E., Hardison, N. L., Lonze, B. E., Lyons, S. and DiNapoli, L. (1999). Transgene expression in zebrafish: A comparison of retroviral- vector and DNA-injection approaches. *Developmental Biology* **213:** 207-216.

Lister, J. A., Robertson, C. P., Lepage, T., Johnson, S. L. and Raible, D. W. (1999). *nacre* encodes a zebrafish microphthalmia-related protein that regulates neural-crest-derived pigment cell fate. *Development* **126:** 3757-3767.

Liu, J. P. and Jessell, T. M. (1998). A role for rhoB in the delamination of neural crest cells from the dorsal neural tube. *Development* **125:** 5055-5067.

Liu, Q., Melnikova, I. N., Hu, M. J. and Gardner, P. D. (1999). Cell type-specific activation of neuronal nicotinic acetylcholine receptor subunit genes by Sox10. *Journal of Neuroscience* **19:** 9747-9755.

Lo, L. C. and Anderson, D. J. (1995). Postmigratory Neural Crest Cells expressing c-ret display restricted developmental and proliferative capacities. *Neuron* **15:** 527-539.

Lo, L. C., Sommer, L. and Anderson, D. J. (1997). MASH1 maintains competence for BMP2-induced neuronal differentiation in post-migratory neural crest cells. *Current Biology* **7:** 440-450.

Loh, S. H. Y. and Russell, S. (2000). A Drosophila group E Sox gene is dynamically expressed in the embryonic alimentary canal. *Mechanisms of Development* **93:** 185-188.

Long, Q. M., Meng, A. M., Wang, H., Jessen, J. R., Farrell, M. J. and Lin, S. (1997). *GATA-1* expression pattern can be recapitulated in living transgenic zebrafish using GFP reporter gene. *Development* **124:** 4105-4111.

Luo, R., Gao, J., Wehrle-Haller, B. and Henion, P. D. (2003). Molecular identification of distinct neurogenic and melanogenic neural crest sublineages. *Development* **130:** 321-330.

Luo, R. S., An, M., Arduini, B. L. and Henion, P. D. (2001). Specific pan-neural crest expression of Zebrafish crestin throughout embryonic development. *Developmental Dynamics* **220:** 169-174.

Lyons, S. E., Lawson, N. D., Lei, L., Bennett, P. E., Weinstein, B. M. and Liu, P. P. (2002). A nonsense mutation in zebrafish *gata1* causes the bloodless phenotype in *vlad tepes*. *Proceedings of the National Academy of Sciences of the United States of America* **99:** 5454-5459.

Ma, Q. F., Fode, C., Guillemot, F. and Anderson, D. J. (1999). NEUROGENIN1 and NEUROGENIN2 control two distinct waves of neurogenesis in developing dorsal root ganglia. *Genes & Development* **13:** 1717-1728.

Ma, Q. F., Sommer, L., Cserjesi, P. and Anderson, D. J. (1997). Mash1 and neurogenin1 expression patterns define complementary domains of neuroepithelium in the developing CNS and are correlated with regions expressing notch ligands. *Journal of Neuroscience* **17:** 3644-3652.

Malicki, J., Schier, A. F., SolnicaKrezel, L., Stemple, D. L., Neuhauss, S. C. F., Stainier, D. Y. R., Abdelilah, S., Rangini, Z., Zwartkruis, F. and Driever, W. (1996). Mutations affecting development of the zebrafish ear. *Development* **123:** 275-283.

Maraia, R., Saal, H. M. and Wangsa, D. (1991). A Chromosome-17q Denovo Paracentric Inversion in a Patient with Campomelic Dysplasia - Case-Report and Etiologic Hypothesis. *Clinical Genetics* **39:** 401-408.

Marchant, L., Linker, C., Ruiz, P., Guerrero, N. and Mayor, R. (1998). The inductive properties of mesoderm suggest that the neural crest cells are specified by a BMP gradient. *Developmental Biology* **198:** 319-329.

MarcosGutierrez, C. V., Wilson, S. W., Holder, N. and Pachnis, V. (1997). The zebrafish homologue of the ret receptor and its pattern of expression during embryogenesis. *Oncogene* **14:** 879-889.

Marshall, O. J. and Harley, V. R. (2000). Molecular mechanisms of SOX9 action. *Molecular Genetics and Metabolism* **71:** 455-462.

Marusich, M. F., Furneaux, H. M., Henion, P. D. and Weston, J. A. (1994). Hu Neuronal Proteins Are Expressed in Proliferating Neurogenic Cells. *Journal of Neurobiology* **25:** 143-155.

Mayor, R., Guerrero, N. and Martinez, C. (1997). Role of FGF and noggin in neural crest induction. *Developmental Biology* **189:** 1-12.

Melnikova, I. N., Lin, H. R., Blanchette, A. R. and Gardner, P. D. (2000). Synergistic transcriptional activation by Sox10 and Sp1 family members. *Neuropharmacology* **39:** 2615-2623.

Meng, A. M., Tang, H., Ong, B. A., Farrell, M. J. and Lin, S. (1997). Promoter analysis in living zebrafish embryos identifies a cis- acting motif required for neuronal

expression of GATA-2. *Proceedings of the National Academy of Sciences of the United States of America* **94:** 6267-6272.

Mertin, S., McDowall, S. G. and Harley, V. R. (1999). The DNA-binding specificity of SOX9 and other SOX proteins. *Nucleic Acids Research* **27:** 1359-1364.

Miller, C. T., Schilling, T. F., Lee, K. H., Parker, J. and Kimmel, C. B. (2000). *sucker* encodes a zebrafish Endothelin-1 required for ventral pharyngeal arch development. *Development* **127:** 3815-3828.

Mintzer, K. A., Lee, M. A., Runke, G., Trout, J., Whitman, M. and Mullins, M. C. (2001). *lost-a-fin* encodes a type I BMP receptor, Alk8, acting maternally and zygotically in dorsoventral pattern formation. *Development* **128:** 859-869.

Montero, J. A., Giron, B., Arrechedera, H., Cheng, Y. C., Scotting, P., Chimal-Monroy, J., Garcia-Porrero, J. A. and Hurle, J. M. (2002). Expression of *Sox8*, *Sox9* and *Sox10* in the developing valves and autonomic nerves of the embryonic heart. *Mechanisms of Development* **118:** 199-202.

Morgan, R. and Sargent, M. G. (1997). The role in neural patterning of translation initiation factor eIF4AII; induction of neural fold genes. *Development* **124:** 2751-2760.

Morin-Kensicki, E. M. and Eisen, J. S. (1997). Sclerotome development and peripheral nervous system segmentation in embryonic zebrafish. *Development* **124:** 159-167.

Morrison, S. J., Perez, S. E., Qiao, Z., Verdi, J. M., Hicks, C., Weinmaster, G. and Anderson, D. J. (2000). Transient Notch activation initiates an irreversible switch from neurogenesis to gliogenesis by neural crest stem cells. *Cell* **101:** 499-510.

Mullins, M. C., Hammerschmidt, M., Haffter, P. and Nusslein-Volhard, C. (1994). Large-Scale Mutagenesis in the Zebrafish: in Search of Genes Controlling Development in a Vertebrate. *Current Biology* **4:** 189-202.

Mullins, M. C., Nguyen, V. H., Schmid, B., Connors, S. A., Wagner, D. S., Trout, J. and Ekker, M. (1998). A *bmp2b* pathway of genes in the zebrafish establishes ventral and lateral cell fates of the gastrula, including the neural crest progenitors. *Developmental Biology* **198:** 165.

Muskavitch, M. A. T. (1994). Delta-Notch Signaling and *Drosophila* Cell Fate Choice. *Developmental Biology* **166:** 415-430.

Muyrers, J. P. P., Zhang, Y. M. and Stewart, A. F. (2001). Techniques: Recombinogenic engineering - new options for cloning and manipulating DNA. *Trends in Biochemical Sciences* **26:** 325-331.

Neumann, C. J. and Nuesslein-Volhard, C. (2000). Patterning of the zebrafish retina by a wave of sonic hedgehog activity. *Science* **289:** 2137-2139.

Nguyen, V. H., Schmid, B., Trout, J., Connors, S. A., Ekker, M. and Mullins, M. C. (1998). Ventral and lateral regions of the zebrafish gastrula, including the neural crest progenitors, are established by a *bmp2b/swirl* pathway of genes. *Developmental Biology* **199:** 93-110.

Nobukuni, Y., Watanabe, A., Takeda, K., Skarka, H. and Tachibana, M. (1996). Analyses of loss-of-function mutations of the MITF gene suggest that haploinsufficiency is a cause of Waardenburg syndrome type 2A. *American Journal of Human Genetics* **59:** 76-83.

Norrander, J., Kempe, T. and Messing, J. (1983). Construction of improved M13 vectors using oligodeoxynucleotide-directed mutagenesis. *Gene* **26:** 101-6.

Oakley, R. A., Lasky, C. J., Erickson, C. A. and Tosney, K. W. (1994). Glycoconjugates Mark a Transient Barrier to Neural Crest Migration in the Chicken-Embryo. *Development* **120:** 103-114.

Odenthal, J. and Nusslein-Volhard, C. (1998). *fork head* domain genes in zebrafish. *Development Genes and Evolution* **208:** 245-258.

Ohe, K., Lalli, E. and Sassone-Corsi, P. (2002). A direct role of SRY and SOX proteins in pre-mRNA splicing. *Proceedings of the National Academy of Sciences of the United States of America* **99:** 1146-1151.

Opdecamp, K., Nakayama, A., Nguyen, M. T. T., Hodgkinson, C. A., Pavan, W. J. and Arnheiter, H. (1997). Melanocyte development in vivo and in neural crest cell cultures: Crucial dependence on the Mitf basic-helix-loop- helix-zipper transcription. *Development* **124:** 2377-2386.

Pachnis, V., Mankoo, B. and Constantini, F. (1993). Expression of the *c-Ret* Protooncogene During Mouse Embryogenesis. *Development* **119:** 1005-1017.

Paratore, C., Eichenberger, C., Suter, U. and Sommer, L. (2002). *Sox10* haploinsufficiency affects maintenance of progenitor cells in a mouse model of Hirschsprung disease. *Human Molecular Genetics* **11:** 3075-3085.

Paratore, C., Goerich, D. E., Suter, U., Wegner, M. and Sommer, L. (2001). Survival and glial fate acquisition of neural crest cells are regulated by an interplay between the transcription factor Sox10 and extrinsic combinatorial signaling. *Development* **128:** 3949-3961.

Parichy, D. M., Ransom, D. G., Paw, B., Zon, L. I. and Johnson, S. L. (2000). An orthologue of the *kit*-related gene *fms* is required for development of neural crest-derived xanthophores and a subpopulation of adult melanocytes in the zebrafish, *Danio rerio*. *Development* **127:** 3031-3044.

Parichy, D. M., Rawls, J. F., Pratt, S. J., Whitfield, T. T. and Johnson, S. L. (1999). Zebrafish *sparse* corresponds to an orthologue of *c-kit* and is required for the morphogenesis of a subpopulation of melanocytes, but is not essential for hematopoiesis or primordial germ cell development. *Development* **126:** 3425-3436.

Park, H. C. and Appel, B. (2003). Delta-Notch signaling regulates oligodendrocyte specification. *Development* **130:** 3747-55.

Park, H. C., Kim, C. H., Bae, Y. K., Yee, S. Y., Kim, S. H., Hong, S. K., Shin, J., Yoo, K. W., Hibi, M., Hirano, T. *et al.* (2000). Analysis of upstream elements in the *HuC* promoter leads to the establishment of transgenic zebrafish with fluorescent neurons. *Developmental Biology* **227:** 279-293.

Park, H. C., Mehta, A., Richardson, J. S. and Appel, B. (2002). olig2 is required for zebrafish primary motor neuron and oligodendrocyte development. *Developmental Biology* **248:** 356-368.

Pattyn, A., Morin, X., Cremer, H., Goridis, C. and Brunet, J. F. (1999). The homeobox gene *Phox2b* is essential for the development of autonomic neural crest derivatives. *Nature* **399:** 366-370.

Pauliny, A. (2002). Cloning and molecular characterisation of the zebrafish *colourless* gene. PhD Thesis, University of Bath, Bath, U.K.

Pauls, S., Geldmacher-Voss, B. and Campos-Ortega, J. A. (2001). A zebrafish histone variant H2A.F/Z and a transgenic H2A.F/Z : GFP fusion protein for in vivo studies of embryonic development. *Development Genes and Evolution* **211:** 603-610.

Peirano, R. I., Goerich, D. E., Riethmacher, D. and Wegner, M. (2000). Protein zero gene expression is regulated by the glial transcription factor Sox10. *Molecular and Cellular Biology* **20:** 3198-3209.

Peirano, R. I. and Wegner, M. (2000). The glial transcription factor Sox10 binds to DNA both as monomer and dimer with different functional consequences. *Nucleic Acids Research* **28:** 3047-3055.

Perez, S. E., Rebelo, S. and Anderson, D. J. (1999). Early specification of sensory neuron fate revealed by expression and function of neurogenins in the chick embryo. *Development* **126:** 1715-1728.

Pevny, L. H. and Lovell-Badge, R. (1997). Sox genes find their feet. *Current Opinion in Genetics & Development* **7:** 338-344.

Pfeifer, D., Poulat, F., Holinski-Feder, E., Kooy, F. and Scherer, G. (2000). The SOX8 gene is located within 700 kb of the tip of chromosome 16p and is deleted in a patient with ATR-16 syndrome. *Genomics* **63:** 108-116.

Picker, A., Scholpp, S., Bohli, H., Takeda, H. and Brand, M. (2002). A novel positive transcriptional feedback loop in midbrain- hindbrain boundary development is revealed through analysis of the zebrafish *pax2.1* promoter in transgenic lines. *Development* **129:** 3227-3239.

Pingault, V., Bondurand, N., Kuhlbrodt, K., Goerich, D. E., Prehu, M. O., Puliti, A., Herbarth, B., Hermans-Borgmeyer, I., Legius, E., Matthijs, G. *et al.* (1998). SOX10 mutations in patients with Waardenburg-Hirschsprung disease. *Nature Genetics* **18:** 171-173.

Pingault, V., Bondurand, N., Le Caignec, C., Tardieu, S., Lemort, N., Dubourg, O., Le Guern, E., Goossens, M. and Boespflug-Tanguy, O. (2001a). The SOX10 transcription factor: evaluation as a candidate gene for central and peripheral hereditary myelin disorders. *Journal of Neurology* **248:** 496-499.

Pingault, V., Bondurand, N., Lemort, N., Sancandi, M., Ceccherini, I., Hugot, J. P., Jouk, P. S. and Goossens, M. (2001b). A heterozygous endothelin 3 mutation in Waardenburg- Hirschsprung disease: is there a dosage effect of EDN3/EDNRB gene mutations on neurocristopathy phenotypes? *Journal of Medical Genetics* **38:** 205-208.

Piotrowski, T., Schilling, T. F., Brand, M., Jiang, Y. J., Heisenberg, C. P., Beuchle, D., Grandel, H., vanEeden, F. J. M., FurutaniSeiki, M., Granato, M. *et al.* (1996). Jaw and branchial arch mutants in zebrafish .2. Anterior arches and cartilage differentiation. *Development* **123:** 345-356.

Pissarra, L., Henrique, D. and Duarte, A. (2000). Expression of *hes6*, a new member of the Hairy/Enhancer-of-split family, in mouse development. *Mechanisms of Development* **95:** 275-278.

Podolsky, T., Fong, S. T. and Lee, B. T. O. (1996). Direct selection of tetracycline-sensitive *Escherichia coli* cells using nickel salts. *Plasmid* **36:** 112-115.

Postlethwait, J. H., Yan, Y. L., Gates, M. A., Horne, S., Amores, A., Brownlie, A., Donovan, A., Egan, E. S., Force, A., Gong, Z. Y. *et al.* (1998). Vertebrate genome evolution and the zebrafish gene map. *Nature Genetics* **18:** 345-349.

Potterf, S. B., Furumura, M., Dunn, K. J., Arnheiter, H. and Pavan, W. J. (2000). Transcription factor hierarchy in Waardenburg syndrome: regulation of MITF expression by SOX10 and PAX3. *Human Genetics* **107:** 1-6.

Potterf, S. B., Mollaaghababa, R., Hou, L., Southard-Smith, E. M., Hornyak, T. J., Arnheiter, H. and Pavan, W. J. (2001). Analysis of SOX10 function in neural crest-derived melanocyte development: SOX10-dependent transcriptional control of dopachrome tautomerase. *Developmental Biology* **237:** 245-257.

Poulain, M. and Lepage, T. (2002). Mezzo, a *paired-like* homeobox protein is an immediate target of Nodal signalling and regulates endoderm specification in zebrafish. *Development* **129:** 4901-4914.

Prior, H. M. and Walter, M. A. (1996). SOX genes: Architects of development. *Molecular Medicine* **2:** 405-412.

Puffenberger, E. G., Hosoda, K., Washington, S. S., Nakao, K., Dewit, D., Yanagisawa, M. and Chakravarti, A. (1994). A Missense Mutation of the Endothelin-B Receptor Gene in Multigenic Hirschsprungs-Disease. *Cell* **79:** 1257-1266.

Puliti, A., Prehu, M. O., Simonchazottes, D., Ferkdadji, L., Peuchmaur, M., Goossens, M. and Guenet, J. L. (1995). A High-Resolution Genetic-Map of Mouse Chromosome-15 Encompassing the *Dominant Megacolon* (*Dom*) Locus. *Mammalian Genome* **6:** 763-768.

Pusch, C., Hustert, E., Pfeifer, D., Sudbeck, P., Kist, R., Roe, B., Wang, Z. L., Balling, R., Blin, N. and Scherer, G. (1998). The *SOX10/Sox10* gene from human and mouse: sequence, expression, and transactivation by the encoded HMG domain transcription factor. *Human Genetics* **103:** 115-123.

Raible, D. W. and Eisen, J. S. (1994). Restriction of neural crest cell fate in the trunk of the embryonic zebrafish. *Development* **120:** 495-503.

Raible, D. W. and Eisen, J. S. (1996). Regulative interactions in zebrafish neural crest. *Development* **122:** 501-507.

Raible, D. W., Wood, A., Hodsdon, W., Henion, P. D., Weston, J. A. and Eisen, J. S. (1992). Segregation and early dispersal of neural crest cells in the embryonic zebrafish. *Dev Dyn* **195:** 29-42.

Rebagliati, M. R., Toyama, R., Haffter, P. and Dawid, I. B. (1998). *cyclops* encodes a nodal-related factor involved in midline signaling. *Proceedings of the National Academy of Sciences of the United States of America* **95:** 9932-9937.

Rehberg, S., Lischka, P., Glaser, G., Stamminger, T., Wegner, M. and Rosorius, O. (2002). Sox10 is an active nucleocytoplasmic shuttle protein, and shuttling is crucial for Sox10-mediated transactivation. *Molecular and Cellular Biology* **22:** 5826-5834.

Riethmacher, D., Sonnenberg-Riethmacher, E., Brinkmann, V., Yamaai, T., Lewin, G. R. and Birchmeier, C. (1997). Severe neuropathies in mice with targeted mutations in the ErbB3 receptor. *Nature* **389:** 725-730.

Riley, B. B., Chiang, M. Y., Farmer, L. and Heck, R. (1999). The *deltaA* gene of zebrafish mediates lateral inhibition of hair cells in the inner ear and is regulated by *pax2.1*. *Development* **126:** 5669-5678.

Robinson, V., Smith, A., Flenniken, A. M. and Wilkinson, D. G. (1997). Roles of Eph receptors and ephrins in neural crest pathfinding. *Cell and Tissue Research* **290:** 265-274.

Russell, S. R. H., SanchezSoriano, N., Wright, C. R. and Ashburner, M. (1996). The Dichaete gene of Drosophila melanogaster encodes a SOX- domain protein required for embryonic segmentation. *Development* **122:** 3669-3676.

Sambrook, J., Fritsch, E.F., Maniatis, T. (1989). Molecular cloning. A laboratory manual. New York: Cold Spring Harbour Laboratory Press.

Sanchez-Soriano, N. and Russell, S. (1998). The Drosophila SOX-domain protein Dichaete is required for the development of the central nervous system midline. *Development* **125:** 3989-3996.

Scheer, N., Groth, A., Hans, S. and Campos-Ortega, J. A. (2001). An instructive function for Notch in promoting gliogenesis in the zebrafish retina. *Development* **128:** 1099-1107.

Schepers, G. E., Bullejos, M., Hosking, B. M. and Koopman, P. (2000). Cloning and characterisation of the Sry-related transcription factor gene Sox8. *Nucleic Acids Research* **28:** 1473-1480.

Schilham, M. W., Vaneijk, M., Vandewetering, M. and Clevers, H. C. (1993). The Murine Sox-4 Protein Is Encoded on a Single Exon. *Nucleic Acids Research* **21:** 2009-2009.

Schilling, T. F. and Kimmel, C. B. (1994). Segment and Cell-Type Lineage Restrictions During Pharyngeal Arch Development in the Zebrafish Embryo. *Development* **120:** 483-494.

Schilling, T. F., Piotrowski, T., Grandel, H., Brand, M., Heisenberg, C. P., Jiang, Y. J., Beuchle, D., Hammerschmidt, M., Kane, D. A., Mullins, M. C. ***et al.*** (1996a). Jaw and branchial arch mutants in zebrafish .1. Branchial arches. *Development* **123:** 329-344.

Schilling, T. F., Walker, C. and Kimmel, C. B. (1996b). The chinless mutation and neural crest cell interactions in zebrafish jaw development. *Development* **122:** 1417-26.

Schneider, C., Wicht, H., Enderich, J., Wegner, M. and Rohrer, H. (1999). Bone morphogenetic proteins are required in vivo for the generation of sympathetic neurons. *Neuron* **24:** 861-870.

Schuchardt, A., Dagati, V., Larssonblomberg, L., Costantini, F. and Pachnis, V. (1994). Defects in the Kidney and Enteric Nervous-System of Mice Lacking the Tyrosine Kinase Receptor Ret. *Nature* **367:** 380-383.

Schulte-Merker, S., van Eeden, F. J. M., Halpern, M. E., Kimmel, C. B. and Nusslein-Volhard, C. (1994). *no tail (ntl)* Is the Zebrafish Homolog of the Mouse *T (Brachyury)* Gene. *Development* **120:** 1009-1015.

Sela-Donenfeld, D. and Kalcheim, C. (1999). Regulation of the onset of neural crest migration by coordinated activity of BMP4 and Noggin in the dorsal neural tube. *Development* **126:** 4749-4762.

Selleck, M. A. J. and Bronner-Fraser, M. (1995). Origins of the Avian Neural Crest - the Role of Neural Plate- Epidermal Interactions. *Development* **121:** 525-538.

Seydoux, G. and Greenwald, I. (1989). Cell Autonomy of Lin-12 Function in a Cell Fate Decision in C- Elegans. *Cell* **57:** 1237-1245.

Shah, N. M., Groves, A. K. and Anderson, D. J. (1996). Alternative neural crest cell fates are instructively promoted by TGF beta superfamily members. *Cell* **85:** 331-343.

Shah, N. M., Marchionni, M. A., Isaacs, I., Stroobant, P. and Anderson, D. J. (1994). Glial Growth-Factor Restricts Mammalian Neural Crest Stem-Cells to a Glial Fate. *Cell* **77:** 349-360.

Shimoda, N., Chevrette, M., Ekker, M., Kikuchi, Y., Hotta, Y. and Okamoto, H. (1996). Mermaid: A family of short interspersed repetitive elements widespread in vertebrates. *Biochemical and Biophysical Research Communications* **220:** 226-232.

Smithers, L., Haddon, C., Jiang, Y. J. and Lewis, J. (2000). Sequence and embryonic expression of *deltaC* in the zebrafish. *Mechanisms of Development* **90:** 119-123.

Sock, E., Schmidt, K., Hermanns-Borgmeyer, I., Bosl, M. R. and Wegner, M. (2001). Idiopathic weight reduction in mice deficient in the high- mobility-group transcription factor Sox8. *Molecular and Cellular Biology* **21:** 6951-6959.

Sommer, L., Shah, N., Rao, M. and Anderson, D. J. (1995). The cellular function of MASH1 in autonomic neurogenesis. *Neuron* **15:** 1245-1258.

Sonnenberg-Riethmacher, E., Miehe, M., Stolt, C. C., Goerich, D. E., Wegner, M. and Riethmacher, D. (2001). Development and degeneration of dorsal root ganglia in the absence of the HMG-domain transcription factor Sox10. *Mechanisms of Development* **109:** 253-265.

Soullier, S., Jay, P., Poulat, F., Vanacker, J. M., Berta, P. and Laudet, V. (1999). Diversification pattern of the HMG and SOX family members during evolution. *Journal of Molecular Evolution* **48:** 517-527.

Southard-Smith, E. M., Angrist, M., Ellison, J. S., Agarwala, R., Baxevanis, A. D., Chakravarti, A. and Pavan, W. J. (1999a). The *Sox10^{Dom}* mouse: Modeling the genetic variation of Waardenburg-Shah (WS4) syndrome. *Genome Research* **9:** 215-225.

Southard-Smith, E. M., Collins, J. E., Ellison, J. S., Smith, K. J., Baxevanis, A. D., Touchman, J. W., Green, E. D., Dunham, I. and Pavan, W. J. (1999b). Comparative analyses of the Dominant megacolon-SOX10 genomic interval in mouse and human. *Mammalian Genome* **10:** 744-749.

Southard-Smith, E. M., Kos, L. and Pavan, W. J. (1998). *Sox10* mutation disrupts neural crest development in *Dom* Hirschsprung mouse model. *Nature Genetics* **18:** 60-64.

Spritz, R. A. (1998). Piebaldism, Waardenburg Syndrome, and Related Genetic Disorders-Molecular and Genetic Aspects. In *The Pigmentary System. Physiology and Pathophysiology*, pp. 207-215. New York: Oxford University Press, Inc.

Stanke, M., Junghans, D., Geissen, M., Goridis, C., Ernsberger, U. and Rohrer, H. (1999). The Phox2 homeodomain proteins are sufficient to promote the development of sympathetic neurons. *Development* **126:** 4087-4094.

Stavropoulos, T. A. and Strathdee, C. A. (2001). Synergy between tetA and rpsL provides high-stringency positive and negative selection in bacterial artificial chromosome vectors. *Genomics* **72:** 99-104.

Steel, K. P., Davidson, D. R. and Jackson, I. J. (1992). Trp-2/Dt, a New Early Melanoblast Marker, Shows That Steel Growth-Factor (C-Kit Ligand) Is a Survival Factor. *Development* **115:** 1111-1119.

Stemple, D. L. and Anderson, D. J. (1992). Isolation of a Stem-Cell for Neurons and Glia from the Mammalian Neural Crest. *Cell* **71:** 973-985.

Stolt, C. C., Rehberg, S., Ader, M., Lommes, P., Riethmacher, D., Schachner, M., Bartsch, U. and Wegner, M. (2002). Terminal differentiation of myelin-forming oligodendrocytes depends on the transcription factor Sox10. *Genes & Development* **16:** 165-170.

Strahle, U., Fischer, N. and Blader, P. (1997). Expression and regulation of a *netrin* homologue in the zebrafish embryo. *Mechanisms of Development* **62:** 147-160.

Streit, A. and Stern, C. D. (1999). Establishment and maintenance of the border of the neural plate in the chick: involvement of FGF and BMP activity. *Mechanisms of Development* **82:** 51-66.

Struhl, G. and Greenwald, I. (1999). Presenilin is required for activity and nuclear access of Notch in *Drosophila*. *Nature* **398:** 522-525.

Stuart, G. W., McMurray, J. V. and Westerfield, M. (1988). Replication, Integration and Stable Germ-Line Transmission of Foreign Sequences Injected into Early Zebrafish Embryos. *Development* **103:** 403-412.

Stuart, G. W., Vielkind, J. R., McMurray, J. V. and Westerfield, M. (1990). Stable Lines of Transgenic Zebrafish Exhibit Reproducible Patterns of Transgene Expression. *Development* **109:** 577-584.

Sudbeck, P. and Scherer, G. (1997). Two independent nuclear localization signals are present in the DNA-binding high-mobility group domains of SRY and SOX9. *Journal of Biological Chemistry* **272:** 27848-27852.

Syrris, P., Carter, N. D. and Patton, M. A. (1999). Novel nonsense mutation of the endothelin-B receptor gene in a family with Waardenburg-Hirschsprung disease. *American Journal of Medical Genetics* **87:** 69-71.

Takke, C., Dornseifer, P., Von Weizsacker, E. and Campos-Ortega, J. A. (1999). *her4*, a zebrafish homologue of the *Drosophila* neurogenic gene *E(spl)*, is a target of NOTCH signalling. *Development* **126:** 1811-1821.

Taraviras, S. and Pachnis, V. (1999). Development of the mammalian enteric nervous system. *Current Opinion in Genetics & Development* **9:** 321-327.

Tassabehji, M., Newton, V. E. and Read, A. P. (1994). Waardenburg Syndrome Type-2 Caused by Mutations in the Human Microphthalmia (Mitf) Gene. *Nature Genetics* **8:** 251-255.

Tassabehji, M., Read, A. P., Newton, V. E., Harris, R., Balling, R., Gruss, P. and Strachan, T. (1992). Waardenburg Syndrome Patients Have Mutations in the Human Homolog of the Pax-3 Paired Box Gene. *Nature* **355:** 635-636.

Technau, G. M. and Campos-Ortega, J. A. (1987). Cell Autonomy of Expression of Neurogenic Genes of *Drosophila melanogaster*. *Proceedings of the National Academy of Sciences of the United States of America* **84:** 4500-4504.

Thermes, V., Grabher, C., Ristoratore, F., Bourrat, F., Choulika, A., Wittbrodt, J. and Joly, J. S. (2002). *I-SceI* meganuclease mediates highly efficient transgenesis in fish. *Mechanisms of Development* **118:** 91-98.

Touraine, R. L., Attie-Bitach, T., Manceau, E., Korsch, E., Sarda, P., Pingault, V., Encha-Razavi, F., Pelet, A., Auge, J., Nivelon-Chevallier, A. *et al.* (2000). Neurological phenotype in Waardenburg syndrome type 4 correlates with novel *SOX10* truncating mutations and expression in developing brain. *American Journal of Human Genetics* **66:** 1496-1503.

Tremblay, P., Dietrich, S., Mericskay, M., Schubert, F. R., Li, Z. L. and Paulin, D. (1998). A crucial role for Pax3 in the development of the hypaxial musculature and the long-range migration of muscle precursors. *Developmental Biology* **203:** 49-61.

Uchikawa, M., Kamachi, Y. and Kondoh, H. (1999). Two distinct subgroups of Group B Sox genes for transcriptional activators and repressors: their expression during embryonic organogenesis of the chicken. *Mechanisms of Development* **84:** 103-120.

Udvadia, A. J. and Linney, E. (2003). Windows into development: historic, current, and future perspectives on transgenic zebrafish. *Developmental Biology* **256:** 1-17.

van de Wetering, M. and Clevers, H. (1992). Sequence-Specific Interaction of the Hmg Box Proteins Tcf-1 and Sry Occurs within the Minor Groove of a Watson-Crick Double Helix. *Embo Journal* **11:** 3039-3044.

Veitia, R. A. (2002). Exploring the etiology of haploinsufficiency. *Bioessays* **24:** 175-184.

Vente, A., Korn, B., Zehetner, G., Poustka, A. and Lehrach, H. (1999). Distribution and early development of microarray technology in Europe. *Nature Genetics* **22:** 22-22.

Vogel, A. M. and Gerster, T. (1999). Promoter activity of the zebrafish *bhikhari* retroelement requires an intact activin signaling pathway. *Mechanisms of Development* **85:** 133-146.

Wagner, T., Wirth, J., Meyer, J., Zabel, B., Held, M., Zimmer, J., Pasantes, J., Bricarelli, F. D., Keutel, J., Hustert, E. *et al.* (1994). Autosomal Sex Reversal and Campomelic Dysplasia Are Caused by Mutations in and around the Sry-Related Gene *Sox9*. *Cell* **79:** 1111-1120.

Wakamatsu, Y., Maynard, T. M. and Weston, J. A. (2000). Fate determination of neural crest cells by NOTCH-mediated lateral inhibition and asymmetrical cell division during gangliogenesis. *Development* **127:** 2811-2821.

Wakamatsu, Y., Mochii, M., Vogel, K. S. and Weston, J. A. (1998). Avian neural crest-derived neurogenic precursors undergo apoptosis on the lateral migration pathway. *Development* **125:** 4205-4213.

Wang, H. U. and Anderson, D. J. (1997). Eph family transmembrane ligands can mediate repulsive guidance of trunk neural crest migration and motor axon outgrowth. *Neuron* **18:** 383-396.

Wegner, M. (1999). From head to toes: the multiple facets of Sox proteins. *Nucleic Acids Research* **27:** 1409-1420.

Wehrle-Haller, B. and Weston, J. A. (1995). Soluble and Cell-Bound Forms of Steel Factor Activity Play Distinct Roles in Melanocyte Precursor Dispersal and Survival on the Lateral Neural Crest Migration Pathway. *Development* **121:** 731-742.

Wen, X. M. and Wu, G. D. (2001). Evidence for epigenetic mechanisms that silence both basal and Immune-Stimulated transcription of the IL-8 gene. *Journal of Immunology* **166:** 7290-7299.

Westin, J. and Lardelli, M. (1997). Three novel *Notch* genes in zebrafish: Implications for vertebrate *Notch* gene evolution and function. *Development Genes and Evolution* **207:** 51-63.

Weston, J. A. (1991). Sequential Segregation and Fate of Developmentally Restricted Intermediate Cell-Populations in the Neural Crest Lineage. *Current Topics in Developmental Biology* **25:** 133-153.

Weston, J. A. and Butler, S. L. (1966). Temporal factors affecting localization of neural crest cells in the chicken embryo. *Dev Biol* **14:** 246-66.

Whitfield, T. T., Granato, M., vanEeden, F. J. M., Schach, U., Brand, M., FurutaniSeiki, M., Haffter, P., Hammerschmidt, M., Heisenberg, C. P., Jiang, Y. J. *et al.* (1996). Mutations affecting development of the zebrafish inner ear and lateral line. *Development* **123:** 241-254.

Williams, R., Lendahl, U. and Lardelli, M. (1995). Complementary and Combinatorial Patterns of *Notch* Gene Family Expression During Early Mouse Development. *Mechanisms of Development* **53:** 357-368.

Wilson, M. and Koopman, P. (2002). Matching SOX: partner proteins and co-factors of the SOX family of transcriptional regulators. *Current Opinion in Genetics & Development* **12:** 441-446.

Wirth, J., Wagner, T., Meyer, J., Pfeiffer, R. A., Tietze, H. U., Schempp, W. and Scherer, G. (1996). Translocation breakpoints in three patients with campomelic dysplasia and autosomal sex reversal map more than 130 kb from SOX9. *Human Genetics* **97:** 186-193.

Wright, E., Hargrave, M. R., Christiansen, J., Cooper, L., Kun, J., Evans, T., Gangadharan, U., Greenfield, A. and Koopman, P. (1995). The Sry-Related Gene Sox9 Is Expressed During Chondrogenesis in Mouse Embryos. *Nature Genetics* **9:** 15-20.

Wright, E. M., Snopek, B. and Koopman, P. (1993). 7 New Members of the Sox Gene Family Expressed During Mouse Development. *Nucleic Acids Research* **21:** 744-744.

Wunderle, V. M., Critcher, R., Ashworth, A. and Goodfellow, P. N. (1996). Cloning and characterization of SOX5, a new member of the human SOX gene family. *Genomics* **36:** 354-358.

Wunderle, V. M., Critcher, R., Hastie, N., Goodfellow, P. N. and Schedl, A. (1998). Deletion of long-range regulatory elements upstream of SOX9 causes campomelic dysplasia. *Proceedings of the National Academy of Sciences of the United States of America* **95:** 10649-10654.

Yamashita, A., Suzuki, S., Fujitani, K., Kojima, M., Kanda, H., Ito, M., Takamatsu, N., Yamashita, S. and Shiba, T. (1998). cDNA cloning of a novel rainbow trout SRY-type HMG box protein, rtSox23, and its functional analysis. *Gene* **209:** 193-200.

Yan, Y. L., Miller, C. T., Nissen, R., Singer, A., Liu, D., Kirn, A., Draper, B., Willoughby, J., Morcos, P. A., Amsterdam, A. *et al.* (2002). A zebrafish *sox9* gene required for cartilage morphogenesis. *Development* **129:** 5065-5079.

Yan, Y. L., Talbot, W. S., Egan, E. S. and Postlethwait, J. H. (1998). Mutant rescue by BAC clone injection in zebrafish. *Genomics* **50:** 287-289.

Yang, X. D. W., Model, P. and Heintz, N. (1997). Homologous recombination based modification in *Escherichia coli* and germline transmission in transgenic mice of a bacterial artificial chromosome. *Nature Biotechnology* **15:** 859-865.

Yu, W., Misulovin, Z., Suh, H., Hardy, R. R., Jankovic, M., Yannoutsos, N. and Nussenzweig, M. C. (1999). Coordinate regulation of *RAG1* and *RAG2* by cell type-specific DNA elements 5 ' of *RAG2*. *Science* **285:** 1080-1084.

Zhan, J. H., Xiu, Y., Gu, J. Q., Fang, Z. C. and Hu, X. L. (1999). Expression of RET proto-oncogene and GDNF deficit in Hirschsprung's disease. *Journal of Pediatric Surgery* **34:** 1606-1609.

Zhang, J. J., Talbot, W. S. and Schier, A. F. (1998a). Positional cloning identifies zebrafish *one-eyed pinhead* as a permissive EGF-related ligand required during gastrulation. *Cell* **92:** 241-251.

Zhang, Y. M., Buchholz, F., Muyrers, J. P. P. and Stewart, A. F. (1998b). A new logic for DNA engineering using recombination in *Escherichia coli*. *Nature Genetics* **20:** 123-128.

Zhong, T. P., Kaphingst, K., Akella, U., Haldi, M., Lander, E. S. and Fishman, M. C. (1998). Zebrafish genomic library in yeast artificial chromosomes. *Genomics* **48:** 136-138.

Zilian, O., Saner, C., Hagedorn, L., Lee, H. Y., Sauberli, E., Suter, U., Sommer, L. and Aguet, M. (2001). Multiple roles of mouse Numb in tuning developmental cell fates. *Current Biology* **11:** 494-501.

Zirlinger, M., Lo, L. C., McMahon, J., McMahon, A. P. and Anderson, D. J. (2002). Transient expression of the bHLH factor neurogenin-2 marks a subpopulation of neural crest cells biased for a sensory but not a neuronal fate. *Proceedings of the National Academy of Sciences of the United States of America* **99:** 8084-8089.

Zlotogora, J., Lerer, I., Bardavid, S., Ergaz, Z. and Abeliovich, D. (1995). Homozygosity for Waardenburg Syndrome. *American Journal of Human Genetics* **56:** 1173-1178.

Zuo, J., Treadaway, J., Buckner, T. W. and Fritzsch, B. (1999). Visualization of α9 acetylcholine receptor expression in hair cells of transgenic mice containing a modified bacterial artificial chromosome. *Proceedings of the National Academy of Sciences of the United States of America* **96:** 14100-14105.

Development 128, 4113-4125 (2001)
Printed in Great Britain © The Company of Biologists Limited 2001
DEV1668

Zebrafish *colourless* encodes *sox10* and specifies non-ectomesenchymal neural crest fates

Kirsten A. Dutton[1,*], Angela Pauliny[1,*], Susana S. Lopes[1], Stone Elworthy[1], Tom J. Carney[1], Jörg Rauch[2], Robert Geisler[2], Pascal Haffter[2] and Robert N. Kelsh[1,‡]

[1]Department of Biology and Biochemistry, University of Bath, Claverton Down, Bath BA2 7AY, UK
[2]Max-Planck-Institut für Entwicklungsbiologie, Spemannstraße 35/III, D-72076 Tübingen, Germany
*These authors contributed equally to this work and are to be considered joint first authors
‡Author for correspondence (e-mail: bssrnk@bath.ac.uk)

Accepted 24 July 2001

SUMMARY

Waardenburg-Shah syndrome combines the reduced enteric nervous system characteristic of Hirschsprung's disease with reduced pigment cell number, although the cell biological basis of the disease is unclear. We have analysed a zebrafish Waardenburg-Shah syndrome model. We show that the *colourless* gene encodes a *sox10* homologue, identify *sox10* lesions in mutant alleles and rescue the mutant phenotype by ectopic *sox10* expression. Using iontophoretic labelling of neural crest cells, we demonstrate that *colourless* mutant neural crest cells form ectomesenchymal fates. By contrast, neural crest cells which in wild types form non-ectomesenchymal fates generally fail to migrate and do not overtly differentiate. These cells die by apoptosis between 35 and 45 hours post fertilisation. We provide evidence that melanophore defects in *colourless* mutants can be largely explained by disruption of *nacre/mitf* expression. We propose that all defects of affected crest derivatives are consistent with a primary role for *colourless/sox10* in specification of non-ectomesenchymal crest derivatives. This suggests a novel mechanism for the aetiology of Waardenburg-Shah syndrome in which affected neural crest derivatives fail to be generated from the neural crest.

Key words: *Danio rerio*, Waardenburg-Shah syndrome, Hirschsprung's disease, Pigment cells, Melanophore, Apoptosis

INTRODUCTION

The neural crest is a vertebrate tissue of developmental and medical importance. Developmentally, neural crest is intriguing because the cells are initially multipotent and subsequently form a great diversity of derivative cell types, including ectomesenchymal fates, such as craniofacial skeleton and fin mesenchyme, and non-ectomesenchymal fates, such as neurones, glia and pigment cells (Le Douarin, 1982; Smith et al., 1994). Medically, neural crest is important because some diseases, known as neurocristopathies and including diverse conditions such as albinism, neurofibromatosis and Hirschsprung's disease (aganglionic megacolon), affect cell types derived from this tissue (Bolande, 1974).

Understanding the genetic and embryological basis of neurocristopathies has depended on animal models. Thus, models for Hirschsprung's disease, in which individuals have few or no enteric ganglia in the colon, or the related Waardenburg-Shah syndrome, in which individuals combine Hirschsprung's disease with pigmentary anomalies of the skin, hair and irises, have been described in several species, including mouse and zebrafish (Hosoda et al., 1994; Kelsh and Eisen, 2000). Analysis of such models in mice has identified three loci that are crucial for Waardenburg-Shah syndrome (Attié et al., 1995; Edery et al., 1996; Hofstra et al., 1996; Pingault et al., 1998; Puffenberger et al., 1994; Southard-Smith et al., 1999). Thus, mutations in loci encoding the G-protein-coupled transmembrane receptor protein endothelin receptor B (Ednrb) or its natural ligand endothelin 3 (Edn3) result in aganglionosis of terminal gut in homozygous mutants (Baynash et al., 1994; Hosoda et al., 1994), as do heterozygous mutations in the *Sry*-related transcription factor gene *Sox10* (Herbarth et al., 1998; Southard-Smith et al., 1998). Homozygous *Sox10* mutant animals show a more severe phenotype with aganglionosis of the whole gut (Herbarth et al., 1998; Southard-Smith et al., 1998). Additionally, mutations in all these genes affect body pigmentation (Lane and Liu, 1984; Mayer, 1965; Mayer and Maltby, 1964), but only *Sox10* mutations result in widespread peripheral nervous system defects (Herbarth et al., 1998; Kapur, 1999; Southard-Smith et al., 1998).

The Sox gene family encodes a large family of transcription factors, with vertebrates likely to have more than 20 Sox genes each (Wegner, 1999). Their precise roles are not well understood, although many are presumed to function in cell fate specification (Pevny and Lovell-Badge, 1997). For example, the founding family member, *Sry*, is likely to be responsible for Sertoli cell specification, and thus male sex

determination, in mammals. While *Sox10* is clearly an important transcriptional regulator in neural crest cell (NCC) development, the cellular basis of the *Sox10* mutant phenotype remains unclear. It has been suggested that peripheral nervous system and pigmentation defects result from loss of NCCs (Southard-Smith et al., 1998; Kapur 1999), although the developmental status of these cells at the time of loss is unknown. Furthermore, roles in defining regional identity in the cranial neural crest and in glial cell differentiation have also been proposed (Bondurand et al., 1998; Herbarth et al., 1998; Kuhlbrodt et al., 1998a; Pusch et al., 1998; Southard-Smith et al., 1998; Britsch et al., 2001).

Mutations at the *colourless* (*cls*) locus have been identified in zebrafish mutagenesis screens (Kelsh et al., 1996; Malicki et al., 1996). We have previously characterised the crest derivative defect displayed by *cls* mutants (Kelsh et al., 2000a; Kelsh and Eisen, 2000), noting extensive loss of pigment cells and enteric nervous system, together with large reductions in sensory and sympathetic neurones and putative satellite glia and Schwann cells. By contrast, we found little effect on ectomesenchymal derivatives, craniofacial skeleton and fin mesenchyme. Based on the severity and details of the phenotype, we proposed that *cls* functions in specification, proliferation or survival of a progenitor(s) for all non-ectomesenchymal crest derivatives.

The *cls* phenotype, and the cell-autonomy of *cls* gene action in pigment cell types (Kelsh and Eisen, 2000), suggested *sox10* as a candidate gene. We provide an experimental test of this hypothesis. We report the mapping of the *cls* locus and cloning of a zebrafish *sox10* homologue. We show linkage between *cls* and *sox10*, identify *sox10* lesions in four mutant alleles and show rescue of the *cls* phenotype by *sox10* expression. In addition, we describe iontophoretic labelling experiments to examine the precise cell-biological role of *cls/sox10* gene function in neural crest development. We show in live embryos that NCC clones in *cls* and wild-type embryos differentiated into ectomesenchymal fates after migration to appropriate sites. Remaining NCC clones adopted non-ectomesenchymal fates in wild-type embryos. By contrast, in *cls* embryos differentiation to non-ectomesenchymal fates was rarely observed. Instead, most clones failed to migrate and underwent late cell death by an apoptotic mechanism. Finally, for the melanophore fate, we show disrupted expression in *cls* mutants of genes vital for melanophore specification and migration. Together, these data demonstrate a complex phenotype in *cls* embryos that can be explained by proposing that *cls/sox10* has a primary role in specification of non-ectomesenchymal fates. Defects in cell migration, survival and differentiation are therefore likely to be secondary consequences of an inability of these cells to adopt specific fates.

MATERIALS AND METHODS

Fish husbandry

Embryos were obtained through natural crosses and staged according to Kimmel et al. (Kimmel et al., 1995). We used 4 *cls* alleles (*m618*, *t3*, *tw2* and *tw11*).

Mapping of *cls*

cls^{tw11} heterozygous fish (Tübingen background), were crossed to wild-type strain WIK11 to produce a reference mapping cross. Heterozygous F_1 were incrossed and separate pools of F_2 homozygous *cls* fish and their wild-type siblings were used for simple sequence length polymorphism analysis (Knapik et al., 1996). Linkages from the pools were confirmed and refined by genotyping individual embryos, as described by Rauch et al. (Rauch et al., 1997).

Isolation, sequencing, phylogenetic analysis and radiation hybrid mapping of zebrafish *sox10*

RT-PCR was performed using total RNA of 19 hpf stage wild-type embryos using published conditions and degenerate primers (Yuan et al., 1995). Sequencing of resulting clones identified a *sox10*-like sequence. The *sox10* clone was extended by RACE PCR using gene-specific primers (Clontech, SMART RACE kit) and sequenced on an ABI DNA sequencer. All primer sequences available on request. The full *sox10* cDNA sequence is available in Genbank (Accession Number AF402677. The zebrafish *sox10* homologue was mapped on the radiation hybrid panel LN54 (Hukriede et al., 1999) by PCR with primers 5′-ACCGTGACACACTCTACCAAGATGACC-3′ and 5′-CATGATAAAATTTGCACCCTGAAAAGG-3′, which generate a 931bp 3′ UTR fragment.

For phylogenetic analysis sequences were extracted from Genbank and coding sequences automatically extracted using Genetrans (within GCG9). These were translated and then aligned using ClustalX (Thompson et al., 1997). The nucleotide alignments were reconstructed from the protein alignments using MRTRANS (www.hgmp.mrc.ac.uk/Registered/Option/mrtrans.html). Tree-Puzzle (v 4.0.2) was used to construct an unrooted tree by maximum likelihood (Strimmer and von Haeseler, 1996). It automatically assigns estimations of support to each internal branch, figures for which are presented in the figure. To model the substitution process the Tamura and Nei (Tamura and Nei, 1993) model was employed and all sites were used. Gamma distributed variation in rates of evolution was permitted with eight variable sites and one invariable. Parameters were estimated using quartet sampling and the neighbour-joining tree.

Characterisation of mutant *sox10* alleles

Total RNA from 27 hpf homozygous embryos of mutant alleles cls^{m618}, cls^{tw2} and cls^{tw11} was prepared using TRI reagent (Sigma). First strand cDNA was generated using random hexamers and SuperscriptII RT (GibcoBRL). For each allele four overlapping RT-PCR fragments were sequenced to identify mutant lesions. For *t3*, genomic DNA was extracted from individual cls^{t3} mutant embryos, a genomic fragment encoding the N-terminal of the Sox10 protein was amplified by PCR and sequenced commercially (Oswell, Southampton). The *t3* insertion sequence is available in Genbank (Accession Number, AF404490).

Ectopic expression in zebrafish embryos

The full coding region of cls^{m618} was amplified by RT-PCR using primers *Cla*I-S21 (5′-CCATCGATACCTACCGAAGTCACCTGT-GG-3′) and S27-*Xba*I (5′-GCTCTAGAGTTTGTGTCGATTGTGG-TGC-3′). The 1615bp fragment was subcloned into the *ClaI/XbaI* site of the heatshock vector pCSHSP (Halloran et al., 2000) to generate hs>*sox10(L142Q)*. The wild type *sox10* construct, hs>*sox10*, was generated by site-directed mutagenesis of hs>*sox10(L142Q)* using QuikChange Site Directed Mutagenesis Kit (Stratagene). Sequencing confirmed the successful generation of both clones. DNA purified for injection using Microcon Filter Devices (Millipore) was diluted to a concentration of 25 ng/μl, with 0.1% Phenol Red. cls^{m618} or their wild-type siblings were injected with 2 nl of either hs>*sox10* or hs>*sox10(L142Q)* at the one- to two-cell stage and incubated at 28.5°C. As appropriate, embryos were heatshocked twice (at 10-13 hpf and 22-24 hpf), by incubation at 37°C for 1 hour. *cls* embryos were scored for rescue at 48 hpf using a MZ12 dissecting microscope (Leica). Rescue was defined as the presence of at least one melanophore of wild-type morphology; these are never seen in uninjected mutant embryos.

Iontophoretic labelling and clonal analysis of single neural crest cells

Iontophoretic labelling of individual neural crest cells was performed using essentially the method of Raible et al. (Raible et al., 1992), except that micropipette tips were filled with 3% lysinated rhodamine dextran and 3% biotinylated dextran (both 10×10^3 M_r; Molecular Probes) mixture dissolved in 0.2 M KCl and the needles backfilled with 0.2 M KCl. Embryos from heterozygotes for *cls* alleles *t3*, *tw2 and tw11* were used; no phenotypic differences between these alleles were seen, so we do not distinguish them here. Individual NCCs were labelled by intracellular injection with dye. Premigratory cranial crest cells, between the posterior eye and the anterior boundary of somite 1, were labelled in 4-14 somite (11-16 hours post fertilisation, hpf) embryos, while premigratory trunk NCCs at the level of somite 7 were labelled in 16-22 somite (18-20 hpf) embryos. Premigratory trunk NCCs at the level of somite 14 were labelled in 22-25 somite (20-22 hpf) embryos. Embryos were recovered and raised for several hours at 28.5°C in embryo medium with 1% v/v penicillin/streptomycin solution (Gibco). Embryos were remounted and examined to identify those with only a single labelled NCC; only these embryos were analysed.

Labelled cells were monitored using Nomarski and fluorescence optics on a BX50WI microscope (Olympus), and documented on a Eclipse E800 microscope (Nikon) using low light level, video-enhanced fluorescence microscopy. Labelled cells were monitored twice daily for up to 3 days until progeny could be identified using published morphological criteria (Raible and Eisen, 1994; Raible et al., 1992; Schilling and Kimmel, 1994). Thus, melanophores contained melanin granules; xanthophores were visibly yellow and autofluoresced at a wavelength near that of fluorescein; iridophores contained iridescent granules; dorsal root ganglial neurones were identified by position ventrolateral to the neural tube combined with a visible neurite; sympathetic neurones were positioned ventral and lateral to the notochord and showed neurites; Schwann cells were elongated and positioned along axonal processes, e.g. trigeminal nerve; satellite glia were associated with the ganglionic sheath or appeared to be wrapped around neuronal stomata; craniofacial cartilage formed characteristic stacks of vacuolated cells in the jaw or gill arches; fin mesenchyme occupied a position within the dorsal fin fold and showed characteristic asymmetric organisation of projections (Smith et al., 1994). Cells which could not be assigned to any of the described groups, owing to their position in regions of limited optical resolution or lack of distinctive morphologies, were classified as 'unidentified'. In cranial regions, these cells undoubtedly included cells of connective tissue fates (Schilling and Kimmel, 1994).

TUNEL

TUNEL (terminal deoxynucleotidyl transferase (TdT)-mediated deoxyuridinetriphosphate (dUTP) nick end-labelling) of double-strand DNA fragmentation was used to confirm apoptosis in cells with apoptotic morphology. cls^{t3} and their wild-type siblings were fixed overnight at 4°C in 4% paraformaldehyde and TUNEL performed using fluorescein dUTP and developed using 4-Nitroblue tetrazolium chloride and 5-Bromo-4-chloro-3-indolyl-phosphate (Boehringer Mannheim; Reyes, 1999).

Morpholino injections

AB wild-type embryos at 25, 30 and 35 hpf were injected with either a high (16.5 ng) or low (9 ng) dose of a morpholino designed to knock-down *sox10*, as described previously (Dutton et al., 2001). Effects on *nac/mitf* expression in melanoblasts at 25 hpf were evaluated by counting *nac/mitf*-expressing cells in one half of the trunk in each of 20 embryos at each dose.

Whole-mount in situ hybridisation and antibody staining

RNA in situ hybridisation was performed as described by Kelsh and Eisen (Kelsh and Eisen, 2000), on cls^{m618}, cls^{tw11} and cls^{t3}, their wild-type siblings and morphants. Probes for the following genes were used: *nac/mitf* (Lister et al., 1999), *spa/kit* (Parichy et al., 1999); *dopachrome tautomerase* (*dct*) (Kelsh et al., 2000b); *dlx2* (Akimenko et al., 1994); *forkhead 6* (*fkd6*) (Odenthal and Nuesslein-Volhard, 1998).

Antibody staining with anti-Hu, mAb 16A11 (Marusich et al., 1994), was performed using peroxidase-antiperoxidase (VECTASTAIN® Elite ABC kit) and DAB substrate.

RESULTS

cls and a zebrafish *sox10* homologue map to the same region on Linkage Group 3

The strong phenotypic similarity between $sox10^{Dom}$ mice and *cls* mutants suggested a zebrafish *sox10* homologue as a candidate gene for *cls*. We used RT-PCR to clone a partial *sox10*-like HMG box and RACE RT-PCR to clone 5′ and 3′ regions. Sequencing these clones revealed an open reading frame encoding a *sox10* homologue, which we refer to as *sox10* (Fig. 1A,B).

Genetic mapping of 274 meioses placed *cls* on LG 3 within a 3.9 cM interval between markers z872 and z13387 (Fig. 1C). Two oligonucleotide primers amplified a 931 bp fragment from zebrafish, but not from control mouse genomic DNA. Amplification from the DNAs in the LN54 radiation hybrid mapping panel (Hukriede et al., 1999) with these primers mapped *sox10* to LG 3, 0cR from the marker z8492 (LOD score=17.6; Fig. 1C). The striking linkage of *cls* and *sox10*, together with in situ hybridisation experiments showing *sox10* expression in neural crest (see below), strongly supported our hypothesis that *cls* might encode *sox10*.

sox10 is disrupted in *cls* mutants

We used RT-PCR to amplify the *sox10*-coding region from 27 hpf homozygous mutants of 3 *cls* alleles. Sequencing these PCR products identified sequence differences from wild-type consistent with them causing the mutant phenotype (Fig. 1D,E). Two alleles show an A→T transversion, resulting in a premature Stop codon; the third is a non-conservative substitution (L142Q) of a fully-conserved residue in the HMG domain. A fourth allele, *t3*, showed highly reduced RNA expression using a 3′ probe for whole-mount RNA in situ hybridisation. PCR from genomic DNA identified a 1.5 kb insertion in all *t3* mutants that was not present in wild types. Sequencing genomic DNA from *t3* homozygotes identified a 1397 bp insertion with sequence homology to a transposon first identified in a mutant *no tail* allele (data not shown; Schulte-Merker et al., 1994). The insertion interrupts the *sox10*-coding sequence upstream of the HMG domain and adds eight novel amino acids before prematurely truncating the protein (Fig. 1D).

To test further whether *cls* encodes *sox10*, we attempted to rescue the *cls* phenotype with ectopic *sox10* expression under heat shock control. We took advantage of the consistent absence of large, stellate melanophores in every *cls* embryo. Ectopic expression of wild-type *sox10* rescued 1-40 melanophores to a wild-type morphology in 48% of cls^{m618} mutants, while ectopic mutant *sox10(L142Q)* failed to do so (Table 1; Fig. 2). Furthermore, while *cls* melanophores always remain dorsal to the neural tube, rescued melanophores frequently migrated, even to very distal positions (Fig. 2).

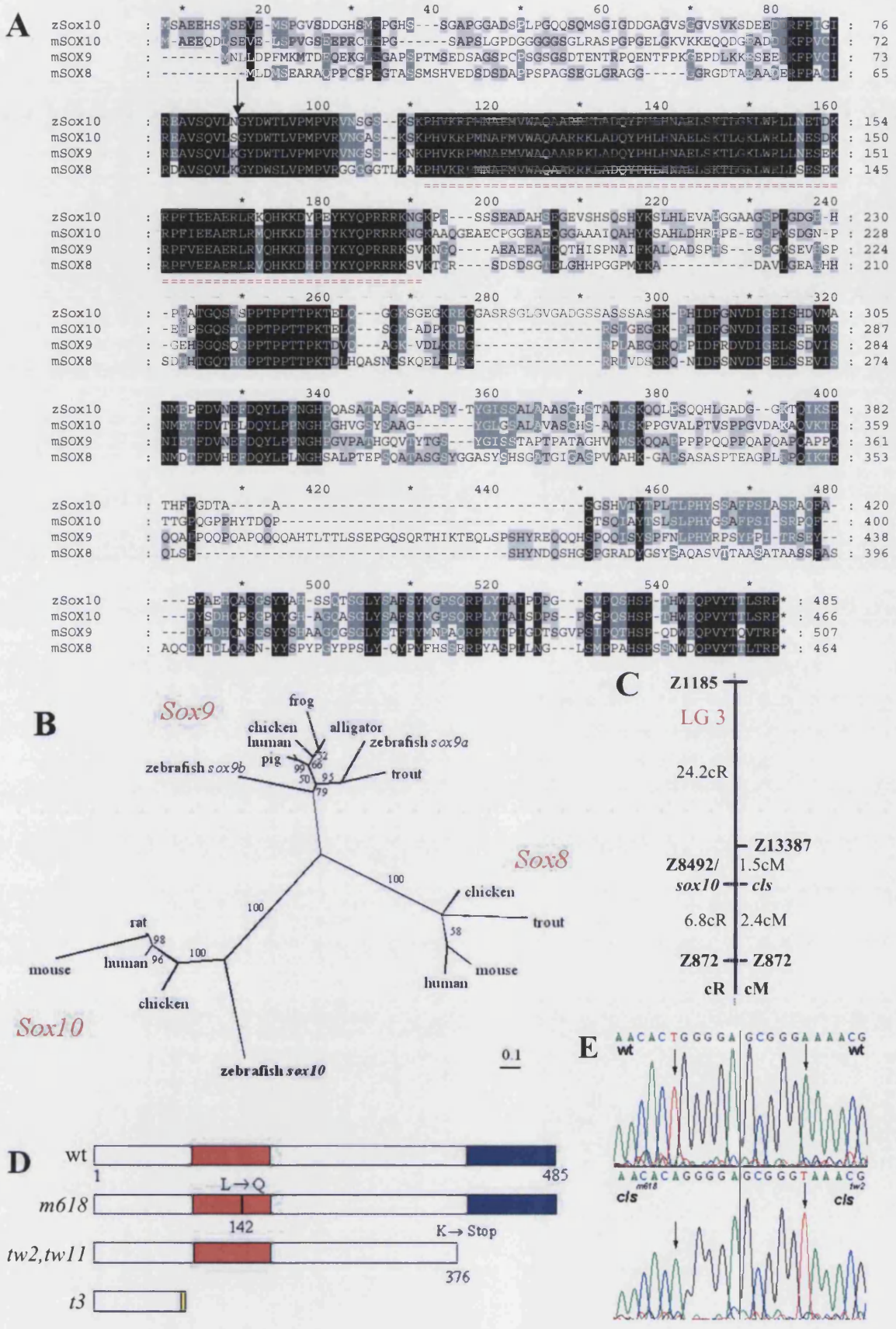
A
zSox10
mSOX10
mSOX9
mSOX8
B
Sox9
frog
chicken
alligator
human
zebrafish sox9a
pig
zebrafish sox9b
trout
Sox8
chicken
trout
rat
mouse
human
human
mouse
chicken
Sox10
zebrafish sox10
0.1
C
Z1185
LG 3
24.2cR
Z13387
Z8492/
1.5cM
sox10
cls
6.8cR
2.4cM
Z872
Z872
cR
cM
D
wt
1
485
L→Q
m618
142
K→ Stop
tw2,tw11
376
t3
E
wt
wt
cls
cls

Fig. 1. A zebrafish *sox10* homologue maps to the region of the *cls* locus. (A) Sequence comparison of predicted zebrafish Sox10 homologue (44, 45 and 60% identity to mouse Sox8, Sox9 and Sox10, respectively). Blocks of identity corresponding to all proposed functional domains can be seen, including the HMG domain (red underline; 95% amino acid identity), N-terminal synergy domain (1-105; 48% identity), dimerisation domain (66-105; 78% identity), C-terminal transcriptional activation domain (395-485; 76% identity) and a domain C-terminal to the HMG domain corresponding to a putative protein-protein interaction domain (234-325; 64% identity; Bondurand et al., 2000; Kuhlbrodt et al., 1998a; Kuhlbrodt et al., 1998b; Liu et al., 1999; Peirano and Wegner, 2000). (B) Maximum likelihood phylogenetic tree of subgroup E Sox genes. Zebrafish *sox10* clusters within the *Sox10* clade of vertebrate Sox genes. The Accession Numbers for the sequences are as follows: chicken *Sox8* (AF228664); trout *SoxP1* (D83256); mouse *Sox8* (AF191325); human *SOX8* (AF226675); frog *Sox9a* (AB035887); alligator *Sox9* (AF106572); trout *Sox9* (AB006448); zebrafish *sox9a* (AF277096); zebrafish *sox9b* (AF277097); chicken *Sox9* (AB012236); pig *Sox9* (AF029696); human *SOX9* (Z46629); zebrafish *sox10* (AF402677); chicken *Sox10* (AF152356); mouse *Sox10* (AF047389); rat *Sox10* (AJ001029); human *SOX10* (NM_006941). (C) Mapping using the LN54 panel placed *sox10* on LG 3 in the region of the *cls* locus identified using microsatellite markers (we found four recombinants between *cls* and z13387 in 274 meioses). Note that z8492 was not polymorphic and could not be analysed in the mapping cross. (D) Schematic to illustrate changes in Sox10 mutant proteins. In cls^{m618} a T425A substitution results in a non-conservative change (Leu142Gln) within the HMG domain (red). In cls^{tw2} and cls^{tw11}, a A1126T substitution introduced a Stop codon truncating the protein just N-terminal to the transactivation domain (blue). Insertion of a 1.4 kb transposon at the site indicated by the arrow in A disrupts *sox10* in cls^{t3} and introduces a C-terminal extension of eight novel amino acids before premature truncation N-terminal to the HMG domain (yellow). (E) Chromatogram traces to show nucleotide changes affecting *sox10*-coding regions in cls^{m618} and cls^{tw2}.

Table 1. Rescue of *cls* phenotype using ectopic *sox10* expression

Construct	Heat shock	Injected cls^- that survived	Rescued cls^- (% rescued)	Mean number of melanophores per rescued embryo
hs>sox10	+	92	44 (48)	15
hs>sox10	–	48	17 (35)*	4.3
hs>sox10(L142Q)	+	122	0 (0)	0

*A similar degree of leakiness with this promoter has been reported by Lister et al. (Lister et al., 1999); note that the degree of rescue is much less in the absence of heat shock.

sox10 expression is disrupted in *cls* mutants

We used in situ hybridisation to examine *sox10* expression in wild-type and *cls* embryos. In wild types, expression was first detected at the one-somite stage in cells in the lateral neural plate (data not shown). Throughout somitogenesis stages, strong *sox10* expression was seen in premigratory NCCs and extended progressively more caudally in older stages (Fig. 3A-C,F). Double RNA in situ hybridisation studies show that there is extensive, but incomplete, overlap of *sox10* and *fkd6*, a marker expressed widely in premigratory NCCs (Fig. 3O,P) (Odenthal and Nuesslein-Volhard, 1998). *sox10* expression was maintained in some migrating NCCs on the medial migration pathway (Fig. 3C,F). By 30-40 hpf *sox10* expression on the medial pathway is organised in segmentally arranged clusters adjacent to the notochord, presumably developing Schwann cells associated with the segmental nerves (Fig. 3Q); *sox10* expression is lost from this site by 48 hpf. Although NCCs are found extensively on the lateral pathway from 24 hpf (Raible et al., 1992), counts of *sox10*-expressing cells show that expression was essentially absent from cells on this pathway (Fig. 3M,N). This demonstrates the rapid downregulation of *sox10* from pigment cell precursors, as NCCs on this pathway form only pigment cells (Raible and Eisen, 1994). Consistent with this, xanthophores and most pigmented melanophores show no detectable *sox10* expression (Fig. 3L), although some weakly expressing melanophores were noted at earlier stages (Fig. 3K). Expression was not seen in fin mesenchyme nor in *dlx2*-expressing craniofacial cartilage precursors (Fig. 3D,E), although differentiating jaw cartilage shows weak expression by 60 hpf (data not shown). Cells expressing *sox10* accumulated in clusters corresponding to the forming cranial ganglia and extending along the posterior lateral line nerve by 24 hpf (Fig. 3F,H), in a pattern reminiscent of *fkd6* expression (Kelsh et al., 2000a), suggesting that *sox10* is expressed in satellite glial and Schwann cells. Consistent with this interpretation, double labelling with anti-Hu antibody confirmed the non-overlapping expression of *sox10* and this neuronal marker (Fig. 3J). *sox10* is maintained in developing Schwann cells on the posterior lateral line nerve up to 60 hpf (data not shown). *sox10* expression was prominent in enteric nervous system precursors at 60 hpf (Fig. 3S).

At early stages, premigratory crest showed equivalent patterns of *sox10*-positive cells in wild-type and cls^{tw11} and cls^{m618} mutant embryos. Counts at 24, 30 and 35 hpf revealed that although in wild type *sox10*-expressing cells were rapidly lost from the premigratory position, they remained here in cls^{m618} mutants; by contrast, *sox10* expression in migrating trunk NCC was broadly comparable between wild type and cls^{m618} mutants (Fig. 3M,N). Additionally, *cls* mutants were

Fig. 2. *cls* phenotype is rescued by ectopic *sox10* expression. Wild-type embryos show many large, strongly pigmented melanophores at 48 hpf (A; close-up of anal region in D), while hs>*sox10(L142Q)*-injected cls^{m618} mutants (B) show only tiny melanised spots in position of premigratory NCCs (arrowheads). (C,E,F) By contrast, cls^{m618} embryos injected with hs>*sox10* and heat-shocked, show mosaic rescue of melanophores. This embryo showed one rescued melanophore in the dorsal stripe (* in C), two in the ventral stripe (arrows in C; close-up in E) and one on the yolk sac (F). Scale bar: 125 μm in A-C; 70 μm in D-F.

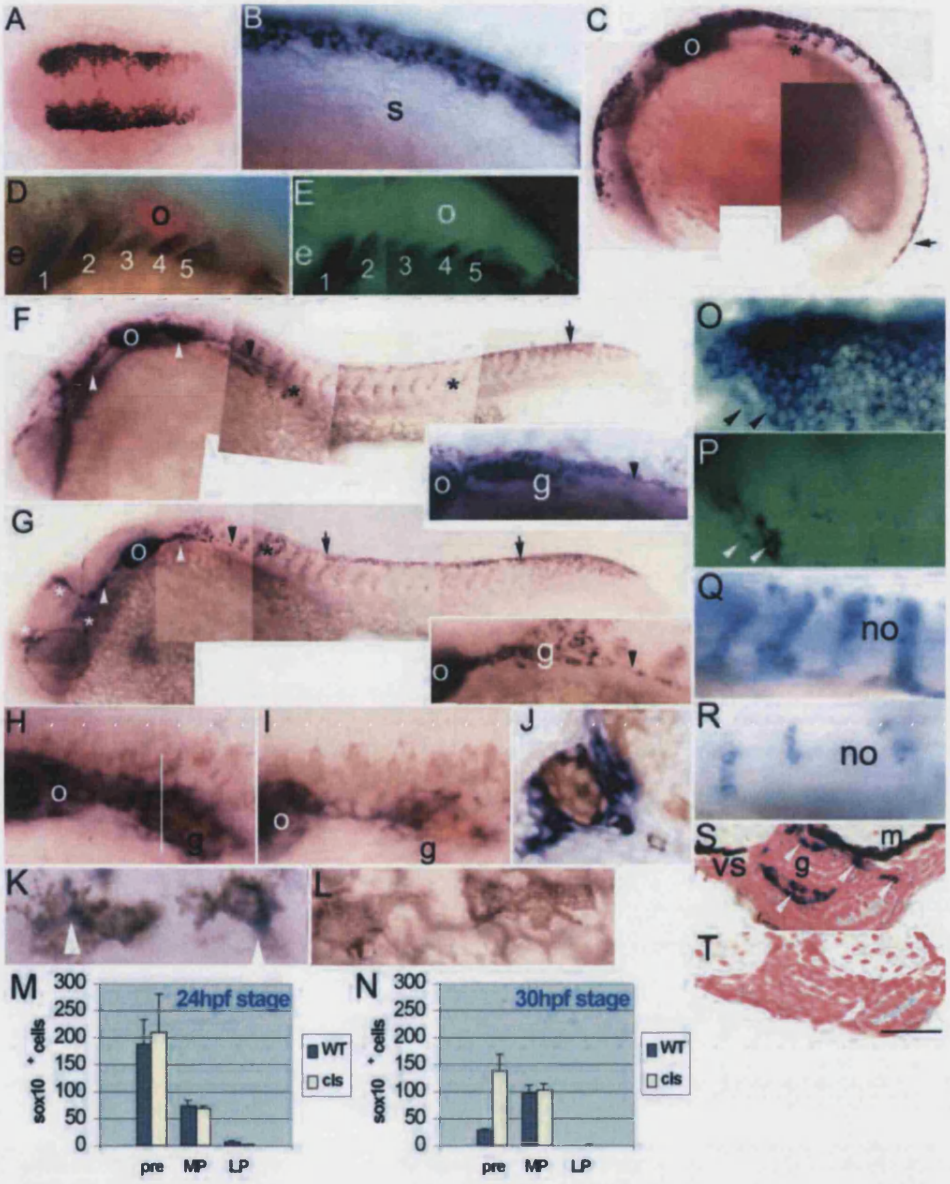

Fig. 3. Embryonic *sox10* expression in wild-type and *cls* embryos. (A,B) *sox10* is expressed in most cranial (A; five-somite stage) and trunk (B; 14-somite stage) premigratory NCCs; double mRNA in situ hybridisation with *fkd6* (O, purple) and *sox10* (P, green) in a six-somite stage embryo reveals extensive overlap, although some individual NCCs lack *sox10* (arrowheads). (C) 18-somite stage embryo shows strong expression in premigratory (black arrow) and migrating (asterisk) NCCs and otic vesicle (o). (D,E) Double mRNA in situ hybridisation with *dlx2* (D, purple) and *sox10* (E, green) in 29 hpf stage embryos shows absence of *sox10* expression in developing branchial arches (1-5). (F) By 24 hpf in wild types, strong expression is associated with cranial ganglia (white arrowheads) and posterior lateral line nerve (black arrowhead; enlarged in inset), otic vesicle (o), migrating NCCs throughout trunk (asterisks) and in premigratory crest (arrow). (G) At 24 hpf in *cls* mutants, expression in the head is clustered (white asterisks) and cranial ganglia have reduced labelling (white arrowheads). Cells expressing *sox10* extend along the posterior lateral line nerve (arrowhead and inset). Rostral trunk shows some migrating cells (black asterisk), but *sox10*-positive cells are clustered dorsal to the neural tube (arrows) in trunk and tail. (H,I) Combined *sox10* in situ hybridisation (purple) and anti-Hu antibody labelling (orange) shows strong *sox10* expression associated with wild-type (H) posterior lateral line ganglion (g), much reduced in *cls* mutant (I). (J) In transverse section of wild-type ganglion (approximate position indicated by white line in H), *sox10* expression is strong peripherally (non-neuronal cells), but absent centrally (neurones). (K,L) 36 hpf wild-type embryos show weak expression in some melanophores, but not all. Thus, weak expression (arrowhead) is seen in some cells of the dorsal stripe (K), but not in cells on the yolk sac (L). (M,N) Number of *sox10*-expressing NCCs in different locations (premigratory, pre; migrating on medial pathway, MP; migrating on lateral pathway, LP) of trunk and anterior tail (somites 1-20) at 24 (M) and 30 hpf (N) in WT and *cls* mutants. (Q,R) Segmentally arranged lines of *sox10*-positive cells lying adjacent to the notochord (no), presumably glia, are abundant in wild type (Q) and only weakly affected in *cls* mutants (R) at 40 hpf. (S,T) Transverse section of trunk of 60 hpf wild-type embryo (S) shows enteric nervous system expression (arrowheads) lateral to the gut (g), absent in *cls* mutant (T). e, eye; m, muscle; s, somite; vs, ventral stripe melanophores. All images are lateral views, rostral towards the left, dorsal upwards, except dorsal views of A,K,O,P. Scale bar: 200 μm in A; 50 μm in B,H-I,K-L; 120 μm in C; 75 μm in D,E; 150 μm in F,G; 35 μm in J; 65 μm in O,P; 55 μm in Q,R; 45 μm in S,T.

distinguishable from 24 hpf by the clustered, not scattered, distribution of *sox10*-positive cells in the head (Fig. 3F,G) and a variable reduction in the number of *sox10*-positive cells in cranial ganglia and on cranial nerves (Fig. 3H,I). By 35 hpf, *cls* mutants were readily distinguished from wild types by their reduced number of *sox10*-positive cells, concentrated in a premigratory position dorsal to the neural tube or clustered near the posterior lateral line ganglia; putative Schwann cells were missing from the posterior lateral line nerve. *cls* mutants showed reduced expression in the putative Schwann cells found as segmental clusters of *sox10*-positive cells (Fig. 3Q,R). Enteric nervous system precursors were absent at 60 hpf (Fig. 3T) in *cls* mutants.

In contrast to the other mutant alleles examined, cls^{t3} mutants consistently show highly reduced *sox10* transcripts when examined using the 3′ *sox10* probe at all stages. When examined using a probe lying 5′ to the insertion site, *sox10* expression levels were comparable with those in other mutant

Table 2. Fates of single neural crest cells injected with lineage tracer

	Trunk (somite 14)				Cranial*			
	Wild type		*colourless*		Wild type		*colourless*	
Fate‡	Number	Percentage	Number	Percentage	Number	Percentage	Number	Percentage
Ectomesenchymal								
Cartilage	–	–	–	–	6	7	2	6
Fin mesenchyme	5	7	2	8	–	–	–	–
Non-ectomesenchymal								
Pigment								
Melanophore	26	34	–	–	12	14	–	–
Xanthophore	9	12	4§	16	12	14	7§	21
Iridophore	3	4	–	–	2	2	–	–
Mixed pigment	10	13	–	–	–	–	–	–
Neural								
Cranial ganglia	–	–	–	–	9	11	–	–
Dorsal root ganglia	6	8	–	–	–	–	–	–
Sympathetic neuron	3	4	–	–	–	–	–	–
Schwann cell	1	1	–	–	–	–	–	–
Mixed neural¶	5	7	–	–	–	–	–	–
Mixed pigment/neural								
Melanophore + Dorsal root ganglia	1	1	–	–	–	–	–	–
Other								
Died	1	1	19§	76	11	13	15§	45
Unidentified	5	7	–	–	33	39	9	27
Total	75	100	25	100	85	100	33	100

*All progeny within a single clone adopted the same fate in every case, as shown previously (Schilling and Kimmel, 1994).

‡Only single injected cells that survived and were identified as NCCs in the afternoon on the day of labelling are included. The numbers represent the number of clones whose cells adopted the indicated fates, using the criteria outlined in the Materials and Methods.

§All xanthophores identified in *cls* embryos subsequently died; hence in total, 23 (92%) and 22 (66%) cells died in the somite 14 and cranial samples.

¶Mixed neural fates include clones with both neuronal and glial derivatives.

alleles, suggesting that insertion of the transposon does not disrupt transcription of 5′ sequences (data not shown).

Outside neural crest, *sox10* expression was particularly strong in otic placode and otic vesicle, and from 11-somite stage onwards (Fig. 3C,F,H), was detected in pectoral fin and in some spinal cord cells from 36 hpf. Expression in the ear was significantly weaker in *cls* mutants by 40 hpf (data not shown).

cls non-ectomesenchymal neural crest cells die prior to differentiation

Previous characterisation of *cls* embryos catalogued a strong reduction in non-ectomesenchymal neural crest derivatives (Kelsh and Eisen, 2000). To analyse the cell biological basis for loss of these neural crest derivatives, we used iontophoretic labelling of single NCCs. We labelled premigratory NCCs in *cls* mutants and their wild-type siblings in two regions that generate ectomesenchymal fates, and scored them for the fate(s) adopted by their progeny (Table 2). In wild-type embryos, almost all (148/160; 93%) labelled cells survived throughout the experiment, and all major derivatives, both ectomesenchymal and non-ectomesenchymal, were identified among the clones. Consistent with our previous analyses, labelled cells generated a similar proportion of ectomesenchymal fates in *cls* mutants (4/58; 7%) and wild-type siblings (11/160; 7%). Furthermore, even in *cls* mutants, cells in these clones migrated and differentiated normally. In wild-type embryos, most cells where fates were identifiable (111/122; 91%) differentiated into recognisable non-ectomesenchymal derivatives. By contrast, most identifiable clones in *cls* embryos (45/49; 92%) died late on the second day (~35-45 hpf). Most showed no sign of morphological differentiation or pigmentation (34/49; 69%). The only exception, clones that developed some xanthophore pigmentation (11/49; 22%), always had abnormal morphology, being rather rounded and blebbed, and died soon after differentiation (Fig. 4N). A series of single cell injections in NCCs at the axial level of somite 7 gave similar results, with 92% of *cls* cells dying by around 48 hpf, in contrast to only 2% in wild-type siblings (data not shown); note that at this axial position no ectomesenchymal fates have been reported (Raible and Eisen, 1994). Our results are consistent with the severe reduction in differentiated non-ectomesenchymal fates in *cls* embryos and suggest that extensive NCC death is associated with the *cls* phenotype.

Non-ectomesenchymal crest derivatives die by apoptosis during a discrete time-window

The morphological appearance of dying cells in our clonal analyses suggested an apoptotic mechanism of death. We combined TUNEL with biotin-detection of the labelled clone in each of five *cls* embryos and showed that the dying cells had fragmented DNA (Fig. 4A-C). We conclude that many non-ectomesenchymal clones in *cls* embryos die by an apoptotic mechanism.

Analysis of cell survival in our cranial NCC data set shows that death of labelled NCCs occurs within a relatively discrete time-window (Fig. 4L). In both *cls* and wild-type embryos, around 10% of labelled clones had died by the morning after injection. In wild-type embryos, the number of surviving

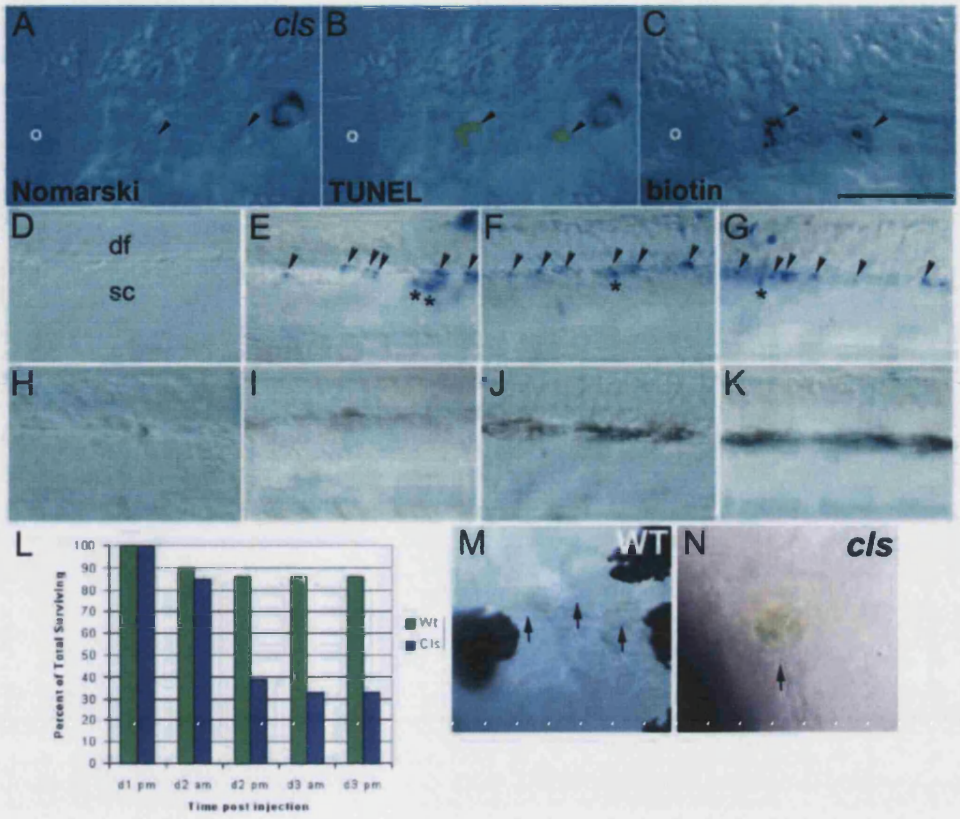

Fig. 4. NCC death in *cls* embryos. (A-C) NCC clones die by an apoptotic mechanism in *cls* embryos. Lateral views of 40 hpf *cls* embryo in which two daughters of a single labelled NCC contributed to the posterior lateral line ganglion, lying just posterior to the otic vesicle (o). In the live embryo, both cells show blebbed morphology typical of apoptotic cells when viewed with Nomarski optics (A). After fixation and processing for TUNEL (B) and detection of the biotinylated-dextran lineage-tracer (C), visible TUNEL signal of these clonal cells indicates DNA fragmentation characteristic of apoptotic cells. (D-K) Whole-mount TUNEL shows NCC apoptosis in *cls* embryos. Lateral views of dorsal spinal cord (sc) in tail of 30 (D,H), 35 (E,I), 40 (F,J) and 45 (G,K) hpf embryos show apoptotic NCCs immediately dorsal to the spinal cord from 35 hpf in *cls* (arrowheads, D-G), but not wild-type (H-K), embryos. Scattered TUNEL-positive cells are prominent in dorsal spinal cord (*) of *cls* embryos (E-G); these are occasionally seen in wild-type siblings at these stages (data not shown). df, dorsal fin. (L) Time-course of labelled single cranial NCC clone survival in *cls* mutants and their wild-type siblings. Percentage of surviving clones is given at each of the five standard time points when embryos were examined. The time points correspond to approximately 16, 32, 40, 56 and 64 hpf, respectively. The first time point includes only single labelled NCCs based on examination within a few hours after labelling. See text for further details. (M,N) Wild-type xanthophores (arrows) at 48 hpf have a very flattened, thin morphology and are only weakly coloured (M), while a dying *cls* xanthophore (arrow) shows characteristic apoptotic morphology and concentrated yellow coloration, which was usually visible by 35 hpf (N). Scale bar: 100 μm in A-C; 50 μm in D-K; 75 μm in M,N.

clones was essentially unchanged at later times. However, in *cls* mutants, the number of surviving clones dropped precipitously to only 40% within the period of around 5-10 hours between the two observational time-points on the second day after labelling (equivalent to ~40 hpf), but then remained constant. We interpret the early (overnight after injection) loss of wild-type and *cls* clones as representing death due to damage during labelling. The subsequent late loss of clones in *cls* embryos corresponds to the time of appearance of apoptotic cells and we attribute this to the *cls* phenotype.

To examine the extent to which apoptosis contributes to the *cls* phenotype, we used whole-mount TUNEL to examine apoptosis of NCCs (Fig. 4D-K). We saw a notable concentration of apoptotic cells dorsal or dorsolateral to the neural tube in *cls* embryos, but not in wild-type control embryos. A timecourse of TUNEL between 20 and 60 hpf indicated that cell death in NCCs becomes apparent by 35 hpf and continues to approximately 45 hpf.

cls neural crest cells fail to migrate before undergoing apoptosis

Our in vivo clonal studies revealed that, while wild-type NCCs migrated extensively on both medial and lateral pathways, most *cls* NCCs failed to leave the premigratory crest area. Thus, excluding ectomesenchymal derivatives (which always migrated normally), only 2/31 (6%) of cranial NCCs appeared to migrate away from their initial positions. At the level of somite 14, all wild-type labelled cells left the premigratory area, and more than 75% migrated at least 50 μm from their original position. Only fin mesenchyme clones migrated normally in *cls* mutants. Of the remaining clones, only 4/23 (17%) migrated away from the premigratory crest; another cell extended towards the horizontal myoseptum, but maintained contact with the premigratory area. Of these five cells, two migrated on the lateral pathway, but underwent apoptosis after moving about half way to the horizontal myoseptum. The other three cells migrated on the medial path. In one case, the cell did not divide, migrated to a position appropriate for a dorsal root ganglion, then died before overt differentiation. The other two cells divided once; in each clone, one sister cell remained dorsal to the neural tube, and may have been an extramedullary cell (Kelsh and Eisen, 2000), while the other migrated to a dorsal root ganglial position, but failed to undergo axonogenesis, consistent with the impaired touch response of 5 dpf larvae. We obtained similar results for labelled NCCs from the region of somite 7 (data not shown). This direct observation of failed NCC migration in *cls* embryos is consistent with our observation of *dct*-expressing melanoblasts and *sox10*-expressing NCCs concentrated dorsal to the neural tube in mutant embryos (Kelsh et al., 2000b) (this work).

cls mutants and *sox10* morphants fail to express genes critical for melanophore specification and migration

cls mutants combine an extensive failure of NCC migration with late apoptotic death of non-ectomesenchymal derivatives. Three recent studies suggested a possible molecular genetic mechanism for these aspects of the phenotype. *sparse* (*spa*), a *kit* homologue, is crucial for survival and migration of melanophores and melanoblasts (Parichy et al., 1999; Kelsh et al., 2000b) and *nacre* (*nac*), a *microphthalmia transcription factor* (*mitf*) homologue, is crucial for melanophore specification and required for *spa* expression (Lister et al., 1999). We used in situ hybridisation at 20-35 hpf to ask whether *spa* or *nac* expression was disrupted in *cls* embryos (Fig. 5). We found that both *spa* and *nac* expression were absent from NCCs, even at a time when many *dct*-positive cells are present, suggesting that the *cls* melanophore phenotype might result from loss of *nac* expression. By contrast, *spa* expression in intermediate cell mass and *nac* expression in the pigmented retinal epithelium are unaffected in *cls* mutants.

We have recently shown that injection of *sox10* morpholino oligonucleotides phenocopies the *cls* mutant phenotype (Dutton et al., 2001). The morphant phenotype varies depending upon the amount of morpholino injected, with high doses phenocopying all aspects of the phenotype of the strong *cls* alleles. Injection of lower doses results in a phenocopy of the weak *cls* allele phenotype, with embryos showing some melanophores, concentrated in dorsal positions (Dutton et al., 2001; Malicki et al., 1996). The number of *nac/mitf*-expressing cells in embryos injected with a low dose of *sox10* morpholino (median number=78; n=20) is significantly higher than in embryos injected with a high dose (median number=20; n=20; Mann-Whitney U-test, P<0.05; Fig. 5C,D), consistent with the differences in melanophore phenotype.

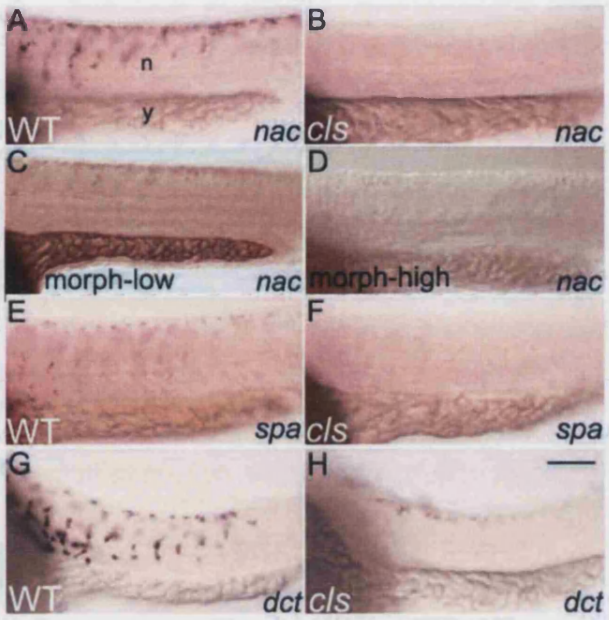

Fig. 5. *cls* mutants lack *nac* and *spa* expression. Lateral views of caudal trunk of 25 hpf wild-type and *cls* embryos after in situ hybridisation with *nac* (A,B), *spa* (E,F) and *dct* (G,H) probes. (C,D) *nac/mitf* expression is decreased weakly (C) or strongly (D) after injection with either a low or high dose, respectively, of *sox10* morpholino. n, neural tube; y, yolk sac. Scale bar: 75 μm.

DISCUSSION

Studies in mice have led to identification of *Sox10* as a key gene in human Waardenburg-Shah syndrome. We have shown that the zebrafish *cls* locus is a *sox10* homologue predicted to encode a protein with all the major domains identified in mammals (Fig. 1). We have identified the molecular lesion likely to cause the mutant phenotype in 4 *cls* alleles. In two cases, *tw2* and *tw11*, both originating from the same mutagenised male (Haffter et al., 1996; Kelsh et al., 1996), the lesions are identical and are presumably independent isolations of the same allele. The zebrafish Lys376Stop lesions resemble the human *059* allele (delGA) in lacking the transactivation domain, although they lack the C-terminal extension present in the human allele. In transient transfection assays human 059 mutant protein has been shown to have no transcriptional activation (Bondurand et al., 2000; Kuhlbrodt et al., 1998b; Liu et al., 1999). The *m618* allele substitutes Leu142 in the second alpha helix of the HMG domain and there is no similar mammalian mutation. The *t3* allele results in a severely truncated protein that lacks both the DNA-binding and transcriptional activation domains. It is thus reminiscent of the human Y83X allele which has been proposed to be a functional null (Kuhlbrodt et al., 1998b; Potterf et al., 2000). All four mutant alleles described here show similar, strong phenotypes (Kelsh et al., 1996; Malicki et al., 1996) (data not shown). These considerations, combined with the similarity of these phenotypes with the maximal morphant phenocopy generated with a *sox10* morpholino, lead us to suggest that these alleles are all likely null alleles. Analysis of the activities of these mutant proteins will be interesting to test this proposal.

Zebrafish *sox10* expression is consistent with cell types affected in *cls* mutants and strongly reminiscent of that in mammals. We have taken advantage of the higher resolution of such studies in zebrafish, to define more precisely the extent of *sox10* expression throughout the neural crest at different stages. In wild type, expression is extensive in premigratory neural crest, but comparison with *fkd6* expression shows that a minority of premigratory NCCs lack *sox10* expression. Expression persists in some migrating cells on the medial migration pathway, but is rapidly downregulated in differentiating pigment cells. Glia of the developing peripheral nervous system show strong expression, as has also been described in mice (Kuhlbrodt et al., 1998a; Britsch et al., 2001). Crest cells in forming branchial arches and fin mesenchyme do not show expression, in agreement with mouse, but not human, expression studies (Bondurand et al., 1998; Kuhlbrodt et al., 1998a; Southard-Smith et al., 1998). Late expression in cranial cartilages is intriguing, but will require further study to evaluate its role. In *cls* mutants, *sox10*-expression in premigratory NCCs is initially unaffected but, unlike in wild-type siblings, *sox10*-expressing cells soon accumulate in this position. In the trunk *sox10*-expressing cells migrating on the medial pathway are seen and presumably contribute to the neurones and glia of the dorsal root ganglia, which are detectable in mutants (Kelsh and Eisen, 2000) (this

study). NCCs tend to become clustered in premigratory positions in *cls* mutants, consistent with the observed defect in NCC migration revealed by our single-cell labelling studies.

Outside the neural crest, *sox10* expression is also largely conserved. Thus, expression in the developing inner ear epithelium is seen in zebrafish as well as in mammals (Bondurand et al., 1998; Southard-Smith et al., 1998). In zebrafish, this expression is remarkably strong and persistent in wild type, but is downregulated in *cls* mutants by 40 hpf. As pronounced otic defects are morphologically detectable in *cls* mutants by 48 hpf (R. N. K., unpublished), we suggest that *sox10* is crucial for development of otic epithelium. Limited expression in embryonic central nervous system is seen in zebrafish and mice (Kuhlbrodt et al., 1998a), although detailed studies will be required to establish the cell types involved in each case.

Our single cell labelling studies at three rostrocaudal positions make clear that defects in *cls* mutants are not limited to one axial position, but instead affect non-ectomesenchymal rather than ectomesenchymal crest derivatives. Most NCCs in *cls* mutants show restricted migration and poor or no differentiation before dying by an apoptotic mechanism within a discrete time-window. We interpret the dying cells as being those that would in wild-type siblings form non-ectomesenchymal fates. Thus, in *cls* embryos, NCCs that would normally yield these missing neural crest derivatives are present in premigratory neural crest in normal numbers, but then die before differentiating, usually without migrating. This confirms and extends reports that putative NCCs apoptose during migration in mouse *sox10* mutants (Kapur, 1999; Southard-Smith et al., 1998).

The *sox10* expression pattern in *cls* mutants may appear contradictory to our single cell label results, as the expression studies show normal numbers of *sox10*-positive NCCs migrating on the medial pathway, while the single cell labelling studies show a strong migration defect in the neural crest. However, our data suggest that *sox10* is expressed in almost all premigratory cells, but is rapidly downregulated in ectomesenchymal and pigment cell precursors as they start to migrate. Thus, *sox10* expression in migrating cells reflects just the neural precursors. Our studies show that these cells are much less defective in migration in *cls* mutants. Consistent with this, the labelled cells in *cls* mutants that did migrate normally all took the medial migration pathway and, if they survived, adopted a position consistent with a dorsal root ganglial fate. By contrast, most labelled NCC clones generated pigment cells, consistent with former studies in zebrafish. These pigment cells are severely defective in migration, as shown by molecular markers for xanthophore (*gdh*; Parichy et al., 2000) and melanophore (*dct*; Fig. 5) cell fates (M. Hawkins and R. N. K., unpublished) (Kelsh and Eisen, 2000). Further work will be required to investigate the specification status of the migrating neural precursors in wild-type and mutant embryos.

We have demonstrated the complexity of NCC defects in *cls* embryos, with survival, migration and differentiation of non-ectomesenchymal cell types all affected. Further, a small decrease in clone size suggests that proliferation may also be somewhat affected (K. A. D. and R. N. K., unpublished). This spectrum of defects is not readily consistent with a primary function for wild-type *cls/sox10* in NCC survival, proliferation or differentiation. Although a dying cell might show abnormal migration and proliferation, the timing of appearance of defects in *cls* mutants conflicts with cell survival being the primary defect. We can first distinguish *cls* mutants at 20 hpf (by lack of *nac/mitf* expression), but do not see NCC apoptosis by TUNEL until around 35 hpf; previous work in zebrafish has suggested that the delay between induction of apoptosis and detectable morphological changes and DNA fragmentation is at most 3-4 hours (Ikegami et al., 1999). Likewise the *cls* mutant phenotype cannot be explained as primarily a failure of migration, with subsequent failure of exposure to required trophic factors, because for three subsets of affected cells (three pigment cell types in the stripe dorsal to the neural tube), the premigratory position is also a final location and hence the necessary trophic factors must be available. Despite this, in *cls* mutants all pigment cells, including those of the dorsal stripe, fail to develop properly. Instead, we propose that the primary role of *cls* gene function is in specification of non-ectomesenchymal cell fates; all other defects in *cls* mutants would then be secondary effects of a failure to become properly specified. Thus, in *cls* mutants NCCs are unable to adopt non-ectomesenchymal fates and so fail to differentiate. This differentiation process would include expression of growth and trophic factor receptors, and hence secondary defects might include impaired proliferation and later apoptosis. Our identification of the *cls* gene as a *sox10* transcription factor gene is consistent with this interpretation.

Indeed, for the specific case of melanophore fate, data presented here and elsewhere permit us to propose a molecular model consistent with this interpretation (Fig. 6). In both zebrafish and mammals, Nac/Mitf homologues have been shown to be important transcription factors for specifying melanophore fate (Lister et al., 1999; Opdecamp et al., 1997; Tachibana et al., 1996). We show here that *cls* mutants lack expression of *nac* (indeed it is the earliest defect we have identified). Thus, *sox10* is required for *nac* expression and thus for melanophore lineage specification. In addition, in *nac* mutants, *nac*-positive cells show a failure to migrate highly reminiscent of the *cls* melanoblast phenotype (Lister et al., 1999). Likewise, in both *cls* and *nac* mutants, *spa/kit* expression is lost in melanoblasts. *spa* function is necessary for both melanoblast migration and melanoblast and melanophore survival (Kelsh et al., 2000b; Parichy et al., 1999). Furthermore, the timing of loss of melanoblasts in *spa* mutants, beginning between 30 and 36 hpf, is consistent with the timing of decrease in melanoblast numbers and with the timing of NCC apoptosis in *cls* mutants (Kelsh et al., 2000b; this study). Hence, a simple model can largely explain the *cls* melanophore phenotype. *cls/sox10* has a key role, by direct or indirect activation of *nac/mitf*, in melanophore specification and consequently *cls* mutants lack expression of genes activated by nac, including *spa/kit*, mediating survival and migration, and melanogenic enzymes, mediating pigmentation. In support of this model, injection of *sox10* mRNA into early embryos results in ectopic *nac/mitf* expression and expression of *nac* in *cls* embryos is sufficient to rescue melanophores (S. E. and R. N. K., unpublished). It will be of interest to expand this model to include other targets of *sox10* and *nac*, as well as to extend this model to other non-ectomesenchymal neural crest derivatives affected in *cls* mutants. Our model predicts that the immediate targets of *sox10* will be either master regulators of

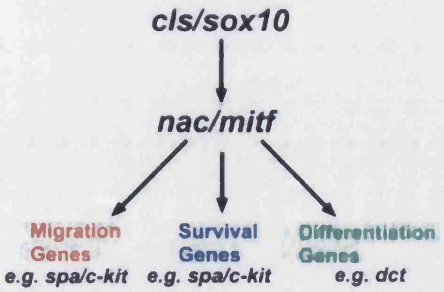

Fig. 6. Model of role of *cls/sox10* in melanophore specification. Formal genetic interactions between selected genes known to function in zebrafish melanophore development are schematised. In *cls* mutants, failure to activate *nac* expression (and thus to specify melanophore fate) results in absence of gene products critical for melanophore survival, migration and differentiation. For details, see main text.

neural crest fate (e.g. *nac*) or a multitude of diverse gene products required within specific crest derivatives for the cellular functions of trophic support, migration and differentiation. Thus, it will be important to identify the direct targets of Sox10 transcriptional regulation.

This specific model is likely to be applicable to mammalian neural crest too. Thus, Sox10 directly regulates *Mitf* expression in mouse (Bondurand et al., 2000; Lee et al., 2000; Potterf et al., 2000; Verastegui et al., 2000). Although *Dct*-positive melanoblasts are not detectable in $Sox10^{Dom}$ mice, some evidence of impaired or delayed migration of some NCCs has been presented (Southard-Smith et al., 1998). Similarly, *Kit* function is critically involved in promoting melanoblast migration and survival, is rapidly lost from melanoblasts in *Mitf* mutants and is known to be a direct target of Mitf, at least in cultured mast cells (Opdecamp et al., 1997; Wehrle-Haller and Weston, 1995; Wehrle-Haller and Weston, 1997). In *Sox10* mutant mice, *Kit* expression in melanoblasts may be absent, although the presence of unaffected cells in the skin, suggested to be mast cells, means that this result needs to be confirmed (Bondurand et al., 2000).

sox10 alone cannot be sufficient to specify each of the non-ectomesenchymal fates. We believe that *sox10*, while crucial for each of them, is not sufficient; instead, we propose that *sox10* is one of a combination of genes that together specify non-ectomesenchymal fates from neural crest. This model helps explain why cells that express molecular markers for affected cell types can be identified in *cls* mutants (Kelsh and Eisen, 2000). For example, although melanophores barely express melanin, xanthophores show much pigment in *cls* mutants. If a combination of transcription factors together specify a cell type, each factor might regulate only partially overlapping subsets of the characteristics of individual fates. In the absence of *sox10* gene function, those aspects of melanophore and xanthophore fate requiring *sox10* function would be affected (e.g. synthesis of melanin and trophic machinery, respectively), while others would remain at least partly unaffected (e.g. *dct* expression and pteridine pigment synthesis, respectively). A directly analogous mechanism has been proposed for autonomic neurone specification from the neural crest, with different genes regulating pan-neuronal and subtype specific cell properties (Anderson et al., 1997). Factors that interact with Sox10 to regulate target genes have been described, including the paired box transcription factor Pax3 and the POU-domain protein Tst-1/Oct6/SCIP (Bondurand et al., 2000; Kuhlbrodt et al., 1998a). However, it remains to be seen whether these co-factors have any role in distinguishing non-ectomesenchymal fates. Identification of combinations of transcription factors required to specify each fate will be a promising line of future research.

Our specification model predicts that *sox10* function is required only in NCCs fated to non-ectomesenchymal derivatives. *fkd6* is expressed very broadly in premigratory NCCs (Odenthal and Nuesslein-Volhard, 1998) and shows extensive, but incomplete, overlap with *sox10*. Further studies will be required to test whether *sox10-; fkd6+* NCCs represent ectomesenchymal precursors. However, our results do show that, consistent with our model, expression is, at least, rapidly downregulated in cells that adopt ectomesenchymal fates. In mammals, *Sox10* has sometimes been assumed to be a generic NCC marker (Pattyn et al., 1999), but our results show that, in fish, overlap with other NC markers is incomplete, even at premigratory stages.

In many respects, zebrafish neural crest development is typical of neural crest development in all vertebrates (Raible et al., 1992). In contrast to mouse and human *Sox10* mutations, none of the fish *sox10* mutations show dominant effects on melanophore number or pattern (R. N. K., unpublished). In mice, expressivity of the *sox10* haploinsufficiency phenotype is dependent on the genetic background (Lane and Liu, 1984). Presumably, in the AB background in zebrafish heterozygotes have sufficient Sox10 for normal melanophore development. Nevertheless, the conserved expression pattern and homozygous phenotypes in the two species suggest that the detailed cell-biological basis for the *cls* phenotype proposed here illuminates a possible mechanism behind Waardenburg-Shah syndrome and Hirschsprung's disease, in which reduced SOX10 function may reduce the number of melanoblasts and enteric precursors specified.

We thank J. James for fish husbandry, L. D. Hurst for generation of Fig. 1B, D. Raible for pCSHSP, and C. Miller, D. Parichy and D. Raible for cDNA clones. We also gratefully acknowledge J. Eisen, D. Raible, J. M. W. Slack, R. Adams, W. Bennett, A. Ward and J. R. Dutton for helpful criticism and discussion of the manuscript. R. G. thanks S. Rudolph-Geiger for technical assistance. This work was supported by a Praxis XXI PhD Studentship (S. S. L.), a University of Bath studentship and ORS award (T. J. C.), a Royal Society Research Grant, Wellcome Trust Project Grant 050602/Z, a MRC Co-operative Group Component Grant G9810985, and MRC Co-operative Group Grant G9721903. R. G. and P. H. were supported by the German Human Genome Project (DHGP Grant 01 KW 9919).

REFERENCES

Akimenko, M. A., Ekker, M., Wegner, J., Lin, W. and Westerfield, M. (1994). Combinatorial expression of three zebrafish genes related to distal-less: part of a homeobox gene code for the head. *J. Neurosci.* **14**, 3475-3486.

Anderson, D. J., Groves, A., Lo, L., Rao, M., Shah, N. M. and Sommer, L. (1997). Cell lineage determination and the control of neuronal identity in the crest. *Cold Spring Harbor Symp. Quant. Biol.* **LXII**, 493-504.

Attié, T., Till, M., Pelet, A., Amiel, J., Edery, P., Boutrand, L., Munnich, A. and Lyonnet, S. (1995). Mutation of the endothelin-receptor B gene in Waardenburg-Hirschsprung disease. *Hum. Mol. Genet.* **4**, 2407-2409.

Baynash, A. G., Hosoda, K., Giaid, A., Richardson, J. A., Emoto, N.,

Hammer, R. E. and Yanagisawa, M. (1994). Interaction of endothelin-3 with endothelin-B receptor is essential for development of epidermal melanocytes and enteric neurons. *Cell* **79**, 1277-1285.

Bolande, R. P. (1974). The neurocristopathies: a unifying concept of disease arising in neural crest maldevelopment. *Hum. Pathol.* **5**, 409-429.

Bondurand, N., Kobetz, A., Pingault, V., Lemort, N., EnchaRazavi, F., Couly, G., Goerich, D. E., Wegner, M., Abitbol, M. and Goossens, M. (1998). Expression of the SOX10 gene during human development. *FEBS Lett.* **432**, 168-172.

Bondurand, N., Pingault, V., Goerich, D. E., Lemort, N., Sock, E., Caignec, C. L., Wegner, M. and Goossens, M. (2000). Interaction among SOX10, PAX3 and MITF, three genes altered in Waardenburg syndrome. *Hum. Mol. Genet.* **9**, 1907-1917.

Britsch, S., Goerich, D. E., Riethmacher, D., Peirano, R. I., Rossner, M., Nave, K. A., Birchmeier, C. and Wegner, M. (2001). The transcription factor Sox10 is a key regulator of peripheral glial development. *Genes Dev.* **15**, 66-78.

Dutton, K., Dutton, J. R., Pauliny, A. and Kelsh, R. N. (2001). A morpholino phenocopy of the *colourless* mutant. *Genesis* **30**, 188-189.

Edery, P., Atti'e, T., Amiel, J., Pelet, A., Eng, C., Hofstra, R. M., Martelli, H., Bidaud, C., Munnich, A. and Lyonnet, S. (1996). Mutation of the endothelin-3 gene in the Waardenburg-Hirschsprung disease (Shah-Waardenburg syndrome). *Nat. Genet.* **12**, 442-444.

Haffter, P., Granato, M., Brand, M., Mullins, M., Hammerschmidt, M., Kane, D., Odenthal, J., van Eeden, F., Jiang, Y., Heisenberg, C. et al. (1996). The identification of genes with unique and essential functions in the development of the zebrafish, Danio rerio. *Development* **123**, 1-36.

Halloran, M., Sato-Maeda, M., Warren, J., Su, F., Lele, Z., Krone, P., Kuwada, J. and Shoji, W. (2000). Laser-induced gene expression in specific cells of transgenic zebrafish. *Development* **127**, 1953-1960.

Herbarth, B., Pingault, V., Bondurand, N., Kuhlbrodt, K., Hermans-Borgmeyer, I., Puliti, A., Lemort, N., Goossens, M. and Wegner, M. (1998). Mutation of the Sry-related Sox10 gene in Dominant megacolon, a mouse model for human Hirschsprung disease. *Proc. Natl. Acad. Sci. USA* **95**, 5161-5165.

Hofstra, R. M., Osinga, J., Tan Sindhunata, G., Wu, Y., Kamsteeg, E. J., Stulp, R. P., van Ravenswaaij Arts, C., Majoor Krakauer, D., Angrist, M., Chakravarti, A. et al. (1996). A homozygous mutation in the endothelin-3 gene associated with a combined Waardenburg type 2 and Hirschsprung phenotype (Shah-Waardenburg syndrome). *Nat. Genet.* **12**, 445-447.

Hosoda, K., Hammer, R. E., Richardson, J. A., Baynash, A. G., Cheung, J. C., Giaid, A. and Yanagisawa, M. (1994). Targeted and natural (piebald-lethal) mutations of endothelin-B receptor gene produce megacolon associated with spotted coat color in mice. *Cell* **79**, 1267-1276.

Hukriede, N. A., Joly, L., Tsang, M., Miles, J., Tellis, P., Epstein, J. A., Barbazuk, W. B., Li, F. N., Paw, B., Postlethwait, J. H. et al. (1999). Radiation hybrid mapping of the zebrafish genome. *Proc. Natl. Acad. Sci. USA* **96**, 9745-9750.

Ikegami, R., Hunter, P. and Yager, T. D. (1999). Developmental activation of the capability to undergo checkpoint-induced apoptosis in the early zebrafish embryo. *Dev. Biol.* **209**, 409-433.

Kapur, R. P. (1999). Early death of neural crest cells is responsible for total enteric aganglionosis in Sox10(Dom)/Sox10(Dom) mouse embryos. *Pediatr. Dev. Pathol.* **2**, 559-569.

Kelsh, R. N., Brand, M., Jiang, Y.-J., Heisenberg, C. P., Lin, S., Haffter, P., Odenthal, J., Mullins, M. C., van Eeden, F. J., Furutani-Seiki, M. et al. (1996). Zebrafish pigmentation mutations and the processes of neural crest development. *Development* **123**, 369-389.

Kelsh, R. N. and Eisen, J. S. (2000). The zebrafish *colourless* gene regulates development of non-ectomesenchymal neural crest derivatives. *Development* **127**, 515-525.

Kelsh, R. N., Dutton, K., Medlin, J. and Eisen, J. S. (2000a). Expression of zebrafish *fkd6* in neural crest-derived glia. *Mech. Dev.* **93**, 161-164.

Kelsh, R. N., Schmid, B. and Eisen, J. S. (2000b). Genetic analysis of melanophore development in zebrafish embryos. *Dev. Biol.* **225**, 277-293.

Kimmel, C. B., Ballard, W. W., Kimmel, S. R., Ullmann, B. and Schilling, T. F. (1995). Stages of embryonic development of the zebrafish. *Dev. Dyn.* **203**, 253-310.

Knapik, E., Goodman, A., Atkinson, O., Roberts, C., Shiozawa, M., Sim, C., Weksler-Zangen, S., Trolliet, M., Futrell, C., Innes, B. et al. (1996). A reference cross DNA panel for zebrafish (Danio rerio) anchored with simple sequence length polymorphisms. *Development* **123**, 451-460.

Kuhlbrodt, K., Herbarth, B., Sock, E., Hermans-Borgmeyer, I. and Wegner, M. (1998a). Sox10, a novel transcriptional modulator in glial cells. *J. Neurosci.* **18**, 237-250.

Kuhlbrodt, K., Schmidt, C., Sock, E., Pingault, V., Bondurand, N., Goossens, M. and Wegner, M. (1998b). Functional analysis of Sox10 mutations found in human Waardenburg-Hirschsprung patients. *J. Biol. Chem.* **273**, 23033-23038.

Lane, P. W. and Liu, H. M. (1984). Association of megacolon with a new dominant spotting gene (Dom) in the mouse. *J. Hered.* **75**, 435-439.

Le Douarin, N. M. (1982). *The Neural Crest.* Cambridge: Cambridge University Press.

Lee, M., Goodall, J., Verastegui, C., Ballotti, R. and Goding, C. R. (2000). Direct regulation of the microphthalmia promoter by Sox10 links Waardenburg-Shah syndrome (WS4)-associated hypopigmentation and deafness to WS2. *J. Biol. Chem.* **275**, 37978-37983.

Lister, J. A., Robertson, C. P., Lepage, T., Johnson, S. L. and Raible, D. W. (1999). nacre encodes a zebrafish microphthalmia-related protein that regulates neural-crest-derived pigment cell fate. *Development* **126**, 3757-3767.

Liu, Q., Melnikova, I. N., Hu, M. and Gardner, P. D. (1999). Cell type-specific activation of neuronal nicotinic acetylcholine receptor subunit genes by Sox10. *J. Neurosci.* **19**, 9747-9755.

Malicki, J., Schier, A. F., Solnica-Krezel, L., Stemple, D. L., Neuhauss, S. C. F., Stainier, D. Y. R., Abdelilah, S., Rangini, Z., Zwartkruis, F. and Driever, W. (1996). Mutations affecting development of the zebrafish ear. *Development* **123**, 275-283.

Marusich, M. F., Furneaux, H. M., Henion, P. D. and Weston, J. A. (1994). Hu neuronal proteins are expressed in proliferating neurogenic cells. *J. Neurobiol.* **25**, 143-155.

Mayer, T. C. (1965). The development of piebald spotting in mice. *Dev. Biol.* **11**, 319-334.

Mayer, T. C. and Maltby, E. L. (1964). An experimental investigation of pattern development in lethal spotting and belted mouse embryos. *Dev. Biol.* **9**, 269-286.

Odenthal, J. and Nuesslein-Volhard, C. (1998). *fork head* domain genes in zebrafish. *Dev. Genes Evol.* **208**, 245-258.

Opdecamp, K., Nakayama, A., Nguyen, M. T. T., Hodgkinson, C. A., Pavan, W. J. and Arnheiter, H. (1997). Melanocyte development in vivo and in neural crest cell cultures: Crucial dependence on the Mitf basic-helix-loop-helix-zipper transcription. *Development* **124**, 2377-2386.

Parichy, D. M., Rawls, J. F., Pratt, S. J., Whitfield, T. T. and Johnson, S. L. (1999). Zebrafish sparse corresponds to an orthologue of c-kit and is required for the morphogenesis of a subpopulation of melanocytes, but is not essential for hematopoiesis or primordial germ cell development. *Development* **126**, 3425-3436.

Parichy, D. M., Ransom, D. G., Paw, B., Zon, L. I. and Johnson, S. L. (2000). An orthologue of the kit-related gene fms is required for development of neural crest-derived xanthophores and a subpopulation of adult melanocytes in the zebrafish, Danio rerio. *Development* **127**, 3031-3044.

Pattyn, A., Morin, X., Cremer, H., Goridis, C. and Brunet, J.-F. (1999). The homeobox gene *Phox2b* is essential for the development of autonomic neural crest derivatives. *Nature* **399**, 366-370.

Peirano, R. I. and Wegner, M. (2000). The glial transcription factor Sox10 binds to DNA both as monomer and dimer with different functional consequences. *Nucleic Acids Res.* **28**, 3047-3055.

Pevny, L. H. and Lovell-Badge, R. (1997). Sox genes find their feet. *Curr. Opin. Genet Dev.* **7**, 338-44.

Pingault, V., Bondurand, N., Kuhlbrodt, K., Goerich, D. E., Prehu, M. O., Puliti, A., Herbarth, B., Hermans-Borgmeyer, I., Legius, E., Matthijs, G. et al. (1998). SOX10 mutations in patients with Waardenburg-Hirschsprung disease. *Nat. Genet.* **18**, 171-173.

Potterf, S. B., Furumura, M., Dunn, K. J., Arnheiter, H. and Pavan, W. J. (2000). Transcription factor hierarchy in Waardenburg syndrome: regulation of MITF expression by SOX10 and PAX3. *Hum. Genet.* **107**, 1-6.

Puffenberger, E. G., Hosoda, K., Washington, S. S., Nakao, K., deWit, D., Yanagisawa, M. and Chakravarti, A. (1994). A missense mutation of the endothelin-B receptor gene in multigenic Hirschsprung's disease. *Cell* **79**, 1257-1266.

Pusch, C., Hustert, E., Pfeifer, D., Sudbeck, P., Kist, R., Roe, B., Wang, Z., Balling, R., Blin, N. and Scherer, G. (1998). The SOX10/Sox10 gene from human and mouse: sequence, expression, and transactivation by the encoded HMG domain transcription factor. *Hum. Genet.* **103**, 115-123.

Raible, D. W. and Eisen, J. S. (1994). Restriction of neural crest cell fate in the trunk of the embryonic zebrafish. *Development* **120**, 495-503.

Raible, D. W., Wood, A., Hodsdon, W., Henion, P. D., Weston, J. A. and Eisen, J. S. (1992). Segregation and early dispersal of neural crest cells in the embryonic zebrafish. *Dev. Dyn.* **195**, 29-42.

Rauch, G. J., Hammerschmidt, M., Blader, P., Schauerte, H. E., Strahle, U., Ingham, P. W., McMahon, A. P. and Haffter, P. (1997). Wnt5 is required for tail formation in the zebrafish embryo. *Cold Spring Harbor Symp. Quant. Biol.* **62**, 227-234.

Reyes, R. (1999). Development and Death of Zebrafish Rohon-Beard Spinal Sensory Neurons. In *Institute of Neuroscience*, pp. 1-99. Eugene, OR: University of Oregon.

Schilling, T. F. and Kimmel, C. B. (1994). Segment and cell type lineage restrictions during pharyngeal arch development in the zebrafish embryo. *Development* **120**, 483-494.

Schulte-Merker, S., Van Eeden, F. J. M., Halpern, M. E., Kimmel, C. B. and Nüsslein-Volhard, C. (1994). *no tail* (*ntl*) is the zebrafish homologue of the mouse *T* (*Brachyury*) gene. *Development* **120**, 1009-1015.

Smith, M., Hickman, A., Amanze, D., Lumsden, A. and Thorogood, P. (1994). Trunk neural crest origin of caudal fin mesenchyme in the zebrafish *Brachydanio rerio*. *Proc. R. Soc. London B Biol. Sci.* **256**, 137-145.

Southard-Smith, E. M., Kos, L. and Pavan, W. J. (1998). Sox10 mutation disrupts neural crest development in DOM Hirschsprung mouse model. *Nat. Genet.* **18**, 60-64.

Southard-Smith, E. M., Angrist, M., Ellison, J. S., Agarwala, R., Baxevanis, A. D., Chakravarti, A. and Pavan, W. J. (1999). The Sox10(Dom) mouse: modeling the genetic variation of Waardenburg-Shah (WS4) syndrome. *Genome Res.* **9**, 215-225.

Strimmer, K. and von Haeseler, A. (1996). Quartet puzzling: A quartet maximum-likelihood method for reconstructing tree topologies. *Mol. Biol. Evol.* **13**, 964-969.

Tachibana, M., Takeda, K., Nobukuni, Y., Urabe, K., Long, J. E., Meyers, K. A., Aaronson, S. A. and Miki, T. (1996). Ectopic expression of MITF, a gene for Waardenburg syndrome type 2, converts fibroblasts to cells with melanocyte characteristics. *Nature Genet.* **14**, 50-54.

Tamura, K. and Nei, M. (1993). Estimation of the number of nucleotide substitutions in the control region of mitochondrial-DNA in humans and chimpanzees. *Mol. Biol. Evol.* **10**, 512-526.

Thompson, J. D., Gibson, T. J., Plewniak, F., Jeanmougin, F. and Higgins, D. G. (1997). The CLUSTAL_X windows interface: flexible strategies for multiple sequence alignment aided by quality analysis tools. *Nucleic Acids Res.* **25**, 4876-4882.

Verastegui, C., Bille, K., Ortonne, J. P. and Ballotti, R. (2000). Regulation of microphthalmia-associated transcription factor gene by the waardenburg syndrome type 4 Gene, Sox10. *J. Biol. Chem.* **275**, 30757-60.

Wegner, M. (1999). From head to toes: the multiple facets of Sox proteins. *Nucleic Acids Res.* **27**, 1409-1420.

Wehrle-Haller, B. and Weston, J. A. (1995). Soluble and cell-bound forms of steel factor activity play distinct roles in melanocyte precursor dispersal and survival on the lateral neural crest migration pathway. *Development* **121**, 731-742.

Wehrle-Haller, B. and Weston, J. A. (1997). Receptor tyrosine kinase-dependent neural crest migration in response to differentially localized growth factors. *BioEssays* **19**, 337-345.

Yuan, H., Corbi, N., Basilico, C. and Dailey, L. (1995). Developmental-specific activity of the FGF-4 enhancer requires the synergistic action of Sox2 and Oct-3. *Genes Dev.* **9**, 2635-2645.

Development 130, 2809-2818

doi:10.1242/dev.00461

DEVELOPMENT AND DISEASE

Transcriptional regulation of *mitfa* accounts for the *sox10* requirement in zebrafish melanophore development

Stone Elworthy[1,*,†], James A. Lister[2,†], Tom J. Carney[1], David W. Raible[2,‡] and Robert N. Kelsh[1,‡]

[1]Department of Biology and Biochemistry, University of Bath, Bath BA2 7AY, UK
[2]Department of Biological Structure, University of Washington, Seattle, WA 98195-7420, USA
*Present address: Centre for Developmental Genetics, Department of Biomedical Science, University of Sheffield, Sheffield S10 2TN, UK
†These authors contributed equally to this work and are joint first authors
‡Authors for correspondence (e-mail: bssrnk@bath.ac.uk and draible@u.washington.edu)

Accepted 26 February 2003

SUMMARY

The transcription factor Sox10 is required for the specification, migration and survival of all nonectomesenchymal neural crest derivatives including melanophores. *sox10*$^{-/-}$ zebrafish lack expression of the transcription factor *mitfa*, which itself is required for melanophore development. We demonstrate that the zebrafish *mitfa* promoter has sox10 binding sites necessary for activity in vitro, consistent with studies using mammalian cell cultures that have shown that *Sox10* directly regulates *Mitf* expression. In addition, we demonstrate that these sites are necessary for promoter activity in vivo. We show that reintroduction of *mitfa* expression in neural crest cells can rescue melanophore development in *sox10*$^{-/-}$ embryos. This rescue of melanophores in *sox10*$^{-/-}$ embryos is quantitatively indistinguishable from rescue in *mitfa*$^{-/-}$ embryos. These findings show that the essential function of *sox10* in melanophore development is limited to transcriptional regulation of *mitfa*. We propose that the dominant melanophore phenotype in Waardenburg syndrome IV individuals with *SOX10* mutations is likely to result from failure to activate *MITF* in the normal number of melanoblasts.

Key words: Zebrafish, *Danio rerio*, Neural crest, Fate specification, Melanocyte, *sox10*, *colourless*, *mitf*, *nacre*, Survival, Transcriptional regulation

INTRODUCTION

During vertebrate embryogenesis neural crest cells delaminate from the dorsal neural tube, migrate throughout the body and differentiate into a remarkably diverse array of cell types (Le Douarin and Kalcheim, 1999; Smith et al., 1994). These neural crest fates can be broadly categorized as ectomesenchymal and nonectomesenchymal. The ectomesenchymal neural crest fates include cranial cartilage and fin mesenchyme (in fish) whereas the nonectomesenchymal fates include neurons and glia of the peripheral nervous system and pigment cells. Defects in neural crest development are a significant cause of human disease and the resulting syndromes are termed neurocristopathies (Le Douarin and Kalcheim, 1999). One such neurocristopathy is Waardenburg's Syndrome, in which individuals have dominant pigmentation defects. Waardenburg's Syndrome types IIa and IV are associated with haploinsufficiency for the transcription factor genes *MITF* and *SOX10*, respectively (Pingault et al., 1998; Tachibana et al., 1994; Tassabehji et al., 1994).

Zebrafish or mice homozygous for mutations in the *sox10* transcription factor gene [previously called *colourless* (*cls*) in zebrafish] have severe defects in all the nonectomesenchymal neural crest cell fates (Dutton et al., 2001; Herbarth et al., 1998; Kelsh and Eisen, 2000; Southard-Smith et al., 1998). In *cls/sox10*$^{-/-}$ zebrafish many neural crest cells undergo apoptotic cell death near the neural tube. They do so after failing to become specified or migrate (Dutton et al., 2001). Apoptotic death of cells on the neural crest migration pathways has also been reported in *Sox10*$^{-/-}$ mouse embryos (Kapur, 1999). In *cls/sox10*$^{-/-}$ zebrafish and in *Sox10*$^{-/-}$ mouse embryos some of the nonectomesenchymal neural crest cell fates such as melanocytes (also called melanophores in zebrafish) and peripheral glia are essentially absent whereas others such as the dorsal root ganglia sensory neurons do form but with fewer and disorganized cells (Britsch et al., 2001; Kelsh and Eisen, 2000; Sonnenberg-Riethmacher et al., 2001; Southard-Smith et al., 1998).

In mammalian systems it has been shown that in the case of the peripheral glia a major requirement of *Sox10* is to directly regulate expression of terminal differentiation genes such as *P0* and *Cx32* (*Gjb1* – Mouse Genome Informatics) (Bondurand et al., 2001; Peirano et al., 2000). *Sox10* also regulates expression of the neuregulin receptor gene, *Erbb3* (Britsch et al., 2001). Signaling through *Erbb3* promotes acquisition of the glial fate

by neural crest cells and is required for peripheral glial cell migration and survival (Paratore et al., 2001). However it is not known whether this *Erbb3* regulation by *Sox10* is direct.

In the case of melanocytes it is not clear to what extent *Sox10* is required for direct transcriptional regulation of terminal differentiation genes. One plausible hypothesis is that in the melanocyte lineage *Sox10* is simply required for direct activation of the *Mitf* transcription factor gene, which then acts as a master regulator of melanocyte cell fate. Evidence for the pivotal role of Mitf in melanocyte development has come from studies with both mammals and zebrafish. In mammalian systems Mitf transactivates expression of melanogenic enzyme genes such as *Tyr* and *Trp1* as well as the receptor tyrosine kinase gene *Kit*. Kit signaling potentiates Mitf activity in turn and is also required for melanocyte proliferation and survival in both zebrafish and mice (Goding, 2000; Hemesath et al., 1998; Hou et al., 2000; Opdecamp et al., 1997; Parichy et al., 1999; Steel et al., 1992; Yasumoto et al., 1997). In mammalian systems Mitf also directly regulates expression of the antiapoptotic factor gene *Bcl2* required for melanocyte survival (McGill et al., 2002). Similarly, ectopic *mitfa* (previously known as *nac*) expression in zebrafish embryos causes ectopic expression of the melanogenic enzyme gene *dct* (Lister et al., 1999). Forced expression of *Mitf* in cultured mouse fibroblasts can induce some aspects of melanocyte differentiation and ectopic *nac/mitfa* expression in zebrafish embryos causes ectopic abnormal melanized cells (Lister et al., 1999; Tachibana et al., 1996).

In cultured mammalian cells, Sox10 can directly activate expression from the mouse or human *Mitf* promoter (Bondurand et al., 2000; Lee et al., 2000; Potterf et al., 2000; Verastegui et al., 2000). *Sox10*$^{-/-}$ zebrafish or mouse embryos lack *Mitf* expression and *nac/mitfa*$^{-/-}$ zebrafish or *Mitf*$^{-/-}$ mouse embryos have melanocyte defects at least as severe as those in *Sox10*$^{-/-}$ mutant embryos (Dutton et al., 2001; Hodgkinson et al., 1993; Lister et al., 1999; Potterf et al., 2001). Thus loss of *mitf* expression would be sufficient to account for the melanocyte defect in *sox10*$^{-/-}$ mutant embryos.

Although regulation of *Mitf* expression is clearly part of the *Sox10* requirement in the melanocyte lineage it is also possible that there are other essential *Sox10* functions in this lineage. Unlike zebrafish, mice show a haploinsufficiency phenotype when heterozygous for *Sox10* mutations (Britsch et al., 2001). This phenotype includes a mild melanocyte deficiency. Melanocytes from these mice show little reduction in *Mitf* expression and yet transiently have a severe reduction in expression of the melanogenic enzyme gene *Dct* (Potterf et al., 2001). In addition, *Sox10* can transactivate expression from a *Dct* promoter construct in cultured cells (Britsch et al., 2001; Potterf et al., 2001). These findings could suggest a requirement for *Sox10* in regulating *Dct* expression that is not mediated via *Mitf*. A critical question is whether any such non-*Mitf*-mediated effects of *Sox10* have a significant role in melanocyte development.

We show here that the direct regulation of *Mitf* expression by *Sox10* reported in cultured mammalian cells also occurs in developing melanophores in zebrafish embryos. We extend these studies by showing that forced expression of *nac/mitfa* in the neural crest of *cls/sox10*$^{-/-}$ mutant zebrafish embryos is sufficient to rescue melanophore development. Furthermore, we show that rescue of melanophores in *cls/sox10*$^{-/-}$ embryos is quantitatively indistinguishable from rescue in *nac/mitfa*$^{-/-}$ embryos. Together, these data suggest that regulation of *nac/mitfa* by *cls/sox10* can fully account for the *cls/sox10* requirement in the zebrafish melanophore lineage.

MATERIALS AND METHODS

Fish

Embryos were obtained through natural crosses and staged according to Kimmel et al. (Kimmel et al., 1995). We used three *cls* alleles (*m618*, *t3* and *tw2*) which all have equally strong phenotypes (Dutton et al., 2001). We used the *nac*^{w2} allele (Lister et al., 1999) except where it is stated that we used the *nac*^{b692} allele (Lister et al., 2001).

PCR genotyping

Embryos were tested for heterozygosity or homozygosity of the *nac* mutations by PCR on genomic DNA. The *nac*^{w2} test used PCR primers cattcttgggttcatggatgcaggac and ggcaggcttgaggggcaggag followed by digestion with *Dra*I which cleaves the mutant allele (Lister et al., 1999). The *nac*^{b692} test used PCR primers gcagaagtaagagccctggc and acggatcatttgacttgggaattaaag followed by digestion with BsrD1 which cleaves the mutant allele.

Whole-mount in situ hybridization

Embryos were processed for whole-mount in situ hybridization with *nac/mitfa* digoxigenin-labeled riboprobe as in Dutton et al. (Dutton et al., 2001).

Cell culture and luciferase assays

Promoter truncations were made from plasmid nac>luc (Dorsky et al., 2000) using the restriction sites indicated in Fig. 3. Mutation to the M1 sequence (see Table 1) was made by replacing the *Spe*1-*Age*1 region with the annealed oligonucleotides ctagtaacccatcgtcggcggtaggcttttgtcgaatcgga and ccggtccgattcgacaaaagcctaccgccgacgatgggtta. The QuickChange kit (Stratagene) was used for mutation to the M2, M3 or M4 sequences (see Table 1). pCS2sox10 and pCS2sox10L142Q were constructed by cloning the *Cla*I/*Xba*I fragments from hs>*sox10* or hs>*sox10L142Q* (Dutton et al., 2001) into pCS2+.

Transfection of NIH3T3 cells and luciferase assays were performed essentially as described previously (Lister et al., 2001). Transfections were performed on cells in 24-well dishes, with each well receiving 300 ng *sox10* expression vector, 100 ng *mitfa*-promoter>luciferase reporter, and 50 ng pCMV-βgal as internal control.

Electrophoretic mobility shift assays

The pCls/Sox10-GST expression plasmid was constructed by cloning a PCR product amplified from hs>*sox10* (Dutton et al., 2001) (using primers cgggatcccgatgtcggcggaggagcacag and gcgaattcaggaacccggtttgccgtt) between the BamH1 and EcoR1 sites of pGEX-3X (Amersham Pharmacia). Cls/Sox10-GST fusion protein was expressed in *E. coli* BL21(RIL) (Stratagene) and affinity purified using glutathione agarose following the manufacturer's instructions (Amersham Pharmacia). Approximate relative concentrations of Cls/Sox10-GST protein were estimated by comparison to a dilution series of bovine serum albumin (BSA) standard using Coomassie-stained polyacrylamide gel electrophoresis (PAGE). The SpeAge DNA probe was oligonucleotides ctagtaacccatcgtcaaagaggcttttgtcgaatcgga and ccgattcgacaaaagcctctttgagacgacgatgggttact annealed together, end labeled with [γ-^{32}P] ATP using T4 polynucleotide kinase and native PAGE purified. For electrophoretic mobility shift assays (EMSA), a 20 μl reaction mixture (containing Cls/Sox10-GST protein, 2000 c.p.m. of [^{32}P]DNA, 330 ng poly(dG-dC)•poly(dG-dC) (Amersham Pharmacia), 50 mM NaCl, 3% (w/v) Ficol (Amersham Pharmacia), 10 mM HEPES (pH 7.9), 5 mM $MgCl_2$,

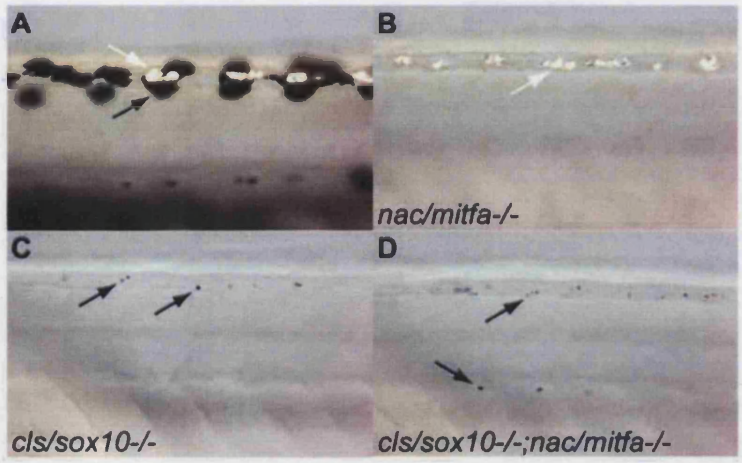

Fig. 1. Pigment cell defects in *cls/sox10*$^{-/-}$, *nac/mitfa*$^{-/-}$ and *cls/sox10*$^{-/-}$;*nac/mitfa*$^{-/-}$ mutant embryos. Lateral views of the dorsal trunk of 3 dpf wild type (A), *nac/mitfa*$^{b692/b692}$ (B), *cls/sox10*$^{t3/t3}$ (C) and *cls/sox10*$^{t3/t3}$;*nac/mitfa*$^{b692/b692}$ (D) embryos. Wild-type embryos have large flat melanophores (black arrow), *cls/sox10*$^{-/-}$ and *cls/sox10*$^{-/-}$;*nac/mitfa*$^{-/-}$ embryos have a few tiny rounded melanophores (black arrows), but *nac/mitfa*$^{-/-}$ embryos lack melanophores. Iridophores (white arrows) are not reduced in *nac/mitfa*$^{-/-}$ embryos but are severely reduced in *cls/sox10*$^{-/-}$ and *cls/sox10*$^{-/-}$;*nac/mitfa*$^{-/-}$. Double mutant embryos were identified by PCR genotyping.

0.5 mM EDTA, 0.1 mM dithiothreitol, 1 mg/ml BSA and sometimes specific competitor oligonucleotide) was incubated on ice for 20 minutes then electrophoresed on a gel (5% (w/v) polyacrylamide (37:1), 0.5% TBE) at 120 V, at 4°C, for 3 hours. Dried gels were exposed to Biomax MS film (Kodak) for autoradiography.

Embryo injections

One- or two-cell stage embryos were injected with plasmids and/or RNA using standard methods as in Dutton et al. (Dutton et al., 2001). RNA was produced using the mMESSAGE mMACHINE kit (Ambion) from hs>*sox10* or hs>*sox10(L142Q)* templates (Dutton et al., 2001) linearized with Asp718.

Plasmids nac>GFP and nac>nac were generated as follows: the SV40 promoter of pGL3-Promoter (Promega) was replaced by a fragment of the *mitfa* promoter from the plasmid pNP-P+ (Lister et al., 2001) via *Sal*I and *Hin*dIII sites to make pGL3-NP. The luciferase gene of pGL3-NP was then excised with *Hin*dIII and *Xba*I and replaced with GFP (from pCS2-BE-GFP) or *mitfa* (from pHS-MT3A.1) (Lister et al., 1999). Plasmids nac>GFP and nac>nac were mutated to the M1, M2, M3, M4, M1M3 and M3M4 sequences by replacing the appropriate *nac* promoter fragments with those from the corresponding Fspnac>luc constructs (see above). cls>nac was constructed by PCR amplifying the *nac/mitfa* coding sequence with N-terminal myc tags from pHS-MT3A.1 (Lister et al., 1999) and cloning the PCR fragment into the Xba1 site of CS26.8. CS26.8 has the Sal1-Xba CMV promoter fragment of pCS2+ replaced by 6.8 kb of sequence extending upstream from the *cls/sox10* translational start site.

GFP fluorescence was scored in gastrulas using an MZ12 dissecting microscope (Leica). GFP fluorescence was scored in 24 hours-post-fertilization (hpf) embryos using an Axioplan 2 microscope (Zeiss) with the embryos anesthetized using 0.003% MS222 (Sigma) and mounted between bridged coverslips. Melanophore rescue was scored at 48 hpf or at 72 hpf in the case when the *cls/sox10*$^{-/-}$ iridophore phenotype was also being scored. Melanophores were only scored as rescued if they had wild-type morphology.

Photography

Live embryos were anesthetized with 0.003% MS222 (Sigma), mounted in methylcellulose or between bridged coverslips and photographed using a Spot digital camera mounted on an Eclipse E800 microscope (Nikon) or Axioplan 2 microscope (Zeiss) with DIC optics. Embryo whole-mount in situ hybridization specimens were photographed using a Spot digital camera mounted on a MZ12 microscope (Leica) with epi-illumination. The GFP fluorescent gastrula image was captured using a LSM510 confocal microscope (Zeiss) with DIC and confocal fluorescence images superimposed.

RESULTS

nac/mitfa$^{-/-}$;*cls/sox10*$^{-/-}$ double mutant embryos have minute melanophores

cls/sox10$^{-/-}$ embryos show no *nac/mitfa* expression detectable by in situ hybridization and *nac/mitfa*$^{-/-}$ embryos have a complete absence of melanophores (Dutton et al., 2001; Lister et al., 1999). Although *cls/sox10*$^{-/-}$ embryos never have any normal melanophores, they do have a small number of tiny rounded cells expressing melanin (Kelsh et al., 1996; Kelsh et al., 2000). To determine whether these melanized cells result from residual *mitfa* expression below the sensitivity of in situ hybridization, we examined *nac/mitfa*$^{-/-}$;*cls/sox10*$^{-/-}$ double mutant embryos.

Intercrossing *nac/mitfa*$^{+/b692}$;*cls/sox10*$^{+/t3}$ parents gave embryos with three different phenotypes: wild-type (Fig. 1A), embryos with the typical *nac/mitfa*$^{-/-}$ phenotype of complete loss of all melanophores but no reduction in iridophores (Fig. 1B), and embryos with the typical *cls/sox10*$^{-/-}$ phenotype of a severe reduction in all pigment types including iridophores but a persistence of tiny melanized spots (Fig. 1C,D). All embryos classified as having a *cls* phenotype were similar, having at least five tiny melanophores, and importantly we did not observe any embryos with both a complete absence of these tiny melanized cells and loss of iridophores. The numbers of embryos with these specific phenotypes, 168 wild type: 59 *nac*: 67 *cls*, fits the ratio of 9:3:4 expected if embryos with the genotype *cls*$^{-/-}$;*nac*$^{-/-}$ exhibit the *cls* phenotype (p=0.64 by chi-square analysis). We confirmed that some of these embryos were indeed *nac/mitfa*$^{-/-}$ homozygotes by PCR genotyping. Of the 27 such embryos we tested, four were *nac/mitfa*$^{-/-}$;*cls/sox10*$^{-/-}$ (Fig. 1D), 14 were *nac/mitfa*$^{+/-}$;*cls/sox10*$^{-/-}$ and nine were *nac/mitfa*$^{+/+}$;*cls/sox10*$^{-/-}$.

To test whether this surprising result was also observed with other *nac/mitfa* and *cls/sox10* alleles we crossed *nac/mitfa*$^{w2/w2}$;*cls/sox10*$^{+/tw2}$ and *nac/mitfa*$^{+/w2}$;*cls/sox10*$^{+/tw2}$ parents. This gave 36 wild-type embryos, 39 embryos with the typical *nac/mitfa*$^{-/-}$ phenotype and 18 embryos with a severe reduction in all pigment types. These 18 embryos each had at least five tiny melanophores and PCR genotyping showed that of the 17 such embryos we tested, 12 were *nac/mitfa*$^{-/-}$;*cls/sox10*$^{-/-}$ and five were *nac/mitfa*$^{+/-}$;*cls/sox10*$^{-/-}$.

These results suggest that the less severe melanophore defect observed in *cls/sox10*$^{-/-}$ embryos as compared to *nac/mitfa*$^{-/-}$

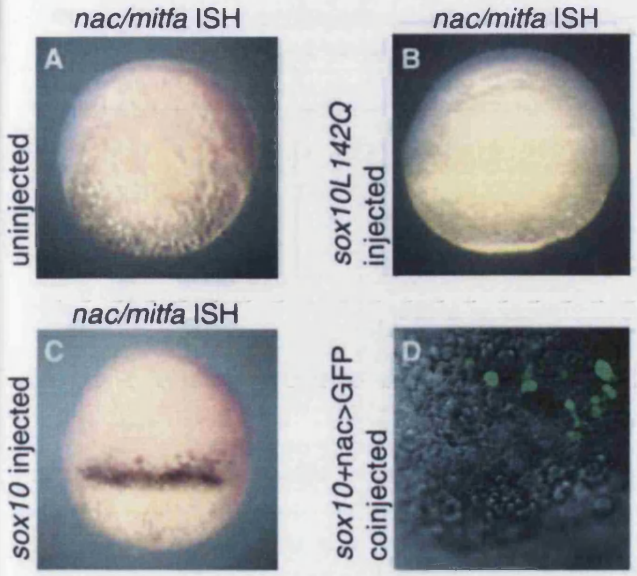

Fig. 2. Precocious *nac/mitfa* expression in 6 h.p.f embryos following injection with *cls/sox10* RNA. Lateral views of uninjected (A), *cls/sox10L142Q* RNA injected (250 pg per embryo; B) and *cls/sox10* RNA injected (250 pg per embryo; C) 6 hpf embryos following *in situ* hybridization with a *nac/mitfa* probe. Spots and/or patches of *nac/mitfa* expression were detected in 39% of *cls/sox10* RNA injected embryos (n=136) but not in any of the uninjected embryos (n=58) nor in any of the *cls/sox10L142Q* RNA injected embryos (n=92). (D) Superimposed fluorescent confocal and DIC images of an animal/lateral view of a 6 hpf embryo coinjected with *cls/sox10* RNA (250 pg per embryo) and nac>GFP reporter plasmid (150 pg per embryo) show cells with GFP fluorescence. GFP fluorescence was observed in 75% (n=224) of embryos coinjected with *cls/sox10* RNA and nac>GFP.

embryos cannot be attributed to residual *nac/mitfa* expression in *cls/sox10*$^{-/-}$ mutant embryos.

Ectopic *cls/sox10* expression in the embryo can induce ectopic *nac/mitfa* expression

In zebrafish embryos *cls/sox10* has been shown to be necessary for *nac/mitfa* expression (Dutton et al., 2001). In mammalian cells *Sox10* has also been reported to directly activate *Mitf* expression (Bondurand et al., 2000; Lee et al., 2000; Potterf et al., 2000; Verastegui et al., 2000). We used forced ectopic expression of *cls/sox10* to test whether *cls/sox10* was also sufficient to induce *nac/mitfa* expression in the zebrafish embryo. Embryos injected with *cls/sox10* RNA were probed for *nac/mitfa* expression by in situ hybridization. *cls/sox10* RNA injection induced *nac/mitfa* transcription at 6 hpf (Fig. 2C), 12 hours before the onset of endogenous *nac/mitfa* expression (Lister et al., 1999). The induced *nac/mitfa* expression was unevenly distributed as patches or spots, with the pattern of expression varying greatly from embryo to embryo. Ectopic *nac/mitfa* expression was not seen when embryos were injected with point mutant *cls/sox10L142Q* RNA (Fig. 2B), the mutation in the *cls*^{m618} allele (Dutton et al., 2001). These results show that *cls/sox10* can induce *nac/mitfa* expression in embryonic contexts other than the neural crest cells where *nac/mitfa* is normally expressed.

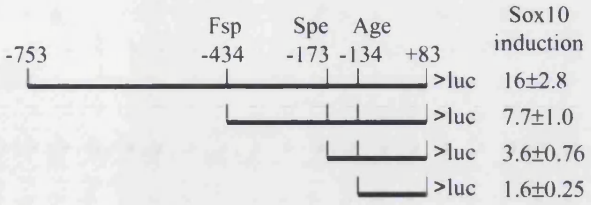

Fig. 3. Distribution of cls/sox10 response elements in the nac/mitfa promoter. Schematic diagram represents the 836 b.p. *nac/mitfa* promoter luciferase reporter construct (nac>luc) and derivative constructs with truncations of the *nac/mitfa* promoter. Co-transfection of the cls/sox10 expression plasmid pCS2sox10 into NIH3T3 cells with these constructs led to higher levels of induction with the full length promoter and incrementally lower levels with incremental 5′ truncations of the promoter. Sox10 induction was measured as: (luciferase activity with co-transfected pCS2sox10)/(luciferase activity with co-transfected pCS2sox10L142Q). The values shown are means±s.e.m. from at least four repetitions of each experiment.

nac/mitfa upstream sequence responds to *cls/sox10*

To establish whether *cls/sox10* acts directly or indirectly on *nac/mitfa* transcription it was necessary to identify sequence elements in the *nac/mitfa* promoter mediating *cls/sox10* responsiveness. Dorsky et al. (Dorsky et al., 2000) showed that an 836 b.p. *nac/mitfa* promoter (extending from –753 to +83 b.p. relative to the transcriptional start site) was able to direct expression from a GFP reporter plasmid (nac>GFP) to melanophores. We found that this reporter responded to *cls/sox10* RNA coinjection (Fig. 2D), but not *cls/sox10L142Q* RNA coinjection (n=146 embryos), in gastrula embryos, recapitulating the ectopic expression of *nac/mitfa*. This indicates that this 836 b.p. region of the *nac/mitfa* promoter contains sequence elements responsible for the *cls/sox10* response in zebrafish embryos. We used a cell line transfection assay to further localize sequence elements in the *nac/mitfa* promoter responsible for *cls/sox10* responsiveness. In transfected NIH3T3 cells a luciferase reporter construct with the 836 b.p. *nac/mitfa* promoter (nac>luc) was activated by a co-transfected zebrafish *cls/sox10* expression construct (pCS2sox10). All *cls/sox10* transfections were compared with the baseline value obtained by co-transfection with the point mutant construct pCS2sox10L142Q. Successive 5′ truncations of the *nac/mitfa* promoter resulted in incremental decreases in the level of induction in response to *cls/sox10* (Fig. 3). Thus elements conferring response to *cls/sox10* appeared to be widely distributed throughout the 836 b.p. *nac/mitfa* promoter. We chose to focus on the most proximal regions that conferred *cls/sox10* response. A promoter with a 5′ truncation to the *Spe*1 site (at –173 b.p.) could still respond to *cls/sox10*, and was significantly different than control transfection (p=0.01), but further truncation to the *Age*1 site (at –134 b.p.) prevented significant response (indistinguishable from control, P>0.1). These results tentatively localized a sequence element(s) responsible for some of the response to *cls/sox10* to this 41 b.p. region of the *nac/mitfa* promoter.

Cls/Sox10 binds *nac/mitfa* promoter sequences in vitro

The 41 b.p. critical region of the *nac/mitfa* promoter between the *Spe*1 and *Age*1 sites contains a sequence element (site S1)

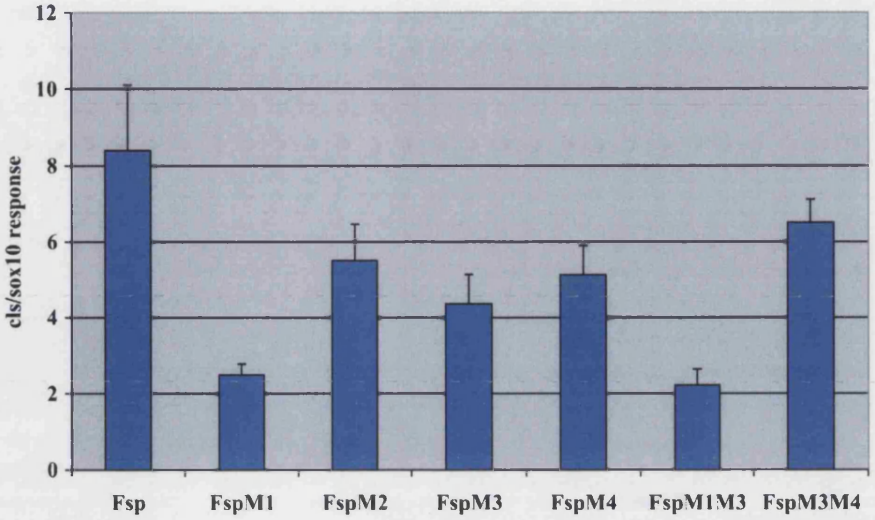

Fig. 5. *cls/sox10* response of *nac/mitfa* promoter luciferase reporter constructs with mutated Cls/Sox10 binding sites (see Table 1). *cls/sox10* response is measured as: (luciferase activity in NIH3T3 cells co-transfected with reporter and pCS2Sox10)/(activity with reporter and pCS2Sox10L142Q). Mean values from five or more repetitions of each experiment are shown for Fspnac>luc (Fsp), FspM1nac>luc (FspM1), FspM2nac>luc (FspM2), FspM3nac>luc (FspM3), FspM4nac>luc (FspM4), FspM1M3nac>luc (FspM1M3) and FspM3M4nac>luc. Bars indicate s.e.m.

(making M1nac>nac) greatly reduced the plasmid's effectiveness at melanophore rescue (Table 2). Mutation of sox binding site S3 (making M3nac>nac) caused a less dramatic reduction in effectiveness, whereas mutations of sites S2 or S4 (making M2nac>nac and M4nac>nac) had little effect (Table 2). We combined the S1 and S3 mutations (making M1M3nac>nac) which had more effect than mutating S1 alone ($P<0.0001$ by chi-square analysis). Combining the S3 and S4 mutations (making M3M4nac>nac) had no more effect than mutating S3 alone ($P>0.5$). These results show that the ability of a binding site to act as a response element in vivo is not accurately reflected by binding affinity in vitro, because sites S2 and S4 compete effectively for Cls/Sox10-GST protein binding in vitro (Fig. 4C) and yet show little evidence of being *cls/sox10* response elements in vivo (Table 2). Presumably other characteristics such as the context of the binding site in the promoter are just as important in defining a site as active in vivo.

We used the GFP reporter plasmid nac>GFP to further test the effect of mutating sox binding sites S1 and S3. As shown by Dorsky et al. (Dorsky et al., 2000), the 836 b.p. *nac/mitfa* promoter in nac>GFP directs expression of GFP to prospective pigment cells in injected embryos at 24 hpf. This assay differs from the nac>nac melanophore rescue assay in that it assesses promoter function in melanoblasts at an earlier developmental stage. Mutation of sox binding site S1 in nac>GFP (making M1nac>GFP) markedly reduced GFP reporter expression (Table 3). Mutation of site S3 (making M3>GFP) also reduced GFP reporter expression and combining the two mutations (making M1M3nac>GFP) had more effect than mutating S1 alone. The mutant rescue and GFP expression assays are different and so it is not prudent to compare the magnitude of the effects observed with each. However, both assays show similar trends in which mutating site S1 has a major effect, mutating site S3 has less of an effect, and mutating both sites has more effect than mutating S1 alone.

These results demonstrate that the *nac/mitfa* promoter contains a Cls/Sox10 protein binding site (site S1) that acts as a *cls/sox10* response element and that is necessary for adequate *nac/mitfa* expression in developing melanophores in the zebrafish embryo. The Cls/Sox10 protein binding site S3 also contributes to activation of *nac/mitfa* expression but to a lesser extent. These results suggest that in zebrafish neural crest cells in the embryo, Cls/Sox10 activates *nac/mitfa* expression by directly binding to the *nac/mitfa* promoter.

Table 2. Melanophore rescue at 48 hpf from *nac/mitfa* promoter constructs with mutated Cls/Sox10-binding sites

Injected plasmid*	Number of *nac/mitfa*$^{-/-}$ embryos injected	Number of embryos with one or more rescued melanophores (%)
nac>nac	658	373 (57)
M1nac>nac	568	50 (8.8)
M2nac>nac	429	235 (55)
M3nac>nac	405	94 (23)
M4nac>nac	371	163 (44)
M3M4nac>nac	338	75 (22)
M1M3nac>nac	485	10 (2.1)

*50 pg plasmid injected per embryo.

Table 3. GFP expression in wild type embryos from a *nac/mitfa* promoter construct is reduced by mutating a Cls/Sox10-binding site in the promoter of the plasmid

Injected plasmid*	Number of embryos injected	Number of embryos with GFP fluorescent crest cells at 24 hpf (%)
nac>nac	132	87 (66)
M1nac>nac	179	29 (16)
M3nac>nac	139	55 (40)
M1M3nac>nac	153	10 (6.5)

*25 pg plasmid injected per embryo.

Forced *nac/mitfa* expression rescues the *cls/sox10*$^{-/-}$ melanophore phenotype

cls/sox10$^{-/-}$ mutant embryos lack *nac/mitfa* expression and *nac/mitfa*$^{-/-}$ mutant embryos lack melanophores (Dutton et al., 2001; Lister et al., 1999). This prompted us to investigate whether activation of *nac/mitfa* transcription could account for

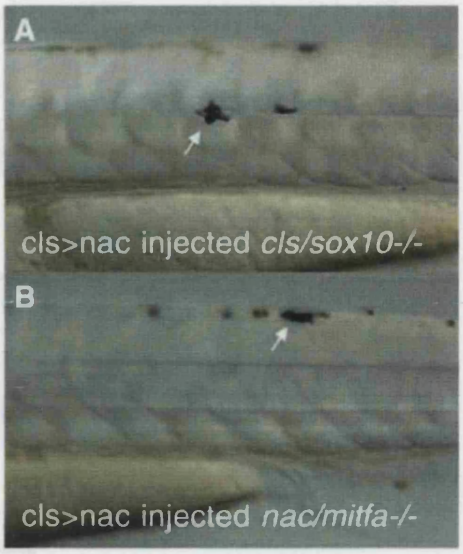

Fig. 6. In vivo melanophore rescue by forced *nac/mitfa* expression in the premigratory neural crest. Lateral views of the posterior trunk of 2 dpf, *cls/sox10*$^{-/-}$ (A) and *nac/mitfa*$^{-/-}$ (B) embryos that had been injected with cls>nac (15 pg per embryo). Rescued melanophores (arrows) have normal position and morphology.

the required role of *cls/sox10* in the melanophore lineage. We tested this by forcing *nac/mitfa* expression in *cls/sox10*$^{-/-}$ embryos, thus bypassing the role of *cls/sox10* in activating *nac/mitfa* expression. Because ectopic expression of *mitf* can confer some melanophore characteristics upon other cell types (Lister et al., 1999; Tachibana et al., 1996), we wanted to express *nac/mitfa* specifically in neural crest cells. We constructed a plasmid with the *nac/mitfa* cDNA under control of a *cls/sox10* promoter (cls>nac). The *cls/sox10* promoter used had previously been shown to target expression of a GFP reporter plasmid to the endogenous sites of *cls/sox10* expression such as neural crest and otic vesicle (T.J.C., J. Dutton and R.N.K., unpublished). Injected cls>nac was able to rescue melanophores with normal morphology and migratory ability in *cls/sox10*$^{-/-}$ mutant embryos and in *nac/mitfa*$^{-/-}$ mutant embryos (Fig. 6). In both genotypes, and in agreement with previous rescue studies of *mitf/nac*$^{-/-}$ (Lister et al., 1999), only a few melanophores were rescued in each embryo, presumably because of the highly mosaic distribution of injected DNA typical for zebrafish injection experiments. These results show that reintroduction of *nac/mitfa* expression rescues the differentiation, migration and survival deficiencies of *cls/sox10*$^{-/-}$ neural crest cells in the melanophore lineage. We were also able to rescue melanophores by expression of *nac/mitfa* using a hsp70 promoter construct (Lister et al., 1999) (data not shown).

We tested whether forced expression of *nac/mitfa* was as effective at rescuing melanophores in *cls/sox10*$^{-/-}$ embryos as in *nac/mitfa*$^{-/-}$ embryos. We injected cls>nac into embryos from intercrossed *cls/sox10*$^{+/-}$;*nac/mitfa*$^{+/-}$ double heterozygous parent fish to compare rescue in *cls/sox10*$^{-/-}$ and *nac/mitfa*$^{-/-}$ siblings that were laid, injected and raised together. Because both *cls/sox10*$^{-/-}$ and *nac/mitfa*$^{-/-}$ embryos have melanophore defects, we used the iridophore phenotype of the *cls/sox10*$^{-/-}$ embryos to distinguish them from embryos

Table 4. Melanophore rescue from forced *nac/mitfa* expression in embryos from intercrossed *cls/sox10*$^{+/-}$,*nac/mitfa*$^{+/-}$ double heterozygous parent fish

	Number of embryos injected* with cls>nac	Number of mutant embryos with one or more rescued melanophores (%)
Wild-type embryos	450	Not applicable
Embryos with melanophore and iridophore defects	210	68 (32)
Embryos with melanophore but not iridophore defects	161	48 (30)

*15 pg plasmid injected per embryo.

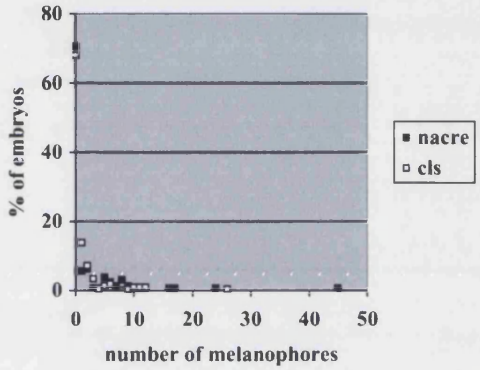

Fig. 7. Melanophore rescue by forced *nac/mitfa* expression in the neural crest of embryos from intercrossed *cls/sox10*$^{+/-}$,*nac/mitfa*$^{+/-}$ double heterozygous parent fish. The plot shows what number of melanophores were rescued in what percentage of *cls/sox10*$^{-/-}$ embryos (white squares) and embryos mutant for *nac/mitfa* but not *cls/sox10* (black squares). The numbers of each class of embryo are shown in Table 4. A Mann-Whitney rank sum test shows no significant difference in the extent of rescue of these two classes of mutant (P=0.876).

mutant for *nac/mitfa* alone (see Fig. 1). As mentioned above, double homozygous *cls/sox10*$^{-/-}$;*nac/mitfa*$^{-/-}$ embryos have melanophore and iridophore defects as in *cls/sox10*$^{-/-}$ embryos and this is reflected in the ratio of phenotypes (Table 4). The *cls/sox10*$^{-/-}$ embryos were rescued to the same extent as the embryos mutant for *nac/mitfa*$^{-/-}$ alone, both in terms of the proportion of embryos showing any rescued melanophores and in terms of the number of rescued melanophores per embryo (Table 4, Fig. 7). This result indicates that in the melanophore lineage, *cls/sox10* is required only to induce *nac/mitfa* expression.

DISCUSSION

cls/sox10$^{-/-}$*; nac/mitfa*$^{-/-}$ embryos have a less severe melanophore phenotype than *nac/mitfa*$^{-/-}$

Previous reports indicated that *nac/mitfa*$^{-/-}$ embryos lack all melanophores whereas *cls/sox10*$^{-/-}$ embryos still have a few tiny, rounded, melanized cells that fail to migrate (Kelsh and Eisen, 2000; Kelsh et al., 2000; Lister et al., 1999). We report

here that the presence of these melanized cells cannot be attributed to putative residual *nac/mitfa* expression in *cls/sox10*$^{-/-}$ embryos because they are also found in *cls/sox10*$^{-/-}$; *nac/mitfa*$^{-/-}$ embryos. The stronger phenotype of *nac/mitfa*$^{-/-}$ embryos may, therefore, imply the presence of a *cls/sox10*-dependent activity that inhibits melanophore development. Obviously, in normal development any such effect must be greatly outweighed by the positive activation of melanophore development mediated by *cls/sox10*. The source of any such inhibitory activity is completely unknown. However, *nac/mitfa*$^{-/-}$ embryos have an increased number of iridophores (Lister et al., 1999) and so it is conceivable that there might be some mechanism for mutual repression between pigment cell types. Sox10 is expressed in neural crest lineages other than that giving rise to melanophores, and perhaps the inhibitory activity functions to prevent expression of melanogenic genes in these cell types.

Role of *sox10* in nonectomesenchymal crest fate specification

Several groups have shown that *Sox10* can directly activate *Mitf* expression in cultured mammalian cells (Bondurand et al., 2000; Lee et al., 2000; Potterf et al., 2000; Verastegui et al., 2000). We found that the zebrafish *nac/mitfa* promoter is also directly activated by zebrafish Cls/Sox10 and that this direct regulation is necessary for expression from the zebrafish *nac/mitfa* promoter in neural crest cells in the developing embryo. Most significantly we found that this activation of *nac/mitfa* expression can account quantitatively for all of the *cls/sox10* requirement in the melanophore lineage. Studies in zebrafish and in mice have revealed defects in neural crest cell fate specification, migration, survival and differentiation in *sox10* mutants. We have previously proposed that the complex phenotype of *cls/sox10* mutants might be explained by a primary defect in specification of nonectomesenchymal crest fates, with defects in migration, survival and differentiation being secondary consequences of this (Dutton et al., 2001; Kelsh and Raible, 2002). Our demonstration here that *cls/sox10* directly activates *nac/mitfa*, a key gene in melanophore fate specification, and that this is vital for melanophore rescue in *nac/mitfa* mutants, is clearly consistent with our model.

Although not usually interpreted in the same way, the mouse *Sox10* mutant phenotype is plainly consistent with the model proposed. For example, the recent demonstration that *Mitf* regulates the antiapoptotic gene *Bcl2* provides a molecular explanation for the apoptosis of melanoblast progenitors in *Sox10* mutants (McGill et al., 2002). Furthermore, in mice the regulation of *Erbb3* (directly or indirectly) by *Sox10* (Britsch et al., 2001) provides evidence that *Sox10* regulates glial fate specification, because neuregulin signaling has been shown to direct neural crest stem cells to a glial fate (Shah and Anderson, 1997; Shah et al., 1994).

At first glance, our findings with the melanophore lineage contrast with the body of work establishing that *Sox10* directly activates a variety of differentiation genes in developing glia. However, these findings are consistent with the observation that *cls/sox10* expression is downregulated in melanoblasts but retained in developing peripheral glia (Dutton et al., 2001), and suggests that in addition to its roles in nonectomesenchymal fate specification, *sox10* is also required for glial cell differentiation.

Only a subset of *sox10*-expressing neural crest cells express *mitfa* and become melanophores. Dorsky et al. (Dorsky et al., 2000) showed that wnt signaling also directly activated *nac/mitfa* expression. These findings are consistent with a model for *cls/sox10* function in the melanophore lineage in which *sox10* is required in conjunction with Wnt signaling to activate *nac/mitfa* expression in neural crest cells (Kelsh and Raible, 2002). *nac/mitfa* then in turn specifies the melanophore fate by activating expression of differentiation genes such as *dct* and genes such as *spa/kit* required for survival and migration. The NIH3T3 cell transfection work described here was conducted in the absence of any known Wnt signaling. Furthermore, eliminating the Tcf/Lef binding sites as described by Dorsky et al. (Dorsky et al., 2000) from the *nac/mitfa* promoter reporter construct did not prevent the observed *cls/sox10* response in NIH3T3 cells (data not shown). Recently, Saito et al. (Saito et al., 2002) have shown that LEF-1 activates transcription from the *MITF* promoter in Hela cells much more effectively when bound together as a complex with the MITF-M protein itself. Future studies using coexpression of *sox10*, *mitfa* and Wnt signaling components could help to reveal how Wnt signaling and *sox10* interact to establish *mitfa* expression. Work by others using mammalian systems has also shown that the transcription factors *Pax3*, *OC-2* and *CREB* transactivate *Mitf* transcription (Bertolotto et al., 1998; Jacquemin et al., 2001; Potterf et al., 2000; Watanabe et al., 1998).

SOX10, *MITF* and human disease

Our demonstration that *sox10* function in melanophores may be limited to regulation of *mitfa* helps to explain the similar pigmentation defects of the Waardenburg Syndromes IIa and IV. Waardenburg Syndromes IIa and IV are associated with human haploinsufficiency for *MITF* and *SOX10*, respectively (Pingault et al., 1998; Tachibana et al., 1994; Tassabehji et al., 1994). Although zebrafish *cls/sox10* mutants have no dominant phenotype, our results suggest a model for the aetiology of Waardenburg Syndrome IV. We propose that in heterozygous *SOX10* mutant humans, activation of *MITF* by SOX10 is less efficient, resulting in specification of fewer melanoblasts. Consistent with this, in heterozygous *Sox10* mutant mice, which share the dominant pigment defects of human individuals, *Kit*-positive melanoblasts are reduced in number (Potterf et al., 2001); although not reported in these studies, we predict that the number of *Mitf*-expressing cells would be reduced in these mice compared to wild-types.

That we can, in zebrafish, account quantitatively for the role of *sox10* in the melanophore lineage by its activation of *mitfa* is perhaps surprising in view of the reports that the mouse *Dct* promoter can be directly regulated by Sox10 (Britsch et al., 2001; Potterf et al., 2001). However, these studies used co-transfection assays in cultured cells and thus leave open the question of whether *Dct* is regulated directly by Sox10 in the developing neural crest. Our findings strongly suggest that even if Sox10 does directly regulate *dct* expression in vivo, this requirement may be dispensable for melanophore development. Such an interpretation is consistent with the phenotype in heterozygous *Sox10* mutant mice. Thus, a transient reduction in *Dct* expression seen in developing melanoblasts was attributed to an effect of the reduced levels of Sox10 (Potterf et al., 2001), although an alternative explanation that sub-wild-type levels of *Mitf* expression result

in lowered *Dct* expression cannot be ruled out; indeed, more recent studies in culture show that MITF interacts with LEF-1 to directly coactivate the *DCT* promoter (Yasumoto et al., 2002). However, regardless of the mechanism mediating this reduction in detectable *Dct* expression, the *Dct* phenotype rapidly recovers, suggesting that in melanophores in which *Mitf* expression is above a threshold level, the requirement for *Sox10* is only transient and non-essential. The alternative explanation, that the precise contributions of *Sox10* and *Mitf* in melanocyte development may not be fully conserved between zebrafish and mice, is less attractive because of the striking similarities in the genetic control of melanocyte development already demonstrated between mouse and zebrafish (Rawls et al., 2001).

We thank Andrew Ward, Richard Adams, Richard Dorsky and members of the Kelsh and Raible laboratories for invaluable reagents and discussions. This work was supported by grants from the Medical Research Council (S.E. and R.N.K.), a University of Bath studentship and ORS award (T.J.C.), and the National Institutes of Health (J.A.L. and D.W.R.).

REFERENCES

Bertolotto, C., Abbe, P., Hemesath, T. J., Bille, K., Fisher, D. E., Ortonne, J. P. and Ballotti, R. (1998). Microphthalmia gene product as a signal transducer in cAMP-induced differentiation of melanocytes. *J. Cell Biol.* **142**, 827-835.

Bondurand, N., Girard, M., Pingault, V., Lemort, N., Dubourg, O. and Goossens, M. (2001). Human Connexin 32, a gap junction protein altered in the X-linked form of Charcot-Marie-Tooth disease, is directly regulated by the transcription factor SOX10. *Hum. Mol. Genet.* **10**, 2783-2795.

Bondurand, N., Pingault, V., Goerich, D. E., Lemort, N., Sock, E., Caignec, C. L., Wegner, M. and Goossens, M. (2000). Interaction among *SOX10*, *PAX3* and *MITF*, three genes altered in Waardenburg syndrome. *Hum. Mol. Genet.* **9**, 1907-1917.

Britsch, S., Goerich, D. E., Riethmacher, D., Peirano, R. I., Rossner, M., Nave, K. A., Birchmeier, C. and Wegner, M. (2001). The transcription factor Sox10 is a key regulator of peripheral glial development. *Genes Dev.* **15**, 66-78.

Dorsky, R. I., Raible, D. W. and Moon, R. T. (2000). Direct regulation of *nacre*, a zebrafish *MITF* homolog required for pigment cell formation, by the Wnt pathway. *Genes Dev.* **14**, 158-162.

Dutton, K. A., Pauliny, A., Lopes, S. S., Elworthy, S., Carney, T. J., Rauch, J., Geisler, R., Haffter, P. and Kelsh, R. N. (2001). Zebrafish *colourless* encodes *sox10* and specifies non-ectomesenchymal neural crest fates. *Development* **128**, 4113-4125.

Goding, C. R. (2000). Mitf from neural crest to melanoma: signal transduction and transcription in the melanocyte lineage. *Genes Dev.* **14**, 1712-1728.

Hemesath, T. J., Price, E. R., Takemoto, C., Badalian, T. and Fisher, D. E. (1998). MAP kinase links the transcription factor Microphthalmia to c-Kit signalling in melanocytes. *Nature* **391**, 298-301.

Herbarth, B., Pingault, V., Bondurand, N., Kuhlbrodt, K., Hermans-Borgmeyer, I., Puliti, A., Lemort, N., Goossens, M. and Wegner, M. (1998). Mutation of the Sry-related *Sox10* gene in Dominant megacolon, a mouse model for human Hirschsprung disease. *Proc. Natl. Acad. Sci. USA* **95**, 5161-5165.

Hodgkinson, C. A., Moore, K. J., Nakayama, A., Steingr'imsson, E., Copeland, N. G., Jenkins, N. A. and Arnheiter, H. (1993). Mutations at the mouse microphthalmia locus are associated with defects in a gene encoding a novel basic-helix-loop-helix-zipper protein. *Cell* **74**, 395-404.

Hou, L., Panthier, J. and Arnheiter, H. (2000). Signaling and transcriptional regulation in the neural crest-derived melanocyte lineage: interactions between KIT and MITF. *Development* **127**, 5379-5389.

Jacquemin, P., Lannoy, V. J., O'Sullivan, J., Read, A., Lemaigre, F. F. and Rousseau, G. G. (2001). The transcription factor Onecut-2 controls the microphthalmia-associated transcription factor gene. *Biochem. Biophys. Res. Commun.* **285**, 1200-1205.

Kapur, R. P. (1999). Early death of neural crest cells is responsible for total enteric aganglionosis in *Sox10(Dom)/Sox10(Dom)* mouse embryos. *Pediatr. Dev. Pathol.* **2**, 559-569.

Kelsh, R. N., Brand, M., Jiang, Y. J., Heisenberg, C. P., Lin, S., Haffter, P., Odenthal, J., Mullins, M. C., van Eeden, F. J., Furutani-Seiki, M. et al. (1996). Zebrafish pigmentation mutations and the processes of neural crest development. *Development* **123**, 369-389.

Kelsh, R. N. and Eisen, J. S. (2000). The zebrafish *colourless* gene regulates development of non-ectomesenchymal neural crest derivatives. *Development* **127**, 515-525.

Kelsh, R. N. and Raible, D. W. (2002). Specification of zebrafish neural crest. In *Pattern Formation in Zebrafish* (ed. L. Solnicka-Kresel), pp. 216-236. Berlin: Springer-Verlag.

Kelsh, R. N., Schmid, B. and Eisen, J. S. (2000). Genetic analysis of melanophore development in zebrafish embryos. *Dev. Biol.* **225**, 277-293.

Kimmel, C. B., Ballard, W. W., Kimmel, S. R., Ullmann, B. and Schilling, T. F. (1995). Stages of embryonic development of the zebrafish. *Dev. Dyn.* **203**, 253-310.

Le Douarin, N. M. and Kalcheim, C. (1999). *The Neural Crest*. Cambridge: Cambridge University Press.

Lee, M., Goodall, J., Verastegui, C., Ballotti, R. and Goding, C. R. (2000). Direct regulation of the microphthalmia promoter by Sox10 links Waardenburg-Shah syndrome (WS4)-associated hypopigmentation and deafness to WS2. *J. Biol. Chem.* **275**, 37978-37983.

Lister, J. A., Close, J. and Raible, D. W. (2001). Duplicate *mitf* genes in zebrafish: complementary expression and conservation of melanogenic potential. *Dev. Biol.* **237**, 333-344.

Lister, J. A., Robertson, C. P., Lepage, T., Johnson, S. L. and Raible, D. W. (1999). *nacre* encodes a zebrafish microphthalmia-related protein that regulates neural-crest-derived pigment cell fate. *Development* **126**, 3757-3767.

McGill, G. G., Horstmann, M., Wildlund, H. R., Du J., Motyckova G., Nishimra E. K., Lin Y., Ramaswamy S., Avery W., Ding H., Jordan S. A. et al. (2002). Bcl2 regulation by the melanocyte master regulator Mitf Modulates lineage survival and melanoma cell viability. *Cell* **109**, 707-718.

Mertin, S., McDowall, S. G. and Harley, V. R. (1999). The DNA-binding specificity of SOX9 and other SOX proteins. *Nucleic Acids Res.* **27**, 1359-1364.

Opdecamp, K., Nakayama, A., Nguyen, M. T. T., Hodgkinson, C. A., Pavan, W. J. and Arnheiter, H. (1997). Melanocyte development in vivo and in neural crest cell cultures: crucial dependence on the Mitf basic-helix-loop-helix-zipper transcription. *Development* **124**, 2377-2386.

Paratore, C., Goerich, D. E., Suter, U., Wegner, M. and Sommer, L. (2001). Survival and glial fate acquisition of neural crest cells are regulated by an interplay between the transcription factor Sox10 and extrinsic combinatorial signaling. *Development* **128**, 3949-3961.

Parichy, D. M., Rawls, J. F., Pratt, S. J., Whitfield, T. T. and Johnson, S. L. (1999). Zebrafish *sparse* corresponds to an orthologue of *c-kit* and is required for the morphogenesis of a subpopulation of melanocytes, but is not essential for hematopoiesis or primordial germ cell development. *Development* **126**, 3425-3436.

Peirano, R. I., Goerich, D. E., Riethmacher, D. and Wegner, M. (2000). Protein zero gene expression is regulated by the glial transcription factor Sox10. *Mol. Cell. Biol.* **20**, 3198-3209.

Pingault, V., Bondurand, N., Kuhlbrodt, K., Goerich, D. E., Prehu, M. O., Puliti, A., Herbarth, B., Hermans-Borgmeyer, I., Legius, E., Matthijs, G. et al. (1998). *SOX10* mutations in patients with Waardenburg-Hirschsprung disease. *Nat. Genet.* **18**, 171-173.

Potterf, S. B., Mollaaghababa, R., Hou, L., Southard-Smith, E. M., Hornyak, T. J., Arnheiter, H. and Pavan, W. J. (2001). Analysis of SOX10 function in neural crest-derived melanocyte development: Sox10-dependent transcriptional control of dopachrome tautomerase. *Dev. Biol.* **237**, 245-257.

Potterf, S. B., Furumura, M., Dunn, K. J., Arnheiter, H. and Pavan, W. J. (2000). Transcription factor hierarchy in Waardenburg syndrome: regulation of MITF expression by SOX10 and PAX3. *Hum. Genet.* **107**, 1-6.

Rawls, J. F., Mellgren, E. M. and Johnson, S. L. (2001). How the zebrafish gets its stripes. *Dev. Biol.* **240**, 301-314.

Saito, H., Yasumoto, K., Takeda, K., Takhashi, K., Fukushima, A., Orikasa, S. and Shibahara, S. (2002). Melanocyte-specific microphthalmia-associated transcription factor isoform activates its own gene promoter through physical interaction with lymphoid-enhancing factor 1. *J. Biol. Chem.* **277**, 28787-28794.

Shah, N. M. and Anderson, D. J. (1997). Integration of multiple instructive cues by neural crest stem cells reveals cell-intrinsic biases in relative growth factor responsiveness. *Proc. Natl. Acad. Sci. USA* **94**, 11369-11374.

Shah, N. M., Marchionni, M. A., Isaacs, I., Stroobant, P. and Anderson, D. J. (1994). Glial growth-factor restricts mammalian neural crest stem-cells to a glial fate. *Cell* **77**, 349-360.

Smith, M., Hickman, A., Amanze, D., Lumsden, A. and Thorogood, P. (1994). Trunk neural crest origin of caudal fin mesenchyme in the zebrafish *Brachydanio rerio*. *Proc. R. Soc. Lond. B* **256**, 137-145.

Sonnenberg-Riethmacher, E., Miehe, M., Stolt, C. C., Goerich, D. E., Wegner, M. and Riethmacher, D. (2001). Development and degeneration of dorsal root ganglia in the absence of the HMG-domain transcription factor Sox10. *Mech. Dev.* **109**, 253-265.

Southard-Smith, E. M., Kos, L. and Pavan, W. J. (1998). *Sox10* mutation disrupts neural crest development in *Dom* Hirschsprung mouse model. *Nat. Genet.* **18**, 60-64.

Steel, K. P., Davidson, D. R. and Jackson, I. J. (1992). TRP-2/DT, a new early melanoblast marker, shows that steel growth factor (c-kit ligand) is a survival factor. *Development* **115**, 1111-1119.

Tachibana, M., Perez Jurado, L. A., Nakayama, A., Hodgkinson, C. A., Li, X., Schneider, M., Miki, T., Fex, J., Francke, U. and Arnheiter, H. (1994). Cloning of *MITF*, the human homolog of the mouse microphthalmia gene and assignment to chromosome 3p14.1-p12.3. *Hum. Mol. Genet.* **3**, 553-557.

Tachibana, M., Takeda, K., Nobukuni, Y., Urabe, K., Long, J. E., Meyers, K. A., Aaronson, S. A. and Miki, T. (1996). Ectopic expression of *MITF*, a gene for Waardenburg syndrome type 2, converts fibroblasts to cells with melanocyte characteristics. *Nat. Genet.* **14**, 50-54.

Tassabehji, M., Newton, V. E. and Read, A. P. (1994). Waardenburg syndrome type 2 caused by mutations in the human microphthalmia (*MITF*) gene. *Nat. Genet.* **8**, 251-255.

Verastegui, C., Bille, K., Ortonne, J. P. and Ballotti, R. (2000). Regulation of the microphthalmia-associated transcription factor gene by the Waardenburg syndrome type 4 gene, *SOX10*. *J. Biol. Chem.* **275**, 30757-30760.

Watanabe, A., Takeda, K., Ploplis, B. and Tachibana, M. (1998). Epistatic relationship between Waardenburg syndrome genes *MITF* and *PAX3*. *Nat. Genet.* **18**, 283-286.

Yasumoto, K., Yokoyama, K., Takahashi, K., Tomita, Y. and Shibahara, S. (1997). Functional analysis of microphthalmia-associated transcription factor in pigment cell-specific transcription of the human tyrosinase family genes. *J. Biol. Chem.* **272**, 503-509.

Yasumoto, K., Takeda, K., Saito, H., Watanabe, K., Takahashi, K. and Shibahara, S. (2002). Microphthalmia-associated transcription factor interacts with LEF-1, a mediator of Wnt signaling. *EMBO J.* **21**, 2703-2714.